

UNCLASSIFIED

AD 432162

DEFENSE DOCUMENTATION CENTER

FOR

SCIENTIFIC AND TECHNICAL INFORMATION

CAMERON STATION, ALEXANDRIA, VIRGINIA



UNCLASSIFIED

NOTICE: When government or other drawings, specifications or other data are used for any purpose other than in connection with a definitely related government procurement operation, the U. S. Government thereby incurs no responsibility, nor any obligation whatsoever; and the fact that the Government may have formulated, furnished, or in any way supplied the said drawings, specifications, or other data is not to be regarded by implication or otherwise as in any manner licensing the holder or any other person or corporation, or conveying any rights or permission to manufacture, use or sell any patented invention that may in any way be related thereto.



COPY NO. 92

CATALOGED BY DDC 2162

FLUSH AND NONFLUSH MOUNTED TELEMETRY ANTENNAS
FLUSH MOUNTED COMMAND CONTROL ANTENNAS
S-BAND AND C-BAND BEACON TRANSPONDER ANTENNAS
ANTENNA SYSTEMS FOR SPECIFIC MISSILES,
PROBES AND SATELLITES

Project Director H. W. Haas

Project Engineer Henry D. Weinschel

Contract No. AF19(604)-6198

Project 7659
Task 7659C1.

FINAL REPORT
15 October 1963



Prepared for

AIR FORCE CAMBRIDGE RESEARCH LABORATORIES
OFFICE OF AEROSPACE RESEARCH
UNITED STATES AIR FORCE
BEDFORD, MASSACHUSETTS

432162

NEW MEXICO STATE UNIVERSITY
PHYSICAL SCIENCE LABORATORY
UNIVERSITY PARK, NEW MEXICO

Requests for additional copies by Agencies of the Department of Defense, their contractors and other Government agencies should be directed to the

**DEFENSE DOCUMENTATION CENTER
CAMERON STATION
ALEXANDRIA, VIRGINIA**

Department of Defense contractors must be established for DDC services or have their "need to know" certified by the cognizant military agency to their project or contract.

All other persons and organizations should apply to the:

**U. S. DEPARTMENT OF COMMERCE
OFFICE OF TECHNICAL SERVICES
WASHINGTON 25, D. C.**

PHYSICAL SCIENCE LABORATORY
NEW MEXICO STATE UNIVERSITY
University Park, New Mexico

ORY

15 October 1963

FINAL REPORT

The research reported in this document has been sponsored in part by Air Force Cambridge Research Laboratories, Office of Aerospace Research, under Contract No. AF 19(604)-6198. It is published for technical information only, and does not necessarily represent recommendations or conclusions of the sponsoring agency.

has been
Research
h, under
shed for
essarily
s of the

FLUSH AND NONFLUSH MOUNTED TELEMETRY ANTENNAS ANTENNAS
FLUSH MOUNTED COMMAND CONTROL ANTENNAS INNAS
S-BAND AND C-BAND BEACON TRANSPONDER ANTENNAS NTENNAS
ANTENNA SYSTEMS FOR SPECIFIC MISSILES, PROBES AND SATELLITE AND SATELLITES

Project Engineer:

Henry D. Weinschel
Associate Physicist

Approved:
Supervisor
Electromagnetics Group

H. W. Haas H. W. Haas
Senior Engineer Senior Engineer

Prepared for

AIR FORCE CAMBRIDGE RESEARCH LABORATORIES
OFFICE OF AEROSPACE RESEARCH
UNITED STATES AIR FORCE
BEDFORD, MASSACHUSETTS

ORIES

ABSTRACT

The Quarterly Progress Reports for the three year contract period from 1 January 1960 to 31 March 1963 are reviewed. Also, short descriptions of antenna systems which were not part of this contract, but are of interest, are included. The contents are arranged by subject matter rather than chronological order. However, the indexes in Appendix I and II provide an easy reference to the progress reports.

A photograph and/or assembly drawing is provided for each antenna discussed. The electrical characteristics of the various antenna types are presented by impedance versus frequency curves, by VSWR versus frequency curves, by patterns of the principle plane and by power contour plots.

In Section 3.0 the various antenna series are discussed with the emphasis on the distinguishing features of the antenna models. Section 4.0 is a discussion of the antenna types. Section 5.0 pertains to special applications or antenna systems.

The Tables in the Appendices show the pertinent antenna information, such as operating or tuning range and weights for easy reference.

ABSTRACT

The Quarterly Progress Reports for the three year contract period from 1 January 1960 to 31 March 1963 are reviewed. Also, short descriptions of antenna systems which were not part of this contract, but are of interest, are included. The contents are arranged by subject matter rather than chronological order. However, the indexes in Appendix I and II provide an easy reference to the progress reports.

A photograph and/or assembly drawing is provided for each antenna discussed. The electrical characteristics of the various antenna types are presented by impedance versus frequency curves, by VSWR versus frequency curves, by patterns of the principle plane cuts and by power contour plots.

In Section 3.0 the various antenna series are discussed with the emphasis on the distinguishing feature of the antenna models. Section 4.0 is a discussion of the antenna types. Section 5.0 pertains to special applications or antenna systems.

The Tables in the Appendices show the pertinent antenna information, such as operating or tuning range and weights for easy reference.

TABLE OF CONTENTS

	Page
1.0 Problem Statement and Scope of Work	1
2.0 Introduction	2
3.0 Discussion of the Various Antenna Models	2
3. 1 The 2,000 Series 1.5-Inch High Telemetry Quadraloop Antennas	3
3. 2 The 2,000 Series 1.0-Inch High Quadraloop Telemetry Antennas	4
3. 3 The 2,000 Series 0.5-Inch High Quadraloop Telemetry Antennas	5
3. 4 The 3,000 Series Flush Mounted Quadraloop Telemetry Antennas	6
3. 5 The 4,000 Series Command Control Quadraloop Antennas	7
3. 6 The 5,000 Series Semiflush Mounted Telemetry Quadraloop Antennas	7
3. 7 The 6,000 Series S-Band Beacon Antennas	8
3. 8 The 7,000 Series C-Band Beacon Antennas	9
3. 9 The 10,000 Series Circumferential Quadraloop Antennas	10
3.10 The 17,000 Series P-Band Quadraloop Antennas	10
3.11 The 20,000 Series Quadraloop Antennas in the 145 Mc/ sec Frequency Range	10
3.12 The 23,000 Series Gap Fed Oblique Stub Antennas	10
3.13 The 24,000 Series Light Weight Telemetry Quadraloop ..	11
4.0 Discussion of the Common Properties of Antenna Types	11
4. 1 Outline of Section 4.0	11
4. 2 Common Properties of the Quadraloop Antennas	11
4.2.1 The Antenna Mounting	11
4.2.2 The Antenna Impedance	12
4.2.3 The Phasing Harness	12
4.2.4 The Antenna Pattern	13
4.2.5 Radio Frequency Breakdown	14
4. 3 The 2,000 Series, 1.5-Inch High Quadraloop Telemetry Antenna	15
4. 4 The 2,000 Series, 1.0-Inch High Quadraloop Telemetry Antenna	15
4. 5 The 2,000 Series, 0.5-Inch High Telemetry Quadraloop Antennas	16

TABLE OF CONTENTS
(Continued)

	Page
4.6 The 3.000 and 5.000 Series Flush and Semiflush Mounted Telemetry Quadraloop Antennas	17
4.7 The 4.000 Series Command Control Quadraloop Antennas	17
4.7.1 The Flush Mounted Type	17
4.7.2 The Nonflush Mounted Type	17
4.8 The 6.000 Series S-Band Beacon Antennas	17
4.8.1 The Quadraloop Type Antenna	17
4.8.2 The Folded Valentine Antenna	18
4.9 The 17.000 Series Quadraloop Beacon Antennas in the 300 Mc/sec Frequency Range	19
5.0 Special Applications and Designs	19
5.1 Outline	19
5.2 The Model 2.025 Telemetry Antennas for the AP/3	19
5.3 The Model 23.006 and 23.007 Telemetry Antennas for the AP/5	20
5.4 The Model 20.004 Quadraloop Antennas for the AO/10 and the AO/15	20
5.5 The Model 2.036 Quadraloop Telemetry Antennas for Exos	21
5.6 The DOVAP Antennas for the Javelin and the Telemetry Antennas for the Cajun	21
6.0 The Command Control Notch Antenna for the Aerobee 150	21
7.0 Graphs and Tables	22
8.0 Summary	22
Appendix I - Antenna Reference Index to the Quarterly Progress Reports	290
Appendix II - Vehicle Reference Index to the Quarterly Progress Reports	295
Appendix III - Antenna Model Listings	298

TABLE OF CONTENTS
(Continued)

	Page
Appendix IV - "Standard" Antenna Models.....	303
Appendix V - List of Antenna Shipments	305
Appendix VI - Antenna Information Work Sheet	308
Acknowledgement	327
Bibliography	328
Distribution List	330

LIST OF ILLUSTRATIONS

	Page
Fig. 1 Photograph of Model II Short Telemetry Quadraloop Antenna	24
Fig. 2 Assembly Drawing of Model II Short Telemetry Quadraloop Antenna	25
Fig. 3 Assembly Drawing of Model II Short Telemetry Quadraloop Antenna	26
Fig. 4 Assembly Drawing of Model II Short Telemetry Quadraloop Antenna	27
Fig. 5 Assembly Drawing of Model II Short Telemetry Quadraloop Antenna	28
Fig. 6 Assembly Drawing of Model II Short Telemetry Quadraloop Antenna	29
Fig. 7 Assembly Drawing of Model II Short Telemetry Quadraloop Antenna	30
Fig. 8 Assembly Drawing of Model II Short Telemetry Quadraloop Antenna	31
Fig. 9 Assembly Drawing of Model 2.002 Telemetry Quadraloop Antenna	32
Fig. 10 Assembly Drawing of Model II - D Telemetry Quadraloop Antenna	33
Fig. 11 Assembly Drawing of Model 2.037 Telemetry Quadraloop Antenna	34
Fig. 12 Assembly Drawing of Model II - B Telemetry Quadraloop Antenna	35
Fig. 13 Assembly Drawing of Model II - C Telemetry Quadraloop Antenna	36
Fig. 14 Assembly Drawing of Model II - E Telemetry Quadraloop Antenna	37

LIST OF ILLUSTRATIONS
(Continued)

		Page
Fig. 15	Photograph of Model 2. 010 Telemetry Quadraloop Antenna	38
Fig. 16	Assembly Drawing of Model 2. 010 Telemetry Quadraloop Antenna	39
Fig. 17	Assembly Drawing of Model 2. 018 Telemetry Quadraloop Antenna	40
Fig. 18	Photograph of Model 2. 013 Telemetry Quadraloop Antenna	41
Fig. 19	Assembly Drawing of Model 2. 013 Telemetry Quadraloop Antenna	42
Fig. 20	Photograph of Model 2. 014 Telemetry Quadraloop Antenna	43
Fig. 21	Assembly Drawing of Model 2. 014 Telemetry Quadraloop Antenna	44
Fig. 22	Photograph of Model 2. 008 Telemetry Quadraloop Antenna	45
Fig. 23	Assembly Drawing of Model 2. 008 Telemetry Quadraloop Antenna	46
Fig. 24	Photograph of Model 2. 012 Telemetry Quadraloop Antenna	47
Fig. 25	Assembly Drawing of Model 2. 012 Telemetry Quadraloop Antenna	48
Fig. 26	Photograph of Model 2. 011 Telemetry Quadraloop Antenna	49
Fig. 27	Assembly Drawing of Model 2. 011 Telemetry Quadraloop Antenna	50
Fig. 28	Photograph of Model A-2 Telemetry Quadraloop Antenna	51

LIST OF ILLUSTRATIONS
(Continued)

		Page
Fig. 29	Assembly Drawing of Model A-3 Telemetry Quadraloop Antenna	52
Fig. 30	Photograph of Model 2.001 Telemetry Quadraloop Antenna	53
Fig. 31	Assembly Drawing of Model 2.001 Telemetry Quadraloop Antenna	54
Fig. 32	Assembly Drawing of Model 2.004 Telemetry Quadraloop Antenna	55
Fig. 33	Assembly Drawing of Model 2.009 Telemetry Quadraloop Antenna	56
Fig. 34	Assembly Drawing of Model 2.023 Telemetry Quadraloop Antenna	57
Fig. 35	Photograph of Model 2.003 Telemetry Quadraloop Antenna	58
Fig. 36	Assembly Drawing of Model 2.003 Telemetry Quadraloop Antenna	59
Fig. 37	Photograph of Model 2.005 Telemetry Quadraloop Antenna	60
Fig. 38	Assembly Drawing of Model 2.005 Telemetry Quadraloop Antenna	61
Fig. 39	Photograph of Model 2.006 Telemetry Quadraloop Antenna	62
Fig. 40	Assembly Drawing of Model 2.006 Telemetry Quadraloop Antenna	63
Fig. 41	Photograph of Model 2.007 Telemetry Quadraloop Antenna	64
Fig. 42	Assembly drawing of Model 2.007 Telemetry Quadraloop Antenna	65

LIST OF ILLUSTRATIONS
(Continued)

		Page
Fig. 43	Photograph of Model 2.025 Telemetry Quadraloop Antenna	66
Fig. 44	Assembly Drawing of Model 2.025 Telemetry Quadraloop Antenna	67
Fig. 45	Photograph of Model 2.032 Telemetry Quadraloop Antenna	68
Fig. 46	Assembly Drawing of Model 2.032 Telemetry Quadraloop Antenna	69
Fig. 47	Photograph of Model 2.035 Telemetry Quadraloop Antenna	70
Fig. 48	Photograph of Model 2.036 Telemetry Quadraloop Antenna	71
Fig. 49	Assembly Drawing of Model 2.036 Telemetry Quadraloop Antenna	72
Fig. 50	Photograph of Model 2.019 Telemetry Quadraloop Antenna	73
Fig. 51	Mounting Drawing of Model 2.019 Telemetry Quadraloop Antenna	74
Fig. 52	Photograph of Model 2.026 Telemetry Quadraloop Antenna	75
Fig. 53	Mounting Drawing of Model 2.026 Telemetry Quadraloop Antenna	76
Fig. 54	Mounting Drawing of Model 2.030 Telemetry Quadraloop Antenna	77
Fig. 55	Photograph of Model 2.031 Telemetry Quadraloop Antenna	78
Fig. 56	Mounting Drawing of Model 2.031 Telemetry Quadraloop Antenna	79

LIST OF ILLUSTRATIONS
(Continued)

		Page
Fig. 57	Photograph of Model III-B Telemetry Quadraloop Antenna	80
Fig. 58	Assembly Drawing of Model III-B Telemetry Quadraloop Antenna	81
Fig. 59	Assembly Drawing of Model III-B-1 Telemetry Quadraloop Antenna	82
Fig. 60	Photograph of Model III-C Telemetry Quadraloop Antenna	83
Fig. 61	Assembly Drawing of Model III-C Telemetry Quadraloop Antenna	84
Fig. 62	Photograph of Model III-D Telemetry Quadraloop Antenna	85
Fig. 63	Assembly Drawing of Model III-D Telemetry Quadraloop Antenna	86
Fig. 64	Photograph of Model III-F Telemetry Quadraloop Antenna	87
Fig. 65	Mounting Drawing of Model III-F Telemetry Quadraloop Antenna	88
Fig. 66	Assembly Drawing of Model III-G Telemetry Quadraloop Antenna	89
Fig. 67	Photograph of Model 3.001 Telemetry Quadraloop Antenna	90
Fig. 68	Assembly Drawing of Model 3.001 Telemetry Quadraloop Antenna	91
Fig. 69	Photograph of IV Command Control Quadraloop Antenna ..	92
Fig. 70	Assembly Drawing of Model IV Command Control Quadraloop Antenna	93

LIST OF ILLUSTRATIONS
(Continued)

		Page
Fig. 71	Assembly Drawing of Model IV-B Command Control Quadraloop Antenna	94
Fig. 72	Photograph of Model 4.001 Command Control Quadraloop Antenna	95
Fig. 73	Assembly Drawing of Model 4.001 Command Control Quadraloop Antenna	96
Fig. 74	Photograph of Model 4.002 Command Control Quadraloop Antenna	97
Fig. 75	Assembly Drawing of Model 4.002 Command Control Quadraloop Antenna	98
Fig. 76	Photograph of Model 4.003 Command Control Quadraloop Antenna	99
Fig. 77	Assembly Drawing of Model 4.003 Command Control Quadraloop Antenna	100
Fig. 78	Photograph of Model V Telemetry Quadraloop Antenna ...	101
Fig. 79	Assembly Drawing of Model V Telemetry Quadraloop Antenna	102
Fig. 80	Photograph of Model V-B Telemetry Quadraloop Antenna	103
Fig. 81	Photograph of Model V-C Telemetry Quadraloop Antenna	104
Fig. 82	Assembly Drawing of Model V-C Telemetry Quadraloop Antenna	105
Fig. 83	Photograph of Model V-F Telemetry Quadraloop Antenna	106
Fig. 84	Assembly Drawing of Model V-G Telemetry Quadraloop Antenna	107

LIST OF ILLUSTRATIONS
(Continued)

		Page
Fig. 85	Photograph of Model IA7b S-Band Quadraloop Antenna....	108
Fig. 86	Assembly Drawing of Models IA7b and IIB7b S-Band Beacon Quadraloop Antenna	109
Fig. 87	Photograph of Model 6.005 S-Band Quadraloop Antenna...	110
Fig. 88	Assembly Drawing of Model 6.005 S-Band Beacon Quadraloop Antenna	111
Fig. 89	Photograph of Model 6.006 S-Band Quadraloop Antenna...	112
Fig. 90	Assembly Drawing of Model 6.006 S-Band Beacon Quadraloop Antenna	113
Fig. 91	Photograph of Model 6.007 Radio Sonde Quadraloop Antenna	114
Fig. 92	Mounting Drawing of Model 6.007 Radio Sonde Quadraloop Antenna	115
Fig. 93	Photograph of Model 6.010 S-Band Folded Valentine Antenna	116
Fig. 94	Assembly Drawing of Model 6.010 S-Band Beacon Folded Valentine Antenna	117
Fig. 95	Photograph of Model 6.011 S-Band Quadraloop Antenna ..	118
Fig. 96	Assembly Drawing of Model 6.011 S-Band Beacon Quadraloop Antenna	119
Fig. 97	Photograph of Model 7.001 C-Band Beacon Scimitar Antenna	120
Fig. 98	Assembly Drawing of Model 7.001 C-Band Beacon Scimitar Antenna	121
Fig. 99	Assembly Drawing of Model 7.003 C-Band Beacon Scimitar Antenna	122

LIST OF ILLUSTRATIONS
(Continued)

		Page
Fig. 100	Photograph of Model 7.002 C-Band Quadraloop Antenna	123
Fig. 101	Assembly Drawing of Model 7.002 C-Band Beacon Quadraloop Antenna	124
Fig. 102	Photograph of Model 7.004 C-Band Beacon Folded Valentine Antenna	125
Fig. 103	Assembly Drawing of Model 7.004 C-Band Beacon Folded Antenna	126
Fig. 104	Assembly Drawing of Model 7.005 C-Band Beacon Folded Valentine Antenna	127
Fig. 105	Assembly Drawing of Model 7.007 C-Band Beacon Quadraloop Antenna	128
Fig. 106	Photograph of Model 7.009 C-Band Beacon Quadraloop Antenna	129
Fig. 107	Assembly Drawing of Model 7.009 Beacon Quadraloop Antenna	130
Fig. 108	Photograph of Model 7.008 C-Band Beacon Folded Valentine Antenna	131
Fig. 109	Mounting Drawing of Model 7.008 C-Band Beacon Folded Valentine Antenna	132
Fig. 110	Photograph of Model 10.004 35 Mc/sec Circumferential Quadraloop Antenna	133
Fig. 111	Photograph of Model 10.005 35 Mc/sec Circumferential Quadraloop Antenna	134
Fig. 112	Photograph of Model 10.006 35 Mc/sec Circumferential Quadraloop Antenna	135
Fig. 113	Photograph of Models 10.009 and 10.016 Circumferential Quadraloop Antenna	136

LIST OF ILLUSTRATIONS
(Continued)

		Page
Fig. 114	Photograph of Models 10.013 and 10.014 Circumferential Quadraloop Antenna	137
Fig. 115	Assembly Drawing of Model 10.023 Circumferential Telemetry Quadraloop Antenna	138
Fig. 116	Photograph of Models 17.001 through 17.004 P-Band Quadraloop Antenna	139
Fig. 117	Assembly Drawing of Model 17.004 P-Band Quadraloop Antenna	140
Fig. 118	Photograph of Model 20.004 Quadraloop Antenna in the 130 Mc/sec Frequency Range	141
Fig. 119	Assembly Drawing of Model 20.004 Quadraloop Antenna	142
Fig. 120	Photograph of Model 23.005 Telemetry Gap Fed Oblique Stub Antenna	143
Fig. 121	Assembly Drawing of Model 23.005 Telemetry Gap Fed Oblique Stub Antenna	144
Fig. 122	Photograph of Models 23.006 and 23.007 Telemetry Gap Fed Oblique Stub Antennas	145
Fig. 123	Assembly Drawing of Model 23.006 Telemetry Gap Fed Oblique Stub Antenna	146
Fig. 124	Photograph of Model 24.001 Telemetry Quadraloop Antenna (Prototype)	147
Fig. 125	Sketch of Model 24.001 Telemetry Quadraloop Antenna (Prototype)	148
Fig. 126	Illustration of Quadraloop Parts and Dimensions	149
Fig. 127	Sketch of Antenna Mountings	150
Fig. 128	Photograph of Diffusion Breakdown	151

LIST OF ILLUSTRATIONS
(Continued)

		Page
Fig. 129	Curve of Altitude Versus Mean Free Path of Molecules from 50,000 to 190,000 Feet Altitude	152
Fig. 130	Curve of Altitude Versus Mean Free Path of Molecules from 180,000 to 320,000 Feet Altitude	153
Fig. 131	Curve of Altitude Versus Mean Free Path of Molecules From 260,000 to 400,000 Feet Altitude	154
Fig. 132	Idealized Impedance Curve of a 2.000 Series, 1.5-Inch High Telemetry Quadraloop Antenna, Mounted on a 15-Inch Diameter Cylinder	155
Fig. 133	Normalized Impedance Curve of a 2.000 Series, 1.5-Inch High Telemetry Quadraloop Antenna	156
Fig. 134	Idealized Impedance Curve of a Two Element Array Fed 180° Out of Phase of the 2.000 Series, 1.5-Inch High Telemetry Quadraloop Mounted on a 15-Inch Diameter Cylinder	157
Fig. 135	Sketch of the Vehicle Mockup for the Model 2.011 Telemetry Quadraloop Antenna Radiation Pattern Measurements	158
Fig. 136	Position Coordinates for the Model 2.011 Antenna Pattern Measurements	159
Fig. 137	Model 2.011 Radiation Patterns	160
Fig. 138	Model 2.011 Radiation Patterns	161
Fig. 139	Model 2.011 Radiation Patterns	162
Fig. 140	Power Contour Plot of the Two Element Array of Model 2.011 Antennas	163
Fig. 141	Representative Diffusion Breakdown Curve of the 2.000 Series, 1.5-Inch High Telemetry Quadraloop Antenna ..	164
Fig. 142	Idealized Impedance Curve of the 2.000 Series, 1.0-Inch High Telemetry Quadraloop Antenna, Mounted on a 15-Inch Diameter Cylinder	165

LIST OF ILLUSTRATIONS
(Continued)

		Page
Fig. 143	Normalized Impedance Curve of the 2.000 Series, 1.0 - Inch High Telemetry Quadraloop Antenna	166
Fig. 144	Idealized Impedance Curve of a Two Element Array Fed 180° Out of Phase of the 2.000 Series, 1.0-Inch High Telemetry Quadraloop Antenna	167
Fig. 145	Photograph of the Vehicle Mockup Used for the Model 2.007 Telemetry Quadraloop Antenna Radiation Pattern Measurements	168
Fig. 146	Sketch of the Vehicle Mockup used for the Model 2.007 Telemetry Quadraloop Antenna Radiation Pattern Measurements	169
Fig. 147	Position Coordinates for the Model 2.007 Antenna Radiation Pattern Measurements	170
Fig. 148	Model 2.007 Radiation Patterns	171
Fig. 149	Model 2.007 Radiation Patterns	172
Fig. 150	Model 2.007 Radiation Patterns	173
Fig. 151	Power Contour Plot of the Two Element Array of Model 2.00 Antennas	174
Fig. 152	Representative Diffusion Breakdown Curve of the 2.000 Series, 1.0-Inch High Telemetry Quadraloop Antenna ...	175
Fig. 153	Idealized Impedance Curve of the 2.000 Series, 0.5-Inch High Telemetry Quadraloop Antenna, Mounted on a 6.8 Inch Diameter Cylinder	176
Fig. 154	Normalized Impedance Curve of the 2.000 Series, 0.5 - Inch High Telemetry Quadraloop Antenna.....	177
Fig. 155	Idealized Impedance Curve of the Two Element Array Fed 180° Out of Phase of the 2.000 Series, 0.5-Inch High Telemetry Quadraloop Mounted on a 6.8-Inch Diameter	178

LIST OF ILLUSTRATIONS
(Continued)

		Page
Fig. 156	Photograph of the Vehicle Mockup Used for the Model 2.031 Telemetry Quadraloop Antenna Radiation Pattern Measurements	179
Fig. 157	Sketch of the Vehicle Mockup Used for the Model 2.031 Telemetry Quadraloop Antenna Radiation Pattern Measurements	180
Fig. 158	Position Coordinates for the Model 2.031 Antenna Radiation Pattern Measurements	181
Fig. 159	Model 2.031 Radiation Patterns	182
Fig. 160	Model 2.031 Radiation Patterns	183
Fig. 161	Model 2.031 Radiation Patterns	184
Fig. 162	Model 2.031 Radiation Patterns	185
Fig. 163	Model 2.031 Radiation Patterns	186
Fig. 164	Model 2.031 Radiation Patterns	187
Fig. 165	Model 2.031 Radiation Patterns	188
Fig. 166	Model 2.031 Radiation Patterns	189
Fig. 167	Model 2.031 Radiation Patterns	190
Fig. 168	Representative Diffusion Breakdown Curve of the 2.000 Series, 0.5-Inch High Telemetry Quadraloop Antenna...	191
Fig. 169	Idealized Impedance Curve of a Two Element Array of the 4.000 Series, Flush Mounted Command Control Quadraloop Antennas Mounted on a 20-Inch Diameter Cylinder	192
Fig. 170	Idealized Impedance Curve for the 4.000 Series, Non-Flush Mounted Command Control Quadraloop Antenna Mounted on a 9-Inch Diameter Cylinder	193

LIST OF ILLUSTRATIONS
(Continued)

		Page
Fig. 171	Normalized Impedance Curve of the 4.000 Series, Non-Flush Mounted Command Control Quadraloop Antenna	194
Fig. 172	Idealized Impedance Curve for the Two Element Array of the 4.000 Series, Nonflush Mounted Command Control Quadraloop Antennas Mounted on a 9-Inch Diameter Cylinder	195
Fig. 173	Photograph of the Payload Mockup Used for the Model 4.001 Radiation Pattern Measurements	196
Fig. 174	Sketch of the Vehicle Mockup for the Model 4.001 Pattern Measurements	197
Fig. 175	Position Coordinates for the Model 4.001 Antenna Radiation Pattern Measurements	198
Fig. 176	Model 4.001 Radiation Patterns	199
Fig. 177	Model 4.001 Radiation Patterns	200
Fig. 178	Power Contour Plot of the Two Element Array of Model 4.001 Antennas	201
Fig. 179	Curve of VSWR Versus Frequency for the Two Element Array of the Model 6.005 Quadraloop Antennas Mounted on a 15-Inch Diameter Cylinder	202
Fig. 180	Photograph of the Vehicle Mockup used for the Model 6.003 Radiation Pattern Measurements	203
Fig. 181	Sketch of the Vehicle Mockup for the Model 6.003 Radiation Pattern Measurements	204
Fig. 182	Position Coordinates for the Model 6.003 Radiation Pattern Measurements	205
Fig. 183	Model 6.003 Radiation Patterns	206
Fig. 184	Model 6.003 Radiation Patterns	207

LIST OF ILLUSTRATIONS
(Continued)

		Page
Fig. 185	Model 6.003 Radiation Patterns	208
Fig. 186	Model 6.003 Radiation Patterns	209
Fig. 187	Power Contour Plot of the Two Element Array of Model 6.003 Antennas, for the $E\theta$ Polarization Vector	210
Fig. 188	Power Contour Plot for the Two Element Array of Model 6.003 Antennas for the $E\phi$ Polarization Vector	211
Fig. 189	Representative Diffusion Breakdown Curve for the 6.000 Series Quadraloop Type C-Band Beacon Antenna	212
Fig. 190	Curve of VSWR Versus Frequency for a Four Element Array Model 6.010 of Folded Valentine Antennas Mounted on a 15-inch Diameter Cylinder	213
Fig. 191	Photograph of the Vehicle Mockup Used for the Model 6.010 C-Band Folded Valentine Antenna Radiation Pattern Measurements	214
Fig. 192	Sketch of the Vehicle Mockup Used for the Model 6.010 C-Band Folded Valentine Antenna Radiation Pattern Measurements	215
Fig. 193	Position Coordinates for the Model 6.010 Antenna Radiation Pattern Measurements	216
Fig. 194	Sketch of the Harness for the Model 6.010 Four Element Array.	217
Fig. 195	Model 6.010 Radiation Patterns	218
Fig. 196	Model 6.010 Radiation Patterns	219
Fig. 197	Model 6.010 Radiation Patterns	220
Fig. 198	Model 6.010 Radiation Patterns	221
Fig. 199	Model 6.010 Radiation Patterns	222

LIST OF ILLUSTRATIONS
(Continued)

		Page
Fig. 200	Power Contour Plot for the Four Element Array of Model 6.010 Antennas for the $E\theta$ Polarization Vector	223
Fig. 201	Power Contour Plot for the Four Element Array of the Model 6.010 Antennas for the $E\phi$ Polarization Vector	224
Fig. 202	Representative Diffusion Breakdown Curve of the 6.000 Series Folded Valentine Antenna	225
Fig. 203	Curve of VSWR Versus Frequency for the Two Element Array of Model 7.004 C-Band Beacon Antennas	226
Fig. 204	Photograph of the Vehicle Mockup Used for the Model 7.004 Radiation Pattern Measurements	227
Fig. 205	Sketch of the Vehicle Mockup Used for the Model 7.004 Radiation Pattern Measurements	228
Fig. 206	Position Coordinates for the Model 7.004 Antenna Radiation Pattern Measurements	229
Fig. 207	Model 7.004 Radiation Patterns	230
Fig. 208	Model 7.004 Radiation Patterns	231
Fig. 209	Model 7.004 Radiation Patterns	232
Fig. 210	Model 7.004 Radiation Patterns	233
Fig. 211	Power Contour Plot of the Two Element Array of Model 7.004 Antennas for the $E\theta$ Polarization Vector	234
Fig. 212	Power Contour Plot of the Two Element Array of Model 7.004 Antennas for the $E\phi$ Polarization Vector	235
Fig. 213	Impedance Curve of a Single Model 17.002 Quadraloop Antenna	236
Fig. 214	Impedance Curve of a Four Element Array of Model 17.004 Quadraloop Antennas Fed in Quadrature	237

LIST OF ILLUSTRATIONS
(Continued)

		Page
Fig. 215	Sketch of the Phasing Harness of the Four Element Array of Model 17.004 Quadraloop Antennas	238
Fig. 216	Photograph of the Vehicle Mockup Used for the Model 17.004 Radiation Pattern Measurements	239
Fig. 217	Sketch of the Vehicle Mockup Used for the Model 17.004 Radiation Pattern Measurements	240
Fig. 218	Position Coordinates for the Model 17.004 Antenna Radiation Pattern Measurements	241
Fig. 219	Model 17.004 Radiation Patterns	242
Fig. 220	Model 17.004 Radiation Patterns	243
Fig. 221	Model 17.004 Radiation Patterns	244
Fig. 222	Power Contour Plot of the Four Element Array of the Model 17.004 Antenna	245
Fig. 223	Representative Diffusion Breakdown Curve for the 17.000 Series Antennas	246
Fig. 224	Photograph of the AP/3 Payload Mockup Used for the Model 2.007 Antenna Pattern Measurements	247
Fig. 225	Sketch of the AP/3 Payload Mockup Used for the Model 2.007 Antenna Pattern Measurements	248
Fig. 226	Position Coordinates for the Model 2.007 Antennas Mounted on the AP/3	249
Fig. 227	Model 2.007 Radiation Patterns AP/3 Payload	250
Fig. 228	Model 2.007 Radiation Patterns AP/3 Payload	251
Fig. 229	Model 2.007 Radiation Patterns AP/3 Payload	252
Fig. 230	Photograph of the AP/5 Payload Mockup	253

LIST OF ILLUSTRATIONS
(Continued)

		Page
Fig. 231	Sketch of the Payload Mockup Used for the AP/5 Radiation Pattern Measurements	254
Fig. 232	Position Coordinates for the Antennas on the AP/5 Payload	255
Fig. 233	Sketch of the Phasing Harness for the Antennas on the AP/5 Payload	256
Fig. 234	Radiation Patterns of the Model 23.006 and 23.007 Array Mounted on AP/5 Flight Payload	257
Fig. 235	Radiation Patterns of the Model 23.006 and 23.007 Array Mounted on the AP/5 Flight Payload	258
Fig. 236	Radiation Patterns of the Model 23.006 and 23.007 Array Mounted on the AP/5 Flight Payload	259
Fig. 237	Photograph of the AO-10 Vehicle Mockup Used for Radiation Pattern Measurements	260
Fig. 238	Sketch of the AO-10 Vehicle Mockup Used for Radiation Pattern Measurements	261
Fig. 239	Position Coordinates of the Model 20.004 Antennas Mounted on the AO-10 Mockup for Radiation Pattern Measurements	262
Fig. 240	Sketch of the Phasing Harness for the Four Element Array of Model 20.004 Antennas	263
Fig. 241	Radiation Patterns of the Model 20.004 Four Element Array	264
Fig. 242	Radiation Patterns of the Model 20.004 Four Element Array	265
Fig. 243	Radiation Patterns of the Model 20.004 Four Element Array	266
Fig. 244	Photograph of the Exos Vehicle Mockup with the Flaps Closed. Used for Radiation Pattern Measurements ...	267

LIST OF ILLUSTRATIONS
(Continued)

		Page
Fig. 245	Sketch of the Exos Vehicle Mockup Used for Radiation Pattern Measurements	268
Fig. 246	Position Coordinates of the Model 2.036 Antennas. Flaps Closed Configuration	269
Fig. 247	Radiation Patterns of the Model 2.036 Two Element Array Mounted on the Exos Vehicle Mockup with the Vehicle Flaps Closed	270
Fig. 248	Radiation Patterns of the Model 2.036 Two Element Array Mounted on the Exos Vehicle Mockup with the Vehicle Flaps Closed.	271
Fig. 249	Radiation Patterns of the Model 2.036 Two Element Array Mounted on the Exos Vehicle Mockup with the Vehicle Flaps Closed	272
Fig. 250	Photograph of the Exos Vehicle Mockup with the Flaps Open Used for Radiation Pattern Measurements	273
Fig. 251	Position Coordinates of the Model 2.036 Antennas. Flaps Open Configuration	274
Fig. 252	Radiation Patterns of the Model 2.036 Two Element Array Mounted on the Exos Vehicle Mockup with the Vehicle Flaps Closed.	275
Fig. 253	Radiation Patterns of the Model 2.036 Two Element Array Mounted on the Exos Vehicle Mockup with the Vehicle Flaps Closed	276
Fig. 254	Radiation Patterns of the Model 2.036 Two Element Array Mounted on the Exos Vehicle Mockup with the Vehicle Flaps Closed	277
Fig. 255	Position Coordinates of the Model 2.007 Antennas on the Exos Vehicle Mockup with the Flaps Open	278
Fig. 256	Radiation Patterns of the Model 2.007 Antenna Mounted on the Exos Vehicle Mockup with the Vehicle Flaps Open	279

LIST OF ILLUSTRATIONS
(Continued)

		Page
Fig. 257	Radiation Patterns of the Model 2, 007 Antenna Mounted on the Exos Vehicle Mockup with the Vehicle Flaps Open.....	280
Fig. 258	Radiation Patterns of the Model 2, 007 Antenna Mounted on the Exos Vehicle Mockup with the Vehicle Flaps Open.....	281
Fig. 259	Position Coordinates of the Command Control Fin Notch Antenna on the Aerobee 150 Mockup for Pattern Measurements	282
Fig. 260	Power Contour Plot of the Command Control Fin Notch Antenna for the Left Circular Components, at 435.0 Mc/sec	283
Fig. 261	Power Contour Plot of the Command Control Fin Notch Antenna for the E_{θ} Component at 435.0 Mc/sec	284
Fig. 262	Power Contour Plot of the Command Control Fin Notch Antenna for the E_{ϕ} Component at 435.0 Mc/sec	285
Fig. 263	Power Contour Plot of the Command Control Fin Notch Antenna for the Left Circular Component at 409.0 Mc/sec	286
Fig. 264	Power Contour Plot of the Command Control Fin Notch Antenna for the E_{θ} Component at 409.0 Mc/sec	287
Fig. 265	Power Contour Plot of the Command Control Fin Notch Antenna for the E_{ϕ} Component at 409.0 Mc/sec	288
Fig. 266	Graph Showing the Tuning Range, the Weight and the Type of Seal for the Standard Antennas in the 135 - 440 Mc/sec Frequency Range	289

1.0 PROBLEM STATEMENT AND SCOPE OF WORK

1.1 The contractor shall supply the necessary personnel, facilities, services and materials to accomplish the following:

1.1.1 Conduct laboratory studies leading to development of antenna designs for research rockets and associated ground instrumentation systems.

1.1.2 Conduct propagation studies leading to the determination of radiation characteristics, voltage breakdown, and heating problems associated with rocket antenna configurations.

1.1.3 Install rocket antennas in research rockets including Aerobee, Cajun, Spaerobee, Exos, Asp, Astrobee and such other rockets as directed by the Contracting Officer.

1.2 Reports are required hereunder and shall be prepared in accordance with the Outline for Geophysics Research Directorate Contract Reports dated 1 April 1958.

1.3 Insofar as practicable, the contractor shall first inform itself of all similar research carried on in other research organizations so as to make use of available information in carrying on its own research and avoid needless duplication.

1.4 The contractor shall be prepared to deliver to the Government models which are constructed and/or writings, sound recordings, pictorial reproduction, drawings or other graphic representations and works of a similar nature which are made as a result of compliance with the statement of work. Periodically, (approximately on the anniversary date of the contract), and upon completion of the contract, at the request of the Contracting Officer, the contractor shall furnish a listing of all models, drawings, etc., developed under the contract and not previously reported. The Contracting Officer, after review of the list, will furnish the contractor disposition instructions.

1.5 Performance of the services called for above shall be under the direct supervision of H. W. Haas. No substitution shall be made without the prior written approval of the Contracting Officer.

1.6 Weather data desired from the Air Weather Service or the United States Weather Bureau will be furnished upon request of the contractor by Air Force Cambridge Research Division.

2.0 INTRODUCTION

The report is organized by subject matter rather than by the chronological order of the quarterly reports. The major divisions are types of antennas and antenna systems for specific vehicles.

During the contract period the antenna model designation was changed from the roman numeral to the decimal system. The roman numeral designated the antenna type and a letter following the variations of the type. The decimal system is similar. The number to the left of the decimal point designates the antenna type and the numbers to the right the variations. The antenna type numbers were not changed. An antenna type designated by a roman numeral III received a model number with the number 3 to the left of the decimal point.

The antenna types discussed in this report are listed below:

Nonflush mounted quadraloop antennas	2.000
Flush mounted quadraloop antennas	3.000
Command control antennas	4.000
Semiflush mounted quadraloop antennas	5.000
S-Band beacon antennas	6.000
C-Band beacon antennas	7.000
Circumferential quadraloop antenna	10.000
Nonflush mounted P-Band quadraloop antenna	17.000
Quadraloop in the 140 Mc range	20.000
Gap fed oblique stub antenna	23.000
Light weight quadraloop	24.000
Command control notch antenna for the Aerobee 150 -No Mod No.	

Since the subject matter is diversified, much of the information is presented in tabulated form. Appendices I and II are references of antenna models and missiles to the quarterly progress reports. Appendix III lists the various antenna models including some that are not mentioned in the quarterly reports but may be of interest. Appendix IV is an extract of Appendix III showing the antenna models most frequently used. Appendix V lists the number and types of antennas shipped during the contract period. Appendix VI is a copy of the antenna information work sheet.

The next few pages contain considerable historical and technical detail which is useful for a better understanding of the pages which follow and further serve to clarify many questions which have arisen from time to time.

3.0 DISCUSSION OF THE VARIOUS ANTENNA MODELS

3.1 The 2,000 Series 1.5-Inch High Telemetry Quadraloop Antennas

The Model II-short, shown in Figs. 1 - 8, designates several variations of the same antenna. They have all flared Teflon inserts but differ by the addition of a stainless steel cuff over the leading edge, by the addition of a mounting plate and by o-ring seals. The antennas were used on various missiles with diameters from 6 to 15 inches. Their most frequent application was for telemetry on the Aerobee 150. The antennas functioned successfully but were discontinued when the more temperature stable Fluorosint dielectric replaced the Teflon.

The Model 2.002, shown in Fig. 9, antenna is a modified Model II-short. It was built for the Astrobee 200 missile. To minimize diffusion breakdown, it was desirable to use a four element array. The time limitation was such that the best approach to the problem was to use the Model II-short antenna and to decrease its height to obtain a 200-ohm driving point impedance. The antennas were then fed in parallel so that the array presented a 50-ohm impedance to the transmitter. Later, four element arrays consisted of standard 100-ohm antennas with 75-ohm, $1/4$ wavelengths matching sections.

Model II-D, shown in Fig. 10 differs from the Model II-short only by the 150-ohm driving point impedance. It is now obsolete.

The early antenna designs with Fluorosint inserts were the Models II-A (2.037), shown in Fig. 11, II-B, shown in Fig. 12, II-C, shown in Fig. 13, II-E shown in Fig. 14, 2.010, shown in Figs. 15 - 16, and 2.018, shown in Fig. 17. All of them were designed for specific applications. At the time very little data was available and no correct frequency scaling factor had been established. Because of the short delivery times it was desirable that the first hardware built could be used for flight. The aim was, therefore, to design the antenna so that the desired frequency would be the center of the tuning range. The result was that the frequency ranges of the various models overlapped. As more data became available, it became possible to design six "standard" models, three pressurized and three not pressurized to cover the frequency range from 215 to 265 Mc/sec. All the models listed at the beginning of the paragraph, except Model II-A (2.037) and II-C, were replaced by the standard antennas.

Model II-A remained unchanged but was given the Model number 2.037 to conform with the decimal system. The first pair was built for NRL and flown on an Aerobee 150 at WSMR. The antennas were recovered and impedance checks showed no detuning.

Model II-C was designed for the Caleb missile. Because of the high radial acceleration, it was thought desirable to replace the nylon screws with an insulated metal screw. The antenna was welded to the missile to

provide a positive air seal. All air spaces in the antenna were vented to permit rapid outgasing.

The standard antennas now in use are Models 2.037, shown in Fig. 11, 2.013, shown in Figs. 18 - 19, and 2.014, shown in Figs. 20 - 21, if an air seal to the missile skin is required. The Models 2.008, shown in Figs. 22 - 23, 2.012, shown in Figs. 24 - 25, and 2.011, shown in Figs. 26 - 27, are identical to the ones above except that the elbow feed connector does not have a glass seal. If at some later date a pressurized elbow connector becomes available only three antennas will be required to cover the frequency range from 215 to 265 Mc/sec.

3.2 The 2.000 Series 1.0-Inch High Quadraloop Telemetry Antennas

The small quadraloop was designed to fill the gap between the flush mounted antennas and the large quadraloop. The flush mounted antenna is an optimum design from the aerodynamic standpoint but carries a corresponding penalty in radiation performance. Compared to the large quadraloop, the gain is generally three db less. On the other hand, the radiation characteristics of the large quadraloop are good, however for small vehicles the drag and lift are sometime excessive.

The first two Models A-2, shown in Fig. 28, and A-3 shown in Fig. 29, differed from the ones that have now become standard. In order to enclose the driven element on three sides by dielectric, the width was reduced to 5/16 inches. The tuning arrangement was a screw to vary the length of the driven element. The main difference between the two models was that the Model A-2 was built with nylon support screws and the Model A-3 with a metal support screw.

Model 2.001, shown in Figs. 30 - 31, is very nearly the same as the ones that have become standard designs. The design of the support screw was mechanically unsatisfactory and the nylon screws were therefore left in the design for additional strength.

Models 2.004, shown in Fig. 32, 2.009, shown in Fig. 33, and 2.023, shown in Fig. 34, are the same as the ones now in use except for changes in slot length. The reasons for their design and their replacements later are the same as the ones given in the third paragraph of Section 3.1.

The standard Models are now 2.003, shown in Figs. 35 - 36, 2.005, shown in Figs. 37 - 38, 2.006, shown in Figs. 39 - 40 and 2.007, shown in Figs. 41 - 42. The frequency range covered is from 210 to 250 Mc/sec by the Models 2.003 and 2.005, from 235 to 275 Mc/sec by the Models 2.006 and 2.007. The Models 2.005 and 2.007 were sealed against the missile skin.

Model 2.025, shown in Figs. 43 - 44, is identical to Model 2.007 except that the nose tip was removed and a crossbar was added for mounting on the AP/3 payload. The crossbar was later removed since the payload configuration was changed and it was no longer required.

Model 2.032, shown in Figs. 45 - 46, is electrically identical to Model 2.007. The mounting was adapted for the Javelin missile. The base of the antenna was widened to a flange and was recessed below the missile skin. This made it possible to mount the antenna under the fiber glass skin without changing the slot or driven element height. One pair of antennas was built and the impedance and pattern measurements were completed. It was later decided to check the patterns of one of the standard antennas mounted on the payload. To date, the payload configuration has not been received.

Model 2.035, shown in Fig. 47, is a prototype antenna. The Fluorosint dielectric of a Model 2.005 antenna was replaced by fused quartz. Impedance and vibration data was obtained. The Model 2.036 antenna for the Exos missile was then designed on the basis of that data.

The Model 2.036, shown in Figs. 48 - 49, antenna was constructed of stainless steel and quartz. It was used on the Exos flight. The antenna was designed as a two element array. During the tests it was decided that it would be more advantageous to excite only one antenna since the pattern of the two antennas produced a null aft of the missile due to doors opening in front of the antennas.

3.3 The 2.000 Series 0.5-Inch High Quadraloop Telemetry Antennas

It was thought desirable for aerodynamic reasons to reduce the height of the antenna for the Cajun vehicle. The small slot and driven element height made efficiency of the antenna comparable to that of the flush mounted antenna. The gain was thought to be acceptable and the design was justified from the aerodynamic point of view.

Model 2.019, shown in Figs. 50 - 51, was the first one built. Only one pair was shipped since the measurements showed that it was desirable to lengthen the antenna by 0.4 inch to have the desired frequency closer to the center of the tuning range.

Model 2.028, shown in Figs. 52 - 53, succeeded Model 2.019 and was identical to it except for the longer slot length. The electrical stability of the antenna was still a problem and it was decided to design two new models.

Models 2.030, shown in Fig. 54, and 2.031, shown in Figs. 55 - 56,

are identical except that Model 2.030 is pressure sealed to the missile skin. The models differ from the ones above by an additional support screw and a less sensitive tuning capacitor. The overall length of the antenna was also increased so that the capacitance at each support screw could be decreased. The purpose of the changes was to increase the tuning stability of the antenna. One pair of Model 2.051 antennas was built. About that time, it was decided to relax the aerodynamic requirements and the development of the antennas was stopped.

3.4 The 3.000 Series Flush Mounted Quadraloop Telemetry Antennas

All antennas in this series mount from the inside of the missile and have no protruding surfaces on the outside of the missile skin. They are ideal from the aerodynamic standpoint but have several undesirable electrical features. They are narrow-banded and are less stable considering applications. The radiation patterns are almost the same shape as that of the nonflush mounted quadraloops but are generally six to eight db lower in gain. This does not rule out the use of the antenna, but care should be taken to insure sufficient signal at the receiver.

Model III-B, shown in Figs. 57 - 58, is one of the early designs with Teflon dielectric. The antenna body is provided with an o-ring gland so that it can be pressurized by choosing the appropriate glass seal feed connector.

Model III-B-1, shown in Fig. 59, is similar to Model III-B. It is 0.175 inch longer to operate in a lower frequency range. One of the nylon support screws was replaced by a stainless steel cuff to secure the Teflon dielectric.

Model III-C, shown in Figs. 60 - 61, is similar to the two antennas above but does not have the o-ring gland for pressurization.

Model III-D, shown in Figs. 62 - 63, has a cavity as the above antennas but is not really a flush mounted antenna since the driven element extends above the missile surface. The reason for the higher driven element was to improve the gain of the antenna.

Model III-F, shown in Figs. 64 - 65, was designed for the Exos missile. The design changes included Fluorosint dielectric in place of Teflon, two metal support screws and a Microdot feed connector.

Model III-G, shown in Fig. 66, is similar to Model III-D except for Fluorosint dielectric, metal support screws and a pressure seal to the missile skin.

Model 3.001, shown in Figs. 67 - 68, is the latest design of

the flush mounted antenna type. One pair of prototype antennas was built and checked. The gain is approximately the same as that for other flush mounted antennas. The tuning range check to date is from 255 to 270 Mc/sec. The project was shelved since there was no immediate application for flush mounted, low gain antennas.

3.5 The 4.000 Series Command Control Quadraloop Antennas

The antennas in this series function generally as receiver antennas in the 390 to 440 Mc/sec frequency range. Flush, semiflush and nonflush mounted antennas are included.

Model IV, shown in Figs. 69 - 70, has a Teflon filled cavity. The antenna body is surrounded by flange so that it can be mounted from the outside of the missile. It is usually referred to as a semiflush mounted antenna.

Model IV-B, shown in Fig. 71, is electrically the same as Model IV but mounts from the inside of the missile. An o-ring gland is provided so that the antenna may be pressurized by using a glass seal feed connector.

Model 4.001, shown in Figs. 72 - 73, is a nonflush mounted quadraloop antenna. From the electrical point of view, it is superior to the flush mounted antennas and should be used whenever the aerodynamic requirements permit it.

Model 4.002, shown in Figs. 74 - 75, is a semiflush mounted antenna similar to Model IV but with a Fluorosint filled cavity and a metal support screw. At the time, the support screw had not been standardized and minor design changes will have to be made if additional antennas are required.

Model 4.003, shown in Figs. 76 - 77, is identical to Model 4.001, but is pressure sealed to the missile skin.

3.6 The 5.000 Series Semiflush Mounted Telemetry Quadraloop Antennas

This antenna type is electrically the same as the one described in Section 3.4. The difference is the method by which they are mounted on the missile. The 3.000 series is mounted from the inside of the missile which is sometime difficult because of the limited space. The 5.000 antenna series has a flange around the antenna body which makes it possible to mount the antenna from the outside of the missile.

Model V, shown in Figs. 78 - 79, was the earliest version. One pair was delivered for flight hardware.

Models V-B, shown in Fig. 80, and V-C, shown in Figs. 81 - 82, are similar. The wall thickness of the cavity was thinned down to decrease the volume and weight of the antenna. The two tuning capacitors of the Model V were replaced by one. Two nylon support screws were added for tuning stability and a more reliable feed connector was used.

Model V-F, shown in Fig. 83, is a prototype antenna. The purpose was to reduce the length by capacitive endloading and to reduce the antenna thickness at the cost of radiation efficiency which was permissible for the intended application. The development of the antenna was stopped, as that of all other flush mounted antennas, when the 1.0-inch high quadraloop became operational.

Model V-G, shown in Fig. 84, is similar to Model V-C but the Teflon dielectric was replaced by Fluorosint and the nylon support screws by insulated metal screws.

3.7 The 6.000 Series S-Band Beacon Antennas

To date the 6.000 series includes two types of antennas, the quadraloop and the folded valentine. The quadraloop has been used more extensively because of its aerodynamic advantages and the ease with which a 100 or 50 ohm driving point impedance can be obtained. These two features are presently lacking for the folded valentine but for some applications are offset by its smoother pattern and larger power handling capability.

Model IA7b, shown in Figs. 85 - 86, is a quadraloop with a flared slot. The driving point impedance is 100 ohms. The feed connector and the tee junction are built at the PSL Machine Shop. The antenna body is aluminum and the dielectric insert is supramica. The antenna is most easily tuned by filing the driven element to the correct length.

Model IIB7b, shown in Fig. 86, is identical to Model IA7b except for the materials. The antenna body is made of stainless steel and the dielectric insert of Alumina.

Model 6.005, shown in Figs. 87 - 88, is a quadraloop antenna. It replaced the Model IA7b above. No tuning is required. The antenna feed is a glass seal connector so that the missile can be pressurized. The driving point impedance is 50 ohms. A Microlab reactive power divider is used for the two element array. The high temperature version of the antenna has not been designed since there has been no demand for it to date.

Model 6.006, shown in Figs. 89 - 90, is similar to Model IA7b. It was designed to fill a flight requirement before the checks on Model 6.005 were completed. The problem was to obtain a better pressure seal than that

of Model IA7b which has a slow leak through the antenna feed. The driven element was made higher to obtain a 50 ohm driving point impedance and the PSL manufactured feed was replaced by a standard glass seal connector. The antennas were then arrayed using a Microlab power divider.

Model 6.007, shown in Figs. 91 - 92, is identical to Model 6.005 except that it is scaled to a lower frequency to be used with the radio sonde transmitter.

Model 6.010, shown in Figs. 93 - 94, is a folded valentine antenna. The antenna was used as a four element array which was fed by a transmitter having a 1000 watts peak power output.

Model 6.011, shown in Figs. 95 - 96, is similar to Model 6.005 except that it mounts from the inside of the missile so that less of the antenna height protrudes above the missile skin. This was essential so that the antenna will fit under the fiber glass shell of the Javelin vehicle.

3.8 The 7.000 Series C-Band Beacon Antennas

The 7.000 series includes scimitar, quadraloop and folded valentine antennas. The scimitar antennas were replaced by the folded valentine antennas which have superior radiation characteristics. The quadraloop antennas are preferred from the aerodynamic point of view.

Models 7.001, shown in Figs. 97 - 98, and 7.003, shown in Fig. 99, are scimitar antennas. They are essentially the same except for the mounting plate and the method for attaching the antenna.

Model 7.002, shown in Figs. 100 - 101, is a quadraloop antenna. It is a prototype antenna and the development was not completed since the folded valentine proved to be very satisfactory.

Model 7.004, shown in Figs. 102 - 103, is a folded valentine antenna and has become the standard C-Band antenna. Its advantages are the pattern shape and the low susceptibility to radio frequency diffusion breakdown.

Model 7.005, shown in Fig. 104, is the pressurized version of Model 7.004.

Model 7.007, shown in Fig. 105, is a quadraloop antenna. It was designed to have good aerodynamic characteristics and high temperature capabilities. The materials are stainless steel and quartz. Because of the delay of the quartz delivery, Model 7.009, shown in Figs. 106 - 107 was built using Fluorosint. Model 7.009 was successfully flown on the Exos vehicle.

Model 7.008, shown in Figs. 108 - 109, is the same as Model 7.004 except for the feed connector and the mounting plate. The plate is constructed so that the antenna mounts from the inside of the vehicle and the antenna base is partially recessed below the surface of the missile skin. This makes it possible to mount the antenna below the fiber glass cover of the Javelin vehicle.

3.9 The 10.000 Series Circumferential Quadraloop Antennas

Basically the antenna geometry is the same as the quadraloops discussed earlier but is mounted so that the long axis of the antenna curves around the missile cylinder. The first prototype antenna was built during the early part of 1961. Impedance and pattern measurements were completed. The further development was delayed due to other development requirements. The investigations were again started during the fall of 1962. Several prototype models are now in existence in the 35 Mc/sec, 75 Mc/sec and 240 Mc/sec frequency ranges. Illustrations are shown in Figs. 110 - 115.

3.10 The 17.000 Series P-Band Quadraloop Antennas

The antennas are of the same type as Model 2.003. They differ in slot length and driven element height because of the particular frequency, driving point impedance and mounting requirements. The final flight model was 17.004, shown in Figs. 116 - 117. It had a 50-ohm driving point impedance and was fed as a four element array.

3.11 The 20.000 Series Quadraloop Antennas in the 145 Mc/sec Frequency Range

The antennas were designed for the A0/10 vehicle. To save weight, the antenna slot was not filled with Fluorosint. Also, the coaxial tuning capacitor was deleted and replaced by a slide to change the driven element length. Models 20.001 through 20.003 are prototype antennas. Model 20.004, shown in Figs. 118 - 119, is flight hardware.

3.12 The 23.000 Series Gap Fed Oblique Stub Antennas

It was found desirable to design an antenna that would have a larger bandwidth and possibly less lift than the "large" quadraloop. One of the possible solutions is the oblique stub antenna. It fulfills the above requirements but does not have a convenient impedance control parameter. It was decided to investigate the properties of an oblique stub antenna fed in the same manner as a quadraloop. Of course it is also possible to think of the antenna as a flared quadraloop.

Prototype antennas for the Cajun and the AP/5 vehicles have

been built. The measurements are still in progress. The prototype antenna for the Cajun is the Model 23.005, shown in Figs. 120 - 121, and the ones for the AP/5 are Models 23.006, and 23.007 shown in Figs. 122 - 123.

3.13 The 24.000 Series Light Weight Telemetry Quadraloop

Since it is often desirable to mount the antennas under a fiber glass shield, it was thought desirable to start an antenna design which would give prime consideration to light weight and none to streamlining. One prototype antenna was built and impedance checks have been made. The antenna was given the model number 24.001, and is shown in Figs. 124 - 125.

4.0 DISCUSSION OF THE COMMON PROPERTIES OF ANTENNA TYPES

4.1 Outline of Section 4.0

In section three the emphasis was on the differences between antenna models. In this section the similarities will be stressed. The nomenclature of the various antenna dimensions and parts is illustrated in Fig. 126. Only nominal values are cited and special designs are neglected. Representative impedance, pattern and breakdown data are included for various antenna series.

The telemetry quadraloop antennas in the 2.000 series are separated in three groups according to antenna height. The semiflush mounted and flush mounted telemetry antennas in the 3.000 and 5.000 series are discussed only briefly and no data are presented since they are currently not in use and the various models have already been mentioned in section 3.0. The command control antennas in the 4.000 series include flush mounted and nonflush mounted antennas. Data are presented for the nonflush mounted antenna only. Data are presented for the S-Band and C-Band antennas in the 6.000 and 7.000 series. The 17.000 series antennas were included as items of interest even though they were not developed as part of this contract.

The quadraloop antennas have many features in common which are outlined in a separate section below to avoid reiteration.

4.2 Common Properties of the Quadraloop Antennas

4.2.1 The Antenna Mounting

Properties that the antennas have in common and that are of primary interest to the user are the antenna mounting, the impedance match, the harness, the antenna radiation pattern, and the radio frequency breakdown characteristics at low pressure.

The three types of antenna mounting are illustrated in Fig. 127. The mounting studs are preferred for strength and simplicity. Whenever screws are used from the inside of the missile, care has to be taken that they are cut to the correct length since the nut in the antenna base has very few threads and all of them have to be used to secure the antenna properly. The base plate mounting is satisfactory but requires the manufacture of an additional part and adds drag and weight to the antenna. About 170 grams should be added to the antenna weights quoted when base plates are used. By the use of o-rings and glass seal feed connectors the antennas can be pressure sealed to the missile skin.

4.2.2 The Antenna Impedance

The driving point impedance of the antenna is defined as the impedance measured at the end of the coaxial cable, i. e. in the plane where the antenna base meets with the dielectric in the slot. It is a function of the antenna dimensions, the feed location, the ground plane configuration and objects located in the near field of the antenna. Depending on the number of antenna elements in the array, the desired driving point impedance is usually selected to be 50 or 100 ohms. It is obtained by the proper choice of the feed location which is well established for cylindrical ground planes. If the ground plane is arbitrary or if various metal objects are located near the antenna, the feed distance has to be determined by impedance measurements. After the impedance is obtained for a given feed location it is possible to estimate the displacement required to obtain the desired impedance.

4.2.3 The Phasing Harness

The phasing harness depends on the number of elements in the array and the desired radiation pattern. The two element array is most frequently used. If the wavelength to missile diameter ratio is greater than one, the antennas are fed in parallel and 180 degree out of phase for good fore and aft coverage or in phase for side coverage. If the wavelength to missile ratio is less than one, the antennas are generally fed in phase with the final choice determined by inspection of the radiation patterns vs application.

In most applications the wavelength to missile diameter ratio is greater than one for telemetry antennas and the unit radiator of the two element array are mounted diagonally opposite on the missile body. If fore and aft coverage is desired, the feed location is chosen for a 100-ohm driving point impedance and the harness consists of $1/2$ wavelength and one wavelength long 50-ohm cable connected at a tee. The parallel impedance of the array is then 50 ohms at the center of the tee and the feed cable from the transmitter to the tee may be cut to an arbitrary length.

A variation of the above harness is to use antenna elements

with a 50-ohm driving point impedance and a harness with $1/4$ and $3/4$ wavelength tee arms of 75-ohm impedance cable. This arrangement is more bothersome since 75-ohm connectors are not readily available and/or applicable.

It is sometimes advantageous to use a four element array to reduce the widths of the nulls in the radiation pattern and/or subdivide power to avoid diffusion breakdown. The antennas are mounted in the same plane circumferentially around the missile in 90 degree intervals. The choice of the array phasing also may depend on the ground station antenna system. If the aspect angle of the vehicle is arbitrary and polarization diversity is not available on the ground, the antennas are designed for 100-ohm driving point impedances and are phased so that the phase difference between adjacent antennas alternates between 0 and 180 degrees. The second part of the harness consists of 75-ohm $1/4$ wavelength cable which transforms the parallel impedance of each pair of antennas back to 100 ohms that are then paralleled to obtain a 50-ohm impedance which is seen by the transmitter.

The second type of harness has antenna elements that are designed for 50-ohm driving point impedances. The cable lengths are cut to obtain $1/4$ wavelength phase difference between adjacent antenna elements and the cable length increasing in clock or counter clockwise direction depending on the desired sense of polarization. Quarter wavelengths, 75-ohm transform sections or a four port power divider is required to obtain a 50-ohm impedance match to the transmitter. The use of this harness results in an increased impedance bandwidth over that of the unit radiator. Also a three db gain is realized in the direction in which the transmitting antenna has the same polarization as the receive antenna when compared to a linearly polarized array on the missile and the usual circularly polarized ground antenna. The disadvantage is that the sense of polarization is reversed in the opposite direction so that both right circular and left circular receiving antennas are required on the ground if a signal is desired for both fore and aft directions of the missile.

4.2.4 The Antenna Pattern

The general pattern shape for a two element array mounted diagonally opposite on cylinder having a diameter less than a wavelength is that of a toroid if the right circular radiation component is recorded. If the antennas are fed 180 degrees out of phase, the axis of the toroid is normal to the axis of the cylinder. If the antennas are fed in phase the toroid is rotated through 90 degrees so that its axis is colinear with the axis of the cylinder.

If the cylinder diameter is larger than a wavelength and the antennas are fed in phase and mounted as above, the pattern for the

linear components is an interference pattern with lobes in all directions but always with nulls fore and aft of the cylinder.

4.2.5 Radio Frequency Breakdown

The quadraloop has a high voltage point at the open end of the antenna. It is therefore susceptible to diffusion breakdown at relatively low powers. Since it is not possible to simulate flight conditions with the available test equipment, the data may not correspond to the flight performance. In the past all indications were that the flight performance was better than that indicated by the measurements in the belljar.

The test is set up as described below. The signal source is usually a Maxon power generator or a transmitter identical to that used in the missile. The transmitter is set for a maximum power output and the radiated power from the antenna is varied by inserting different lengths of lossy cable. The incident and reflected powers are monitored by a Hewlett Packard 430 C and a Sierra 164 power meter. The pressure measurements are obtained with a High Vacuum Measuvac McLeod gage Model TD-1 by Kinney Co. and an Aneroid pressure gage Type CG1-B by Edwards High Vacuum Ltd. The ion source in the vacuum system is an alpha particle emitter or a Tesla coil. The appearance of breakdown is illustrated in Fig. 128. The airglow surrounding the antenna is usually visible, however to avoid ambiguities during faint glows the antenna radiation is monitored by an oscilloscope and breakdown is defined by the observed deterioration of the signal.

The data is presented graphically. The gas pressure and the altitude are plotted along the abscissa and the absorbed power along the ordinate. The absorbed power is defined as the difference between the incident power from the transmitter and the reflected power from the antenna. Two data points are obtained for each power level. The point to the left shows the initiation and the point to the right the recovery of breakdown. Signal deterioration due to breakdown occurs at all altitudes between the two points. The minimum of the curve represents the least power at which breakdown will occur.

The equation below, by J. A. Kane, defines the relationship between frequency and the mean free path for which the breakdown power is a minimum.

$$fL = 1.722$$

where f is the frequency in megacycles per second and L the mean free path of the neutral particles in feet. The correlation between mean free path and altitude is shown in Figs. 125 - 131. The curve was obtained from the tables

in U. S. Standard Atmosphere, 1962, prepared under sponsorship of NASA, U. S. Air Force and the U. S. Weather Bureau.

4.3 The 2.000 Series, 1.5-Inch High Quadraloop Telemetry Antenna

The overall dimensions of the antennas are: height 1.5 inches, width 1.0-inch, and length from 9.0 to 10.0 inches depending on the desired frequency range. The primary materials are aluminum metal and Fluorosint dielectric. The antenna weight varies from 450 to 600 grams depending on the antenna length.

Idealized impedance curves are shown in Figs. 132 - 134. Figure 132 shows the driving point impedance of a single quadraloop as a function of frequency. The antenna is mounted on a 15.0-inch diameter cylinder and the feed location is 0.7 inch from the antenna short. The configuration of the curve remains the same if the diameter of the cylinder is varied and the feed location is properly adjusted. The impedance curve shown in Fig. 133 is identical to that in Fig. 132 except that it is plotted on a normalized chart. It is included to show the impedance bandwidth. Nominal values for the bandwidth are: 1.6 Mc over a 1.5:1 VSWR and 2.8 Mc over a 2.0:1 VSWR. Figure 134 shows the impedance versus frequency curve for the two element array fed 180 degree out of phase.

Representative pattern data are shown in Figs. 135 - 140.

Figure 135 is a sketch of the vehicle mockup showing the antenna location and the mockup dimensions. The antenna position in the coordinate system is shown in Fig. 136. The gain reference, the $\phi = 0^\circ$ cut and the $\phi = 90^\circ$ are shown in Figs. 137 - 139. The complete pattern is shown in Fig. 140 in the form of a power contour plot which was obtained from ϕ cut patterns taken in 10 degree increments.

A representative curve of the diffusion breakdown as a function of power and altitude is shown in Fig. 141.

4.4 The 2.000 Series, 1.0-Inch High Quadraloop Telemetry Antenna

The main differences between the 1.0-inch high quadraloop and the one described in section 4.3 is the reduction in size and the additional capacitive endloading from the metal support screw. The support screw is shown as item 9 in Fig. 36. The discussion below applies to the "standard" models and neglects the early development designs and the special designs, as for example the Model 2.036 for the Exos vehicle.

The overall dimensions of the antennas are: height 1.0 inches, width 0.62-inch, and length from 6.6 to 7.4 inches. The materials are aluminum and Fluorosint. The antenna weight varies from 160 to 190 grams.

The impedance versus frequency curves are shown in Figs. 142 - 144. The nominal impedance bandwidth is 0.7 Mc over a 1.5:1 VSWR and 1.2 Mc over a 2.0:1 VSWR. The reduced bandwidth is due to the decreased driven element and slot heights. The implication of the decreased bandwidth is an increased Q value for the antenna which in turn means that the ratio of the stored to the radiated energy is increased. It is for this reason that it is not practical to decrease the height of the antenna much below the present one.

The pattern data is presented in Figs. 145 - 151. Four antennas were mounted on the mockup but the patterns are that of a two element array fed 180 degrees out of phase. The second pair of antennas were tuned to a different frequency and did not influence the pattern. In the coordinate system, the test antennas are shown solid and the others are line drawings.

A representative diffusion breakdown curve is shown in Fig. 152. There is some indication that the minimum breakdown power is proportional to the driven element height. However, the data are insufficient for a quantitative statement.

4.5 The 2.000 Series, 0.5-Inch High Quadraloop Telemetry Antennas

The antennas are constructed of aluminum and Fluorosint. The weights for single element vary from 110 to 160 grams. The antenna mounting is similar to that of the larger quadraloops with a base plate, except that the base plate is not a separate part. The antenna base is simply widened to provide a flange.

All that has been outlined in the previous 4.3 and 4.4 sections applies to these antennas. The even further reduced slot and driven element height decreased the bandwidth and the gain.

The driving point impedance is 100 ohms since the antenna was to be used as two element arrays. Idealized impedance curves are shown in Figs. 153 - 155. The bandwidth is 0.5 Mc over a 1.5:1 VSWR and 0.9 Mc over a 2.0:1 VSWR.

The patterns are presented, together with the coordinate system and a sketch of the missile mockup, in Figs. 156 - 167. The power contour plot is not included since the patterns were measured in 30 degree increments of phi.

The diffusion breakdown data are shown in Fig. 168. As expected the minimum breakdown power is less than that of the 1.5-inches high or that of the 1.0-inch high quadraloop.

4.6 The 3.000 and 5.000 Series Flush and Semiflush Mounted Telemetry Quadraloop Antennas

Because of the similarities between the 3.000 and 5.000 series antennas they will be discussed in the same section. The antennas are quadraloops recessed in a cavity and the statements in section 4.0 pertain also to these antennas. The mechanical differences were already pointed out in section 3.4 and 3.5, and electrically they are identical. The bandwidth and gain corresponds closely to that of the 0.5-inch high quadraloop discussed in section 4.5.

4.7 The 4.000 Series Command Control Quadraloop Antennas

4.7.1 The Flush Mounted Type

The antennas in this group are scaled versions of the 3.000 and 5.000 series antennas to operate in the 400 Mc/sec frequency region. None of the present models are considered standard designs.

An idealized impedance curve of the two element array fed 180 degrees out of phase is shown in Fig. 169. The impedance bandwidth is 0.6 Mc over a 1.5:1 VSWR and 1.5 Mc over a 2.0:1 VSWR.

4.7.2 The Nonflush Mounted Type

This type antenna is a scaled version of the 2.000 series. The impedance data are shown in Figs. 170 - 172. The impedance bandwidth is 2.0 Mc over a 1.5:1 VSWR and 3.6 Mc over a 2.0:1 VSWR.

No representative patterns with the antennas mounted on a cylindrical ground plane have been obtained to date. However, patterns for a special application with the antennas mounted on a payload are shown in Figs. 173 - 178. This particular task was not part of this contract and the data is presented as a matter of interest.

No diffusion breakdown data has been obtained to date.

4.8 The 6.000 Series S-Band Beacon Antennas

4.8.1 The Quadraloop Type Antenna

The antenna is similar to the quadraloop discussed in section 4.1, but has been scaled to the higher frequency. Since the antenna is small from the aerodynamic point of view, it was possible to increase the bandwidth by increasing the slot and drive element height in terms of wavelength. The support screws were deleted since the structure is rigid enough

without them. To date only the stud mounting has been used, however, with minor redesigns all three types of mounting discussed earlier are possible.

The bandwidth of the antenna is from 2700 Mc to 2960 Mc over a 1.5:1 VSWR and from 2660 to 3020 over a 2:1 VSWR. The desired operating frequencies fall in this range and therefore no antenna tuning is required.

The antennas are designed for a 50-ohm driving point impedance. It is therefore easy to array two or four elements. To date only the two element array has been used. For almost all applications the ratio of missile diameter to wavelength has been greater than one and a more satisfactory pattern is obtained if the two element array is fed in phase. The coaxial transmission line harness consists of 50-ohm cable having tee arms of equal length and a Microlab power divider.

The VSWR and pattern data are presented in Figs. 179 - 188. The diffusion breakdown data are shown in Fig. 189.

4.8.2 The Folded Valentine Antenna

The development of the folded valentine antenna is not part of this contract. They are included as a matter of interest. The antenna has two advantages compared to the quadraloop antenna. It is less susceptible to diffusion breakdown and the radiation pattern is smoother. The disadvantage is an aerodynamic one. It has so far found only one application and the existing data are insufficient to optimize the design.

The driving point impedance is approximately 150-j50 ohms and no satisfactory impedance control parameter has been found to date. However, the particular application required that the feed point region would be potted to decrease further the possibility of breakdown and it was found that the potting changed the antenna impedance to 50 ohms. Peak power rating of this antenna array was greater than 2.0 Kw.

The antennas were then harnessed as a four element array. They were mounted circumferentially at the base of an Aerobee nose cone in 90 degree intervals and phased so that the phase difference between antennas would be alternately 0 and 180 degrees. The second phasing was in quadrature. Patterns were satisfactory for both phasings. The second phasing was chosen because the impedance match was better over a wider frequency range. The patterns are superior to that of a two element quadraloop array and do not show the deep null aft of the missile. VSWR and pattern data are presented in Figs. 190 - 201. The diffusion breakdown data are shown in Fig. 202.

4.9 The 17,000 Series Quadraloop Beacon Antennas in the 300 Mc/sec Frequency Range

The 17,000 series antennas were not part of this contract, but were used on a vehicle for AFCRL and are included as a matter of interest. They are similar to the 2,000 series telemetry antennas but are a good example of a four element array.

The array elements were mounted on a slightly tapered cylinder as shown in Fig. 216. The patterns shown pertain to this particular payload configuration. The flight pattern may have differed from the measured ones since photographs obtained later showed that a number of reflecting objects were located close to the antenna which may have disturbed the pattern and impedance match. The measured patterns are shown in Figs. 218 - 220. Only the principal plane cuts are presented.

The impedance measurements show the increase of the impedance bandwidth due to the 90 degree phase difference between the array elements. For the single element the bandwidth is 1.0 Mc over a 1.5:1 VSWR and 1.9 Mc over a 2.0:1 VSWR. For the array the bandwidth is 5.0 Mc over a 1.5:1 VSWR and 7 Mc over a 2.0:1 VSWR. The impedance curves and a sketch of the phasing harness is shown in Figs. 213 - 215.

5.0 SPECIAL APPLICATIONS AND DESIGNS

5.1 Outline

In this section various special designs for long range probes, a satellite and a high temperature sounding rocket are discussed. The discussion is not complete nor detailed and each application will be covered more fully by a scientific report which will be published at a later date. The long range probes are the AP/3 and the AP/5. The satellites are the AO/10 and the AO/15. The high temperature vehicle is the Exos.

Special antennas which are still in the design stage and for which no data is presented in this report are the DOVAP antennas for the Javelin and the telemetry antennas for the Cajun.

5.2 The Model 2,025 Telemetry Antennas for the AP/3

When the problem was first presented, the plan was to design a tubular quadraloop antenna similar to the Model 24,001. However the time schedule did not permit it and it was decided to adapt the standard Model 2,007 antenna. The leading edge of the antenna was modified for a mounting bracket and the first tests were made with the antenna mounted on a mock-up that simulated the first design of the payload which consisted of a truncated

cone, a short cylinder and a spherical motor. This design was later modified to the configuration shown in Fig. 223. The mounting bracket was no longer required and the antenna was then identical to the Model 2.007 except that part of the aerodynamic leading edge had been removed. However, the model number remained 2.025, to avoid confusion.

The antenna impedance match was rechecked a few weeks before the flight at Cape Canaveral. At that time it became necessary to remove the band that provided a d-c short from the cylindrical section to the spherical motor and it was decided to recheck the patterns. The pattern measurements showed that the change was not detrimental. The gain check, the $\phi = 0$ degrees cut and the $\phi = 90$ degrees cut are shown in Figs. 225 - 228.

5.3 The Model 23.006 and 23.007 Telemetry Antennas for the AP/5

The antenna design had to be revised several times since its conception due to changes of the payload configuration and the pattern requirements. At the start of the problem the emphasis was on minimum antenna weight and a pattern with a major lobe aft of the payload. The payload was to be constructed of Fiberglas with a faraday shield embedded in the walls. Later measurements showed the assumption erroneous that the faraday shield would provide a sufficient ground plane and that it would shield the magnetometers sufficiently from the rf field. It also proved to be desirable to minimize the pattern nulls in the $\theta = 90$ degrees plane. The two element array was replaced by a four element array. Because of the configuration of the payload it was not possible to use antennas with the same flare angle. The array consists, therefore, of two Model 23.006 and two Model 23.007 antennas. To provide a good rf shield and antenna ground plane the payload was gold plated.

The design of the 23.000 series antennas may be interpreted in two ways. It could be considered an oblique stub antenna that is fed across the slot like a quadraloop or as a quadraloop antenna with a variable slot height. The design resulted from the desire to obtain an antenna that could be mounted and impedance matched like a quadraloop and would also approach the radiation efficiency and bandwidth of the stub antenna.

The gain check, the $\phi = 0$ degrees and the $\phi = 90$ degrees cuts are shown in Figs. 233 - 235. The above patterns were measured with the entire surface of the payload gold plated. Earlier patterns measured with the payload configuration as shown in Fig. 229 showed more signal in the $\theta = 90$ degrees plane and a lower gain in the $\theta = 180$ degree direction.

5.4 The Model 20.004 Quadraloop Antennas for the AO/10 and the AO/15

The design emphasis was on light weight, reduced antenna length and an omnidirectional type pattern. The antennas were of a tubular construction and were capacitively endloaded to fit into the available space. Two antenna systems were used each consisting of a four element array and phased in quadrature as shown in Fig. 239. The antennas were mounted on a cylindrical section of the payload as shown in the coordinate system in Fig. 238. The gain check, the $\phi=0$ degrees and the $\phi=90$ degrees cuts are shown in Figs. 240 - 242.

5.5 The Model 2.036 Quadraloop Telemetry Antennas for Exos

The anticipated temperature was such that it was decided to use stainless steel for the antenna body and quartz for the dielectric insert. In all other respects the antennas resemble the Model 2.005 quadraloop. The main problem was the doors opening in front of the antenna. It had been assumed that the doors would act as reflectors and result in an increased gain aft of the missile. Later pattern measurements showed that they acted as directors increasing the gain in the forward direction of the missile. The antenna patterns are shown in Figs. 246 - 248 with the doors on the missile closed and in Figs. 251 - 253 with the doors open. Since at that time it was too late to change the vehicle configuration and it was impossible to move the antennas in the fore or aft direction, it was decided to excite only one antenna of the array. The configuration and the patterns are shown in Figs. 254 - 257. The radiating antenna is shown solid in the coordinate system. Since the Model 2.036 antennas had to be shipped, a Model 2.007 antenna was used for the pattern measurements.

5.6 The DOVAP Antennas for the Javelin and the Telemetry Antennas for the Cajun

Several prototype models in the 10,000 series for DOVAP frequencies have been built. The antennas are similar to the quadraloops, but are curved to fit circumferentially around a cylindrical missile body. Preliminary impedance and pattern checks have been completed. However, to improve the pattern measurements, transmitters are being built to fit into the missile body to eliminate the feed cable leading through the rotator column to the antenna. The patterns should become available during the fall of 1963.

The telemetry antennas for the Cajun are similar to the ones used on AP/5. Several prototype antennas have been built to establish the feed location. No pattern measurements were taken to date. The design is expected to be firm by the fall of 1963.

6.0 THE COMMAND CONTROL NOTCH ANTENNA FOR THE AEROBEE 150

The antennas have been in extensive use for a number of years and

were described in a previous report. However, as a matter of interest power contour plots obtained from recent pattern measurements are shown in Figs. 259 - 264.

7.0 GRAPHS AND TABLES

No additional information is given in this section. The purpose is to present the information most frequently desired by the contractor in an easily accessible form. The tuning range, the weight of a single antenna element and the pressurized or non pressurized mounting for the various standard model in the 135 to 440 Mc/sec frequency range is shown in Fig. 260.

Appendix I lists the antenna models with reference to the quarterly progress reports. Appendix II is a similar index for the vehicles.

Appendix III lists all the antenna models in sequence that were mentioned in the progress reports or could be of interest to the contractor. The antennas that were not mentioned in the progress reports are starred. The tuning ranges and weight are given when available. The assembly drawing numbers and photograph numbers are included for the contractors convenience when requesting additional information. Appendix IV is the condensed version of Appendix III and includes only the presently used standard models.

Appendix V is a list of the number of antenna units shipped during the report period.

Appendix VI is a sample of the ANTENNA INFORMATION WORK SHEET that has been assembled to aid the contracting agency and the contractor when requesting antennas for particular vehicles. It lists the information required to select the correct antenna model or to initiate a new antenna design to produce optimum results with least cost and time.

8.0 SUMMARY

A major part of the effort was devoted to providing operational antennas for the various vehicles at a rate of approximately one antenna unit every third day. At the same time every effort was made to accumulate sufficient data to design the antennas so that the largest number of requirements could be filled with the least number of antenna types. The antennas listed in Appendix IV will now fill nearly all requirements for sounding rockets from telemetry to C-Band beacons. In the future this should provide more engineering applied research and development time for the special designs like DOVAP antennas, high temperature antennas and light weight antennas for covered payloads or for other unforeseeable requirements.

The particular direction which future efforts will take is difficult to foresee since they depend largely on the contractors requirements. However, from the present viewpoint it would seem advisable to direct the efforts toward the investigation of new dielectrics, to investigate various arrays of C-Band antennas, to start the development of telemetry antennas for higher frequencies, and to extend the study of diffusion and multipacting breakdown.

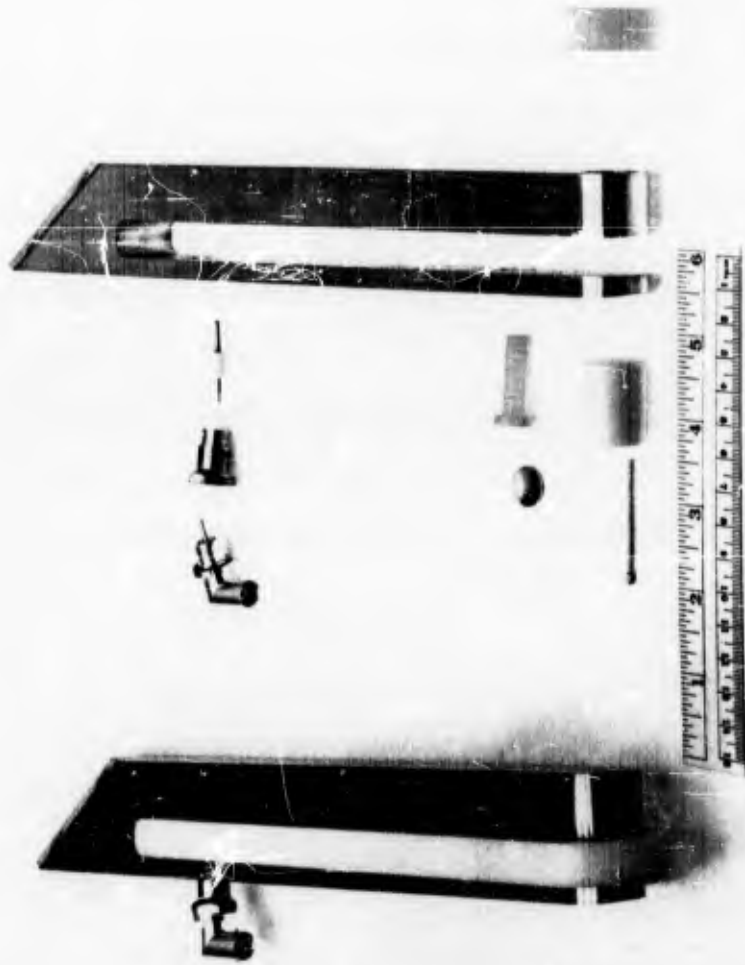


FIG. 1 - PHOTOGRAPH OF MODEL II-SHORT TELEMETRY
QUADRALOOP ANTENNA

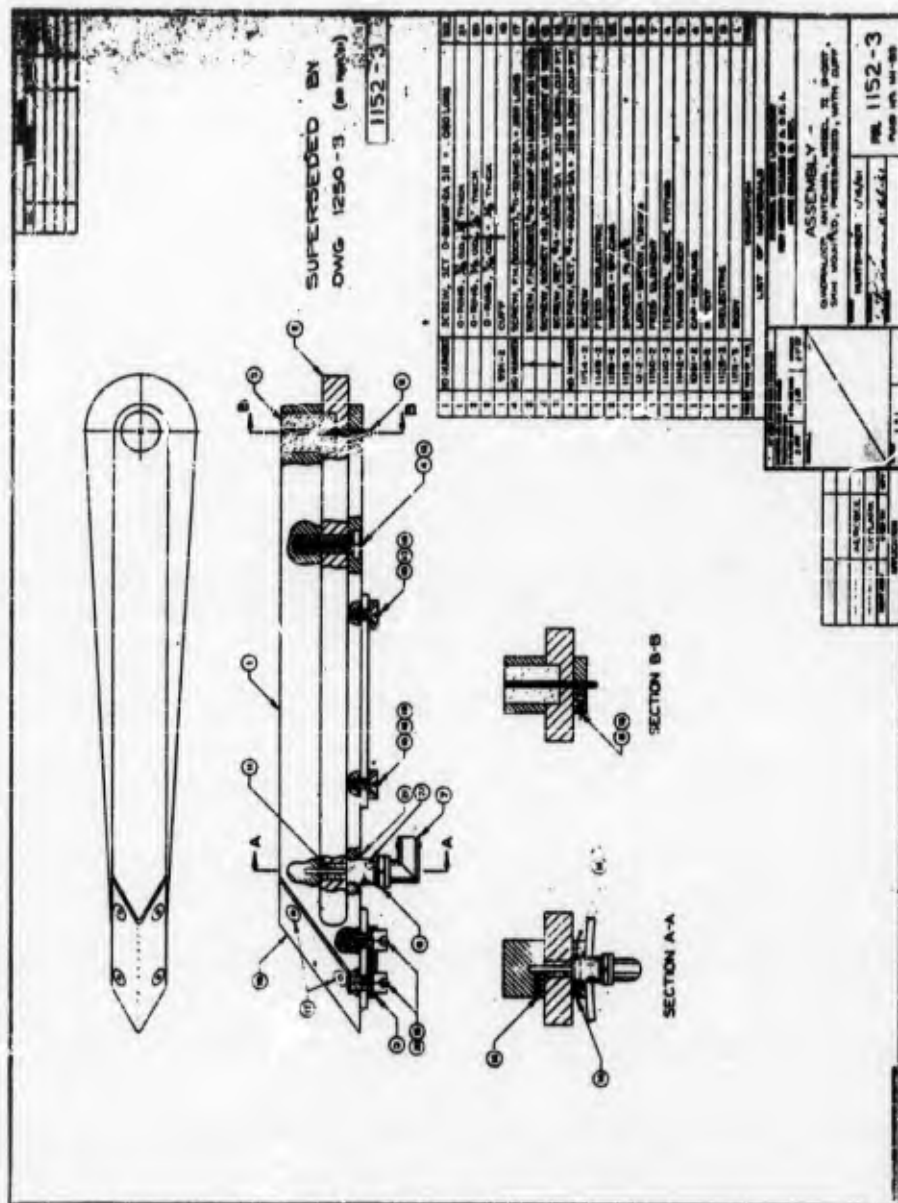


FIG. 2 - MODEL II SHORT TELEMETRY QUADRALOOP ANTENNA

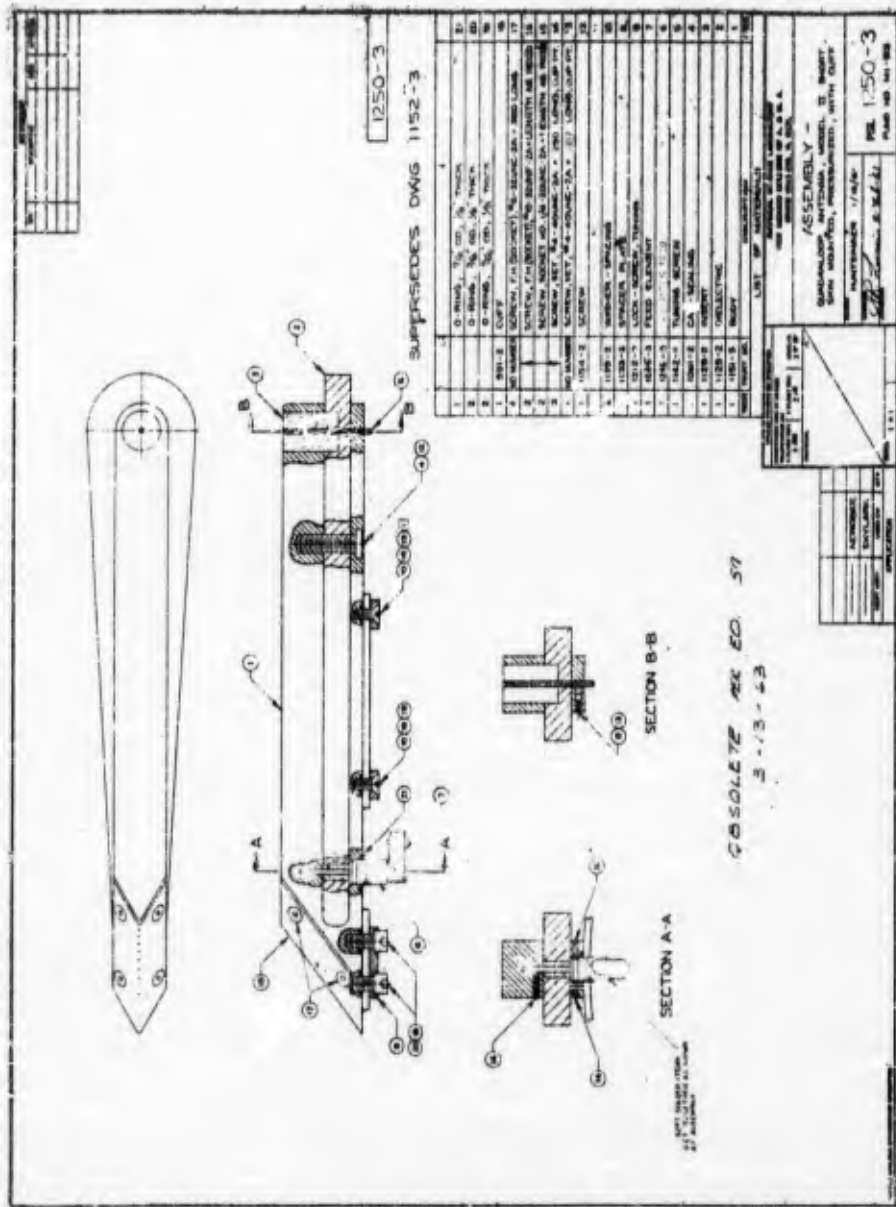


FIG. 3 - MODEL II SHORT TELEMETRY QUADRALOOP ANTENNA

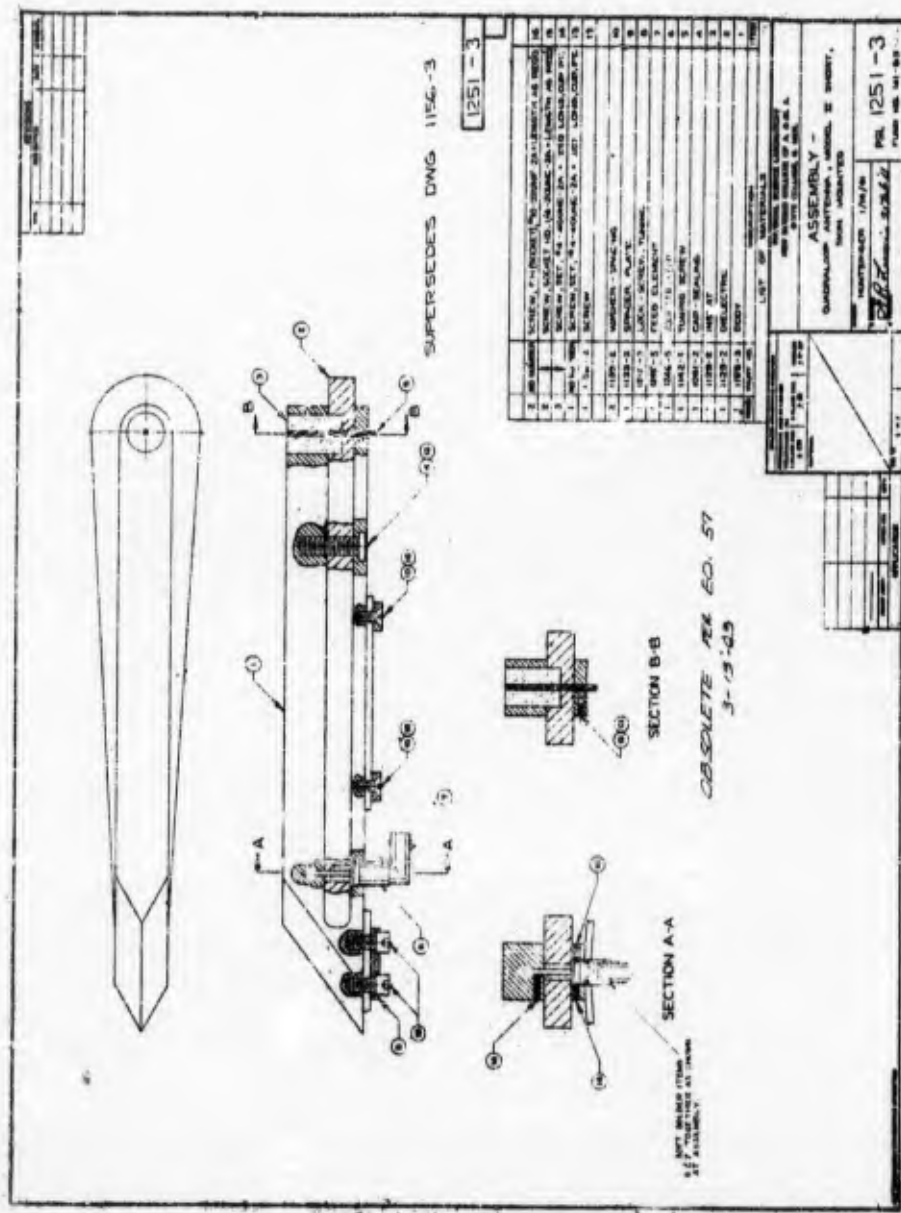


FIG. 4 - MODEL I SHORT TELEMETRY QUADRALOOP ANTENNA

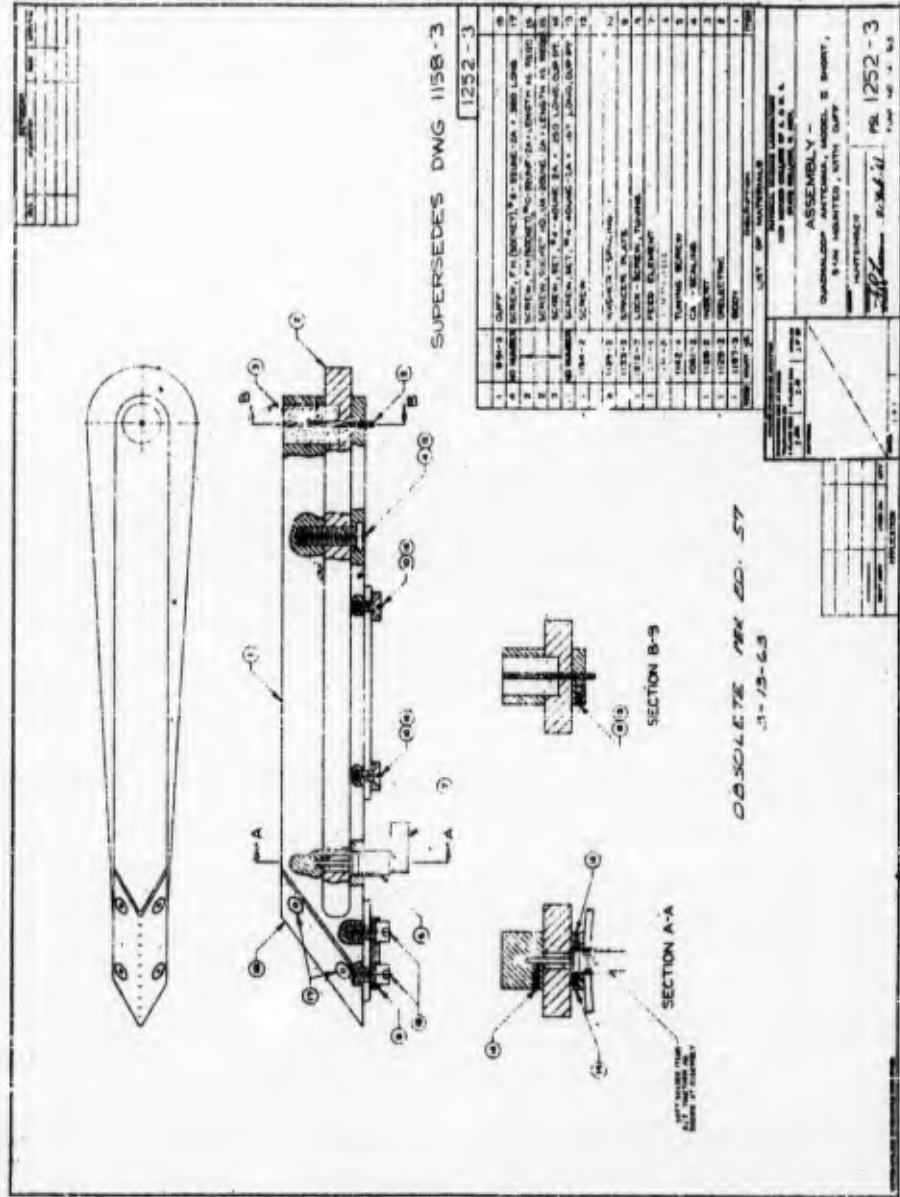


FIG. 5 - MODEL II SHORT TELEMETRY QUADRALOOP ANTENNA

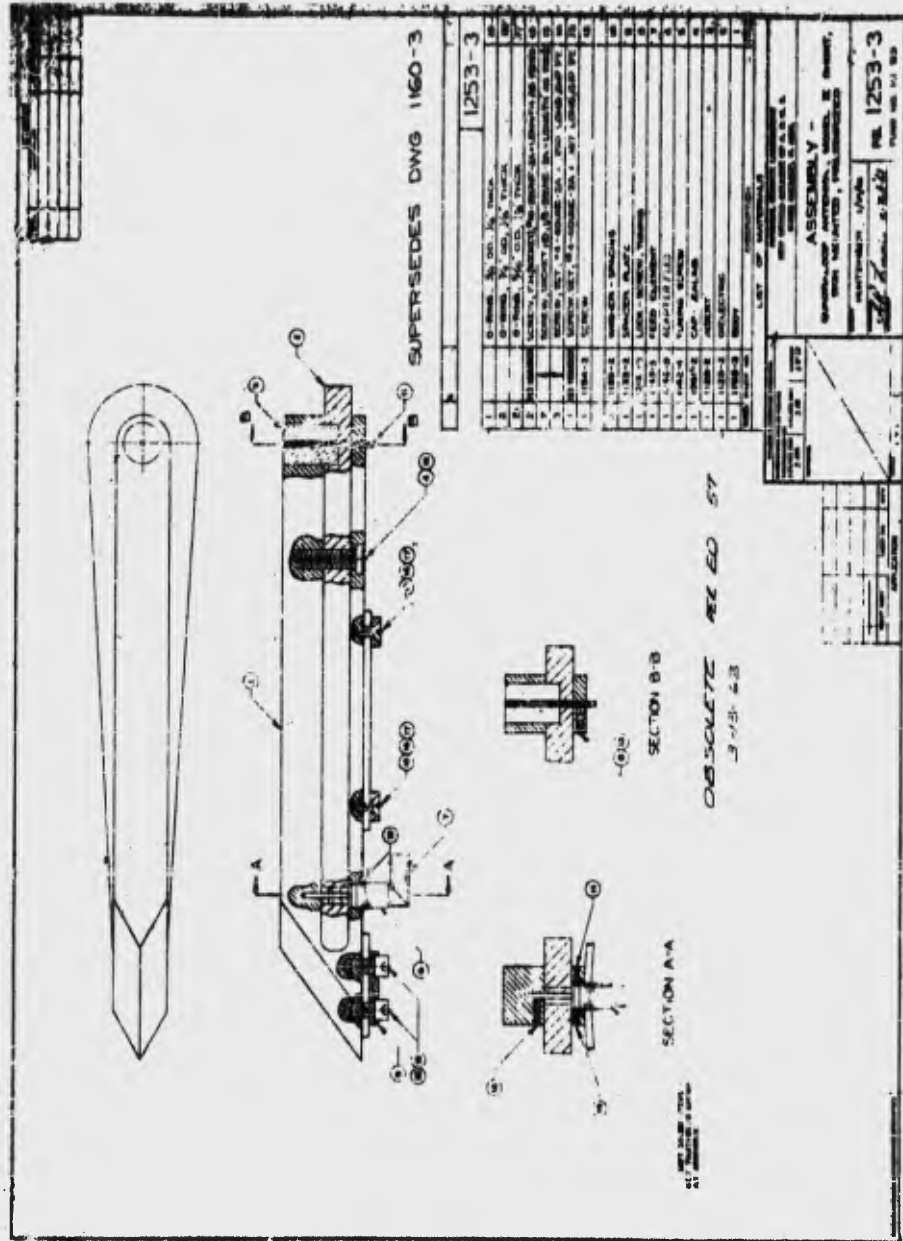


FIG. 6 - MODEL I) SHORT TELEMETRY QUADRALOOP ANTENNA

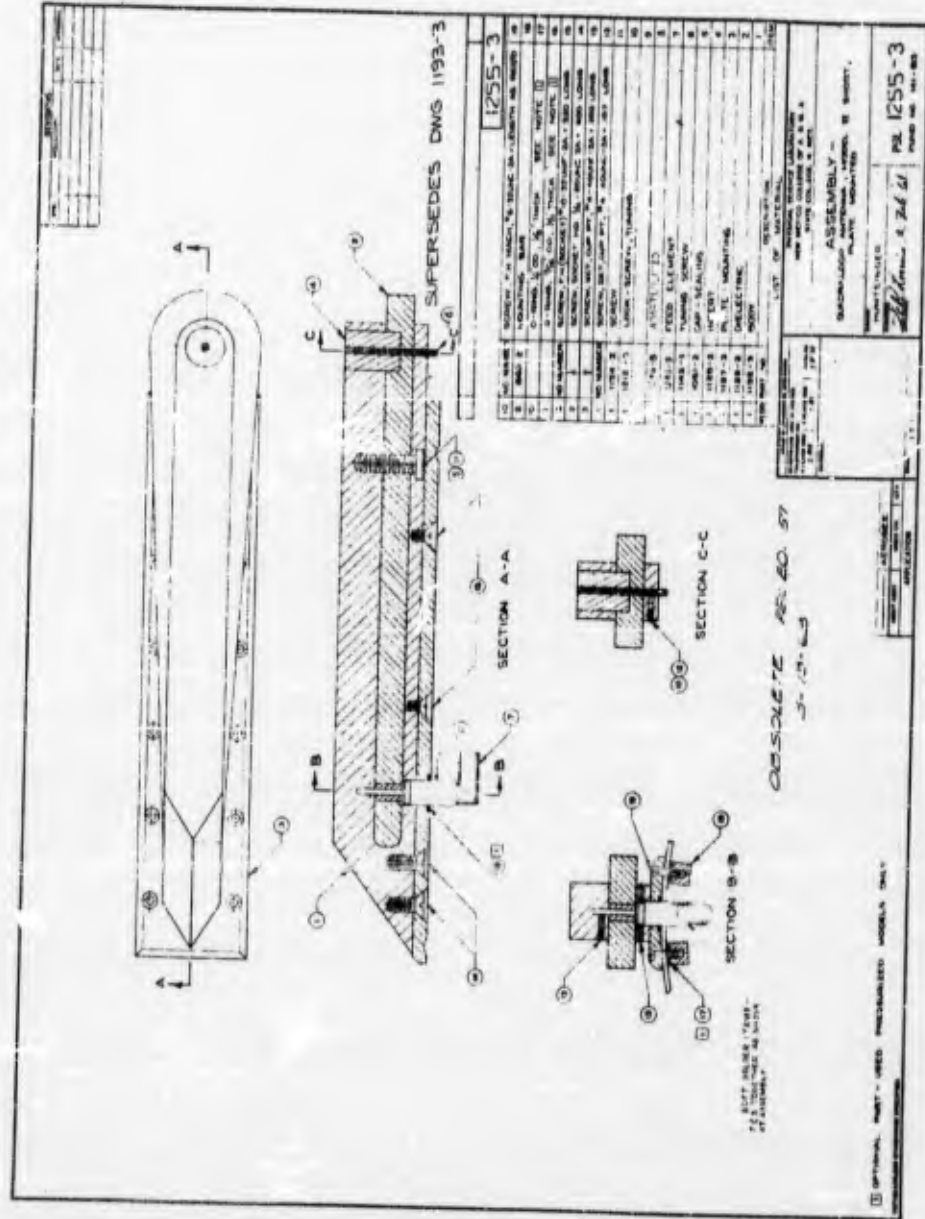


FIG. 8 - MODEL II SHORT TELEMETRY QUADRALOOP ANTENNA

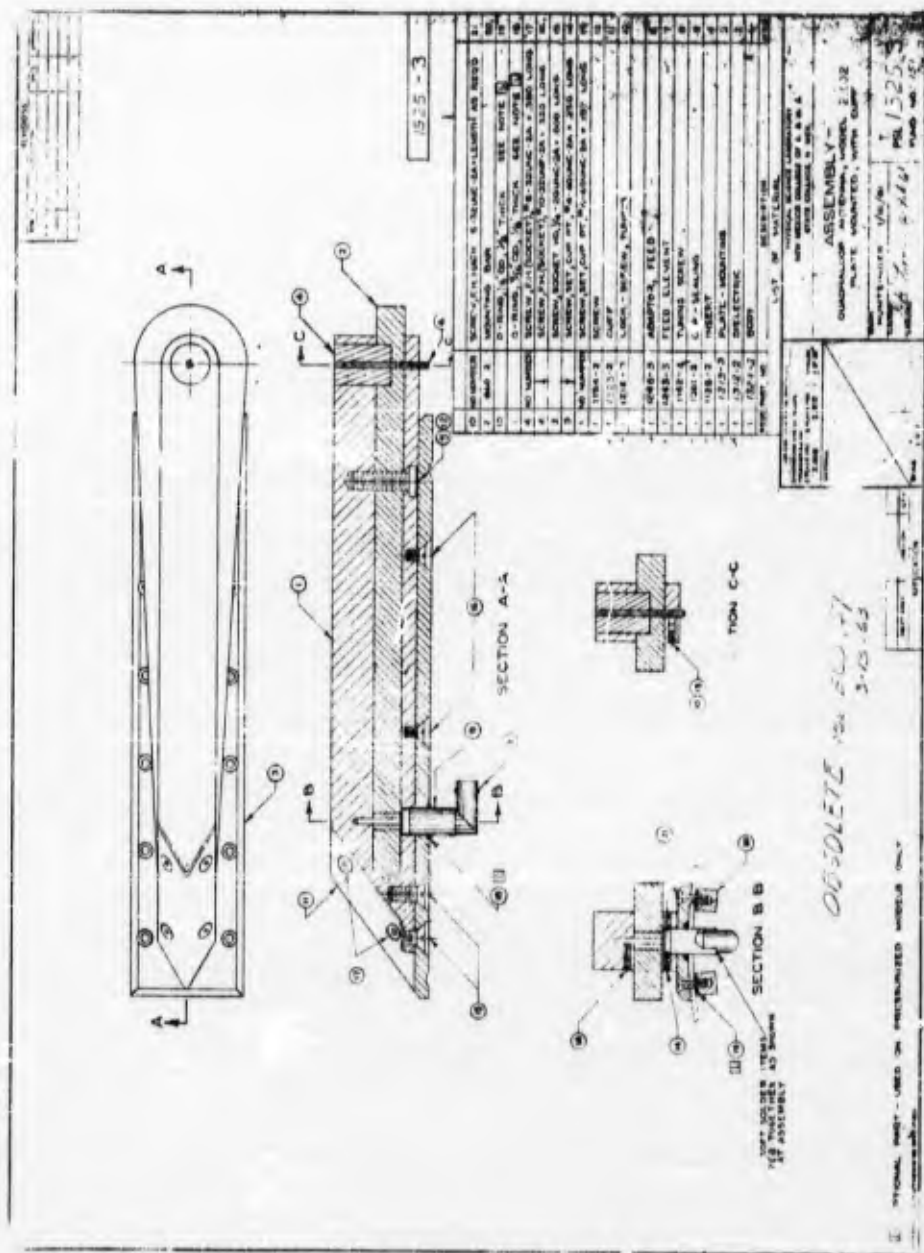


FIG. 9 - MODEL 2.002 TELEMETRY QUADRALOOP ANTENNA

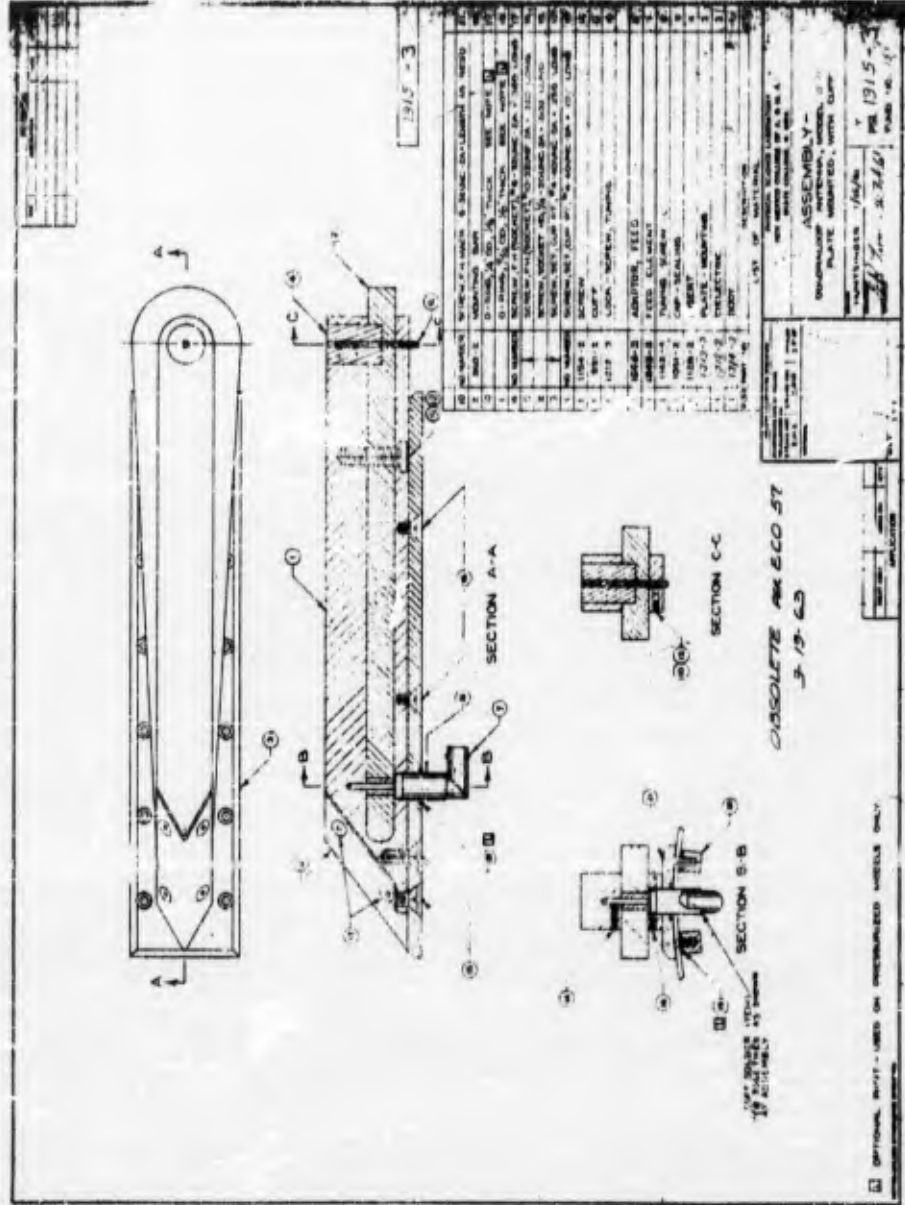


FIG. 10 - MODEL II-D TELEMETRY QUADRALOOP ANTENNA

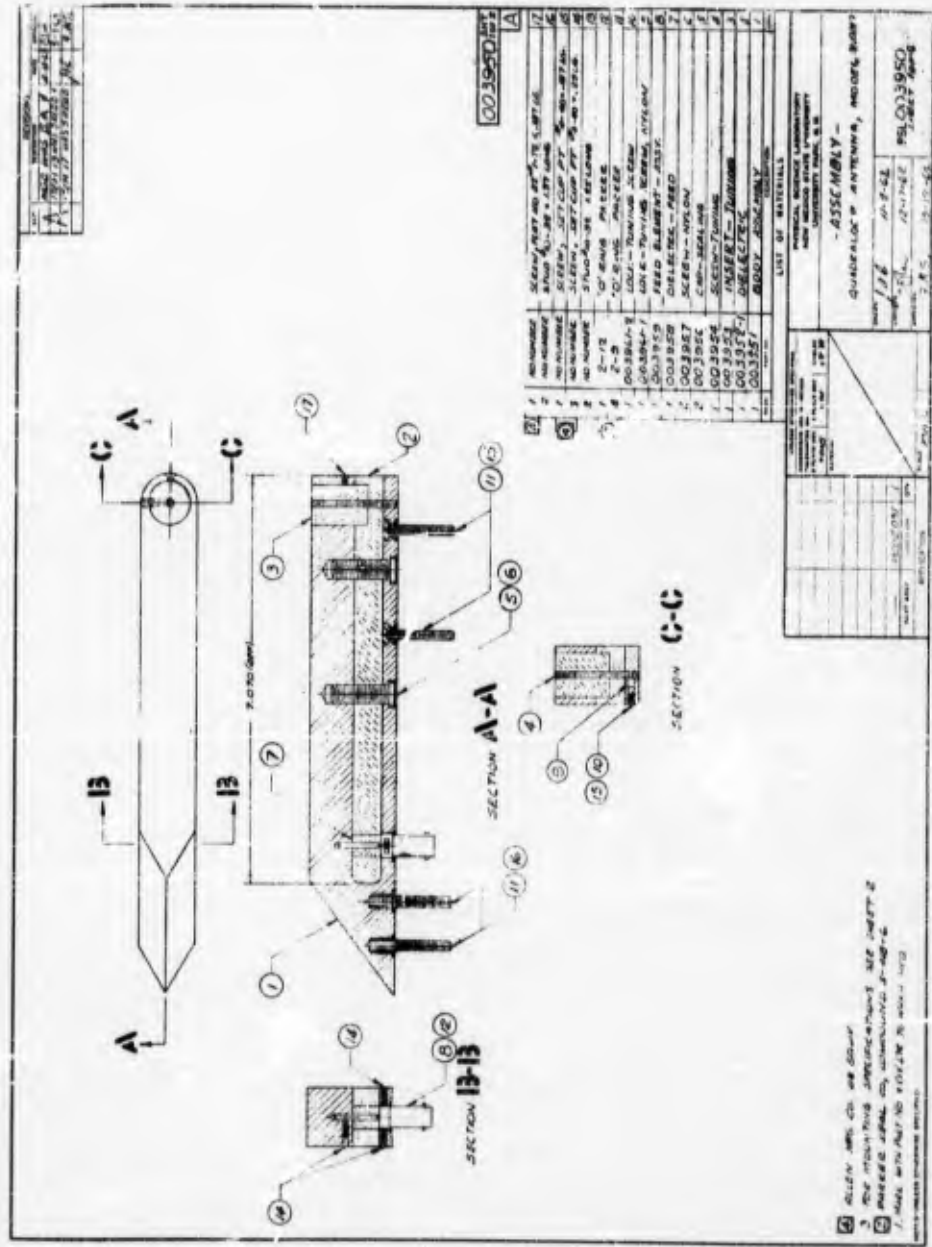


FIG. 11 - MODEL 2.037 TELEMETRY QUADRALOOP ANTENNA

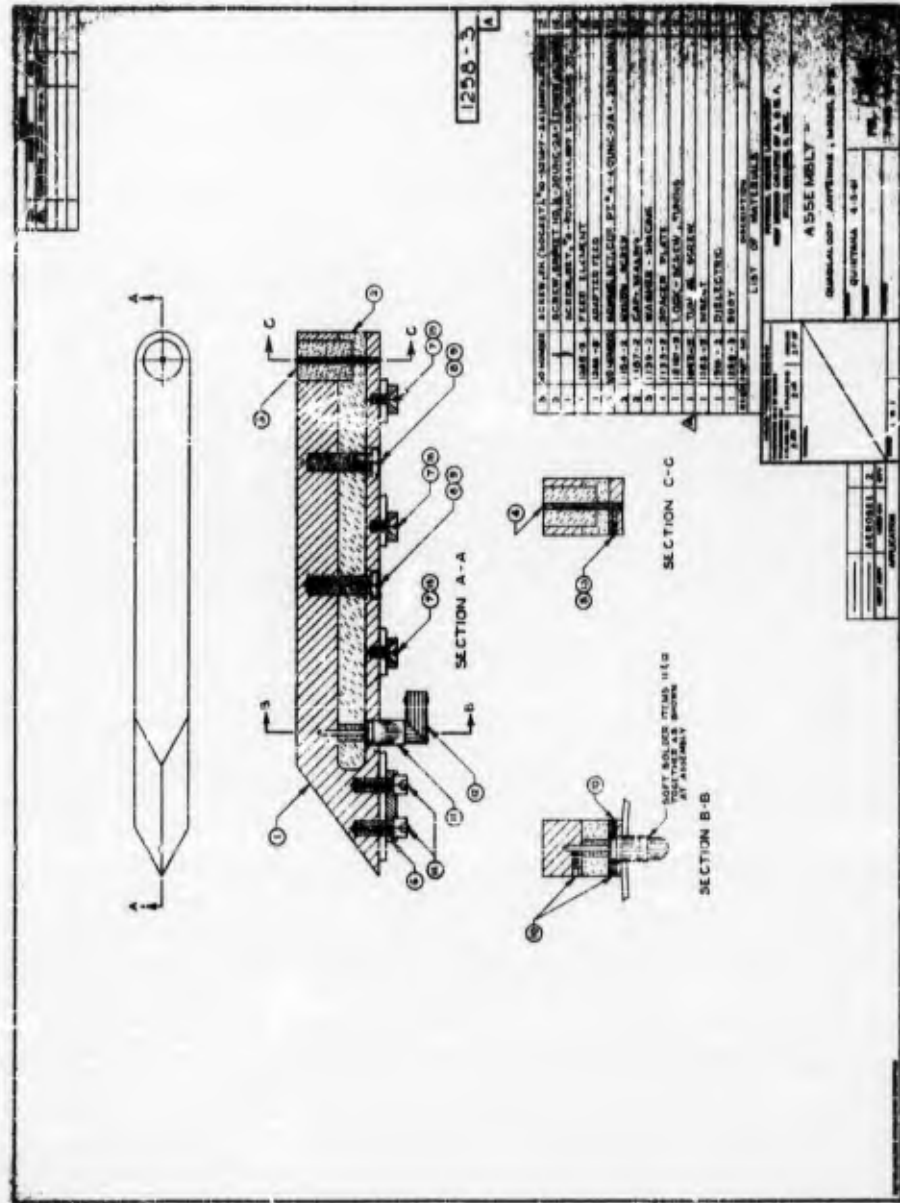


FIG. 12 -- MODEL II-B TELEMETRY QUADRALOOP ANTENNA

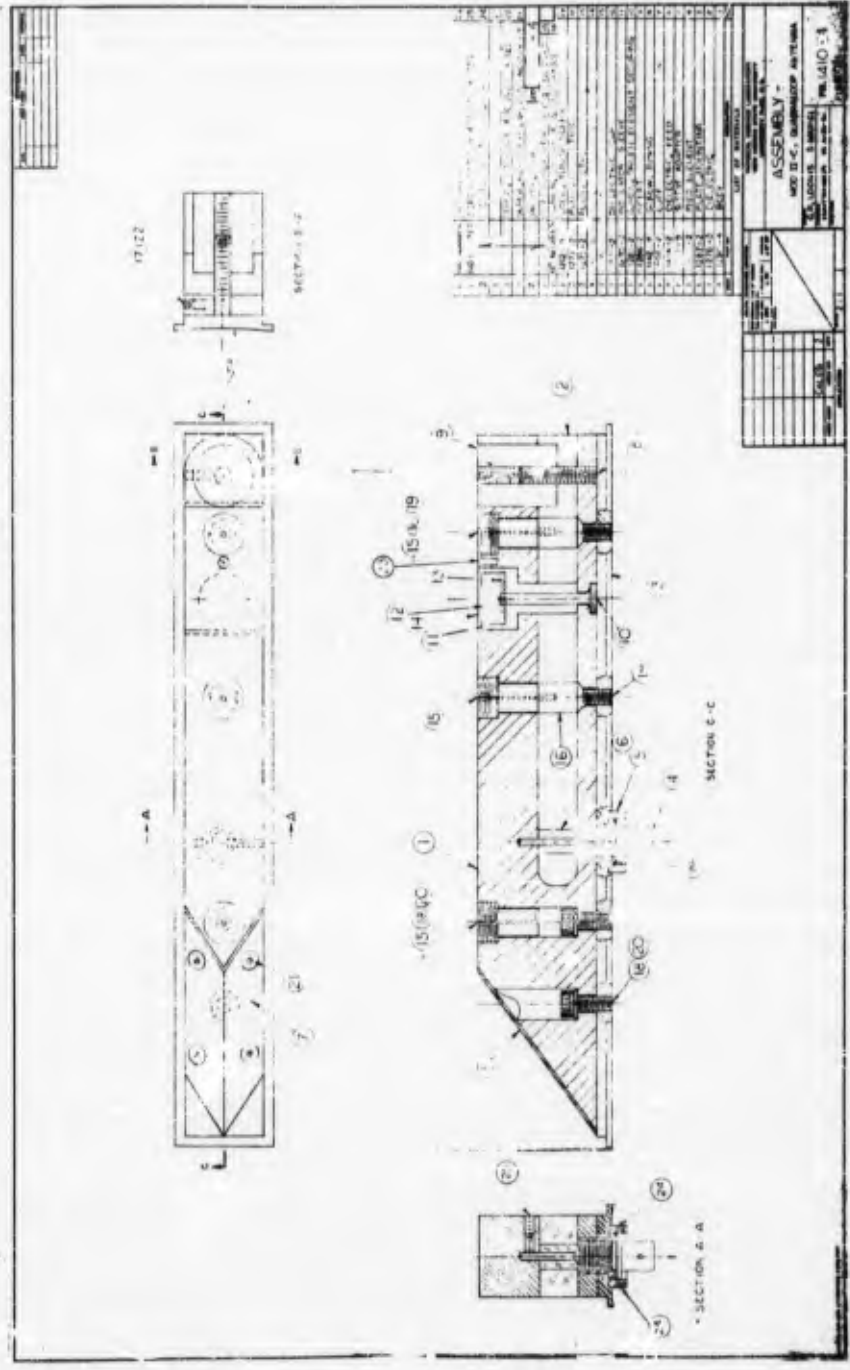


FIG. 13 - MCJEL II-C TELEMETRY QUADRALOOP ANTENNA

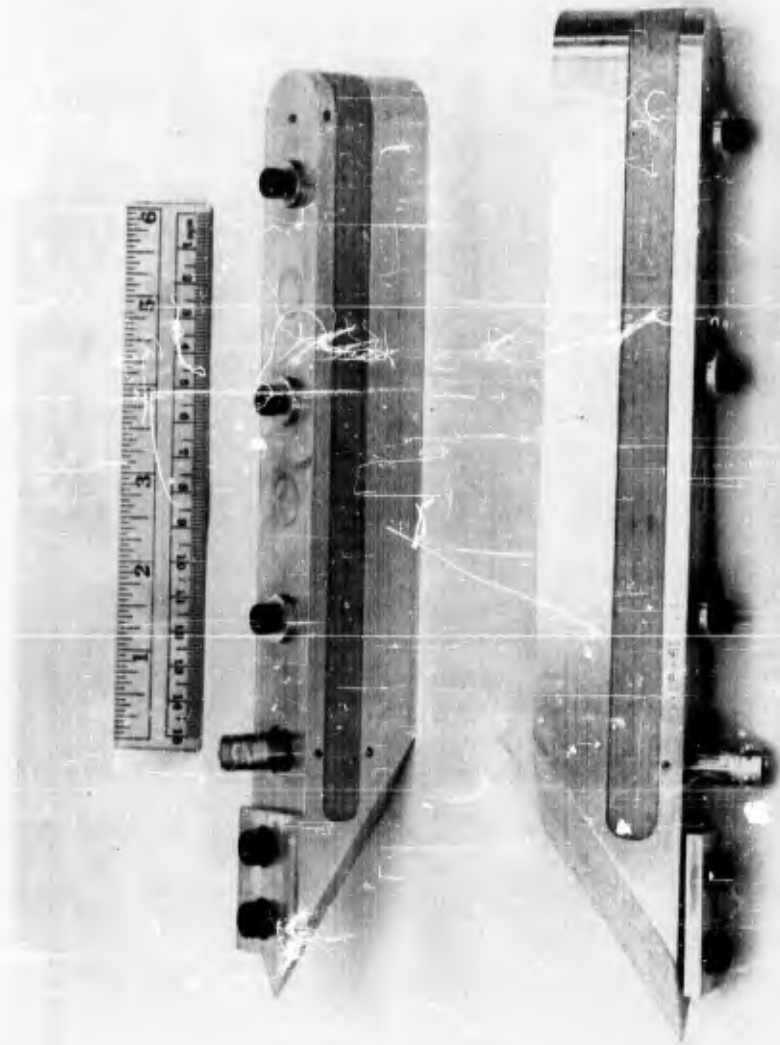


FIG. 15 - PHOTOGRAPH OF MODEL 2.010 TELEMETRY
QUADRALOOP ANTENNA

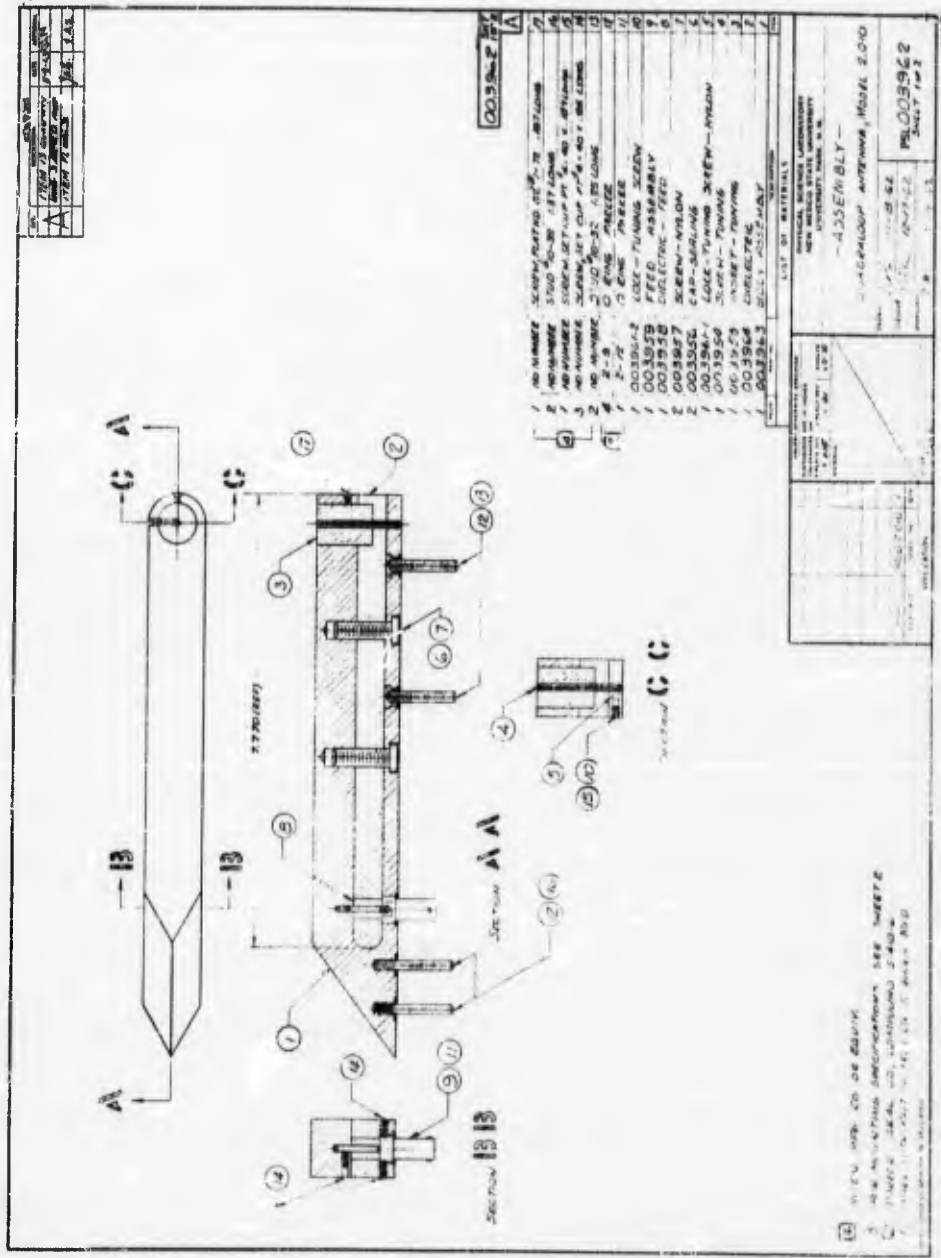


FIG. 16 - MODEL 2,010 TELEMETRY QUADRATURE LOOP ANTENNA

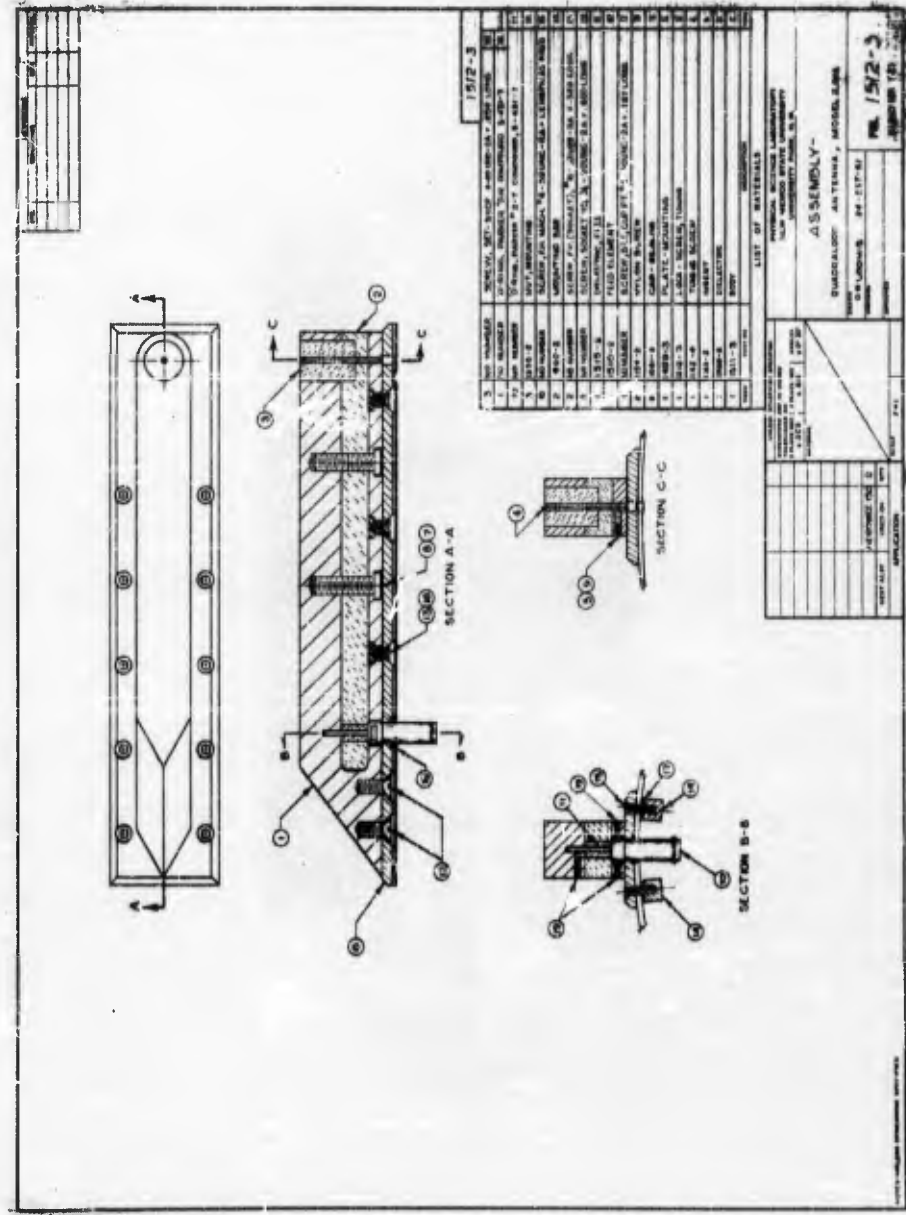


FIG. 17 - MODEL 2.018 TELEMETRY QUADRALOOP ANTENNA

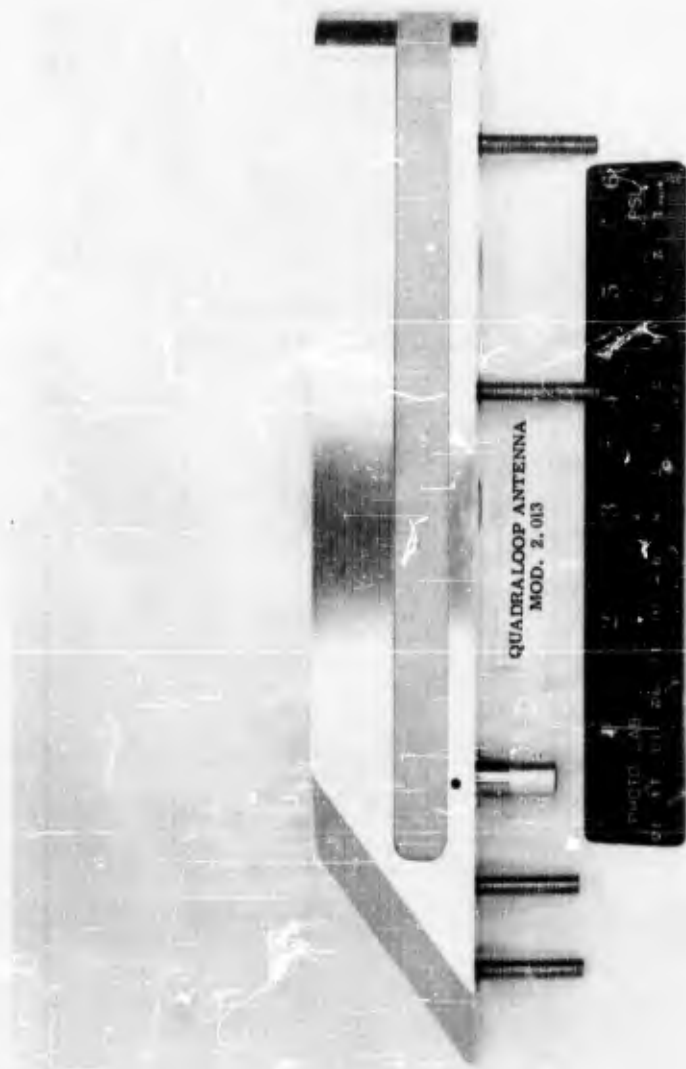


FIG. 18 - PHOTOGRAPH OF MODEL 2.013 TELEMETRY
QUADRALOOP ANTENNA

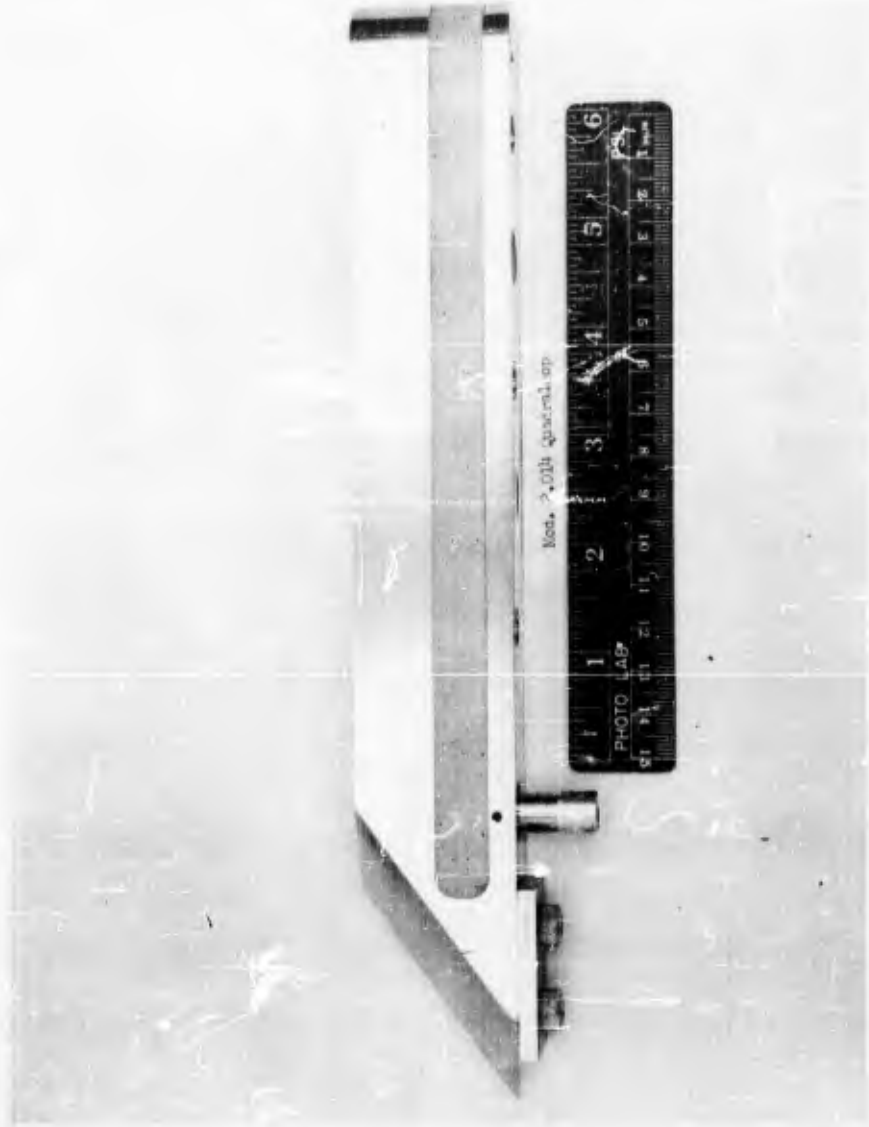


FIG. 20 - PHOTOGRAPH OF MODEL 2.014 TELEMETRY
QUADRALOOP ANTENNA

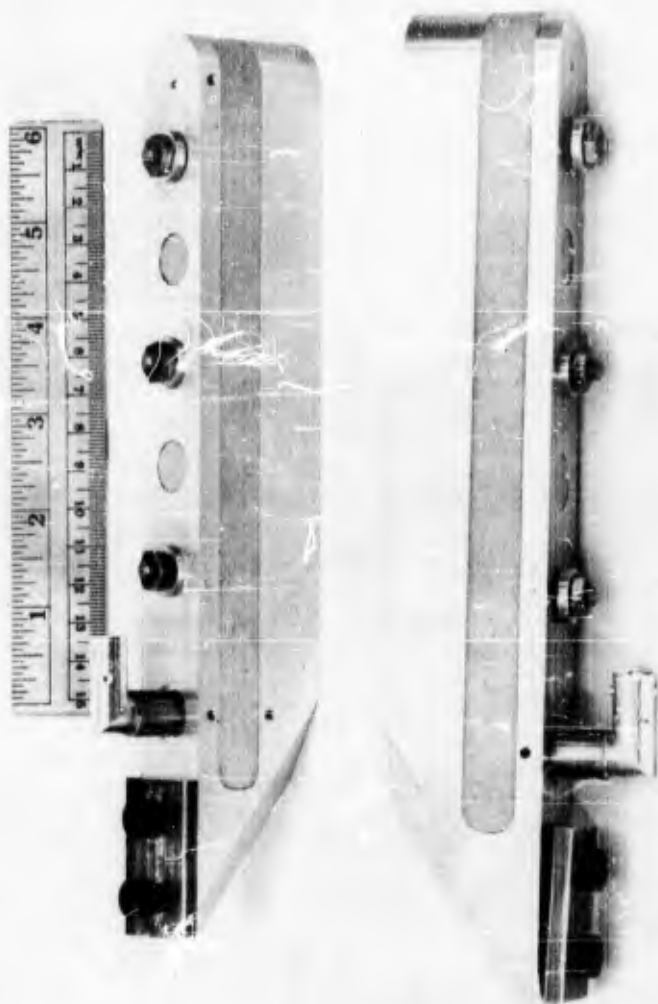


FIG. 22 - PHOTOGRAPH OF MODEL 2.008 TELEMETRY
QUADRALOOP ANTENNA

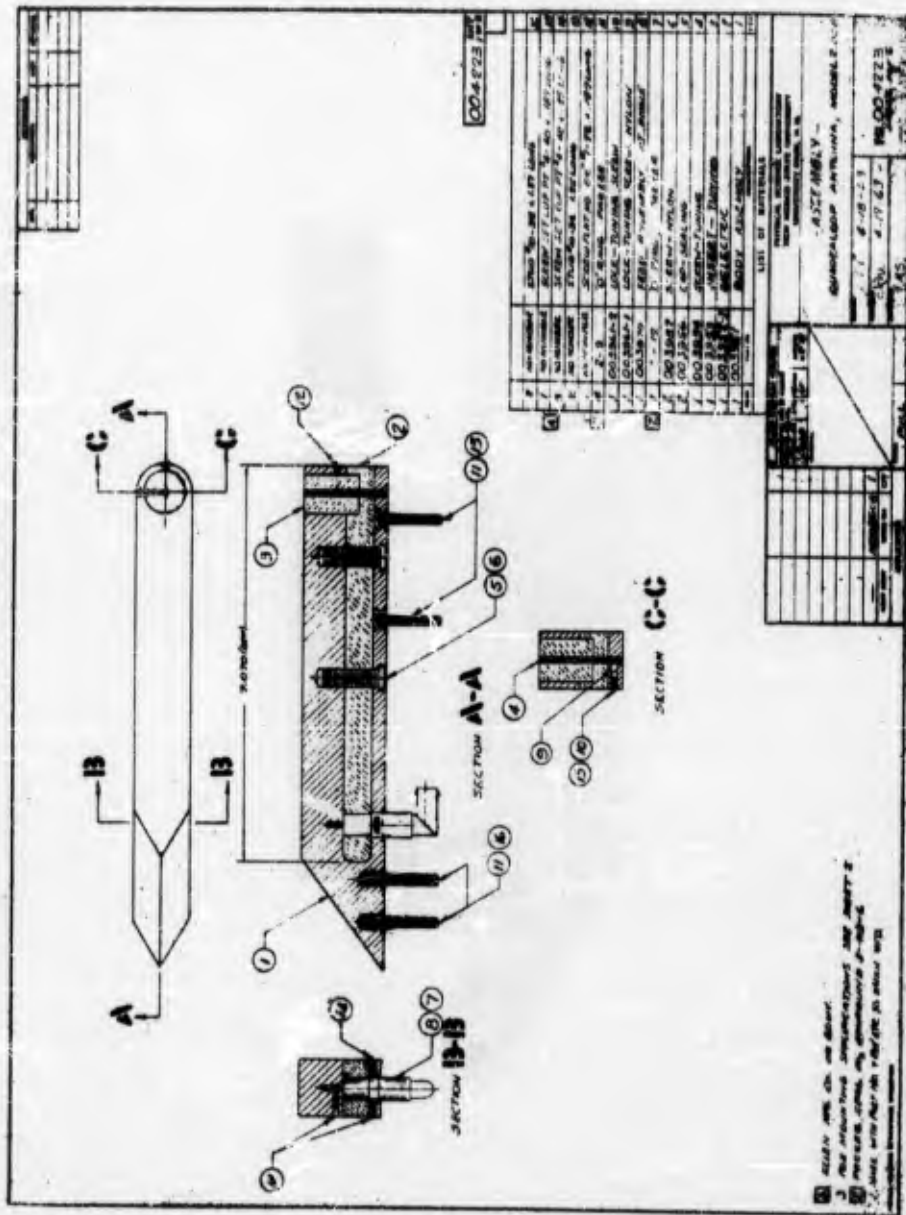


FIG. 23 - MODEL 2.008 TELEMETRY QUADRALOOP ANTENNA

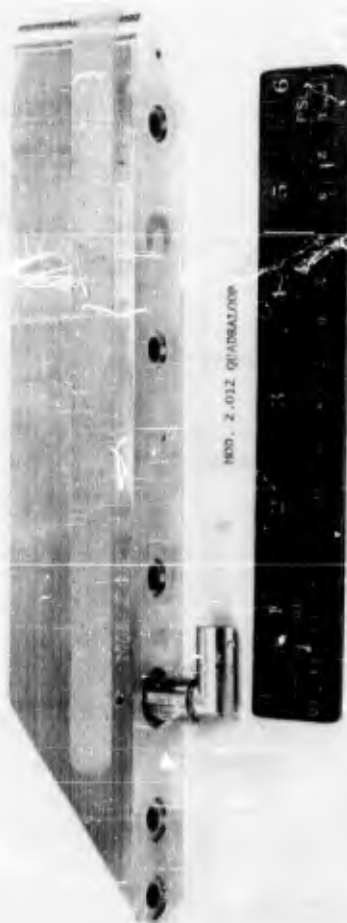


FIG. 24 - PHOTOGRAPH OF MODEL 2.012 TELEMETRY
QUADRALOOP ANTENNA

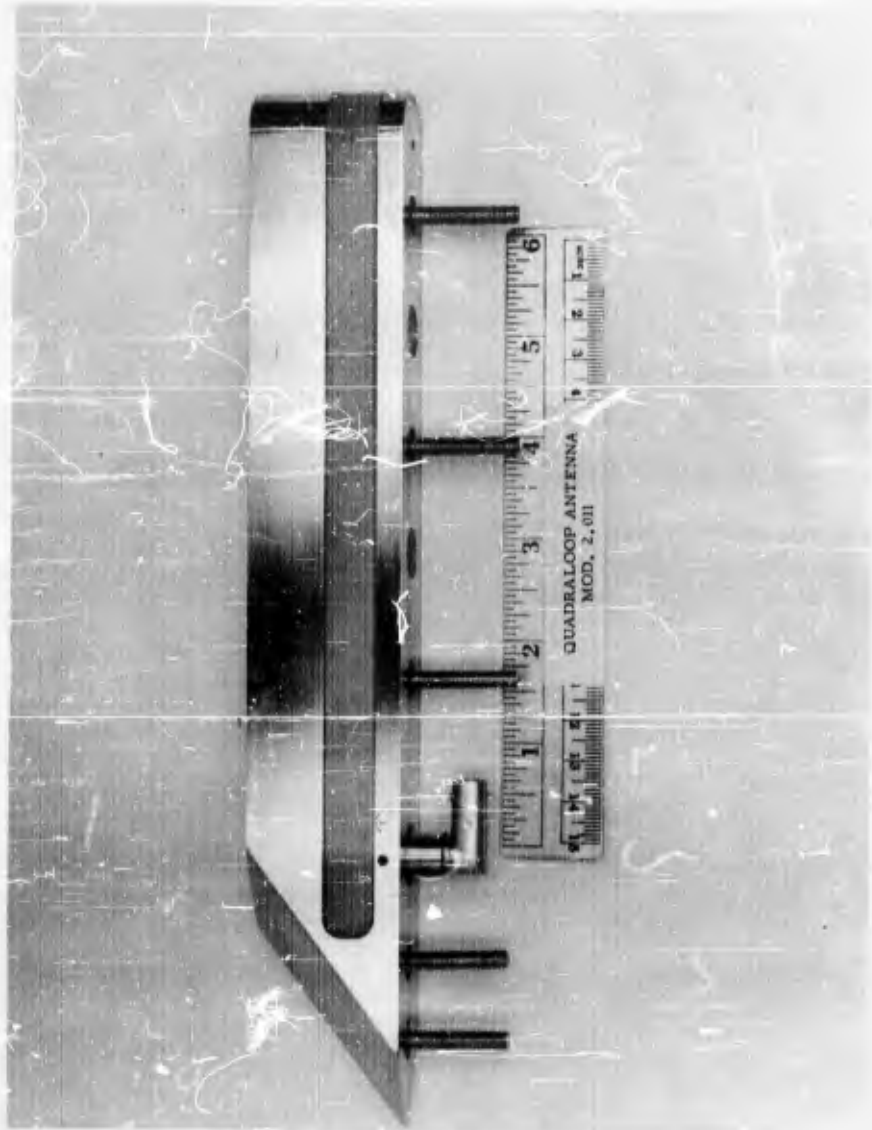


FIG. 26 - PHOTOGRAPH OF MODEL 2.011 TELEMETRY
QUADRALOOP ANTENNA

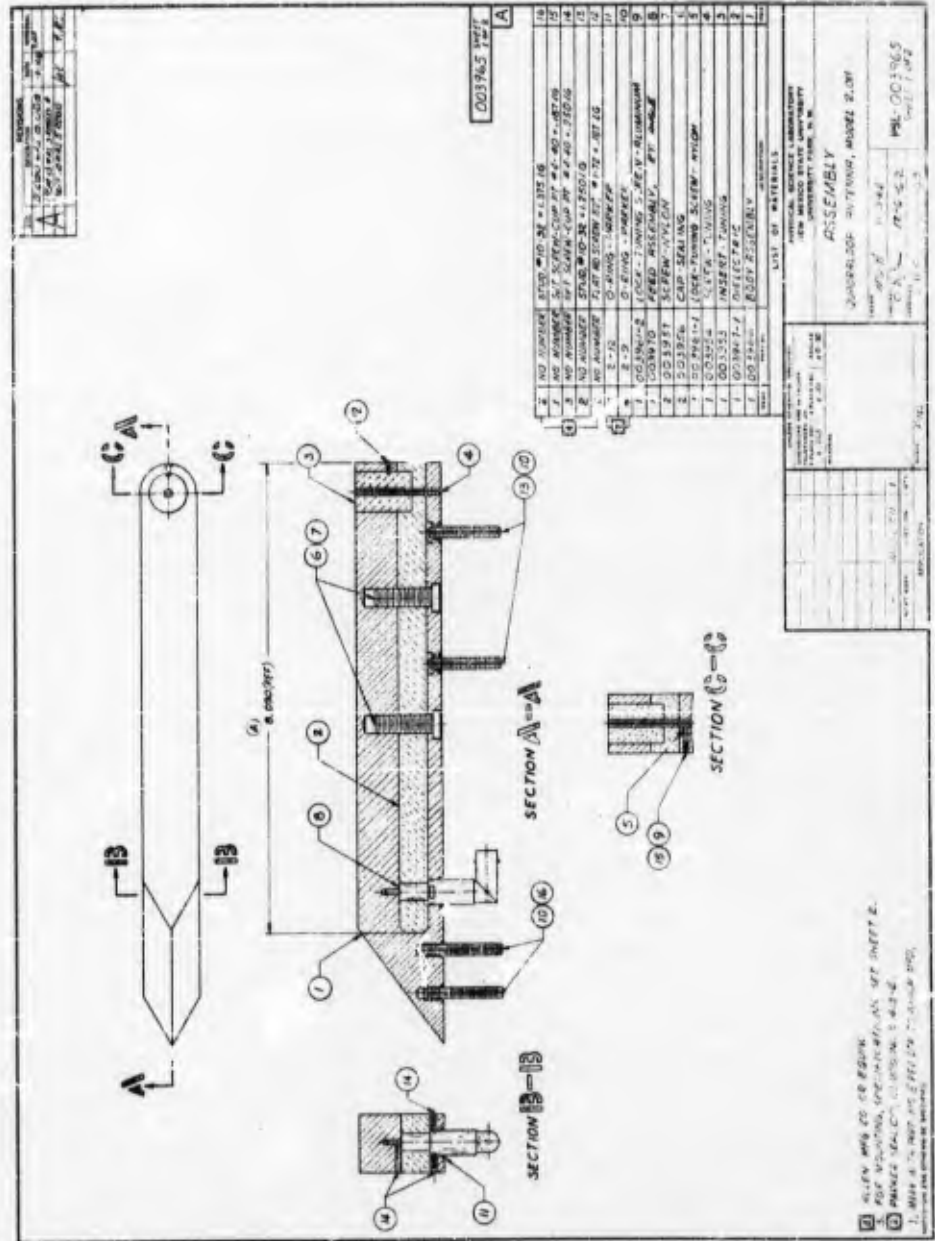


FIG. 27 - MODEL 2.011 TELEMETRY QUADRALOOP ANTENNA



FIG. 28 - PHOTOGRAPH OF MODEL A-2 TELEMETRY
QUADRALOOP ANTENNA

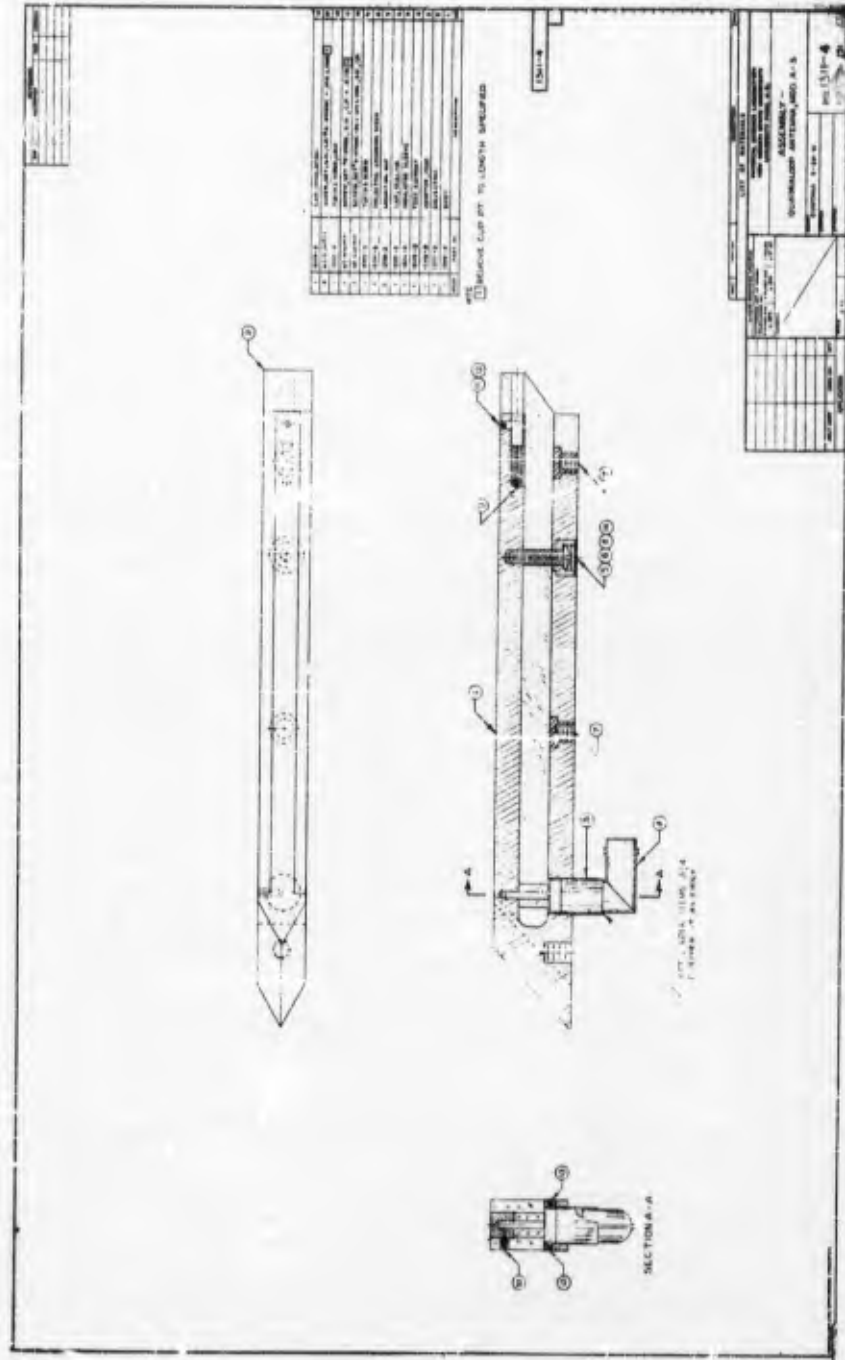


FIG. 29 - MODEL A-3 TELEMETRY QUADRA LOOP ANTENNA



FIG. 30 - PHOTOGRAPH OF MODEL 2.001 TELEMETRY
QUADRALOOP ANTENNA

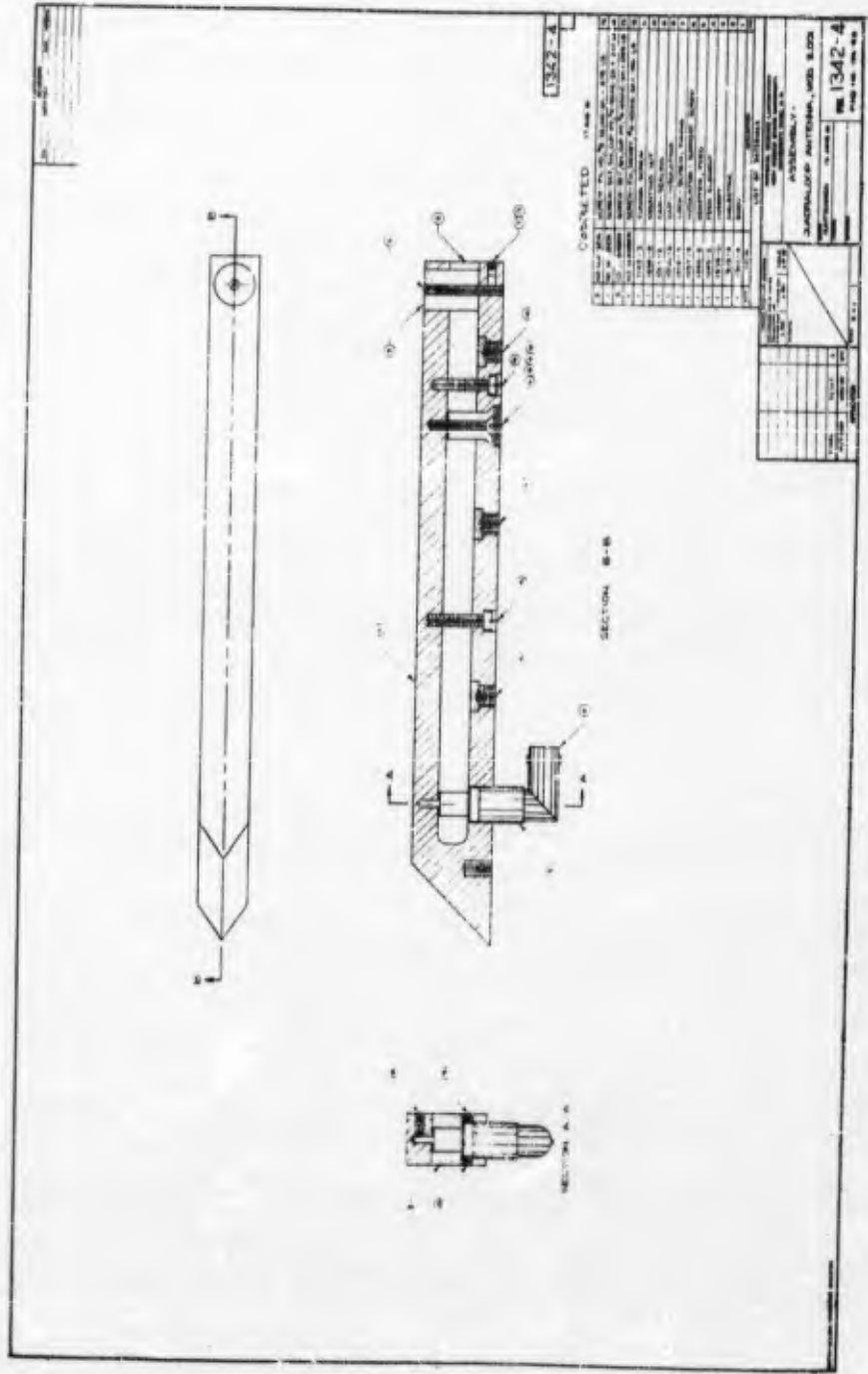


FIG. 31 - MODEL 2.001 TELEMETRY QUADRALOOP ANTENNA

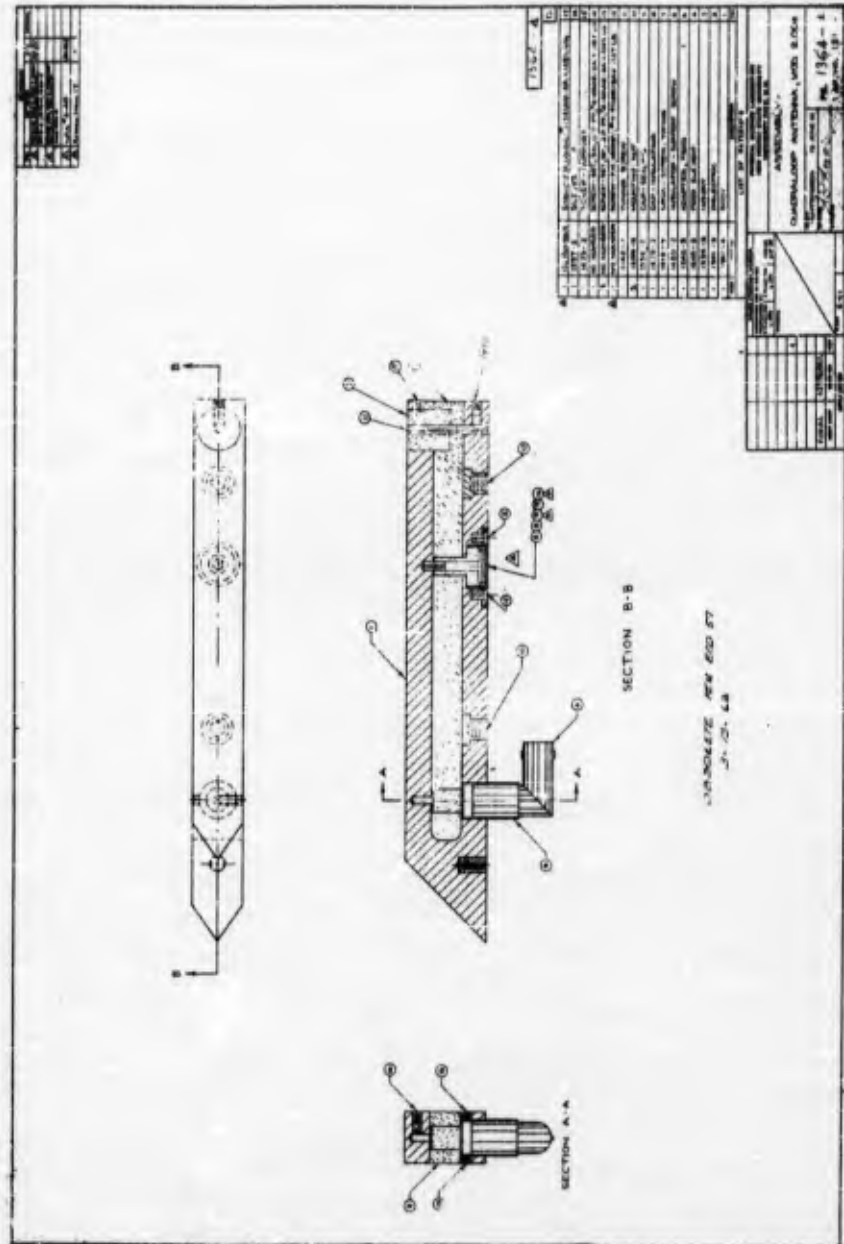


FIG. 32 - MODEL 2.004 TELEMETRY QUADRALOOP ANTENNA

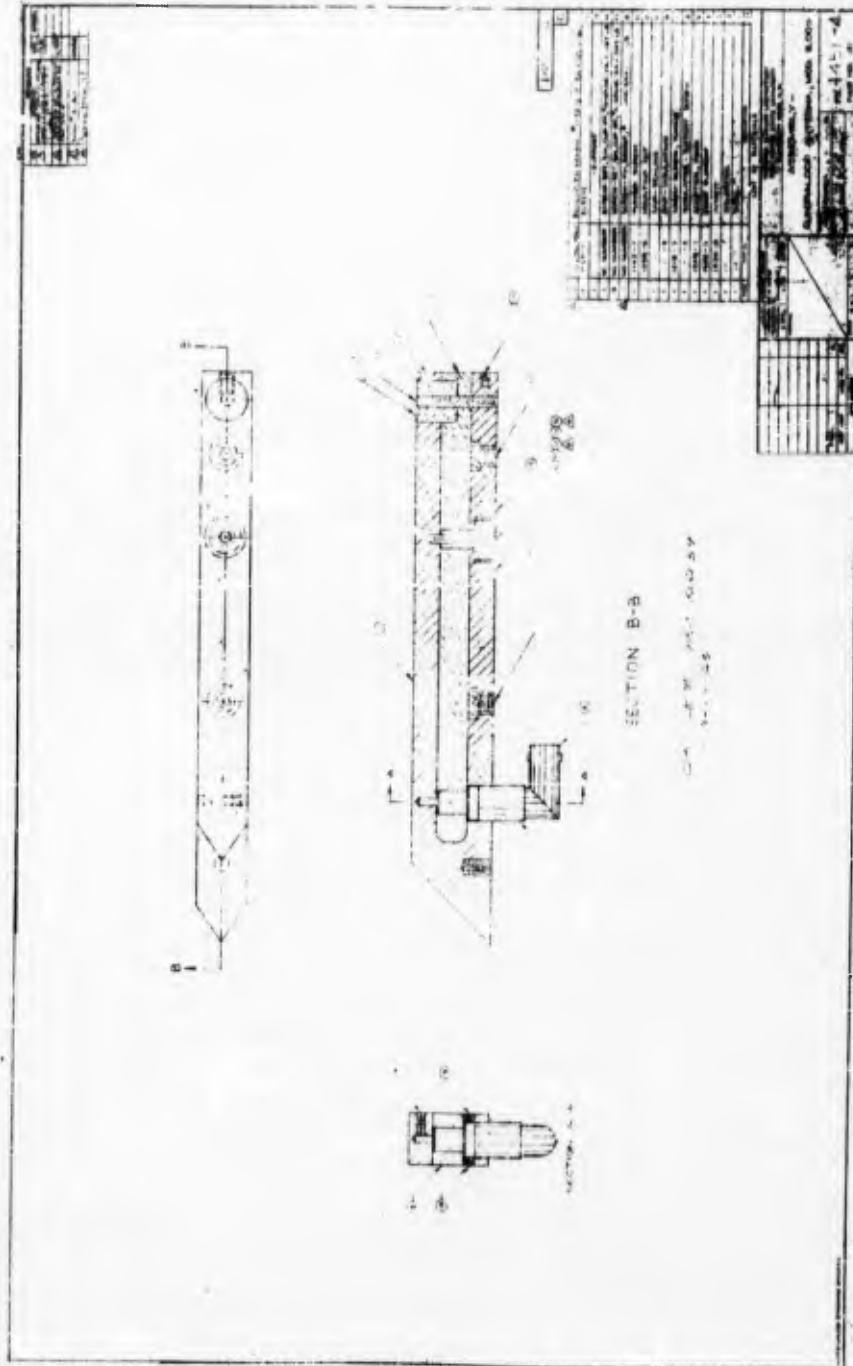


FIG. 33 - MODEL 2.009 TELEMETRY QUADRALOOP ANTENNA

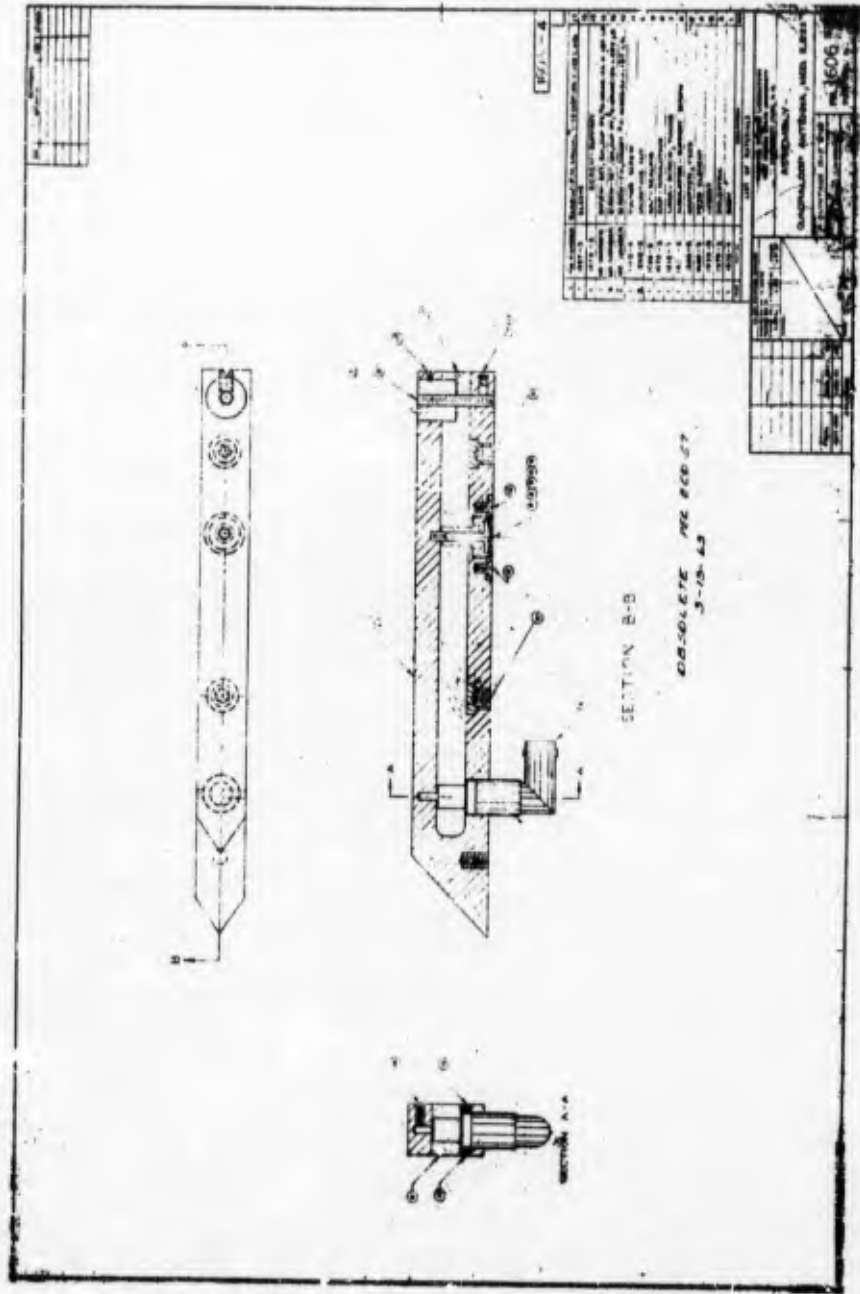


FIG. 34 - MODEL 2.023 TELEMETRY QUADRALOOP ANTENNA

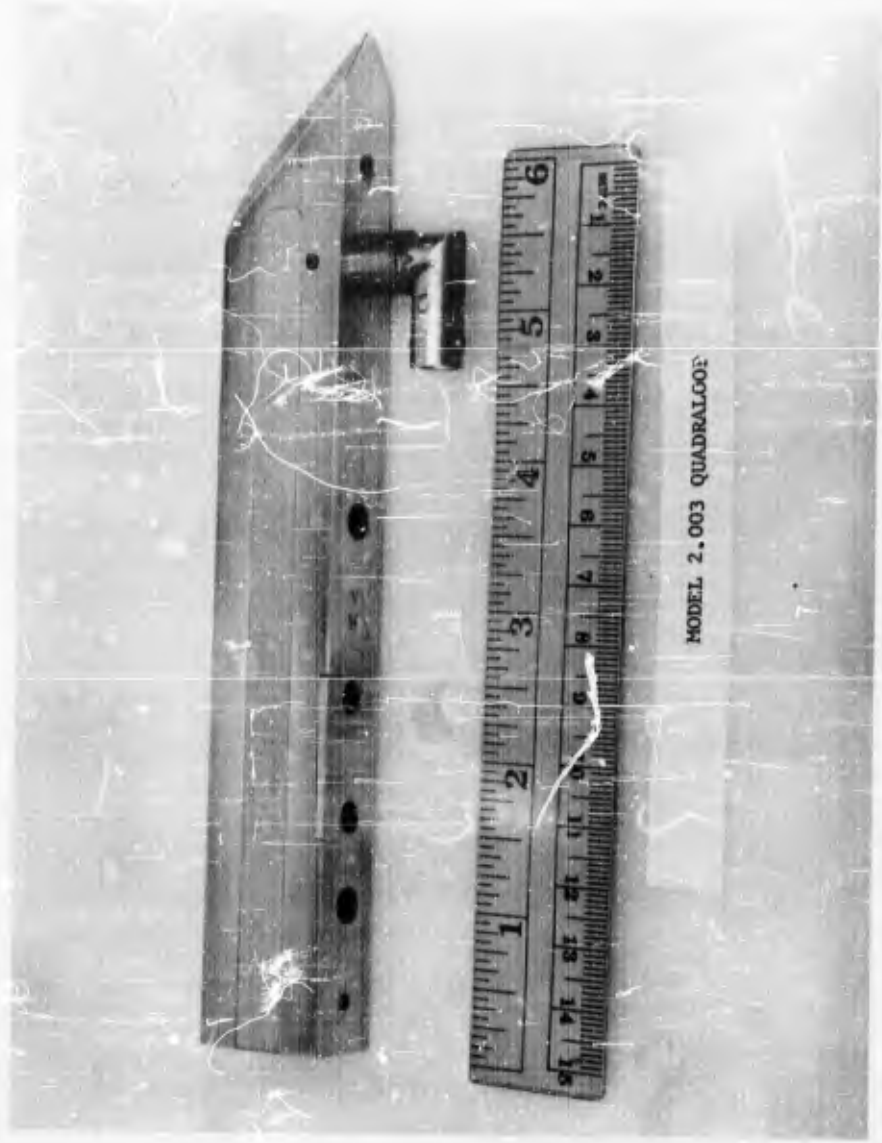


FIG. 35 - PHOTOGRAPH OF MODEL 2.003 TELEMETRY
QUADRALOOP ANTENNA

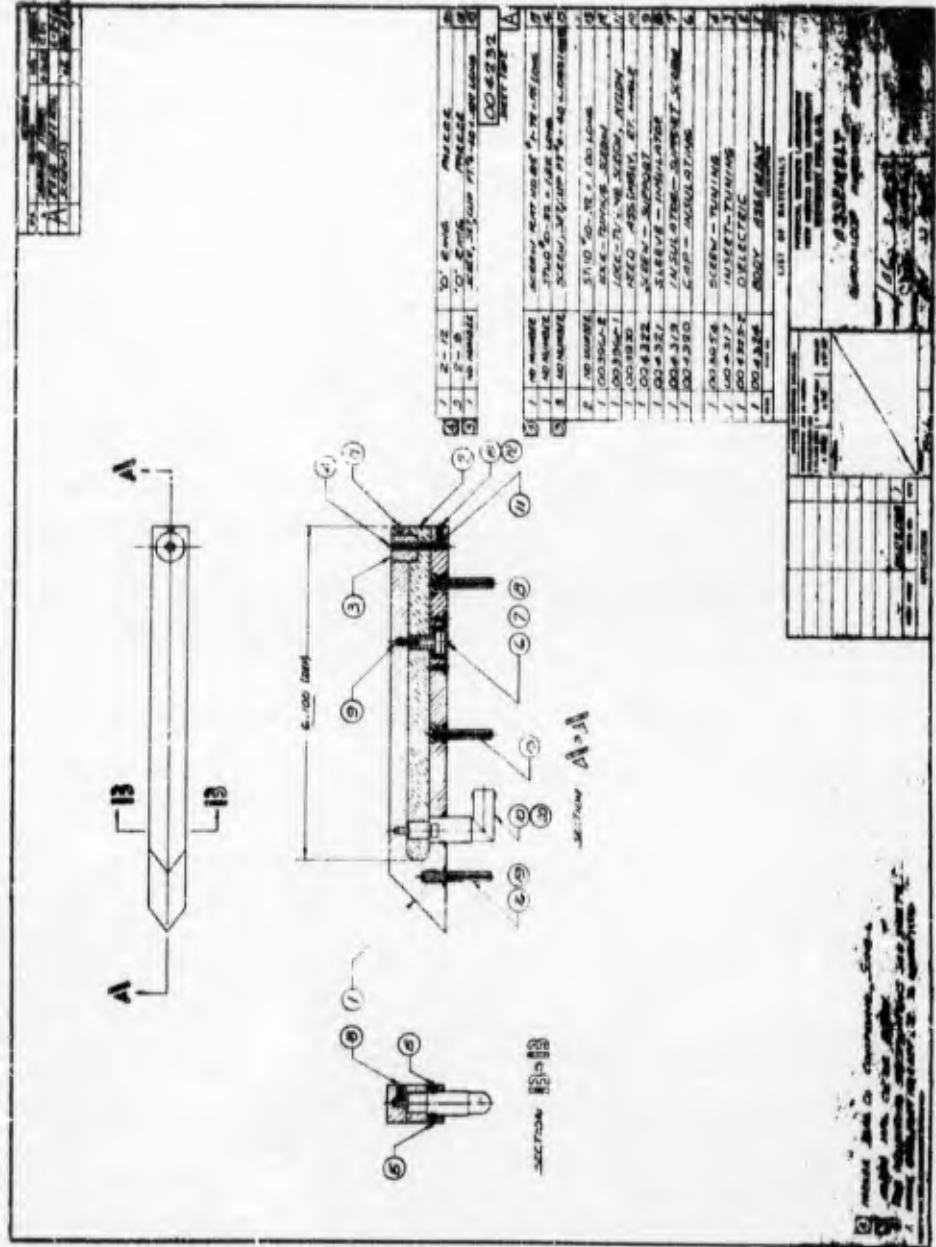


FIG. 36 - MODEL 2.003 TELEMETRY QUADRALOOP ANTENNA

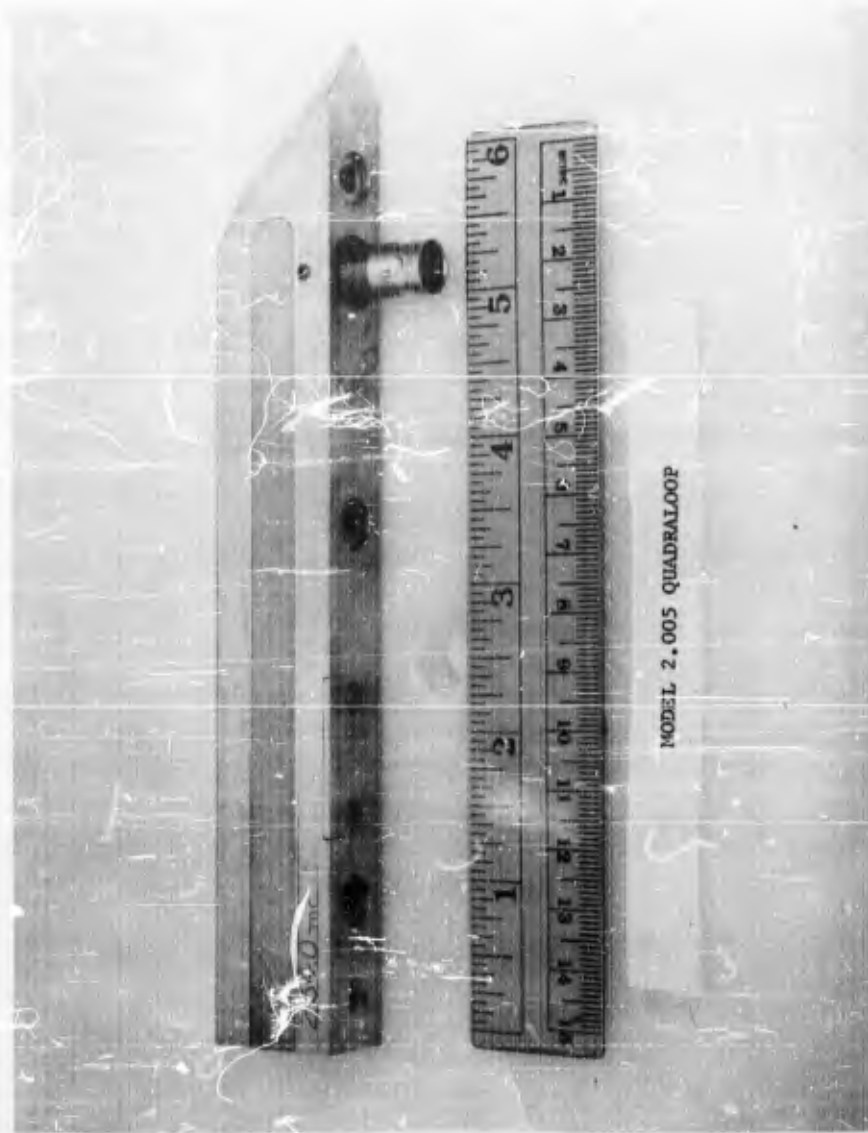


FIG. 37 - PHOTOGRAPH OF MODEL 2.005 TELEMETRY
QUADRALOOP ANTENNA

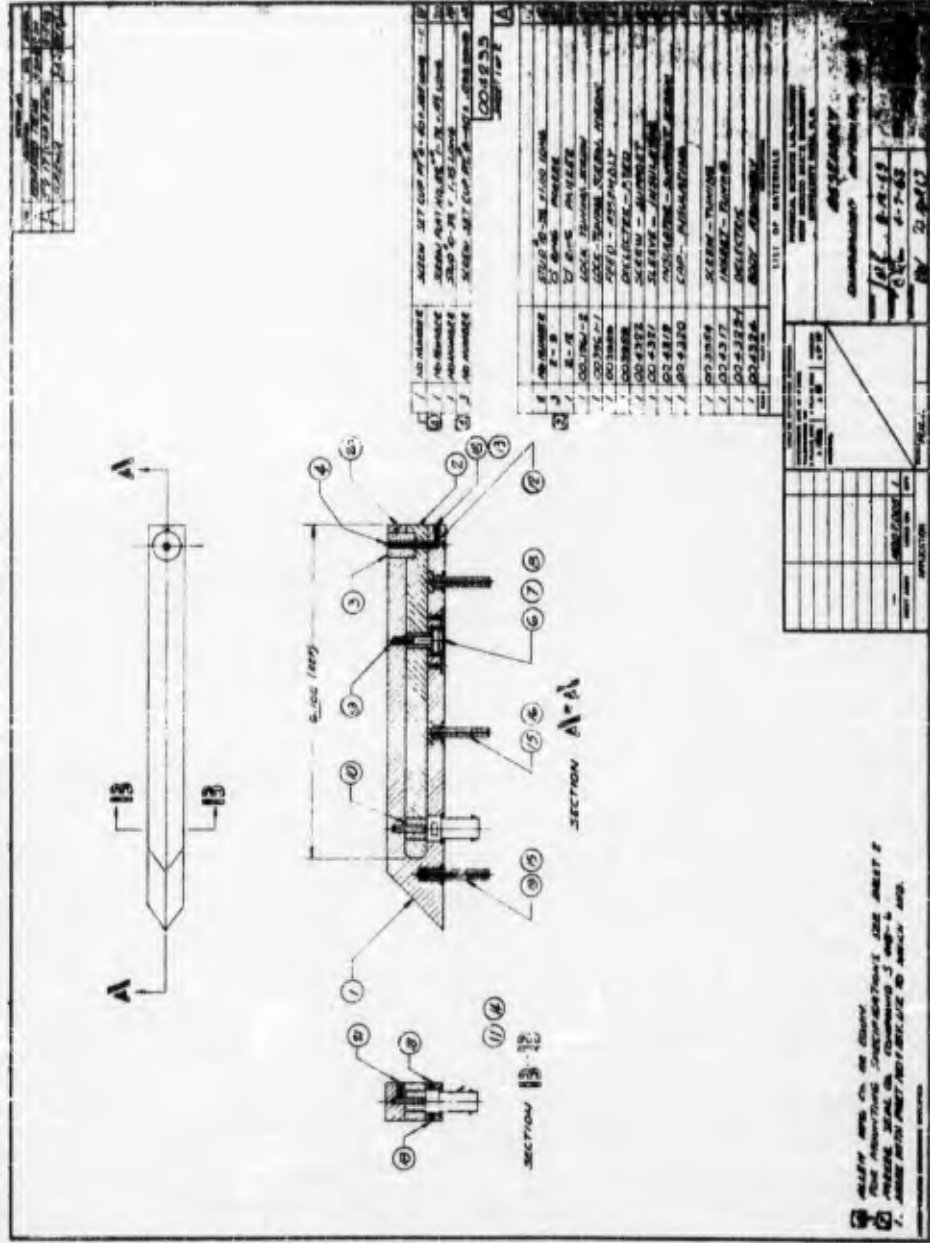


FIG. 38 - MODEL 2.005 TELEMETRY QUADRALOOP ANTENNA

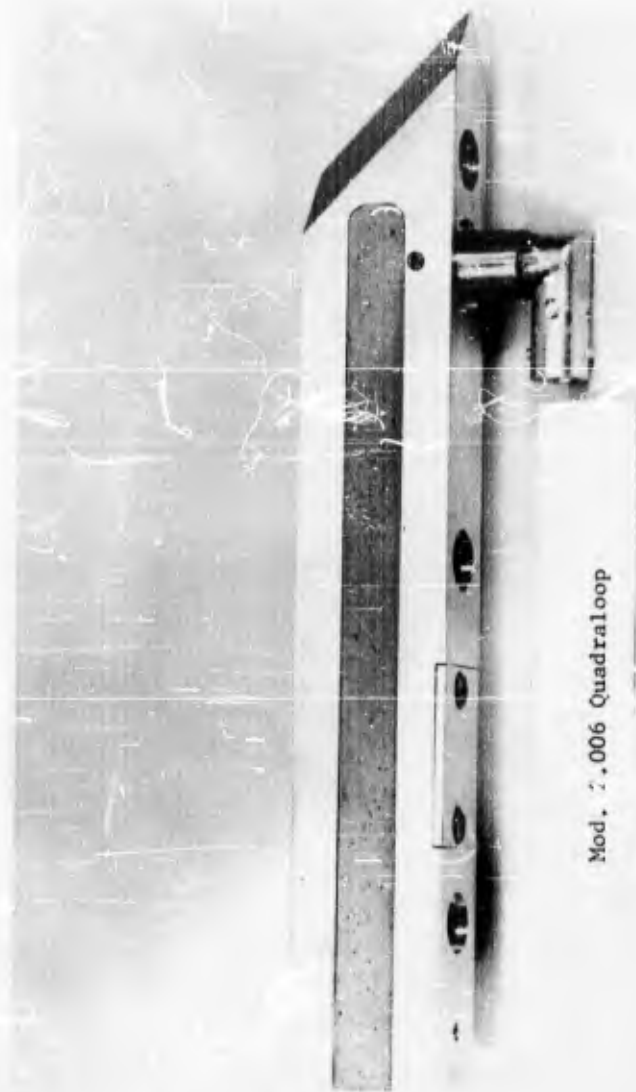


FIG. 39 - PHOTOGRAPH OF MODEL 2,006 TELEMETRY
QUADRALOOP ANTENNA

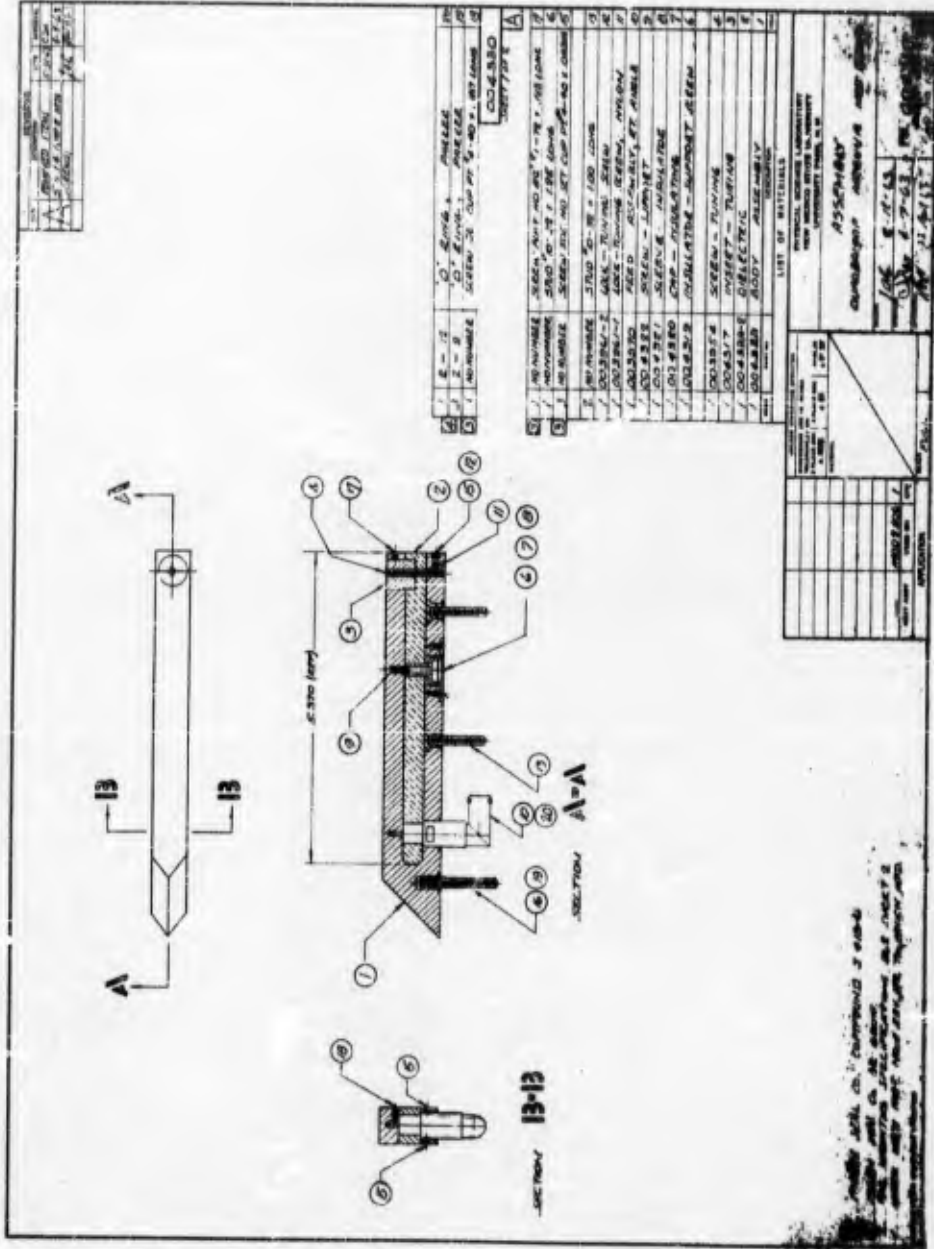


FIG. 40 - MODEL 2.006 TELEMETRY QUADRALOOP ANTENNA

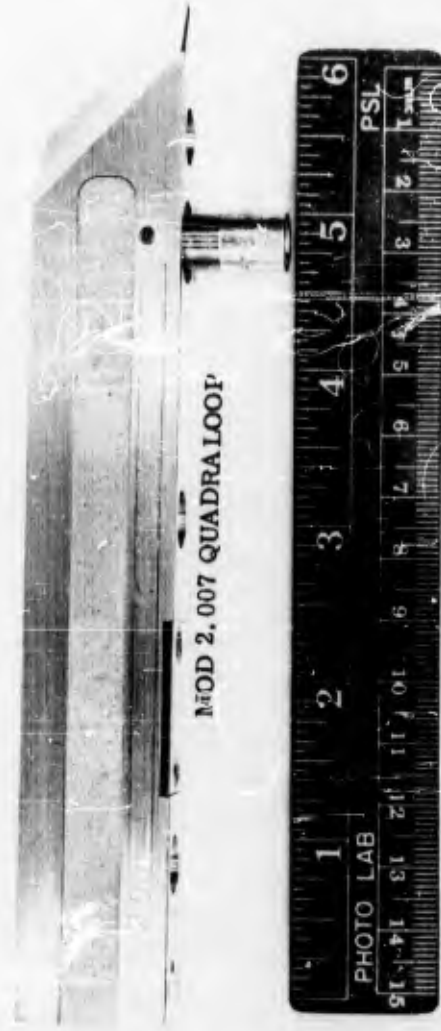


FIG. 41 - PHOTOGRAPH OF MODEL 2.007 TELEMETRY
QUADRALOOP ANTENNA

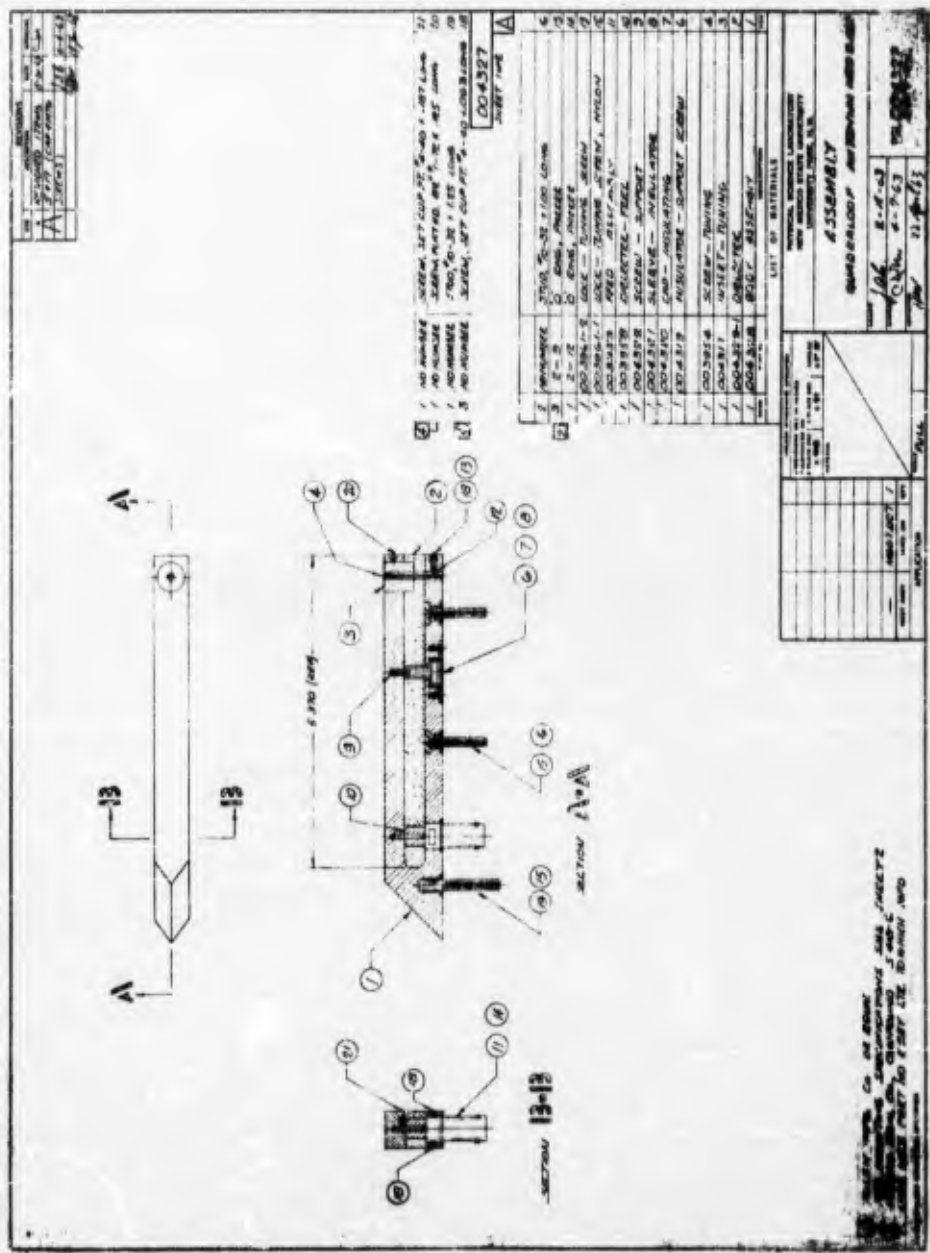




FIG. 43 - PHOTOGRAPH OF MODEL 2.025 TELEMETRY
QUADRALOOP ANTENNA

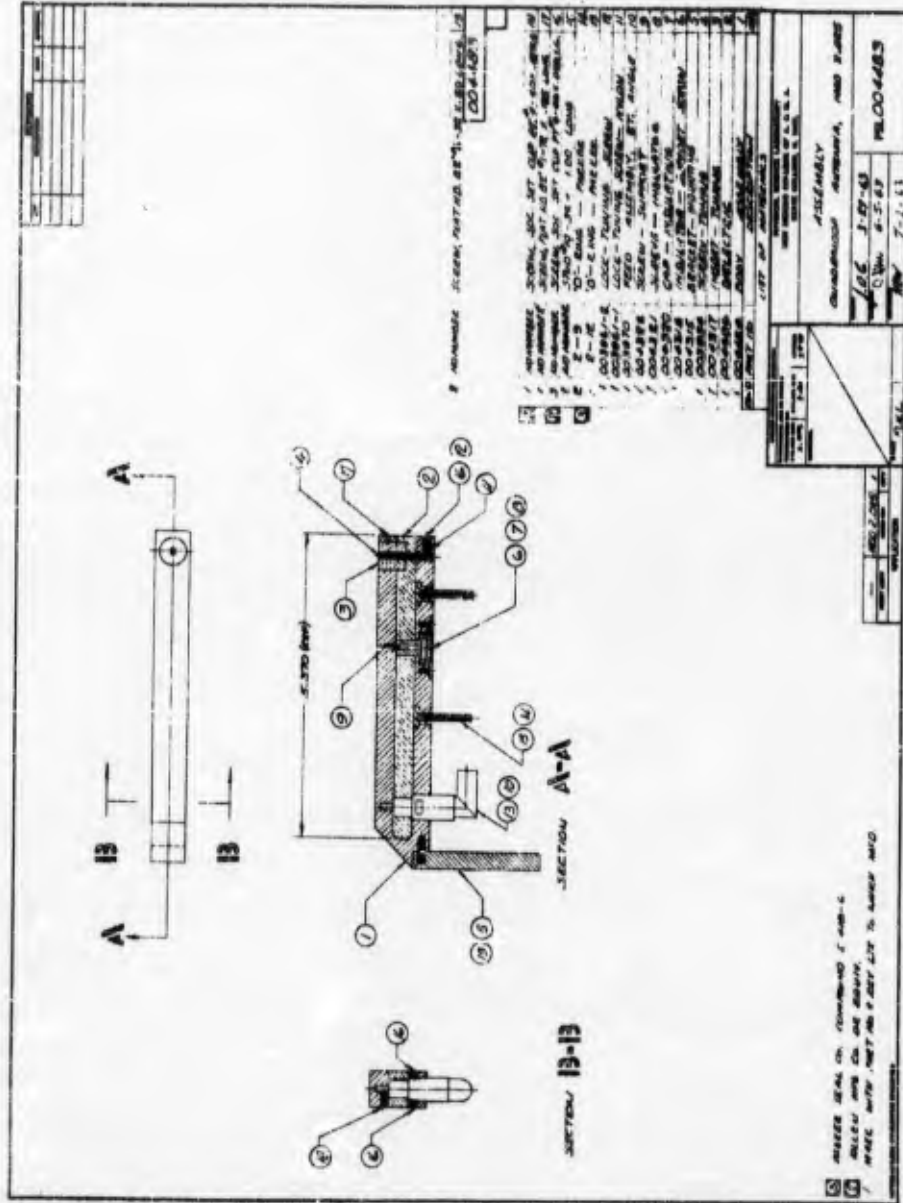


FIG. 44 - MODEL 2.025 TELEMETRY QUADRALOOP ANTENNA



FIG. 45 - PHOTOGRAPH OF MODEL 2.032 TELEMETRY
QUADRALOOP ANTENNA

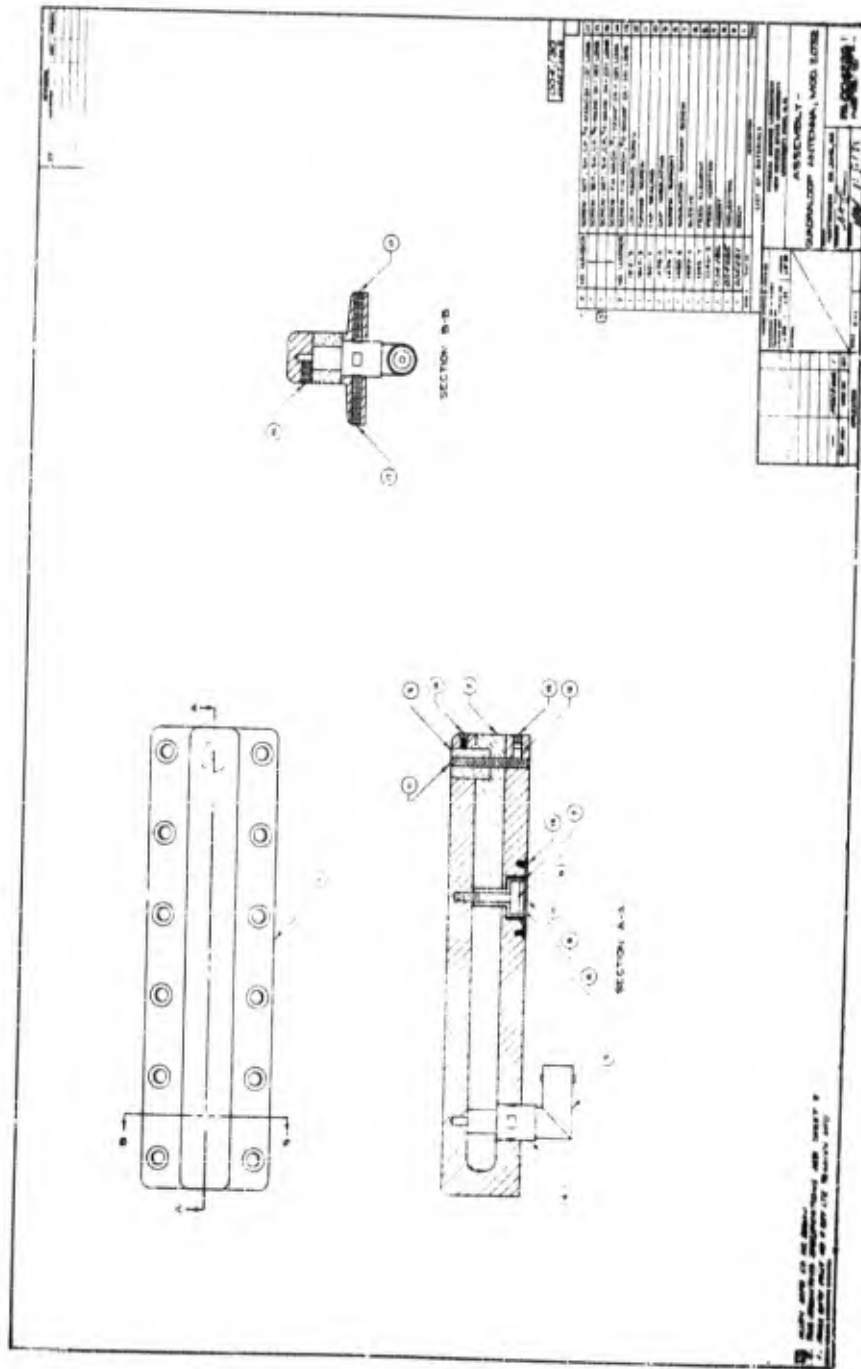


FIG. 46 - MODEL 2.032 TELEMETRY QUADRALOOP ANTENNA

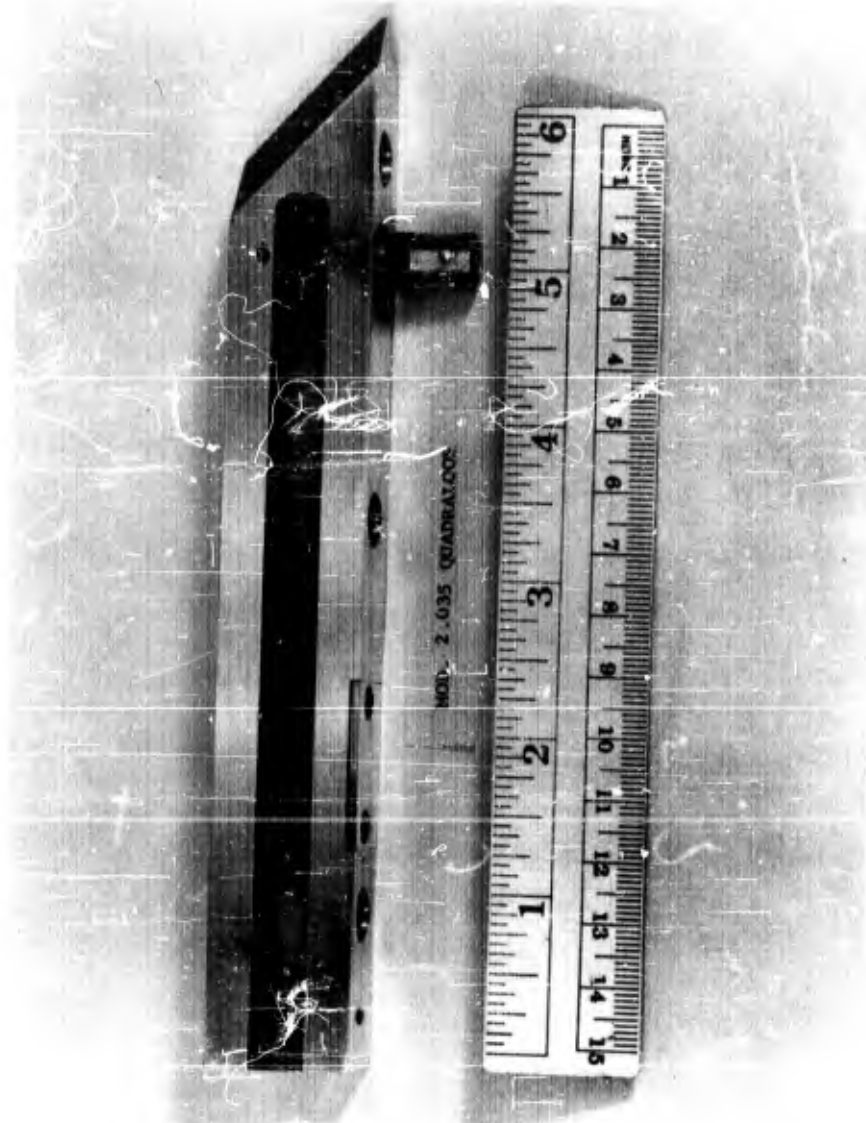


FIG. 47 - PHOTOGRAPH OF MODEL 2.035 TELEMETRY
QUADRALOOP ANTENNA



FIG. 48 - PHOTOGRAPH OF MODEL 2.036 TELEMETRY
QUADRALOOP ANTENNA

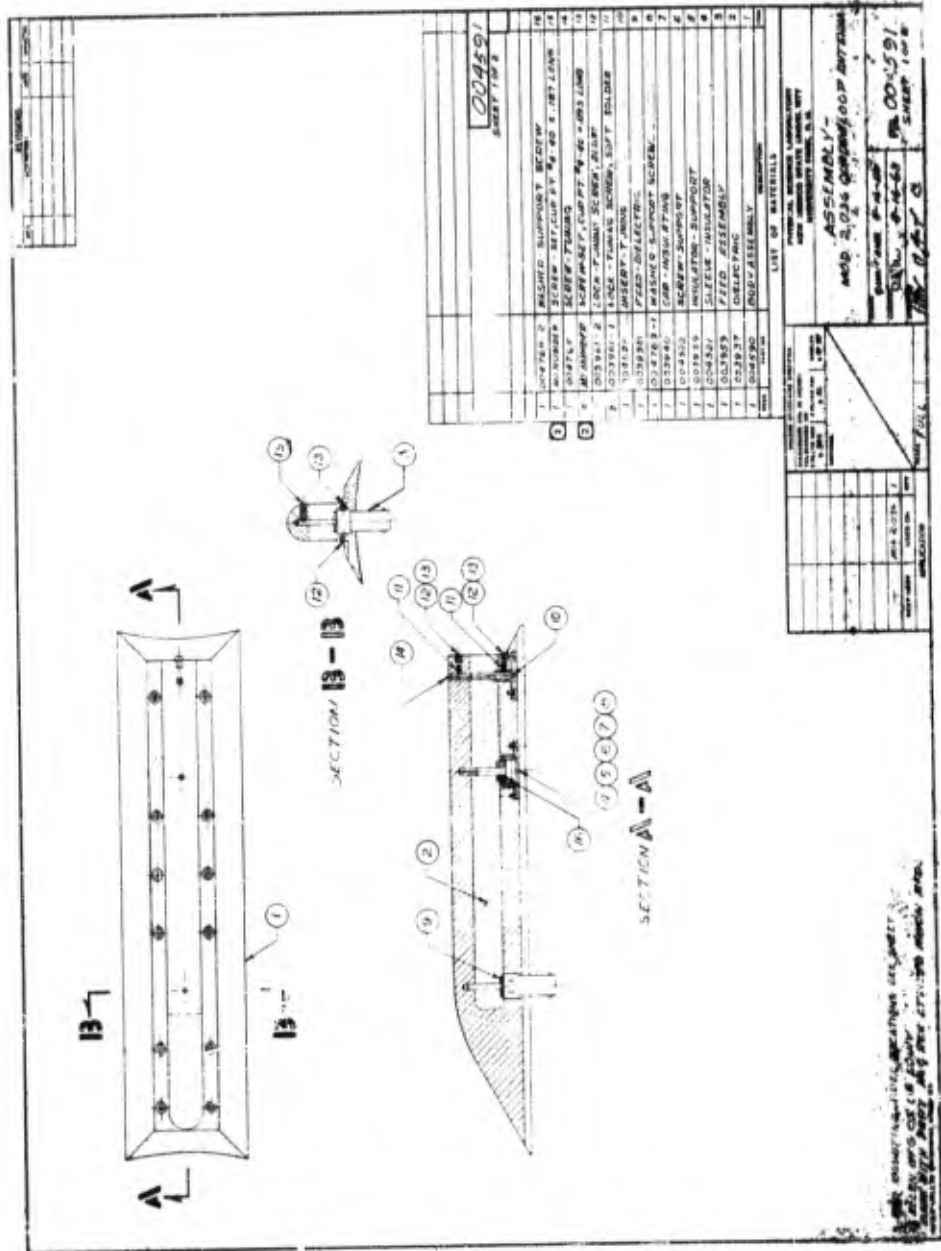


FIG. 49 - MODEL 2 036 TELEMETRY QUADRALOOP ANTENNA

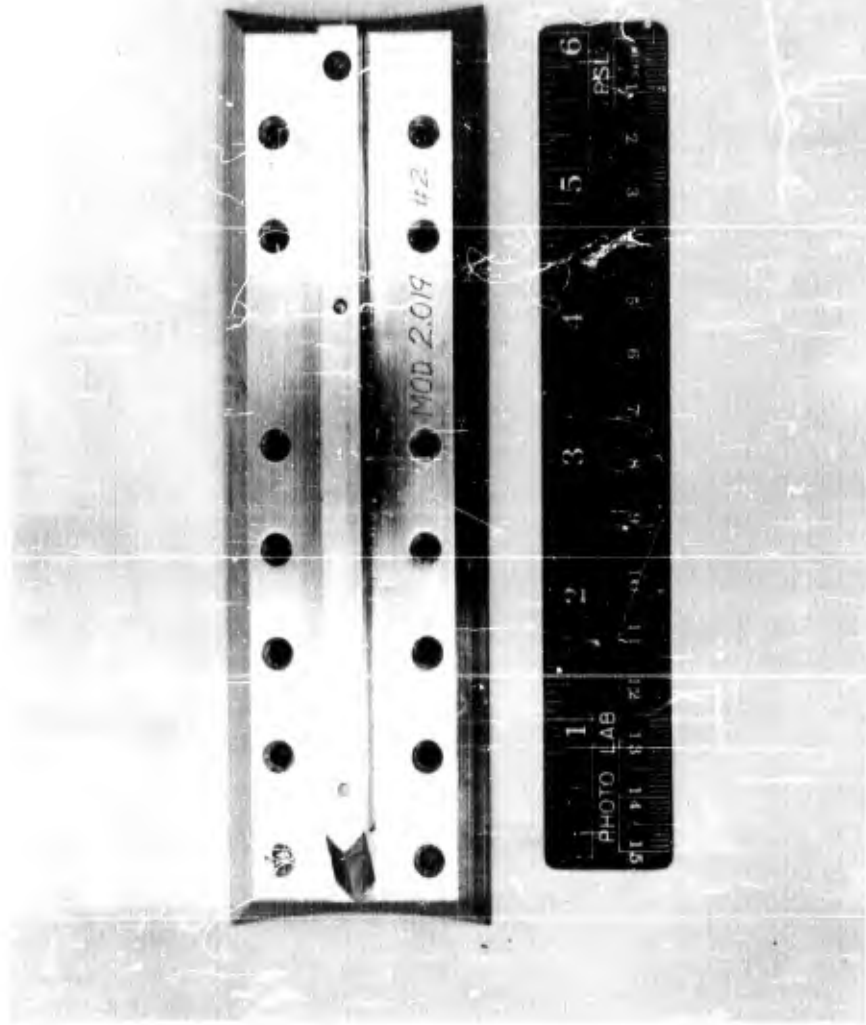


FIG. 50 - PHOTOGRAPH OF MODEL 2.019 TELEMETRY
QUADRALOOP ANTENNA

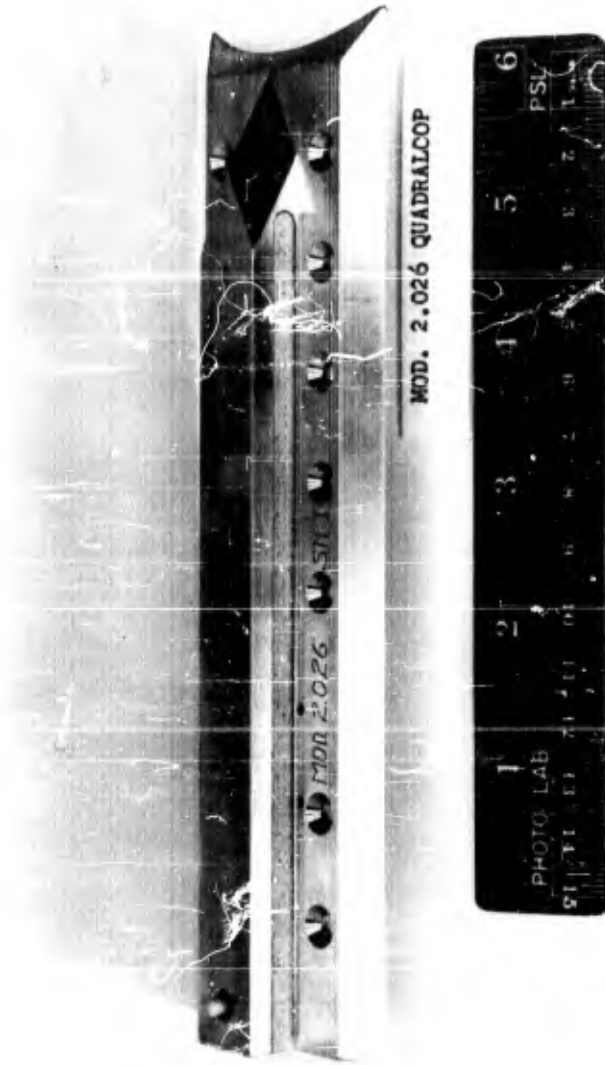


FIG. 52 - PHOTOGRAPH OF MODEL 2.026 TELEMETRY
QUADRALOOP ANTENNA

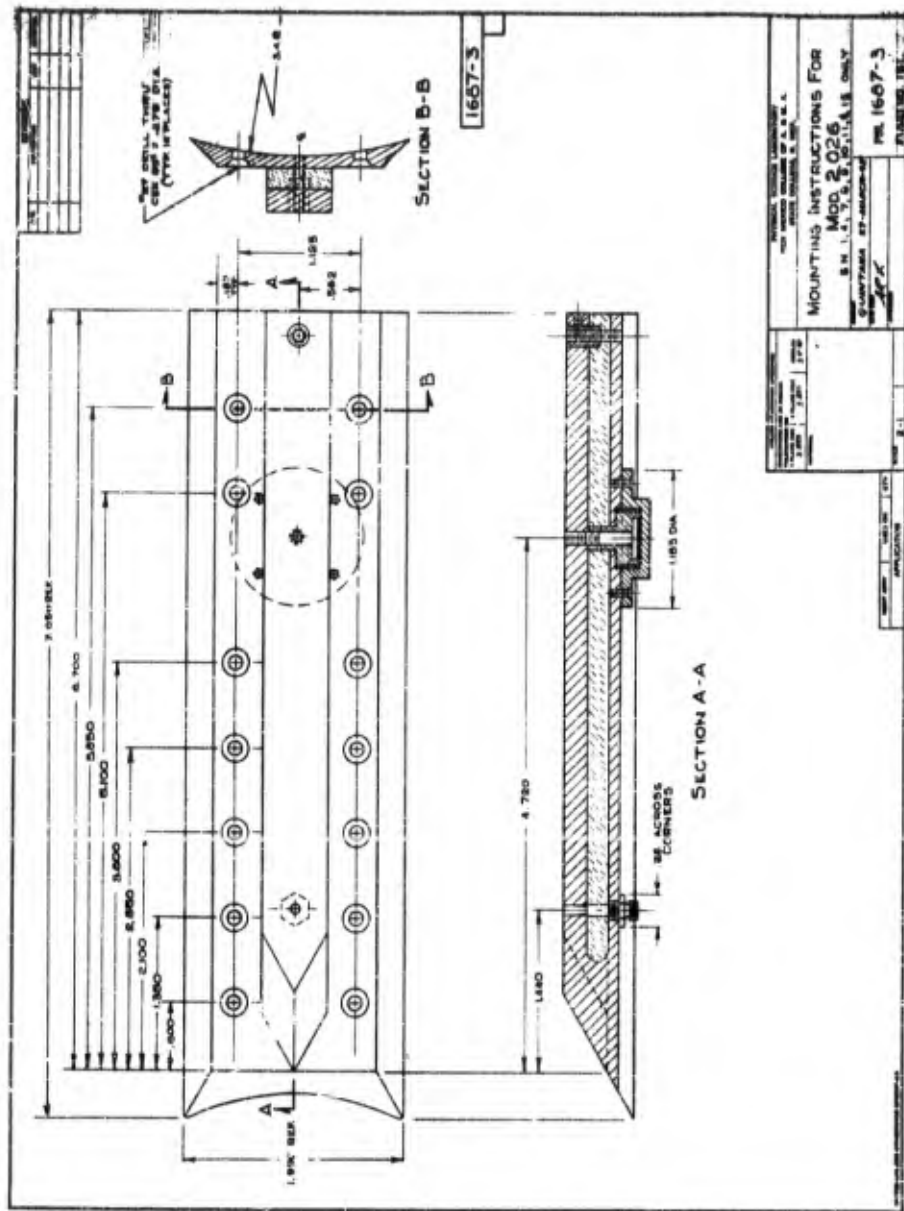


FIG. 53 - MODEL 2.026 TELEMETRY QUADRALOOP ANTENNA

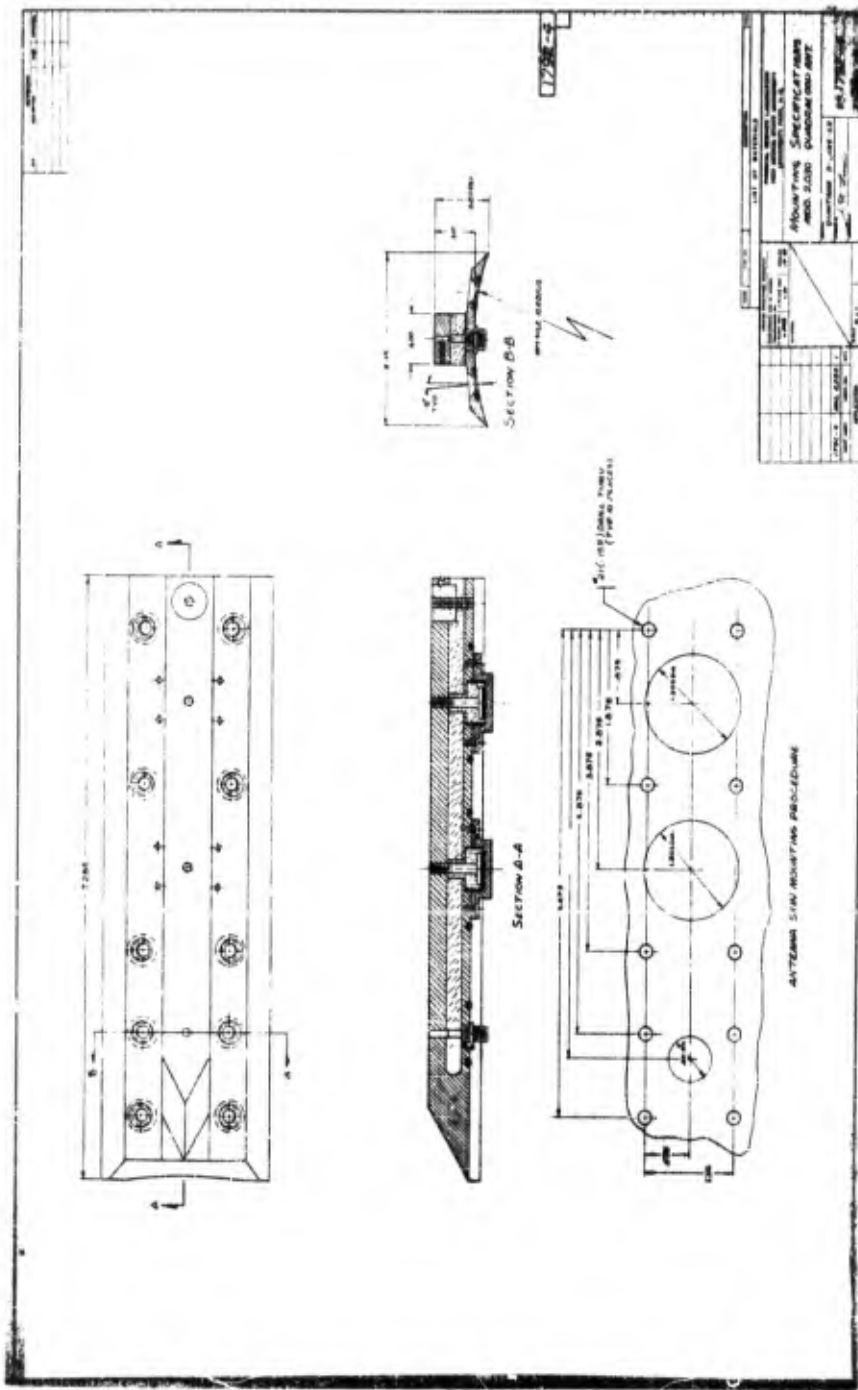


FIG. 54 - MODEL 2.030 TELEMETRY QUADRALOOP ANTENNA



FIG. 55 - PHOTOGRAPH OF MODEL 2.031 TELEMETRY QUADRALOOP ANTENNA

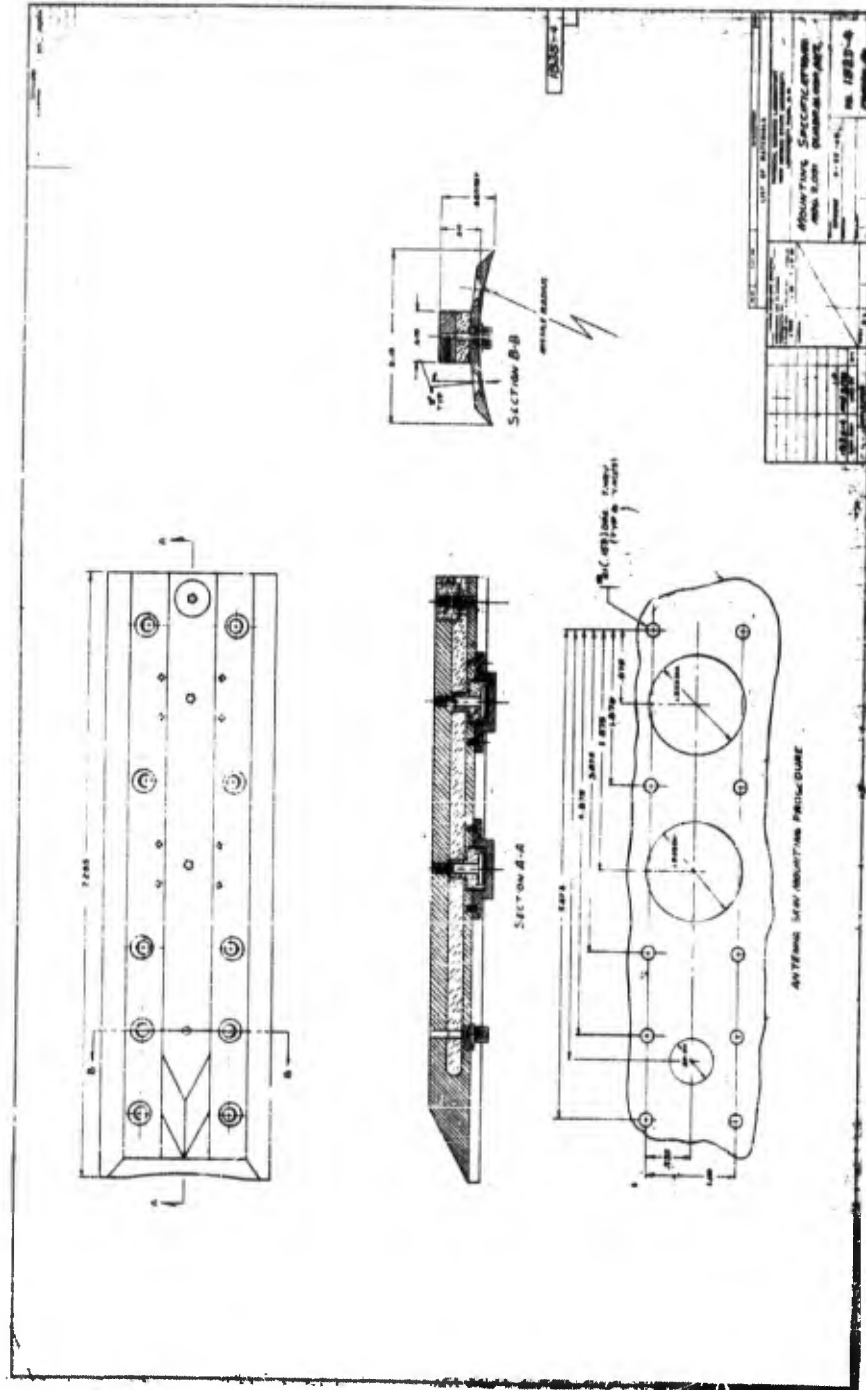


FIG. 56 - MODEL 2.031 TELEMETRY QUADRALOOP ANTENNA



FIG. 57 - PHOTOGRAPH OF MODEL III-B TELEMETRY
QUADRALOOP ANTENNA



FIG. 60 - PHOTOGRAPH OF MODEL III-C TELEMETRY
QUADRALOOP ANTENNA

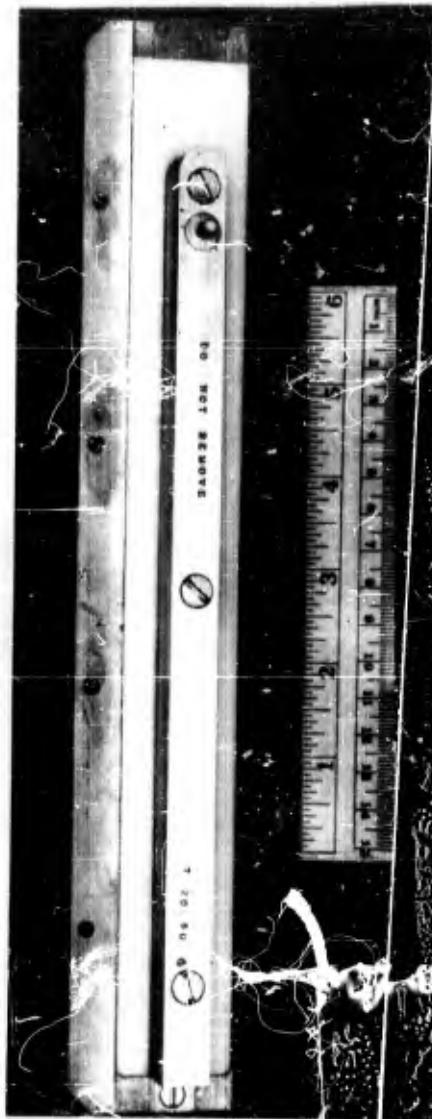


FIG. 62 - PHOTOGRAPH OF MODEL III-D TELEMETRY
QUADRANGLE ANTENNA

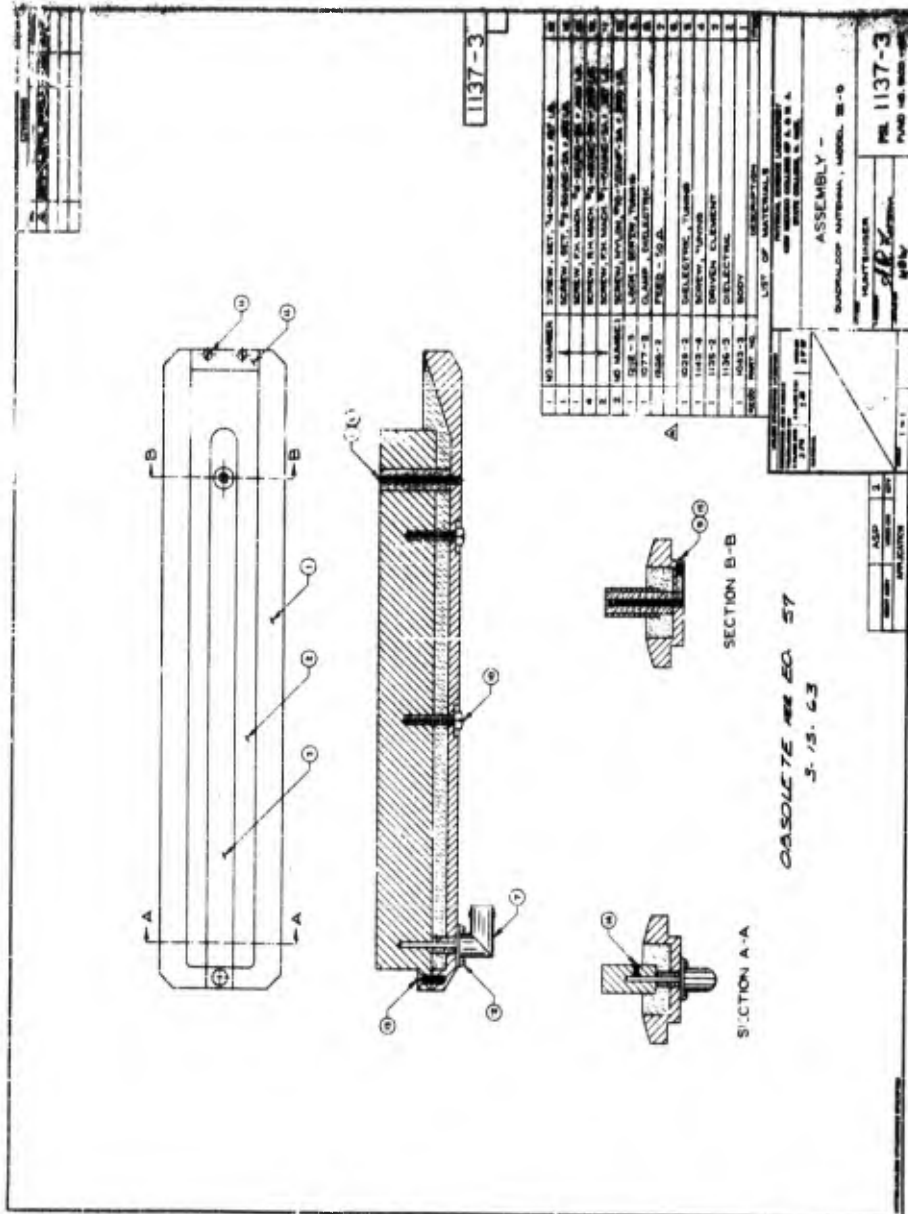


FIG. 63 - MODEL III-D TELEMETRY QUADRALOOP ANTENNA

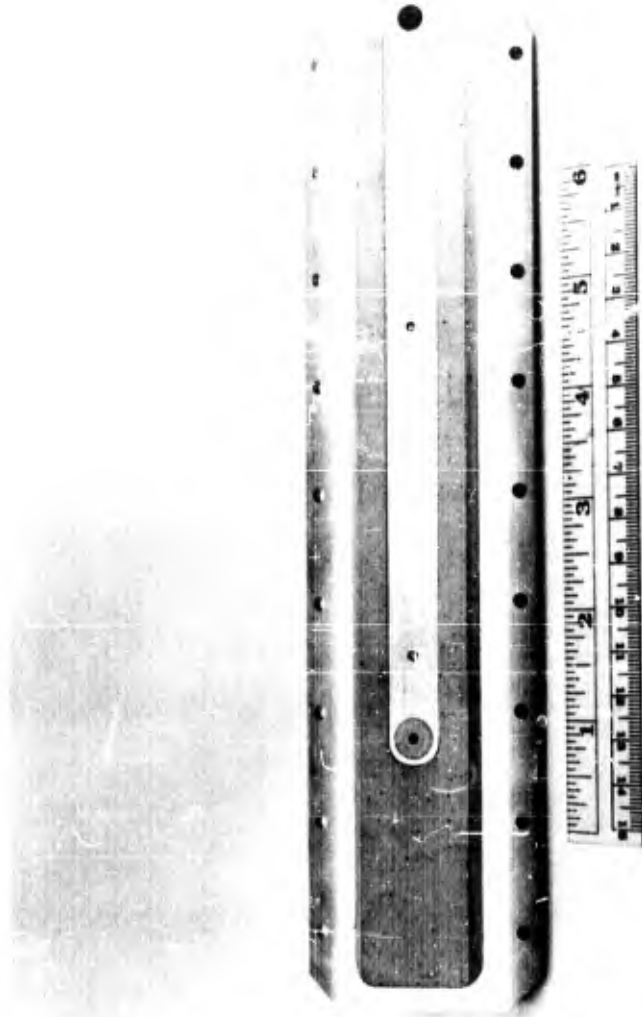


FIG. 64 - PHOTOGRAPH OF MODEL III-F TELEMETRY
QUADRALOOP ANTENNA

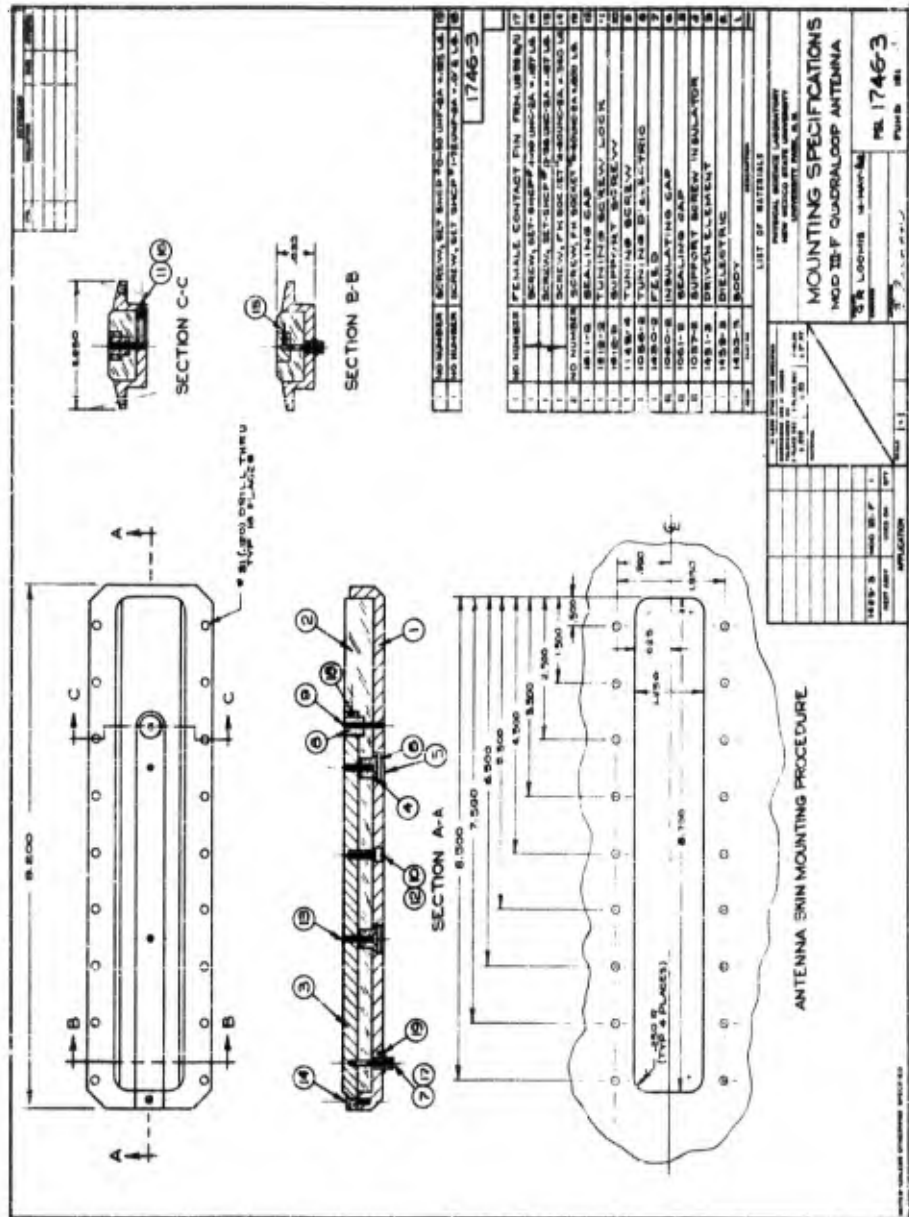


FIG. 65 - MODEL III-F TELEMETRY QUADRALOOP ANTENNA

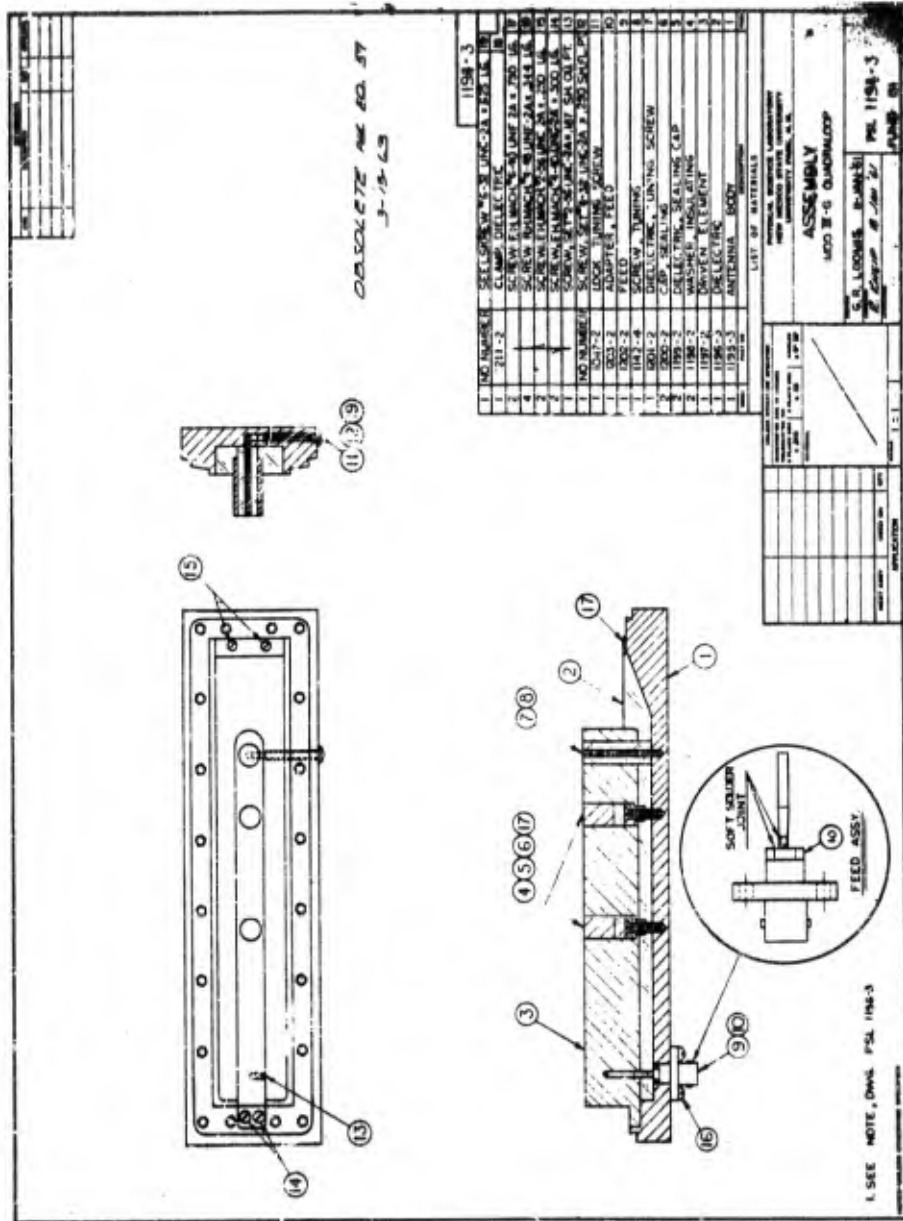


FIG. 66 - MODEL III-G TELEMETRY QUADRALOOP ANTENNA



FIG. 67 - PHOTOGRAPH OF MODEL 3.001 TELEMETRY
QUADRALOOP ANTENNA

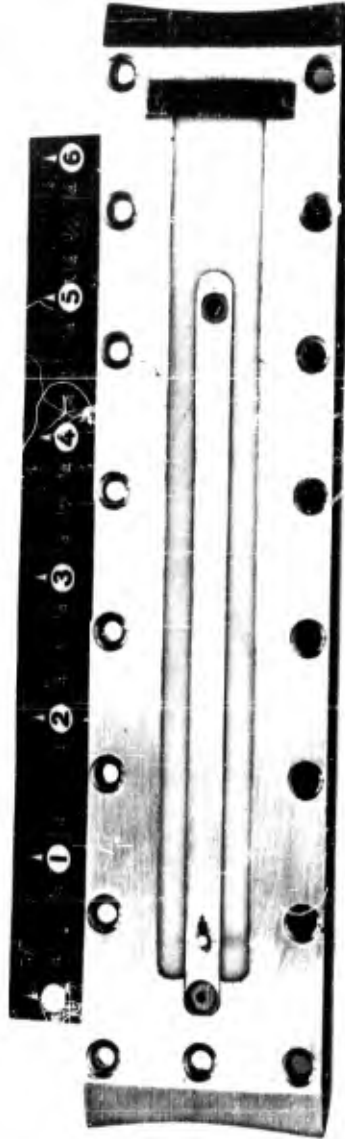


FIG. 69 - PHOTOGRAPH OF MODEL IV COMMAND CONTROL
QUADRALOOP ANTENNA

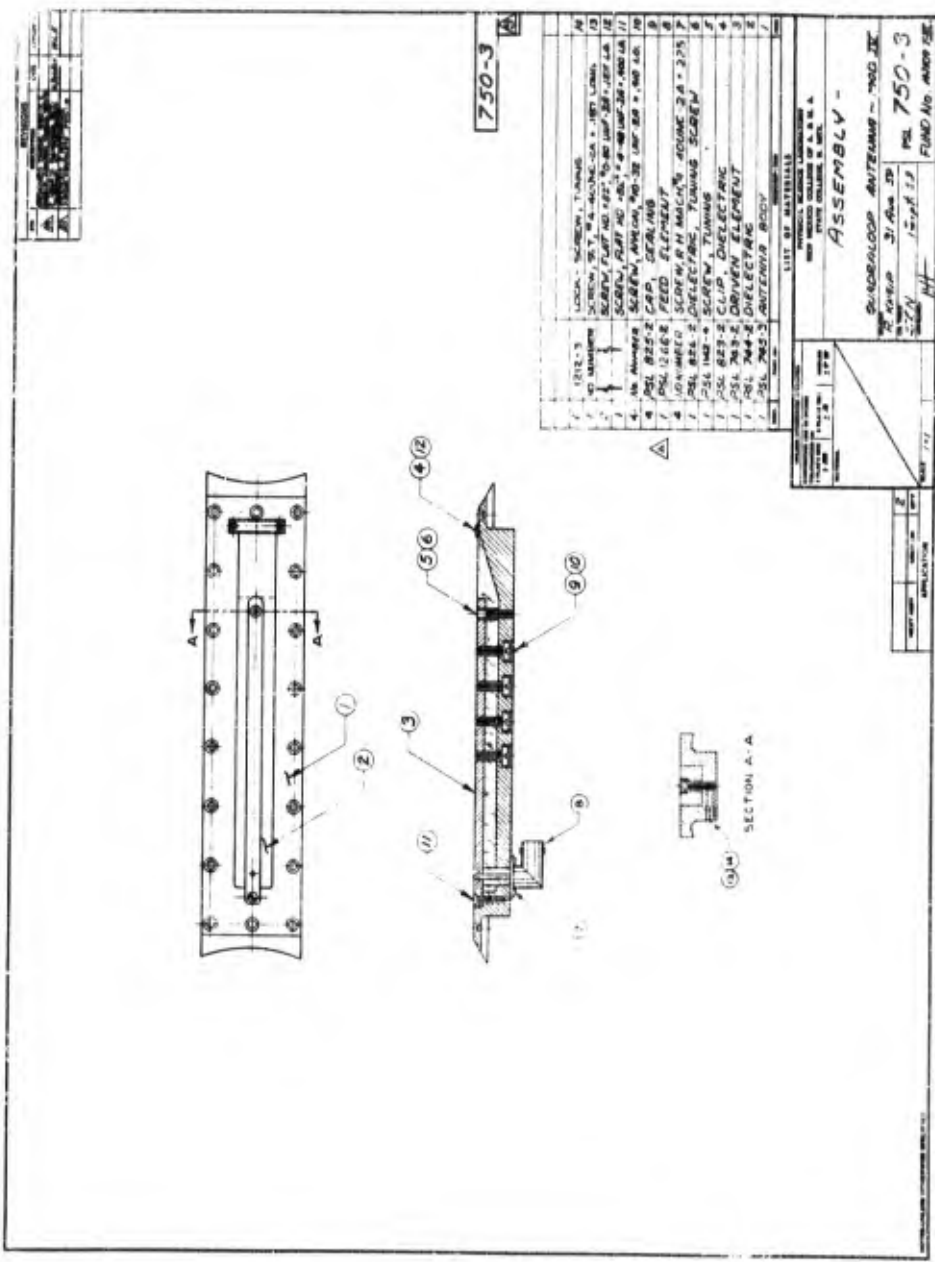


FIG. 70 - MODEL IV COMMAND CONTROL QUADRALOOP ANTENNA

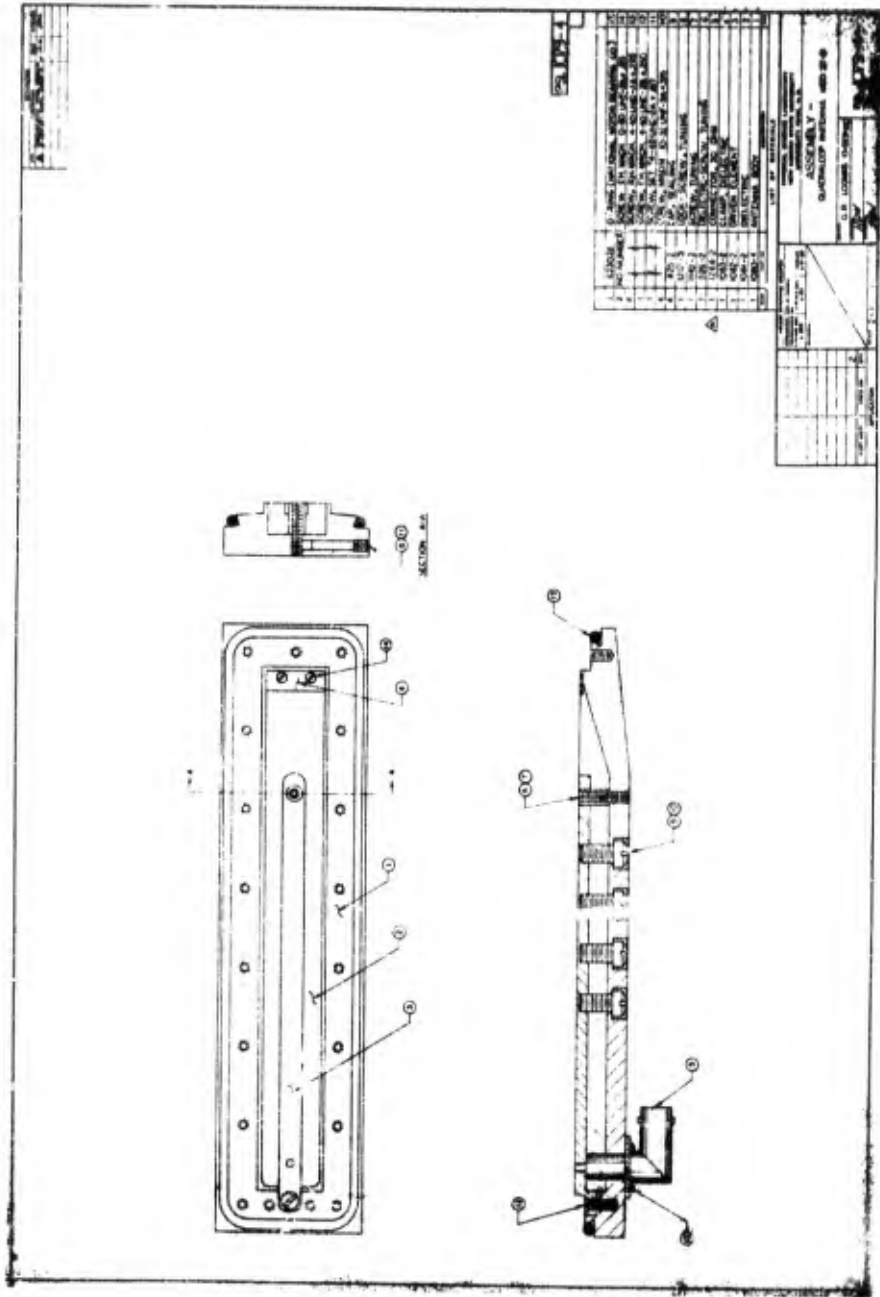


FIG. 71 - MODEL IV-B COMMAND CONTROL QUADRALOOP ANTENNA



FIG. 72 - PHOTOGRAPH OF MODEL 4.001 COMMAND CONTROL QUADRANGLE LOOP ANTENNA



FIG. 74 - PHOTOGRAPH OF MODEL 4,002 COMMAND CONTROL
QUADRALOOP ANTENNA

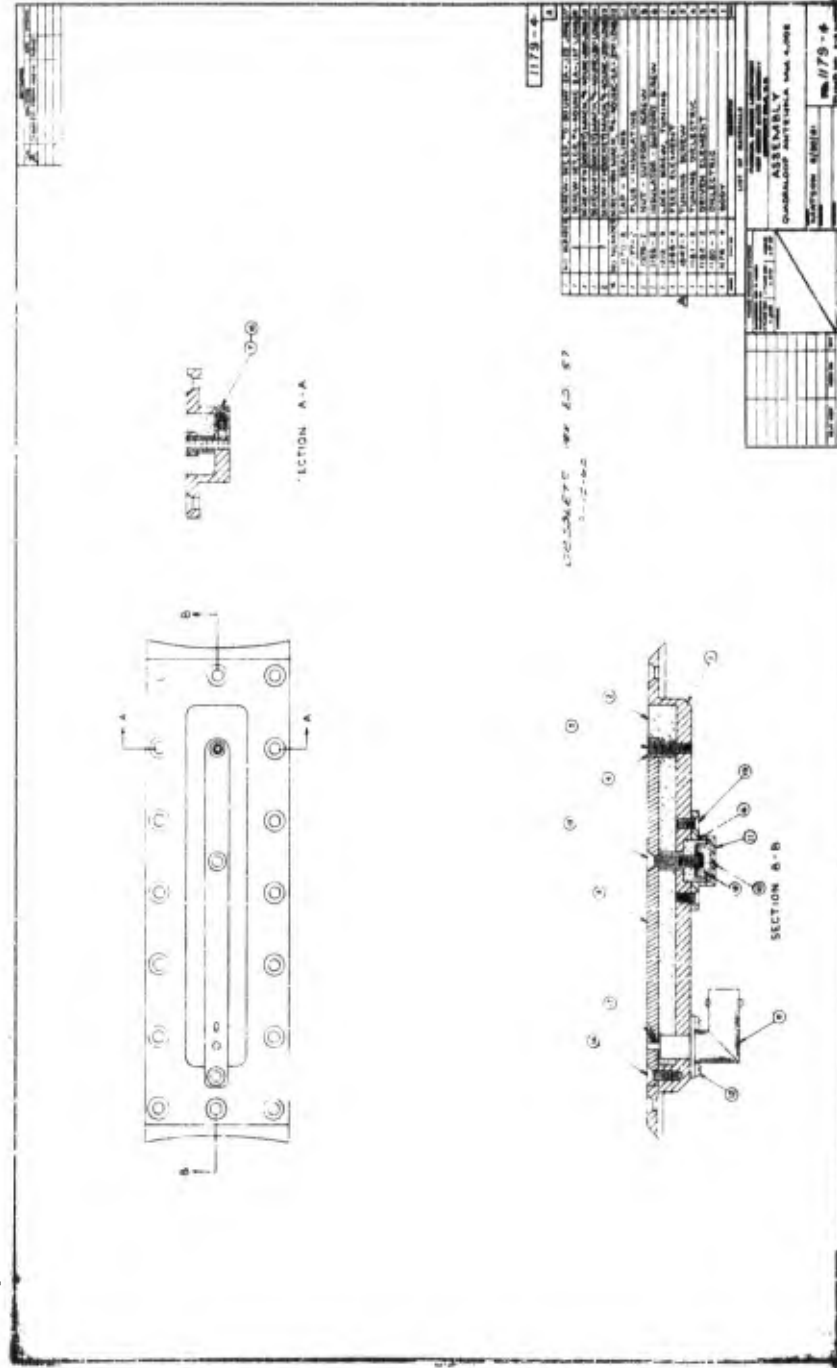


FIG. 75 - MODEL 4,002 COMMAND CONTROL QUADRALOOP ANTENNA

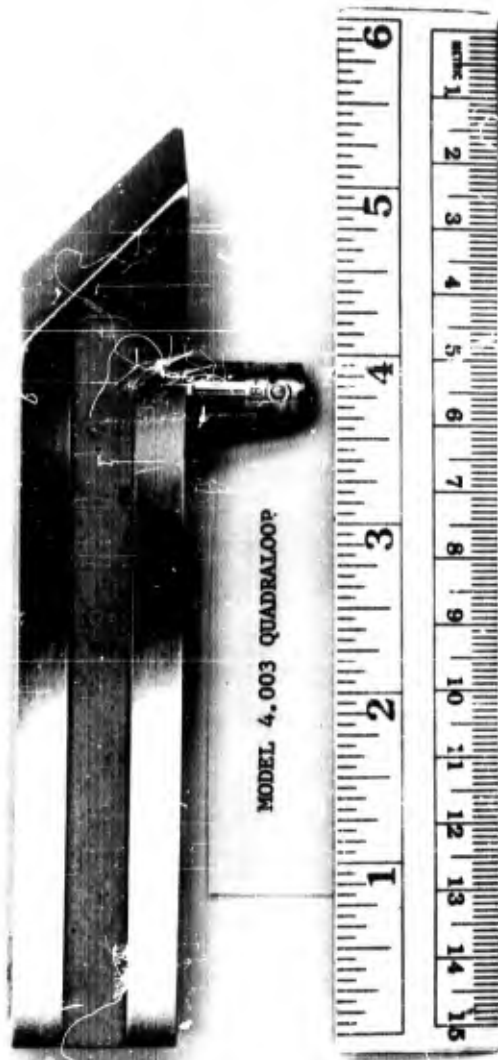


FIG. 76 - PHOTOGRAPH OF MODEL 4.003 COMMAND CONTROL
QUADRALOOP ANTENNA

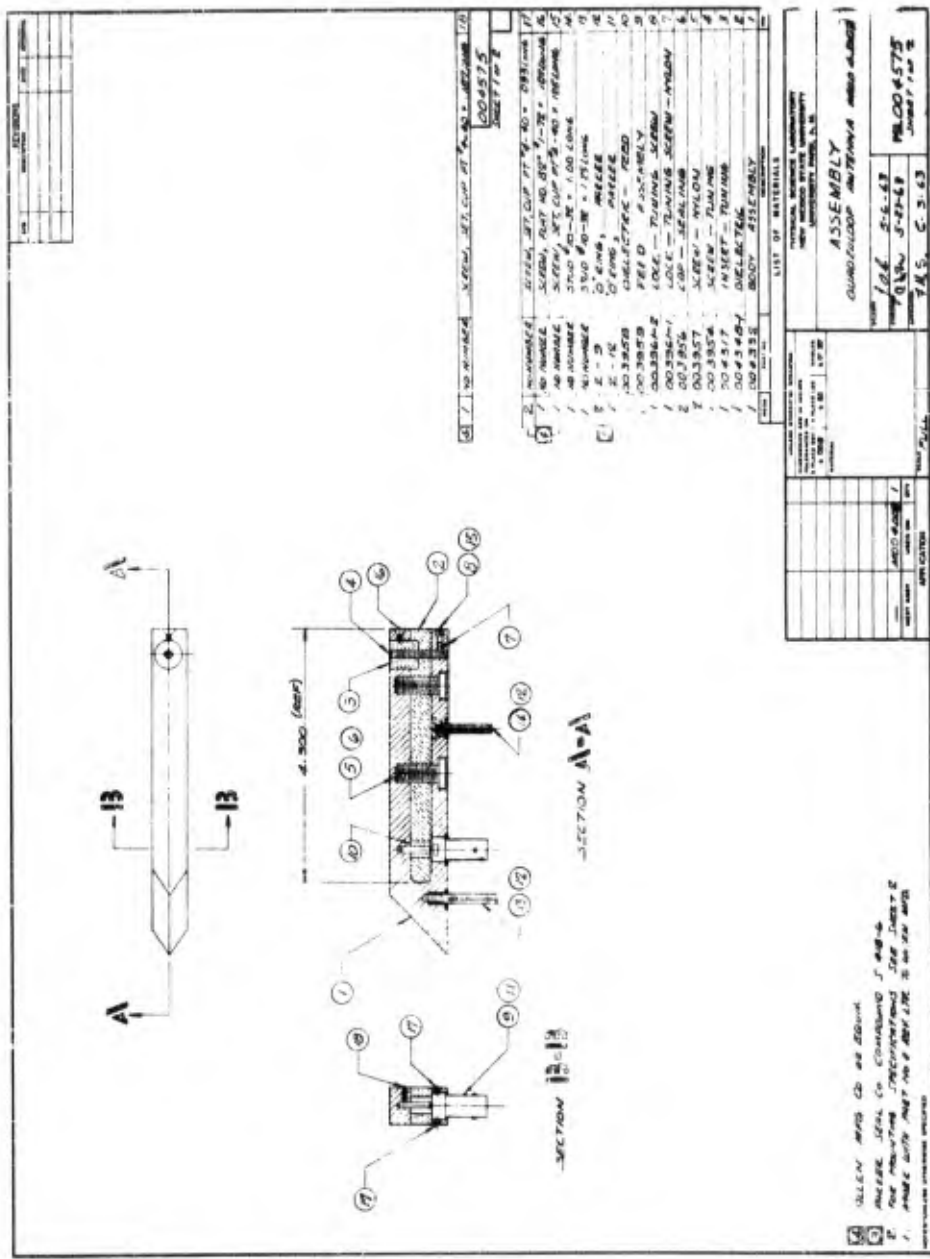


FIG. 77 - MODEL 4.003 COMMAND CONTROL QUADRALOOP ANTENNA

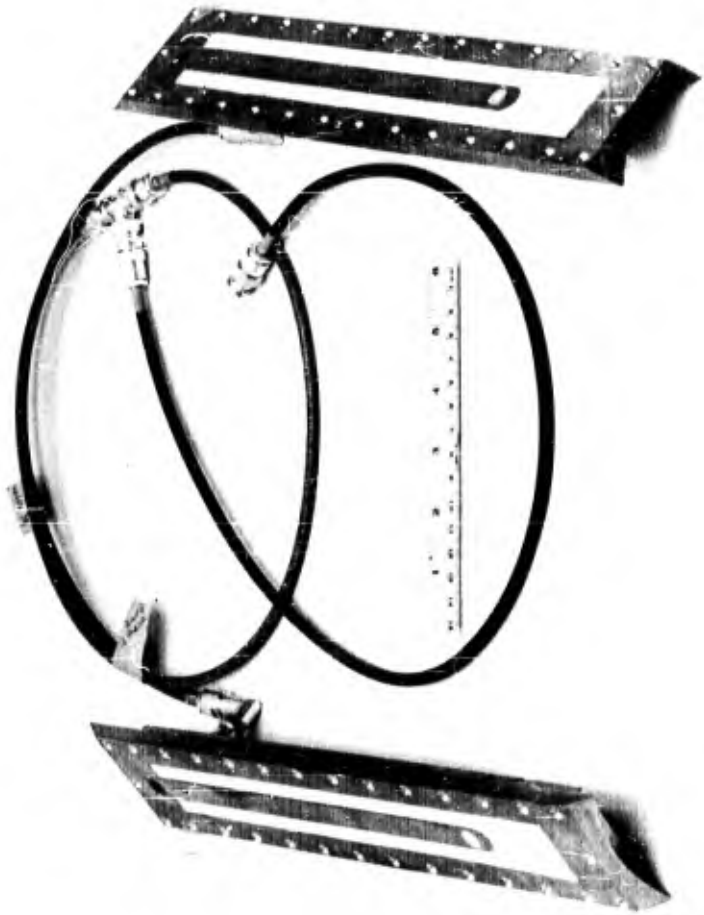


FIG. 78 - PHOTOGRAPH OF MODEL V TELEMETRY
QUADRALOOP ANTENNA

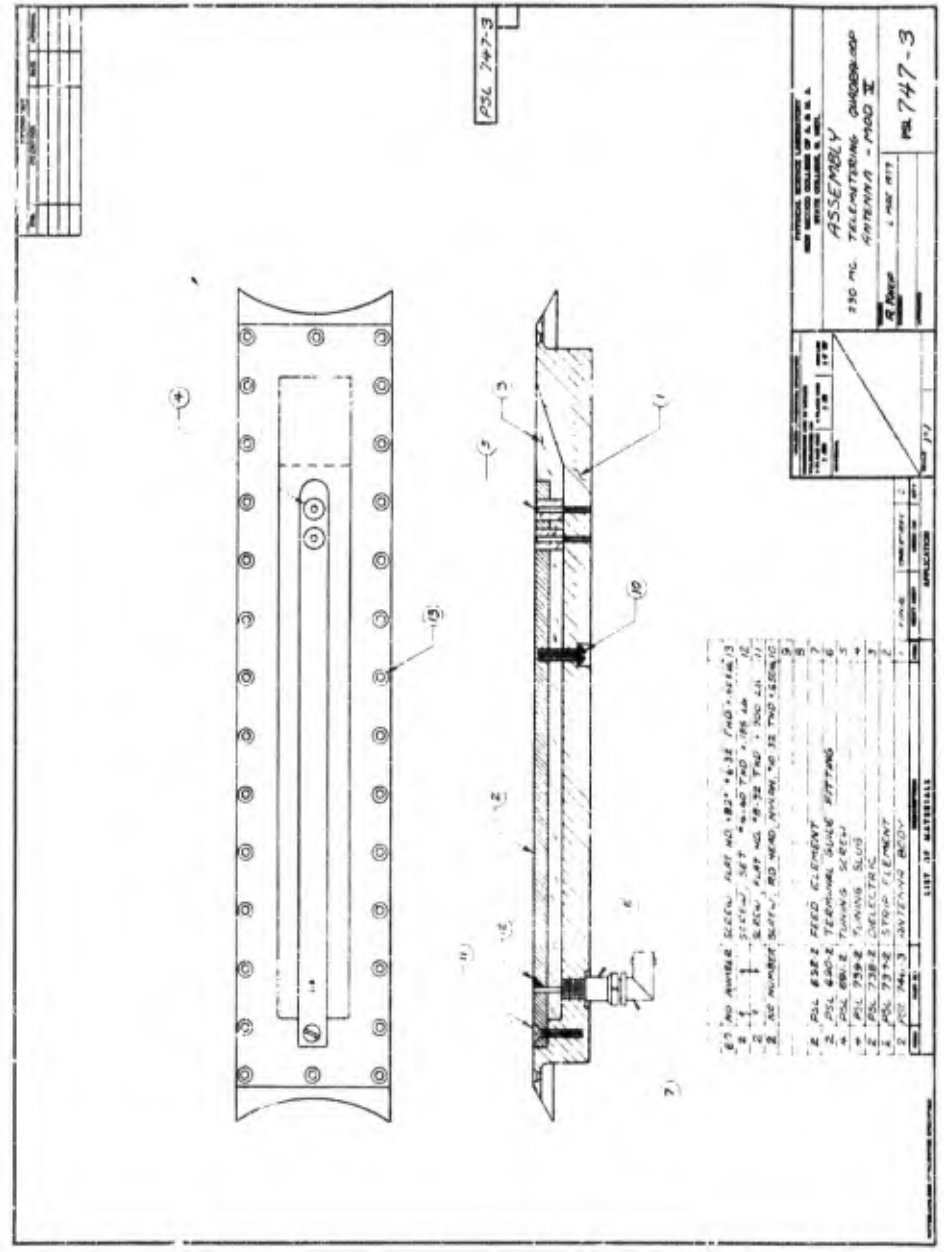


FIG. 79 - MODEL V TELEMETRY QUADRALOOP ANTENNA

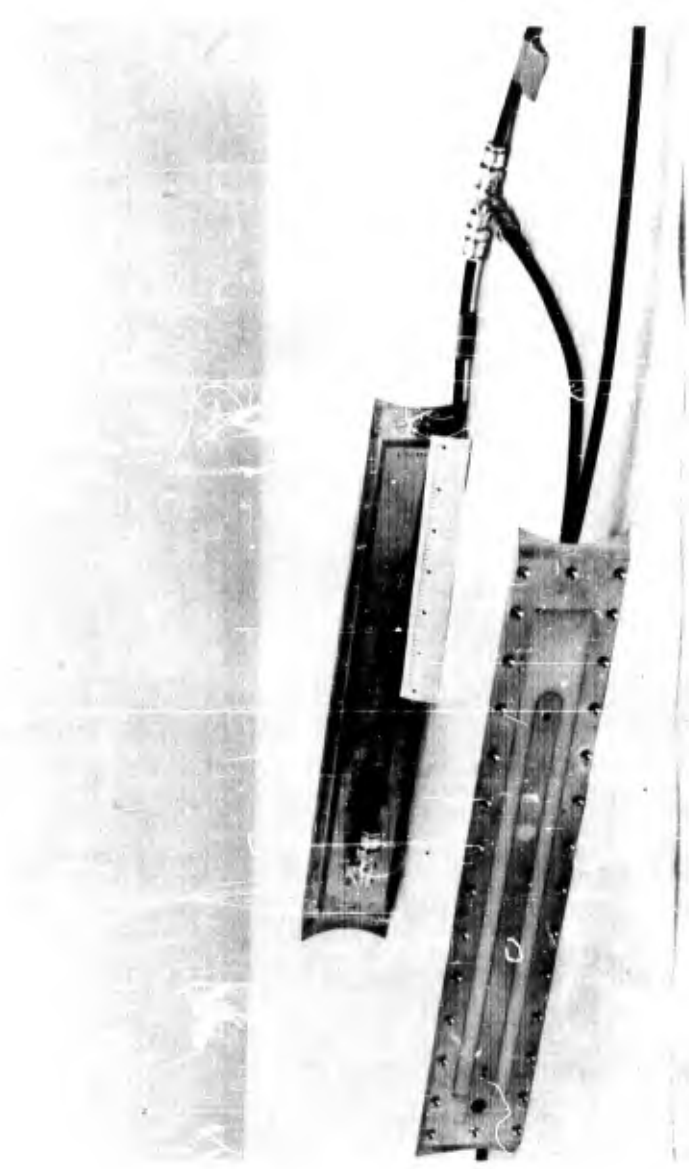


FIG. 30 - PHOTOGRAPH OF MODEL V-B TELEMETRY
QUADRALOOP ANTENNA



FIG. 8' - PHOTOGRAPH OF MODEL V-C TELEMETRY
QUADRALOOP ANTENNA

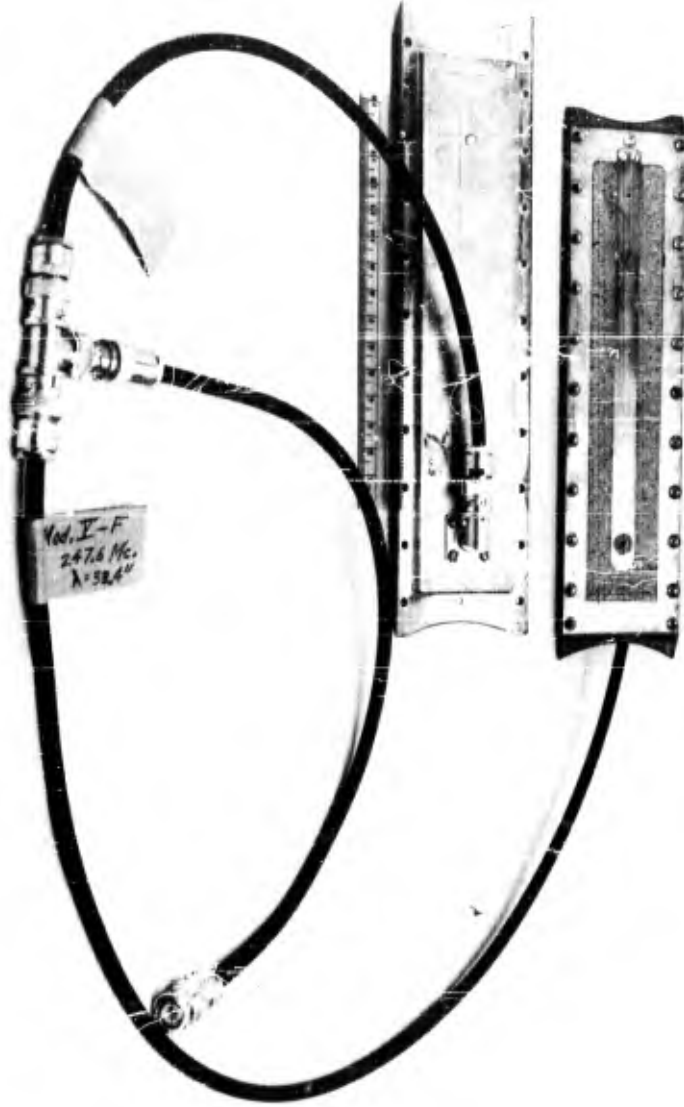


FIG. 83 - PHOTOGRAPH OF MODEL V-F TELEMETRY
QUADRALOOP ANTENNA

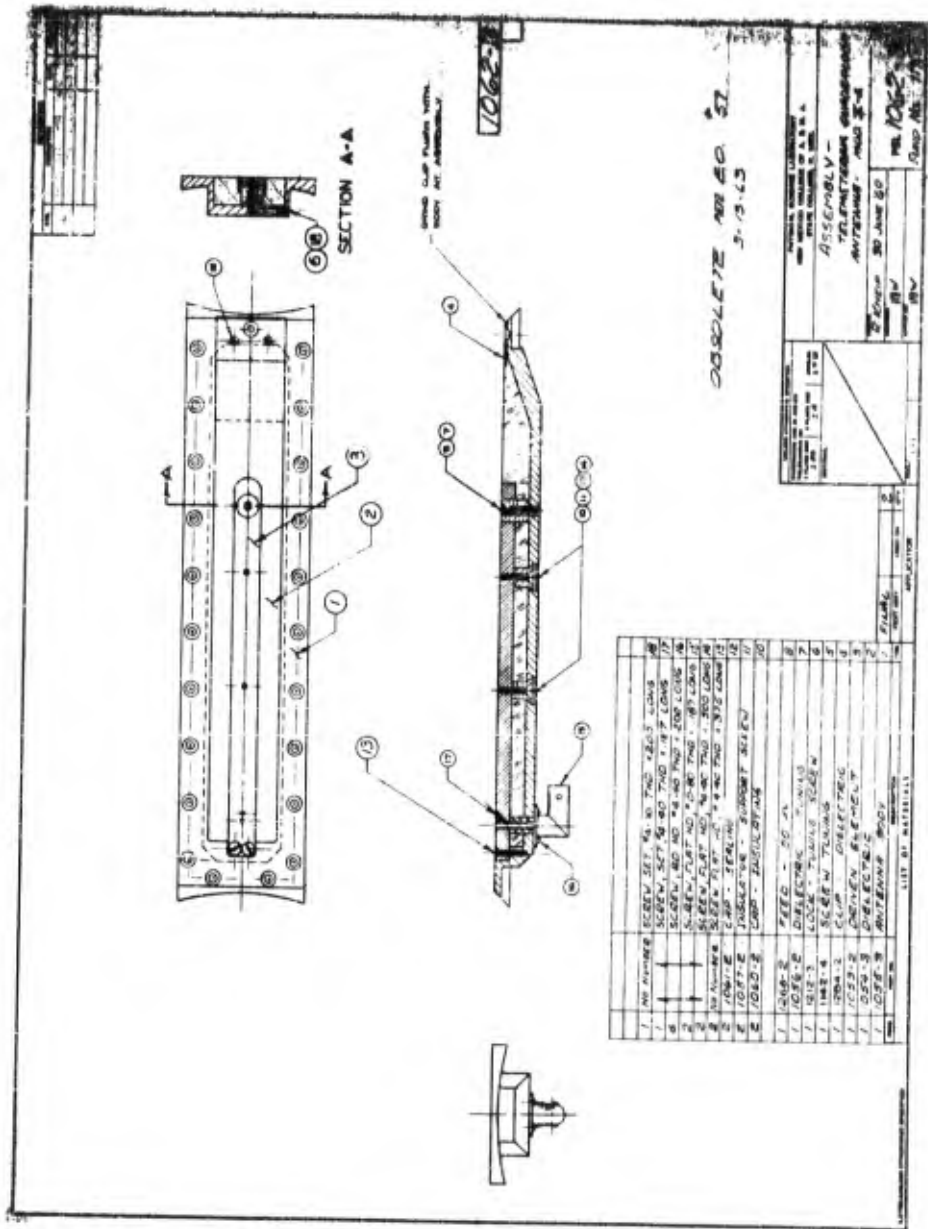


FIG 84 - MODEL V-G TELEMETRY QUADRALOOP ANTENNA



FIG. 85 - PHOTOGRAPH OF MODEL IA7b S-BAND
QUADRALOOP ANTENNA

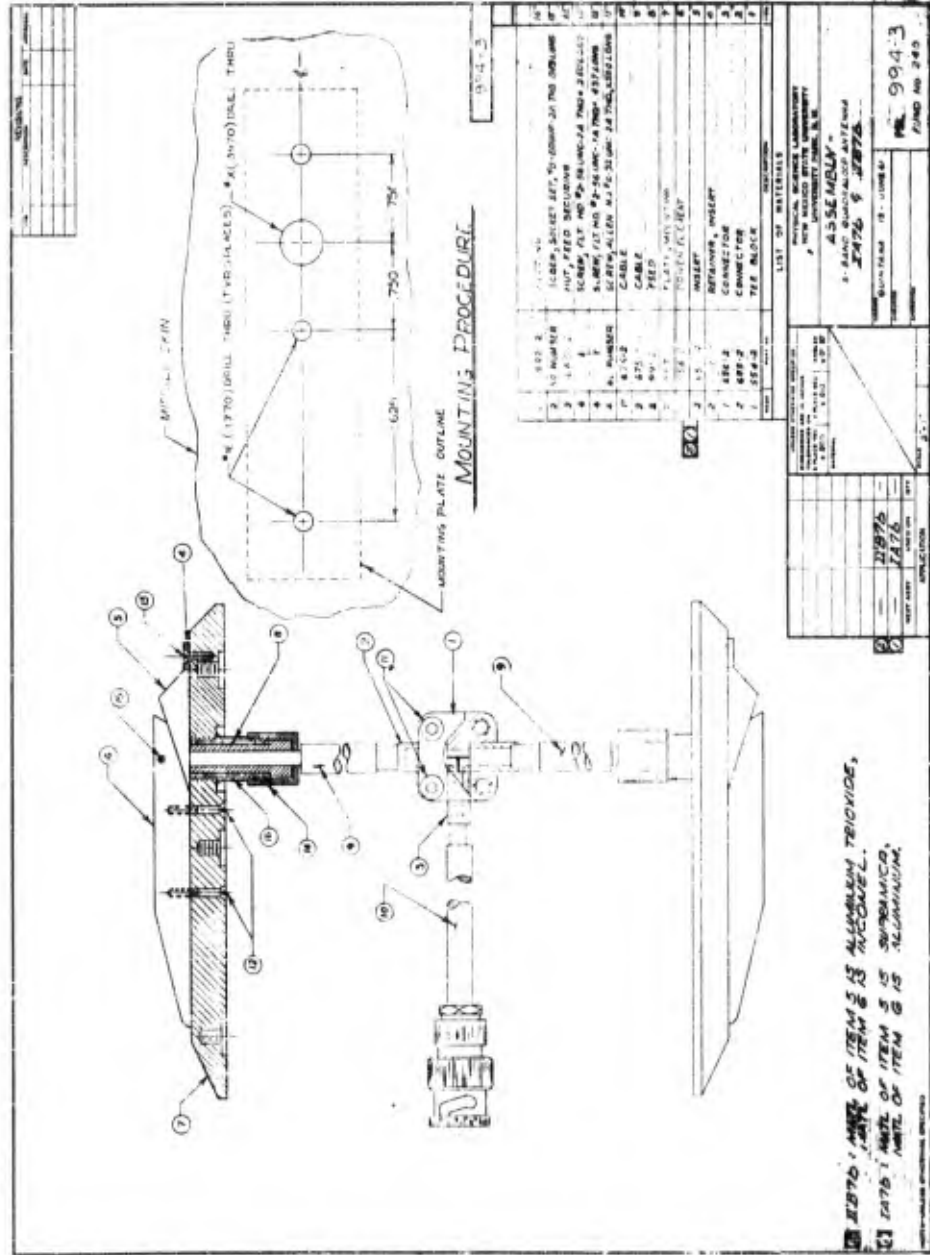


FIG. 86 - MODELS IA7b AND IB7b S-BAND BEACON QUADRALOOP ANTENNA

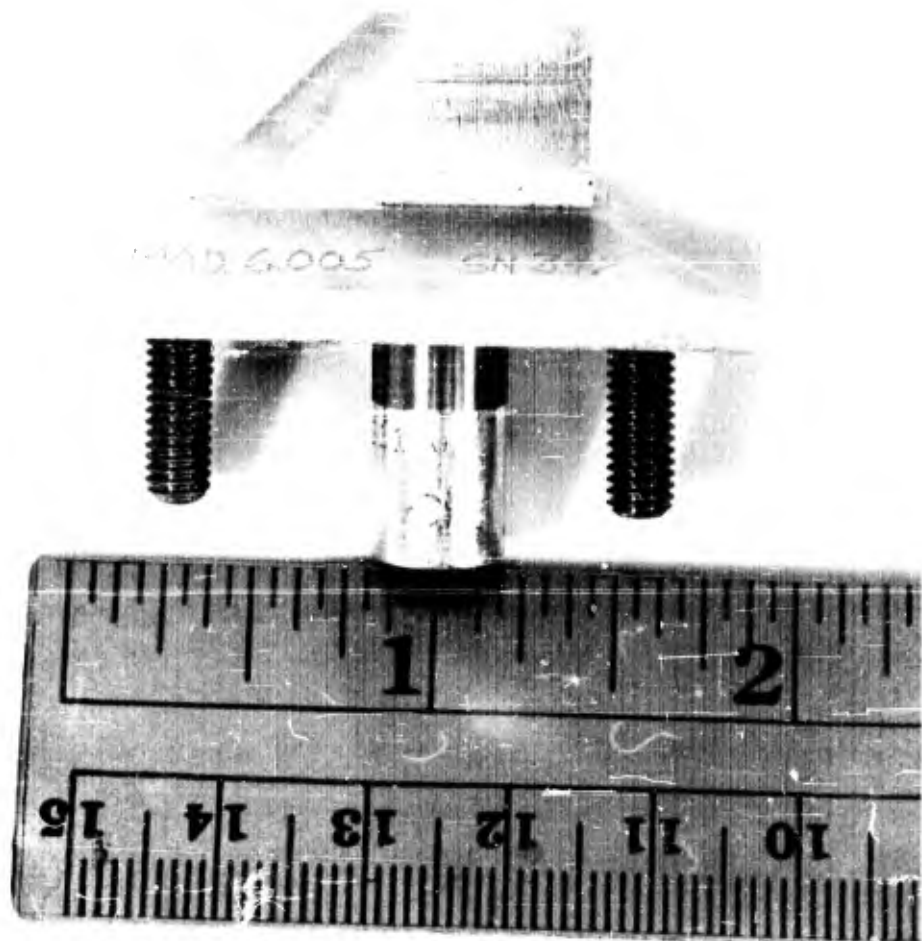


FIG. 87 - PHOTOGRAPH OF MODEL 6.005 S-BAND
QUADRALOOP ANTENNA

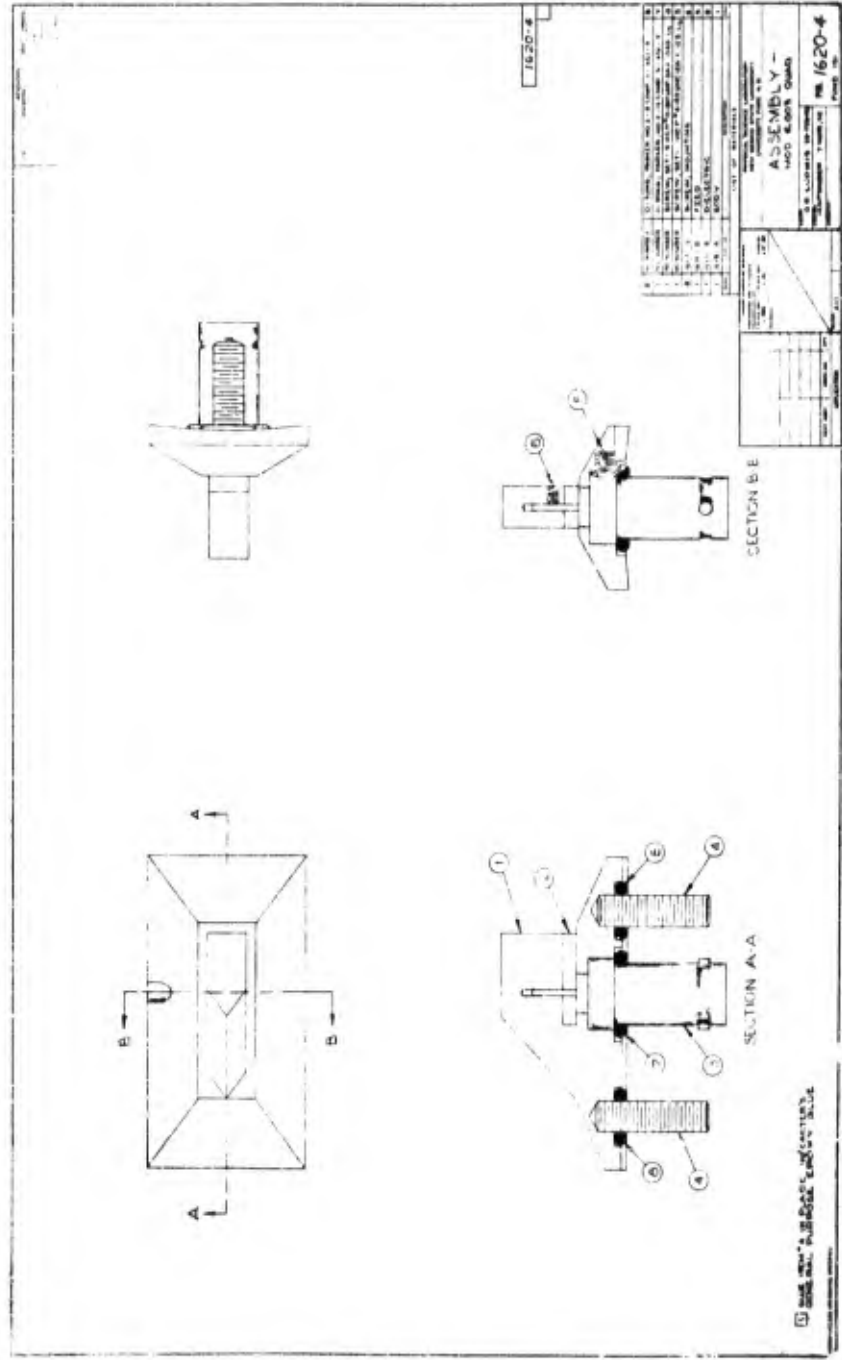


FIG. 88 - MODEL 6.005 S-BAND BEACON QUADRALOOP ANTENNA

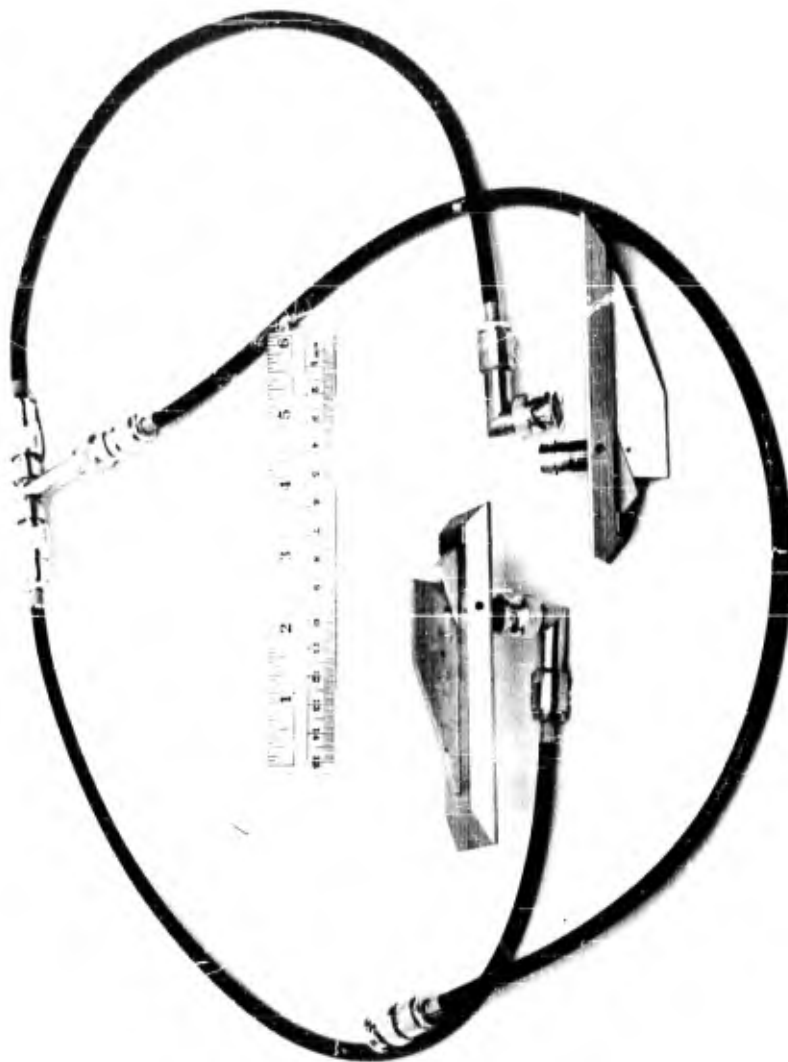


FIG. 89 - PHOTOGRAPH OF MODEL 6.006 S-BAND
QUADRALOOP ANTENNA

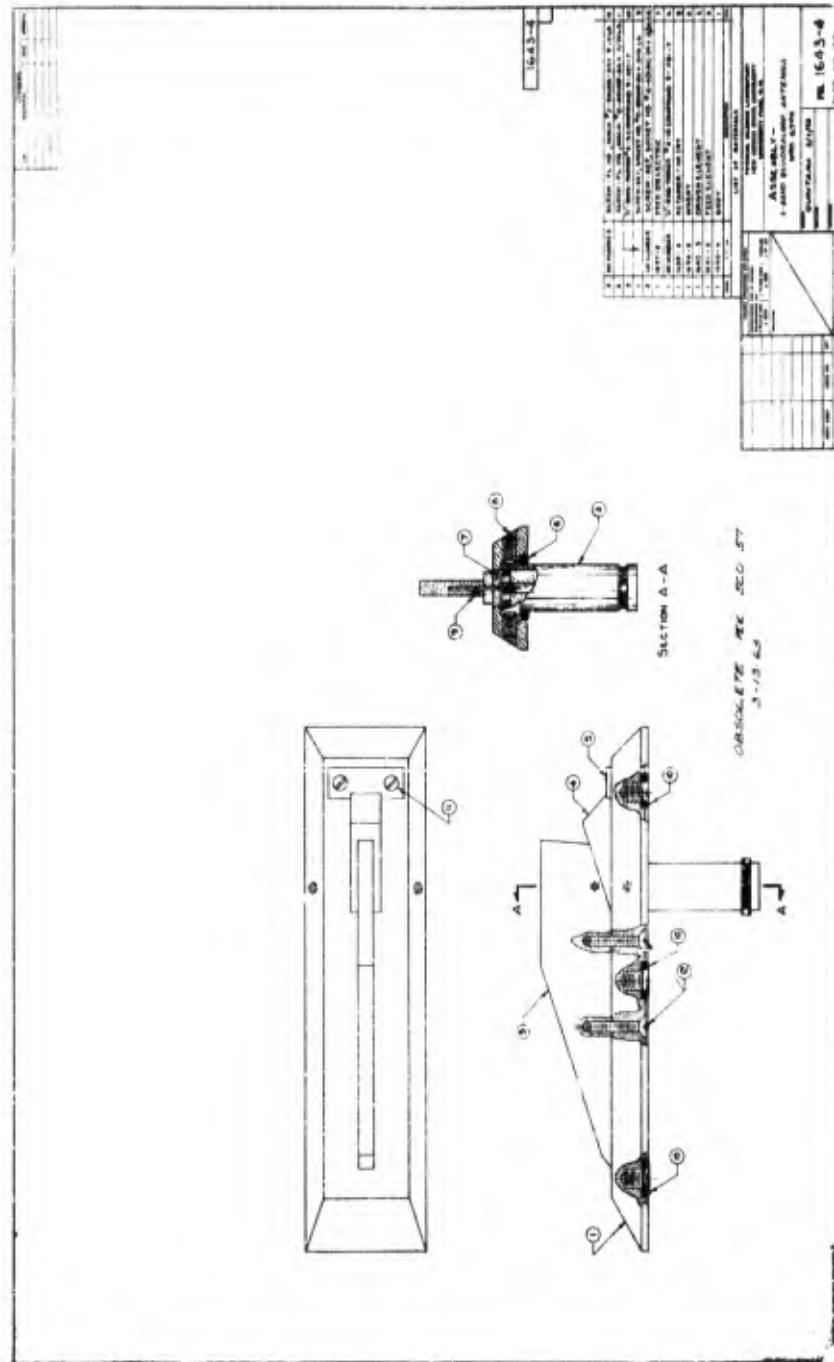


FIG. 90 - MODEL 6.006 S-BAND BEACON QUADRALOOP ANTENNA

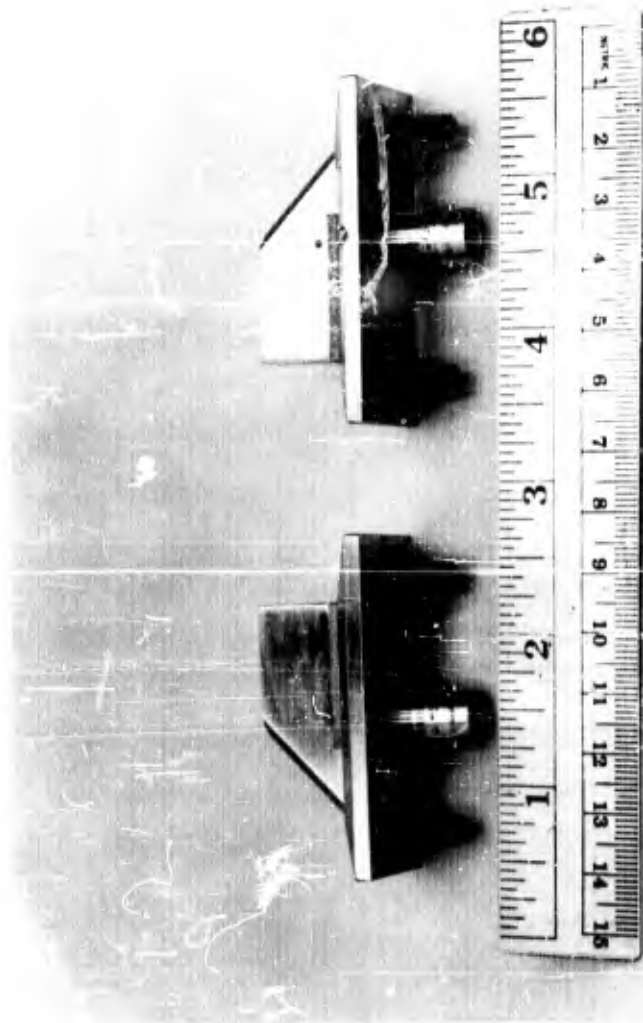


FIG. 91 - PHOTOGRAPH OF MODEL 6.007 RADIO SONDE
QUADRALOOP ANTENNA

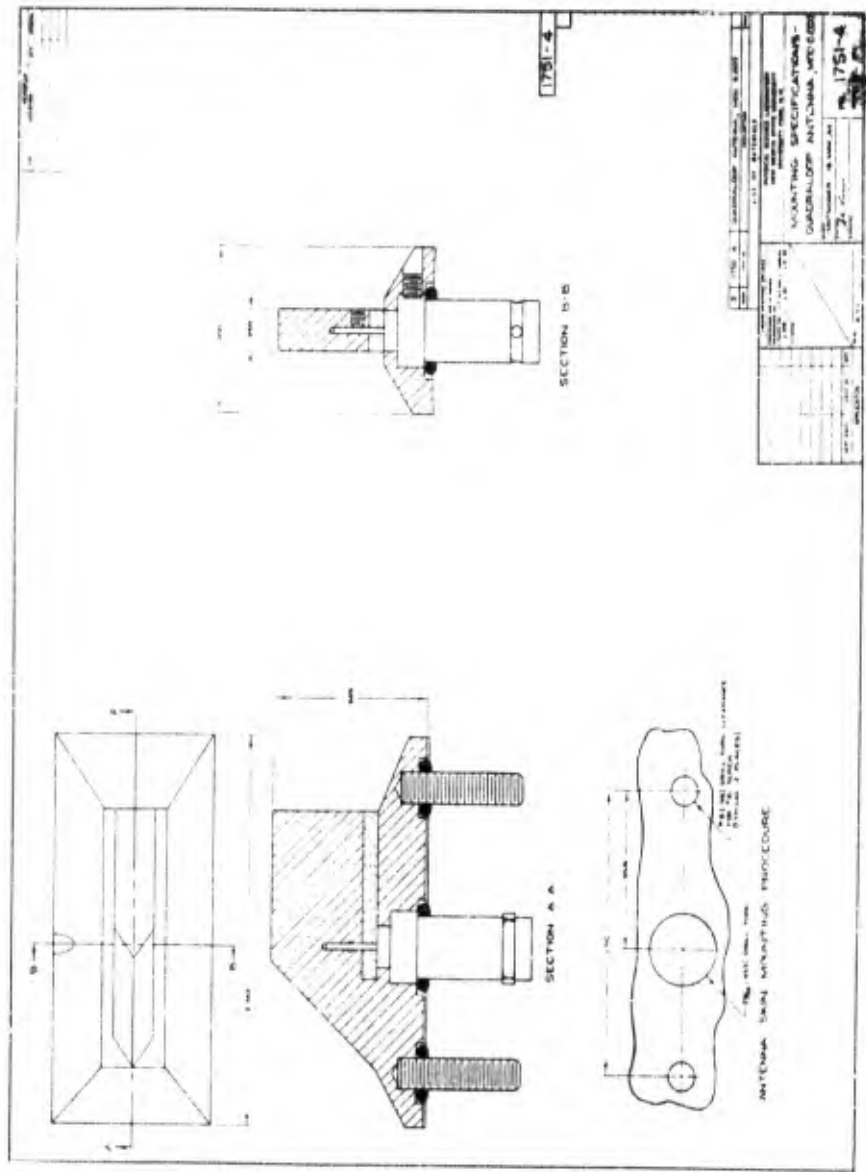


FIG. 92 - MODEL 6.007 RADIO SONDE QUADRA LOOP ANTENNA

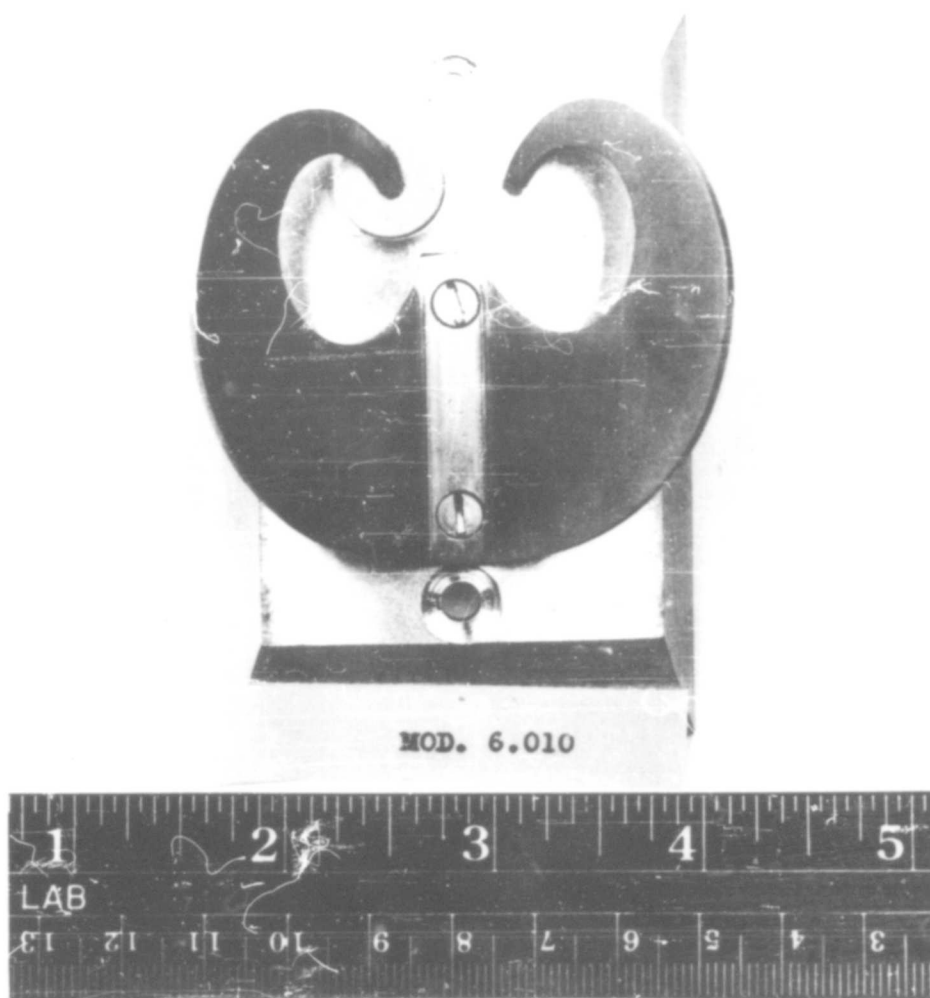


FIG. 93 - PHOTOGRAPH OF MODEL 6.010 S-BAND FOLDED VALENTINE ANTENNA

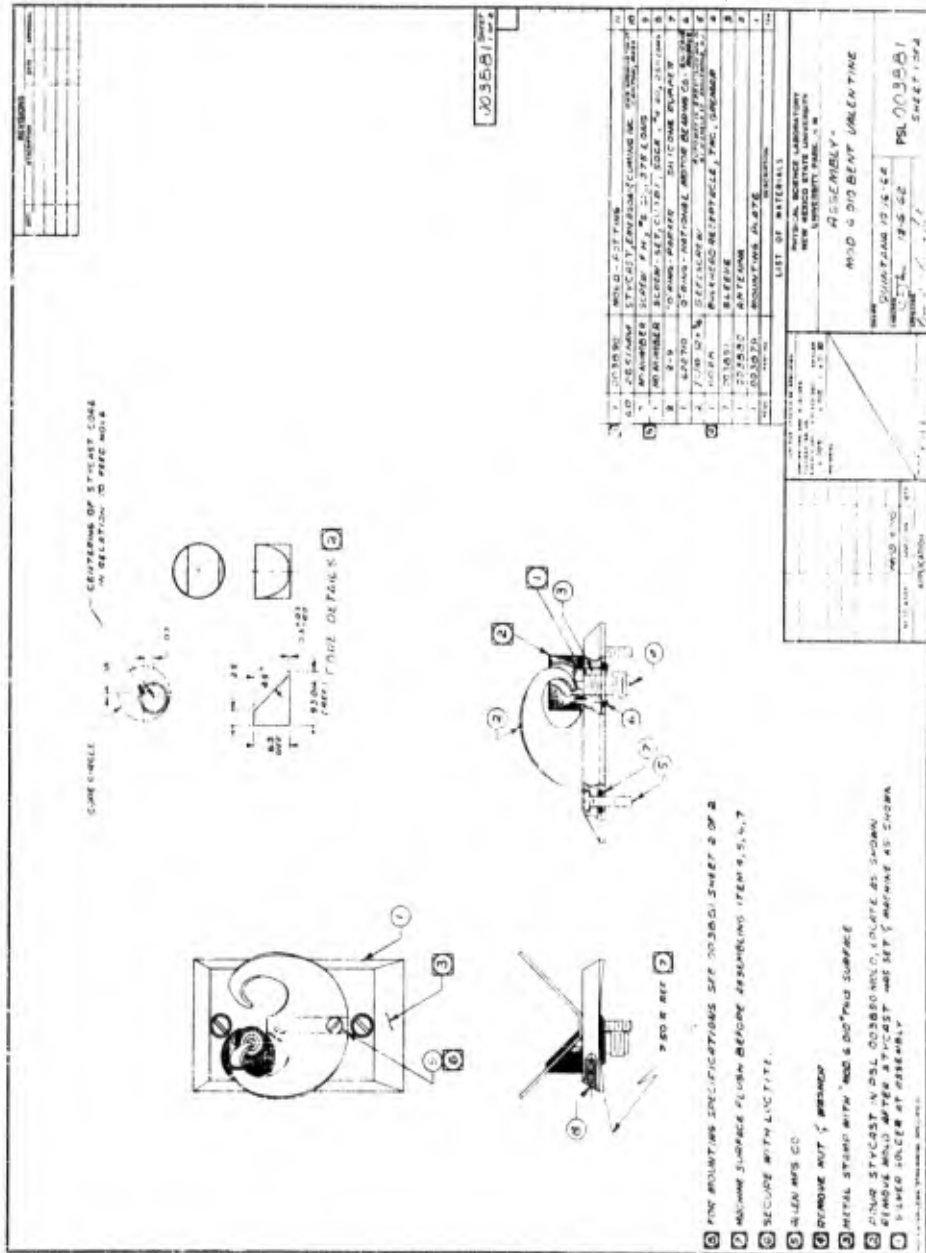


FIG. 94 - MODEL 6, 010 S-BAND BEACON FOLDED VALENTINE ANTENNA

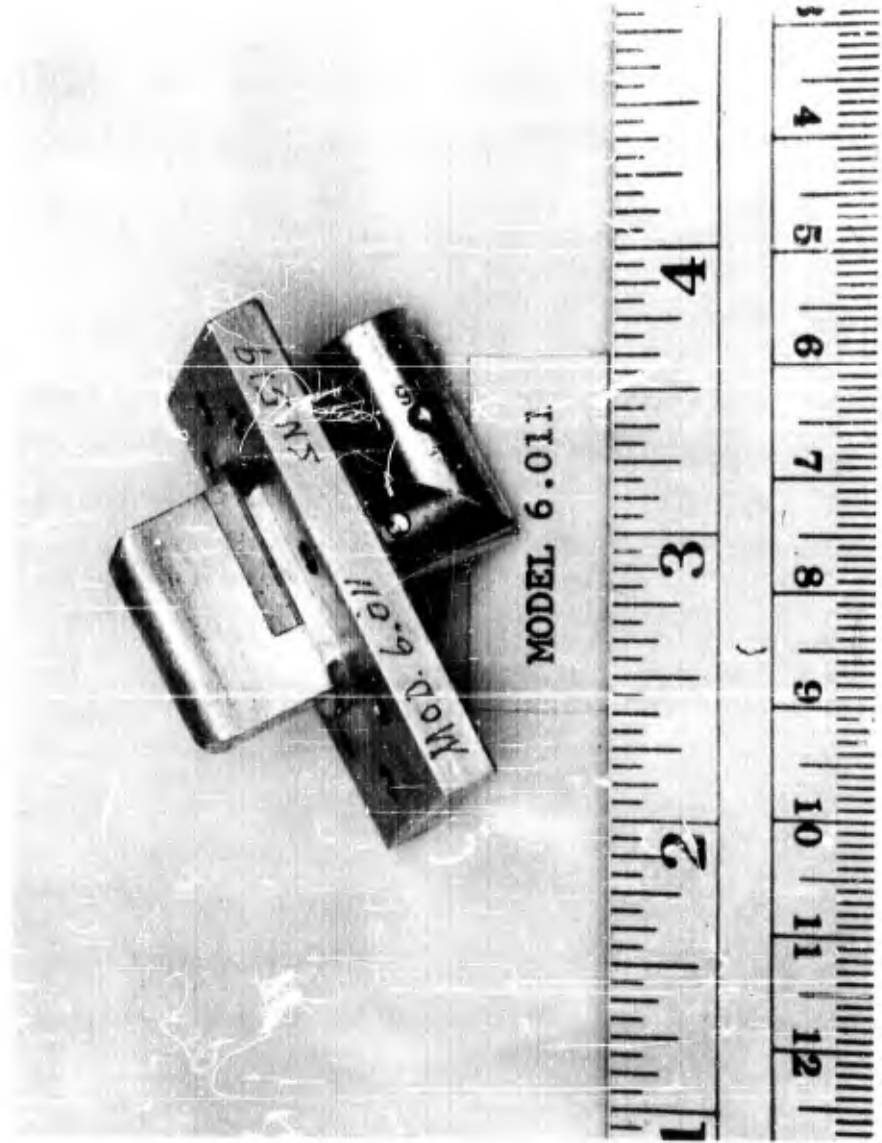


FIG. 95 - PHOTOGRAPH OF MODEL 6.011 S-BAND
QUADRALOOP ANTENNA

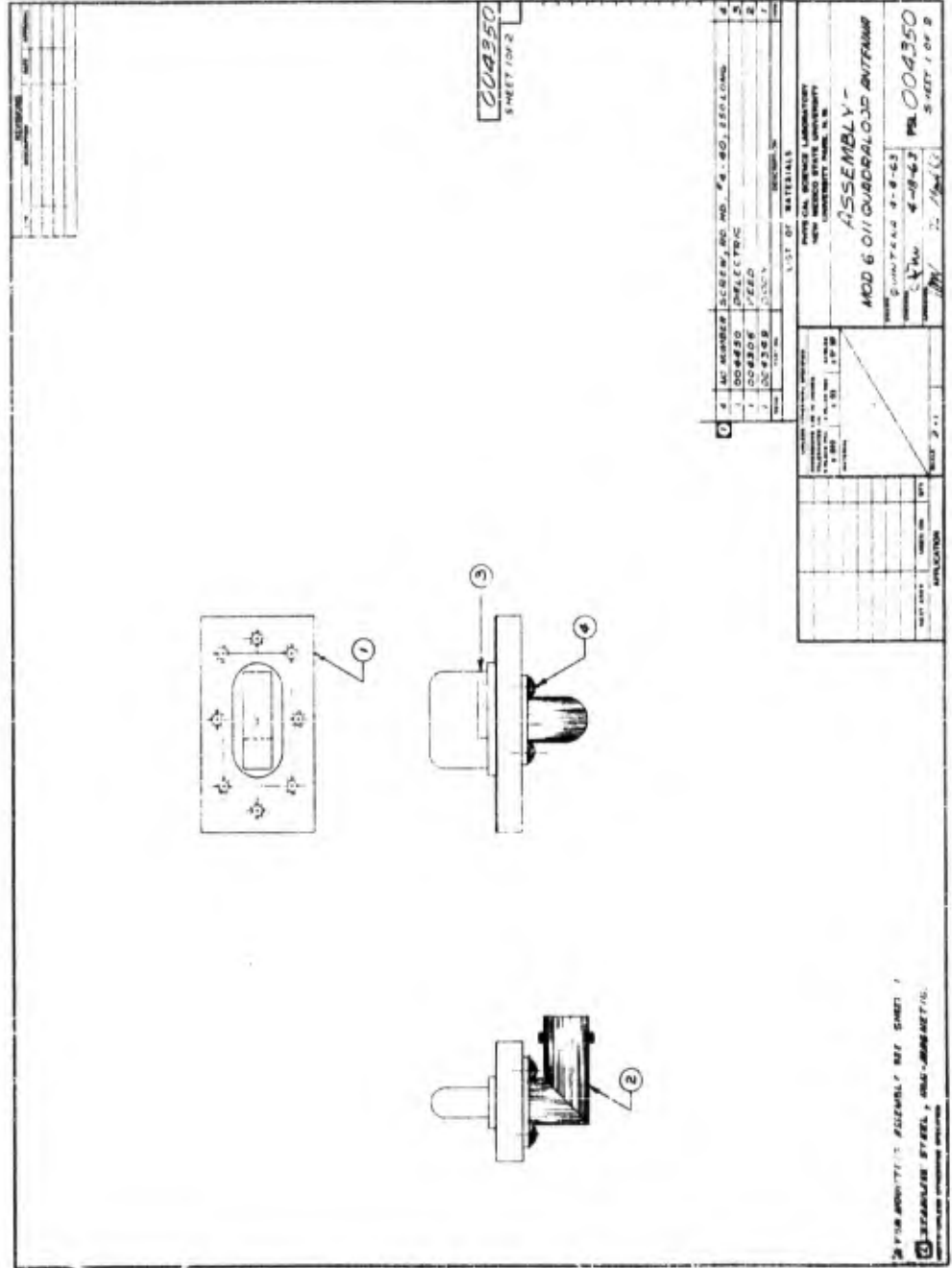


FIG. 96 - MODEL 6 011 S-BAND BEACON QUADRALOOP ANTENNA

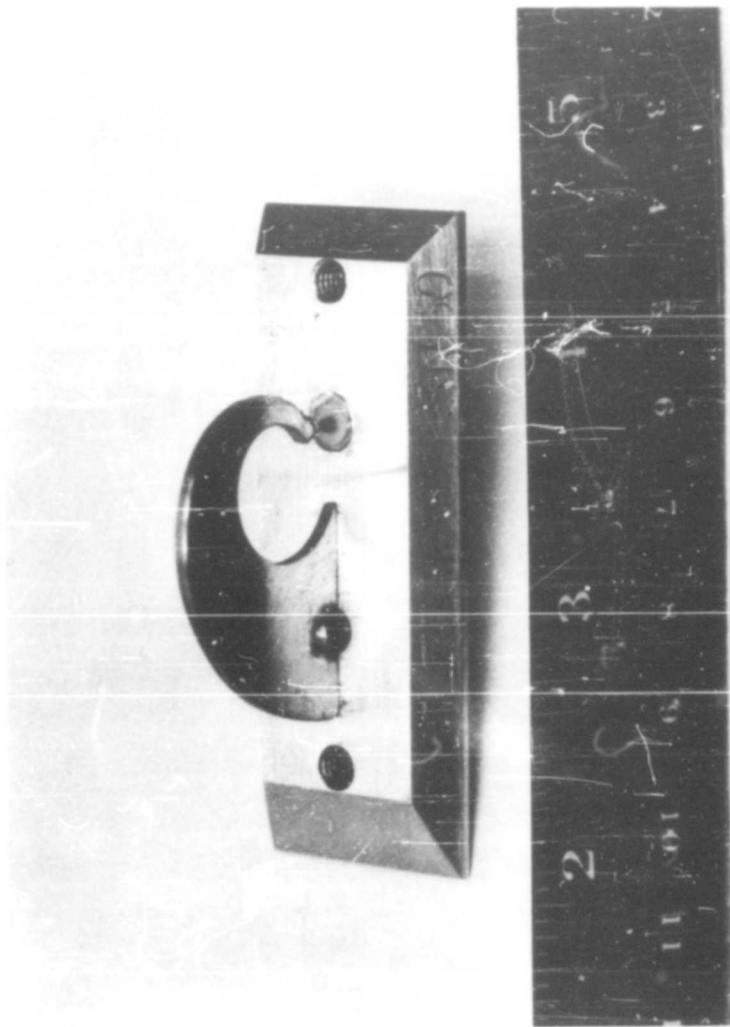


FIG. 97 - PHOTOGRAPH OF MODEL 7.001 C-BAND BEACON
SCIMITAR ANTENNA

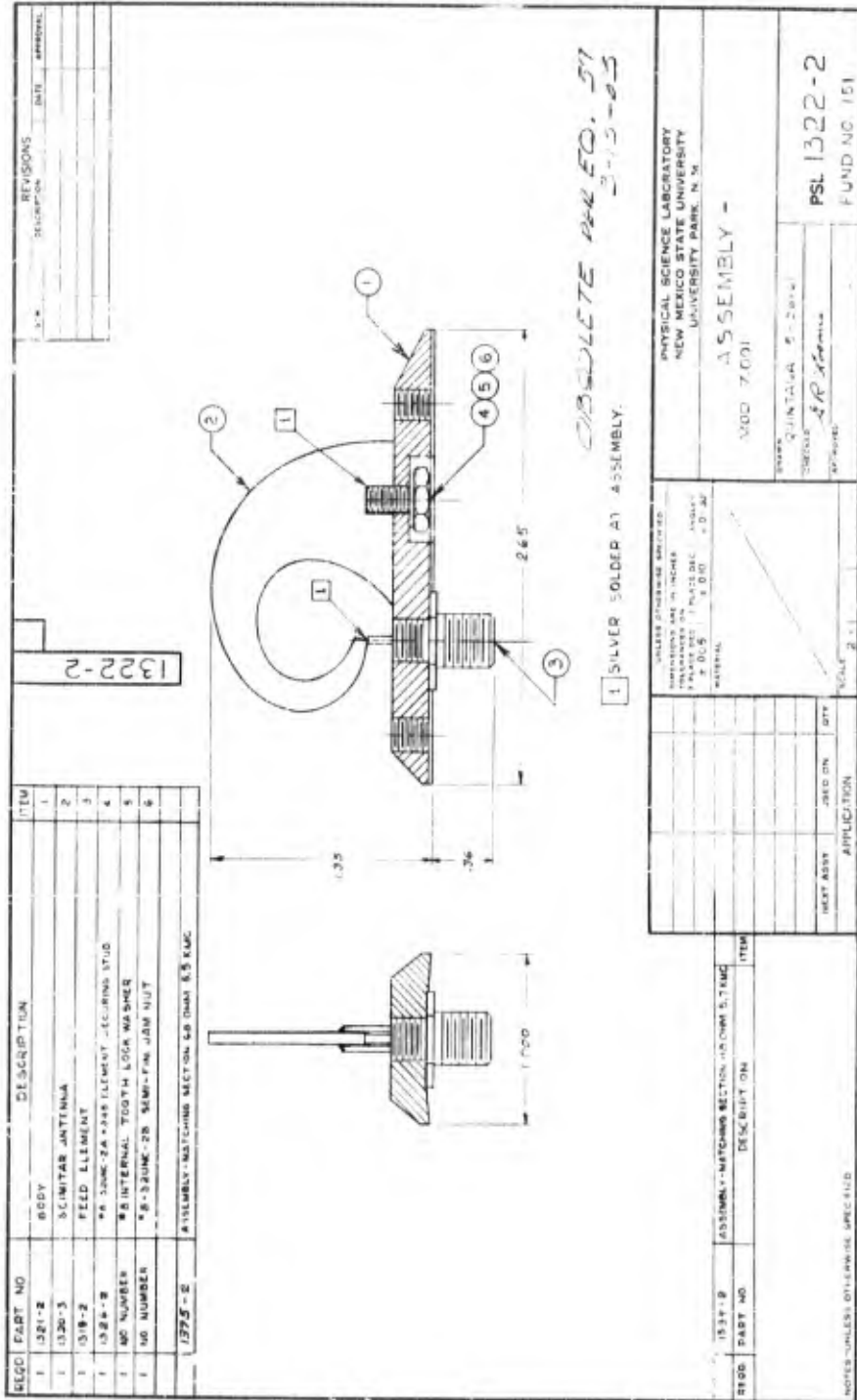


FIG 98 MODEL 7 001 C-BAND BEACON SCIMITAR ANTENNA

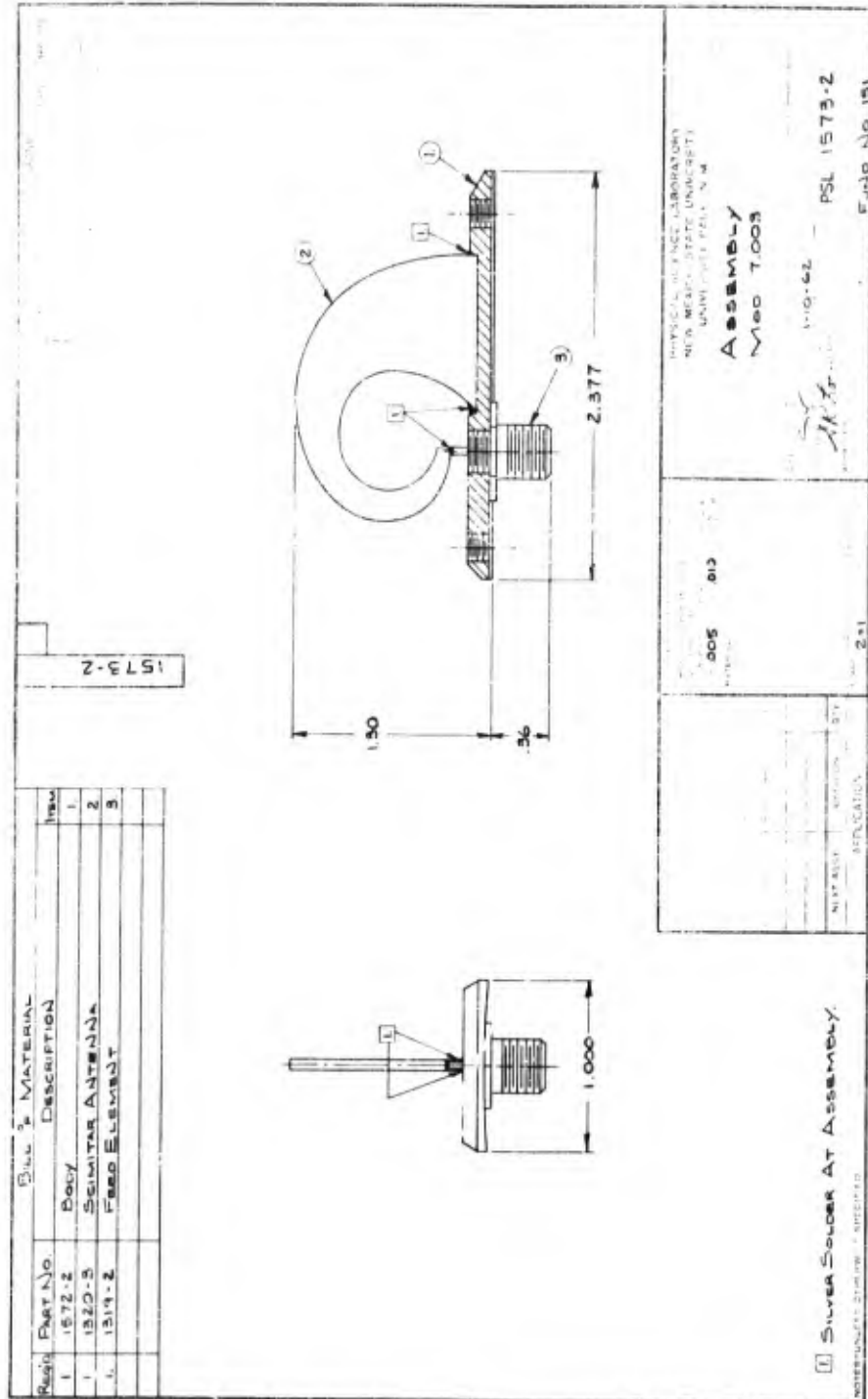


FIG. 99 - MODEL 7.003 C-BAND BEACON SCIMITAR ANTENNA

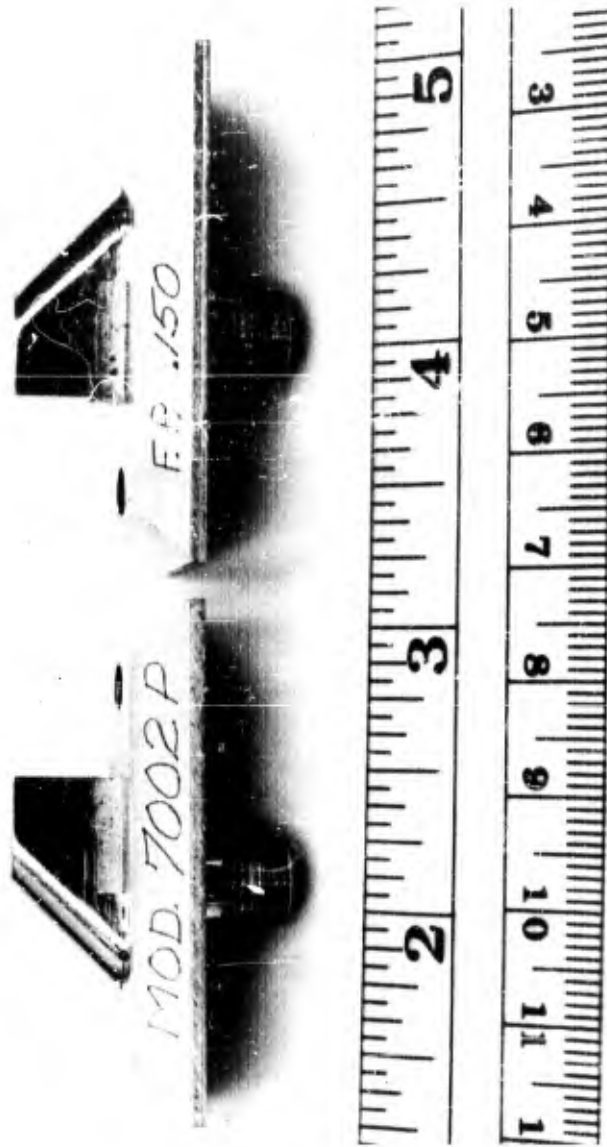


FIG. 100 - PHOTOGRAPH OF MODEL 7.002 C-BAND
QUADRALOOP ANTENNA

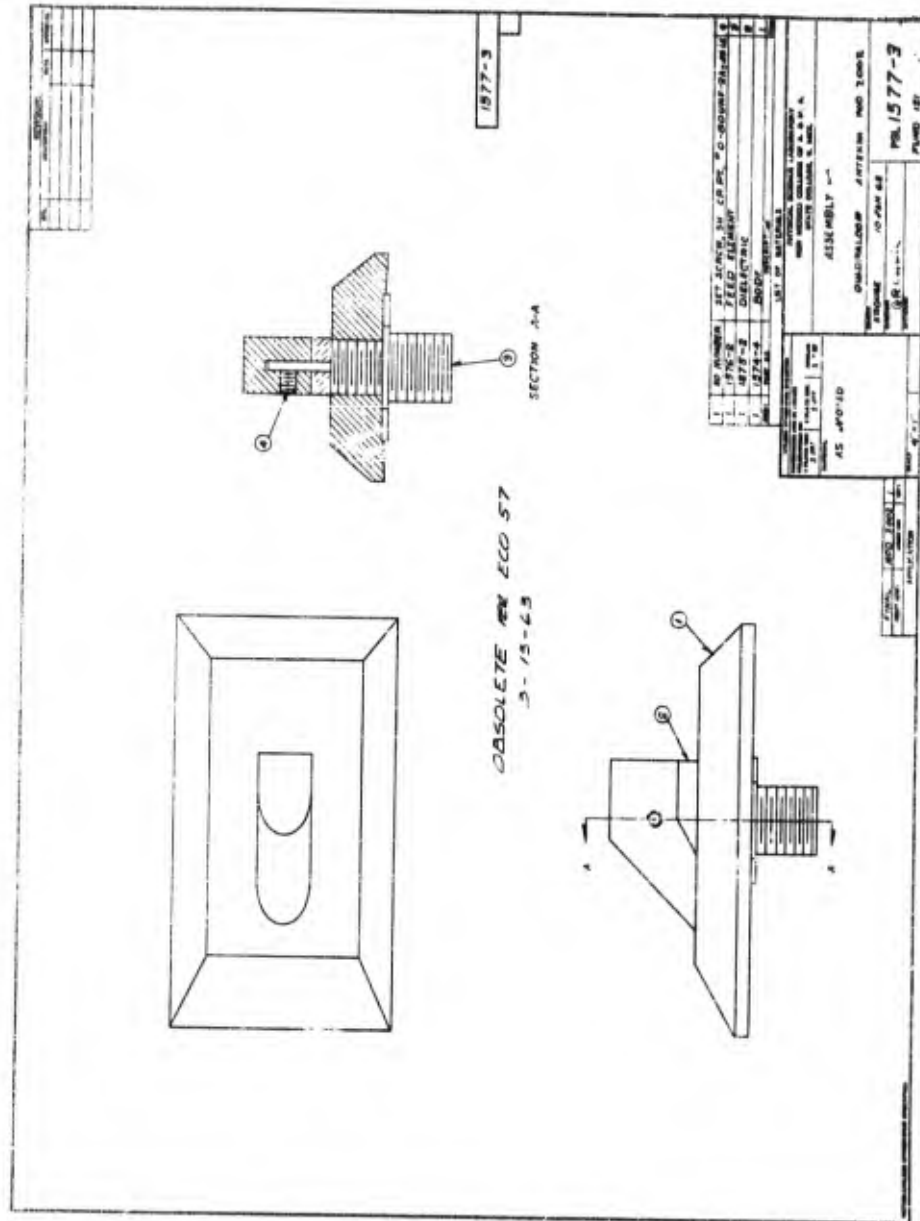


FIG. 101 - MODEL 7.002 C-BAND BEACON QUADRALOOP ANTENNA

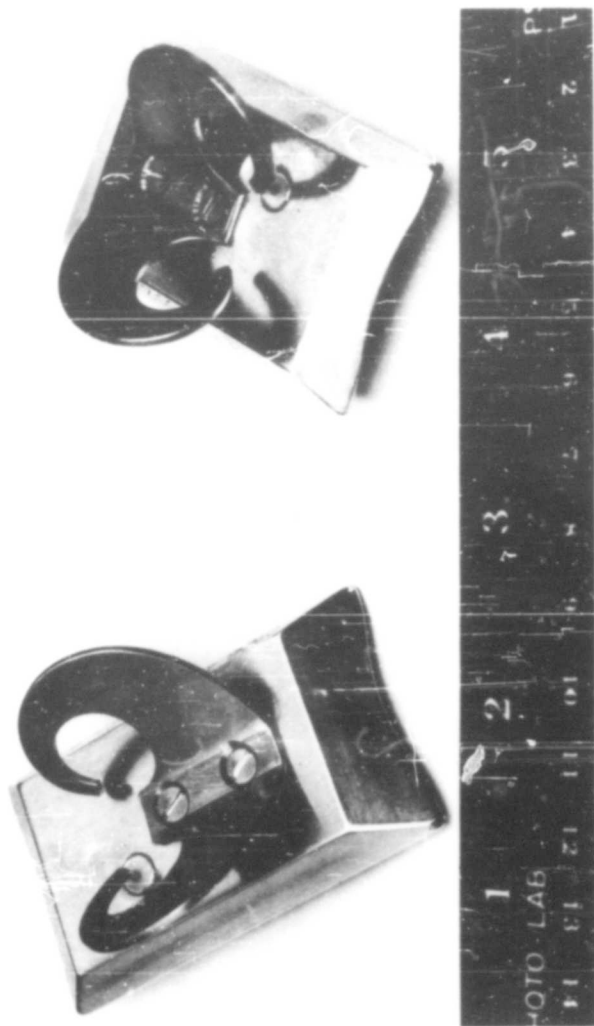


FIG. 102 - PHOTOGRAPH OF MODEL 7.004 C-BAND BEACON FOLDED VALENTINE ANTENNA

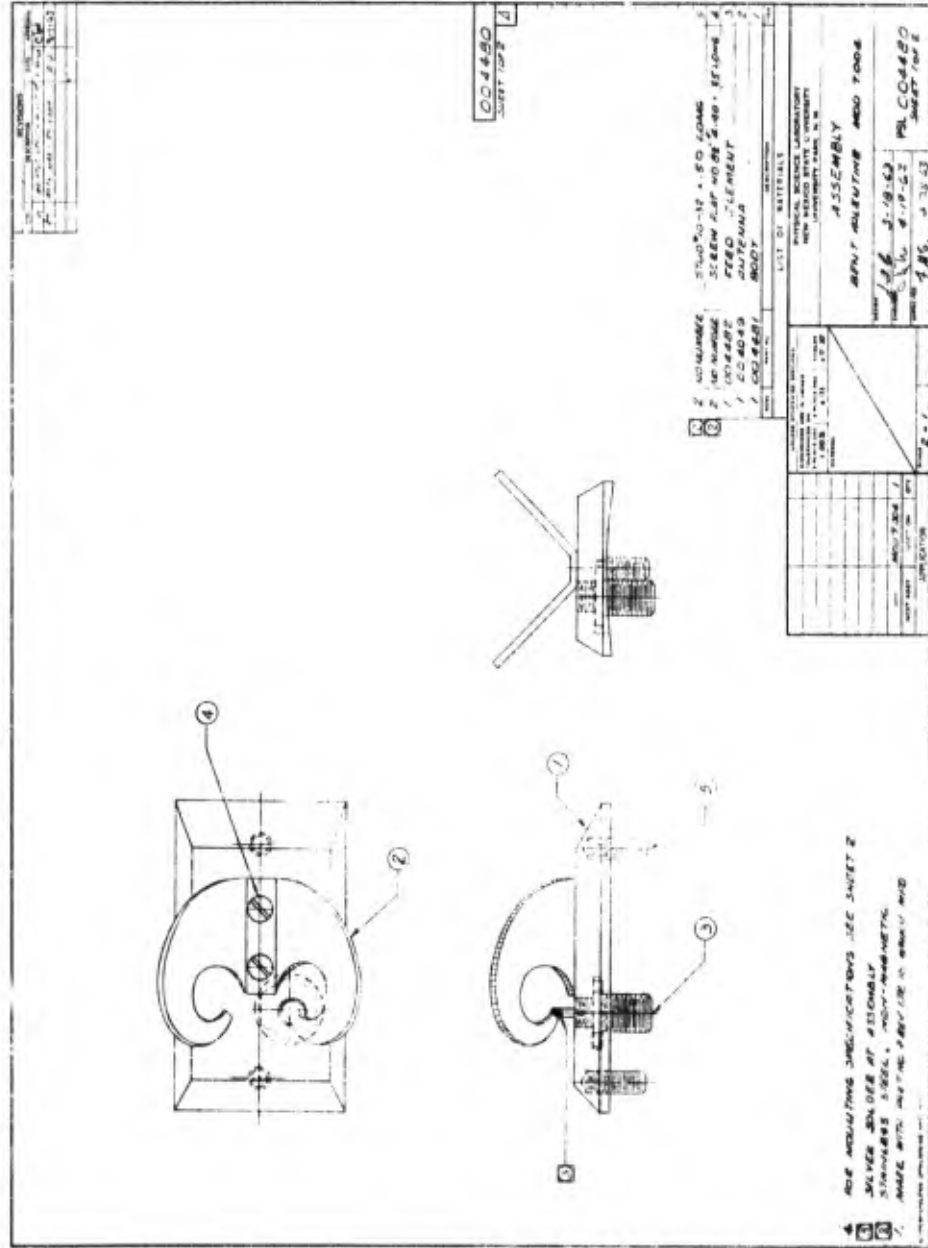


FIG. 103 - MODEL 7,004 C-BAND BEACON FOLDED VALENTINE ANTENNA

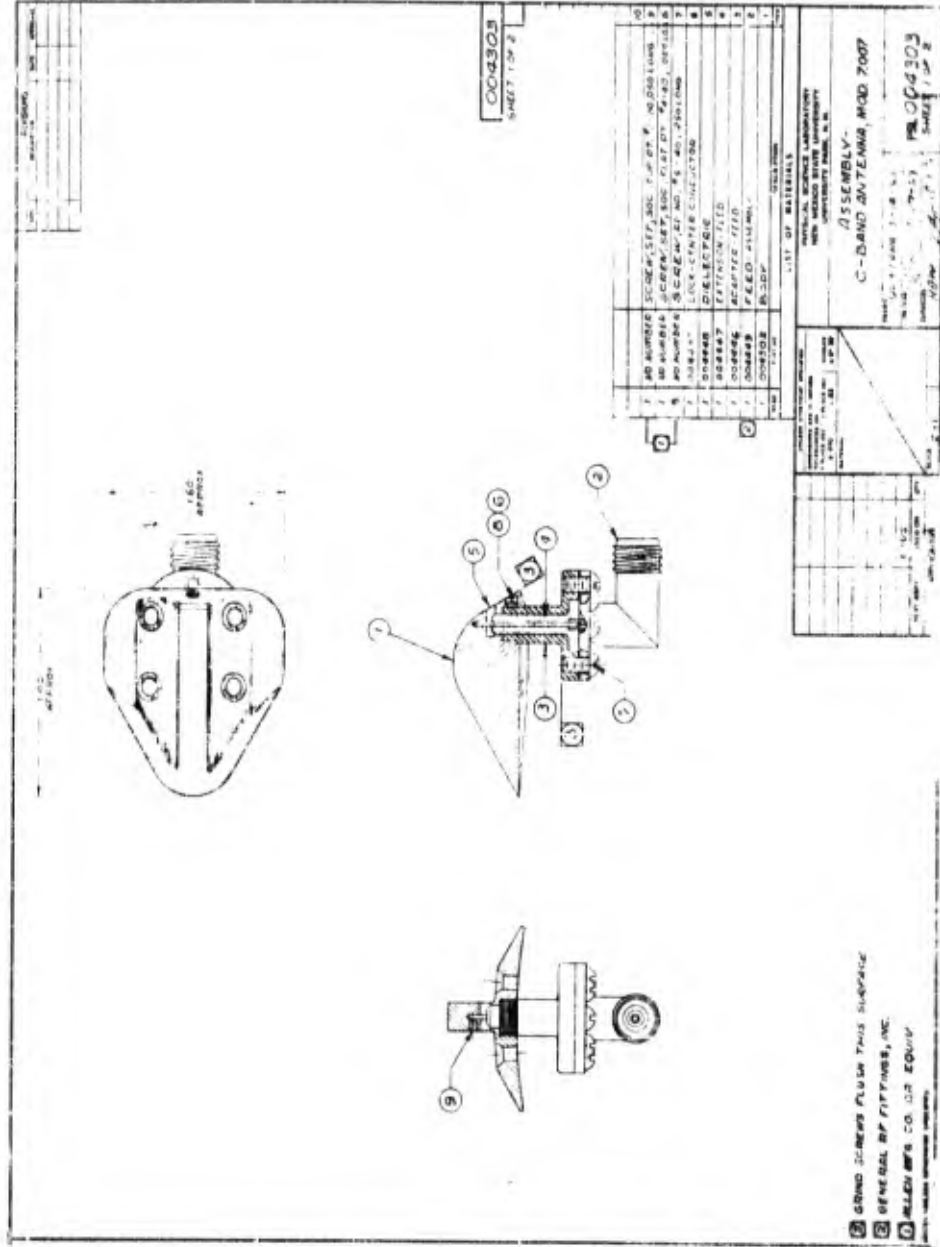
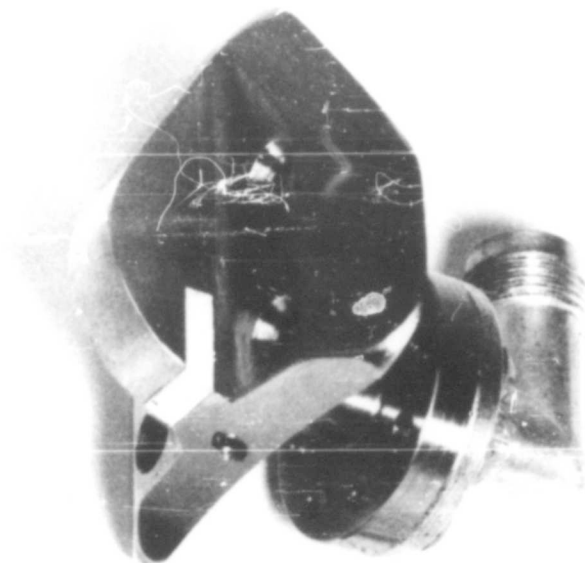


FIG 105 - MODEL 7.007 C-BAND BEACON QUADRALOOP ANTENNA



MOD 7.009 QUADRALOOP



FIG. 106 - PHOTOGRAPH OF MODEL 7.009 C-BAND BEACON QUADRALOOP ANTENNA

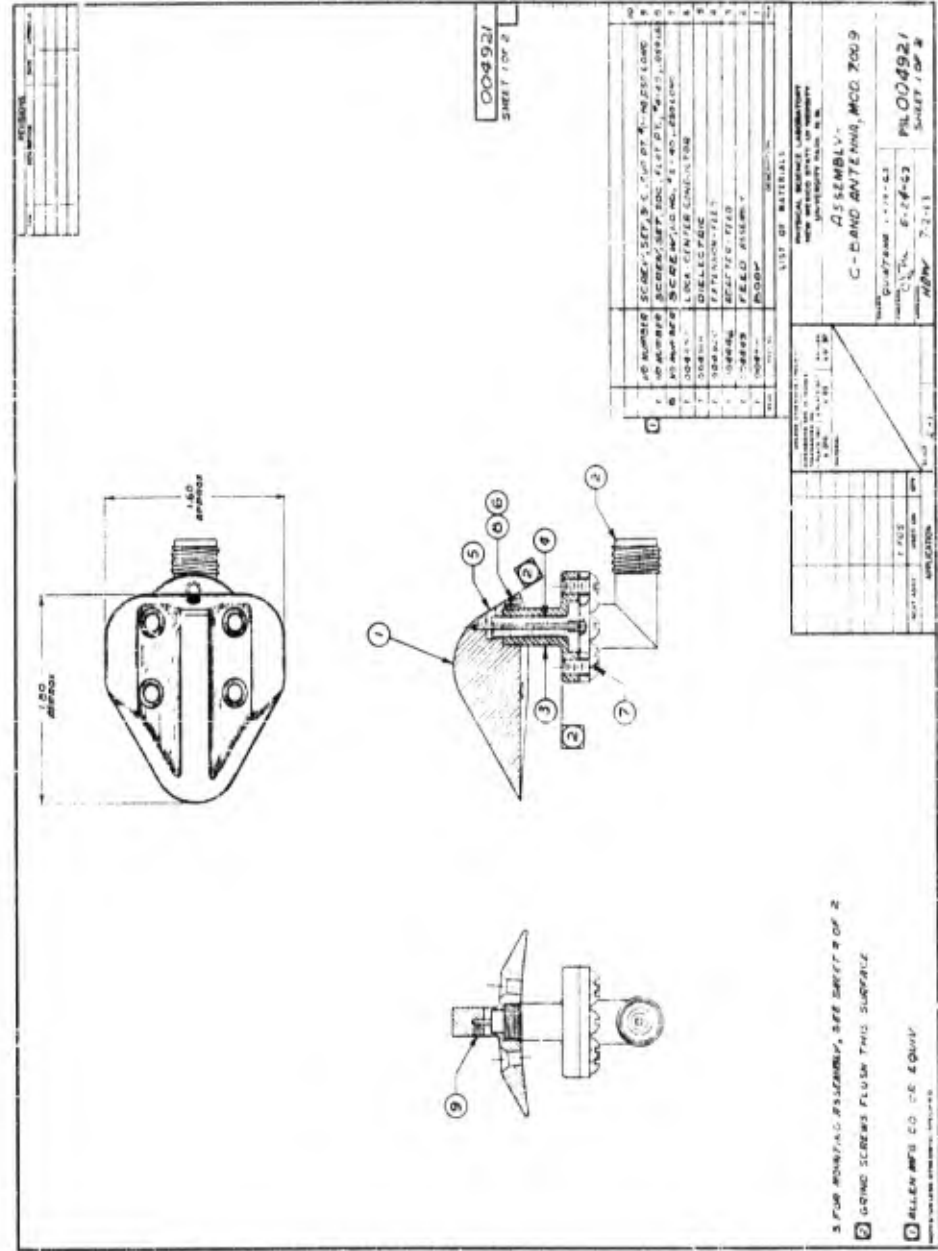


FIG. 107 - MODEL 7.009 C-BAND BEACON QUADRALOOP ANTENNA

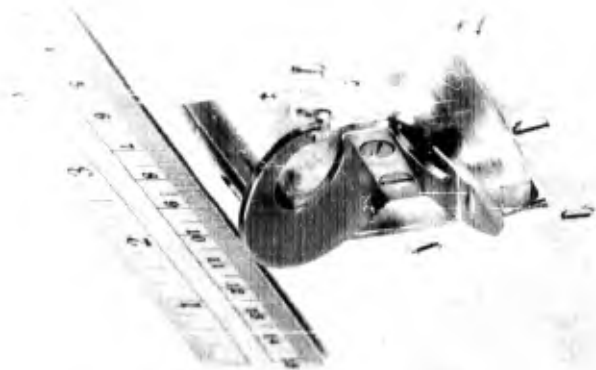


FIG. 108 - PHOTOGRAPH OF MODEL 7.008 C-BAND BEACON FOLDED
VALENTINE ANTENNA

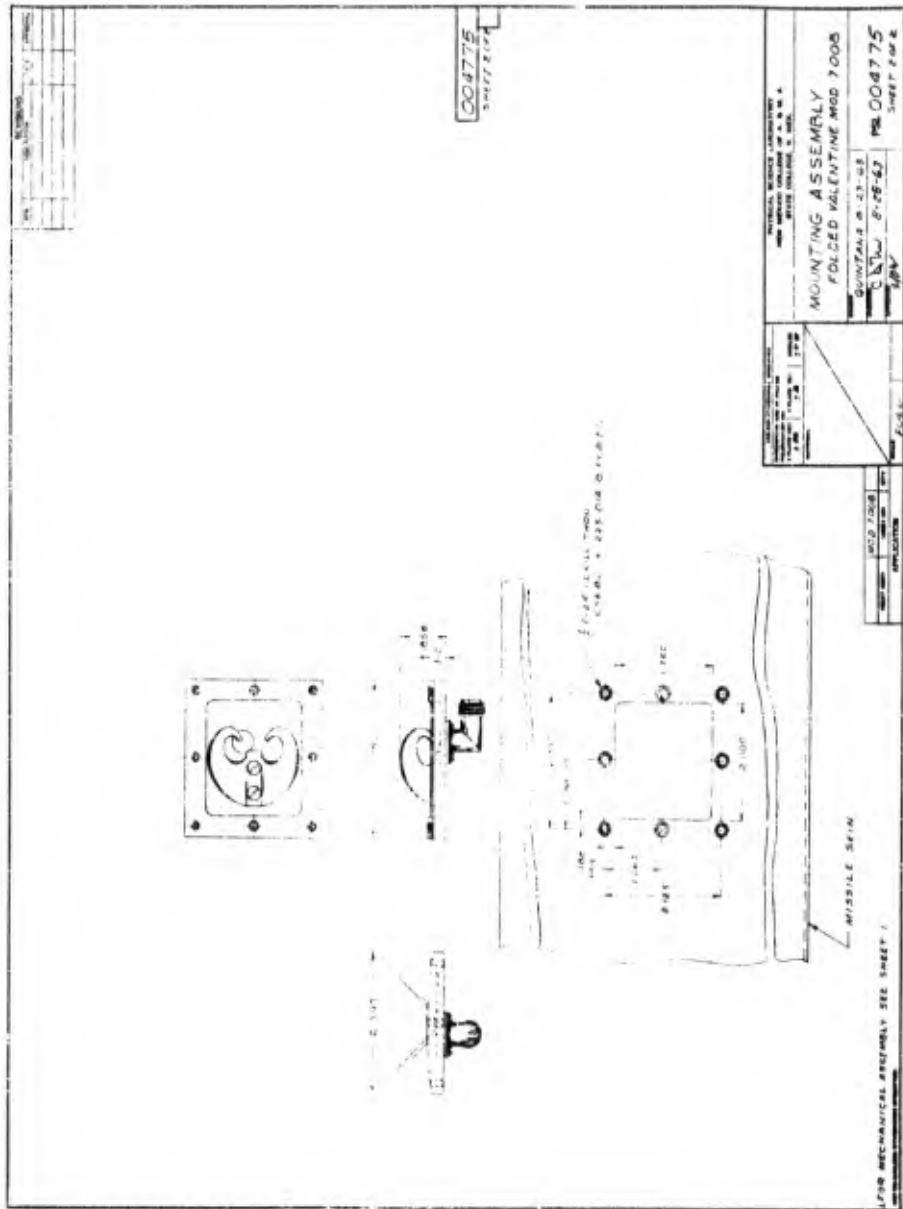


FIG. 109 - MODEL 7.008 C-BAND BEACON FOLDED VALENTINE ANTENNA



FIG. 110 - PHOTOGRAPH OF MODEL 10.004 35 MC/SEC
CIRCUMFERENTIAL QUADRALOOP ANTENNA

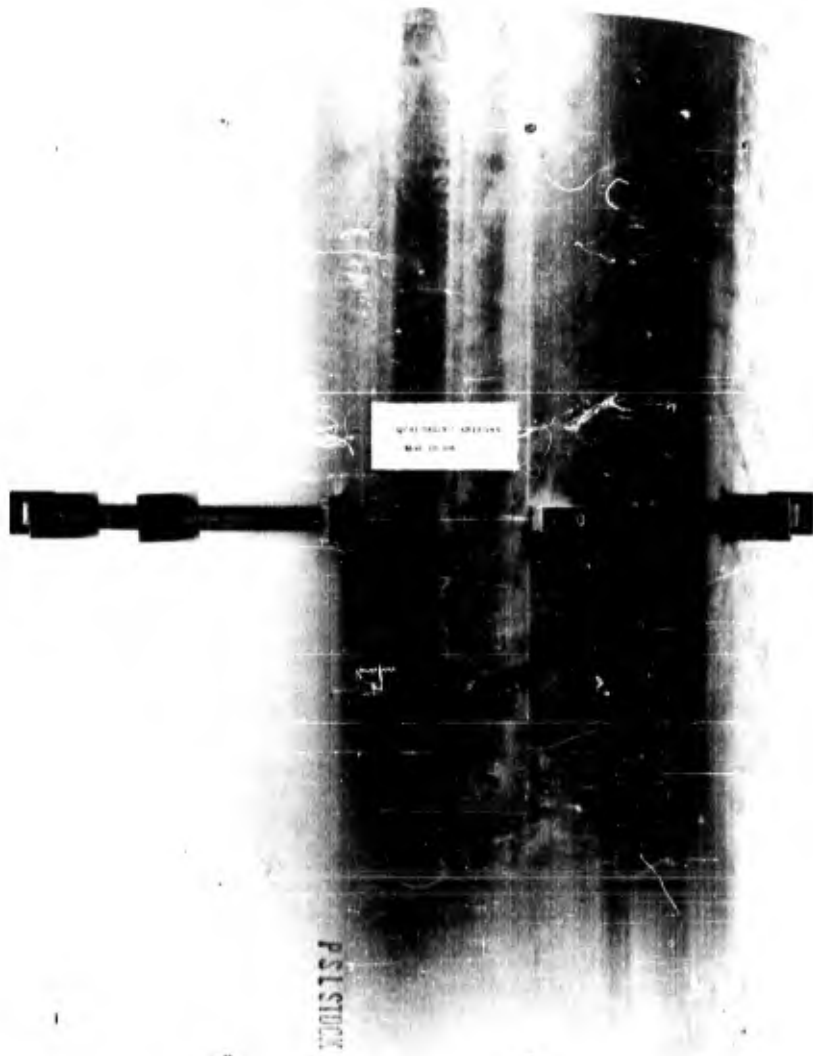


FIG. 112 - PHOTOGRAPH OF MODEL 10.006 35 Mc/SEC
CIRCUMFERENTIAL, QUADRALOOP ANTENNA

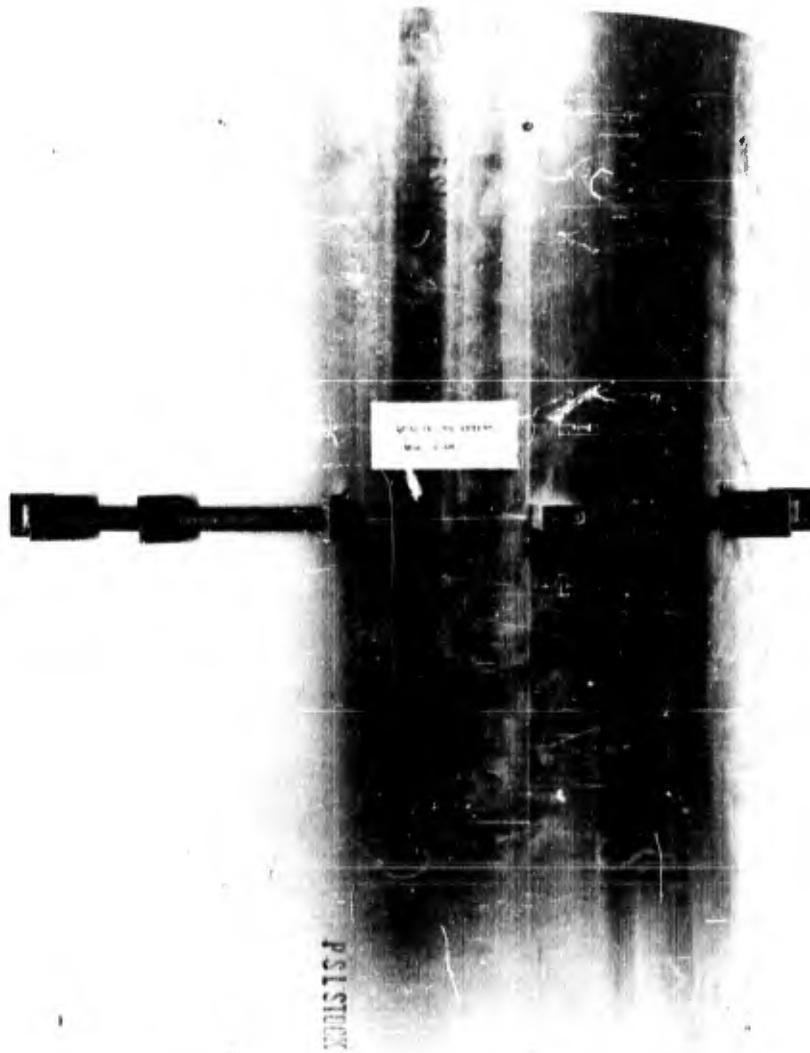


FIG. 112 - PHOTOGRAPH OF MODEL 10.006 35 MC/SEC
CIRCUMFERENTIAL QUADRALOOP ANTENNA

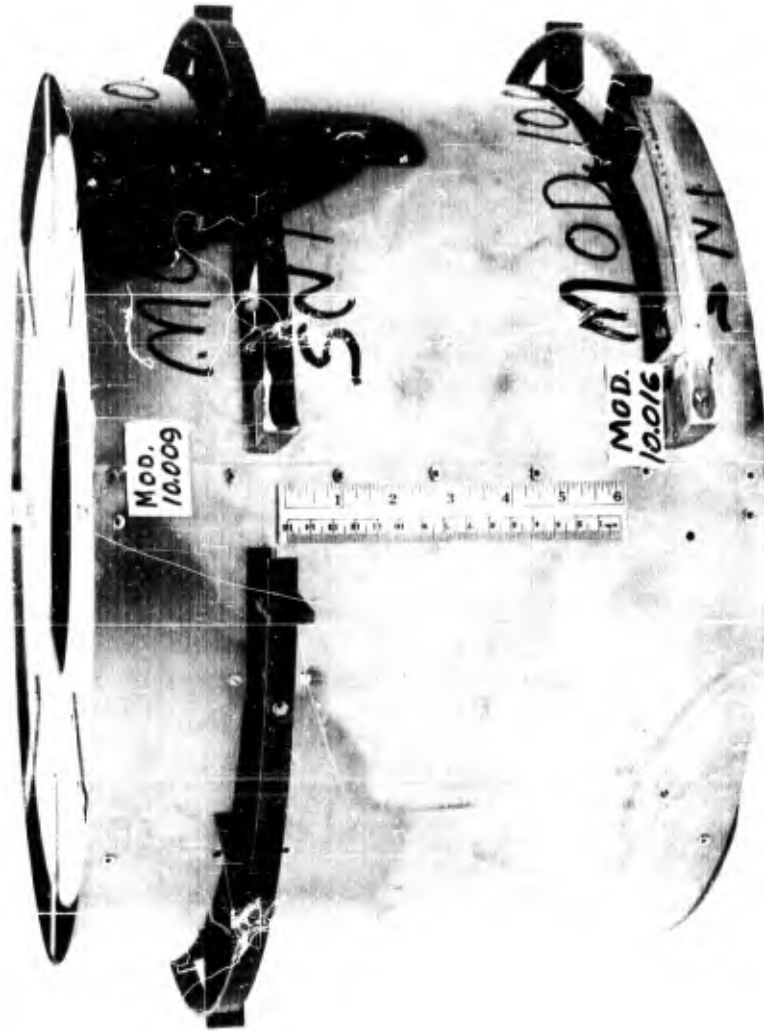


FIG. 113 - PHOTOGRAPH OF MODELS 10.009 AND 10.016
CIRCUMFERENTIAL QUADRALOOP ANTENNA

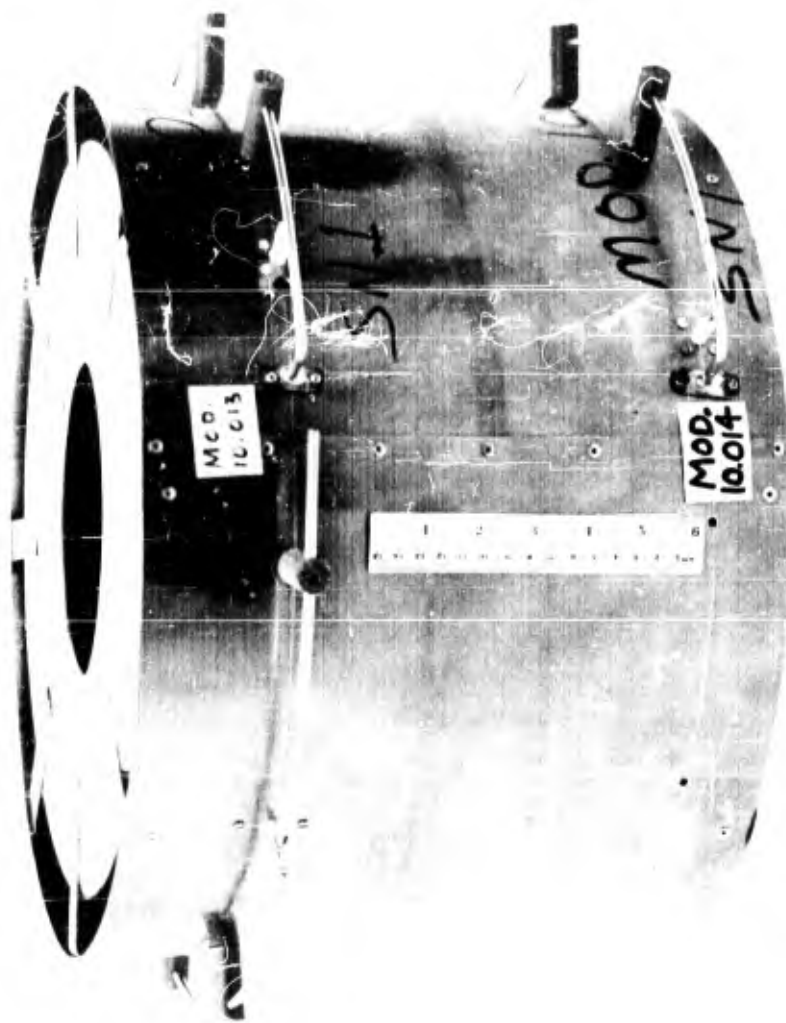


FIG. 114 - PHOTOGRAPH OF MODELS 10.013 AND 10.014
CIRCUMFERENTIAL QUADRALOOP ANTENNA

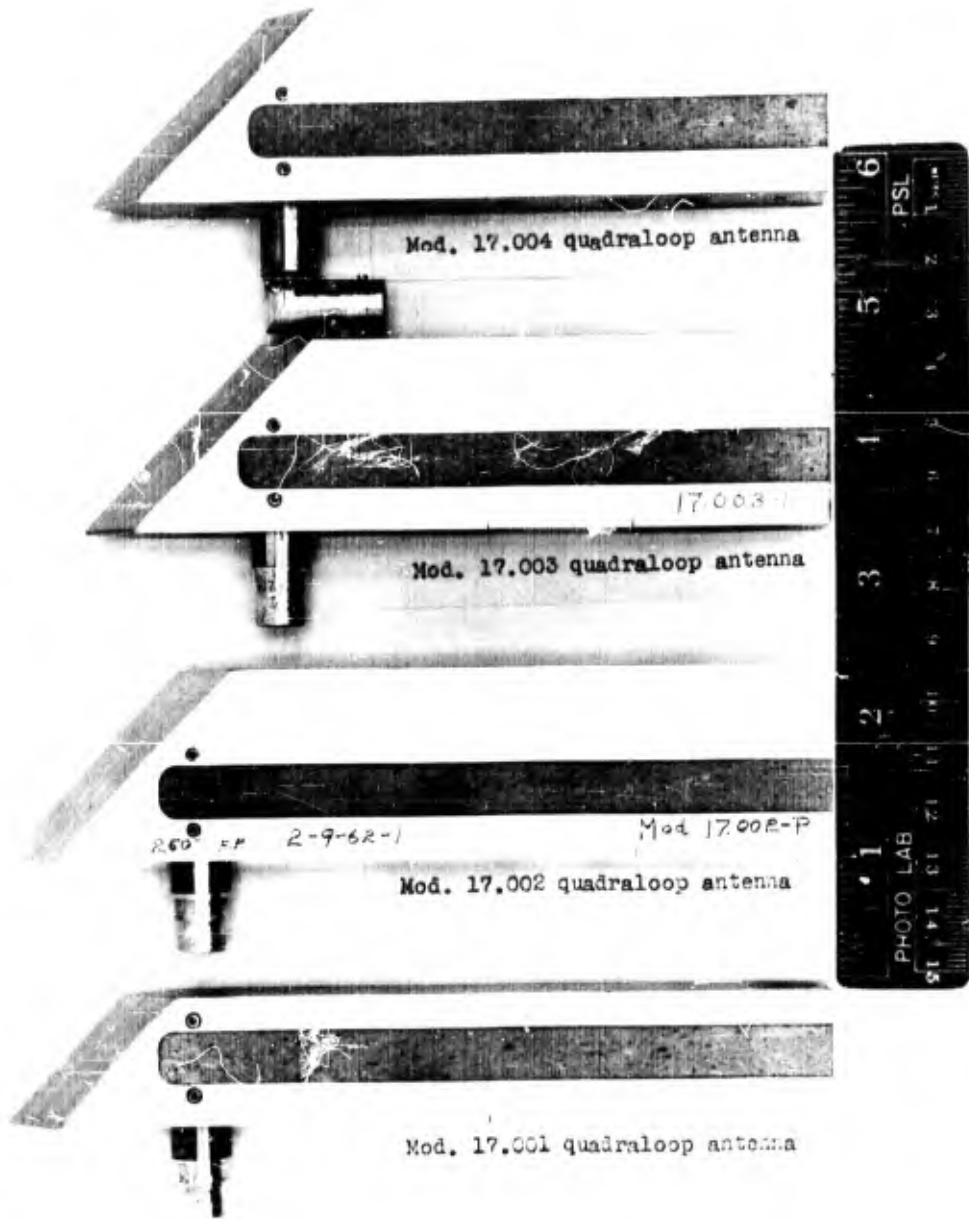


FIG. 116 - PHOTOGRAPH OF MODELS 17.001 THROUGH 17.004
P-BAND QUADRALOOP ANTENNA

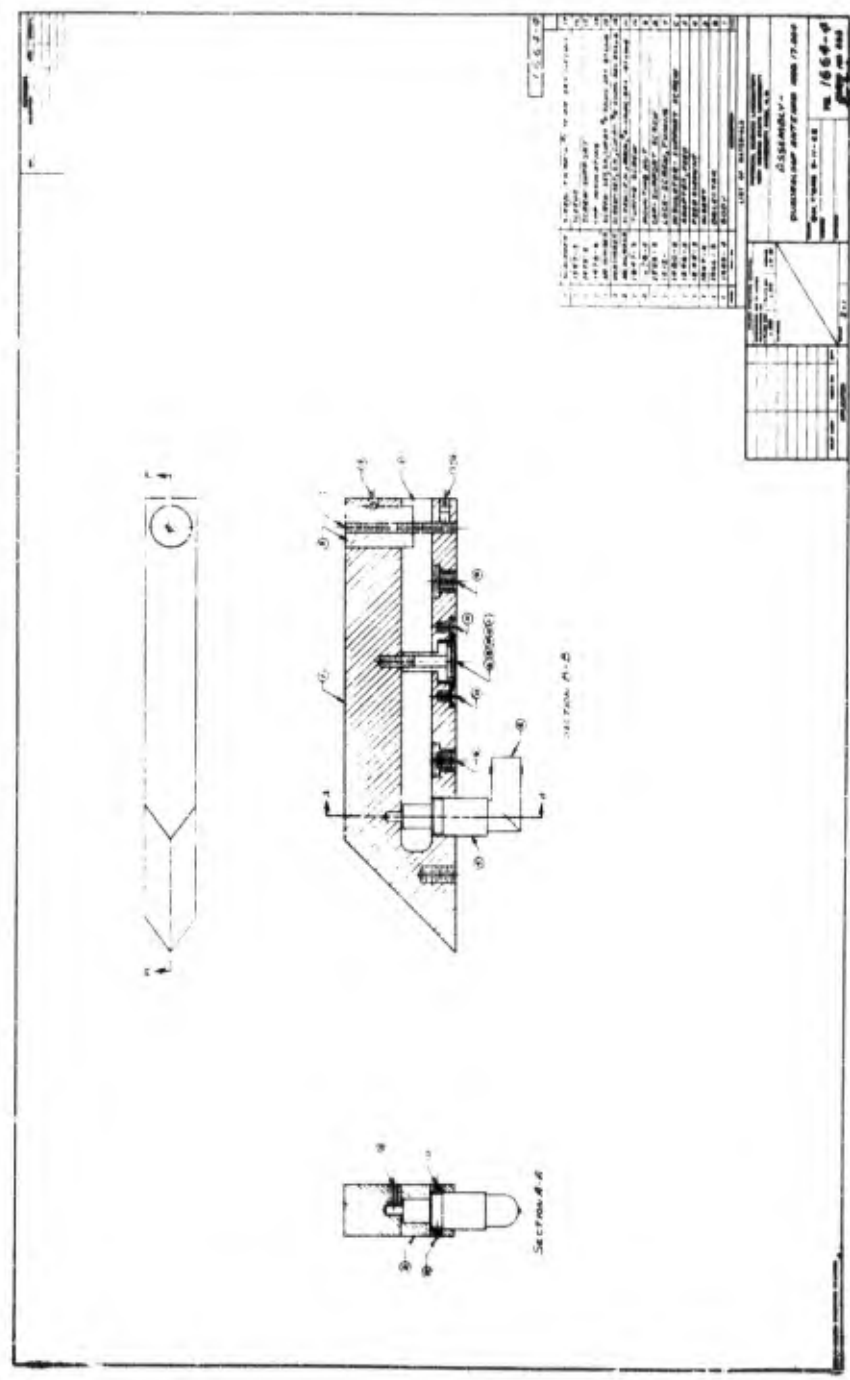


FIG 117 - MODEL 17.004 P-BAND QUADRALOOP ANTENNA

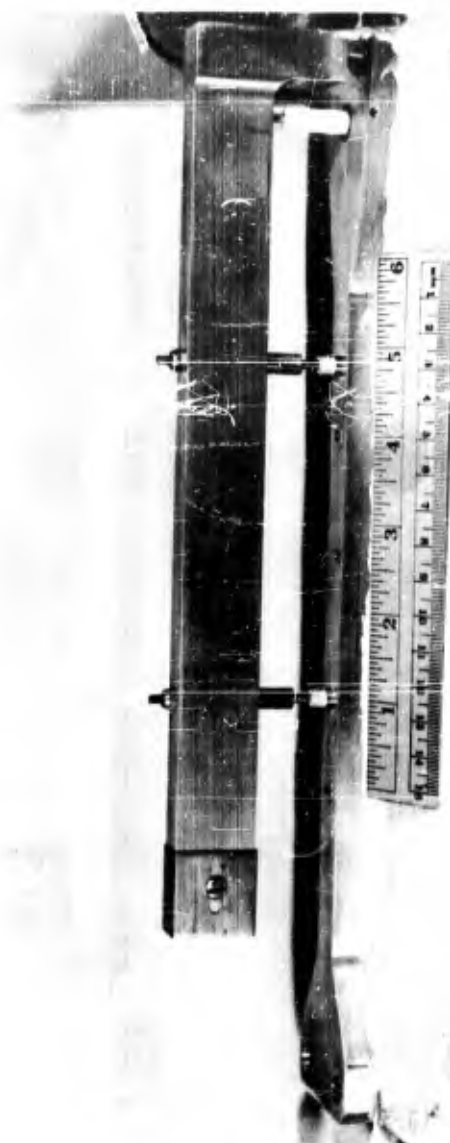


FIG. 118 - PHOTOGRAPH OF MODEL 20,004 QUADRATURE
ANTENNA IN THE 130 MC/SEC FREQUENCY
RANGE

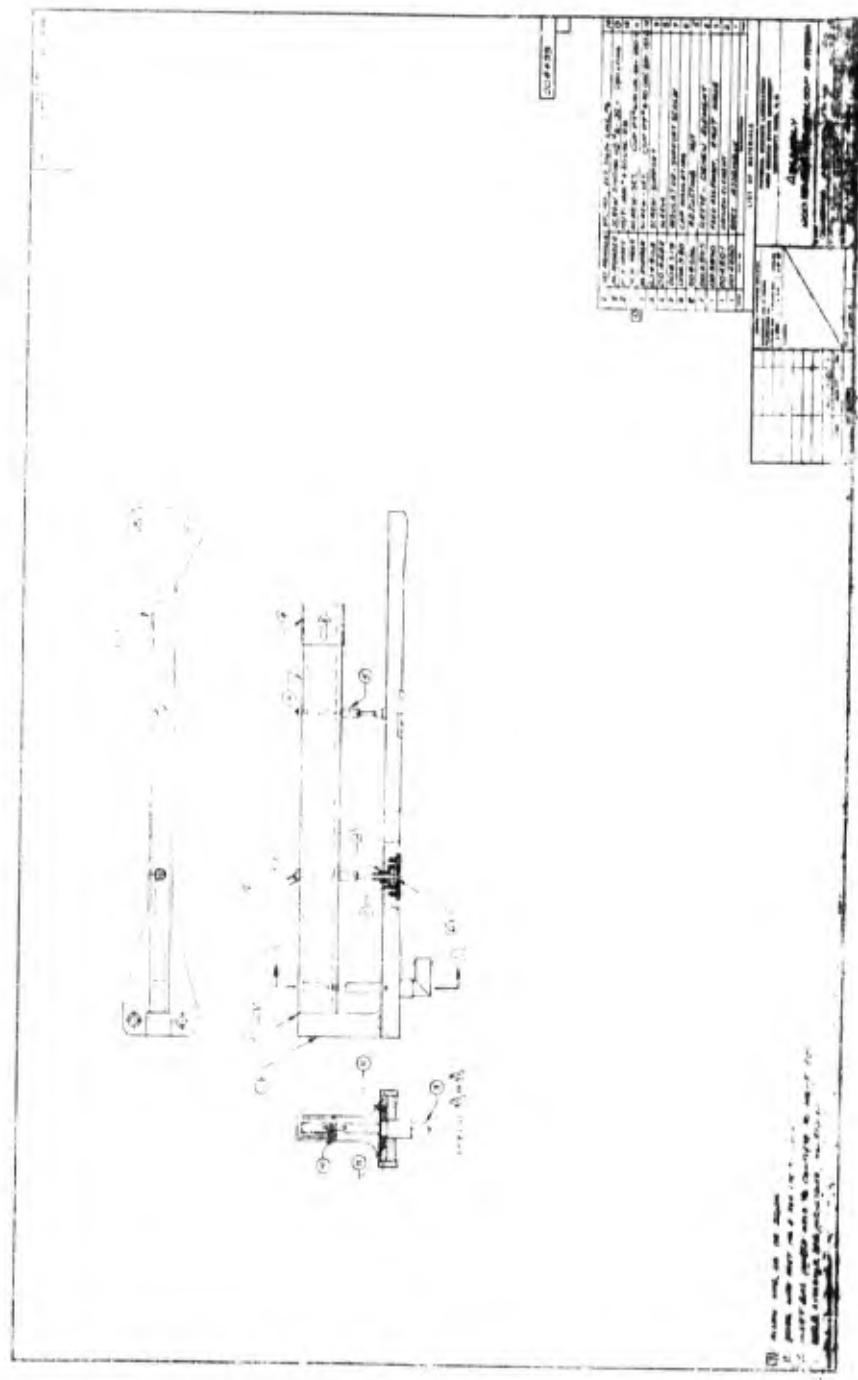


FIG 119 - MODEL 20 004 QUADRALOOP ANTENNA



FIG. 120 - PHOTOGRAPH OF MODEL 23.005 TELEMETRY GAP FED
OBLIQUE STUB ANTENNA

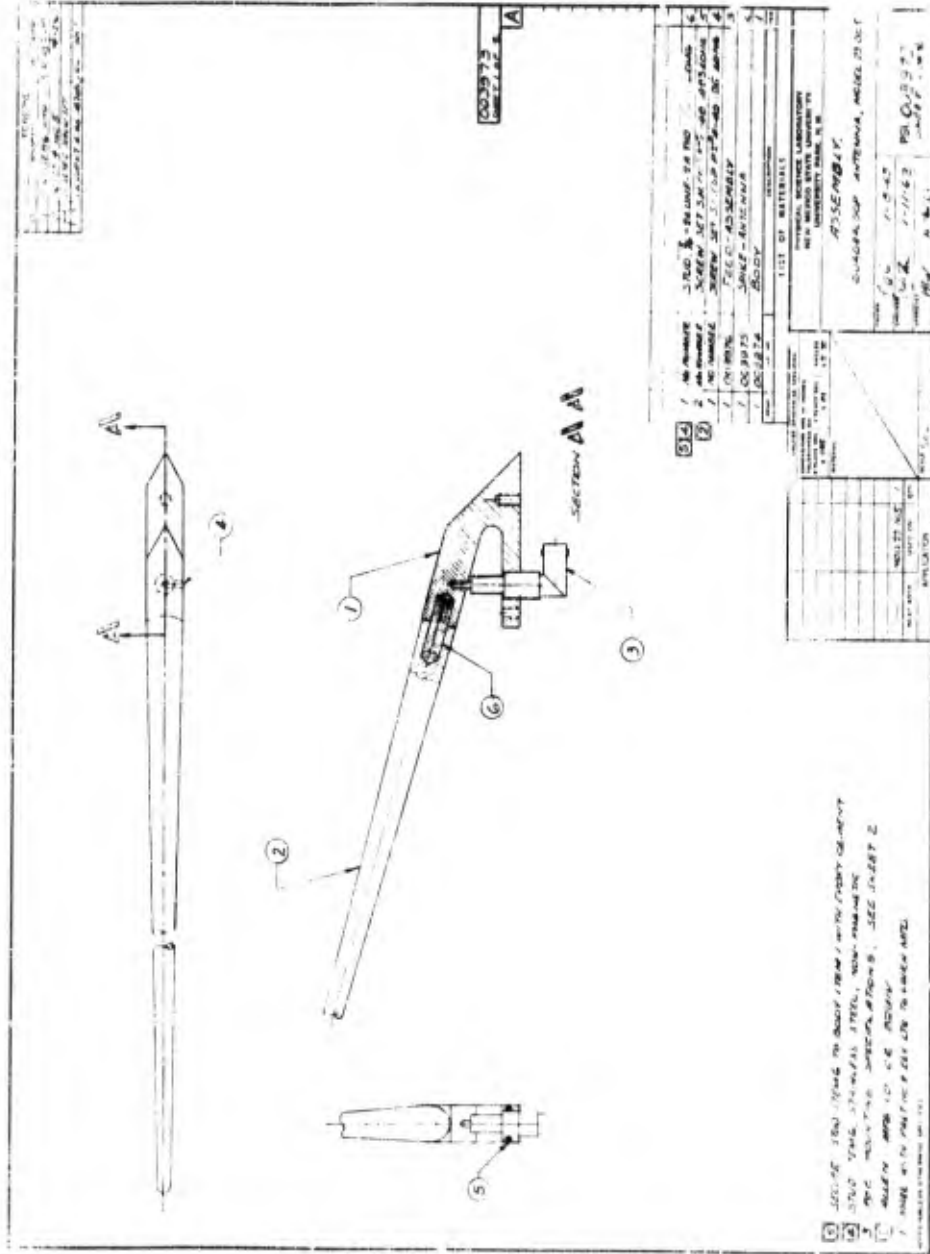


FIG. 121 - MODEL 23.005 TELEMETRY GAP FED OBLIQUE STUB ANTENNA

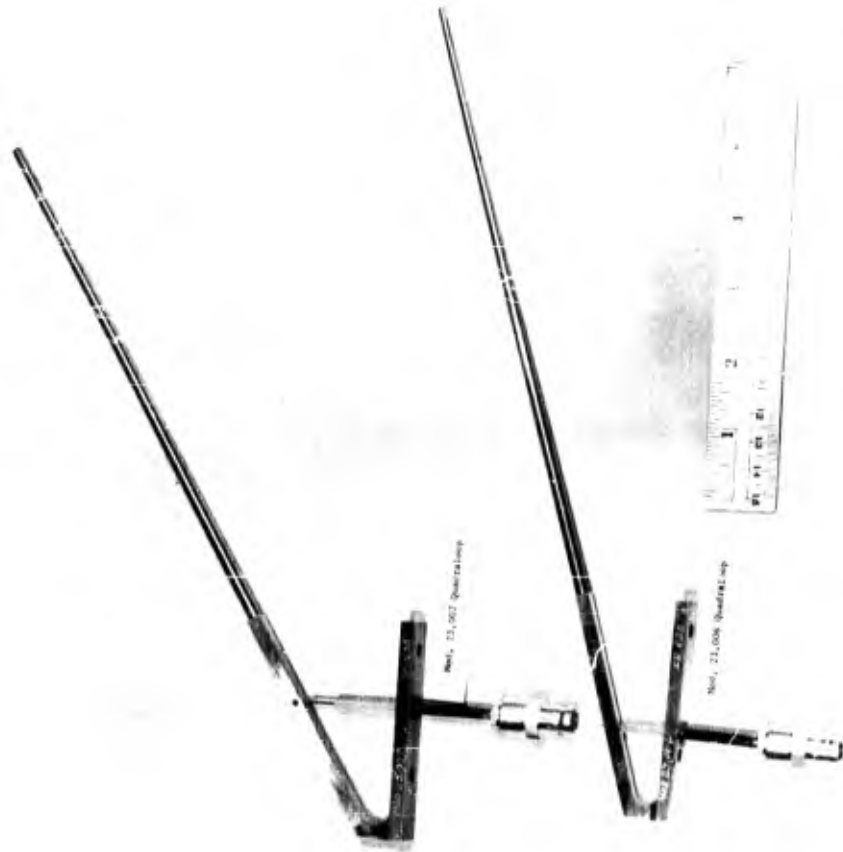


FIG. 122 - PHOTOGRAPH OF MODELS 23.006 AND 23.007 TELEMETRY
GAP FED OBLIQUE STUB ANTENNAS

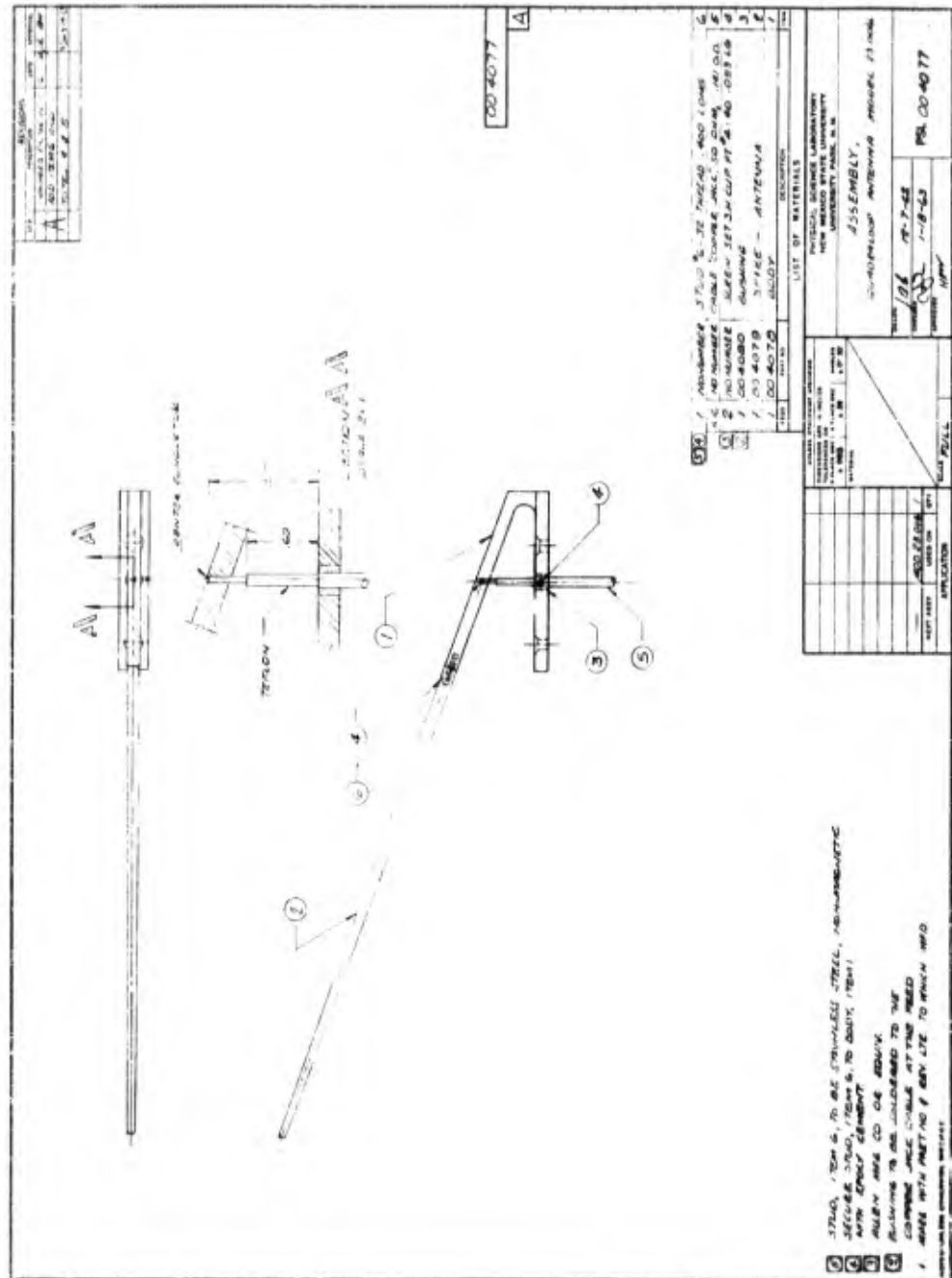


FIG. 123 - MODEL 23.006 TELEMETRY GAP FED OBLIQUE STUB ANTENNA

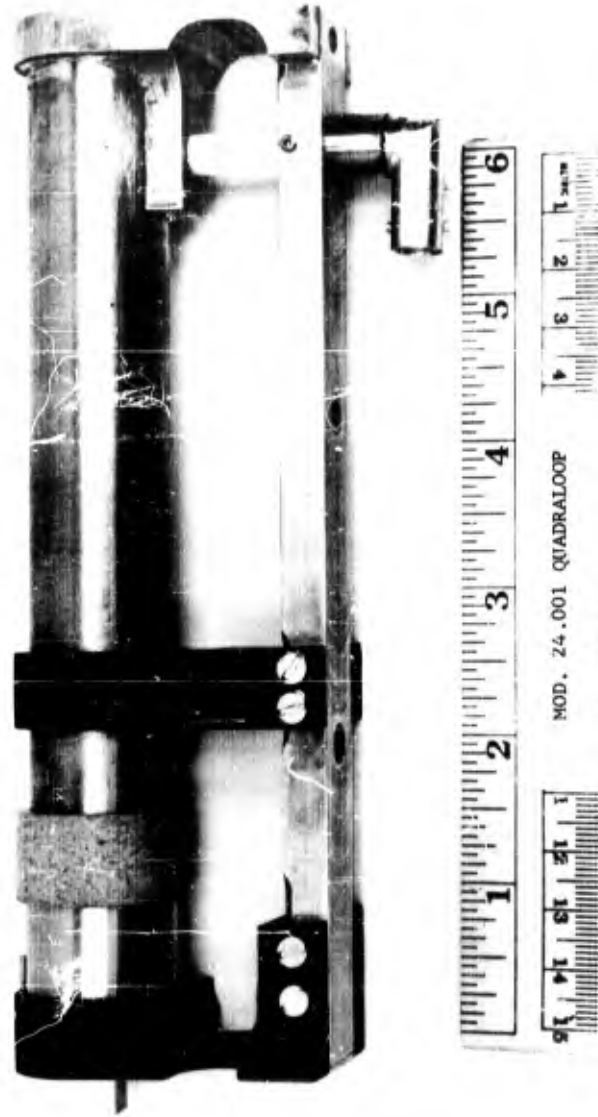


FIG. 124 - PHOTOGRAPH OF MODEL 24,001 TELEMETRY QUADRALOOP ANTENNA (PROTOTYPE)

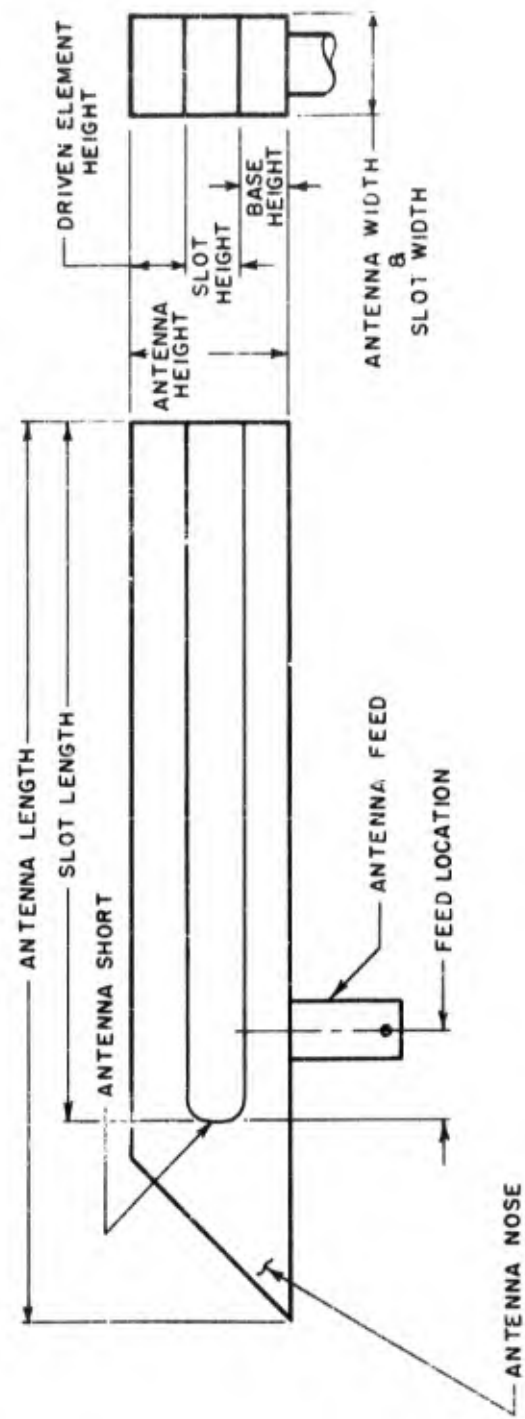


FIG. 126 - ILLUSTRATION OF QUADRALOOP PARTS AND DIMENSIONS

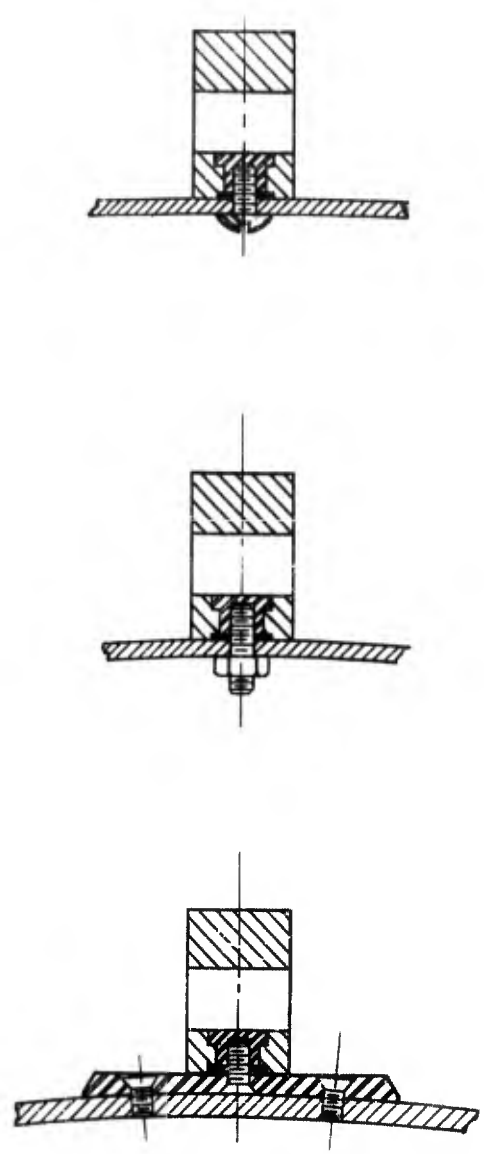


FIG. 127 - SKETCH OF ANTENNA MOUNTING

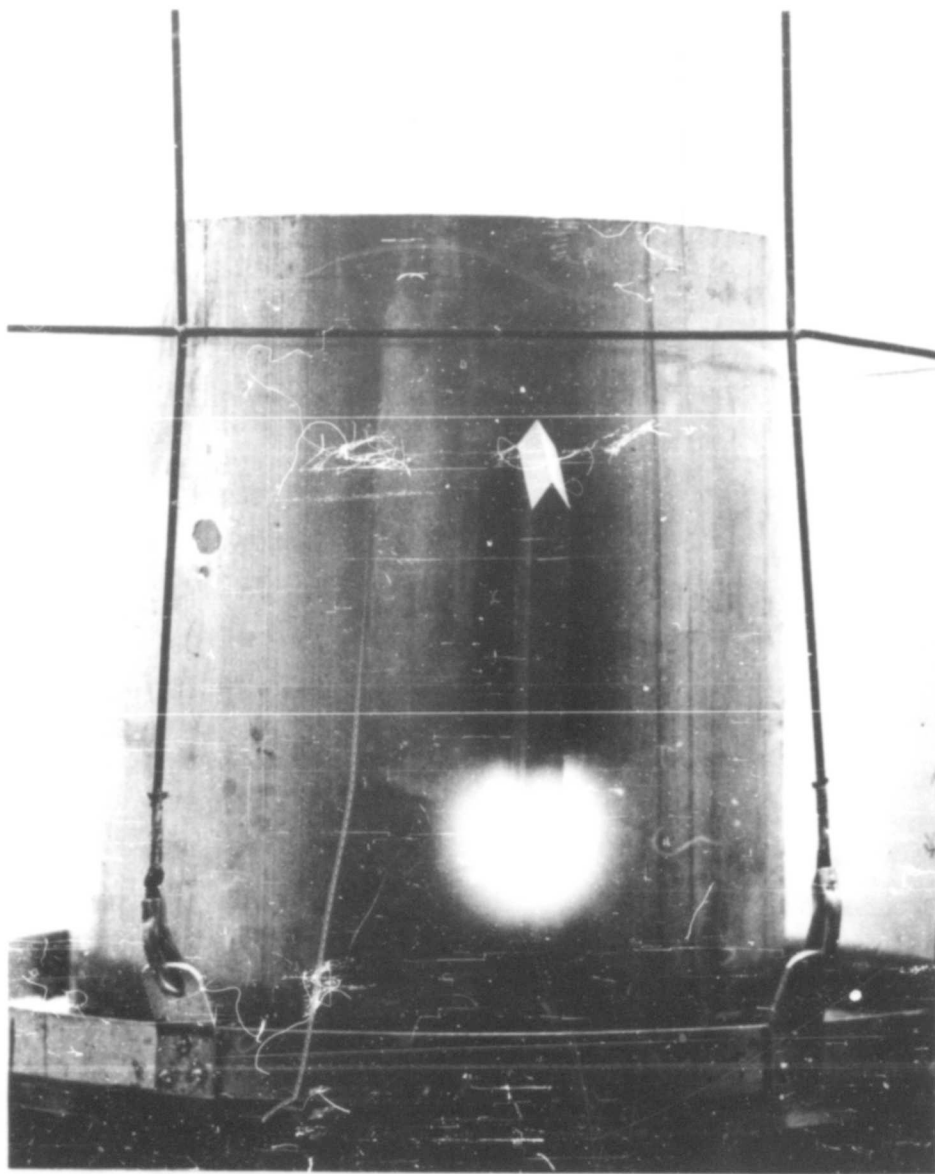


FIG. 128 - PHOTOGRAPH OF DIFFUSION BREAKDOWN

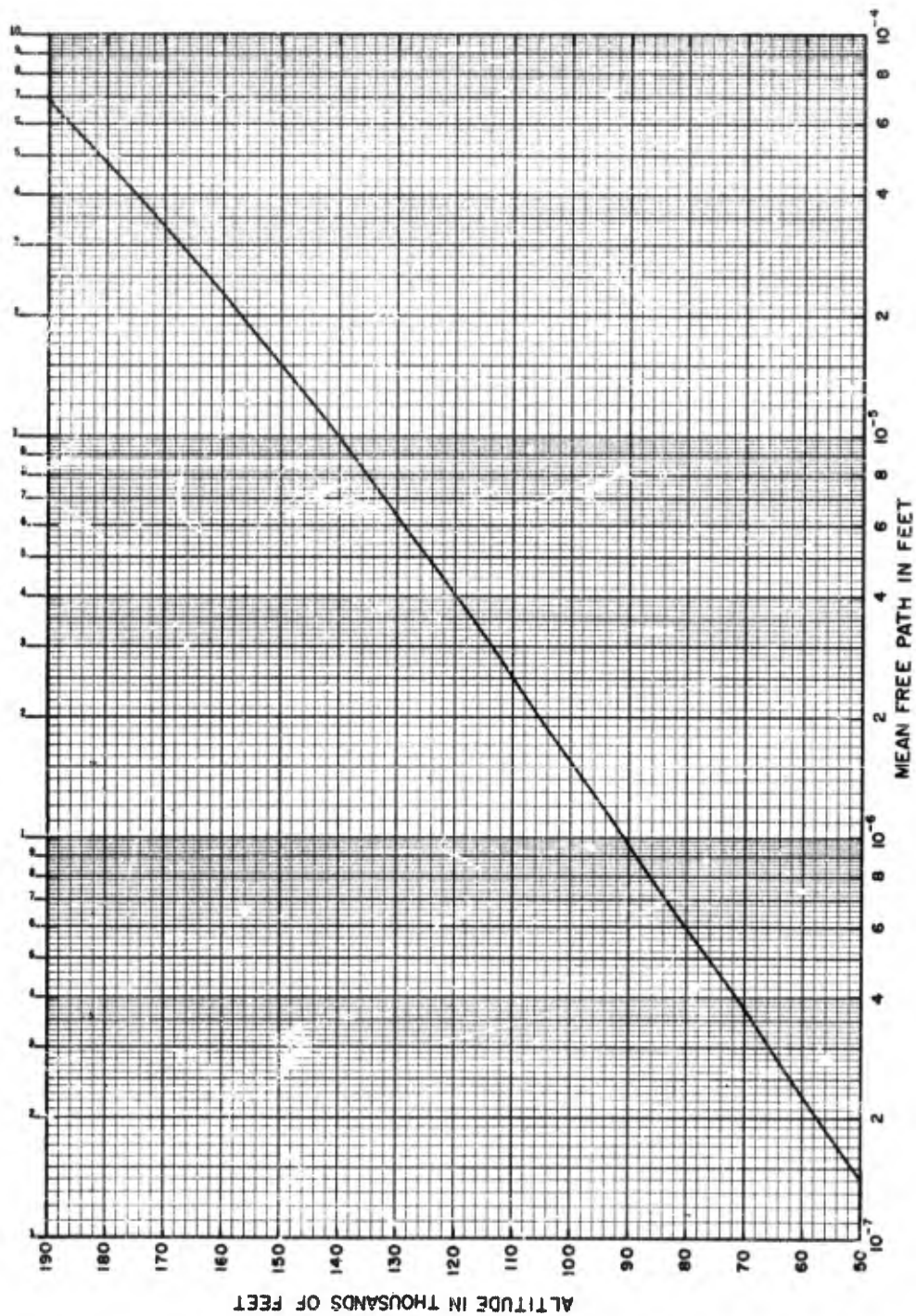


FIG. 129 - CURVE OF ALTITUDE VERSUS MEAN FREE PATH OF MOLECULES FROM 50,000 TO 190,000 FEET ALTITUDE

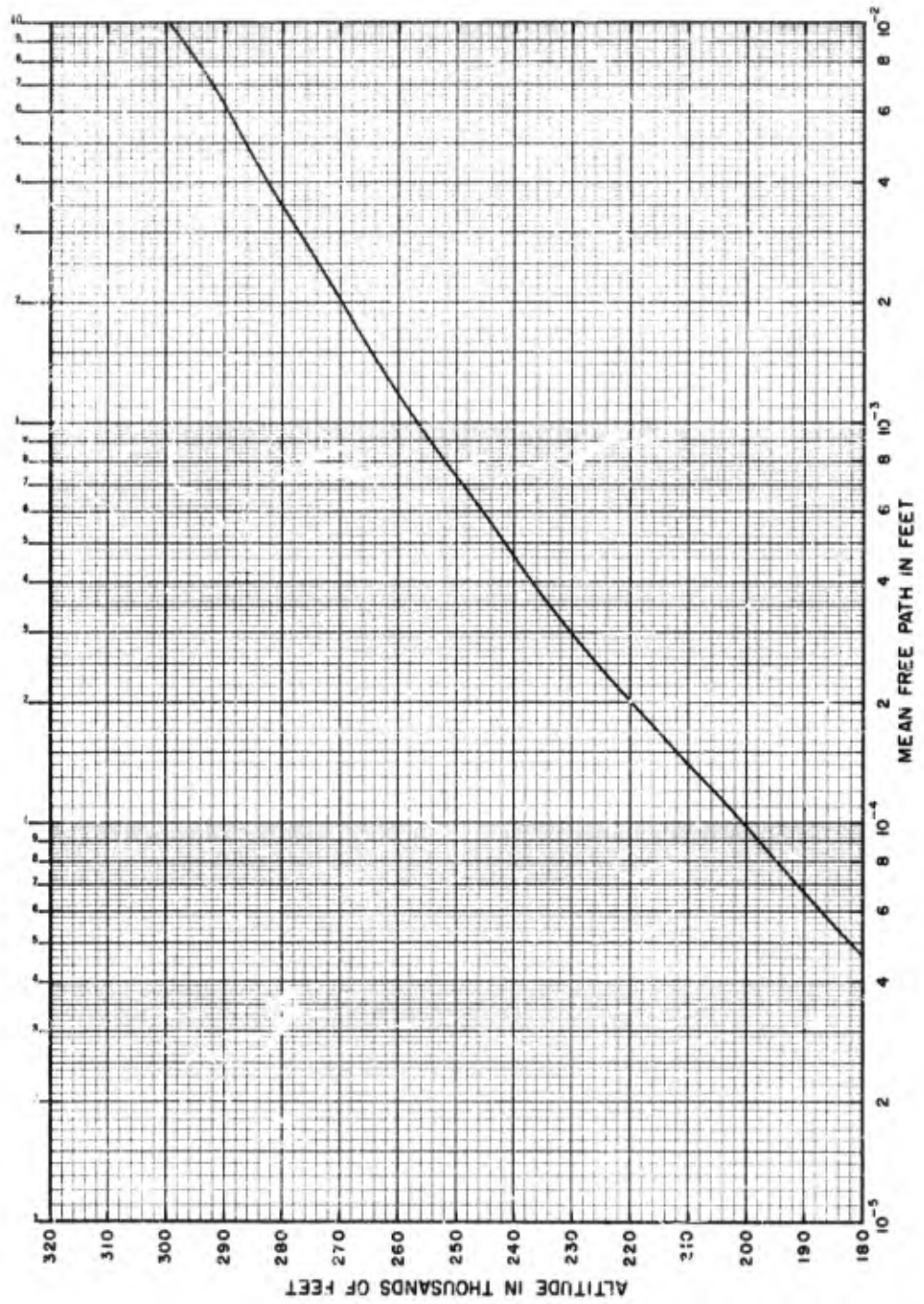


FIG 130 - CURVE OF ALTITUDE VERSUS MEAN FREE PATH OF MOLECULES FROM 180,000 TO 320,000 FEET ALTITUDE

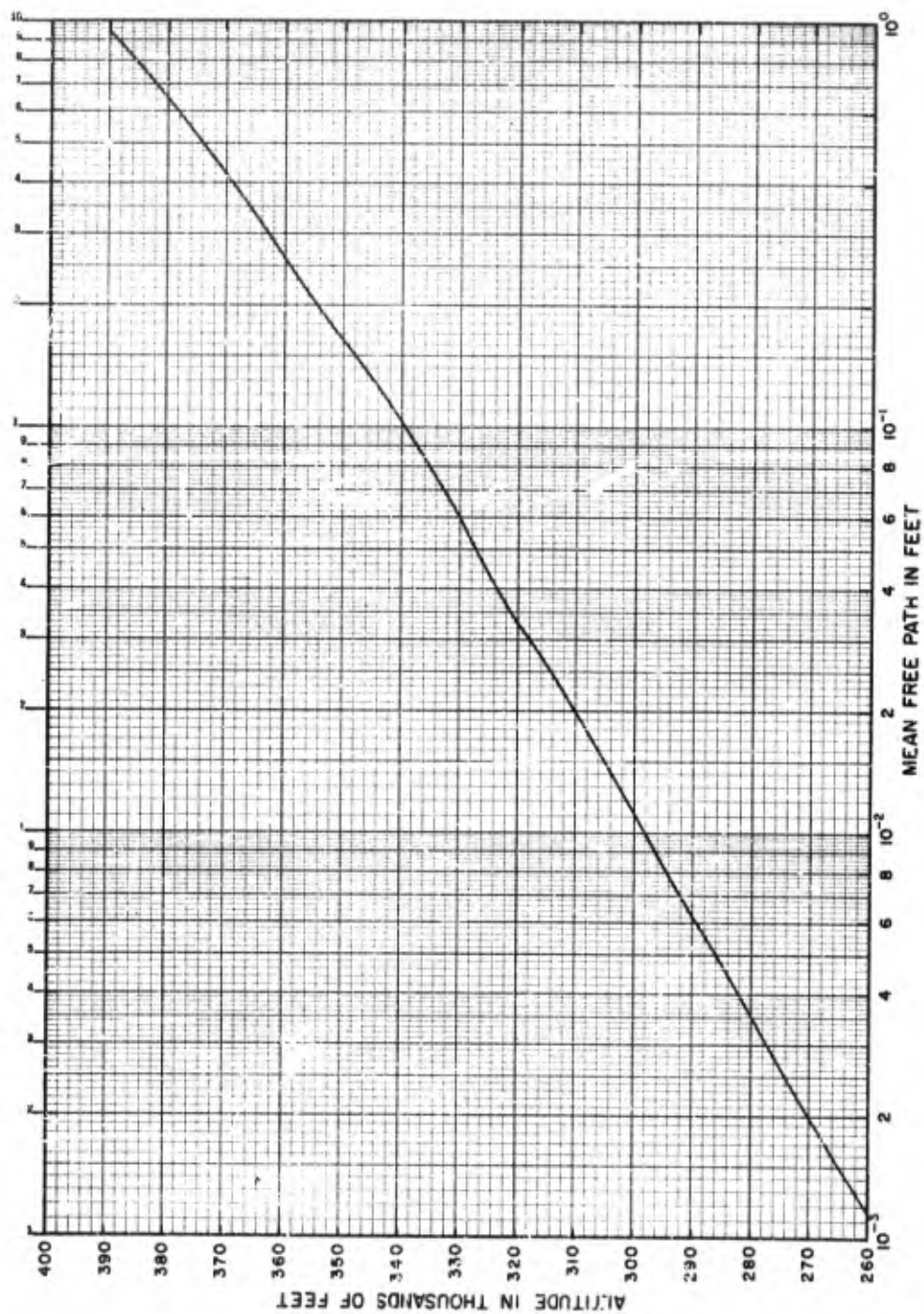


FIG. 131 - CURVE OF ALTITUDE VERSUS MEAN FREE PATH OF MOLECULES
FROM 260,000 TO 400,000 FEET ALTITUDE

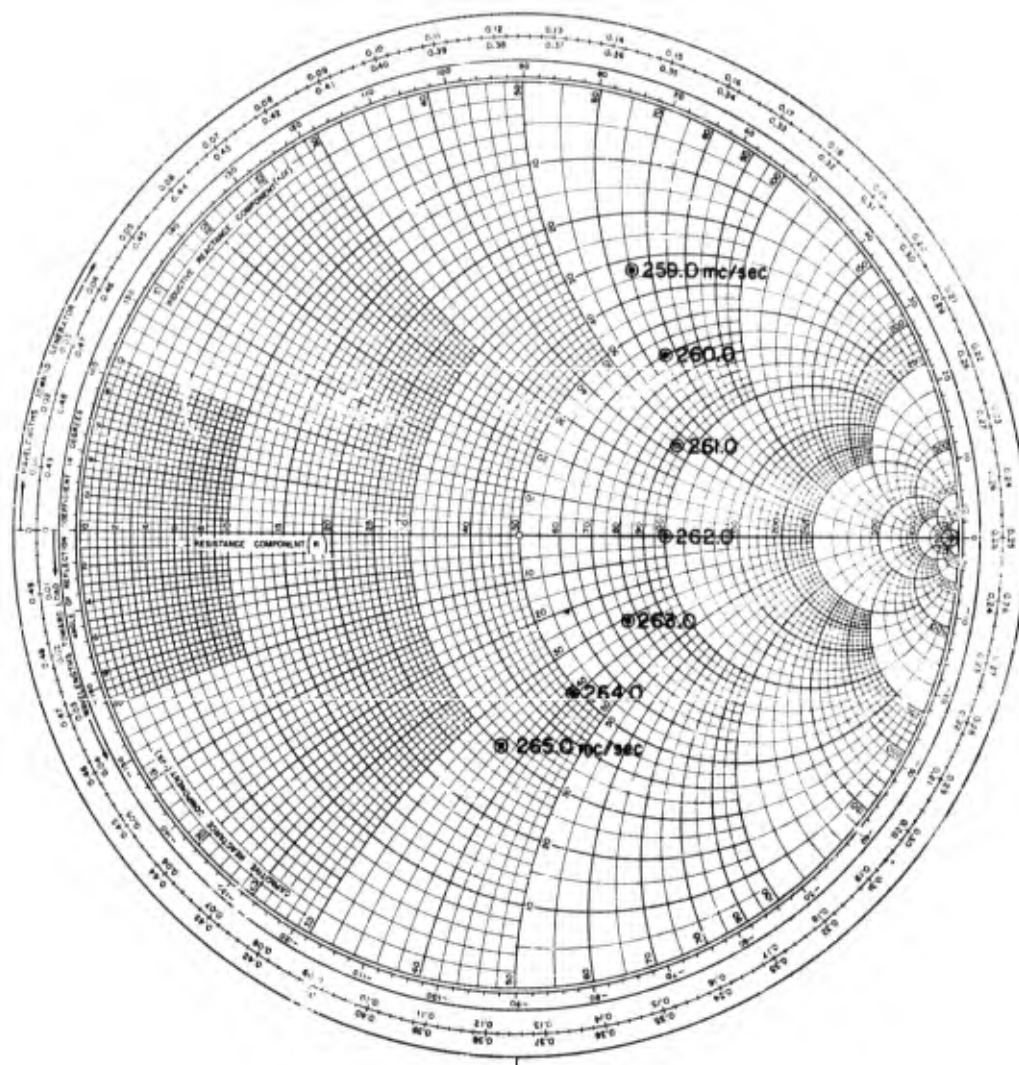


FIG. 132 - IDEALIZED IMPEDANCE CURVE OF A 2.000 SERIES, 1.5-INCH HIGH TELEMETRY QUADRALOOP ANTENNA, MOUNTED ON A 15-INCH DIAMETER CYLINDER

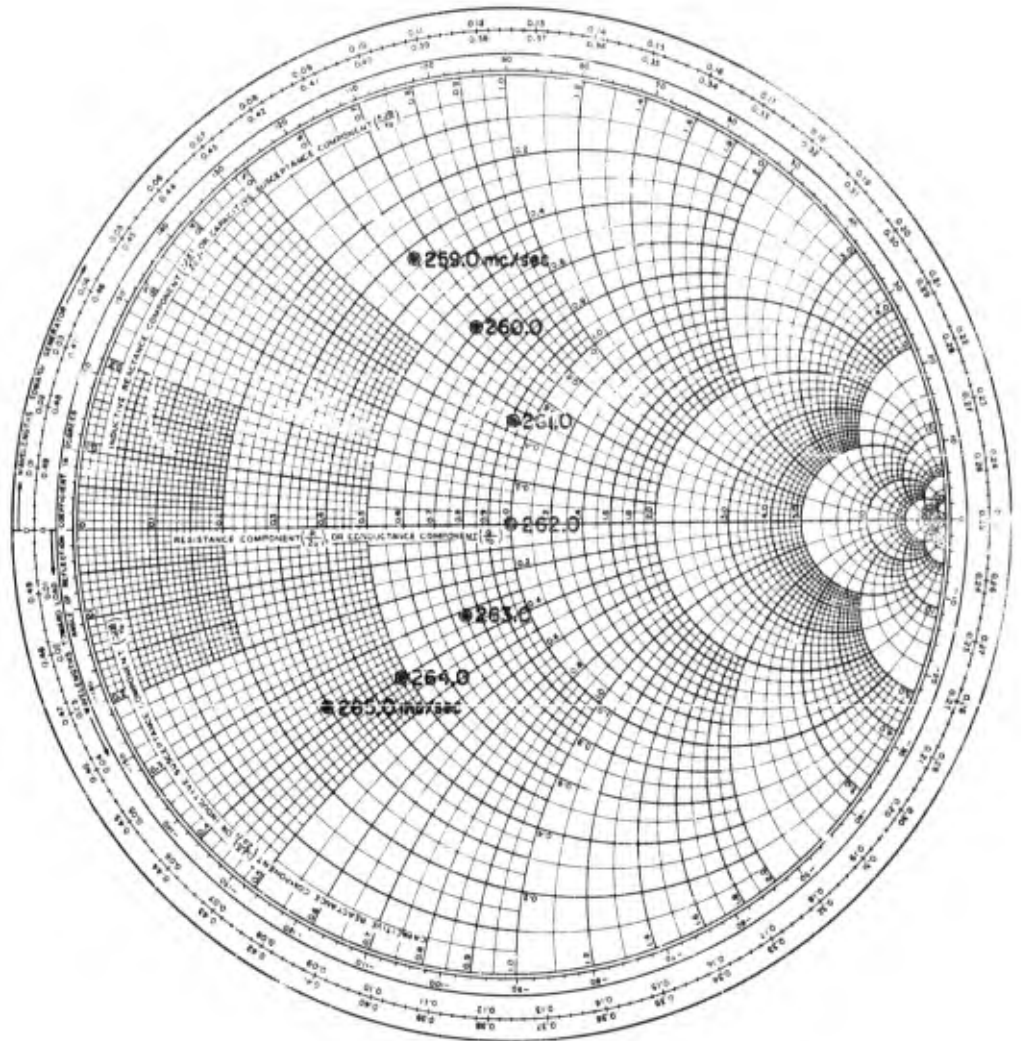


FIG. 133 - NORMALIZED IMPEDANCE CURVE OF A 2.000 SERIES, 1.5-INCH HIGH TELEMETRY QUADRALOOP ANTENNA

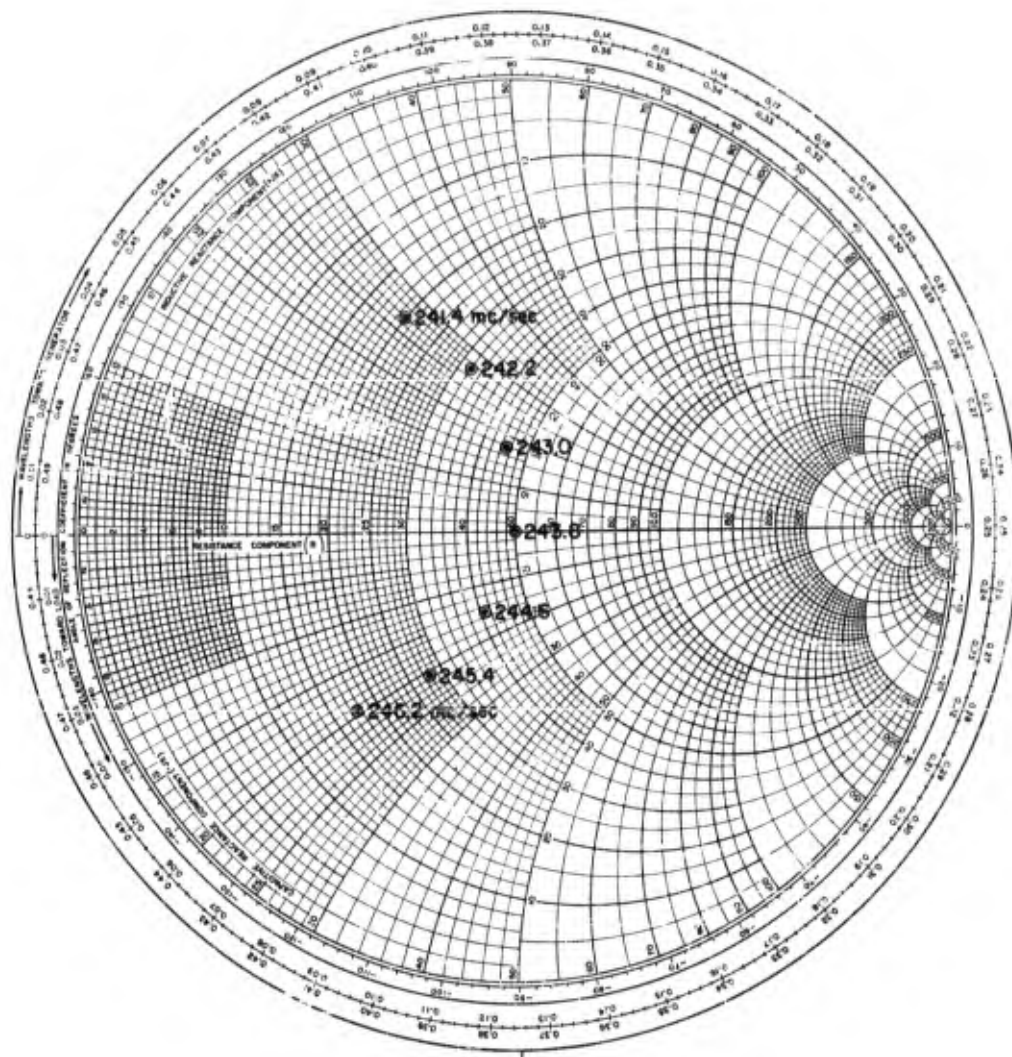


FIG. 134 - IDEALIZED IMPEDANCE CURVE OF A TWO ELEMENT ARRAY
 FED 180° OUT OF PHASE OF THE 2.000 SERIES, 1.5-INCH
 HIGH TELEMETRY QUADFALOOP MOUNTED ON A
 15-INCH DIAMETER CYLINDER

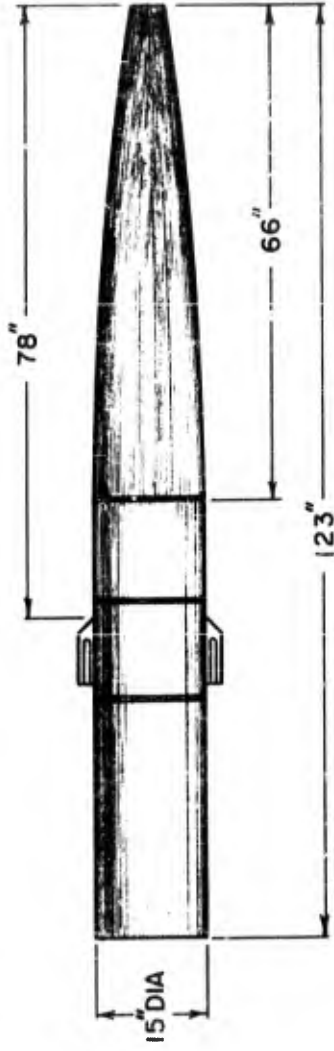


FIG. 135 - SKETCH OF THE VEHICLE MOCKUP FOR THE MODEL 2.011 TELEMETRY
QUADRALOOP ANTENNA RADIATION PATTERN MEASUREMENTS

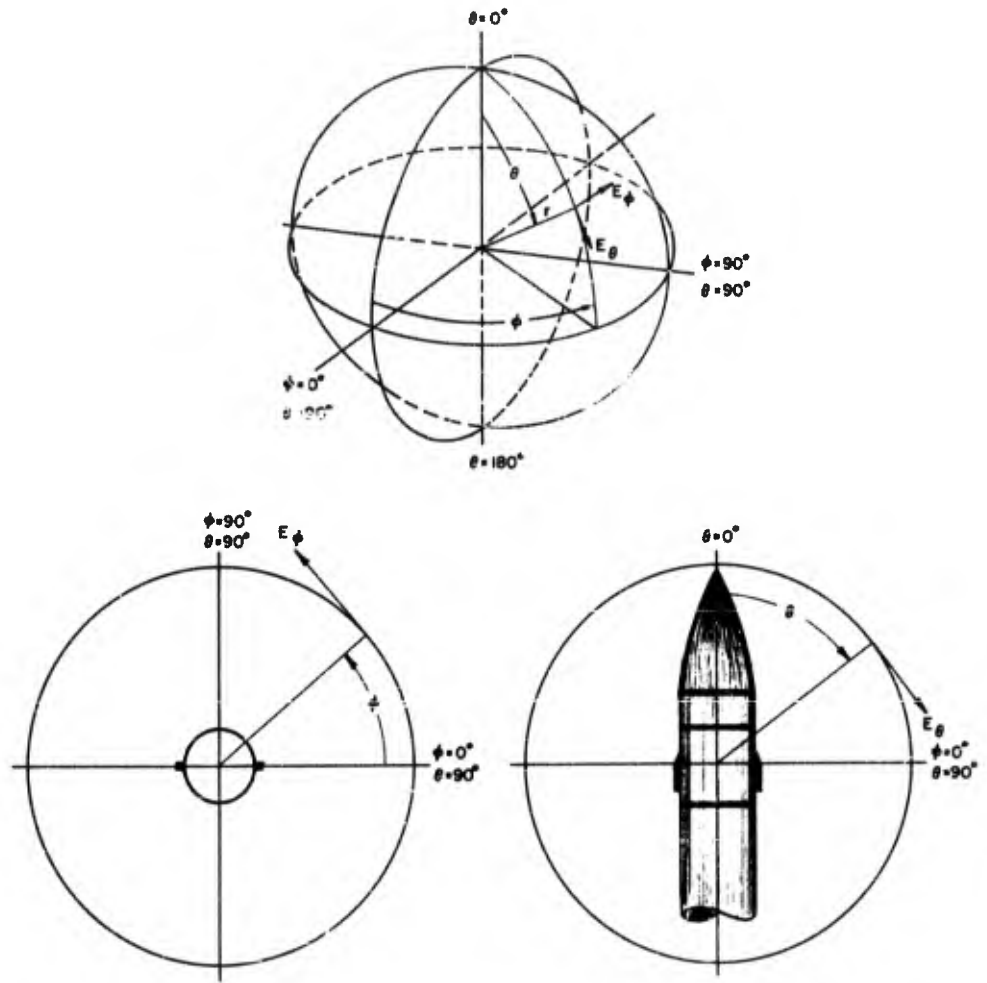


FIG. 136 - POSITION COORDINATES FOR THE MODEL 2.011 ANTENNA PATTERN MEASUREMENTS

POLARIZATION

- GAIN REF - - - - -
 E_{θ} - - - - -
 E_{ϕ} - - - - -
 R.C. - - - - -
 L.C. - - - - -
 OTHER AS NOTED

$\phi = \underline{\hspace{1cm}}^{\circ}$ $\theta = \underline{0}^{\circ}$ COORDINATE REFERENCE

$\phi = \underline{0}^{\circ}$
 $\theta = \underline{90}^{\circ}$

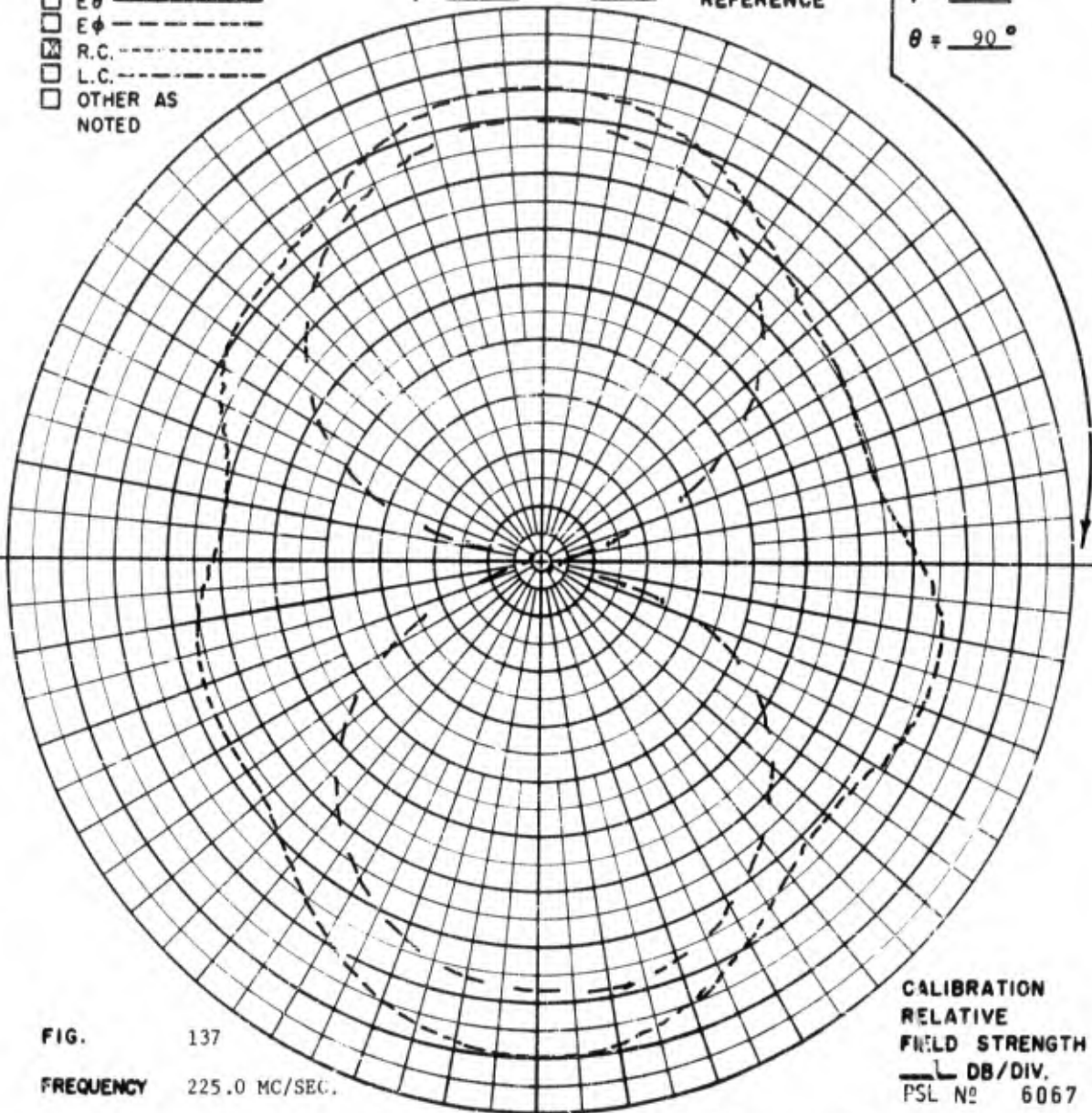


FIG. 137

FREQUENCY 225.0 MC/SEC.

ANTENNA AN ARRAY OF TWO MODEL 2.011 ANTENNAS FED 180° OUT OF PHASE.

REMARKS GAIN REFERENCE IS A STODDART HALF-WAVE DIPOLE ILLUMINATED BY A RIGHT CIRCULAR HELIX.

CALIBRATION
 RELATIVE
 FIELD STRENGTH
 — DB/DIV.
 PSL No 6067

POLARIZATION

- GAIN REF - - - - -
 E_{θ} - - - - -
 E_{ϕ} - - - - -
 R.C. - - - - -
 L.C. - - - - -
 OTHER AS NOTED

$\phi =$ _____ ° $\theta =$ _____ ° COORDINATE REFERENCE

$\phi =$ _____ °
 $\theta =$ _____ °

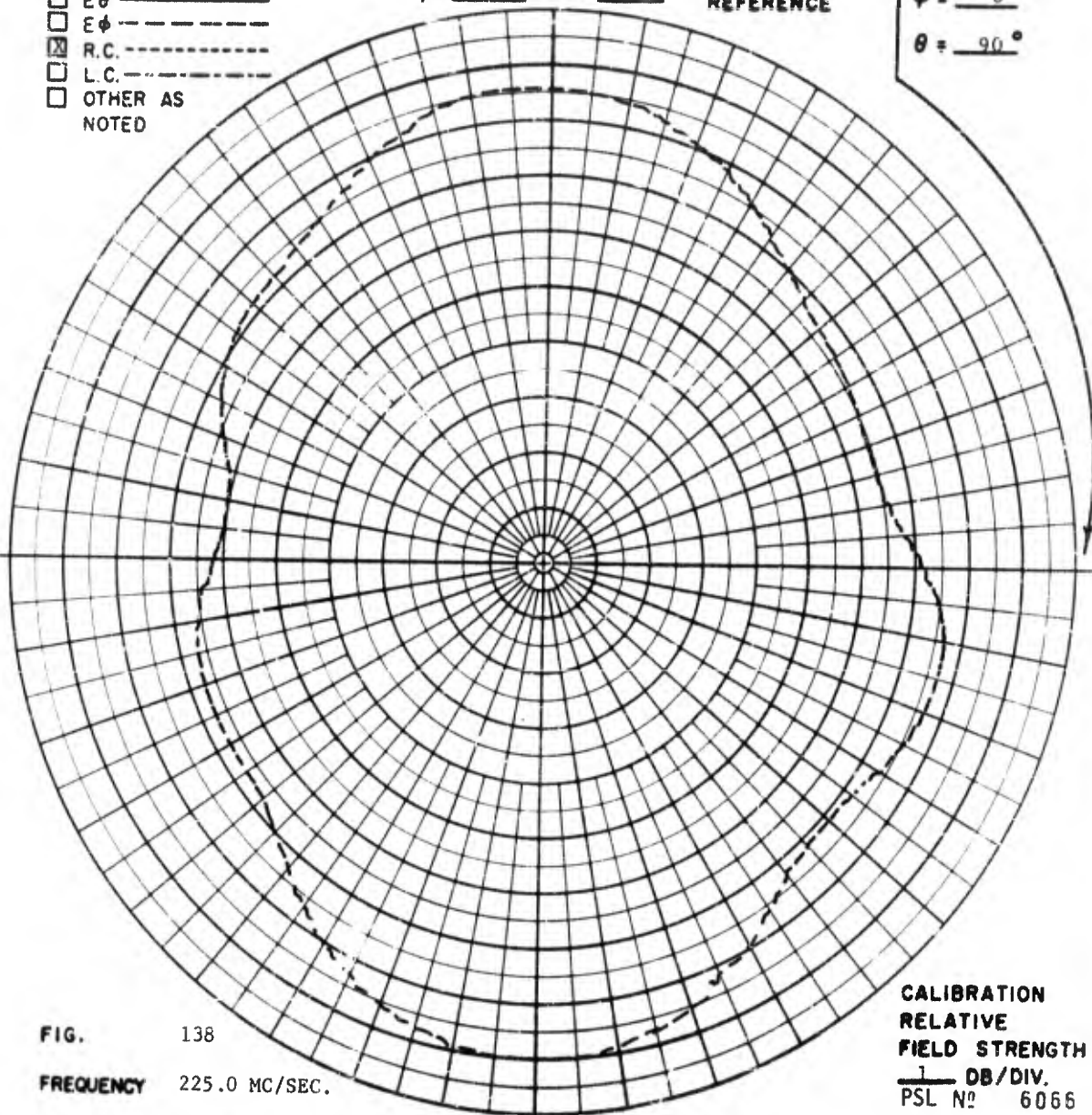


FIG. 138

FREQUENCY 225.0 MC/SEC.

ANTENNA AN ARRAY OF TWO MODEL 2.011 ANTENNAS FED 180° OUT OF PHASE.

REMARKS AT $\theta = 180^\circ$, $\phi = 0^\circ$ THE GAIN IS +2 DB WITH RESPECT TO THE STODDART HALF-WAVE DIPOLE.

CALIBRATION
 RELATIVE
 FIELD STRENGTH
 1 DB/DIV.
 PSL No 6066

POLARIZATION

- GAIN REF - - - -
 E θ - - - -
 E ϕ - - - -
 R.C. - - - -
 L.C. - - - -
 OTHER AS NOTED

$\phi = \underline{\quad}^\circ$ $\theta = \underline{0}^\circ$ COORDINATE REFERENCE

$\phi = \underline{90}^\circ$
 $\theta = \underline{90}^\circ$

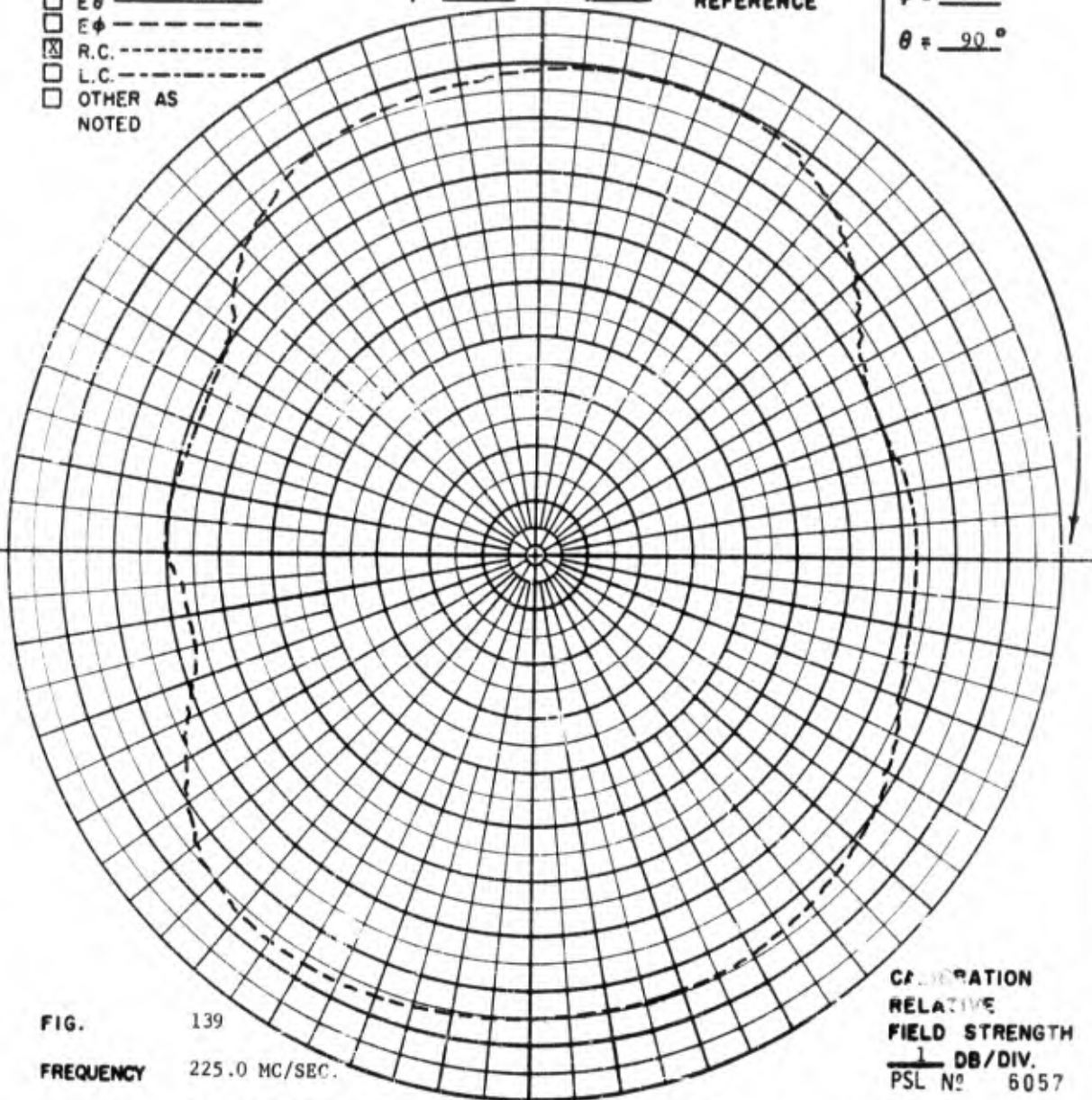


FIG. 139

FREQUENCY 225.0 MC/SEC.

ANTENNA AN ARRAY OF TWO MODEL 2.011 ANTENNAS FED 180° OUT OF PHASE.

REMARKS

CALIBRATION
 RELATIVE
 FIELD STRENGTH
 1 DB/DIV.
 PSL No 6057

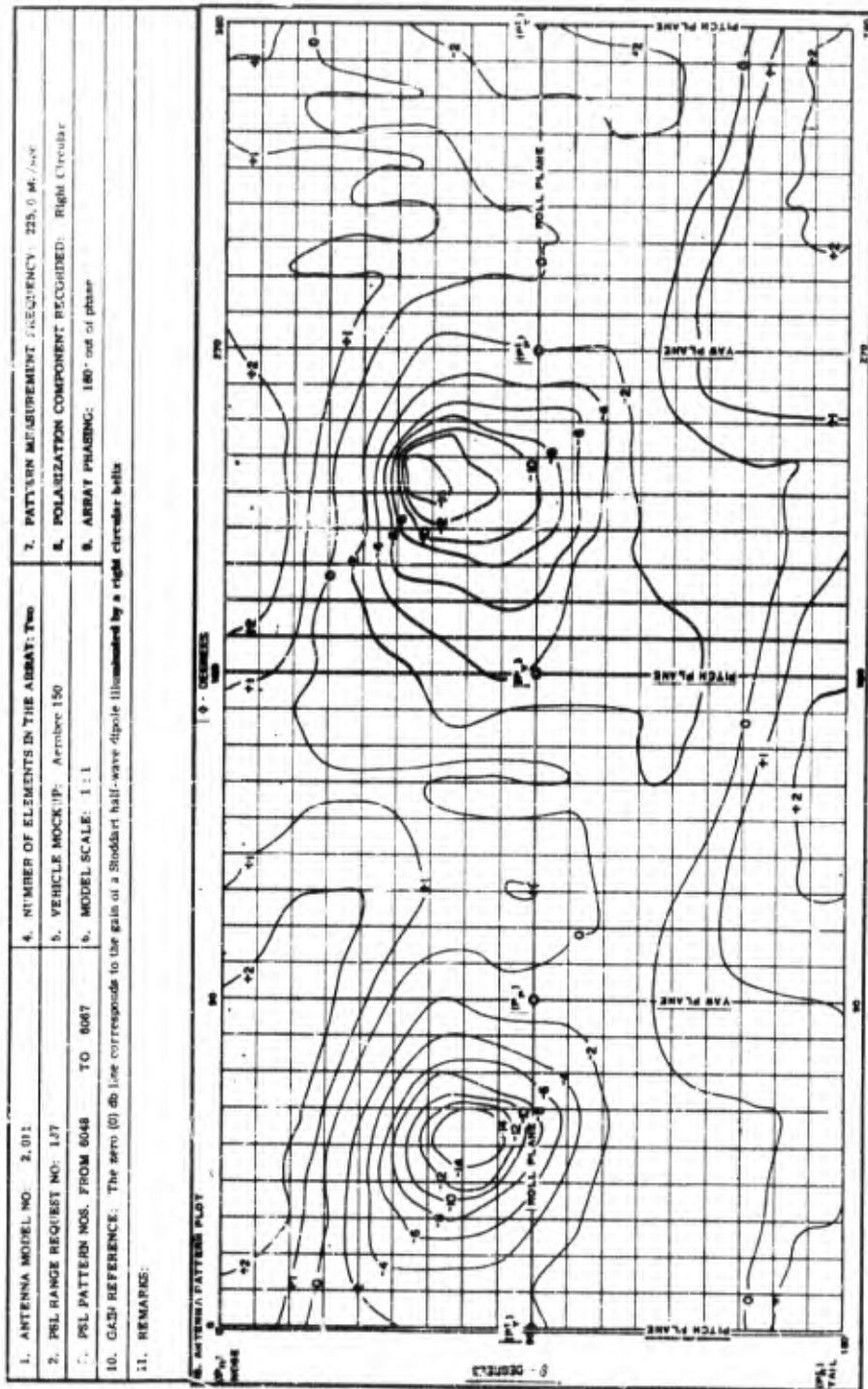


FIG. 140 - POWER CONTOUR PLOT OF THE TWO ELEMENT ARRAY OF MODEL 2,011 ANTENNAS

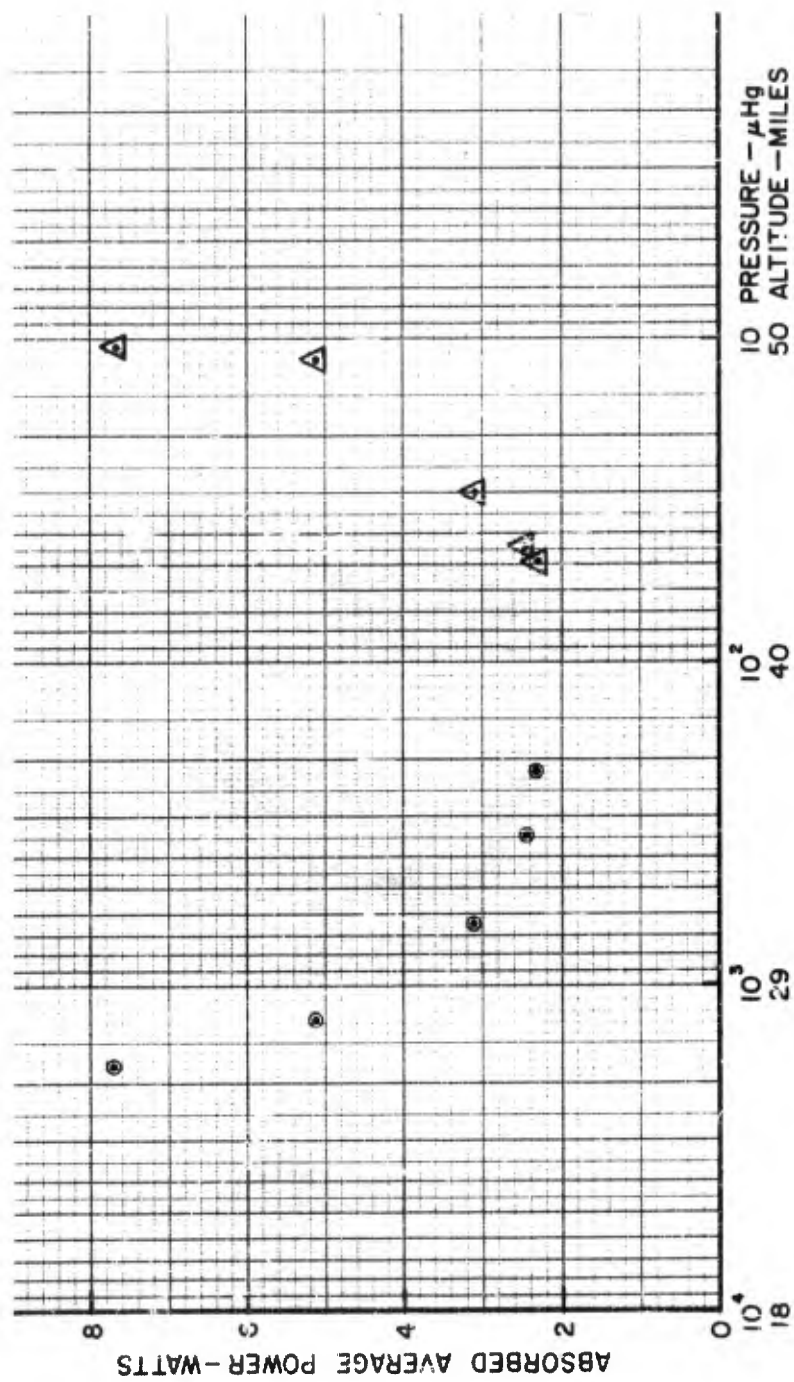


FIG. 141 - REPRESENTATIVE DIFFUSION BREAKDOWN CURVE OF THE 2,000 SERIES, 1.5-INCH HIGH TELEMETRY QUADRALOOP ANTENNAS

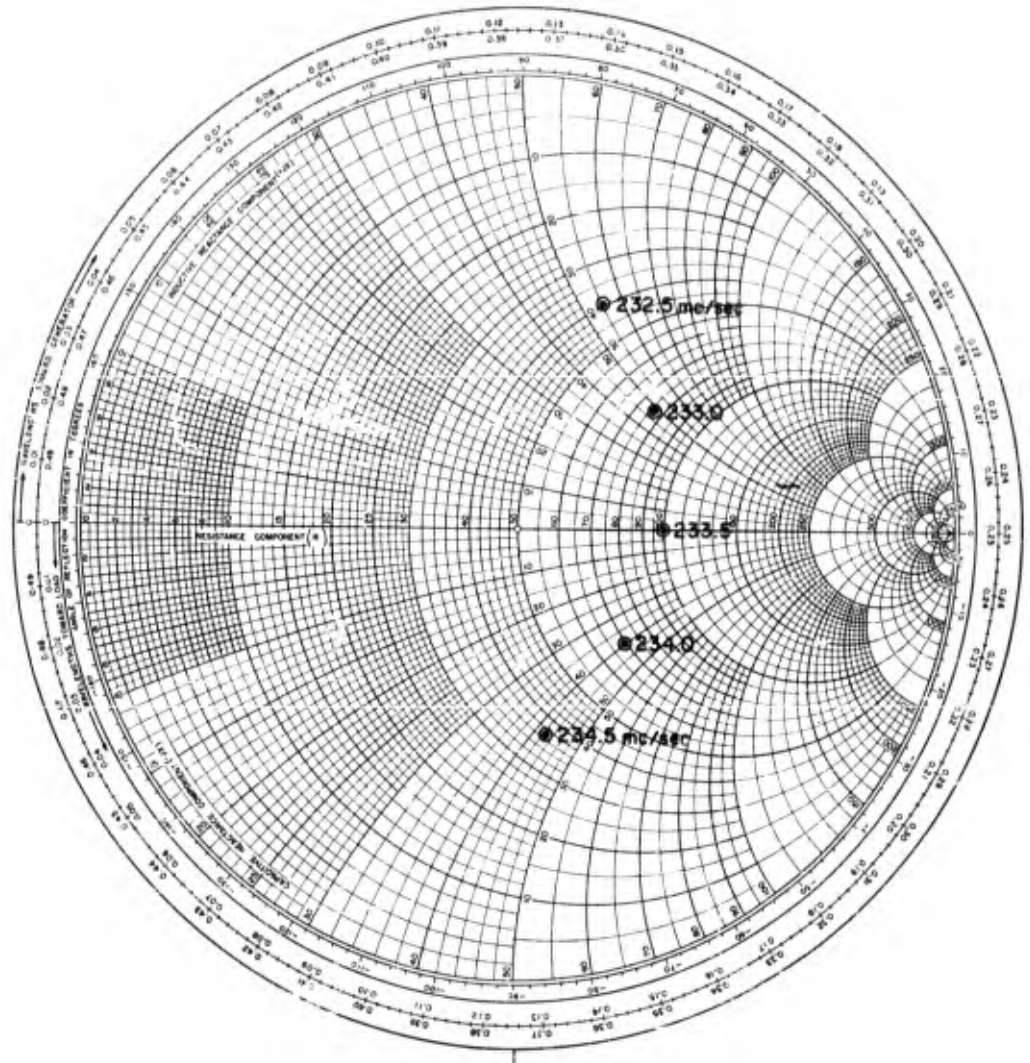


FIG. 142 - IDEALIZED IMPEDANCE CURVE OF THE 2,000 SERIES,
1.0-INCH HIGH TELEMETRY QUADRALOOP ANTENNA,
MOUNTED ON A 15-INCH DIAMETER CYLINDER

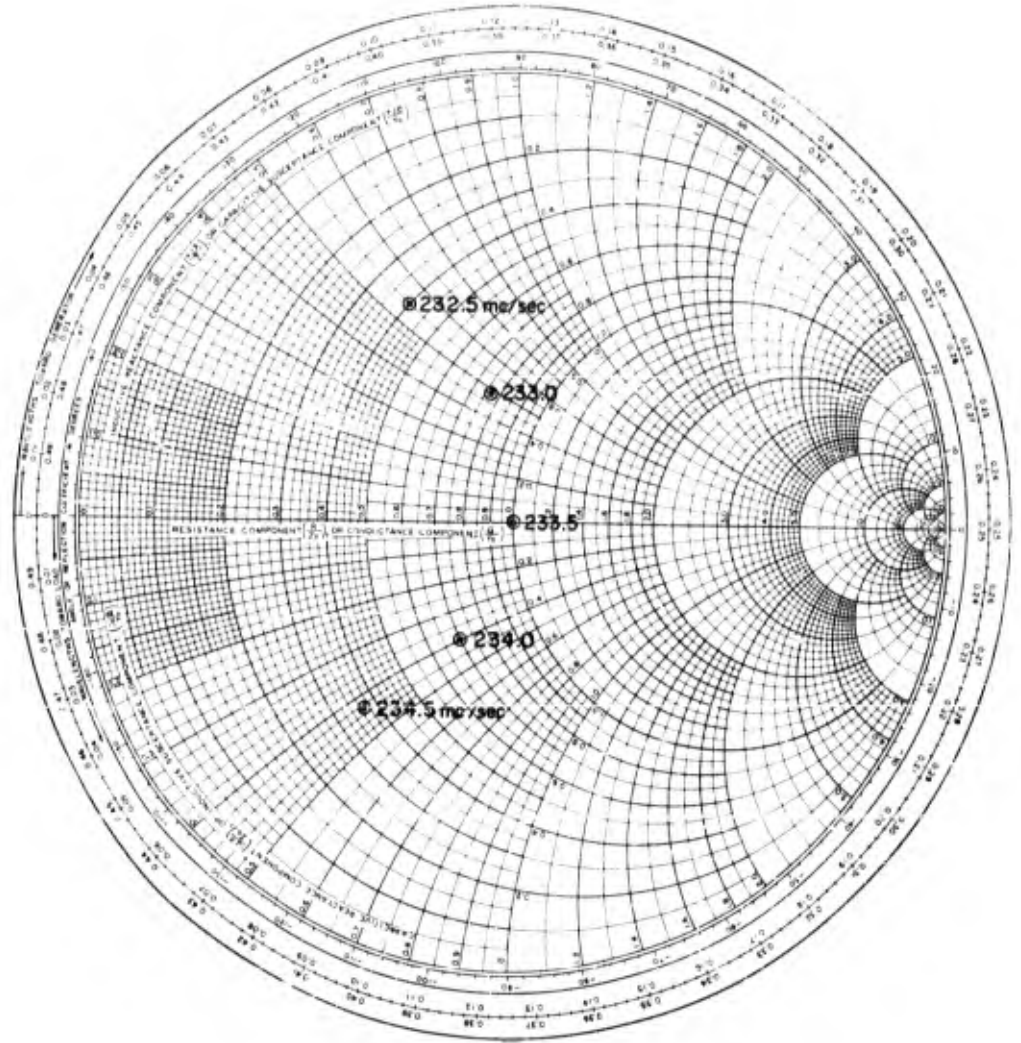


FIG. 143 - NORMALIZED IMPEDANCE CURVE OF THE 2.00C SERIES, 1.0-INCH HIGH TELEMETRY QUADRALOOP ANTENNA

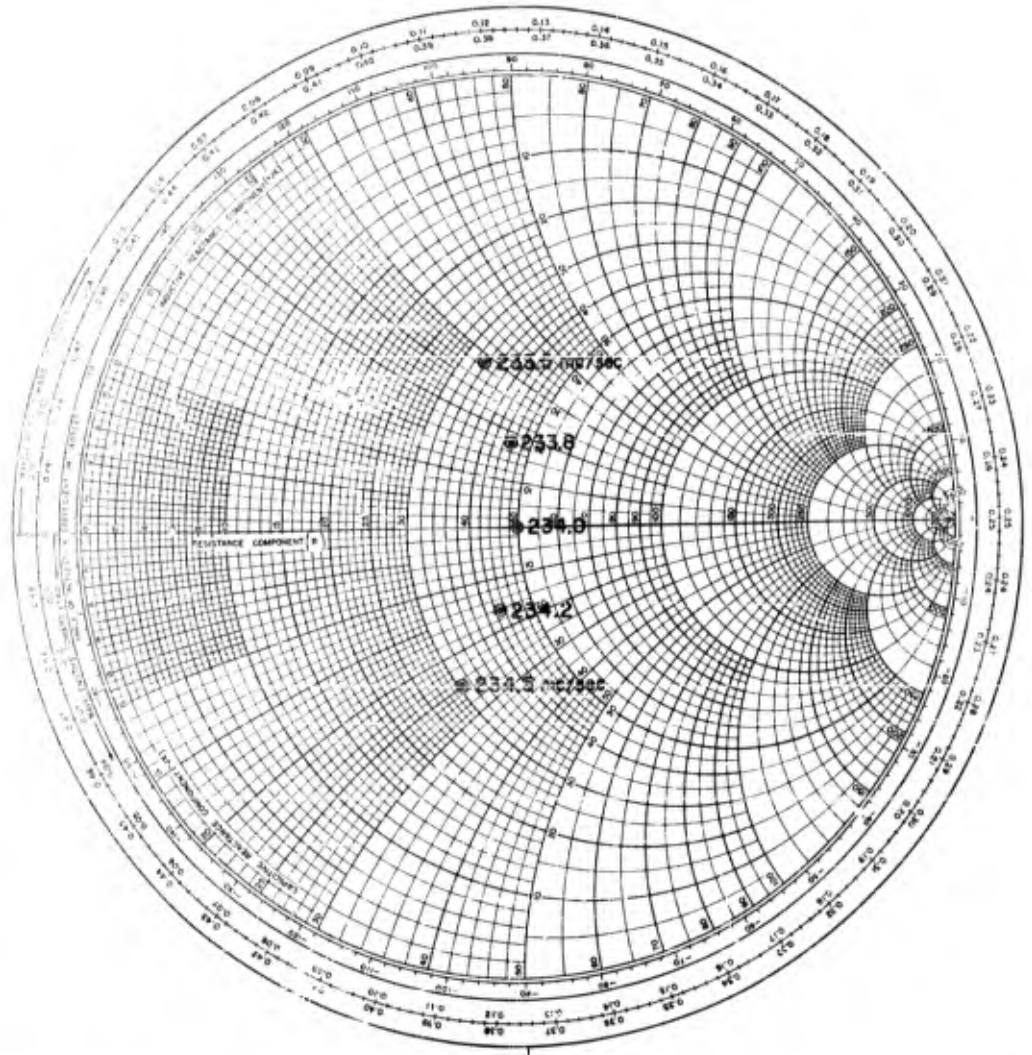


FIG. 144 - IDEALIZED IMPEDANCE CURVE OF A TWO ELEMENT ARRAY
 FED 180° OUT OF PHASE OF THE 2.000 SERIES, 1.0-INCH
 HIGH TELEMETRY QUADRALOOP ANTENNAS

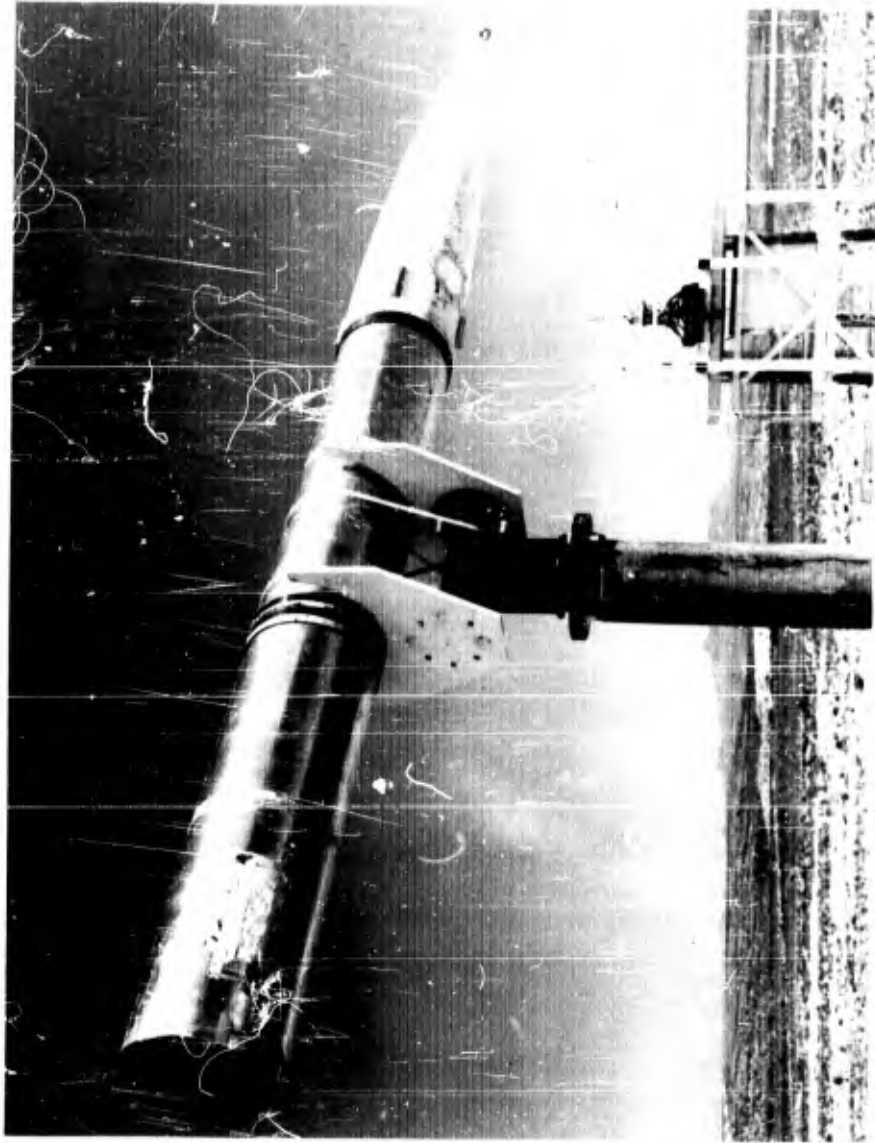


FIG. 145 - PHOTOGRAPH OF THE VEHICLE MOCKUP USED FOR THE MODEL
2.007 TELEMETRY QUADRATURE ANTENNA RADIATION
PATTERN MEASUREMENTS

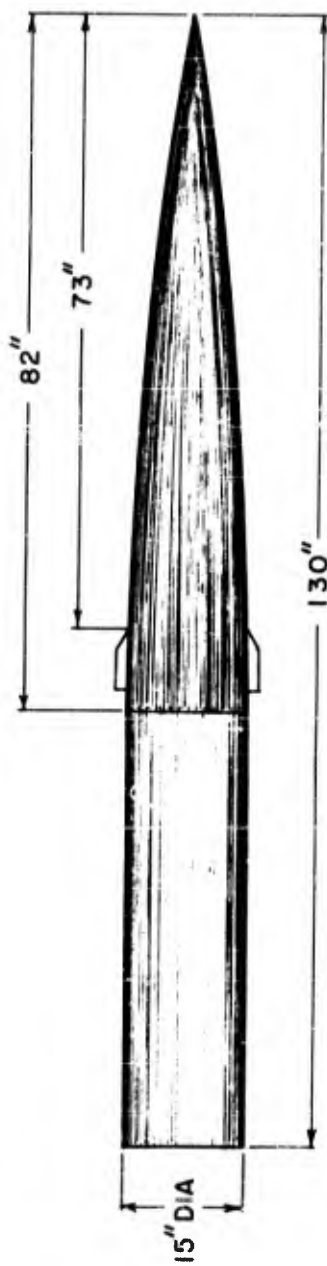


FIG. 146 - SKETCH OF THE VEHICLE MOCKUP USED FOR THE MODEL 2.007 TELEMETRY
QUADRALOOP ANTENNA RADIATION PATTERN MEASUREMENTS

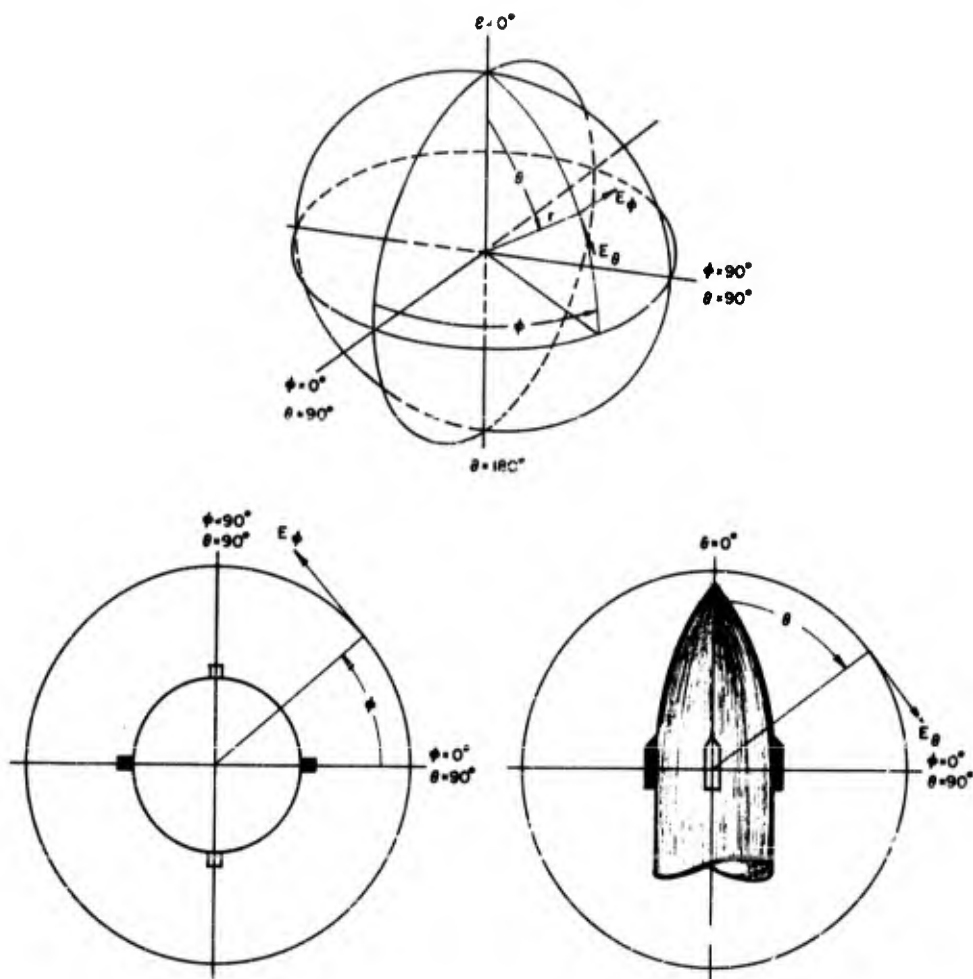


FIG. 147 - POSITION COORDINATES FOR THE MODEL 2.007 ANTENNA RADIATION PATTERN MEASUREMENTS

POLARIZATION

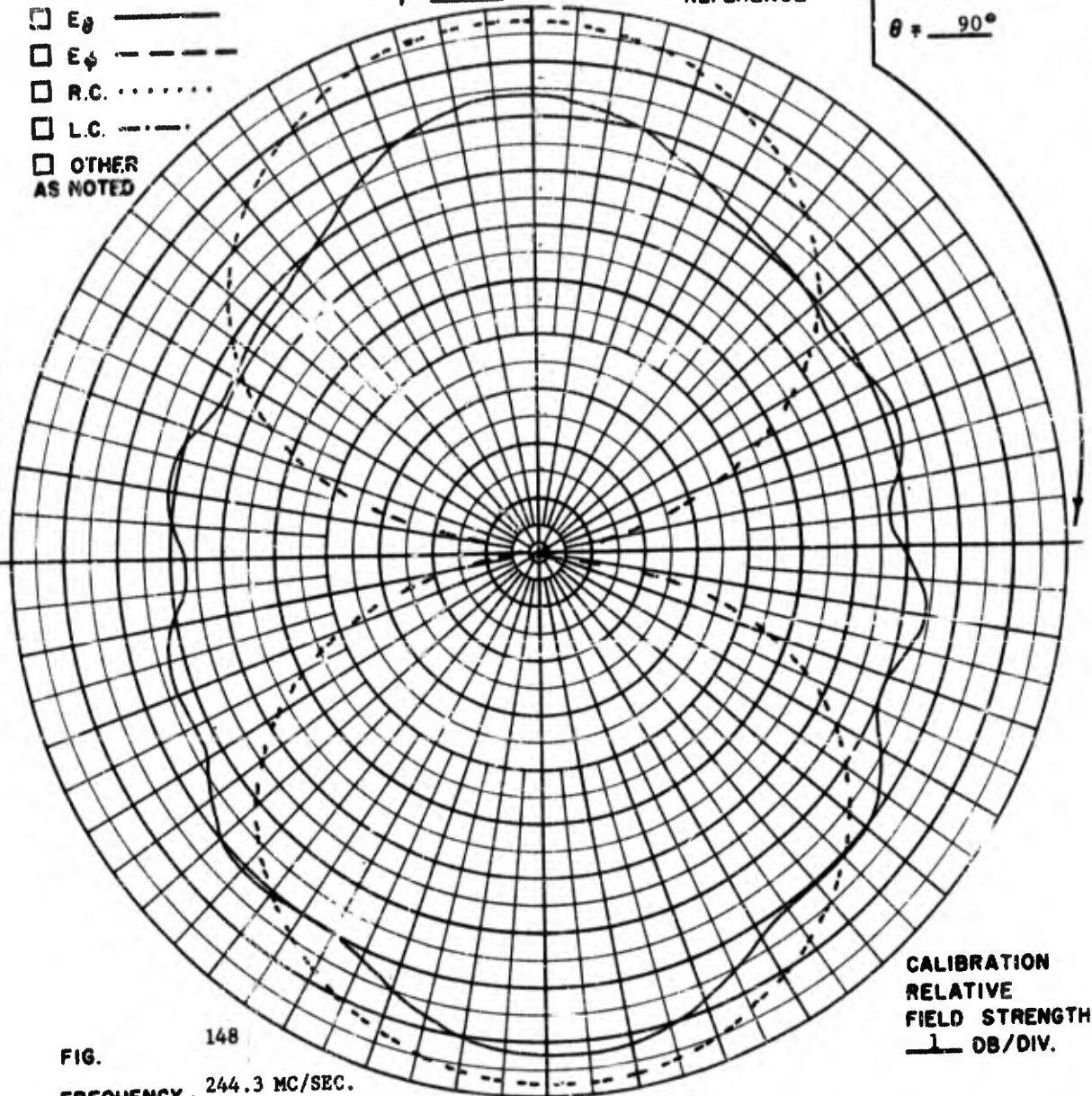
- GAIN REF
- E_{θ} —————
- E_{ϕ} - - - - -
- R.C.
- L.C. - - - - -
- OTHER AS NOTED

$\phi = \underline{\hspace{1cm}}^{\circ}$ $\theta = \underline{0}^{\circ}$

COORDINATE REFERENCE

$\phi = \underline{0}^{\circ}$
 $\theta = \underline{90}^{\circ}$

PSL No 3315



CALIBRATION
RELATIVE
FIELD STRENGTH
1 DB/DIV.

FIG. 148
FREQUENCY 244.3 MC/SEC.
ANTENNA MODEL 2.007 QUADRALOOP TWO ELEMENT ARRAY FED 180° OUT OF PHASE.
REMARKS THE GAIN REFERENCE IS A STODDART HALF WAVE DIPOLE ILLUMINATED BY A RIGHT CIRCULAR HELIX.

POLARIZATION

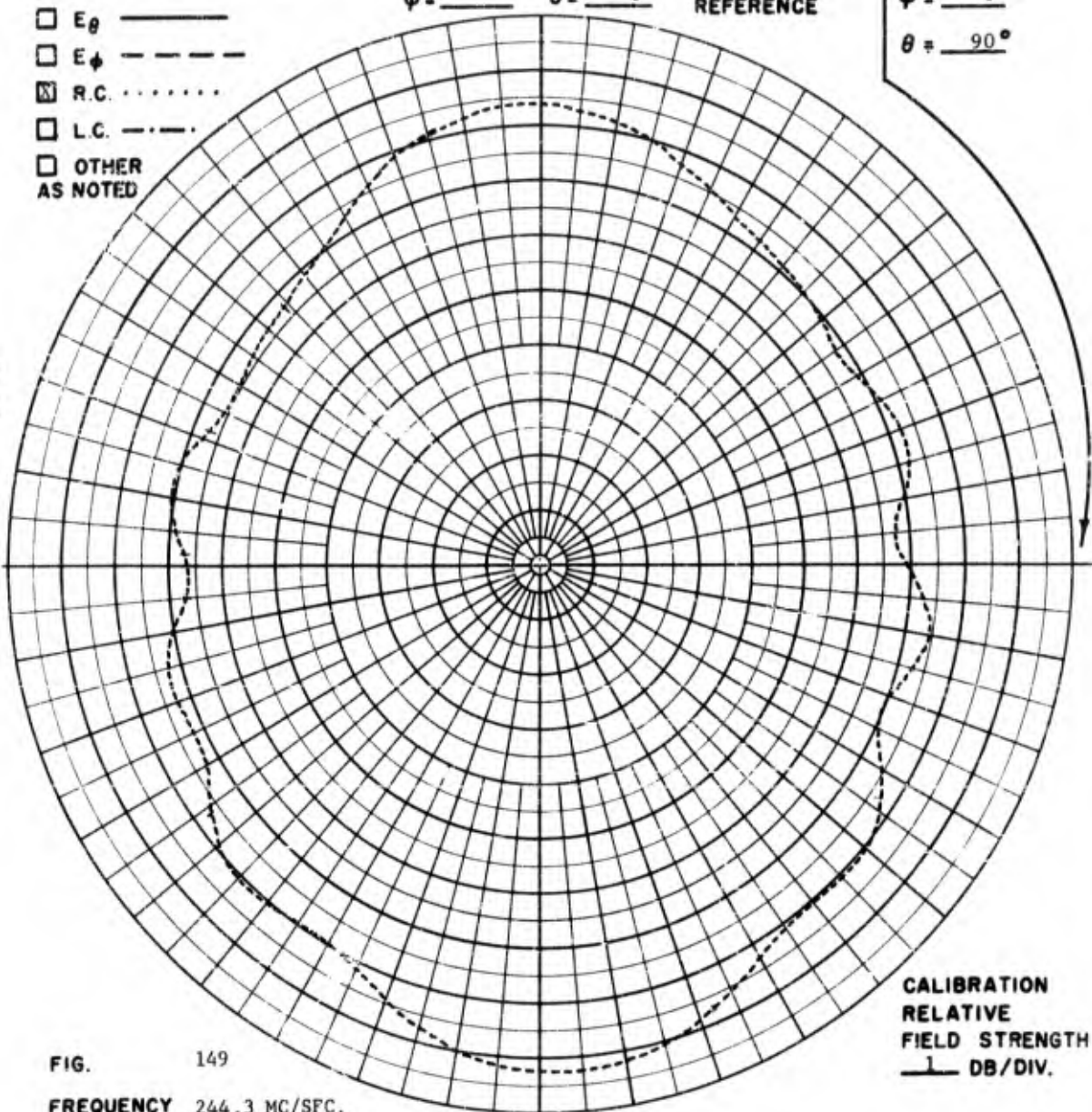
- GAIN REF
- E_{θ} _____
- E_{ϕ} - - - - -
- R.C.
- L.C. - . - . -
- OTHER AS NOTED

$\phi = \underline{\quad}^{\circ}$ $\theta = \underline{0}^{\circ}$

COORDINATE REFERENCE

$\phi = \underline{0}^{\circ}$
 $\theta = \underline{90}^{\circ}$

PSL No. 3316



CALIBRATION
RELATIVE
FIELD STRENGTH
1 DB/DIV.

FIG. 149
FREQUENCY 244.3 MC/SFC.

ANTENNA MODEL 2.007 QUADRALOOP TWO ELEMENT ARRAY FED 180° OUT OF PHASE.

REMARKS AT $\theta = 180^{\circ}$, $\phi = 0^{\circ}$ THE SIGNAL IS -1 DB WITH RESPECT TO THE STODDART HALFWAVE DIPOLE.

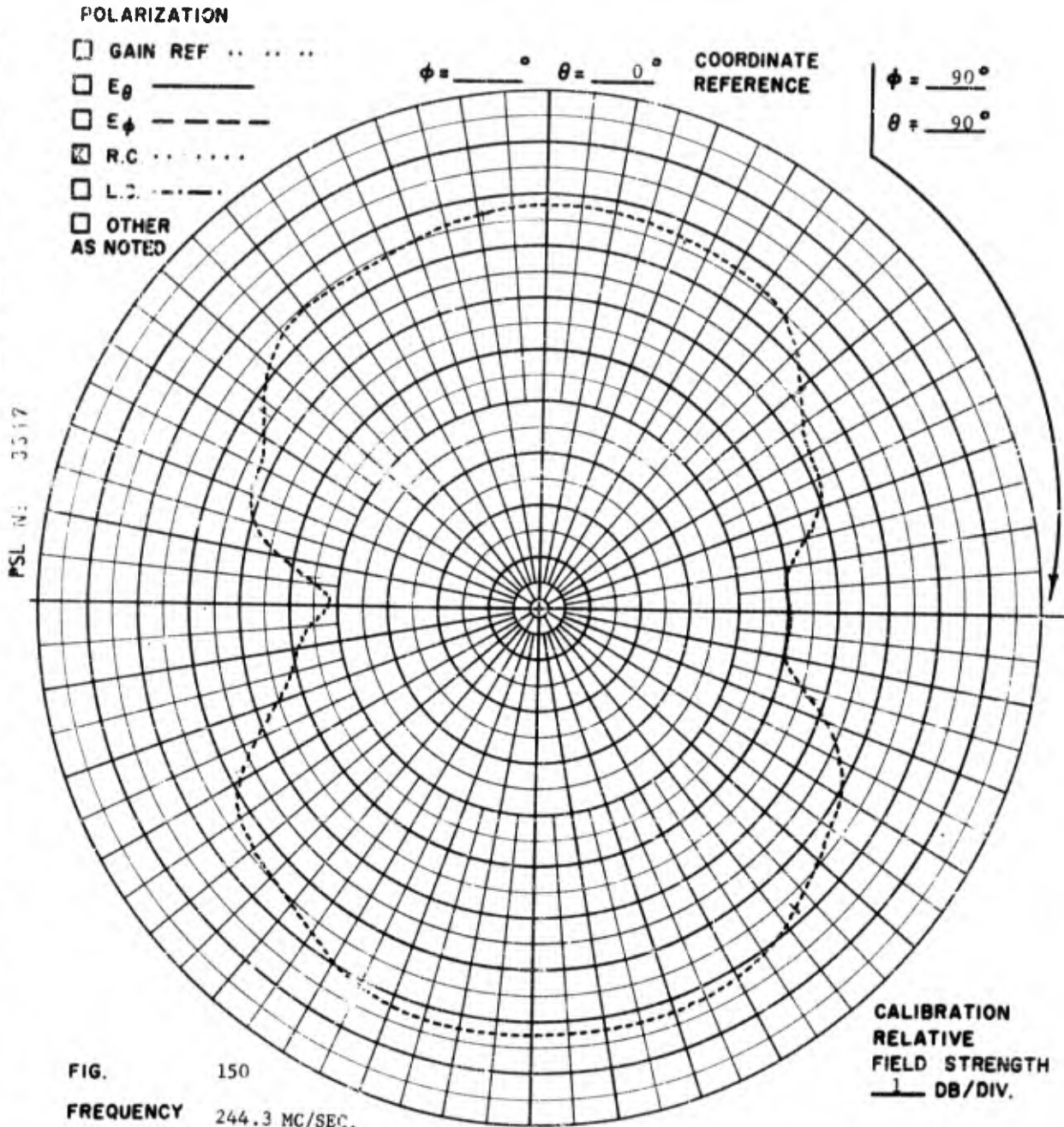


FIG. 150
FREQUENCY 244.3 MC/SEC.
ANTENNA MODEL 2.007 QUADRALOOP TWO ELEMENT ARRAY, FED 180° OUT OF PHASE.
REMARKS

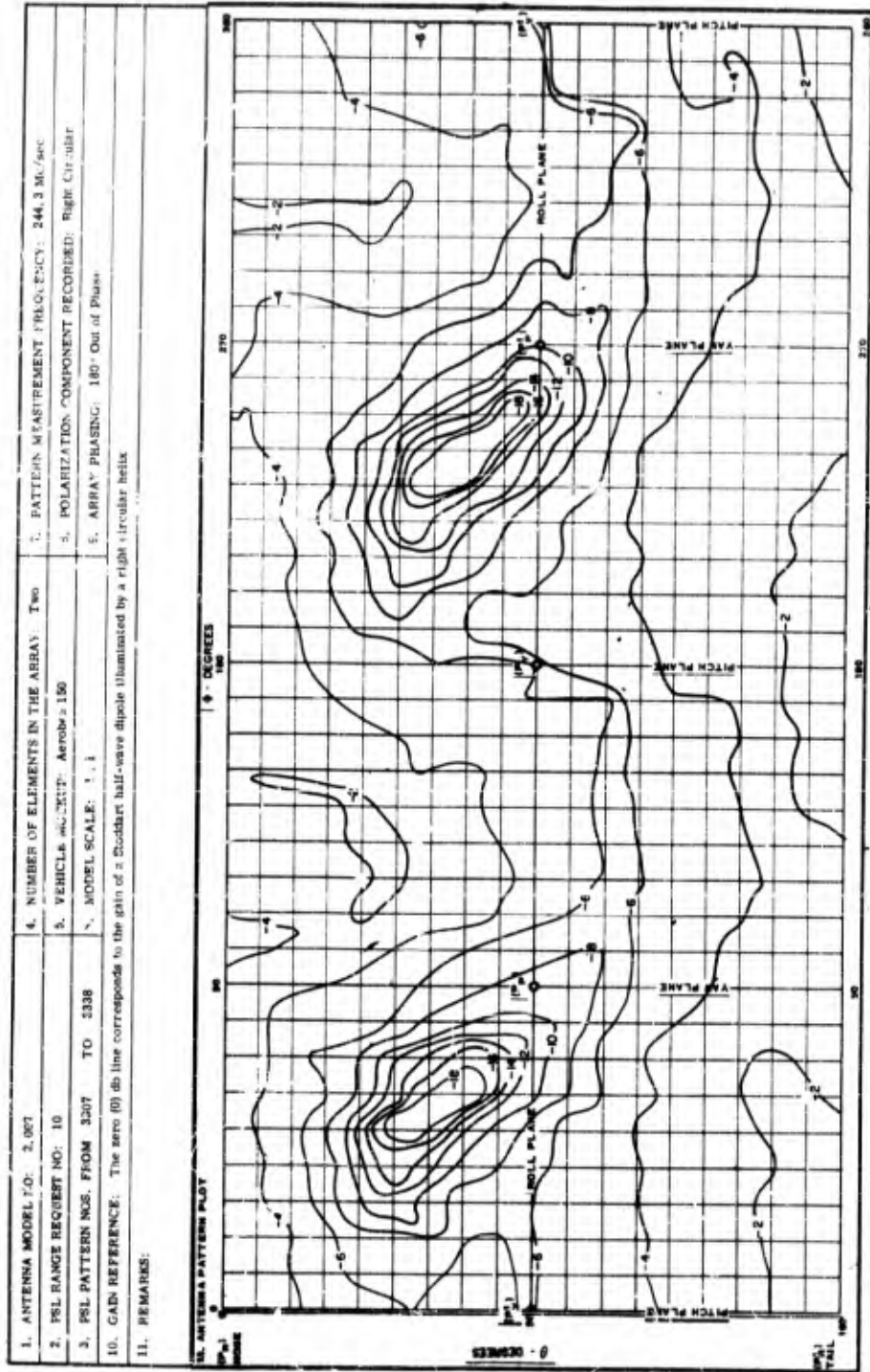


FIG. 151 - POWER CONTOUR PLOT OF THE TWO ELEMENT ARRAY OF
MODEL 2,007 ANTENNAS

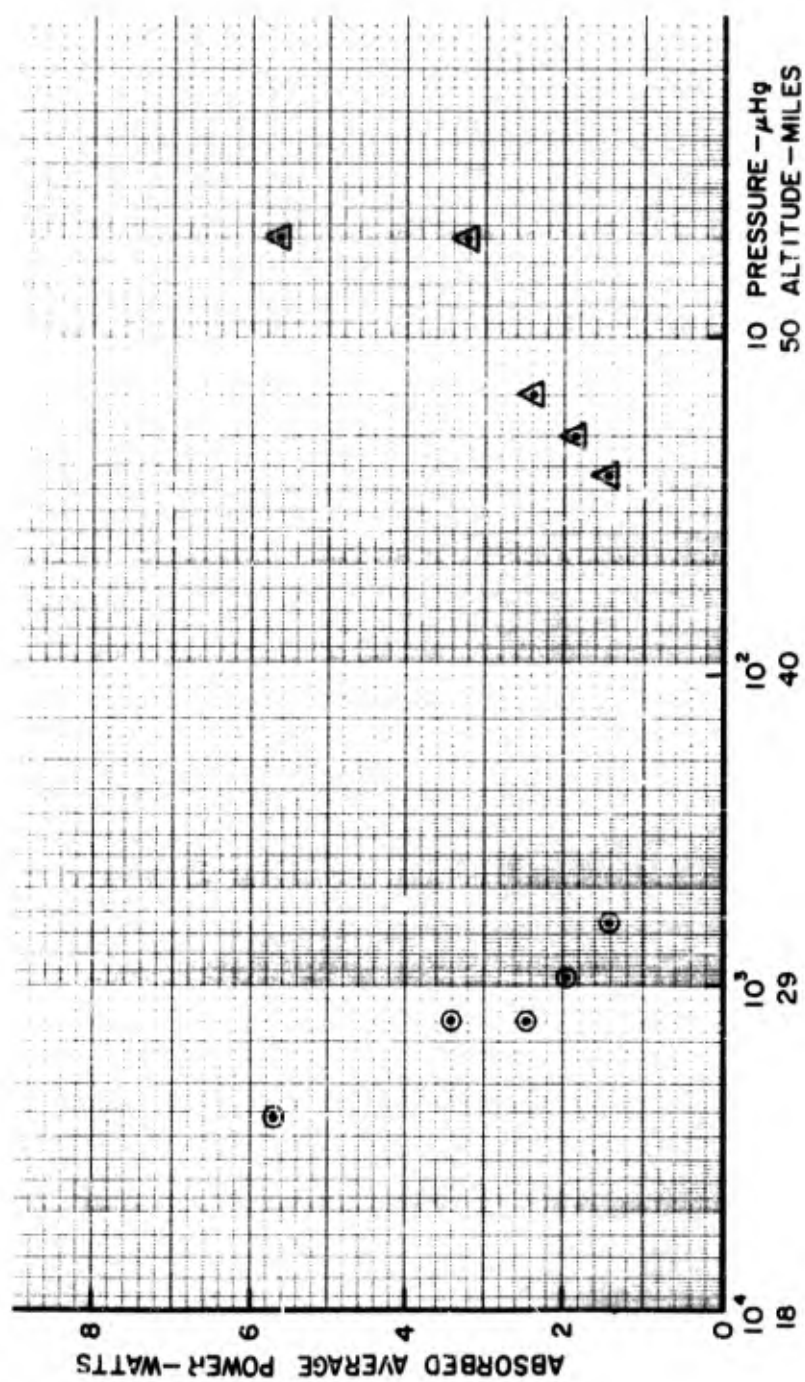


FIG. 152 - REPRESENTATIVE DIFFUSION BREAKDOWN CURVE OF THE 2,000 SERIES, 1.0-INCH HIGH TELEMETRY QUADRALOOP ANTENNA

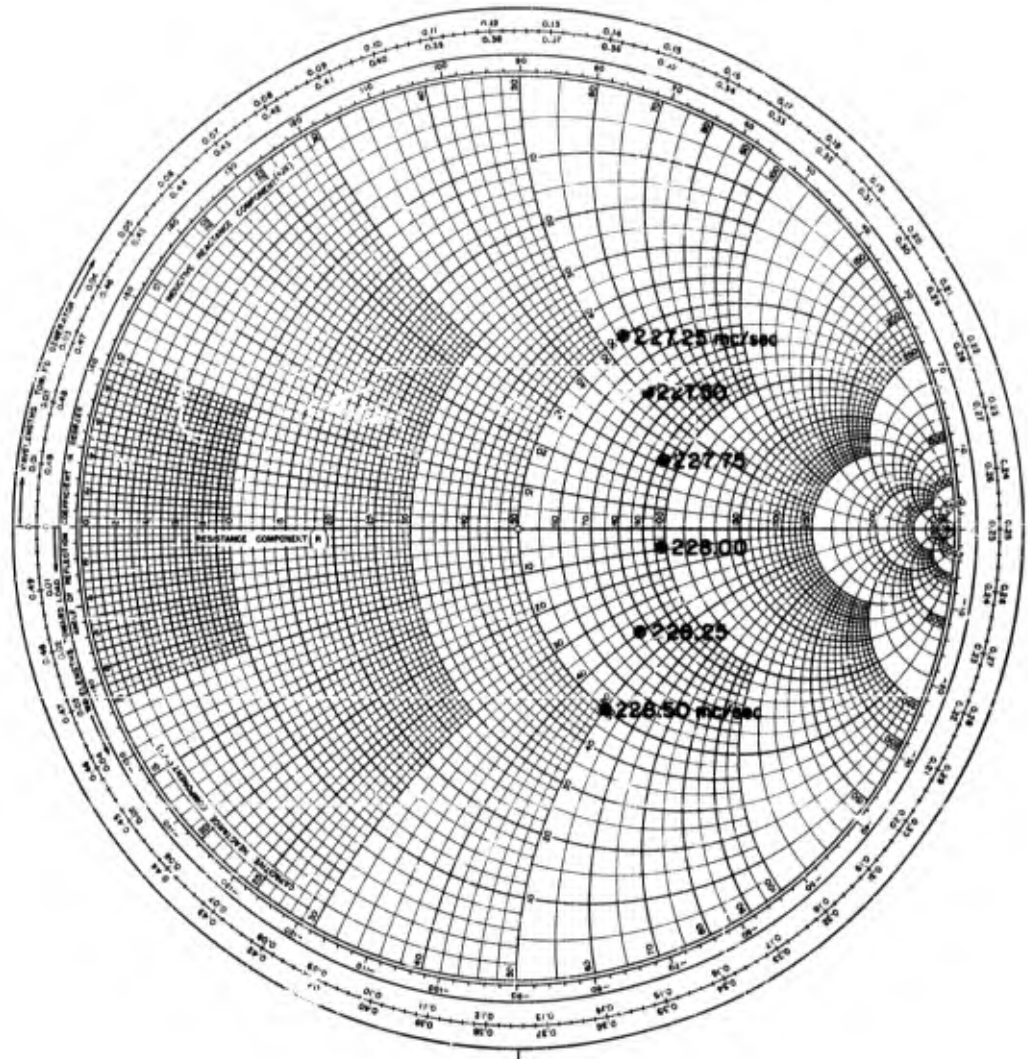


FIG. 153 - IDEALIZED IMPEDANCE CURVE OF THE 2.000 SERIES,
0.5-INCH HIGH TELEMETRY QUADRALOOP ANTENNA
MOUNTED ON A 6.8-INCH DIAMETER CYLINDER

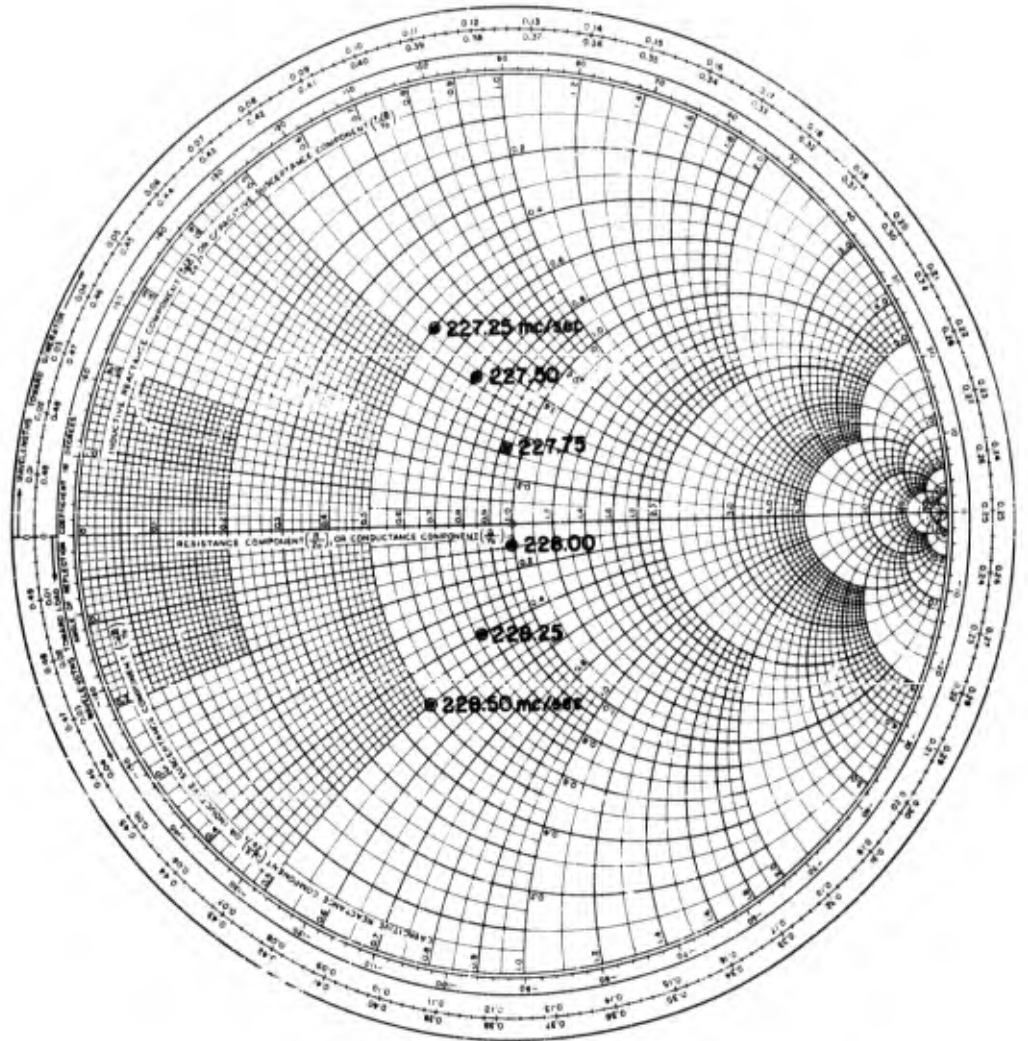


FIG. 154 - NORMALIZED IMPEDANCE CURVE OF THE 2.000 SERIES,
0.5-INCH HIGH TELEMETRY QUADRALOOP ANTENNA

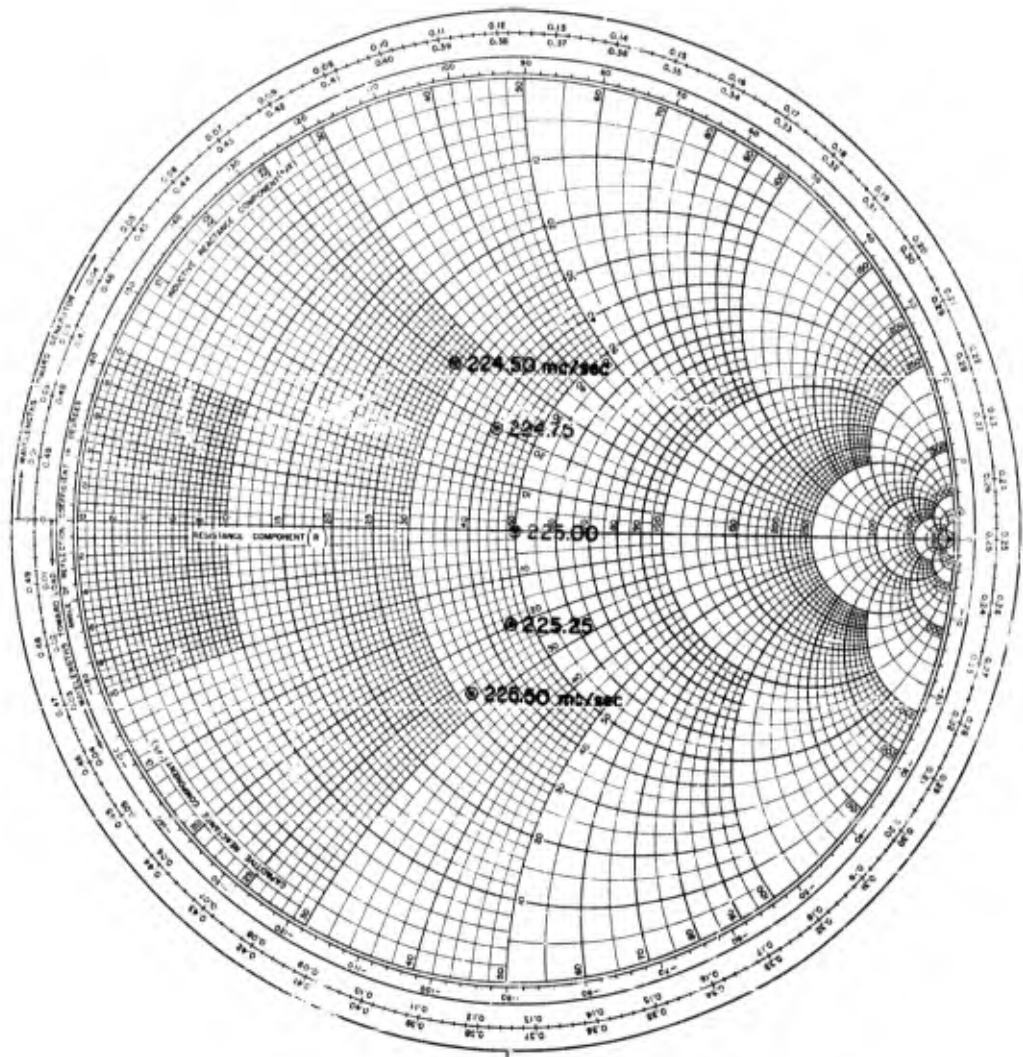


FIG. 155 - IDEALIZED IMPEDANCE CURVE OF THE TWO ELEMENT ARRAY FED 180° OUT OF PHASE OF THE 2.000 SERIES, 0.5-INCH HIGH TELEMETRY QUADRALOOP MOUNTED ON A 6.8-INCH DIAMETER

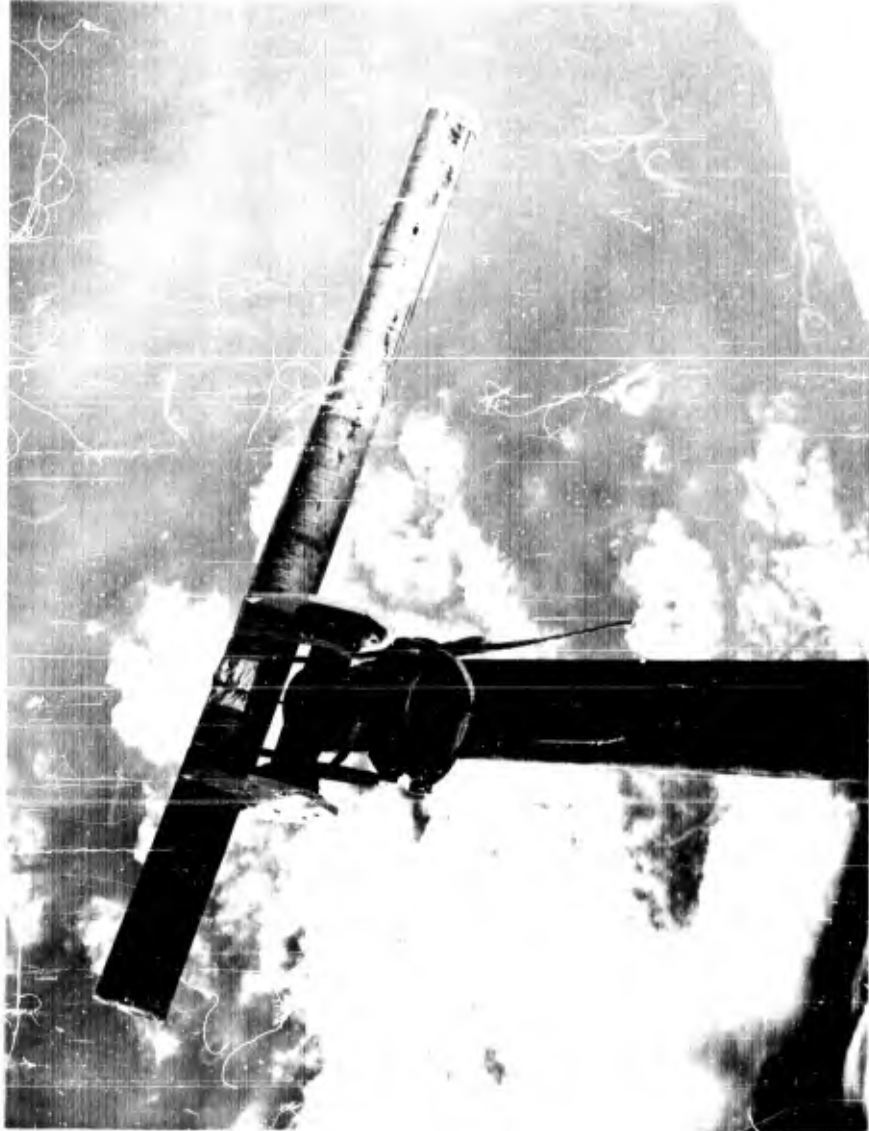


FIG. 156 - PHOTOGRAPH OF THE VEHICLE MOCKUP USED FOR THE MODEL
2.031 TELEMETRY QUADRALOOP ANTENNA RADIATION
PATTERN MEASUREMENTS



FIG. 157 - SKETCH OF THE VEHICLE MOCKUP USED FOR THE MODEL 2.031
ELEMENTARY QUADRALOOP ANTENNA RADIATION
PATTERN MEASUREMENTS

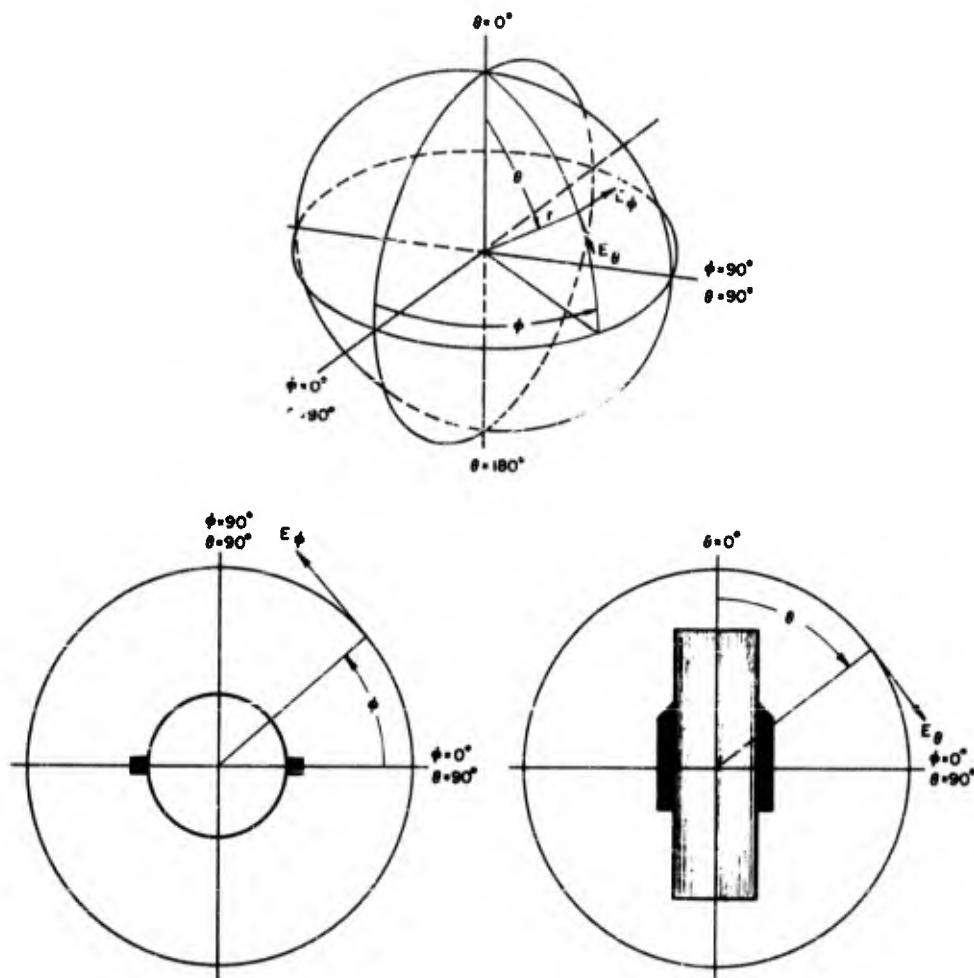


FIG. 158 - POSITION COORDINATES FOR THE MODEL 2.031 ANTENNA RADIATION PATTERN MEASUREMENTS

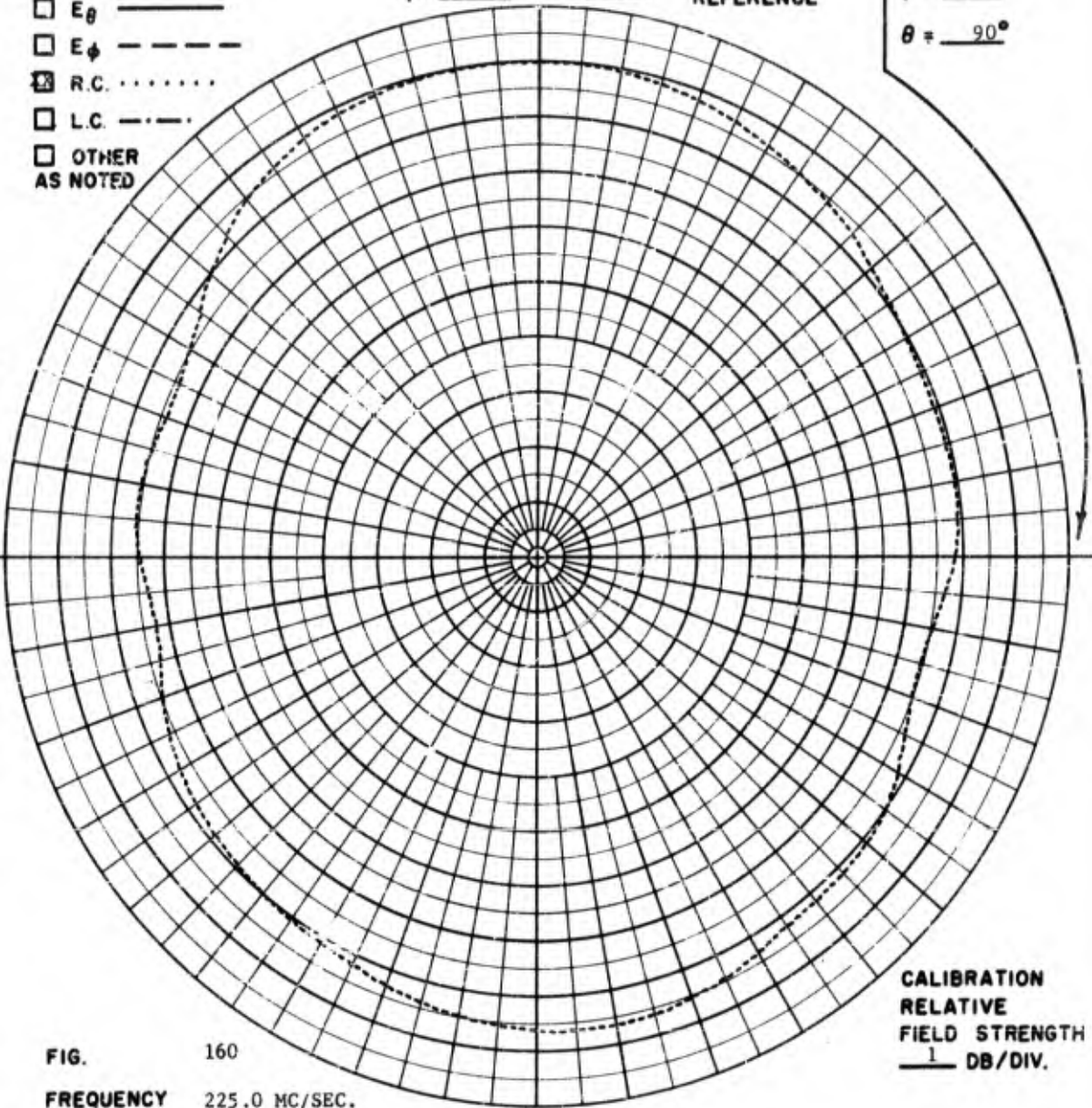
POLARIZATION

- GAIN REF
- E_θ _____
- E_ϕ - - - - -
- R.C.
- L.C. - . - . -
- OTHER AS NOTED

$\phi =$ _____ $\theta =$ _____ 0° COORDINATE REFERENCE

$\phi =$ _____ 0°
 $\theta =$ _____ 90°

PSL N^o 1512



CALIBRATION
RELATIVE
FIELD STRENGTH
1 DB/DIV.

FIG. 160

FREQUENCY 225.0 MC/SEC.

ANTENNA MODEL 2.031 TWO ELEMENT ARRAY FED 180° OUT OF PHASE.

REMARKS AT $\theta = 180^\circ$, $\phi = 0^\circ$ THE GAIN IS -7 DB WITH RESPECT TO THE STODDART HALFWAVE DIPOLE.

POLARIZATION

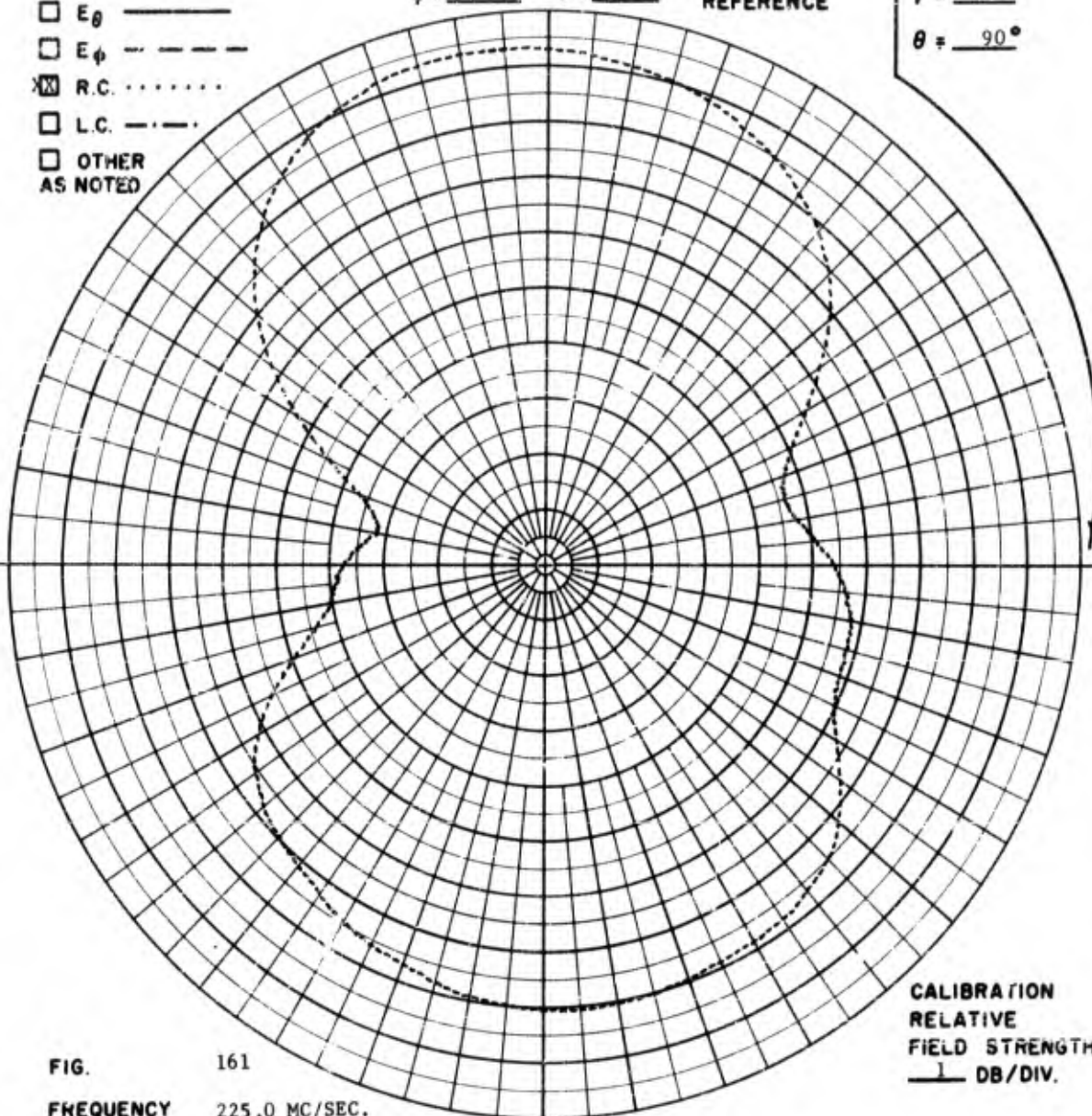
- GAIN REF
- E_{θ} —————
- E_{ϕ} - - - - -
- R.C.
- L.C. - - - - -
- OTHER AS NOTED

$\phi = \underline{\hspace{1cm}}^{\circ}$ $\theta = \underline{0}^{\circ}$

COORDINATE REFERENCE

$\phi = \underline{30}^{\circ}$
 $\theta = \underline{90}^{\circ}$

PSL 11 1512



CALIBRATION
RELATIVE
FIELD STRENGTH
1 DB/DIV.

FIG. 161
FREQUENCY 225.0 MC/SEC.
ANTENNA MODEL 2.031 TWO ELEMENT ARRAY FED 180° OUT OF PHASE.
REMARKS

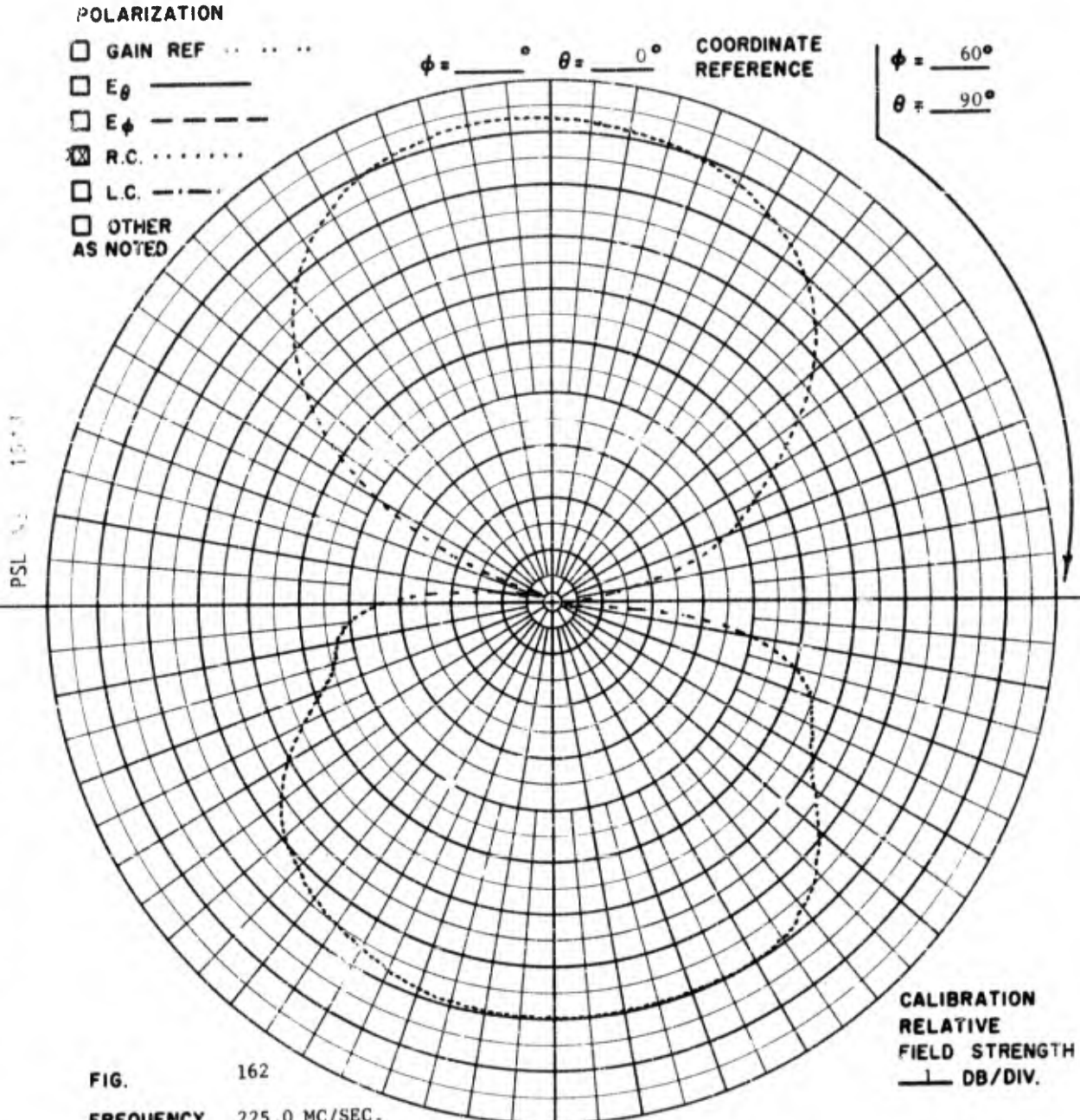


FIG. 162

FREQUENCY 225.0 MC/SEC.

ANTENNA MODEL 2.031 TWO ELEMENT ARRAY FED 180° OUT OF PHASE.

REMARKS

POLARIZATION

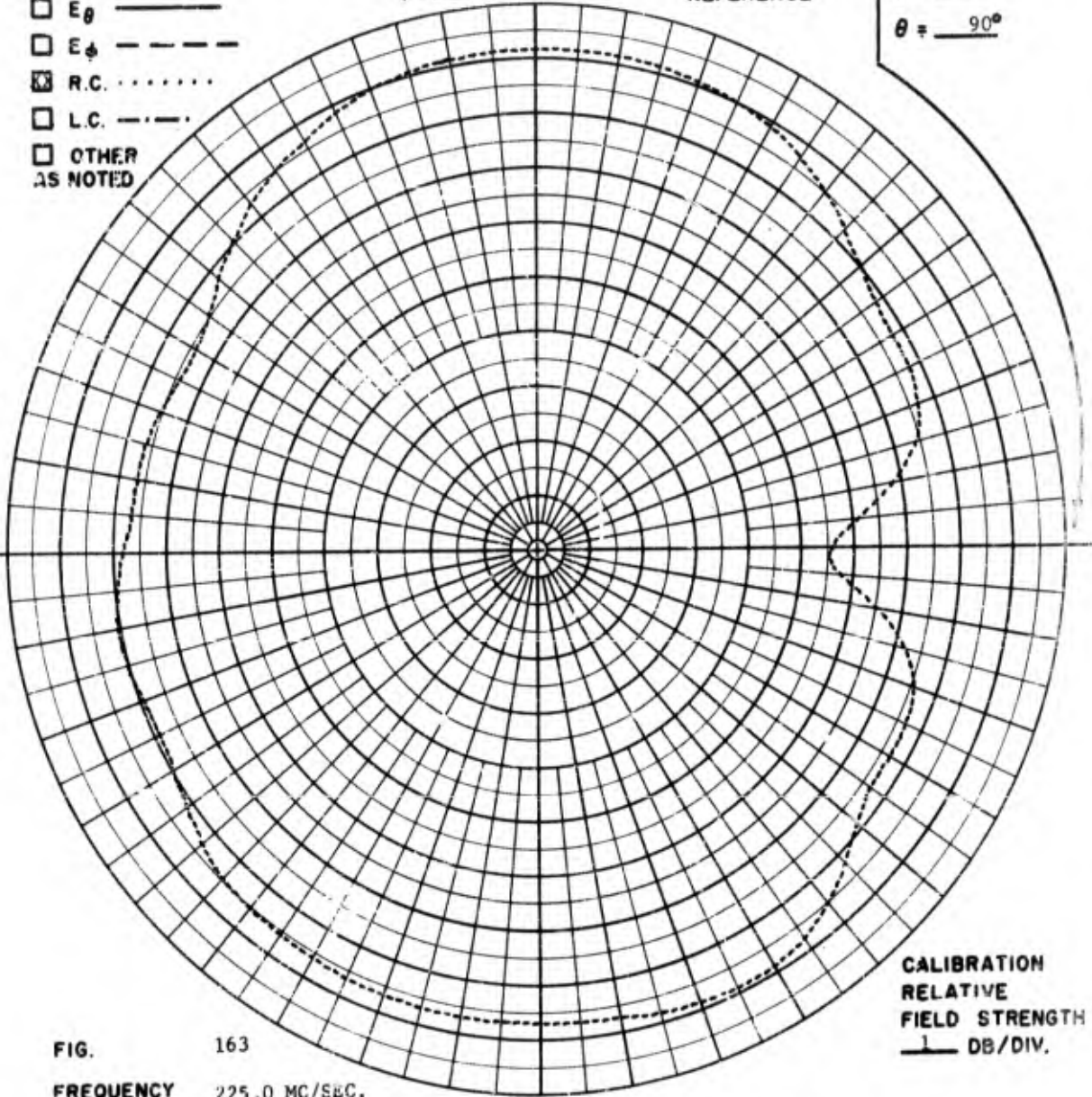
- GAIN REF
- E_{θ} _____
- E_{ϕ} - - - - -
- R.C.
- L.C. - - - - -
- OTHER
AS NOTED

$\phi =$ _____ $\theta =$ _____ 0°

COORDINATE REFERENCE

$\phi = 90^{\circ}$
 $\theta = 90^{\circ}$

PSL 7.2 1513



CALIBRATION
RELATIVE
FIELD STRENGTH
1 DB/DIV.

FIG. 163
FREQUENCY
ANTENNA
REMARKS

225.0 MC/SEC.
MODEL 2.031 TWO ELEMENT ARRAY FED 180° OUT OF PHASE.

POLARIZATION

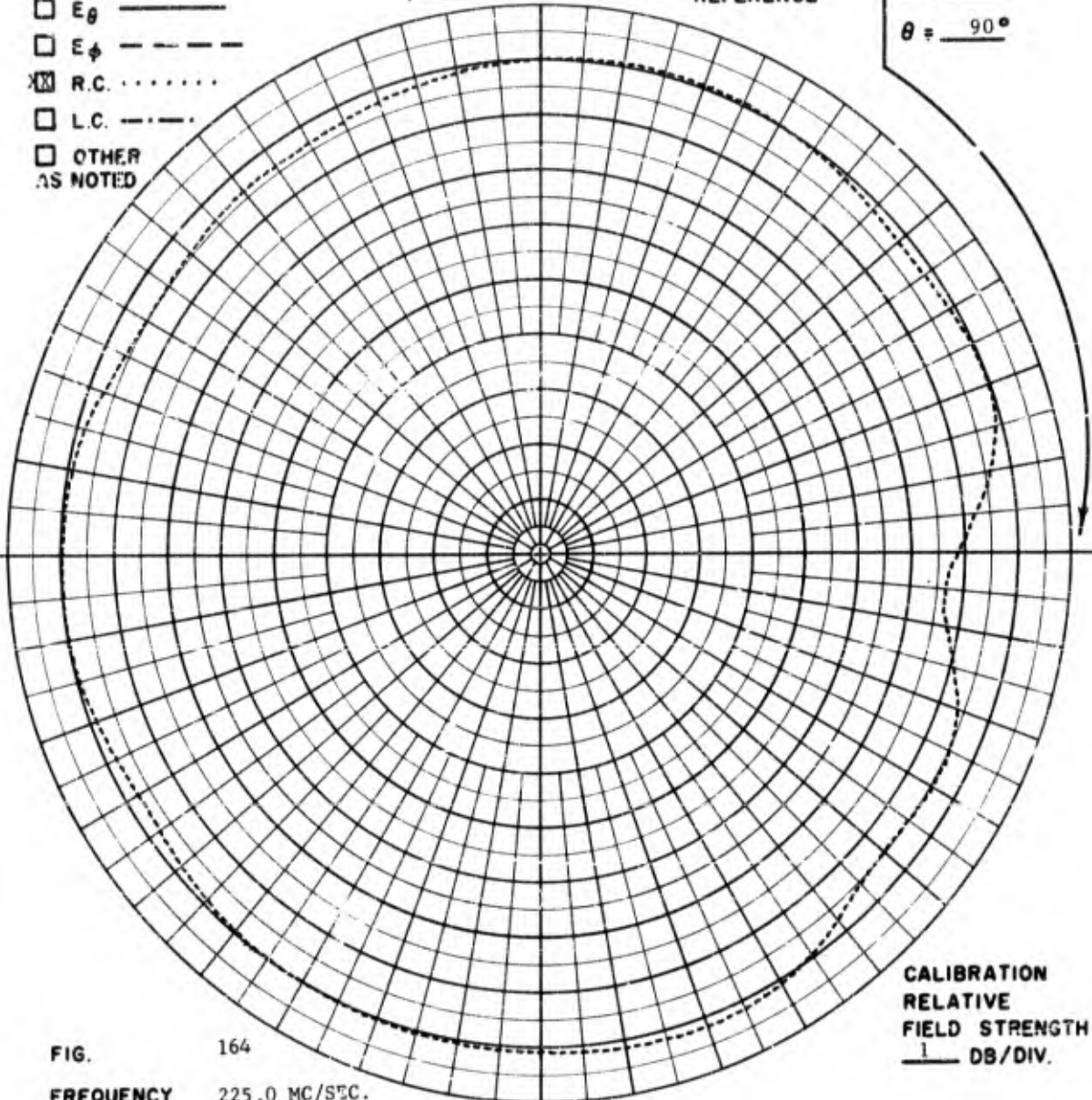
- GAIN REF
- E_{θ} _____
- E_{ϕ} - - - - -
- R.C.
- L.C. - - - - -
- OTHER AS NOTED

$\phi =$ _____ $\theta =$ _____

COORDINATE REFERENCE

$\phi = 120^\circ$
 $\theta = 90^\circ$

PSL 1517



CALIBRATION
RELATIVE
FIELD STRENGTH
1 DB/DIV.

FIG. 164
 FREQUENCY 225.0 MC/SEC.
 ANTENNA MODEL 2.031 TWO ELEMENT ARRAY FED 180° OUT OF PHASE.
 REMARKS

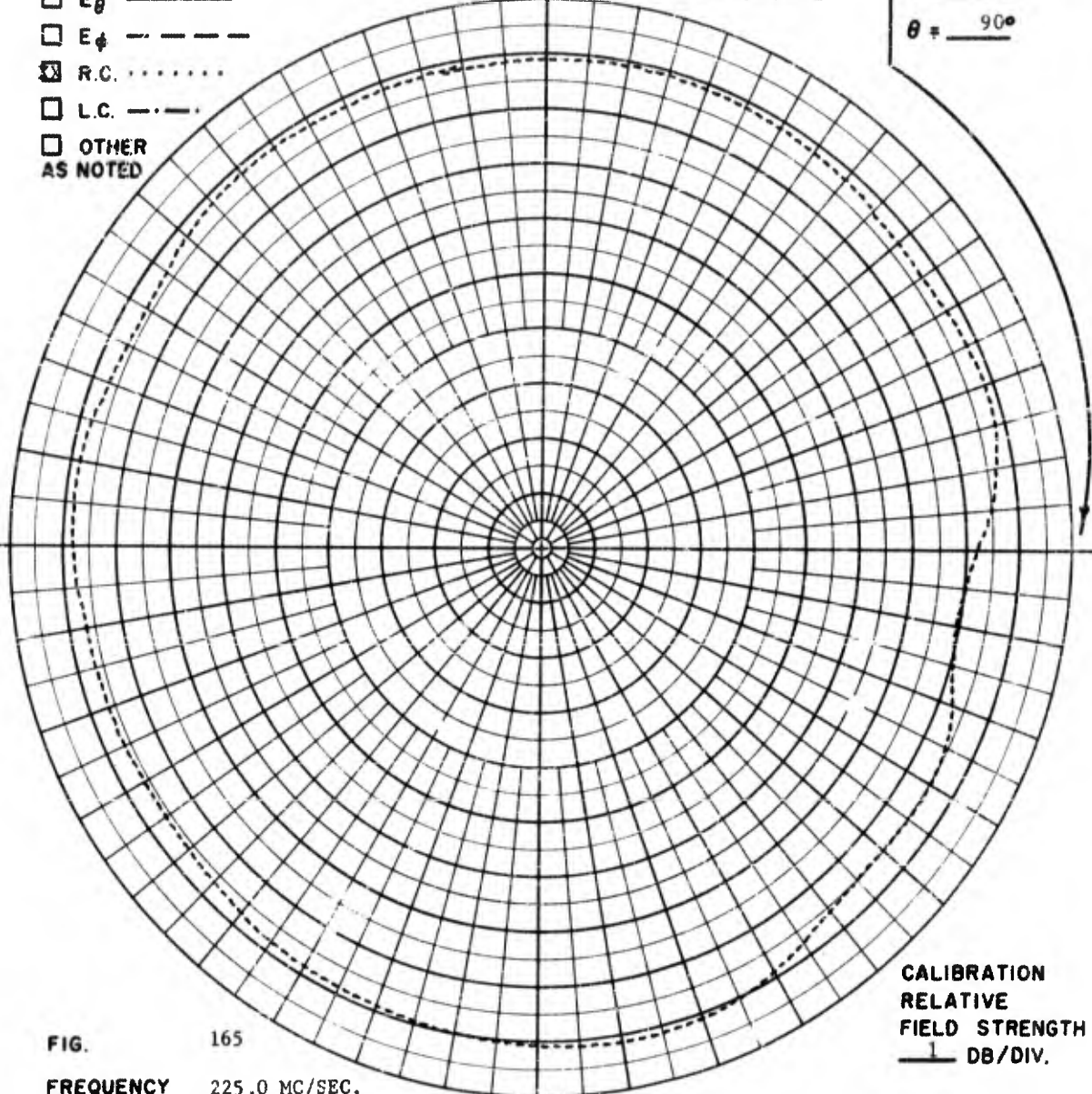
- POLARIZATION**
- GAIN REF
 - E_θ _____
 - E_ϕ - - - - -
 - R.C.
 - L.C. - . - . -
 - OTHER
AS NOTED

$\phi =$ _____ $\theta =$ _____

**COORDINATE
REFERENCE**

$\phi = 150^\circ$
 $\theta = 90^\circ$

PSL 1515



**CALIBRATION
RELATIVE
FIELD STRENGTH
DB/DIV.**

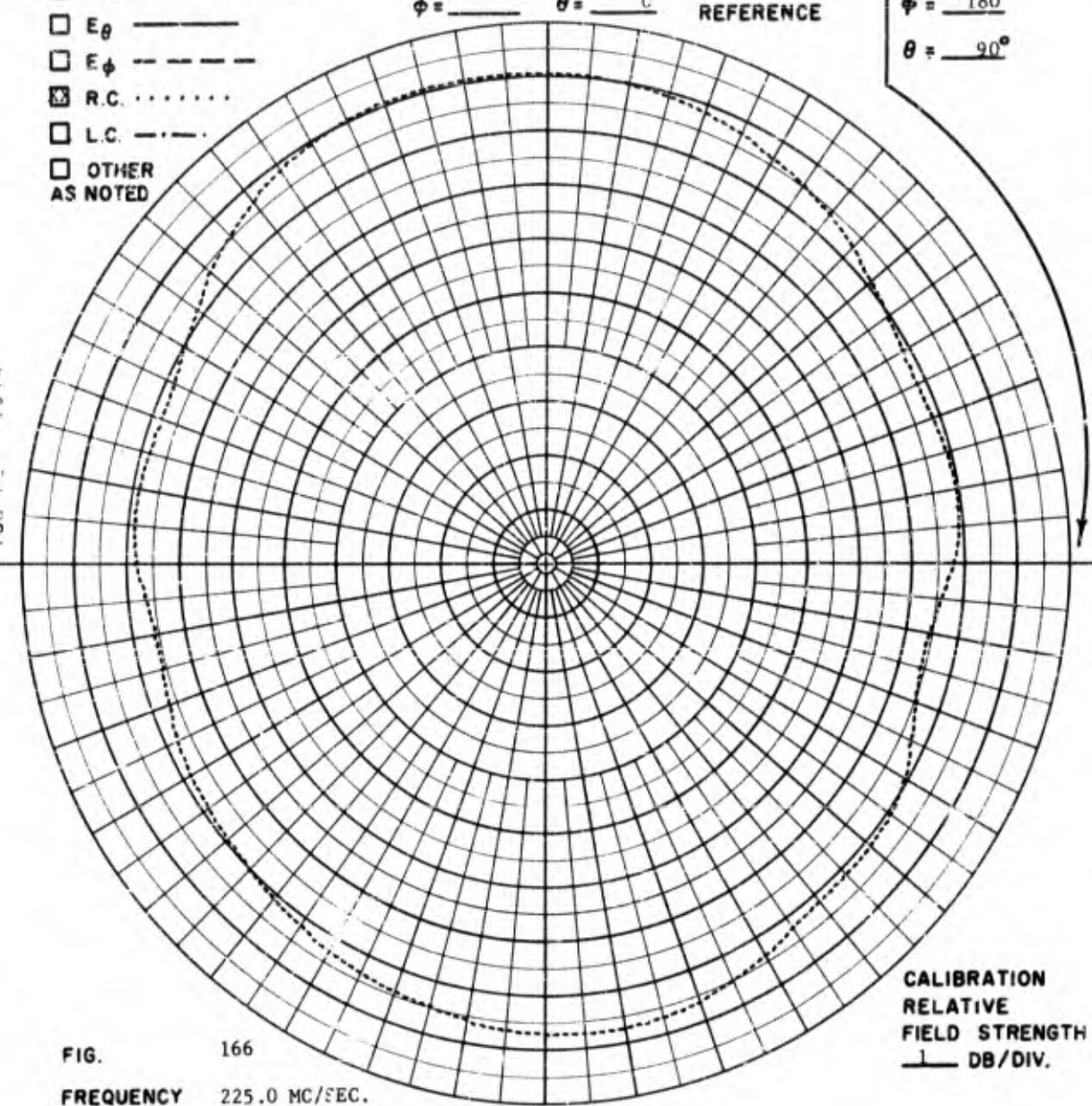
FIG. 165
FREQUENCY 225.0 MC/SEC.
ANTENNA MODEL 2.031 TWO ELEMENT ARRAY FED 180° OUT OF PHASE.
REMARKS

- POLARIZATION**
- GAIN REF
 - E_θ _____
 - E_ϕ - - - - -
 - R.C.
 - L.C. - - - - -
 - OTHER AS NOTED

$\phi =$ _____^o $\theta =$ _____^o **COORDINATE REFERENCE**

$\phi =$ 180^o
 $\theta =$ 90^o

PSL 1-2 1514



CALIBRATION
RELATIVE
FIELD STRENGTH
1 DB/DIV.

FIG. 166
FREQUENCY 225.0 MC/SEC.
ANTENNA MODEL 2.031 TWO ELEMENT ARRAY FED 180° OUT OF PHASE.
REMARKS

POLARIZATION

- GAIN REF
- E_{θ} —————
- E_{ϕ} - - - - -
- R.C.
- L.C. - . - . -
- OTHER
AS NOTED

$\phi = 0^\circ$ $\theta = 90^\circ$ COORDINATE REFERENCE

$\phi = 270^\circ$
 $\theta = 90^\circ$

PSL No 1520

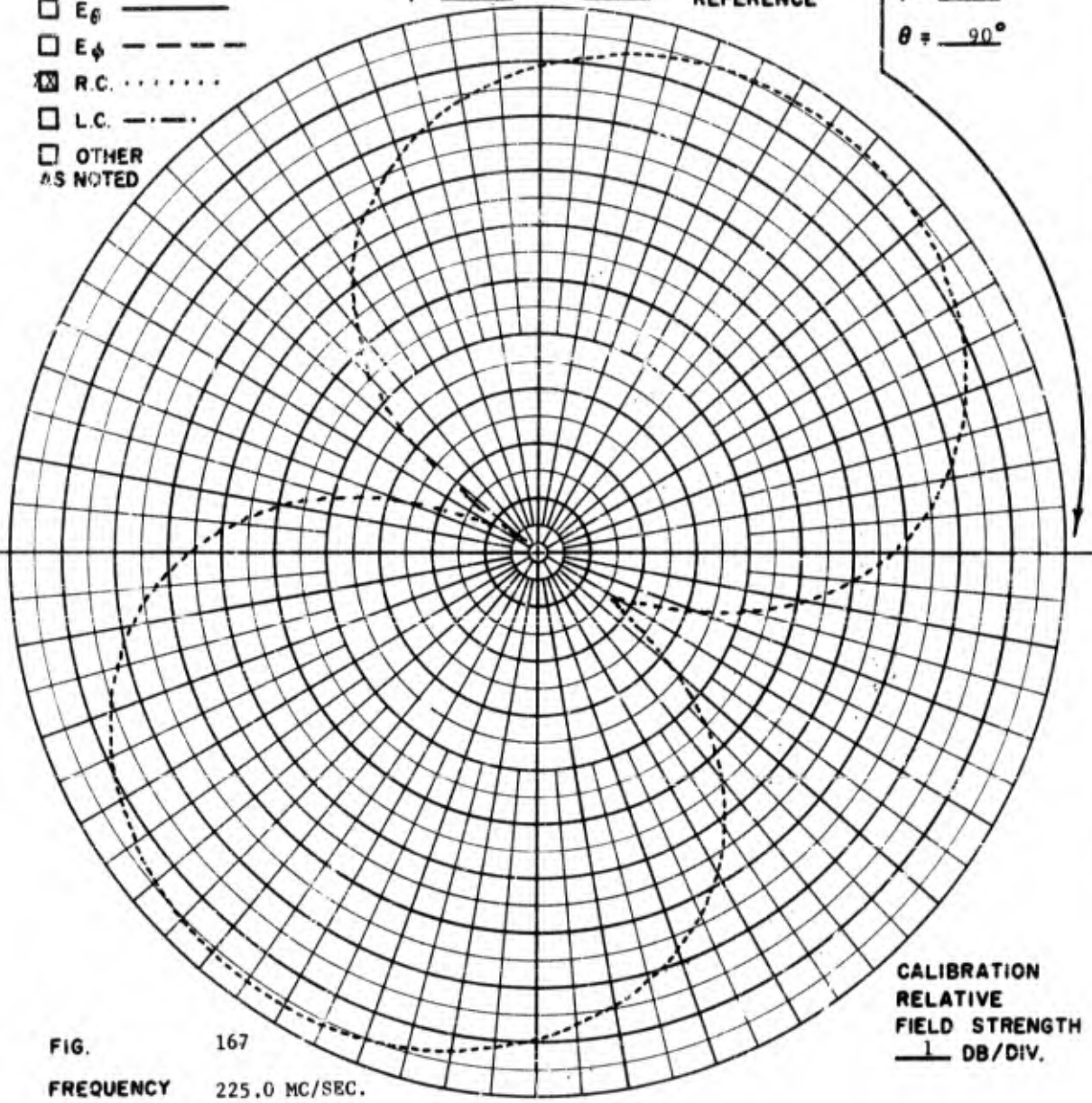
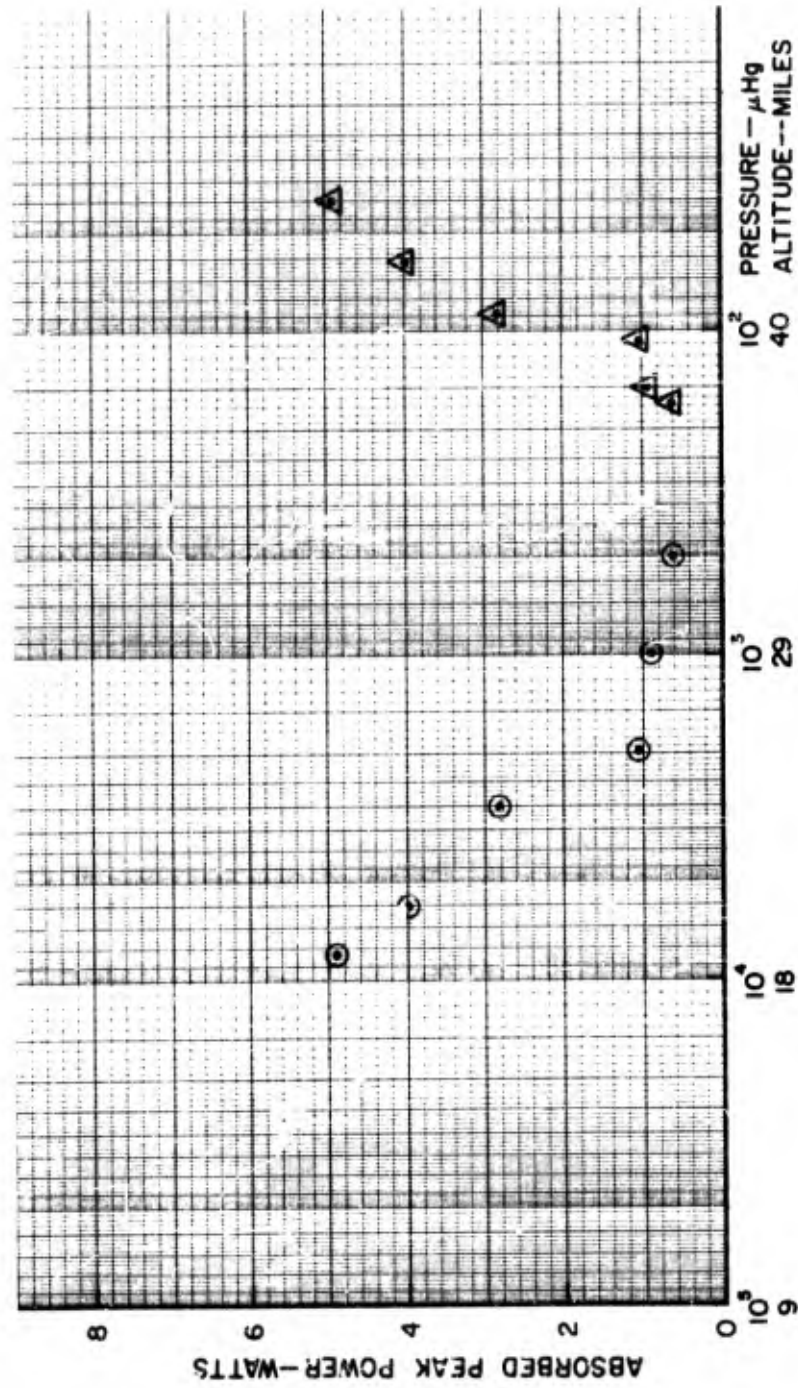


FIG. 167
 FREQUENCY 225.0 MC/SEC.
 ANTENNA MODEL 2.031 TWO ELEMENT ARRAY FED 180° OUT OF PHASE.
 REMARKS

CALIBRATION
RELATIVE
FIELD STRENGTH
1 DB/DIV.



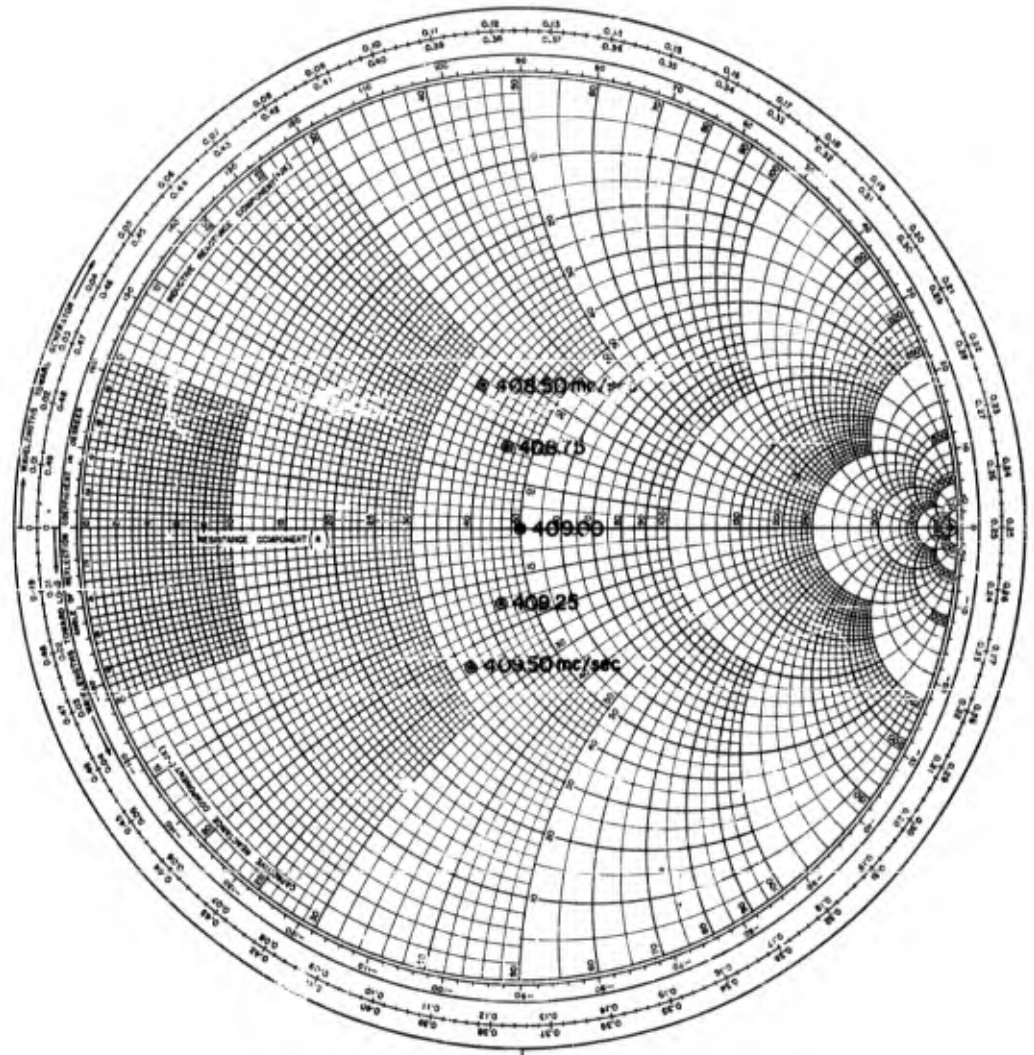


FIG. 169 - IDEALIZED IMPEDANCE CURVE OF A TWO ELEMENT ARRAY OF THE 4.000 SERIES, FLUSH MOUNTED COMMAND CONTROL QUADRALOOP ANTENNAS MOUNTED ON A 20-INCH DIAMETER CYLINDER

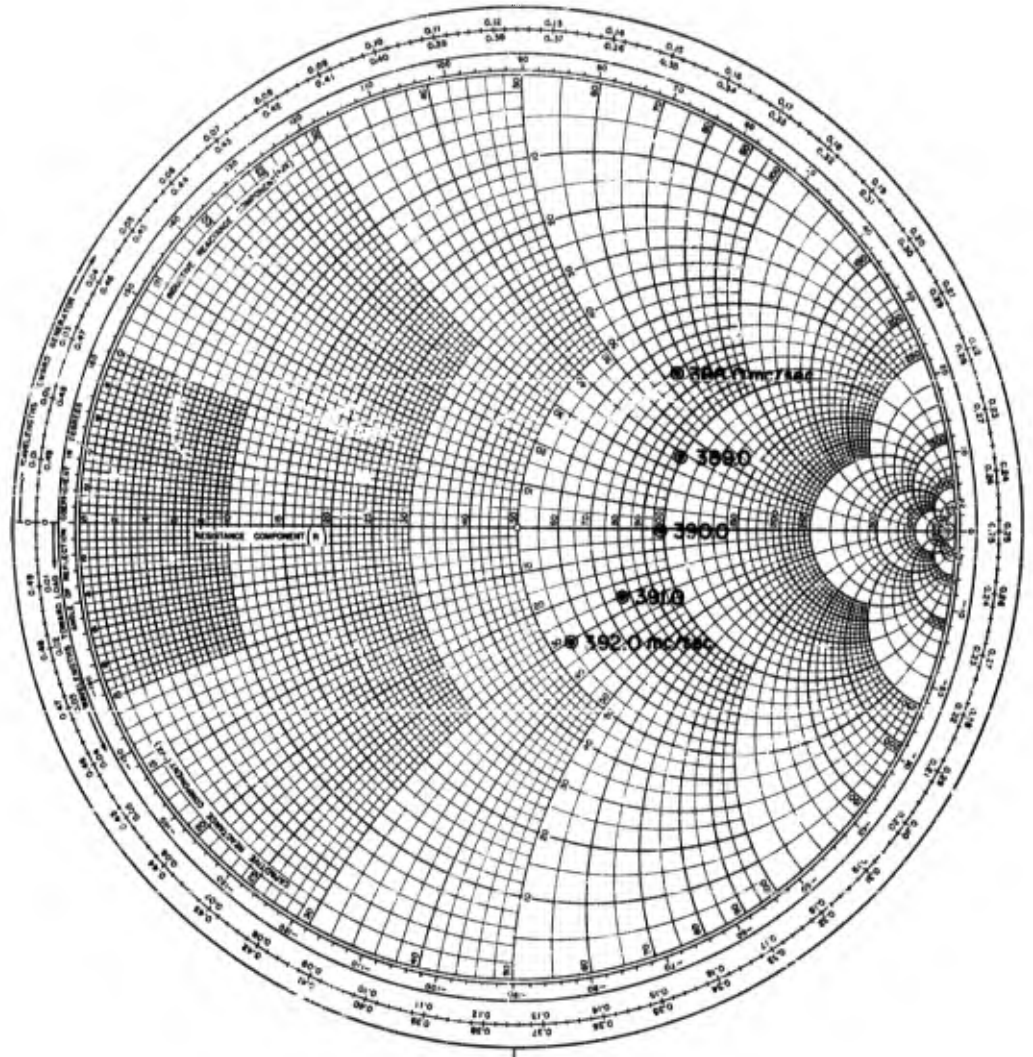


FIG. 170 - IDEALIZED IMPEDANCE CURVE FOR THE 4.000 SERIES, NONFLUSH MOUNTED COMMAND CONTROL QUADRALOOP ANTENNA MOUNTED ON A 9-INCH DIAMETER CYLINDER

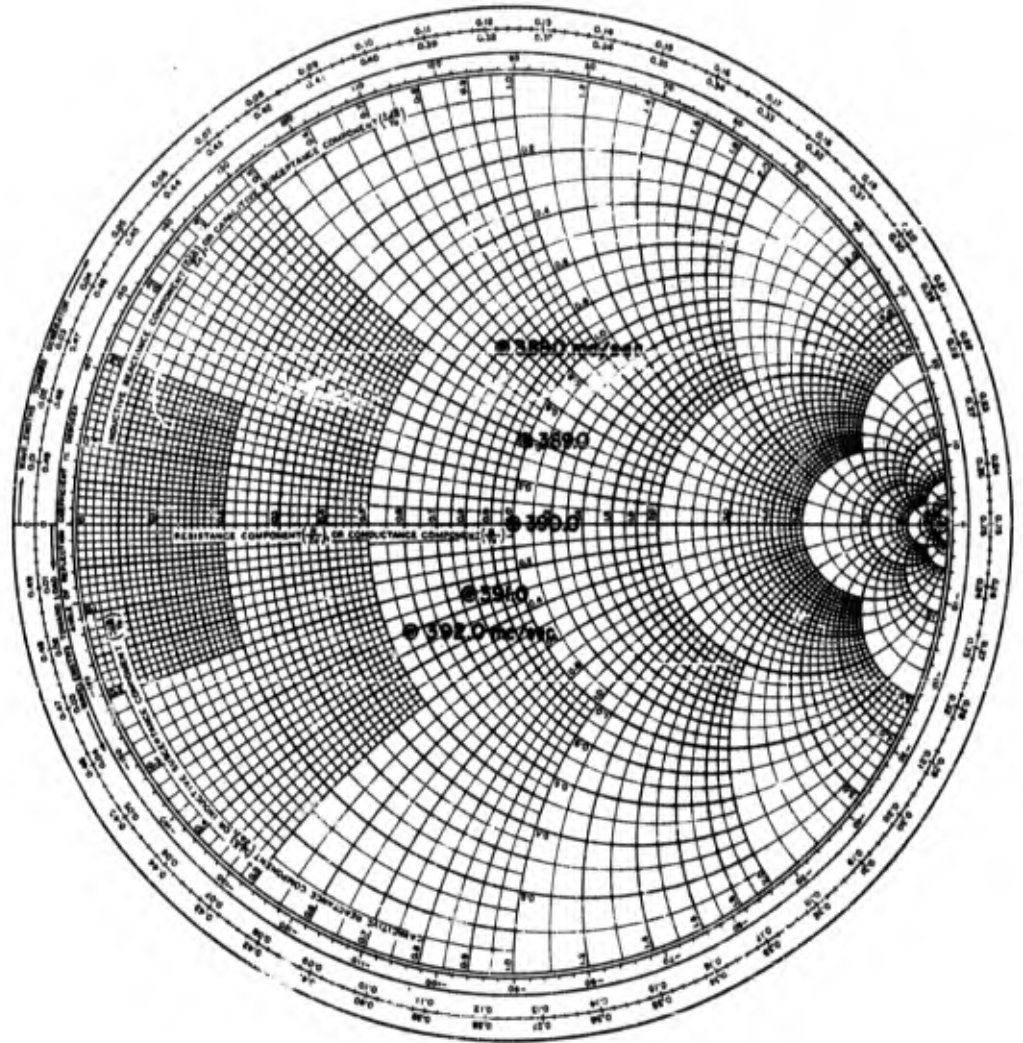


FIG. 171 - NORMALIZED IMPEDANCE CURVE OF THE 4.000 SERIES,
NONFLUSH MOUNTED COMMAND CONTROL
QUADRALOOP ANTENNA

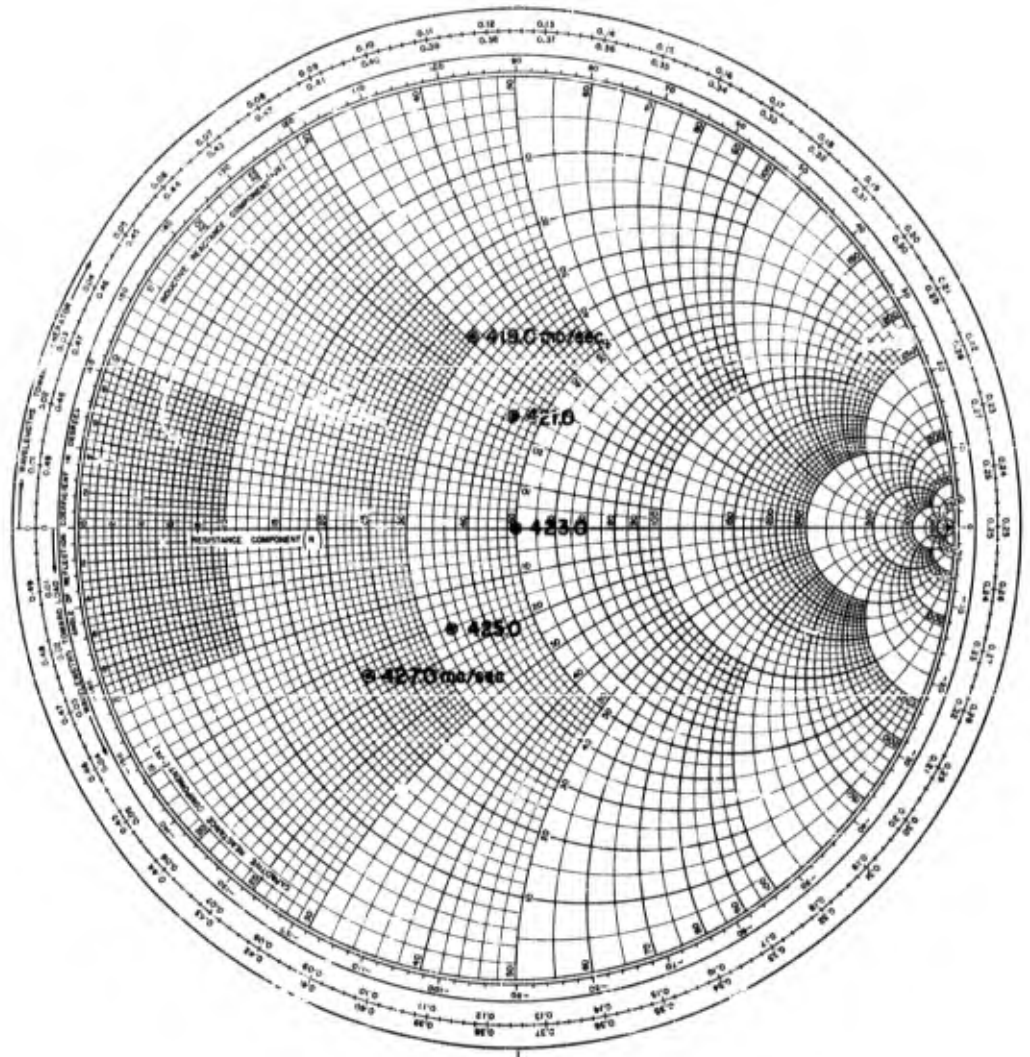


FIG. 172 - IDEALIZED IMPEDANCE CURVE FOR THE TWO ELEMENT
 ARRAY OF THE 4.000 SERIES, NONFLUSH MOUNTED
 COMMAND CONTROL QUADRALOOP ANTENNAS
 MOUNTED ON A 9-INCH DIAMETER CYLINDER

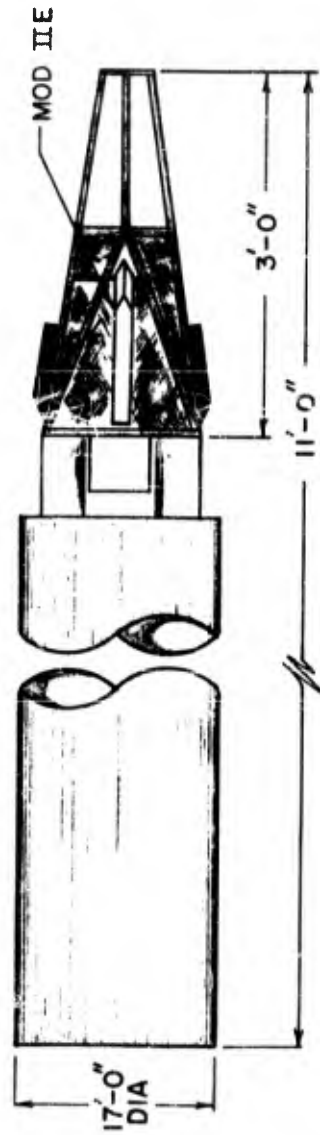


FIG. 174 - SKETCH OF THE VEHICLE MOCKUP FOR THE MODEL 4.001
PATTERN MEASUREMENTS

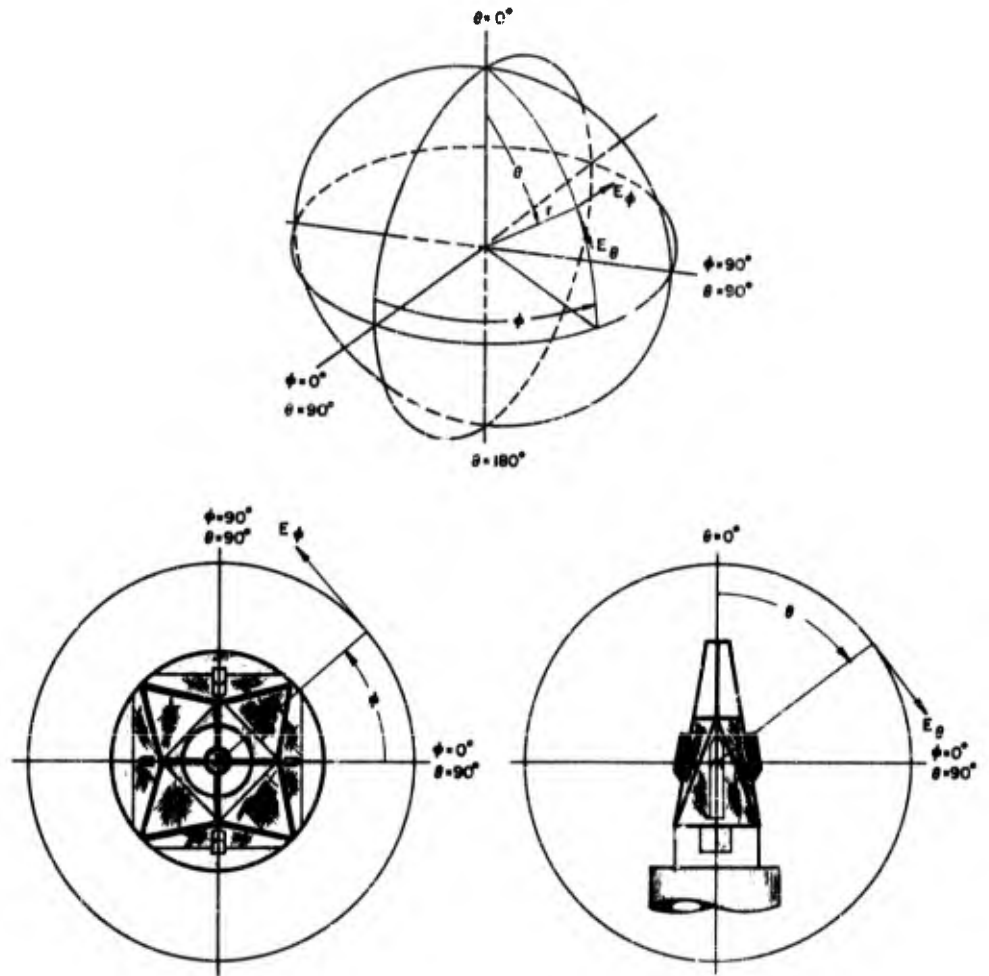


FIG. 175 - POSITION COORDINATES FOR THE MODEL 4.001 ANTENNA RADIATION PATTERN MEASUREMENTS

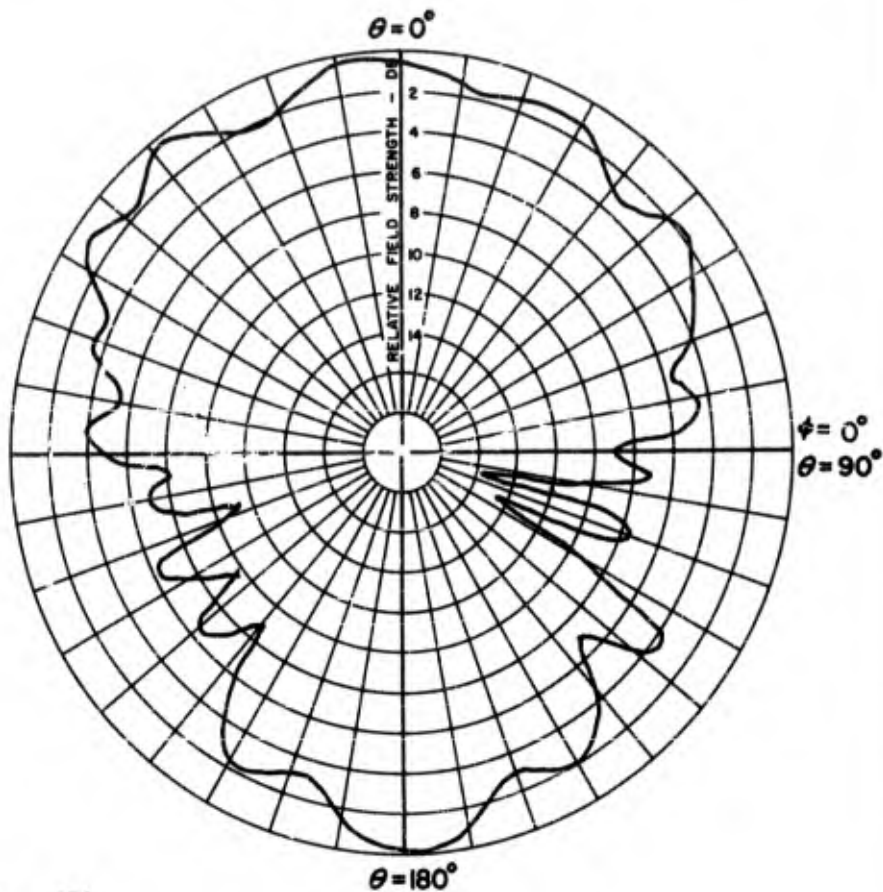


FIG. 176

MISSILE — Javelin

ANTENNA — Mod 4, 001 Quadraloop in an array of two fed 180° out of phase

FREQUENCY — 412.0 Mc

POLARIZATION — RIGHT CIRCULAR

REMARKS — AT $\theta = 180^\circ$, $\theta = 0^\circ$ THE SIGNAL IS -1 DB WITH RESPECT TO A STODDART HALF WAVE DIPOLE ILLUMINATED BY A RIGHT CIRCULAR HELIX.

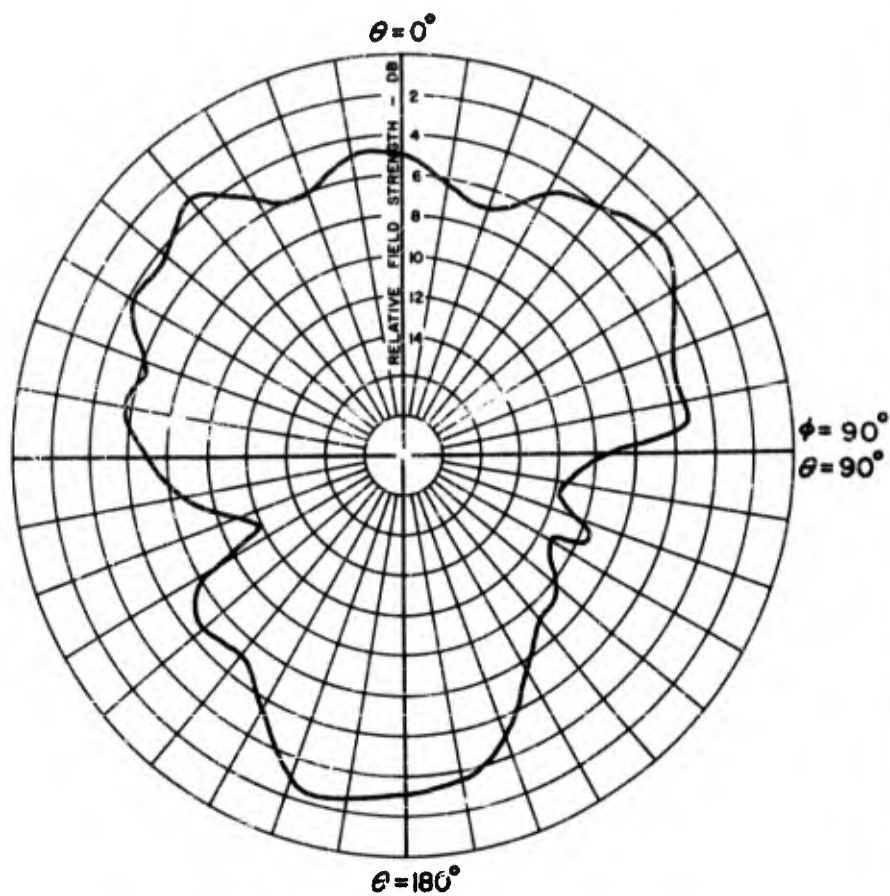


FIG. 177

MISSILE — Javelin

ANTENNA — Mod 4.001 Quadraloop in an array of two fed 180° out of phase

FREQUENCY — 412.0 Mc

POLARIZATION — RIGHT CIRCULAR

REMARKS —

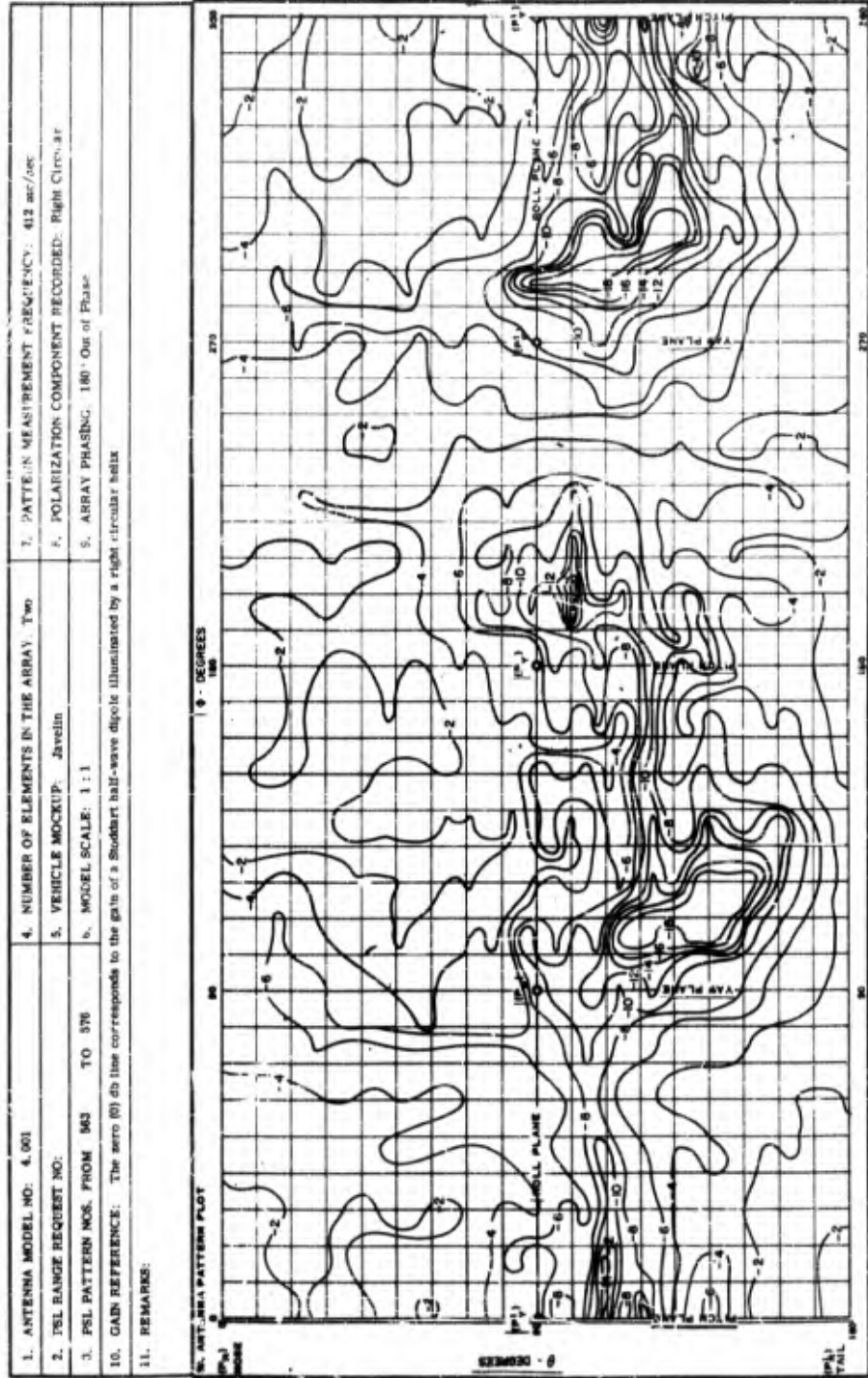


FIG. 178 - POWER CONTOUR PLOT OF THE TWO ELEMENT ARRAY OF MODEL 4.001 ANTENNAS

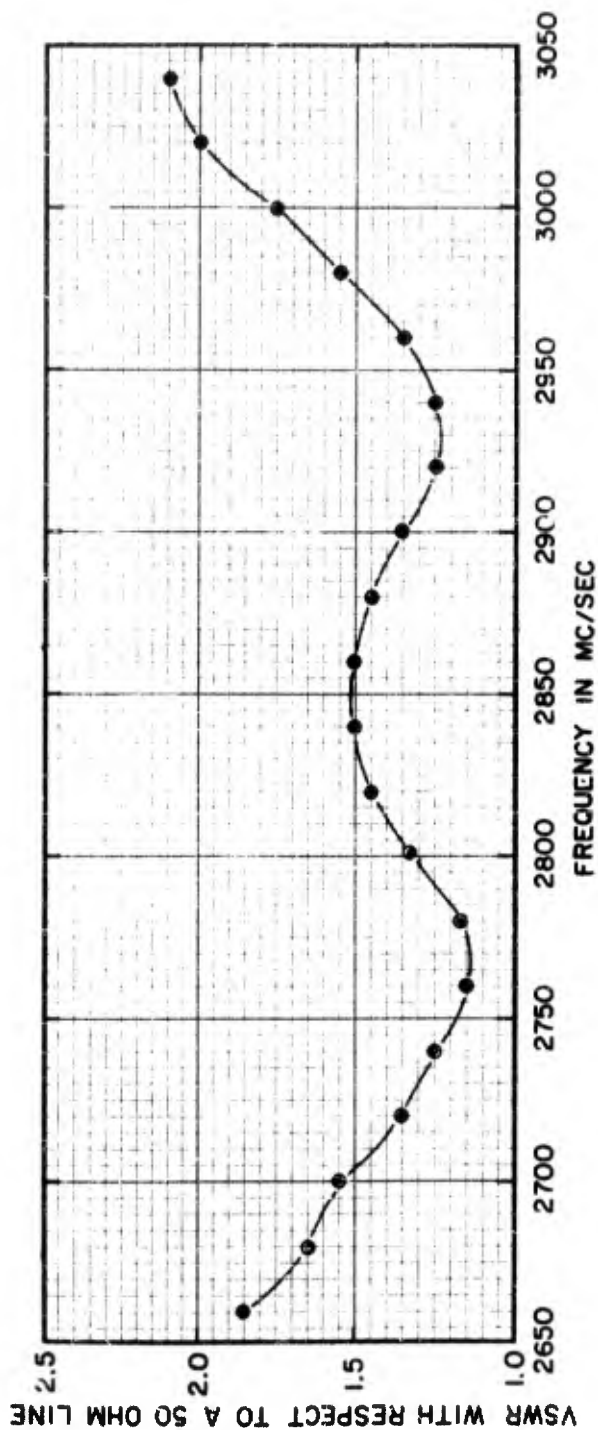


FIG. 179 - CURVE OF VSWR VERSUS FREQUENCY FOR THE TWO ELEMENT ARRAY OF THE MODEL 6.005 QUADRALOOP ANTENNAS MOUNTED ON A 15-INCH DIAMETER CYLINDER

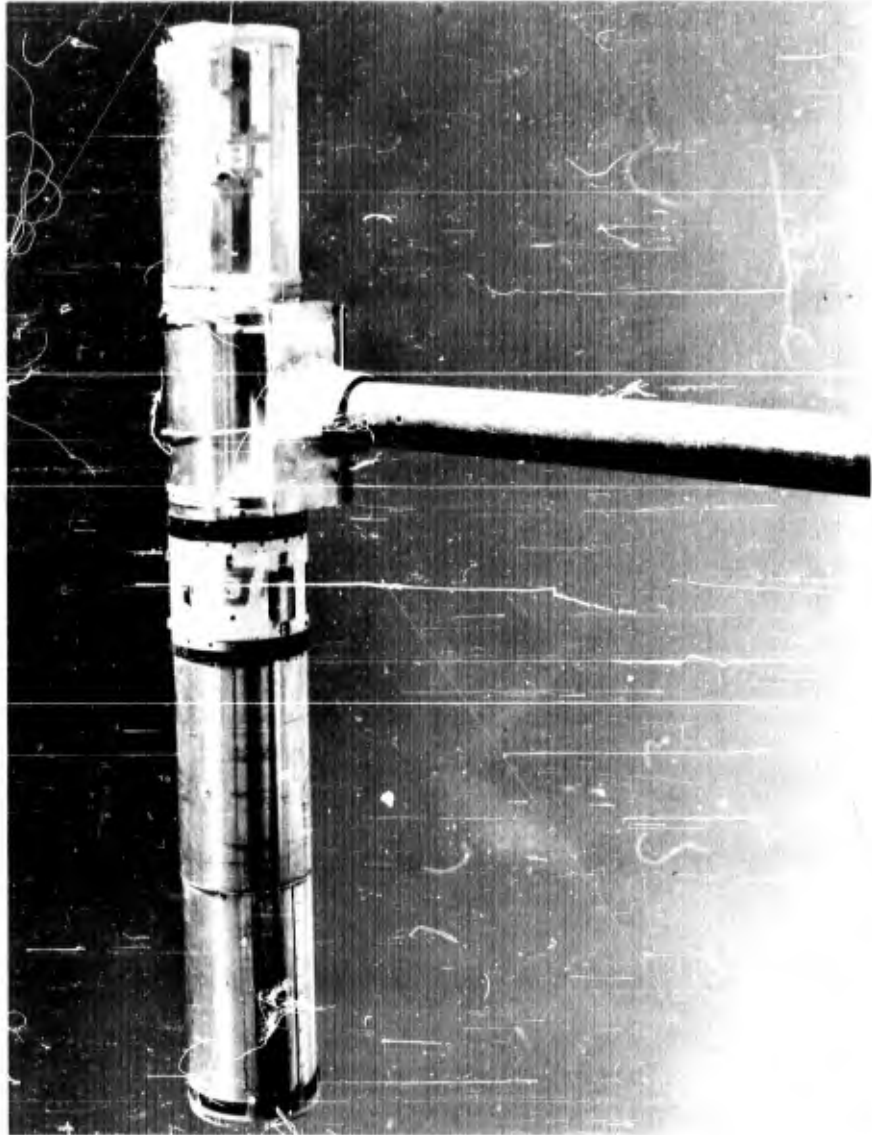


FIG. 180 - PHOTOGRAPH OF THE VEHICLE MOCKUP USED FOR THE MODEL
6.003 RADIATION PATTERN MEASUREMENTS

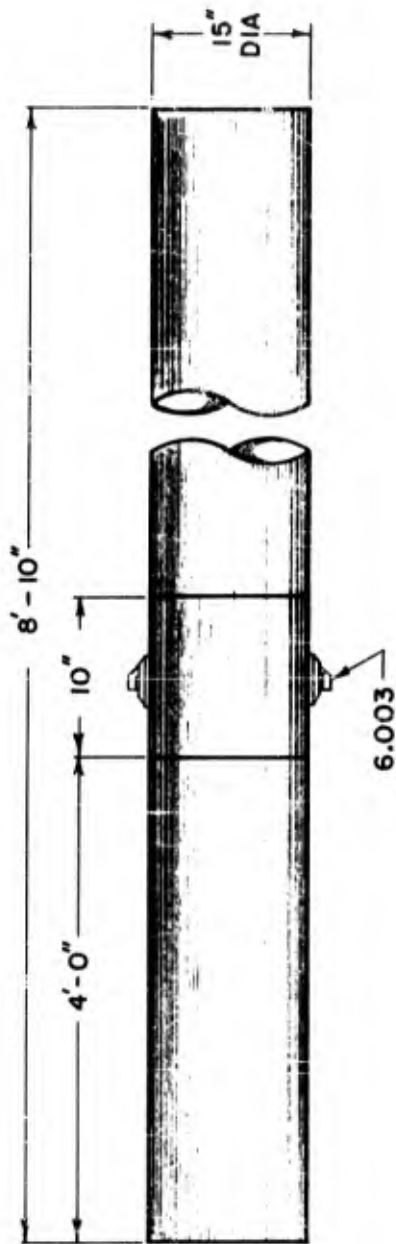


FIG. 181 - SKETCH OF THE VEHICLE MOCKUP FOR THE MODEL 6.003
RADIATION PATTERN MEASUREMENTS

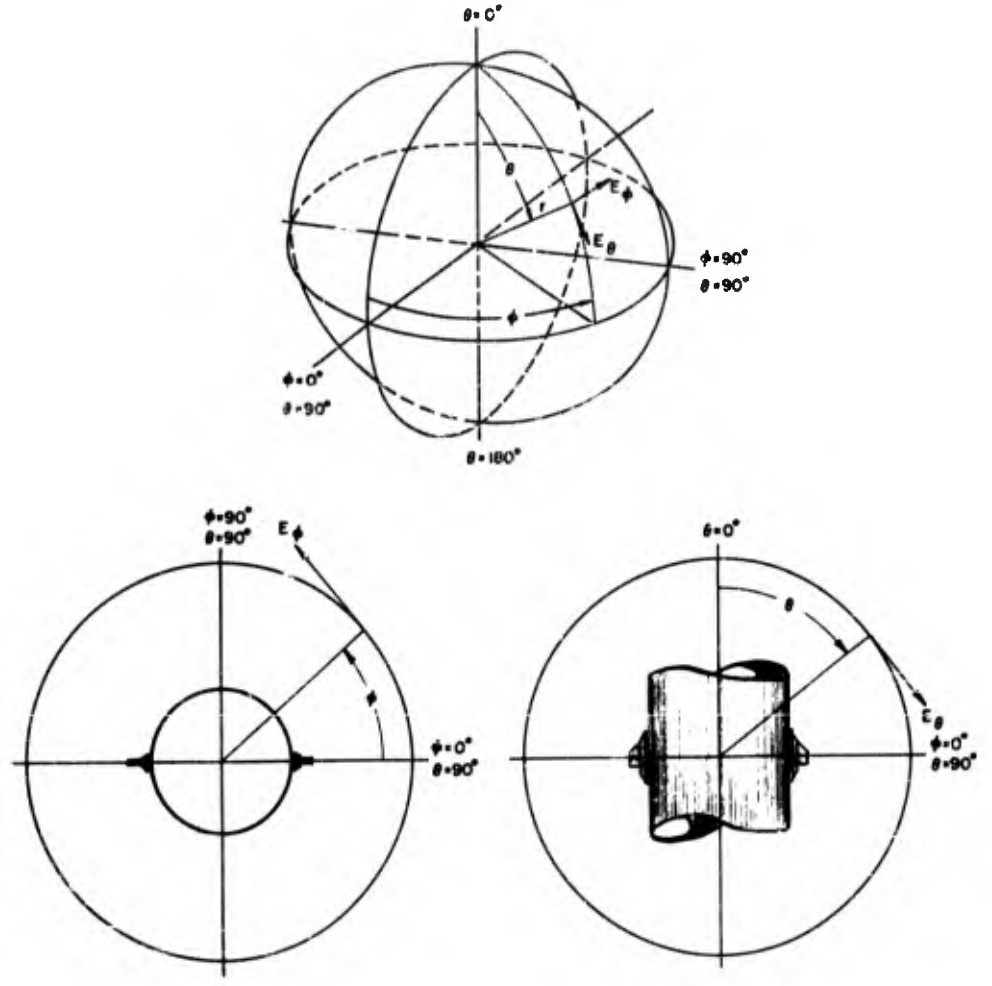


FIG. 182 - POSITION COORDINATES FOR THE MODEL 6.003 RADIATION PATTERN MEASUREMENTS

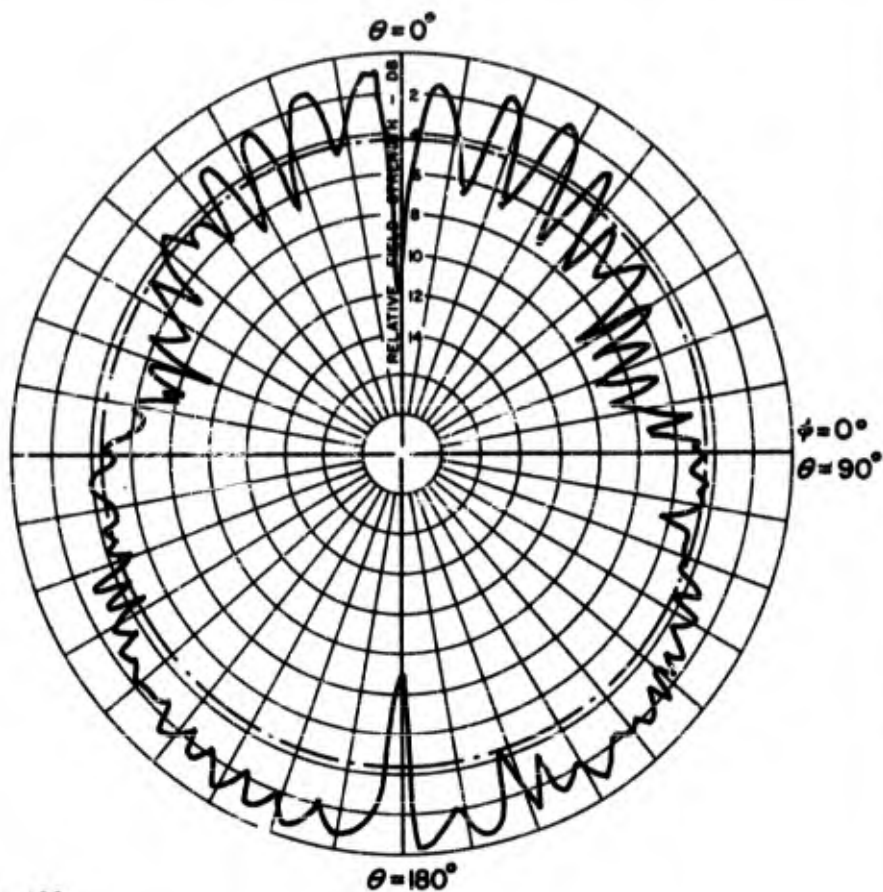


FIG. 183

MISSILE — Aerobee 150, 15" Diameter

ANTENNA — Mod 6.003 two element array fed in phase

FREQUENCY — 2.85 gc

POLARIZATION — E_θ ——— E_ϕ - - - - -

REMARKS — The dash-dot-dash circle indicates the relative gain of an isotropic radiator.

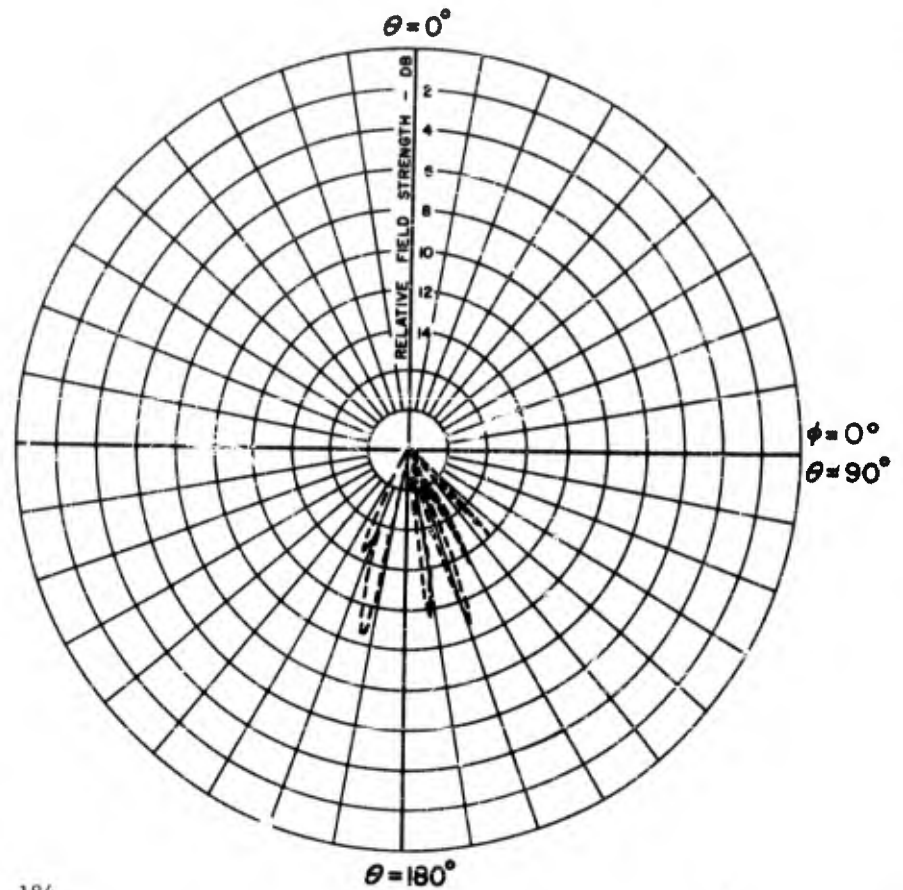


FIG. 184

MISSILE — Aerobee 150, 15' Diameter

ANTENNA — Mod 6.003 two element array fed in phase

FREQUENCY — 2.85 gc

POLARIZATION — E_{θ} _____ E_{ϕ} - - - - -

REMARKS —

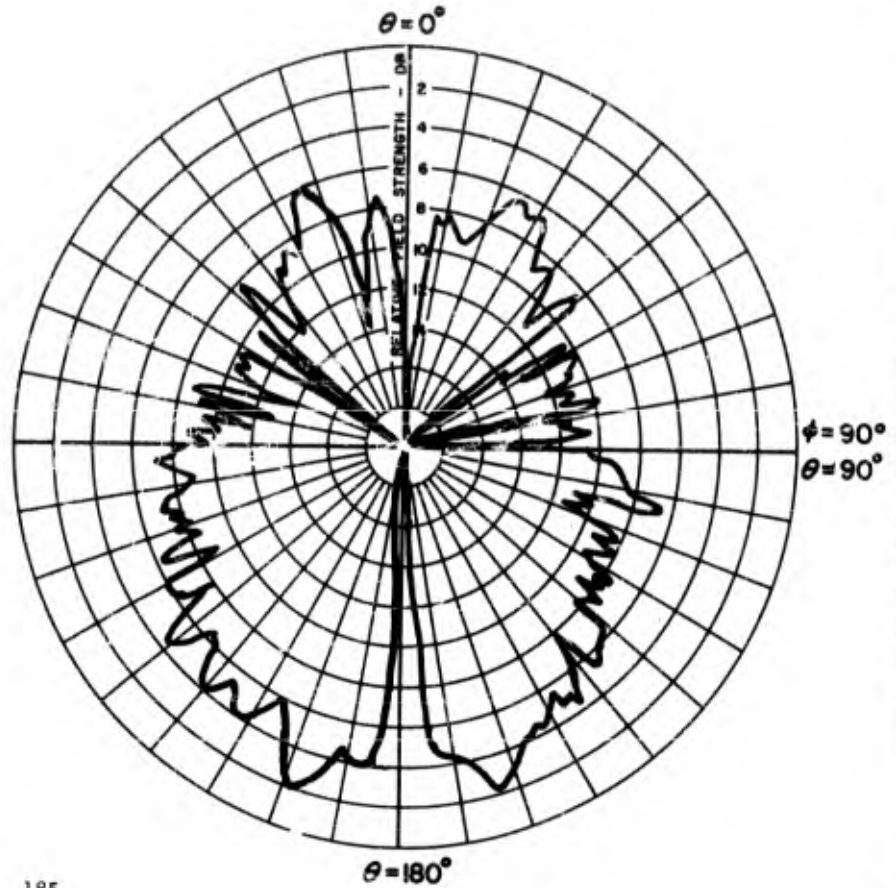


FIG. 185

MISSILE — Aerobee 150, 15" Diameter

ANTENNA — Mod 6.003 two element array fed in phase

FREQUENCY — 2.85 gc

POLARIZATION — E_{θ} ——— E_{ϕ} - - - - -

REMARKS —

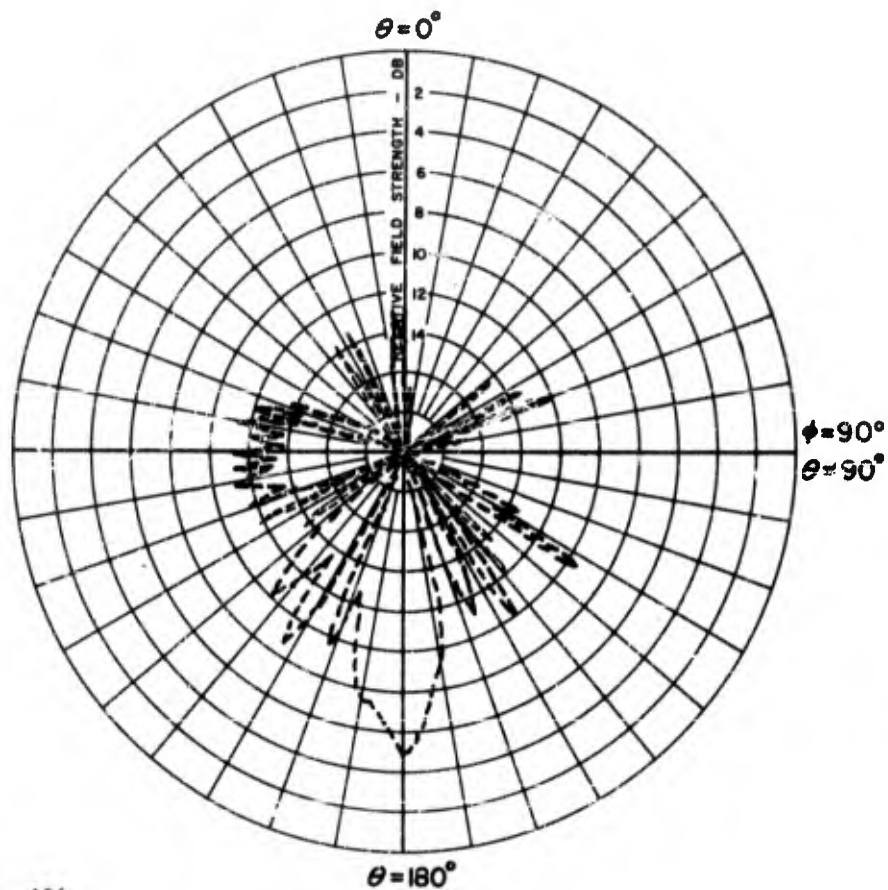


FIG. 186

MISSILE — Aerobee 150, 15" Diameter

ANTENNA — Mod 6.003 two element array fed in phase

FREQUENCY — 2.85 gc

POLARIZATION — E_θ _____ E_ϕ -----

REMARKS —

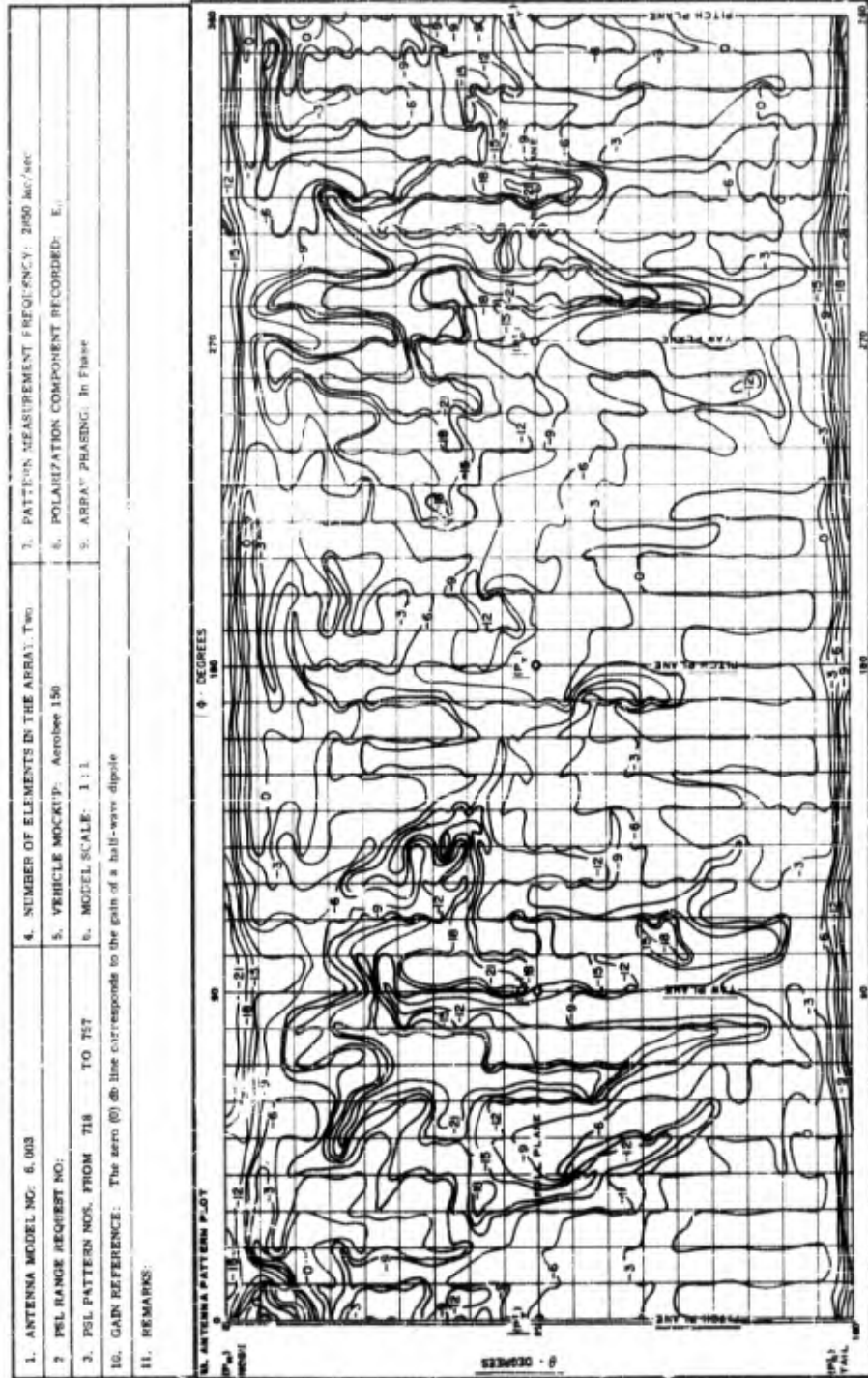


FIG. 187 - POWER CONTOUR PLOT OF THE TWO ELEMENT ARRAY OF MODEL 6 003 ANTENNAS, FOR THE E_z POLARIZATION VECTOR

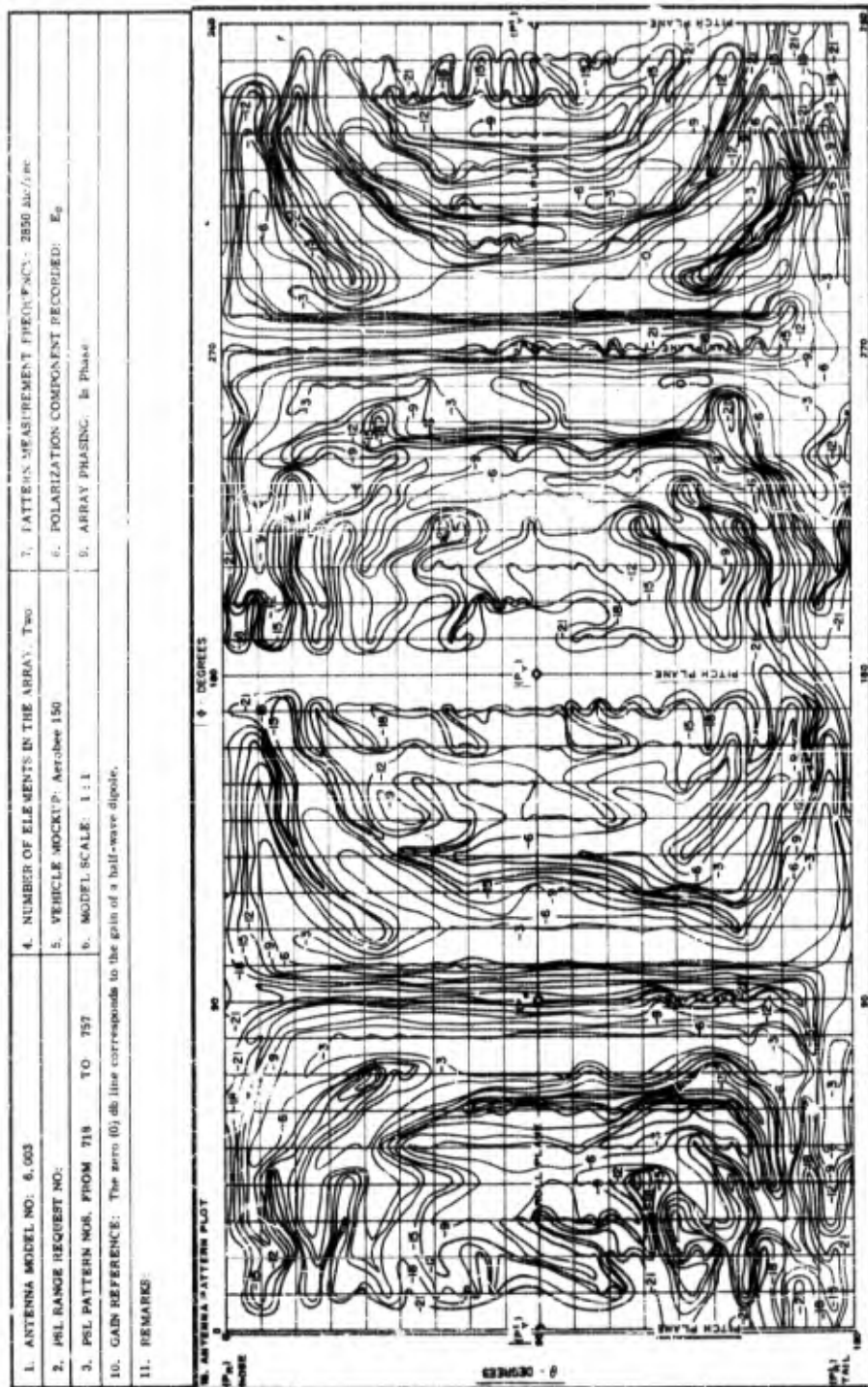


FIG. 188 - POWER CONTOUR PLOT FOR THE TWO ELEMENT ARRAY OF MODEL 6.003 ANTENNAS, FOR THE E_{θ} POLARIZATION VECTOR

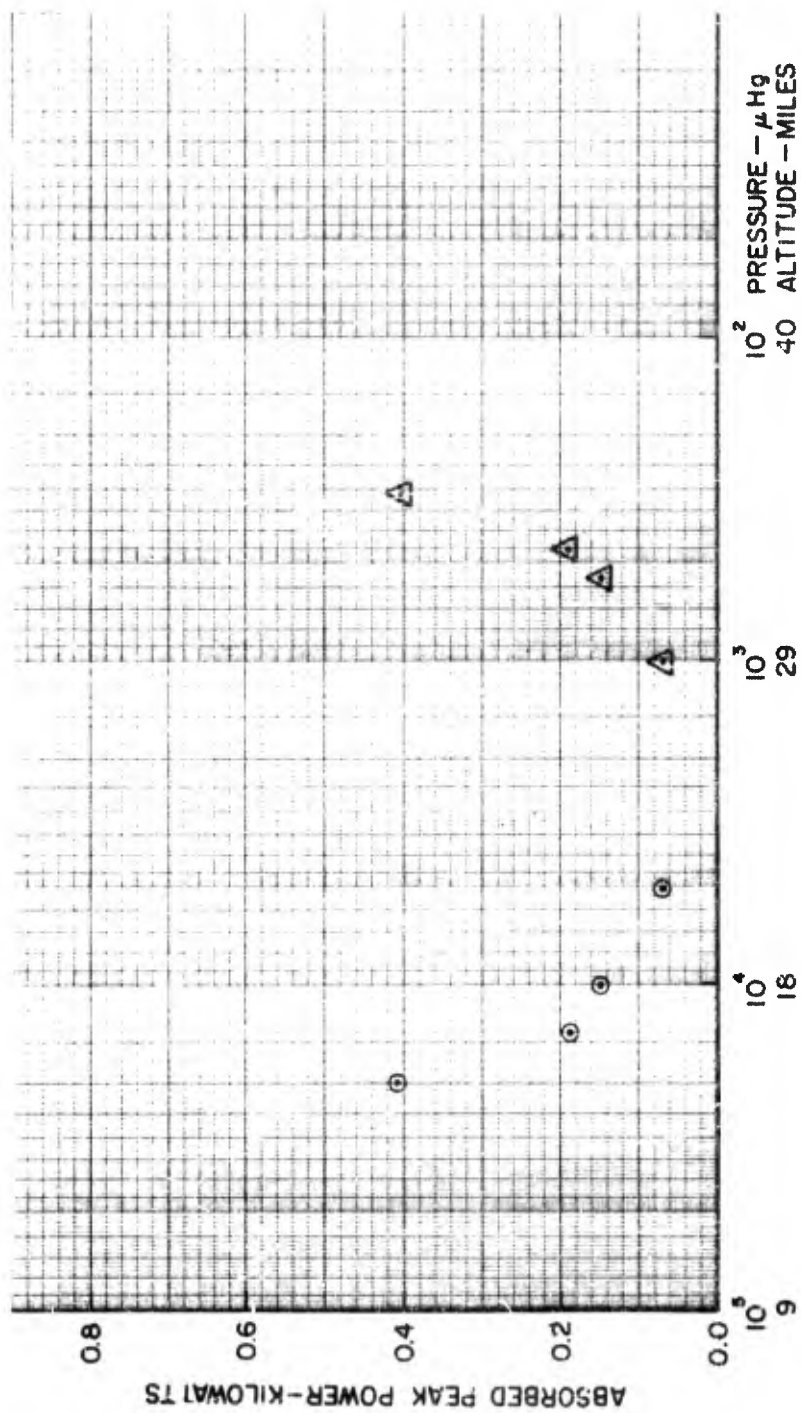


FIG. 189 - REPRESENTATIVE DIFFUSION BREAKDOWN CURVE FOR THE
 6,000 SERIES QUADRALOOP TYPE C-BAND
 BEACON ANTENNA

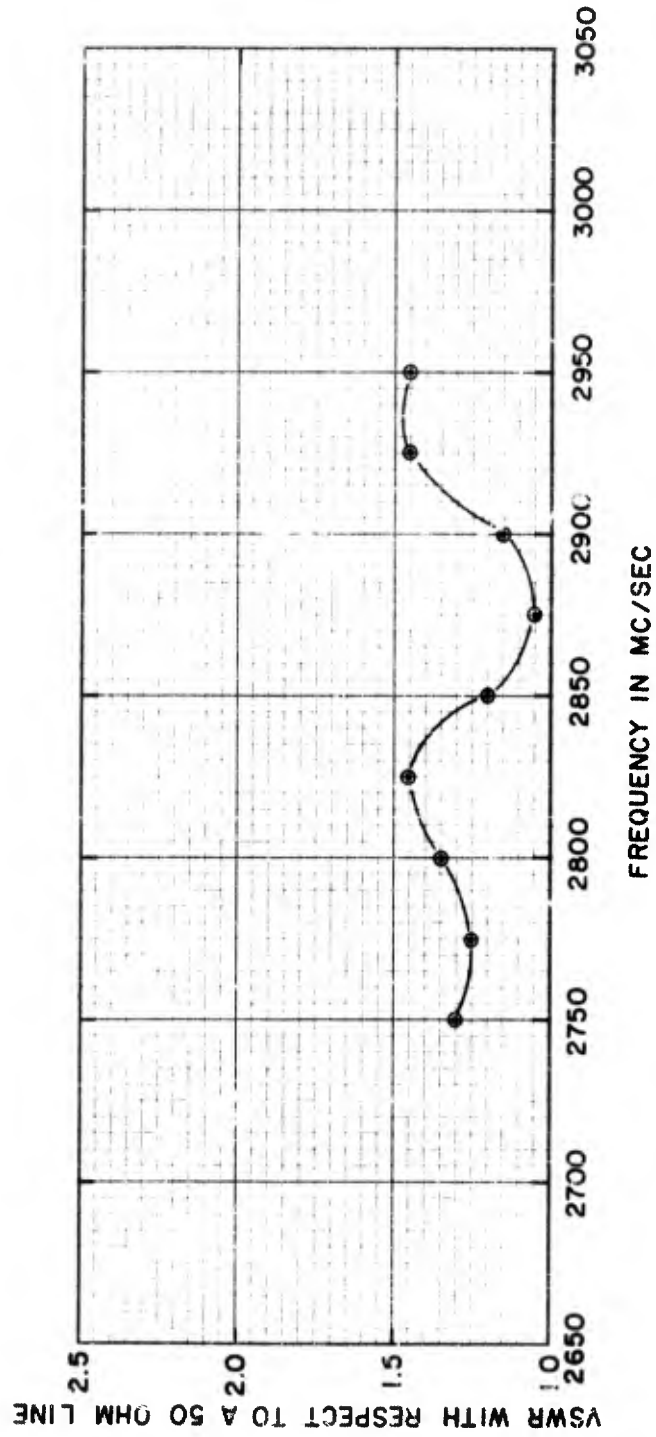


FIG. 190 - CURVE OF VSWR VERSUS FREQUENCY FOR A FOUR ELEMENT ARRAY OF MODEL 6.010 FOLDED VALENTINE ANTENNAS MOUNTED ON A 15-INCH DIAMETER CYLINDER

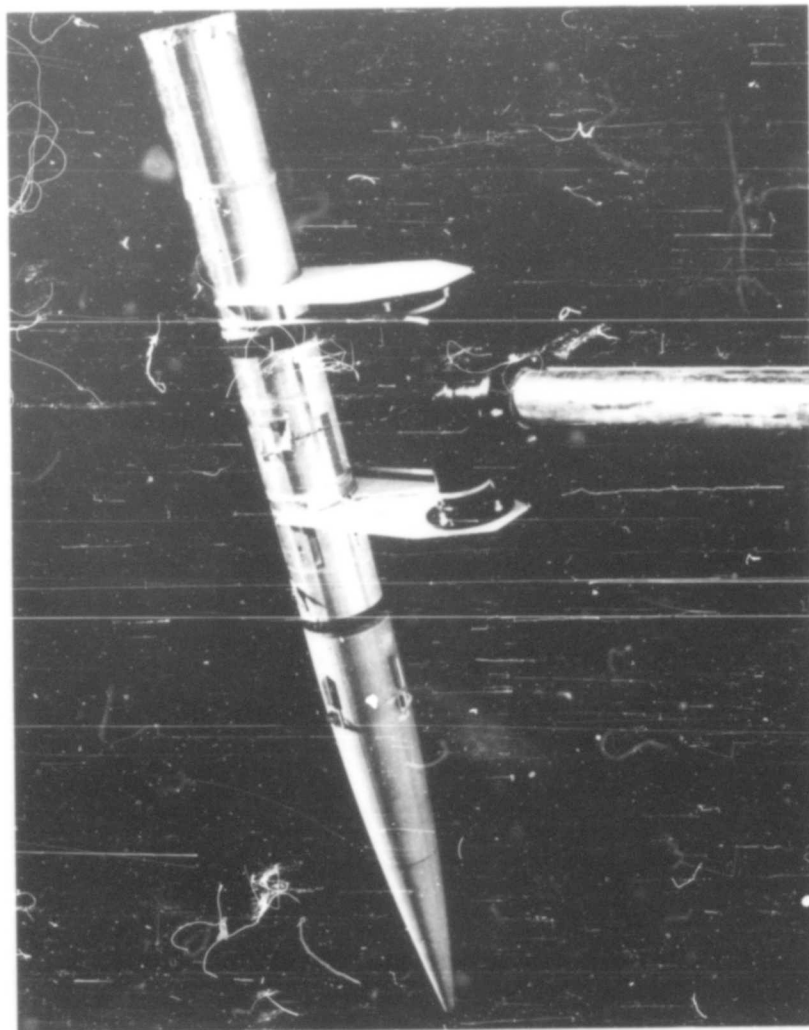


FIG. 191 - PHOTOGRAPH OF THE VEHICLE MOCKUP USED FOR THE MODEL
6.010 C-BAND FOLDED VALENTINE ANTENNA RADIATION
PATTERN MEASUREMENTS

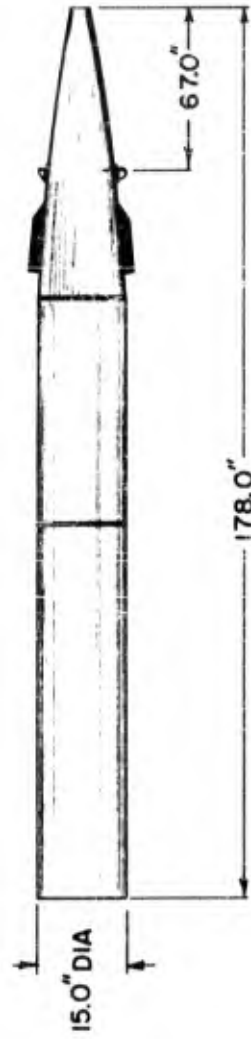


FIG. 192 - SKETCH OF THE VEHICLE MOCKUP USED FOR THE MODEL 6.010 C-BAND FOLDED VALENTINE ANTENNA RADIATION PATTERN MEASUREMENTS

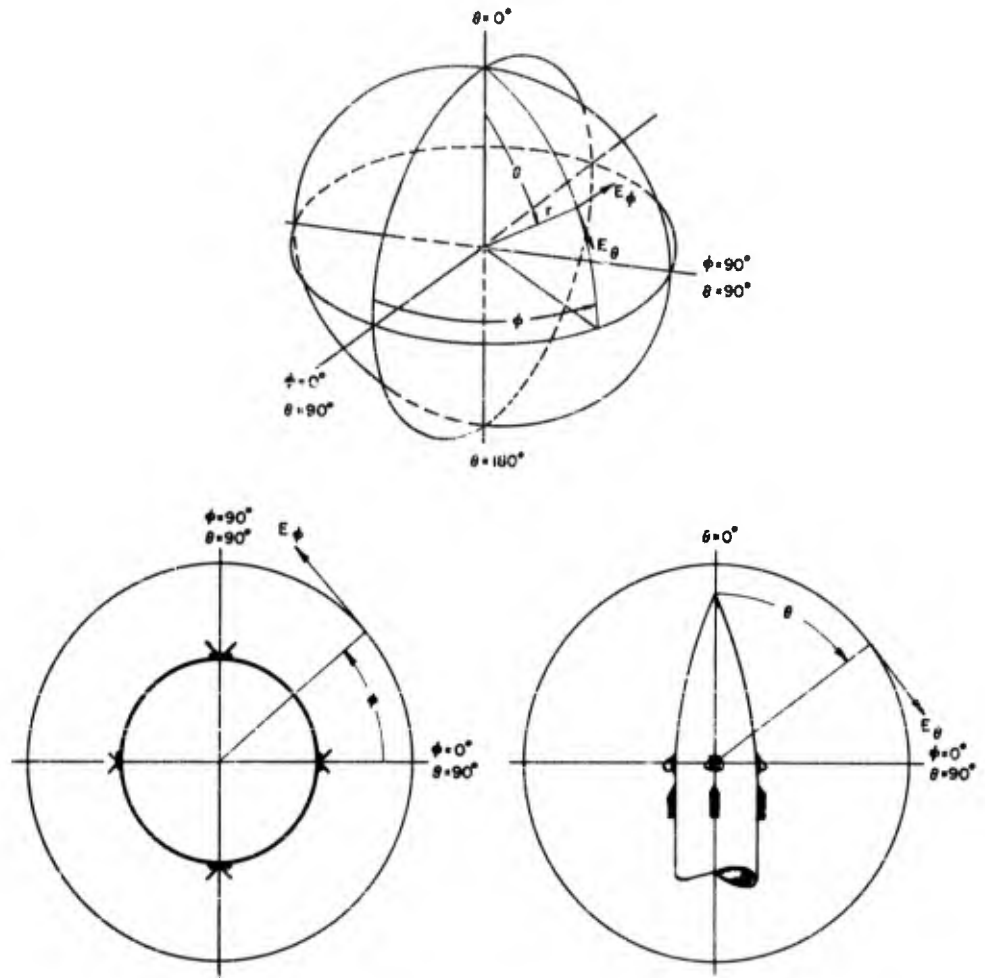
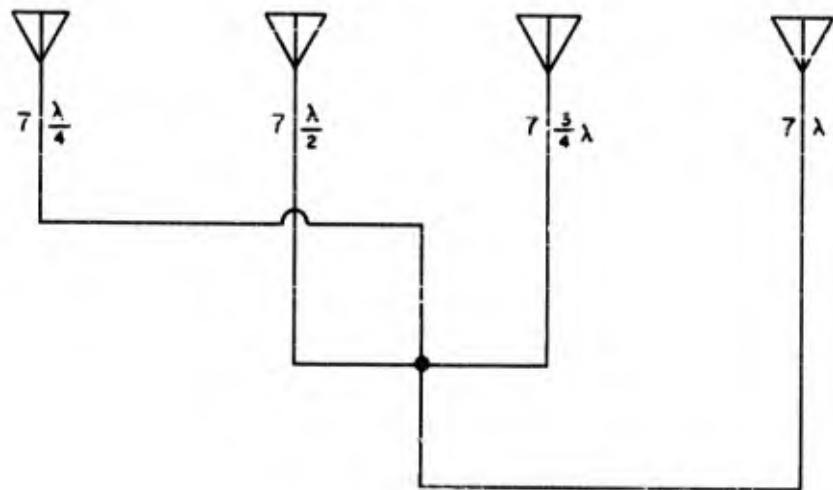
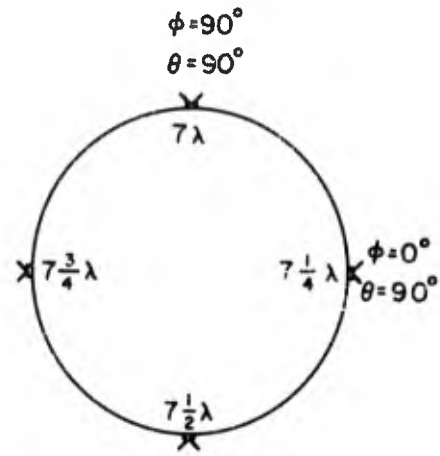


FIG. 193 - POSITION COORDINATES FOR THE MODEL 6.010 ANTENNA RADIATION PATTERN MEASUREMENTS



CHARACTERISTIC IMPEDANCE
OF CABLE IS 50 OHMS

FIG. 194 - SKETCH OF THE HARNESS FOR THE MODEL 6.010
FOUR ELEMENT ARRAY

POLARIZATION

- GAIN, REF - - - - -
- E_{θ} - - - - -
- E_{ϕ} - - - - -
- R.C. - - - - -
- L.C. - - - - -
- OTHER AS NOTED

$\phi = \underline{\hspace{1cm}}^{\circ}$ $\theta = \underline{0}^{\circ}$ COORDINATE REFERENCE

$\phi = \underline{0}^{\circ}$
 $\theta = \underline{90}^{\circ}$

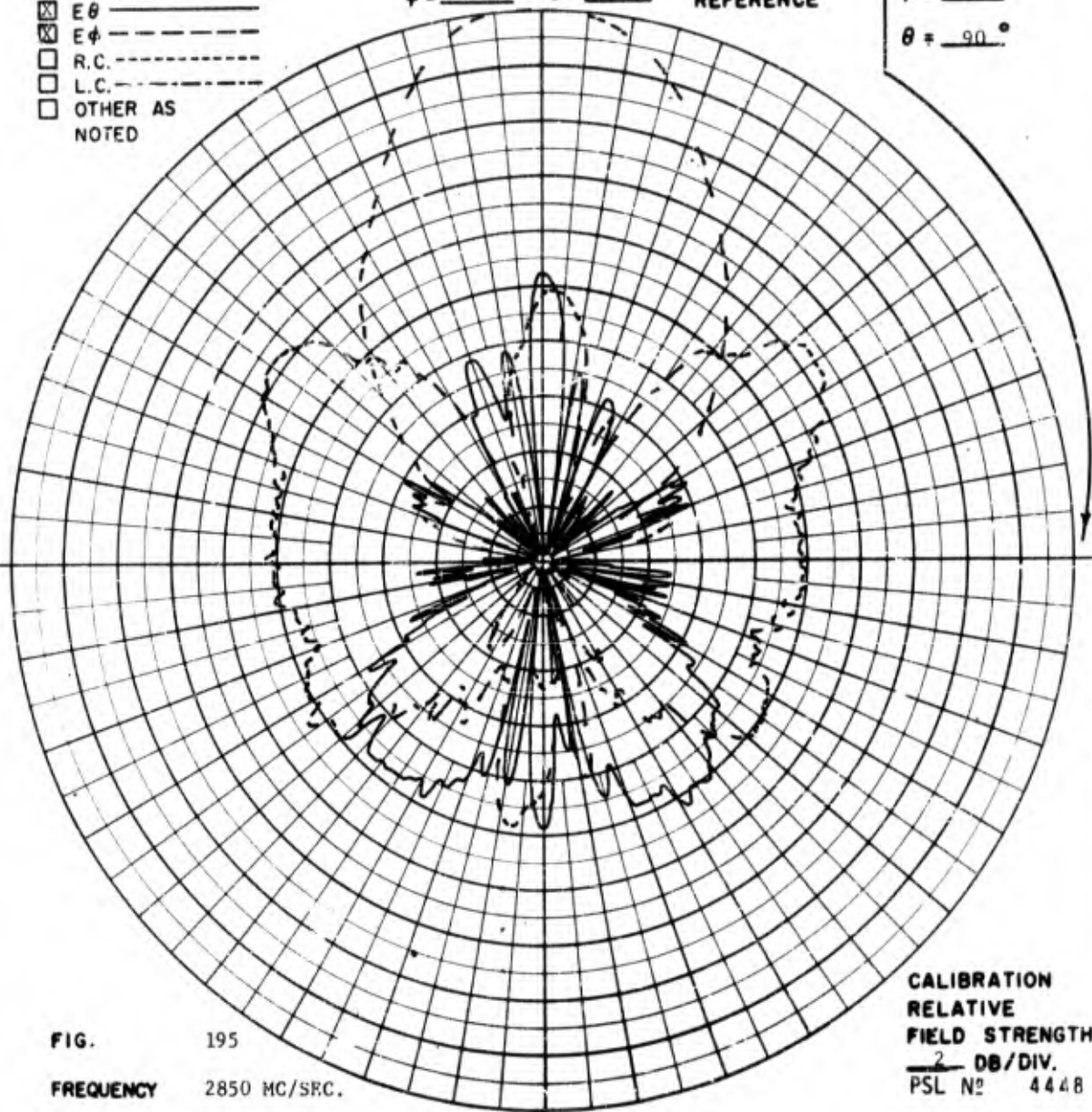


FIG. 195

FREQUENCY 2850 MC/SEC.

ANTENNA MODEL 6.010 FOUR ELEMENT ARRAY.

REMARKS THE REFERENCE IS A SGH 2.6 ANTENNA HAVING A GAIN OF +17.7 DB WITH RESPECT TO ISOTROPIC.

CALIBRATION
RELATIVE
FIELD STRENGTH
2 DB/DIV.
PSL No 4448

POLARIZATION

- GAIN REF - - - -
 E_{θ} - - - -
 E_{ϕ} - - - -
 R.C. - - - -
 L.C. - - - -
 OTHER AS NOTED

$\phi = \underline{\quad}^{\circ}$ $\theta = \underline{0}^{\circ}$ COORDINATE REFERENCE

$\phi = \underline{0}^{\circ}$
 $\theta = \underline{90}^{\circ}$

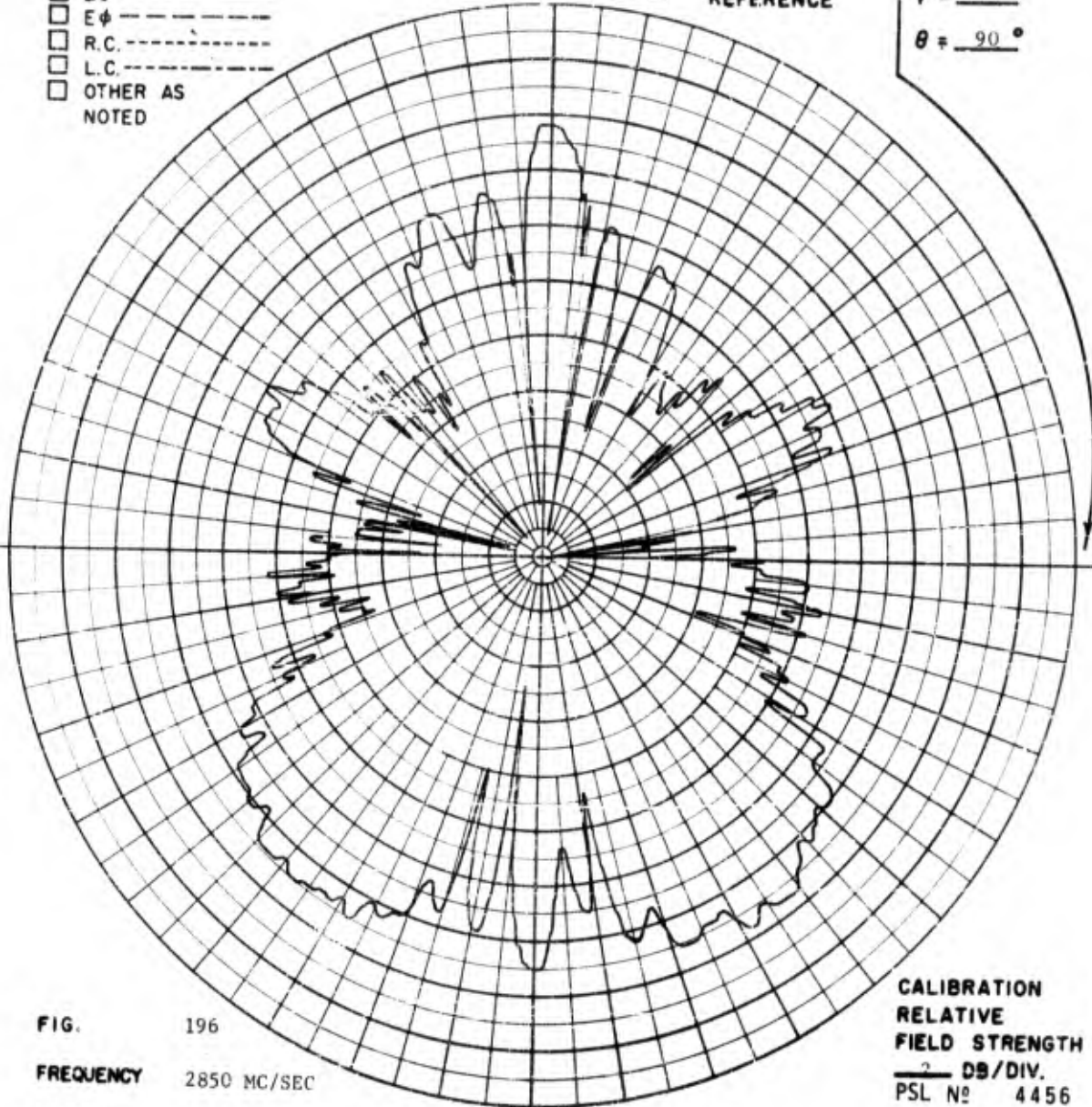


FIG. 196

FREQUENCY 2850 MC/SEC

ANTENNA MODEL 6.010 FOUR ELEMENT ARRAY.

REMARKS RIGHT CIRCULAR PHASING IN THE $\theta = 180^{\circ}$ DIRECTION.

CALIBRATION
 RELATIVE
 FIELD STRENGTH
 2 DB/DIV.
 PSL No 4456

POLARIZATION

- GAIN REF - - - -
 E θ - - - -
 E ϕ - - - -
 R.C. - - - -
 L.C. - - - -
 OTHER AS NOTED

$\phi = \underline{\quad}^\circ$ $\theta = \underline{0}^\circ$

COORDINATE
REFERENCE

$\phi = \underline{0}^\circ$
 $\theta = \underline{90}^\circ$

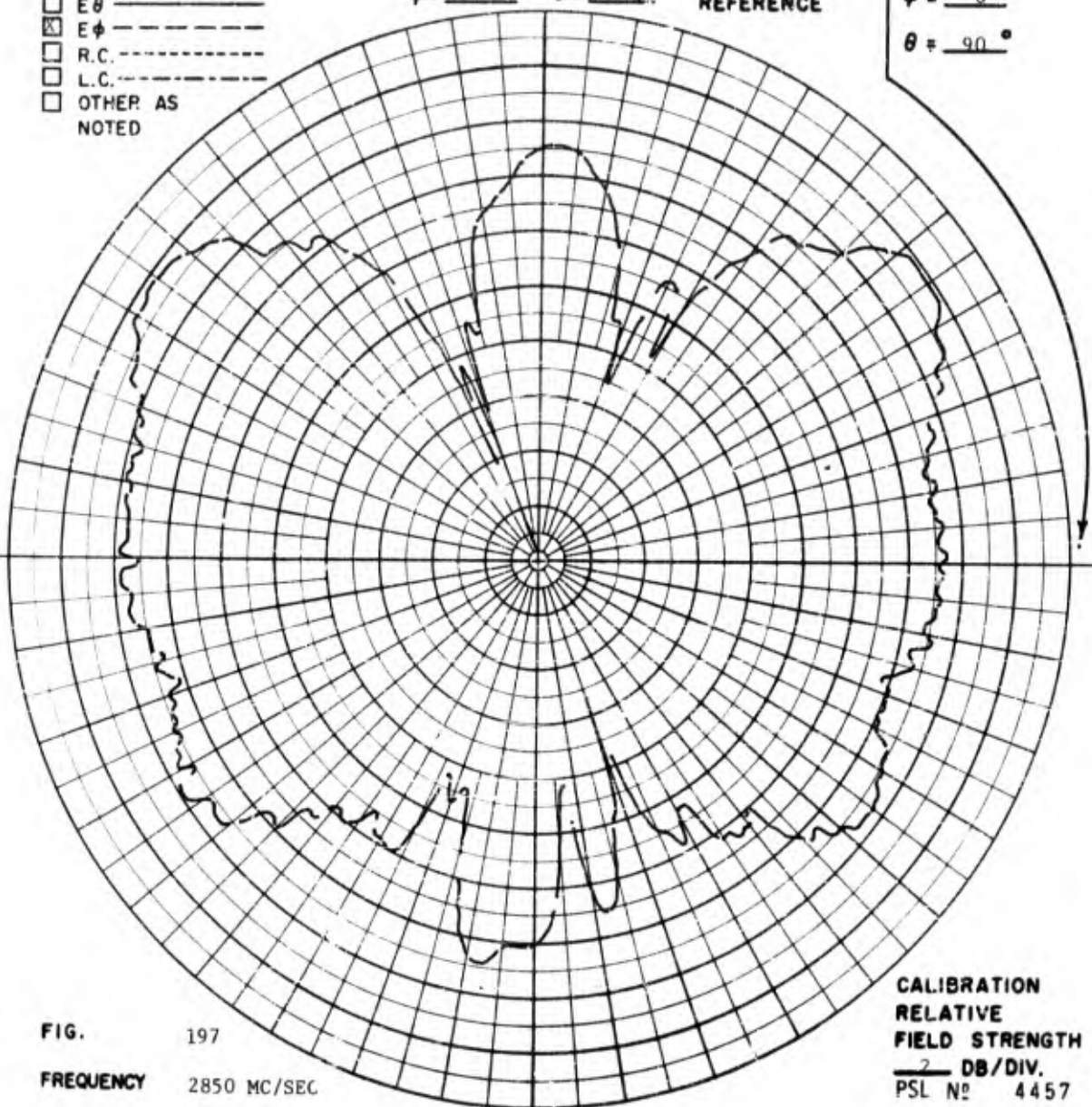


FIG. 197

FREQUENCY 2850 MC/SEC

ANTENNA MODEL 6.010 FOUR ELEMENT ARRAY.

REMARKS

CALIBRATION
 RELATIVE
 FIELD STRENGTH
 2 DB/DIV.
 PSL No 4457

POLARIZATION

- GAIN REF - - - -
 E_{θ} - - - -
 E_{ϕ} - - - -
 R.C. - - - -
 L.C. - - - -
 OTHER AS NOTED

$\phi = \underline{\quad}^{\circ}$ $\theta = \underline{0}^{\circ}$

COORDINATE REFERENCE

$\phi = \underline{90}^{\circ}$
 $\theta = \underline{90}^{\circ}$

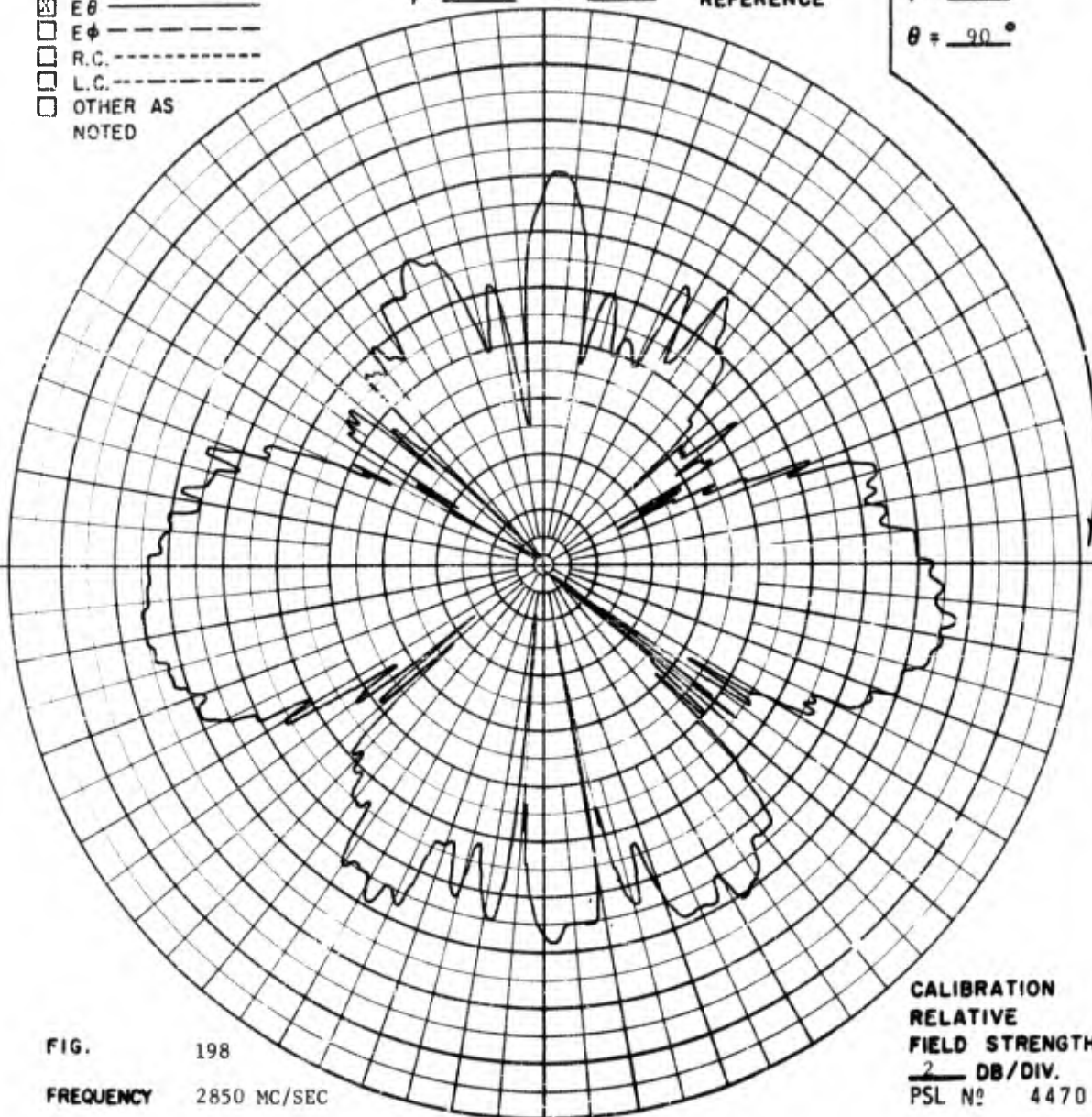


FIG. 198
FREQUENCY 2850 MC/SEC
ANTENNA MODEL 6.010 FOUR ELEMENT ARRAY.
REMARKS

CALIBRATION
RELATIVE
FIELD STRENGTH
 2 DB/DIV.
 PSL No 4470

POLARIZATION

- GAIN REF - - - - -
 E θ - - - - -
 E ϕ - - - - -
 R.C. - - - - -
 L.C. - - - - -
 OTHER AS NOTED

$\phi =$ _____ $\theta =$ 0°
 COORDINATE REFERENCE

$\phi =$ 90°
 $\theta =$ 90°

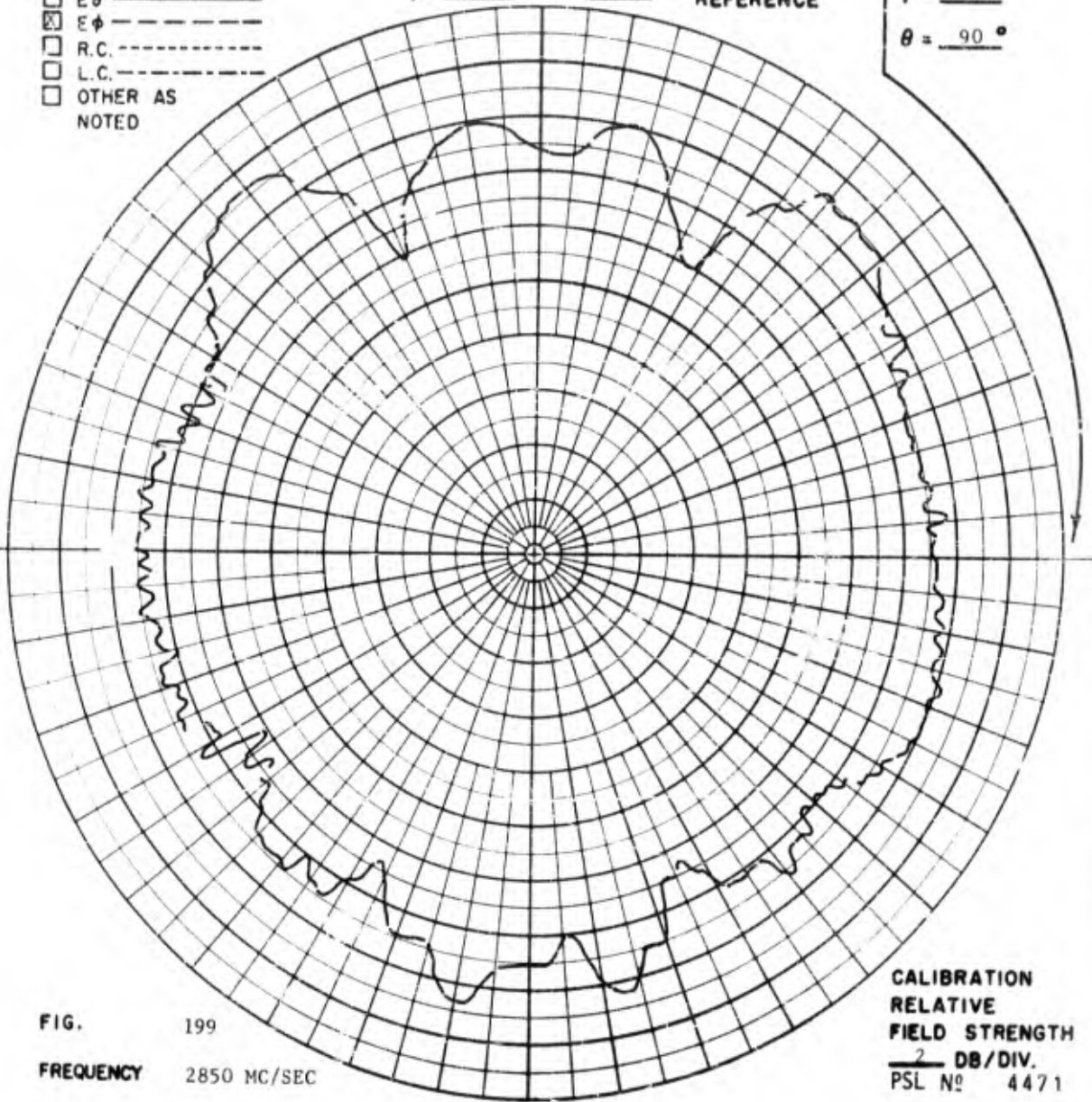


FIG. 199
 FREQUENCY 2850 MC/SEC
 ANTENNA MODEL 6.010 FOUR ELEMENT ARRAY.
 REMARKS

CALIBRATION
 RELATIVE
 FIELD STRENGTH
 2 DB/DIV.
 PSL N° 4471

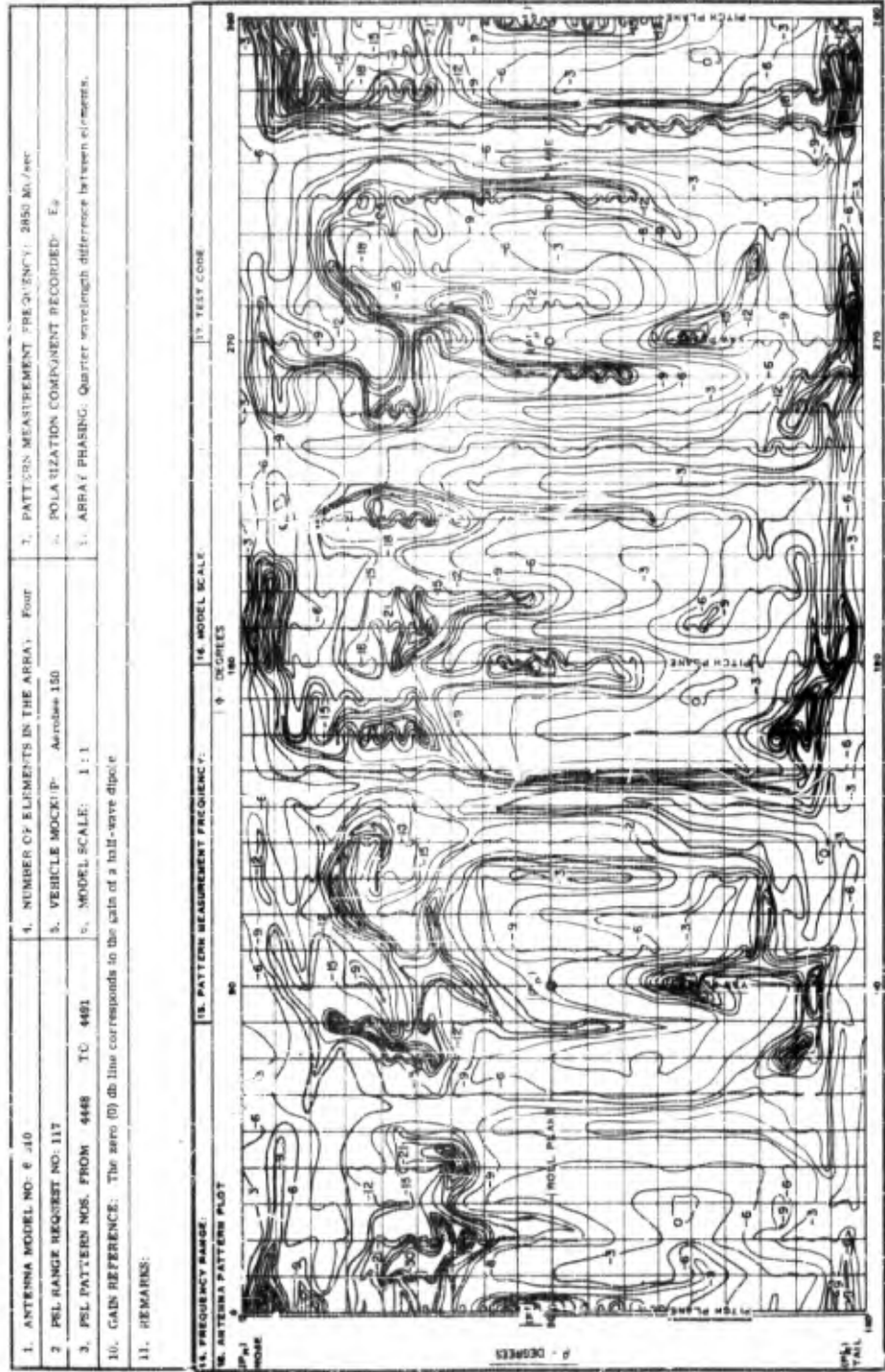


FIG 200 POWER CONTOUR PLOT FOR THE FOUR ELEMENT ARRAY OF MODEL 6 010 ANTENNAS FOR THE E_θ POLARIZATION VECTOR

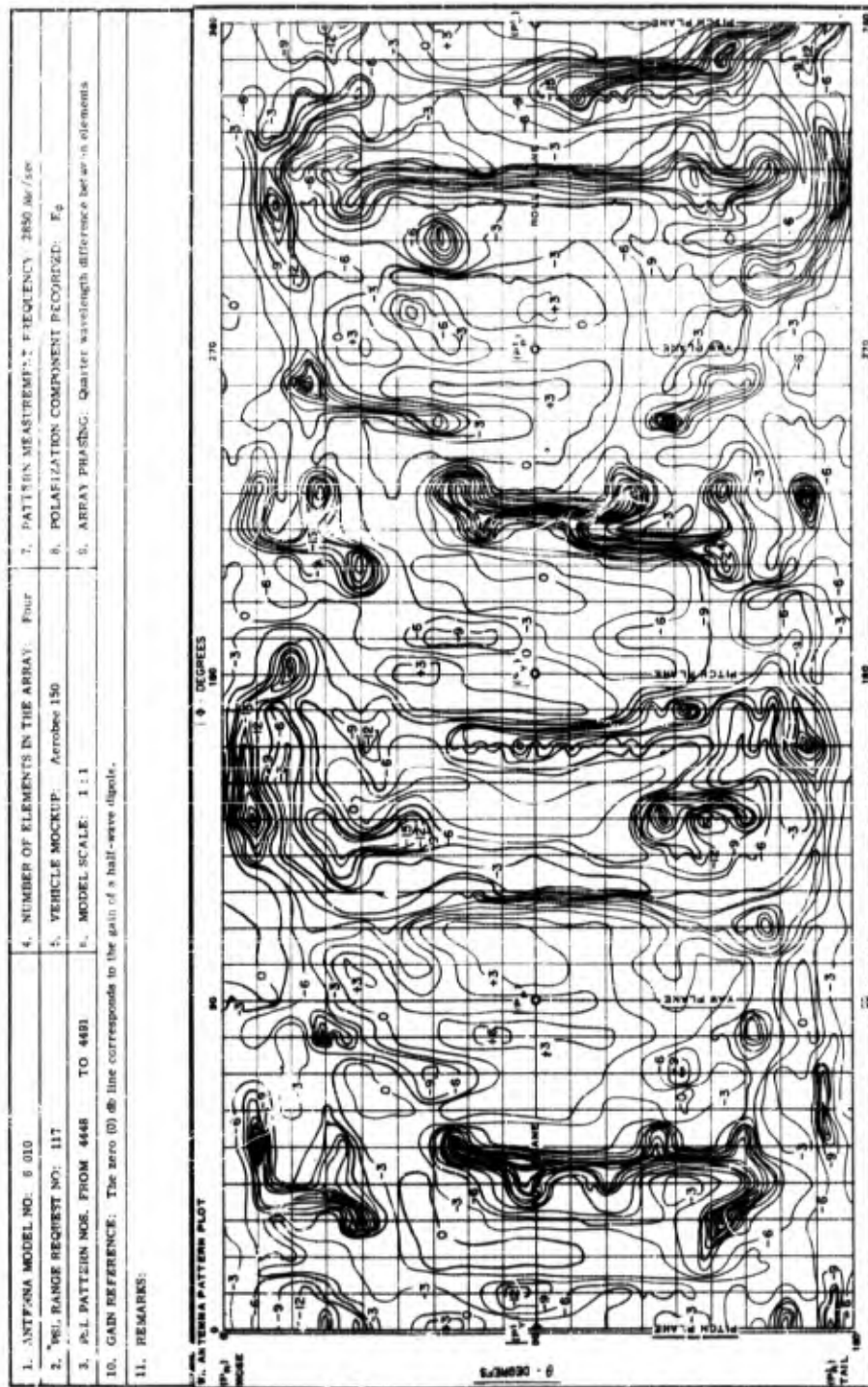


FIG. 201 - POWER CONTOUR PLOT FOR THE FOUR ELEMENT ARRAY OF MODEL 6.010 ANTENNAS FOR THE E_0 POLARIZATION VECTOR

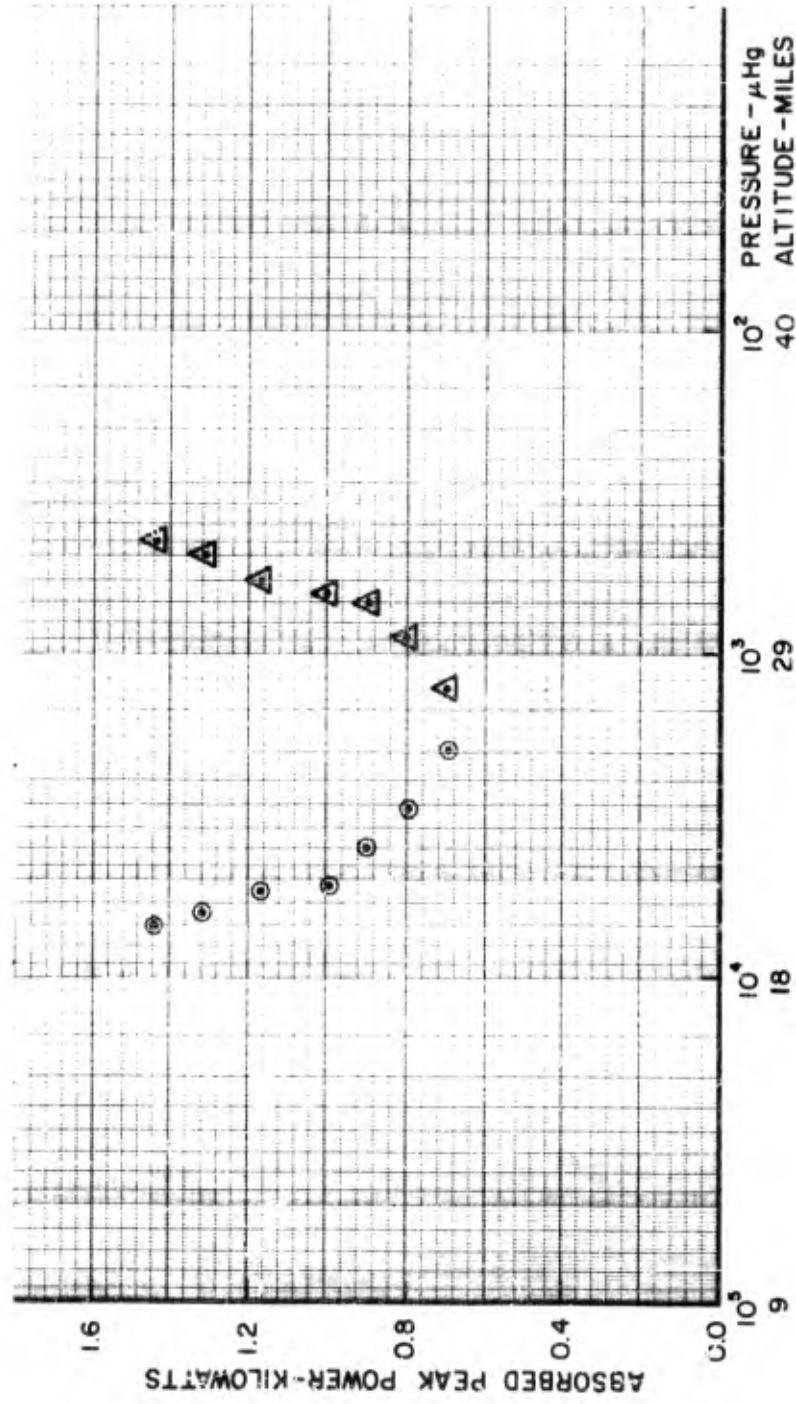


FIG. 202 - REPRESENTATIVE DIFFUSION BREAKDOWN CURVE OF THE 6 000 SERIES FOLDED VALENTINE ANTENNA

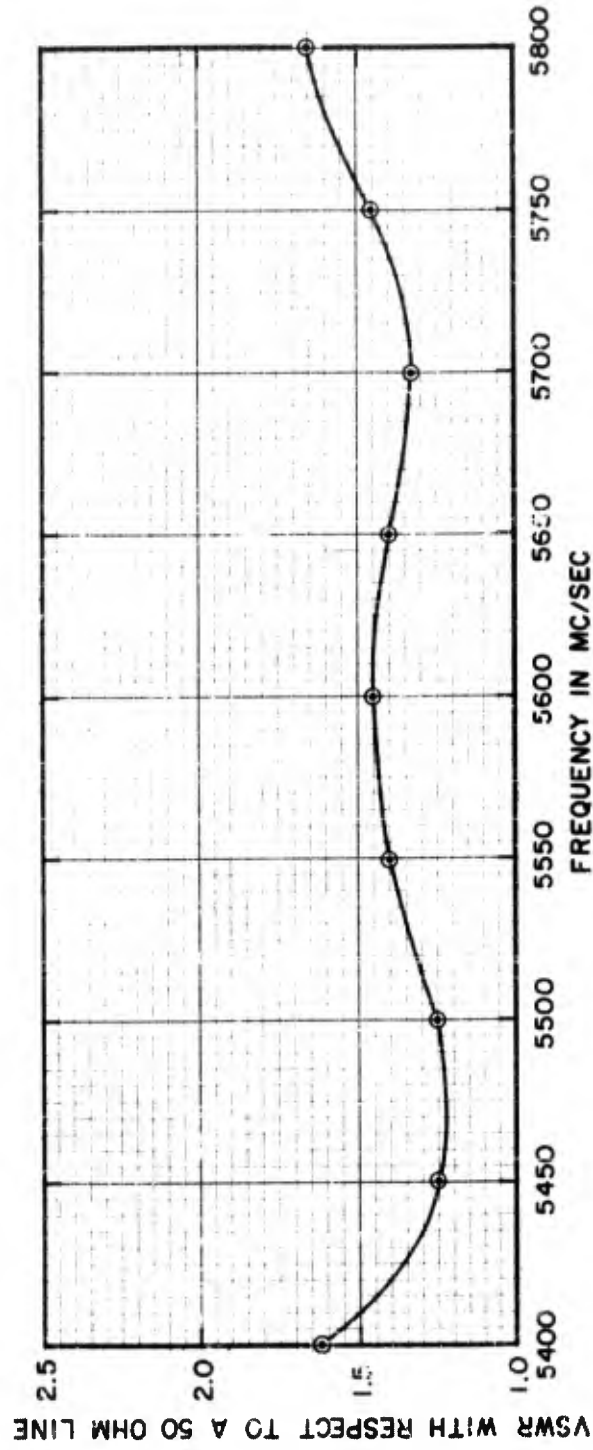


FIG. 203 - CURVE OF VSWR VERSUS FREQUENCY FOR THE TWO ELEMENT ARRAY OF MODEL 7.004 C-BAND BEACON ANTENNAS

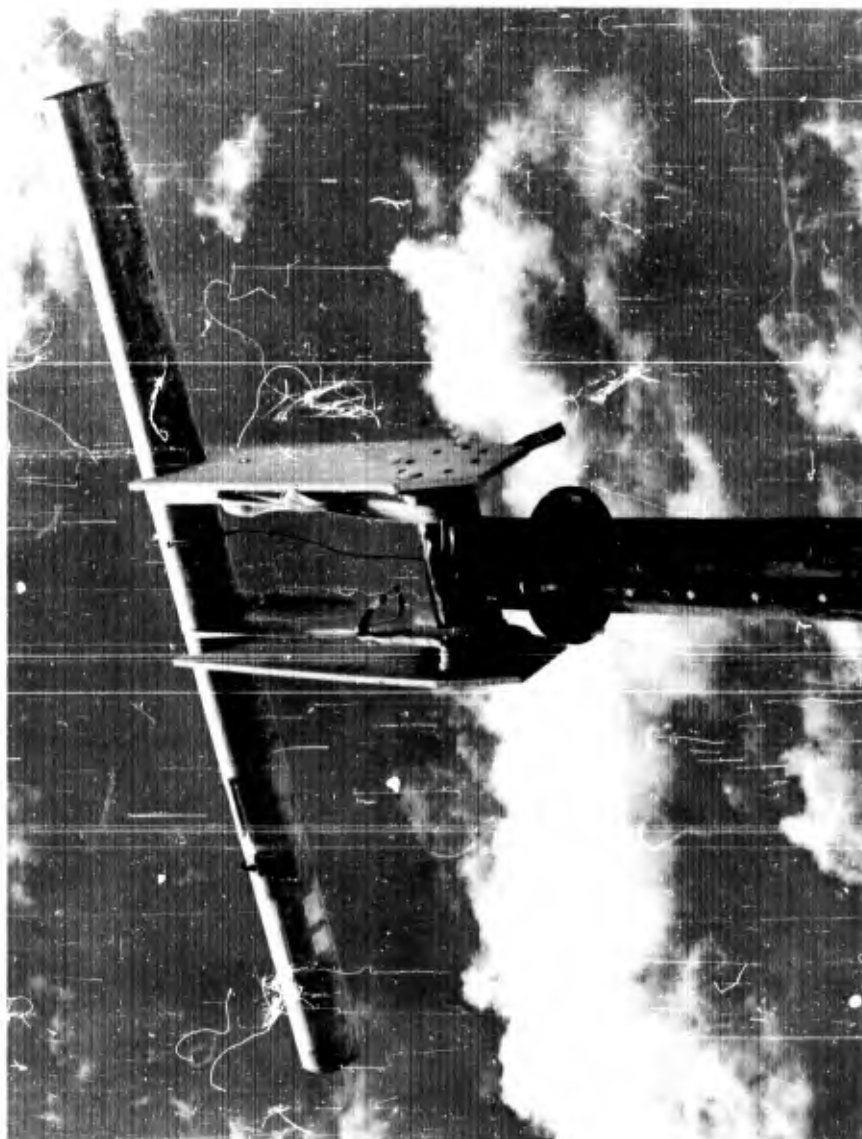


FIG. 204 - PHOTOGRAPH OF THE VEHICLE MOCKUP USED FOR THE MODEL
7.004 RADIATION PATTERN MEASUREMENTS



FIG. 205 - SKETCH OF THE VEHICLE MOCKUP USED FOR THE MODEL 7.004
RADIATION PATTERN MEASUREMENTS

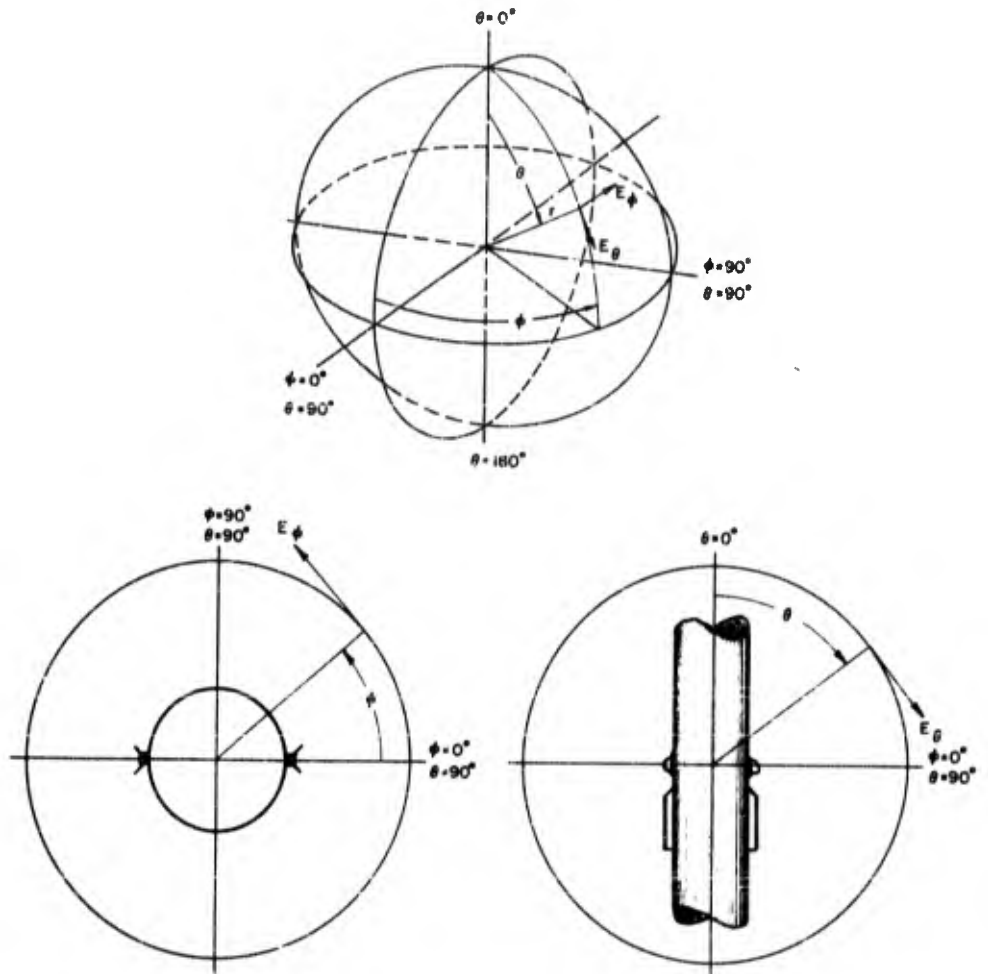


FIG. 206 - POSITION COORDINATES FOR THE MODEL 7.004 ANTENNA RADIATION PATTERN MEASUREMENTS

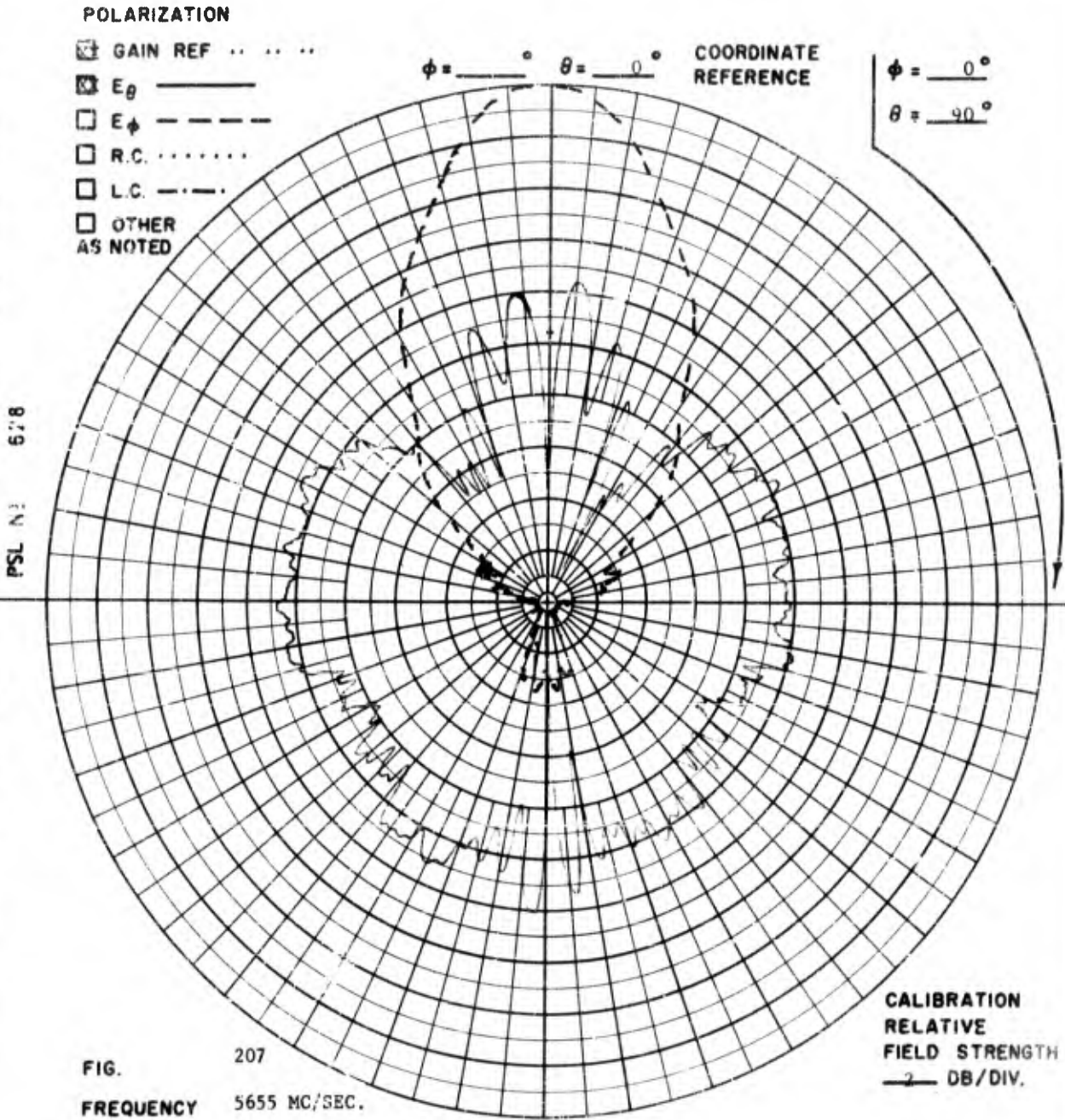


FIG. 207

FREQUENCY 5655 MC/SEC.

ANTENNA MODEL 7.004 TWO ELEMENT ARRAY FED IN PHASE.

REMARKS THE GAIN REFERENCE ANTENNA IS A SCIENTIFIC-ATLANTA HORN, MODEL SGH - 3.95 WHICH HAS A GAIN OF +19.2 DB WITH RESPECT TO ISOTROPIC.

POLARIZATION

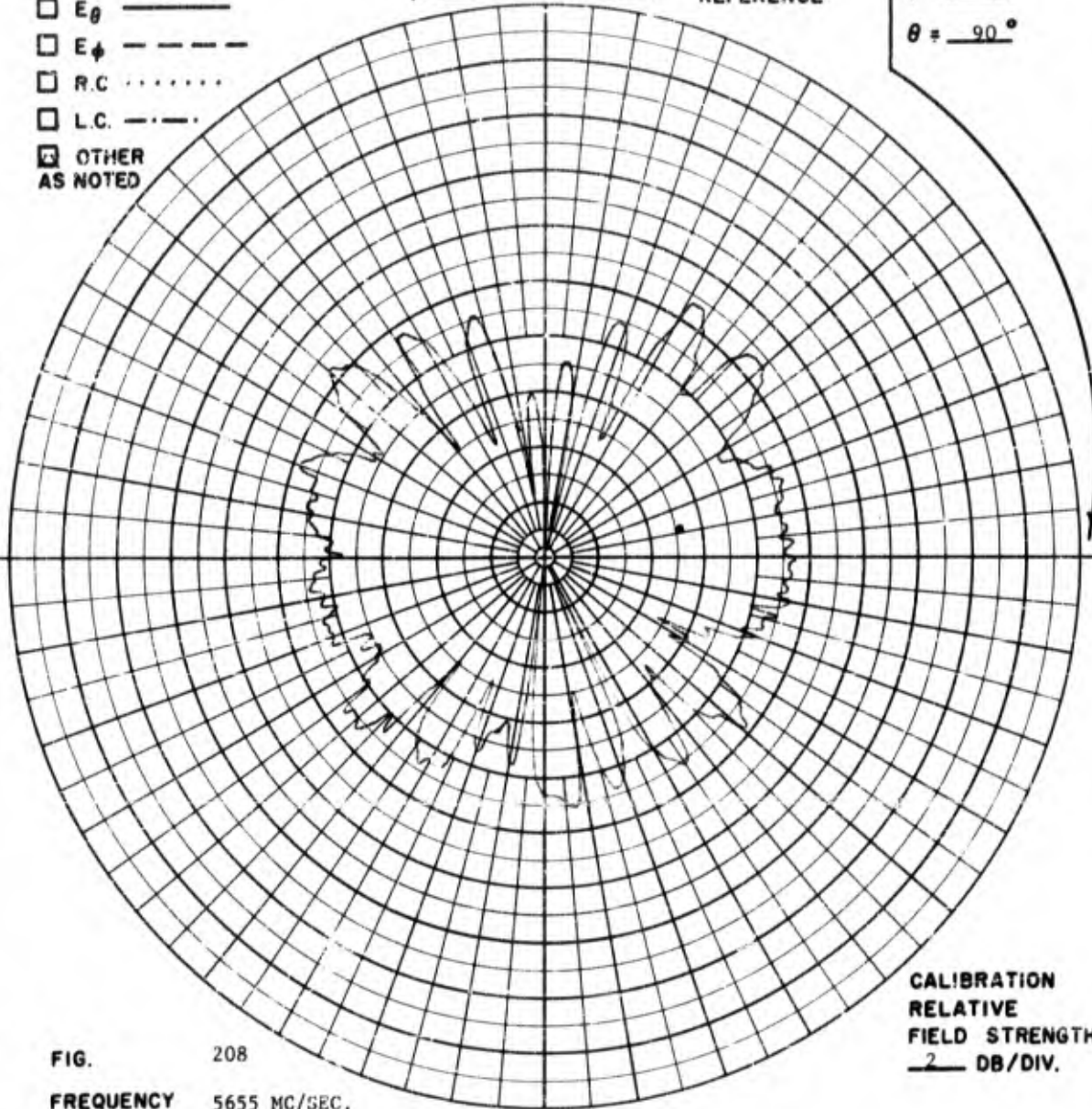
- GAIN REF
- E_θ _____
- E_ϕ - - - - -
- R.C.
- L.C. - . - . -
- OTHER AS NOTED

$\phi =$ _____ $^\circ$ $\theta =$ 0 $^\circ$

COORDINATE REFERENCE

$\phi =$ 0 $^\circ$
 $\theta =$ 90 $^\circ$

PSL No 677



CALIBRATION
RELATIVE
FIELD STRENGTH
2 DB/DIV.

FIG. 208
FREQUENCY 5655 MC/SEC.
ANTENNA MODEL 7.004 TWO ELEMENT ARRAY FED IN PHASE
REMARKS E_θ _____

POLARIZATION

- GAIN REF
- E_{θ} _____
- E_{ϕ} - - - - -
- R.C.
- L.C. - - - - -
- OTHER AS NOTED

$\phi = \text{---}^{\circ}$ $\theta = \text{---}^{\circ}$

COORDINATE REFERENCE

$\phi = 90^{\circ}$
 $\theta = 90^{\circ}$

PSL No 649

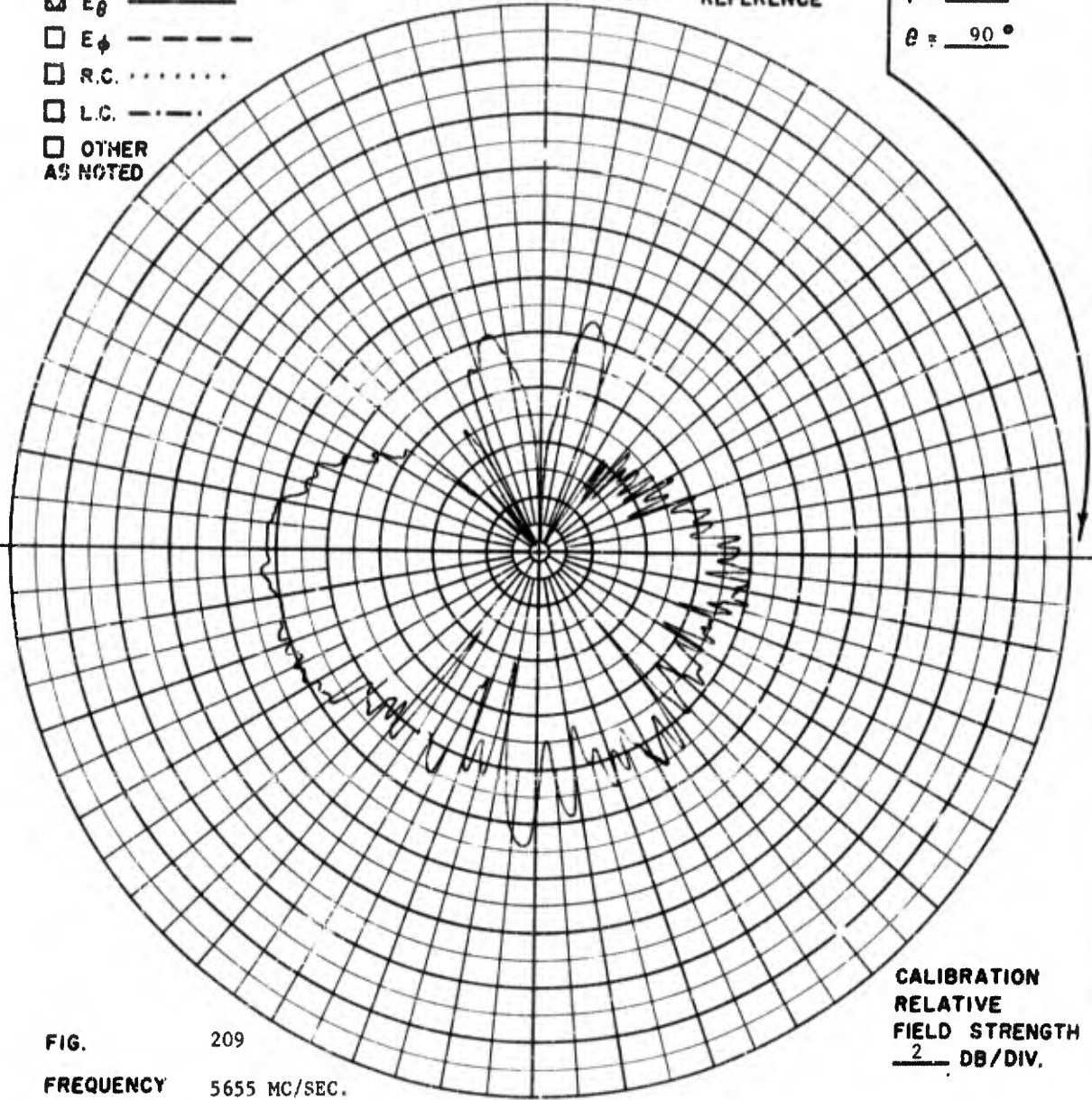
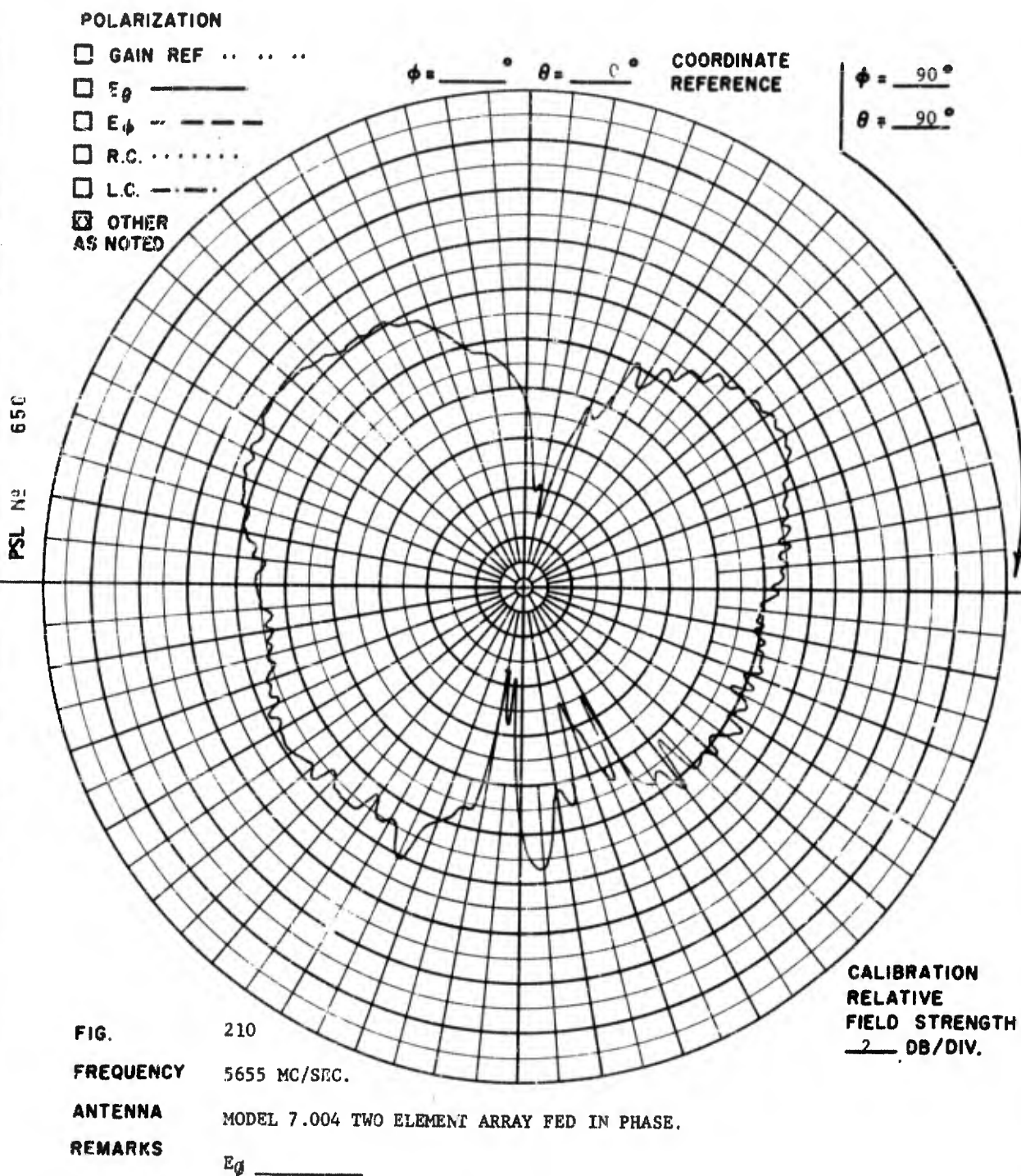


FIG. 209
 FREQUENCY 5655 MC/SEC.
 ANTENNA MODEL 7.004 TWO ELEMENT ARRAY FED IN PHASE.
 REMARKS

CALIBRATION
RELATIVE
FIELD STRENGTH
2 DB/DIV.



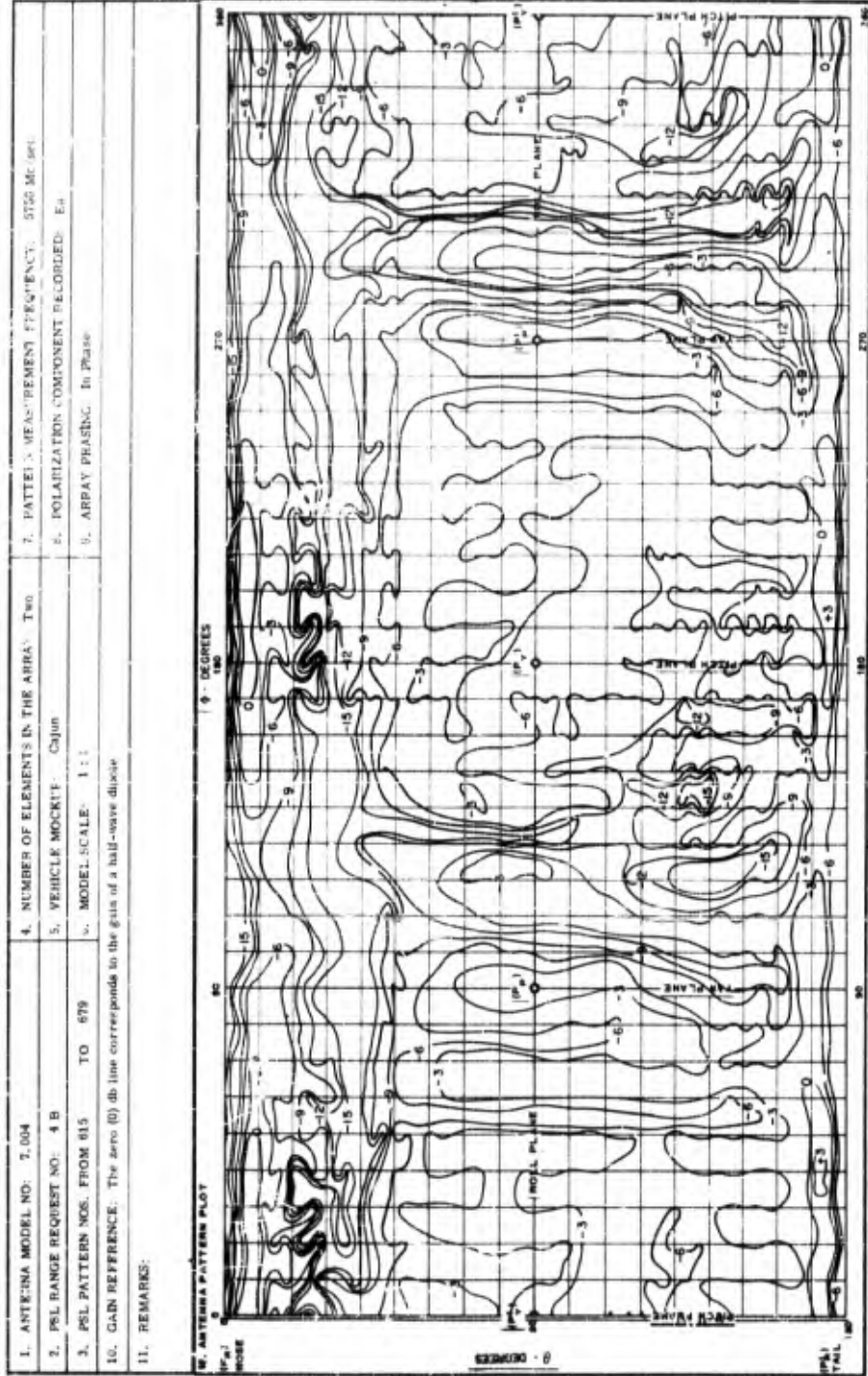


FIG. 211 - POWER CONTOUR PLOT OF THE TWO ELEMENT ARRAY OF MODEL 7 004 ANTENNAS FOR THE E_H POLARIZATION VECTOR

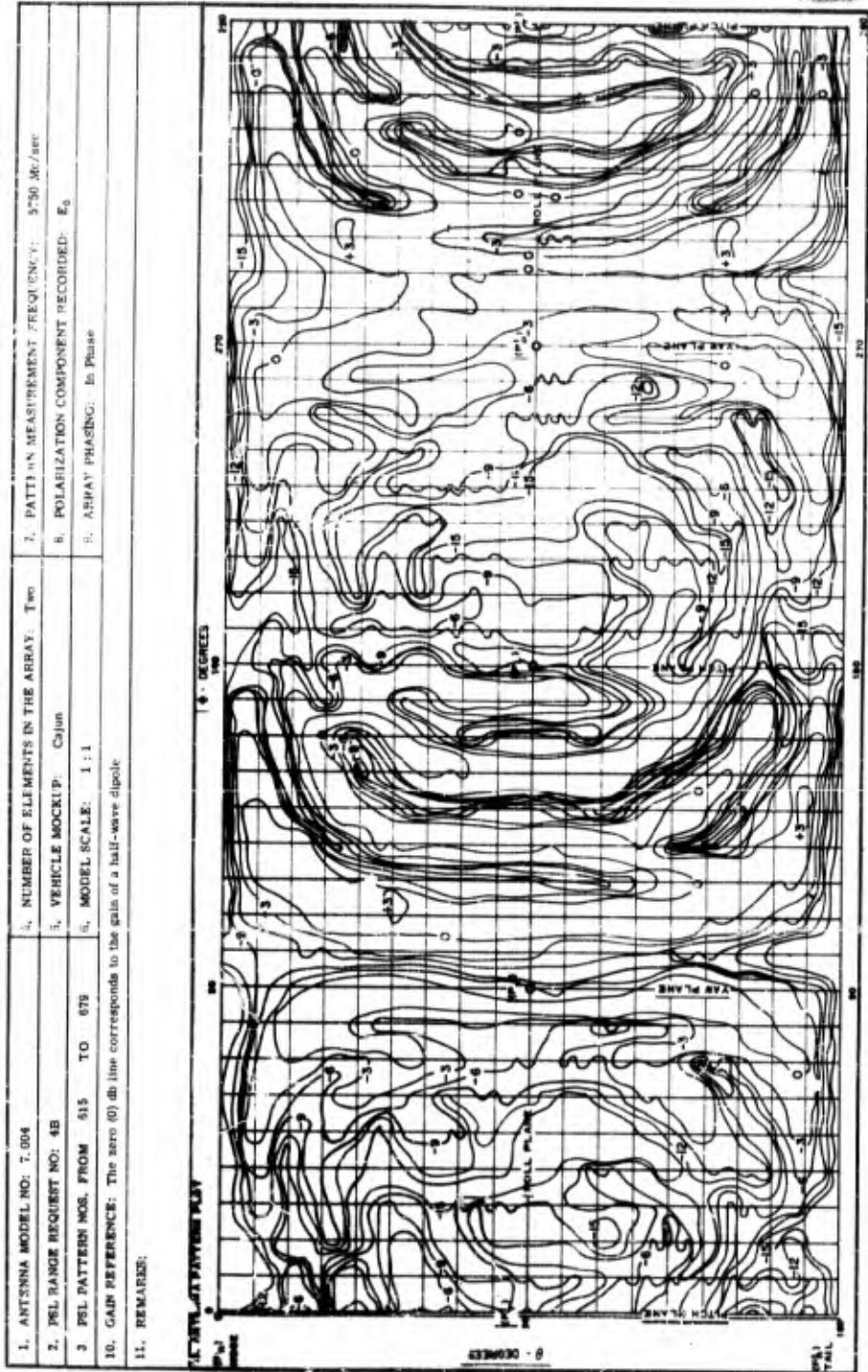


FIG. 212 - POWER CONTOUR PLOT OF THE TWO ELEMENT ARRAY OF MODEL 7.004 ANTENNAS FOR THE E_θ POLARIZATION VECTOR

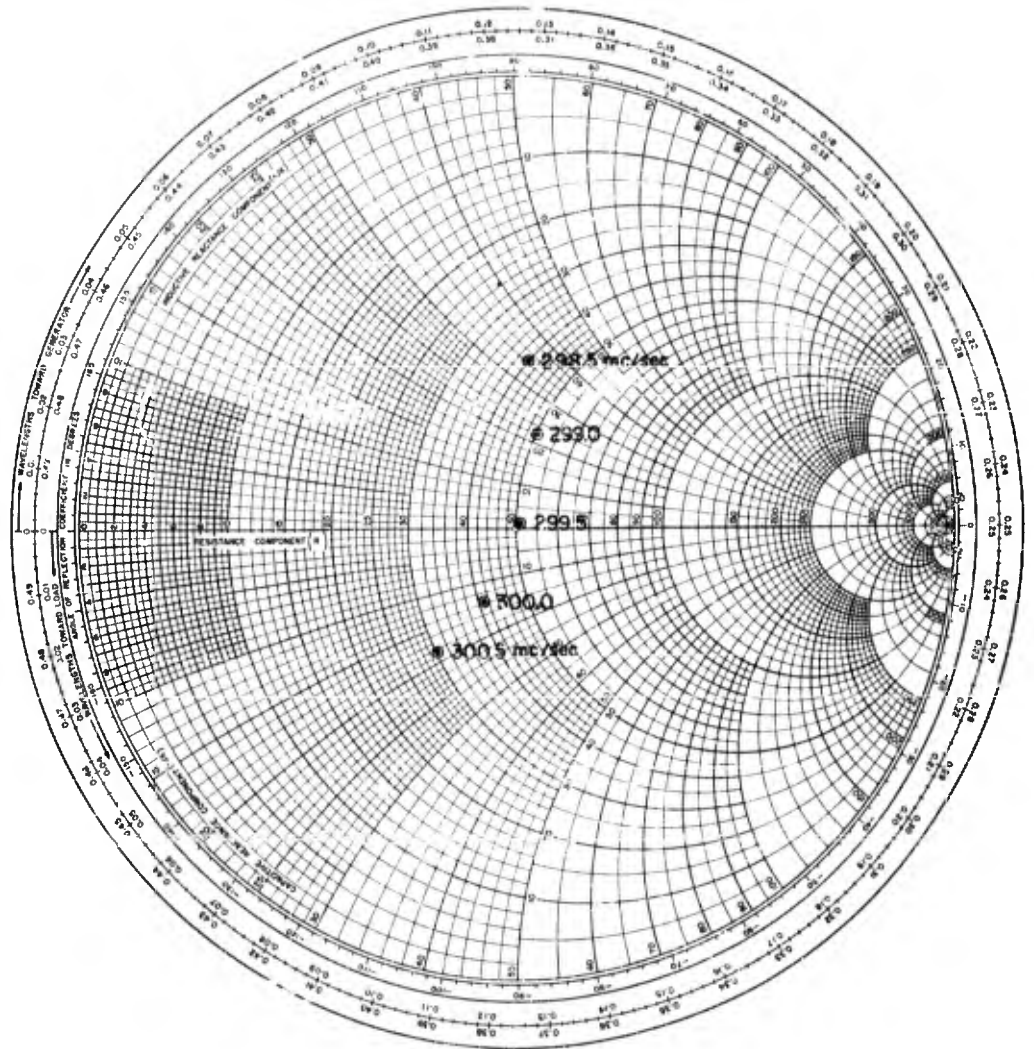


FIG. 213 - IMPEDANCE CURVE OF A SINGLE MODEL 17.002 QUADRALOOP ANTENNA

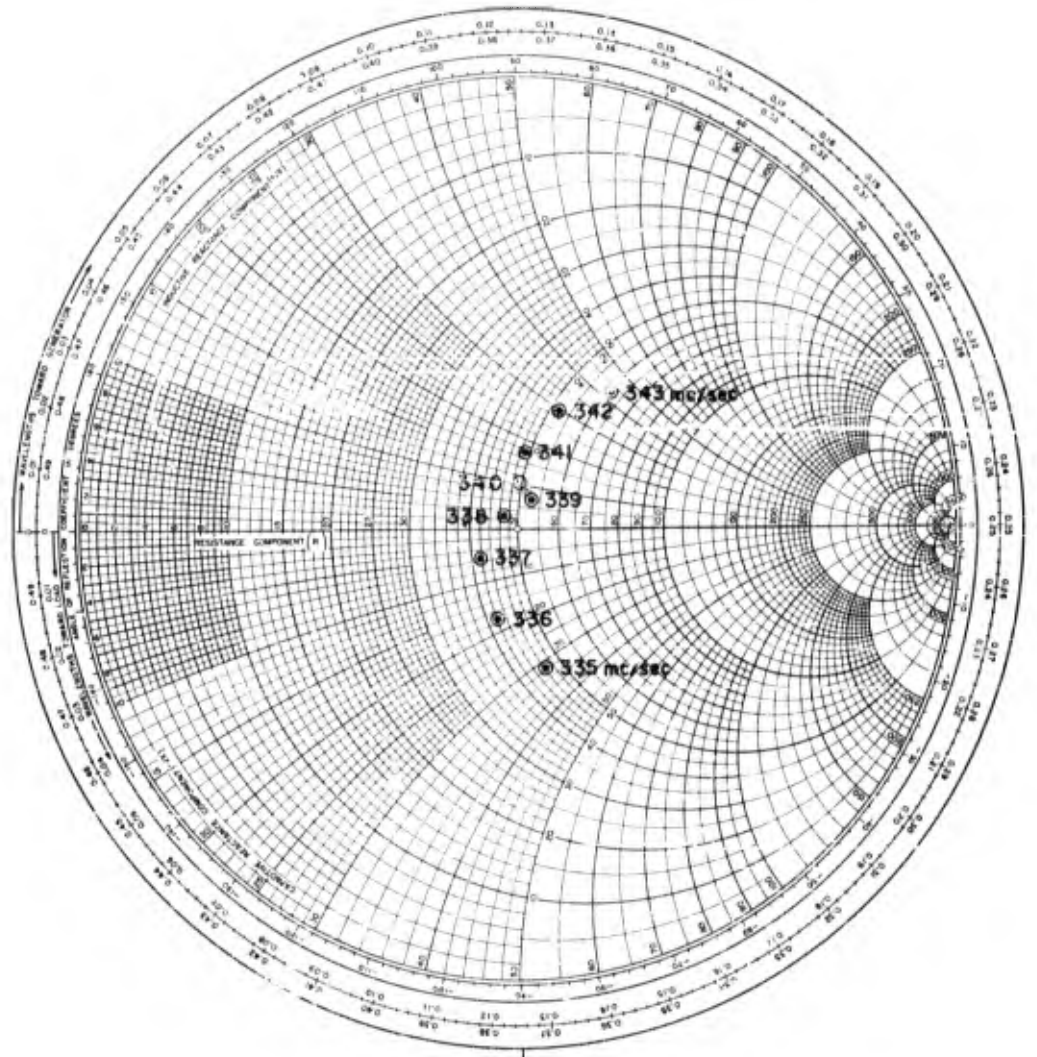


FIG. 214 - IMPEDANCE CURVE OF A FOUR ELEMENT ARRAY OF MODEL 17.004 QUADRALOOP ANTENNAS FED IN QUADRATURE

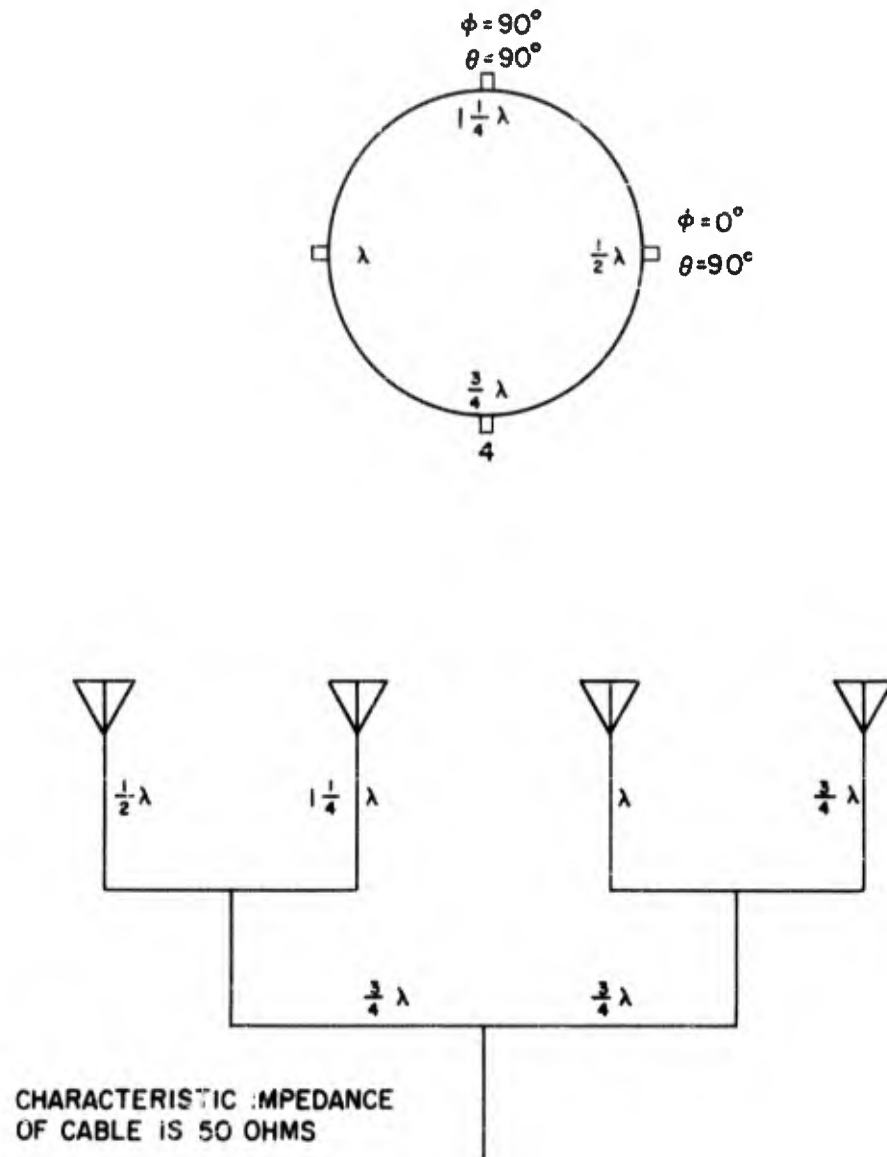


FIG. 215 - SKETCH OF THE PHASING HARNESS OF THE FOUR ELEMENT ARRAY OF MODEL 17.004 QUADRALOOP ANTENNAS

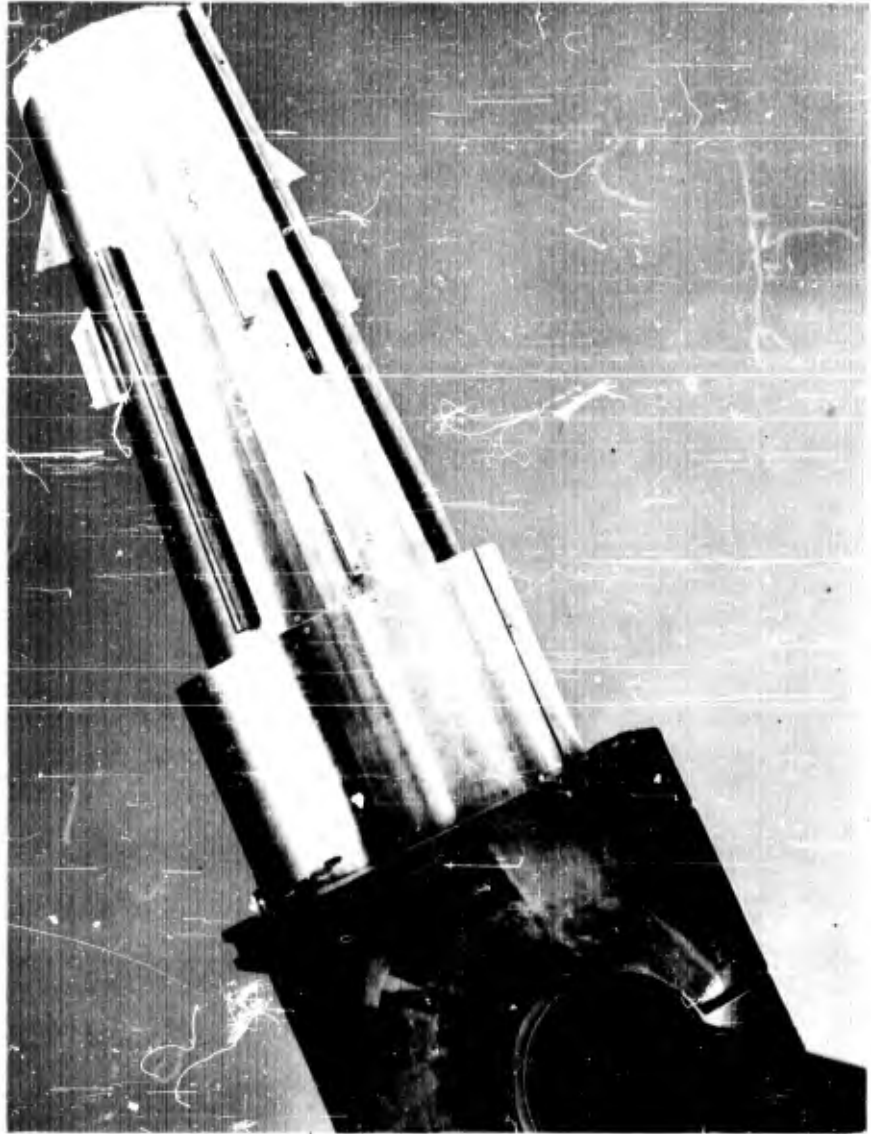


FIG. 216 - PHOTOGRAPH OF THE VEHICLE MOCKUP USED FOR THE MODEL
17.004 RADIATION PATTERN MEASUREMENTS

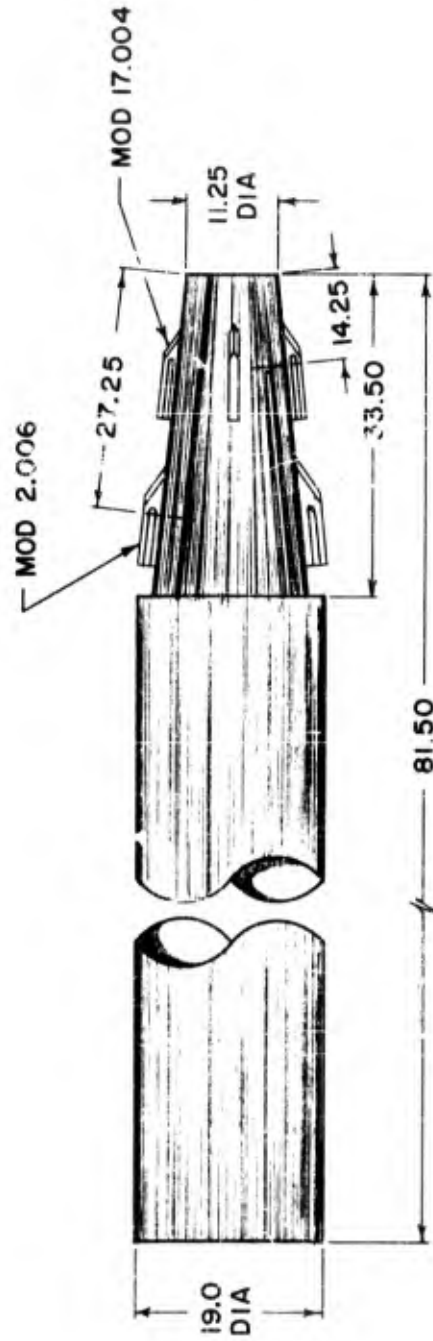


FIG. 217 - SKETCH OF THE VEHICLE MOCKUP USED FOR THE MODEL 17.004
RADIATION PATTERN MEASUREMENTS

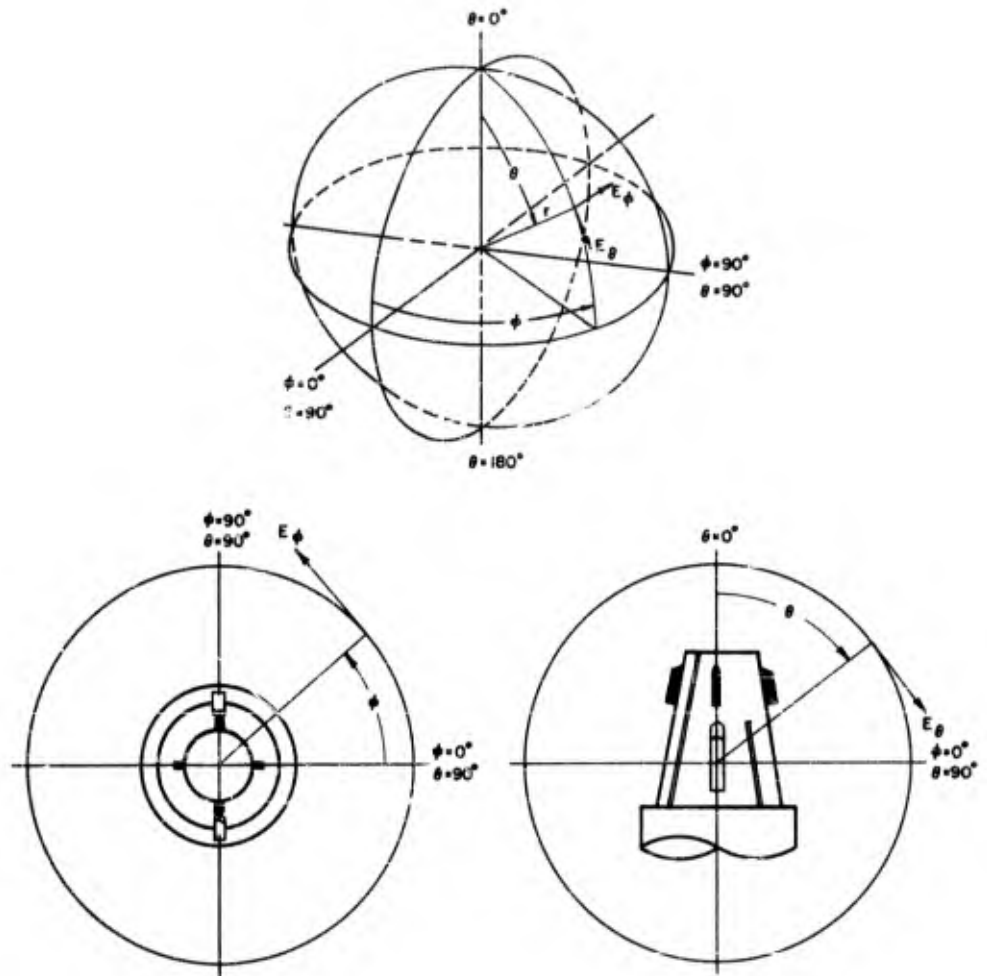


FIG. 218 - POSITION COORDINATES FOR THE MODEL 17,004 ANTENNA RADIATION PATTERN MEASUREMENTS

POLARIZATION

- GAIN REF - - - -
 E_{θ} - - - -
 E_{ϕ} - - - -
 R.C. - - - -
 L.C. - - - -
 OTHER AS NOTED

$\phi =$ _____ ° $\theta =$ _____ ° COORDINATE REFERENCE

$\phi =$ _____ °
 $\theta =$ _____ °

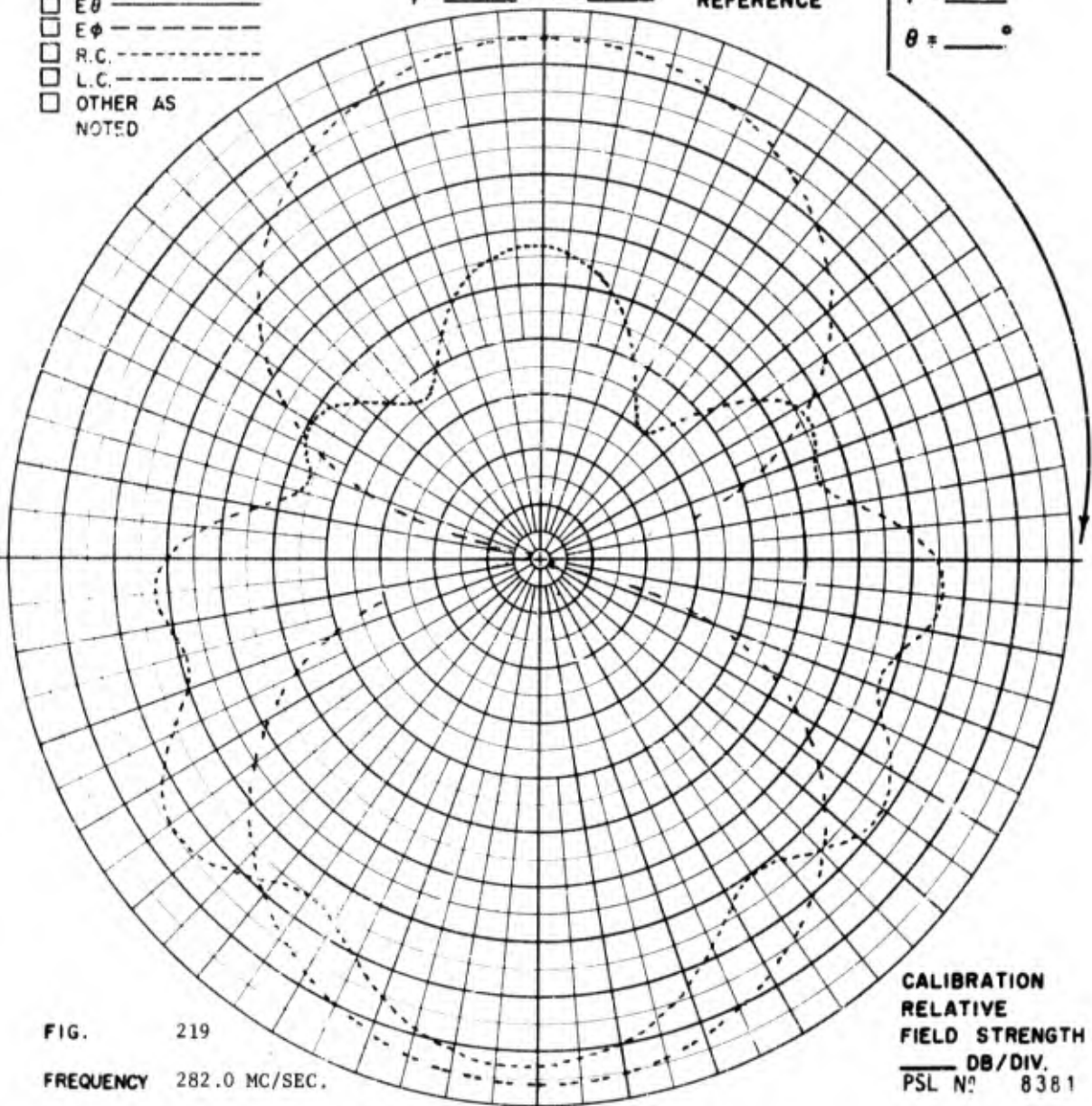


FIG. 219

FREQUENCY 282.0 MC/SEC.

ANTENNA MODEL 17.004 FCJR ELEMENT ARRAY.

REMARKS THE GAIN REFERENCE ANTENNA IS A STODDART HALF-WAVE DIPOLE.
TO COMPARE THE TWO ANTENNAS, ADD 2 DB TO THE TEST ANTENNA PATTERN.

CALIBRATION
 RELATIVE
 FIELD STRENGTH
 _____ DB/DIV.
 PSL No 8381

POLARIZATION

- GAIN REF -----
 E_{θ} -----
 E_{ϕ} -----
 R.C. -----
 L.C. -----
 OTHER AS NOTED

$\phi = \underline{\quad\quad}^{\circ}$ $\theta = \underline{0}^{\circ}$ COORDINATE REFERENCE

$\phi = \underline{0}^{\circ}$
 $\theta = \underline{90}^{\circ}$

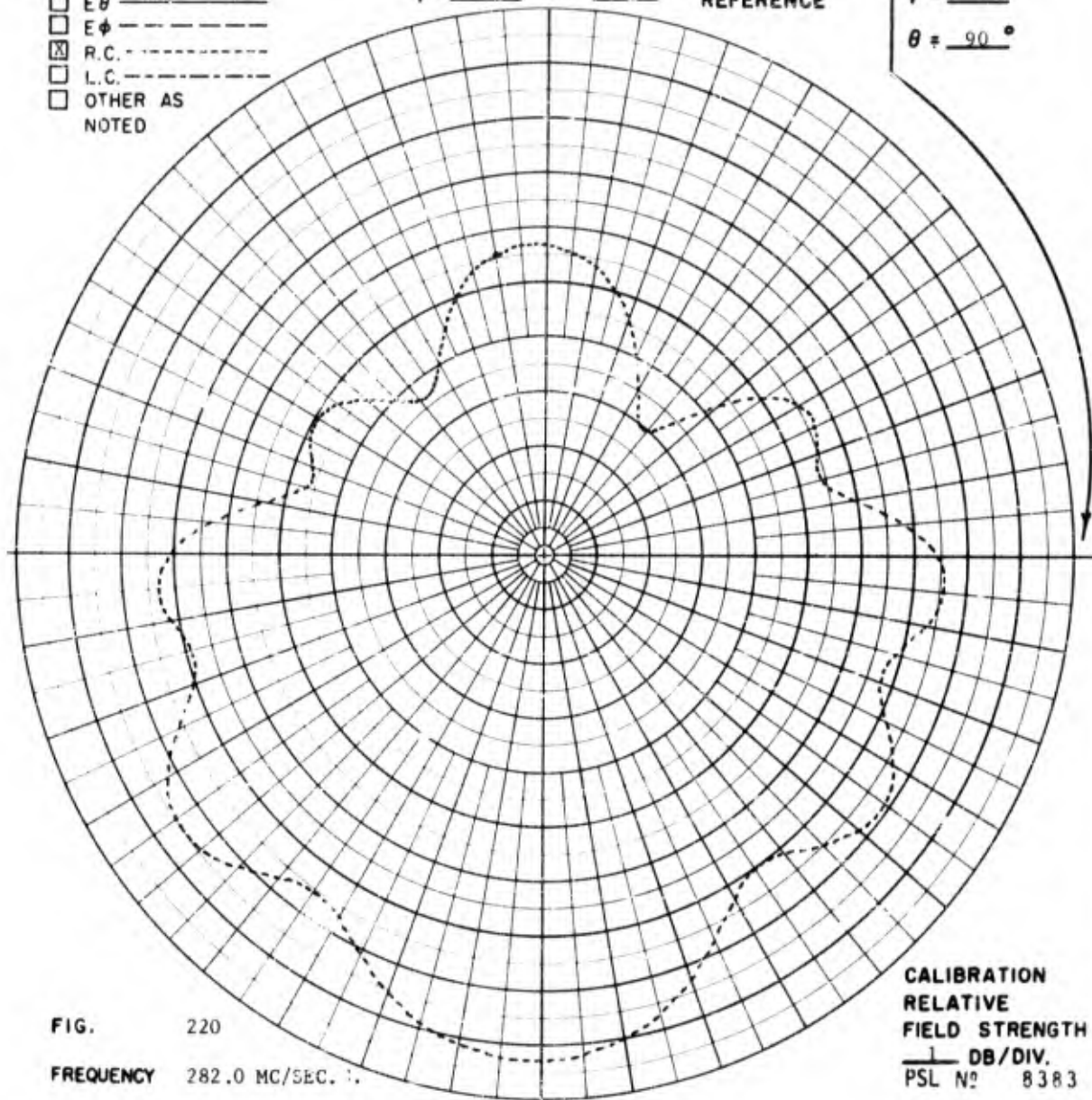


FIG. 220
FREQUENCY 282.0 MC/SEC.

ANTENNA MODEL 17.004 FOUR ELEMENT ARRAY.

REMARKS AT $\theta = 180^{\circ}$, $\phi = 0^{\circ}$ THE SIGNAL IS +1.5 DB WITH RESPECT TO
 A STODDART HALFWAVE DIPOLE ILLUMINATED BY A RIGHT CIRCULAR HELIX.

POLARIZATION

- GAIN REF - - - - -
- E θ _____
- E ϕ - - - - -
- R.C. - - - - -
- L.C. - - - - -
- OTHER AS NOTED

$\phi =$ _____^o $\theta =$ _____^o

COORDINATE REFERENCE

$\phi =$ 90^o
 $\theta =$ 90^o

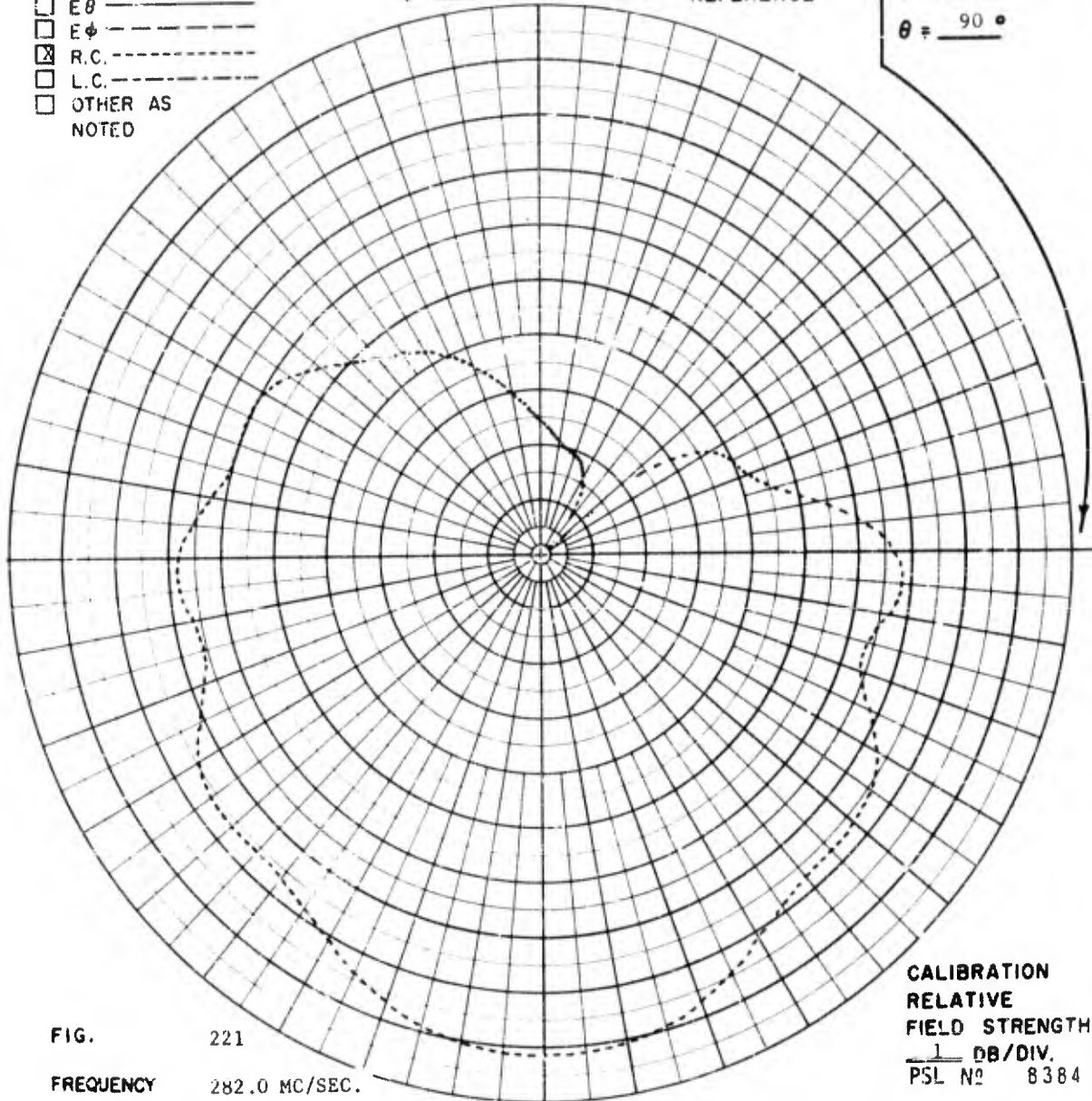


FIG. 221

FREQUENCY 282.0 MC/SEC.

ANTENNA MODEL 17.004 FOUR ELEMENT ARRAY.

REMARKS

CALIBRATION
 RELATIVE
 FIELD STRENGTH
 1 DB/DIV.
 PSL N^o 8384

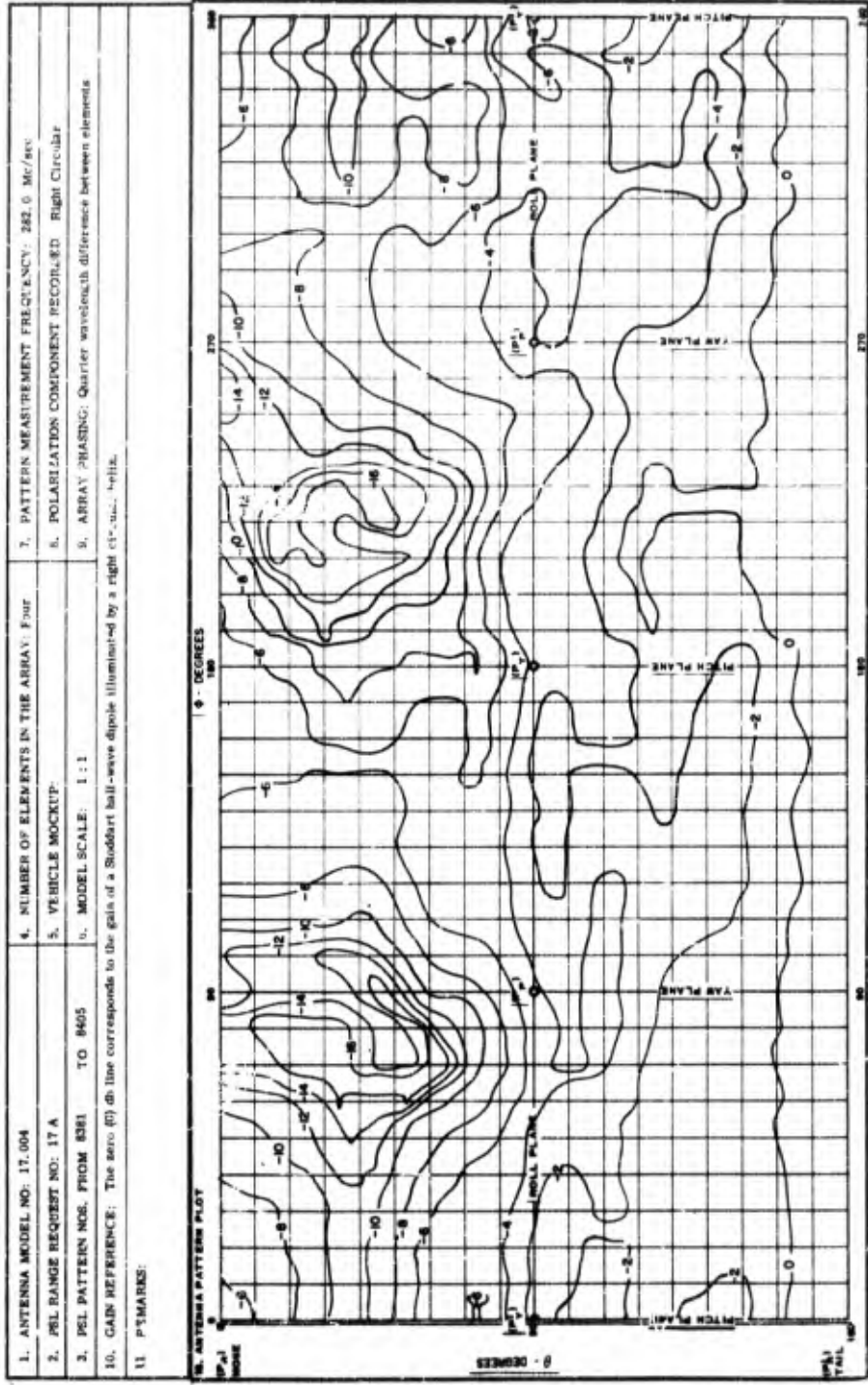


FIG. 222 - POWER CONTOUR PLOT OF THE FOUR ELEMENT ARRAY OF MODEL 17.004 ANTENNAS

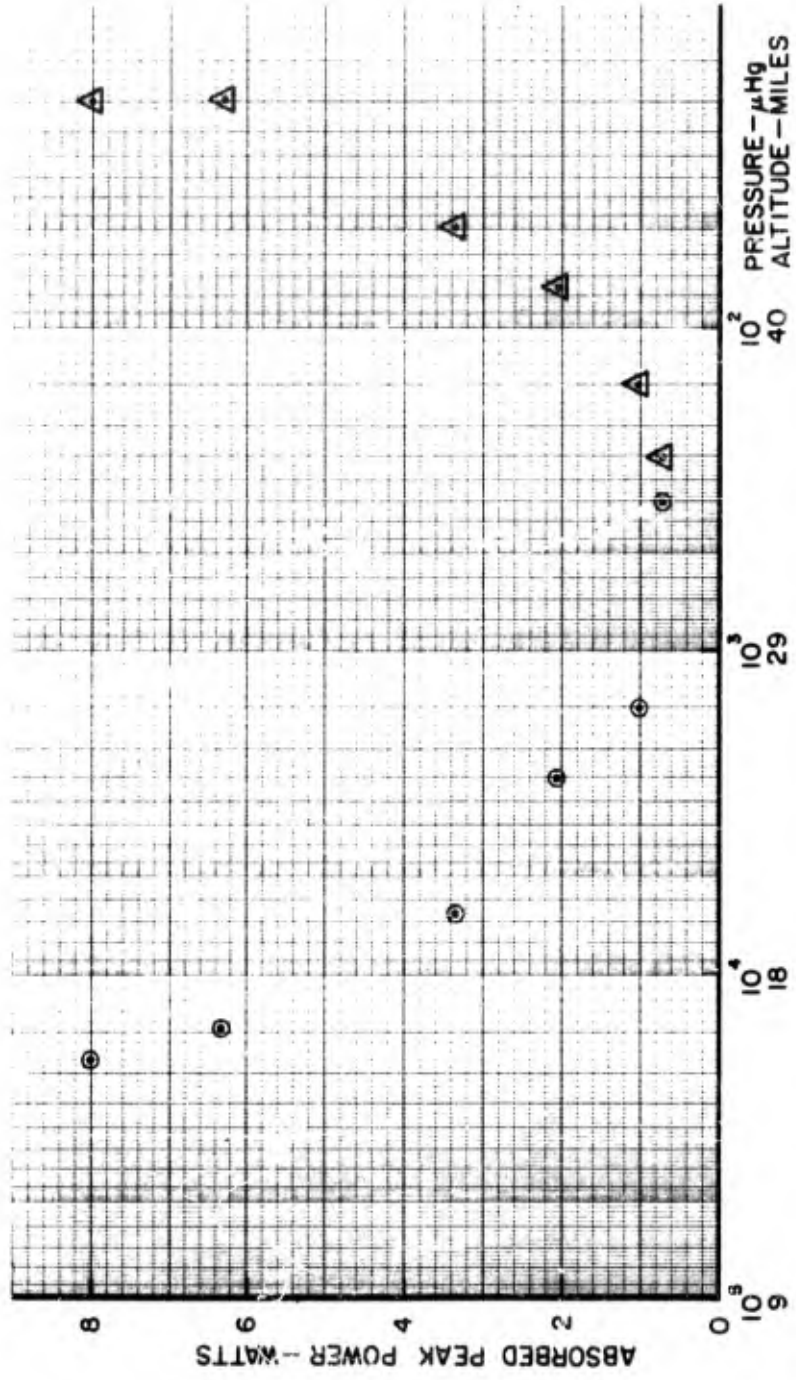


FIG. 223 - REPRESENTATIVE DIFFUSION BREAKDOWN CURVE FOR THE 17,000 SERIES ANTENNAS

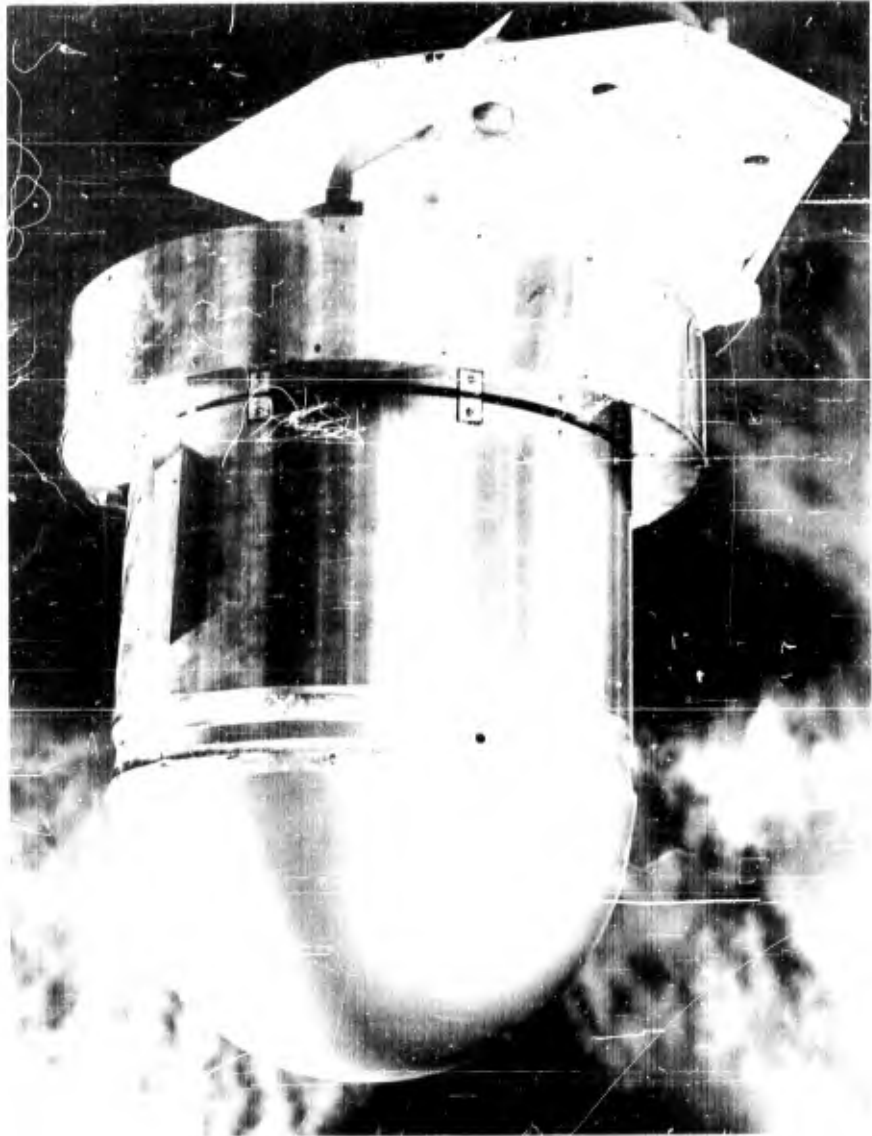


FIG. 224 - PHOTOGRAPH OF THE AP/3 PAYLOAD MOCKUP USED FOR THE MODEL
2.007 ANTENNA PATTERN MEASUREMENTS

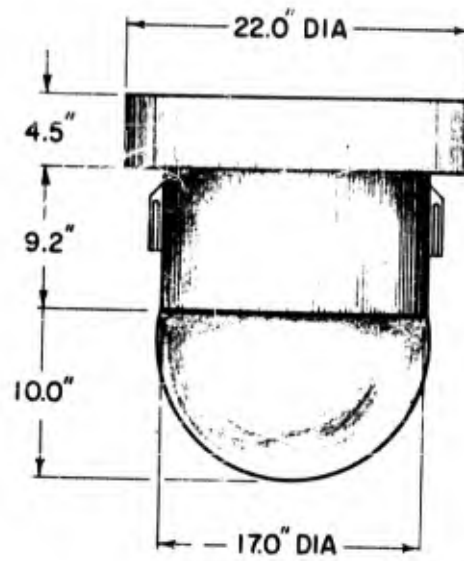


FIG. 225 - SKETCH OF THE AP/3 PAYLOAD MOCKUP USED FOR THE MODEL 2.007 ANTENNA PATTERN MEASUREMENTS

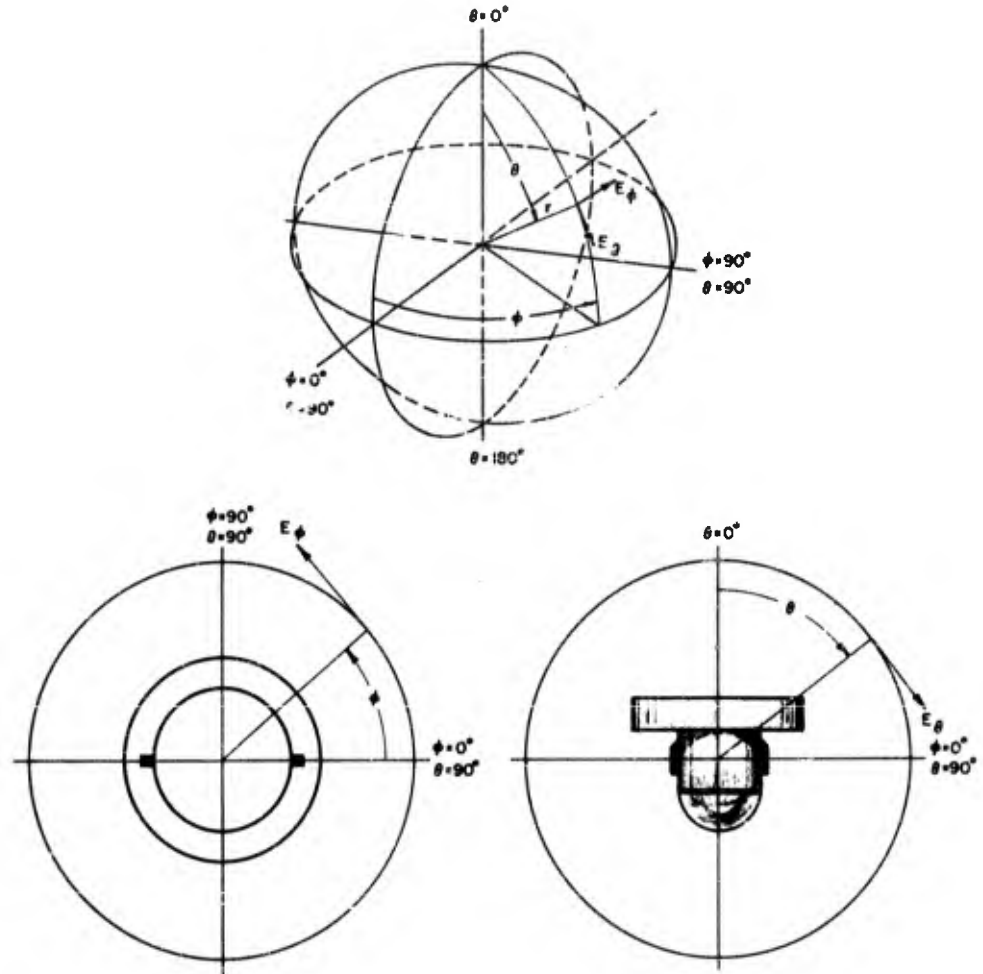


FIG. 226 - POSITION COORDINATES FOR THE MODEL 2.007 ANTENNAS MOUNTED ON THE AP/3 PAYLOAD

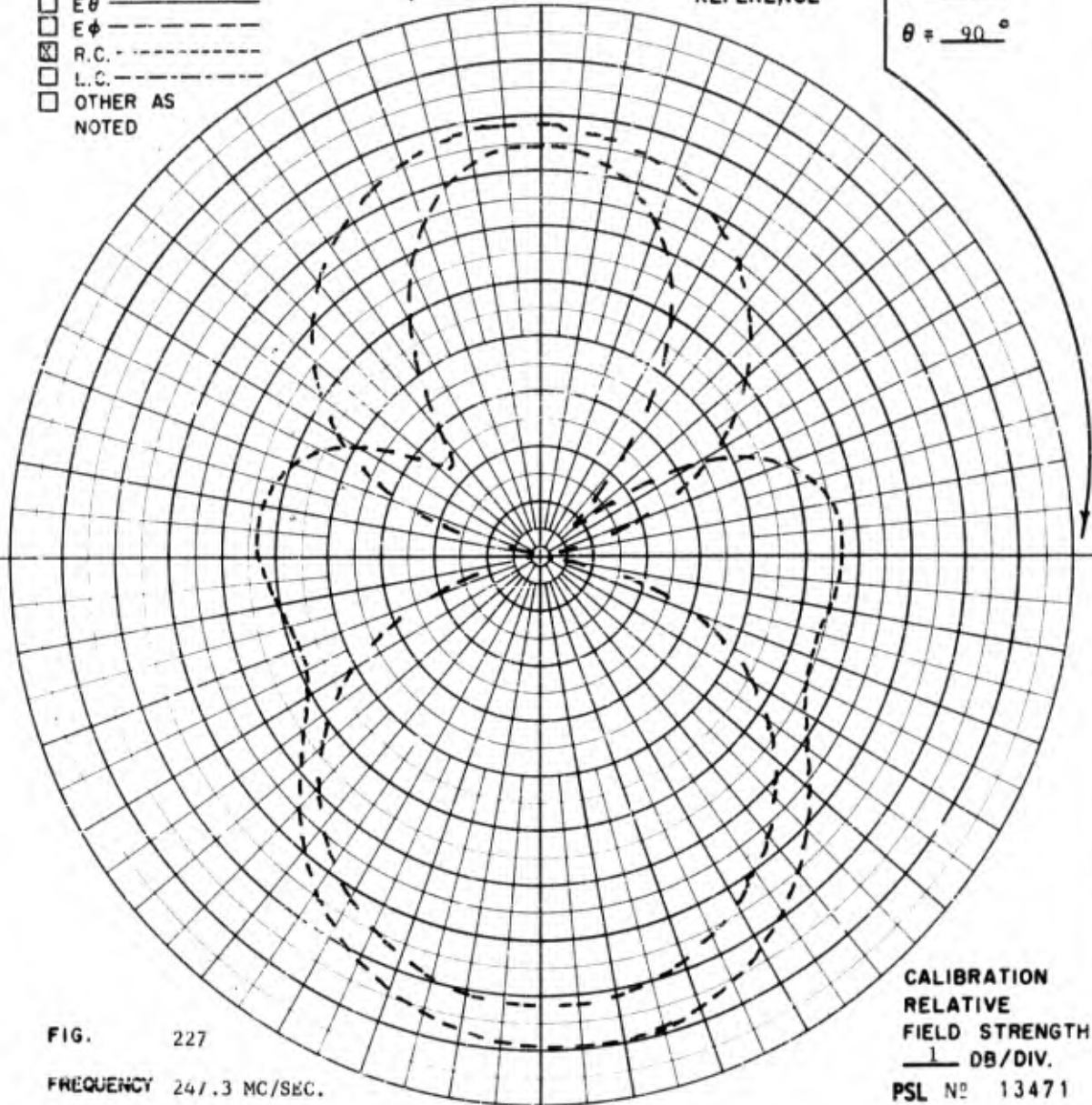
POLARIZATION

- GAIN REF - - - - -
 E θ - - - - -
 E ϕ - - - - -
 R.C. - - - - -
 L.C. - - - - -
 OTHER AS NOTED

$\phi = \underline{\quad\quad}^\circ$ $\theta = \underline{0}^\circ$

COORDINATE REFERENCE

$\phi = \underline{0}^\circ$
 $\theta = \underline{90}^\circ$



CALIBRATION
 RELATIVE
 FIELD STRENGTH
 1 DB/DIV.
 PSL No 13471

FIG. 227

FREQUENCY 247.3 MC/SEC.

ANTENNA MODEL 2.007 TWO ELEMENT ARRAY FED 180° OUT OF PHASE AND MOUNTED ON THE AP-3 MOCKUP.

REMARKS THE GAIN REFERENCE ANTENNA IS A STODDART HALF-WAVE DIPOLE ILLUMINATED BY A RIGHT CIRCULAR HELIX.

POLARIZATION

- GAIN REF - - - - -
- E θ - - - - -
- E ϕ - - - - -
- R.C. - - - - -
- L.C. - - - - -
- OTHER AS NOTED

$\phi = \underline{\hspace{2cm}}^\circ$ $\theta = \underline{0}^\circ$

COORDINATE REFERENCE

$\phi = \underline{0}^\circ$
 $\theta = \underline{90}^\circ$

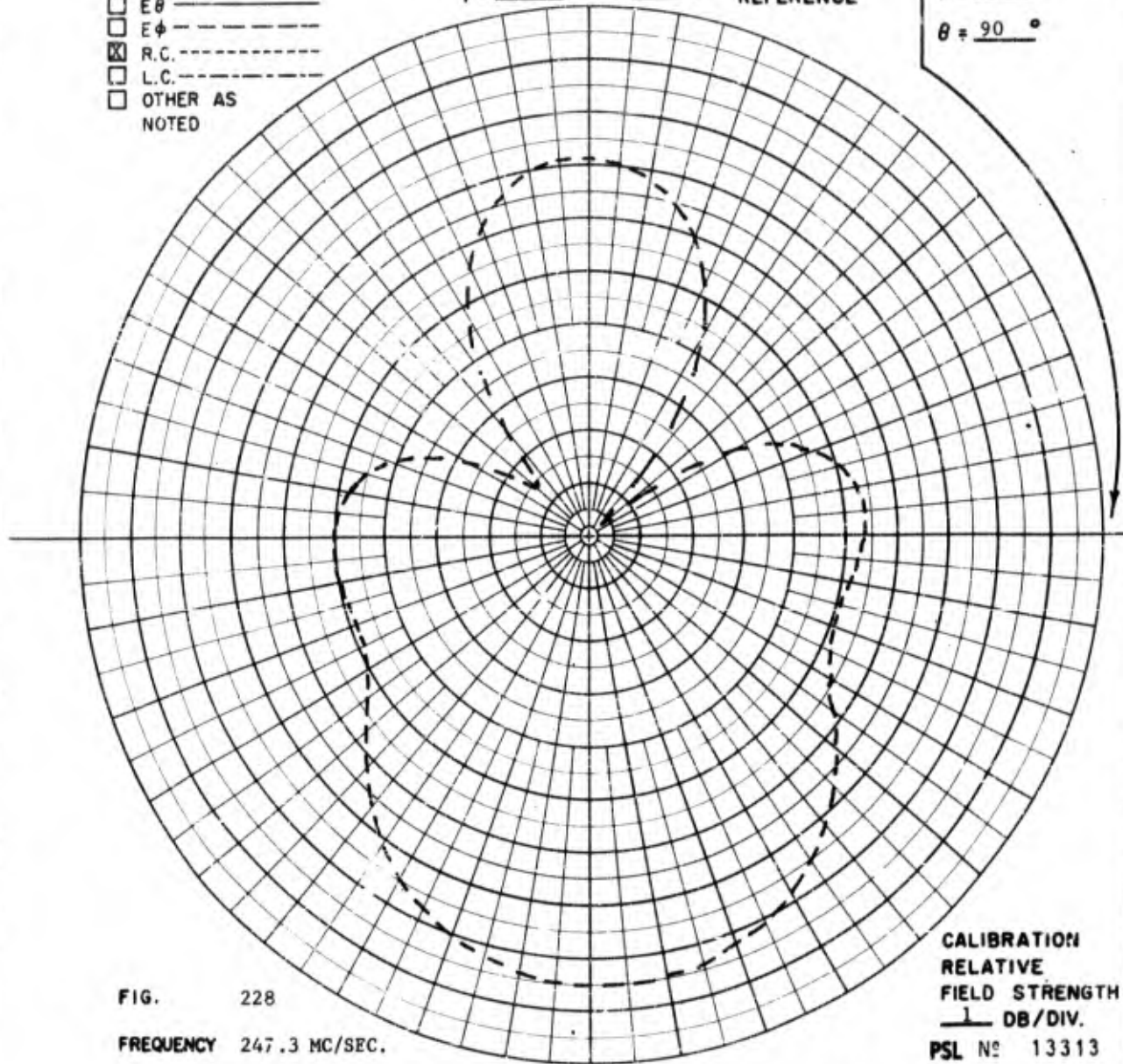


FIG. 228

FREQUENCY 247.3 MC/SEC.

CALIBRATION
RELATIVE
FIELD STRENGTH
1 DB/DIV.
PSL No 13313

ANTENNA MODEL 2.007 TWO ELEMENT ARRAY FED 180° OUT OF PHASE AND MOUNTED ON THE AP-3 MOCKUP.

REMARKS AT $\theta = 180^\circ$, $\theta = 90^\circ$ THE GAIN IS -2 DB WITH RESPECT TO THE REFERENCE DIPOLE. ANTENNA GROUND PLANE SHIPPED TO MOTOR WITH ALUMINIZED TAPE.

POLARIZATION

- GAIN REF -----
- E_{θ} -----
- E_{ϕ} -----
- R.C. -----
- L.C. -----
- OTHER AS NOTED

$\phi = \underline{\hspace{1cm}}^{\circ}$ $\theta = \underline{0}^{\circ}$ **COORDINATE REFERENCE**

$\phi = \underline{90}^{\circ}$
 $\theta = \underline{90}^{\circ}$

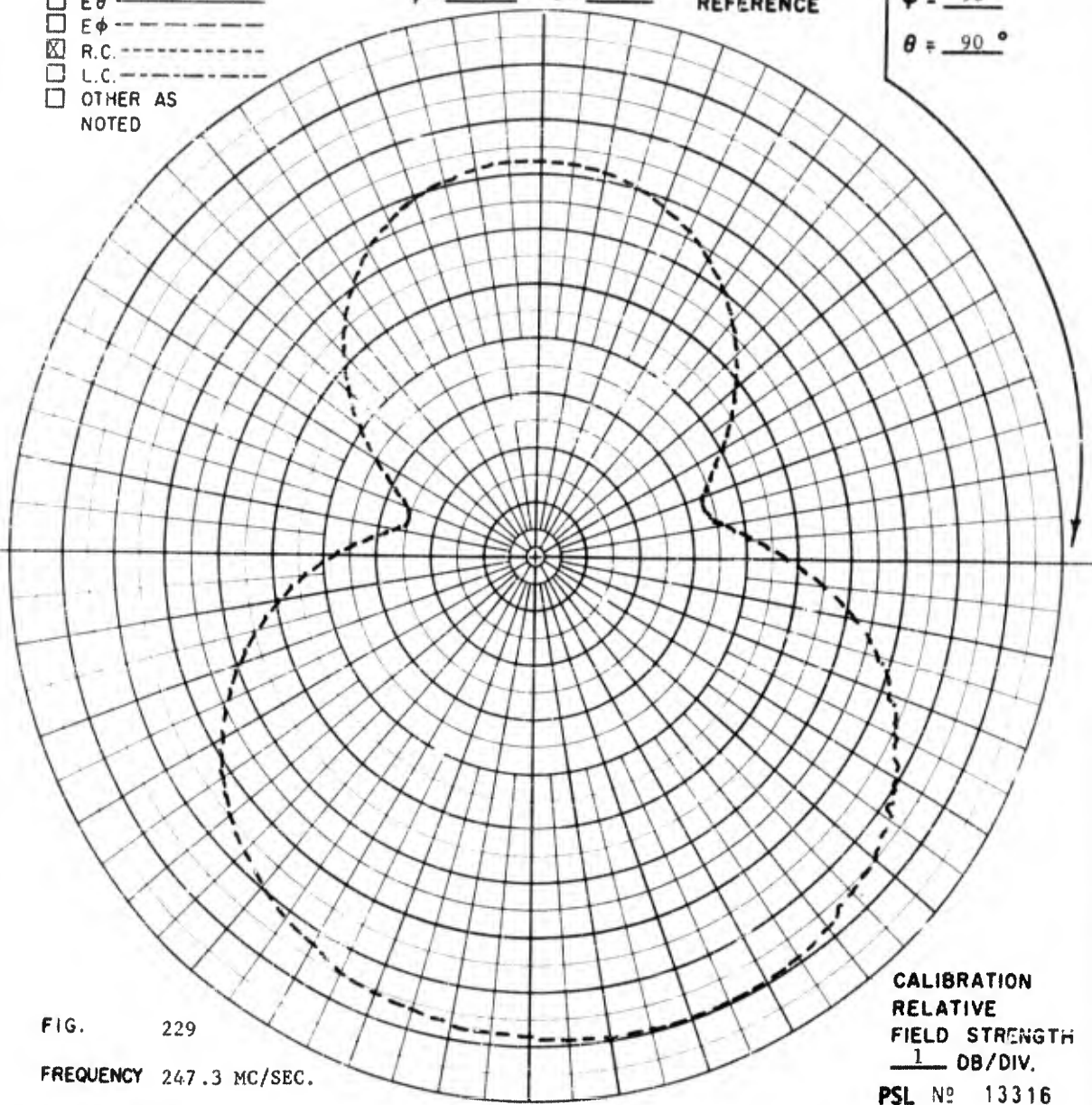


FIG. 229
FREQUENCY 247.3 MC/SEC.
ANTENNA MODEL 2.007 TWO ELEMENT ARRAY FED 180° OUT OF PHASE AND MOUNTED ON THE AP-3 MOCK'UP.
REMARKS

CALIBRATION
RELATIVE
FIELD STRENGTH
1 DB/DIV.
PSL No 13316

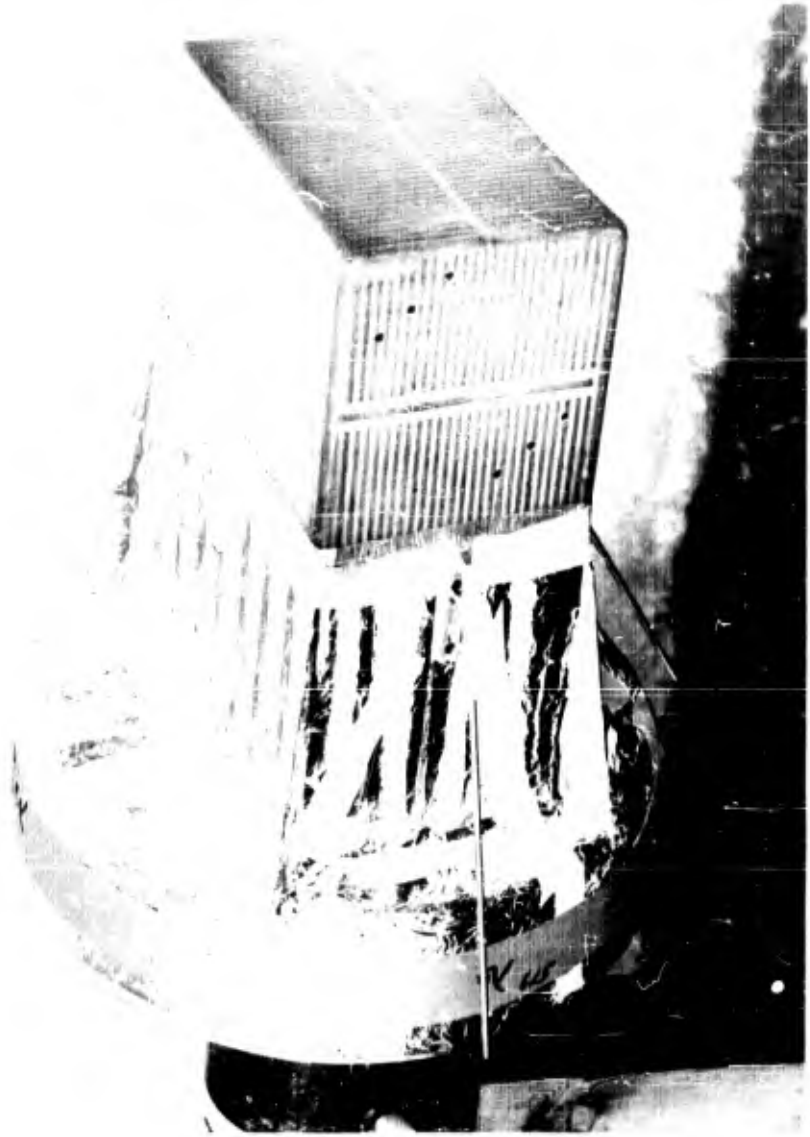


FIG. 230 - PHOTOGRAPH OF THE AP/5 PAYLOAD MOCKUP

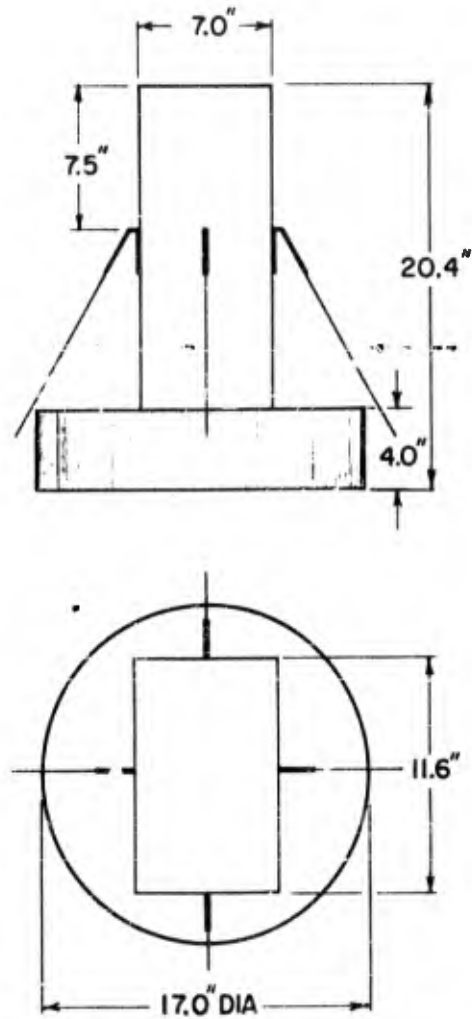


FIG. 231 - SKETCH OF THE PAYLOAD MOCKUP USED FOR THE AP/5 RADIATION PATTERN MEASUREMENTS

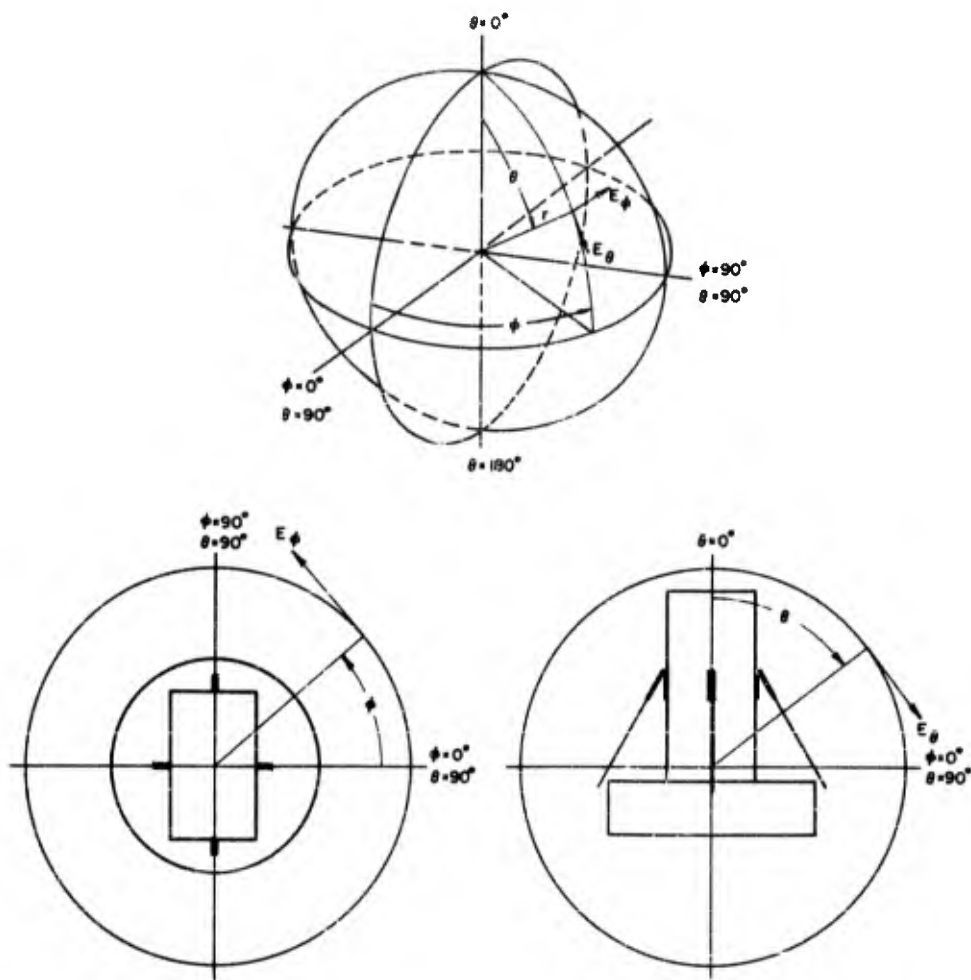


FIG. 232 - POSITION COORDINATES FOR THE ANTENNAS ON THE AP/5 PAYLOADS

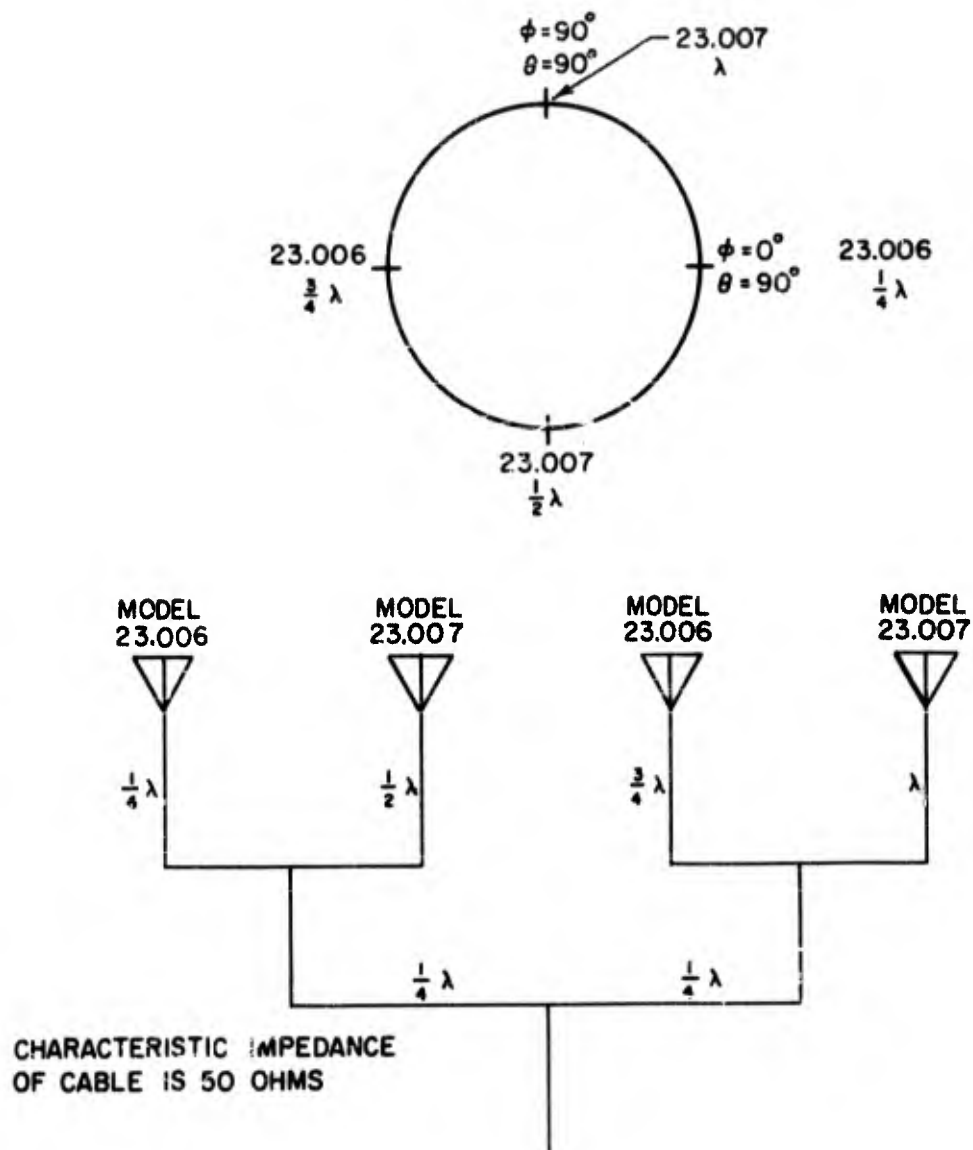


FIG. 233 - SKETCH OF THE PHASING HARNESS FOR THE ANTENNAS ON THE AP/5 PAYLOAD

POLARIZATION

- GAIN REF -----
 $E\theta$ -----
 $E\phi$ -----
 R.C. -----
 L.C. -----
 OTHER AS NOTED

$\phi =$ _____ ° $\theta =$ _____ ° COORDINATE REFERENCE

$\phi =$ _____ °
 $\theta =$ _____ °

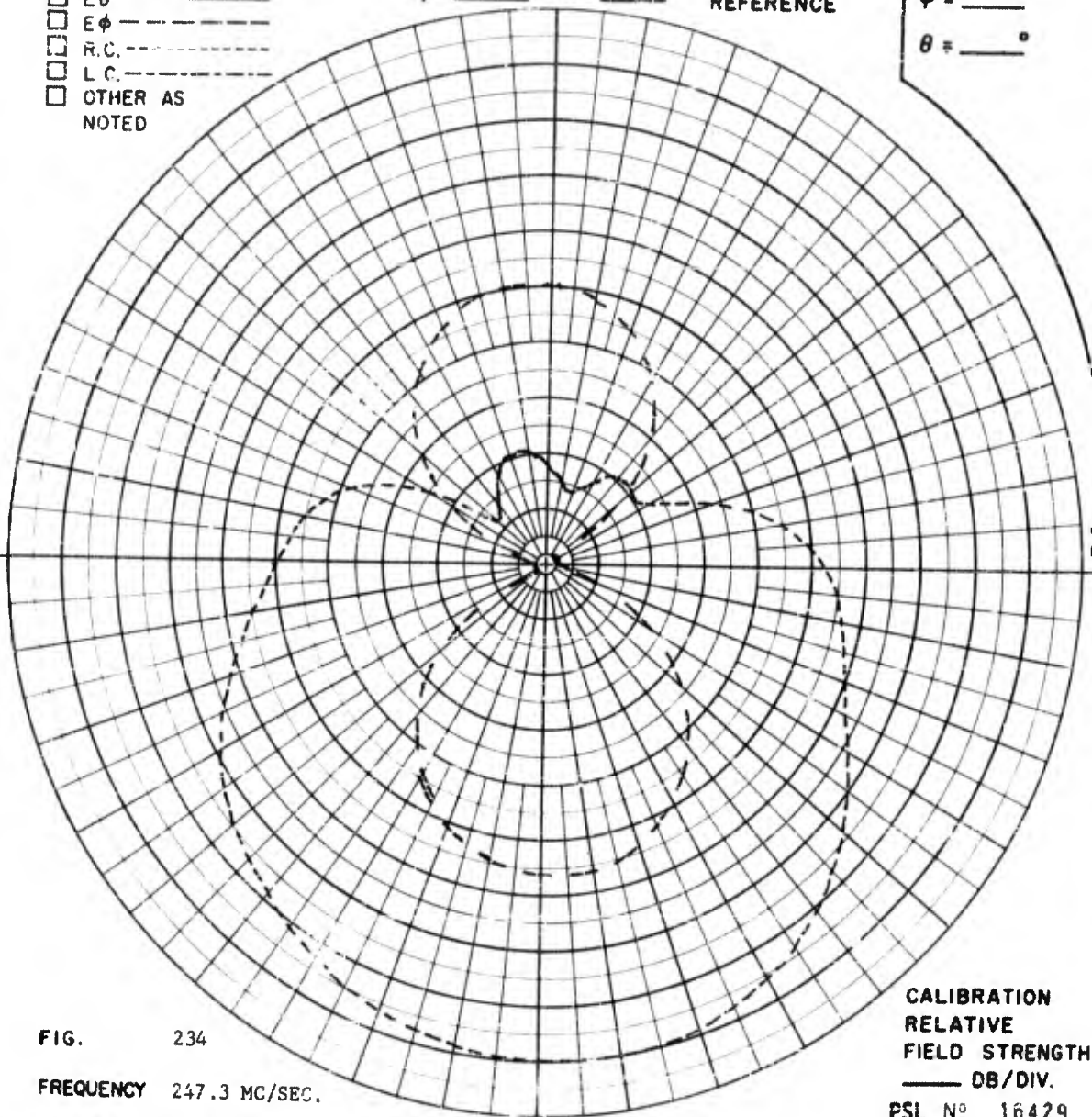


FIG. 234

FREQUENCY 247.3 MC/SEC.

ANTENNA ARRAY OF MODEL 23.006 AND 23.007 ANTENNAS MOUNTED ON THE AP-5 PAYLOAD.

REMARKS THE GAIN REFERENCE ANTENNA IS A STODDART HALF-WAVE DIPOLE ILLUMINATED BY A RIGHT CIRCULAR HELIX.

CALIBRATION
 RELATIVE
 FIELD STRENGTH
 — DB/DIV.

PSL No 16429

POLARIZATION

- GAIN REF - - - - -
 E_{θ} ————
 E_{ϕ} - - - - -
 R.C. - - - - -
 L.C. - - - - -
 OTHER AS NOTED

$\phi = \text{---}^{\circ}$ $\theta = \text{---}^{\circ}$ COORDINATE REFERENCE

$\phi = \text{---}^{\circ}$
 $\theta = \text{---}^{\circ}$

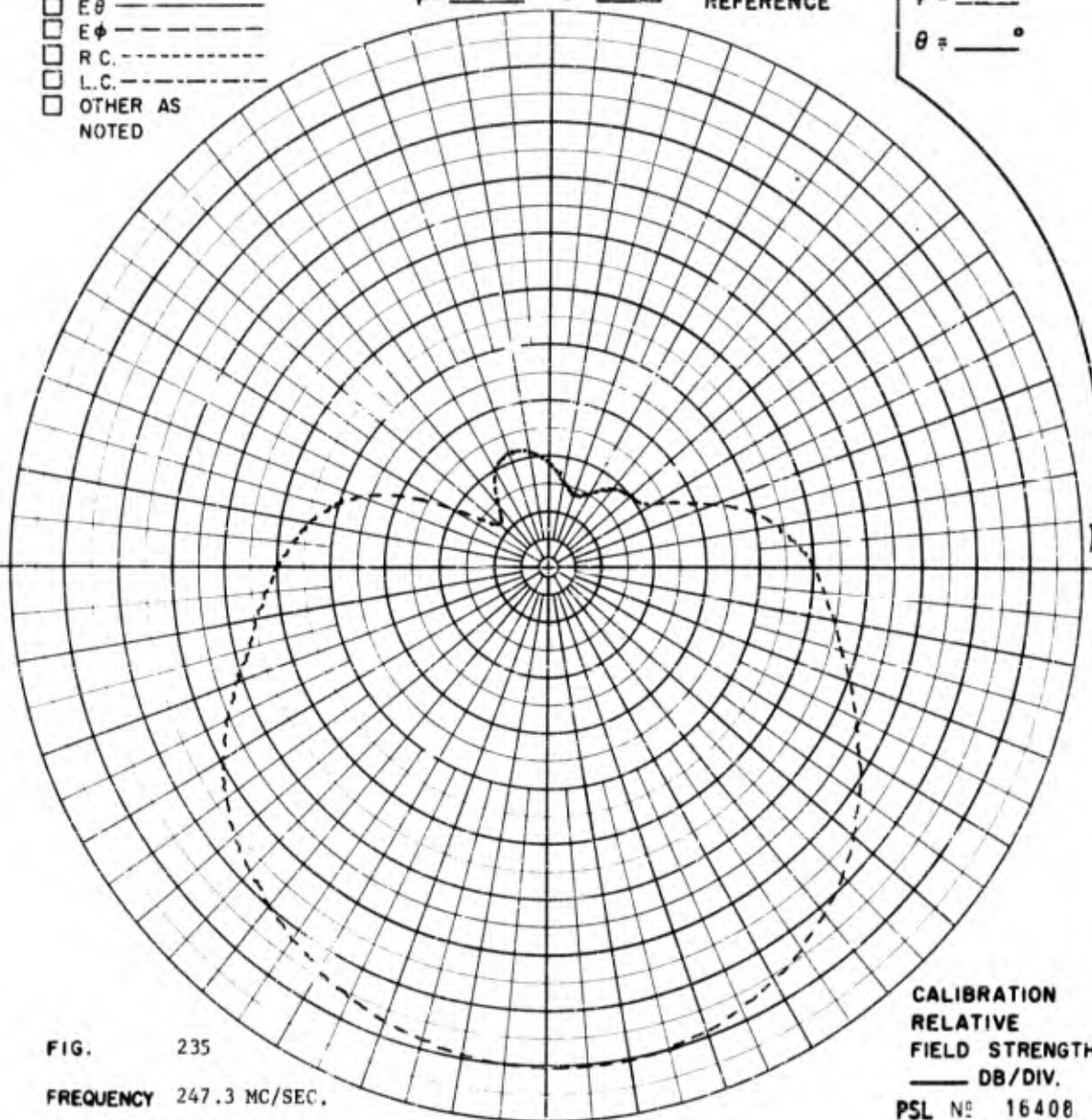


FIG. 235
 FREQUENCY 247.3 MC/SEC.

CALIBRATION
 RELATIVE
 FIELD STRENGTH
 ——— DB/DIV.
 PSL NO 16408

ANTENNA ARRAY OF MODEL 23.006 AND 23.007 ANTENNAS MOUNTED ON THE AP-5 PAYLOAD.

REMARKS AT $\theta = 180^{\circ}$, $\phi = 0^{\circ}$ THE GAIN IS +7 DB WITH RESPECT TO THE REFERENCE DIPOLE.

POLARIZATION

- GAIN REF - - - - -
 E_{θ} - - - - -
 E_{ϕ} - - - - -
 R.C. - - - - -
 L.C. - - - - -
 OTHER AS NOTED

$\phi = \text{---}^{\circ}$ $\theta = \text{---}^{\circ}$

COORDINATE
REFERENCE

$\phi = \text{---}^{\circ}$
 $\theta = \text{---}^{\circ}$

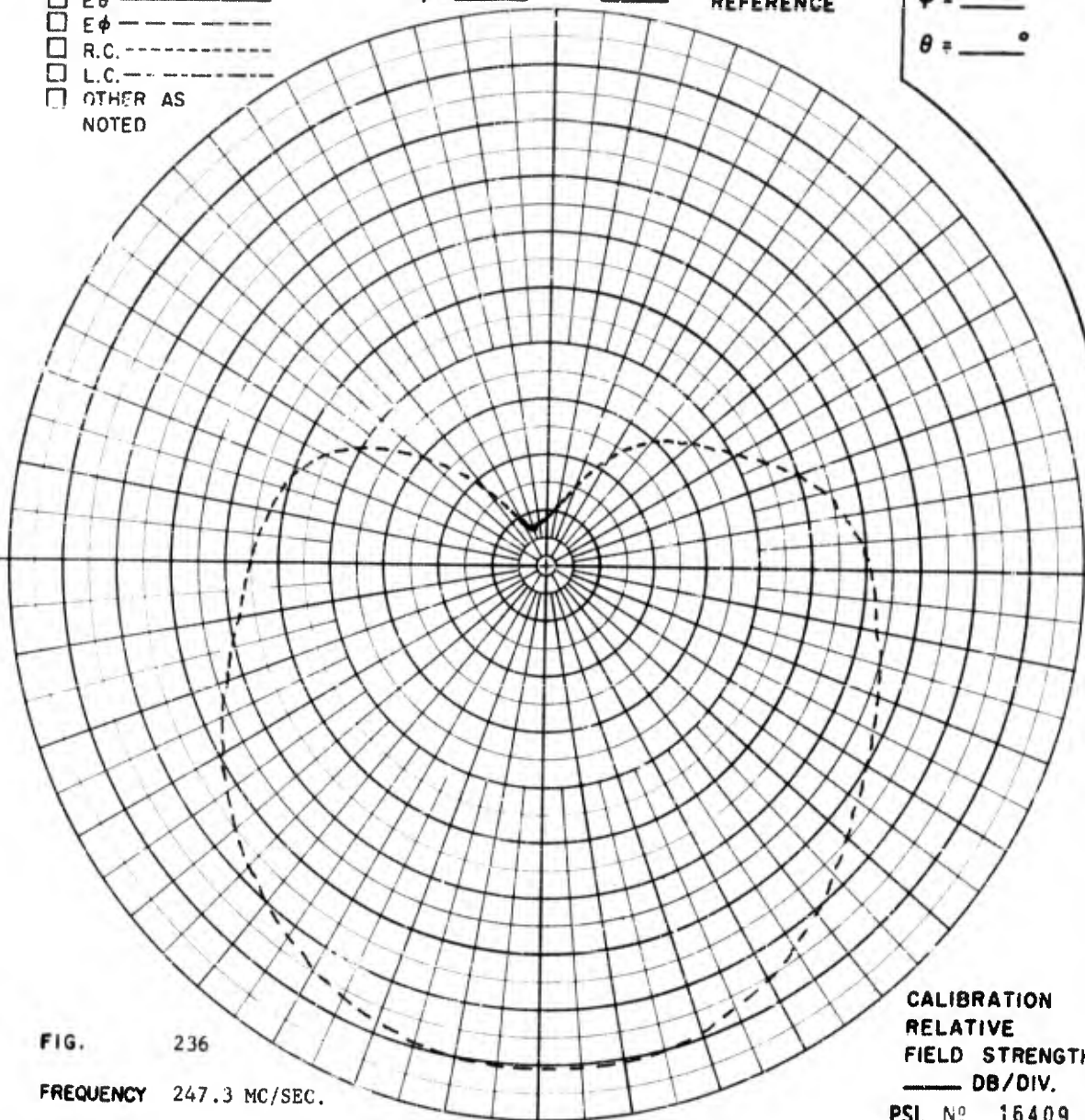


FIG. 236

FREQUENCY 247.3 MC/SEC.

ANTENNA ARRAY OF MODEL 23.006 AND 23.007 ANTENNAS MOUNTED ON THE AP-5 PAYLOAD.

REMARKS

CALIBRATION
 RELATIVE
 FIELD STRENGTH
 — DB/DIV.
 PSL № 16409

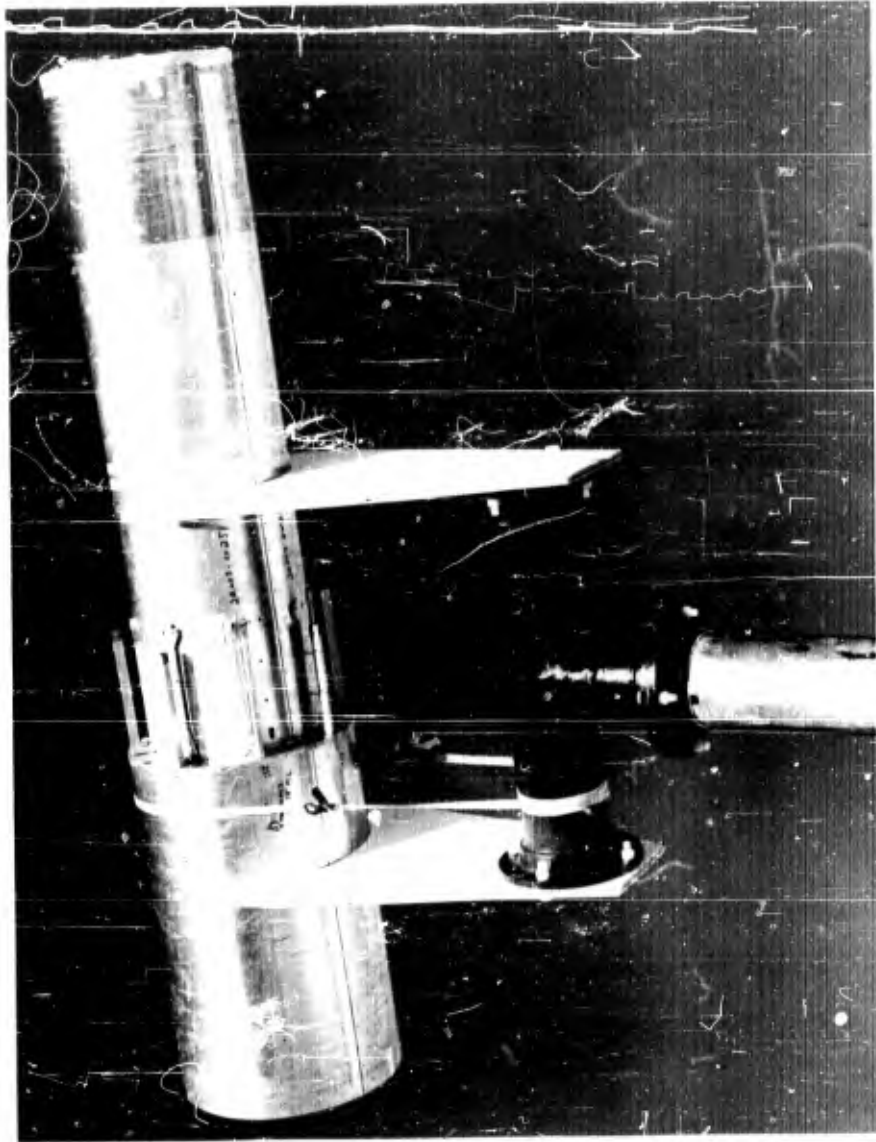


FIG. 237 - PHOTOGRAPH OF THE AO-10 VEHICLE MOCKUP USED FOR RADIATION PATTERN MEASUREMENTS

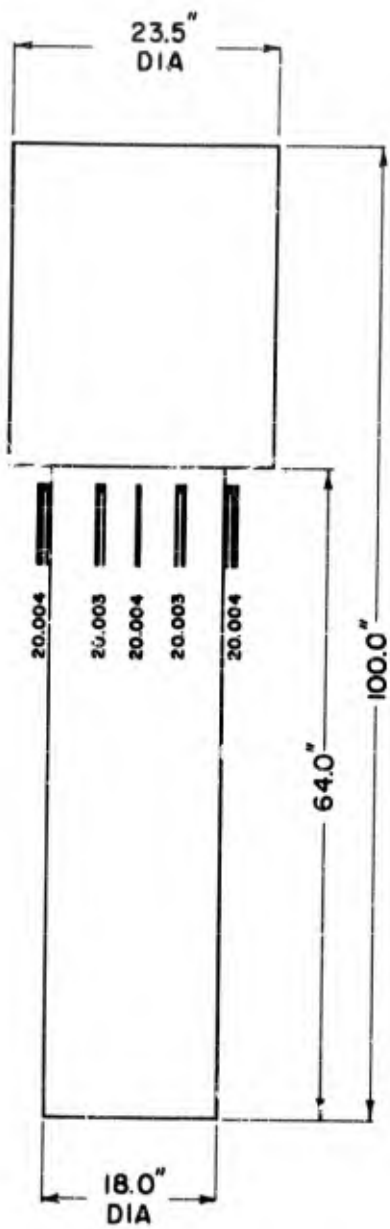


FIG. 238 - SKETCH OF THE AO-10 VEHICLE MOCKUP USED FOR RADIATION PATTERN MEASUREMENTS

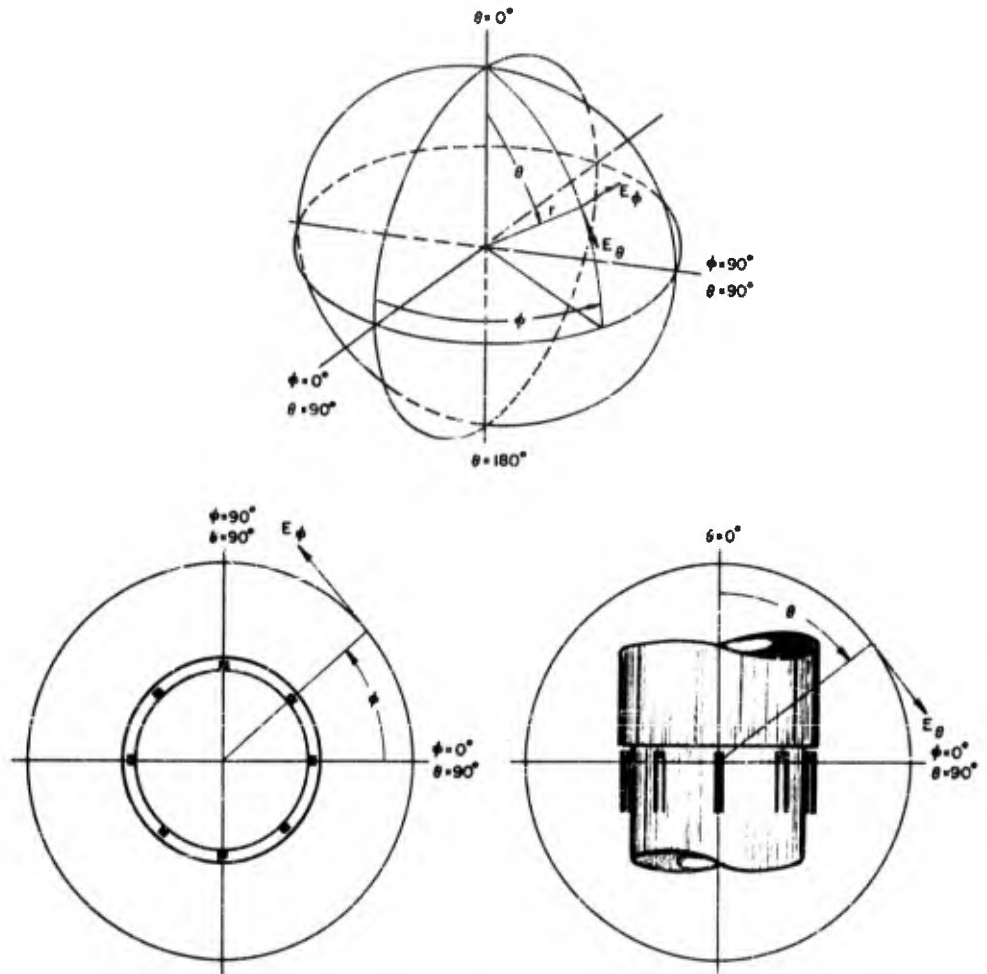


FIG. 239 - POSITION COORDINATES OF THE MODEL 20.004 ANTENNAS MOUNTED ON THE AO-10 MOCKUP FOR RADIATION PATTERN MEASUREMENTS

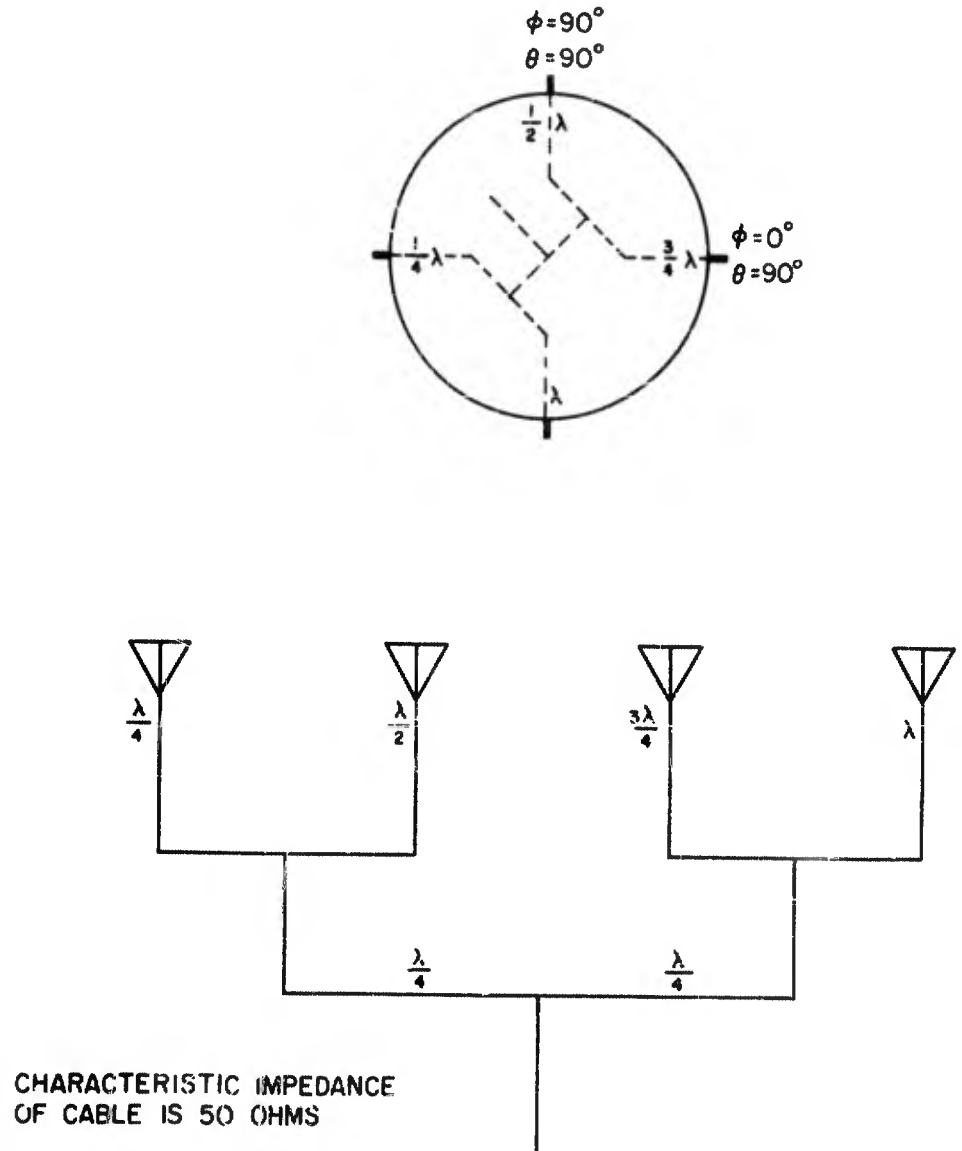


FIG. 240 - SKETCH OF THE PHASING HARNESS FOR THE FOUR ELEMENT ARRAY OF MODEL 20.004 ANTENNAS

POLARIZATION

- GAIN REF -----
- E_θ -----
- E_ϕ -----
- R.C. -----
- L.C. -----
- OTHER AS NOTED

$\phi = \underline{\hspace{1cm}}^\circ$ $\theta = \underline{0}^\circ$ COORDINATE REFERENCE

$\phi = \underline{0}^\circ$
 $\theta = \underline{90}^\circ$

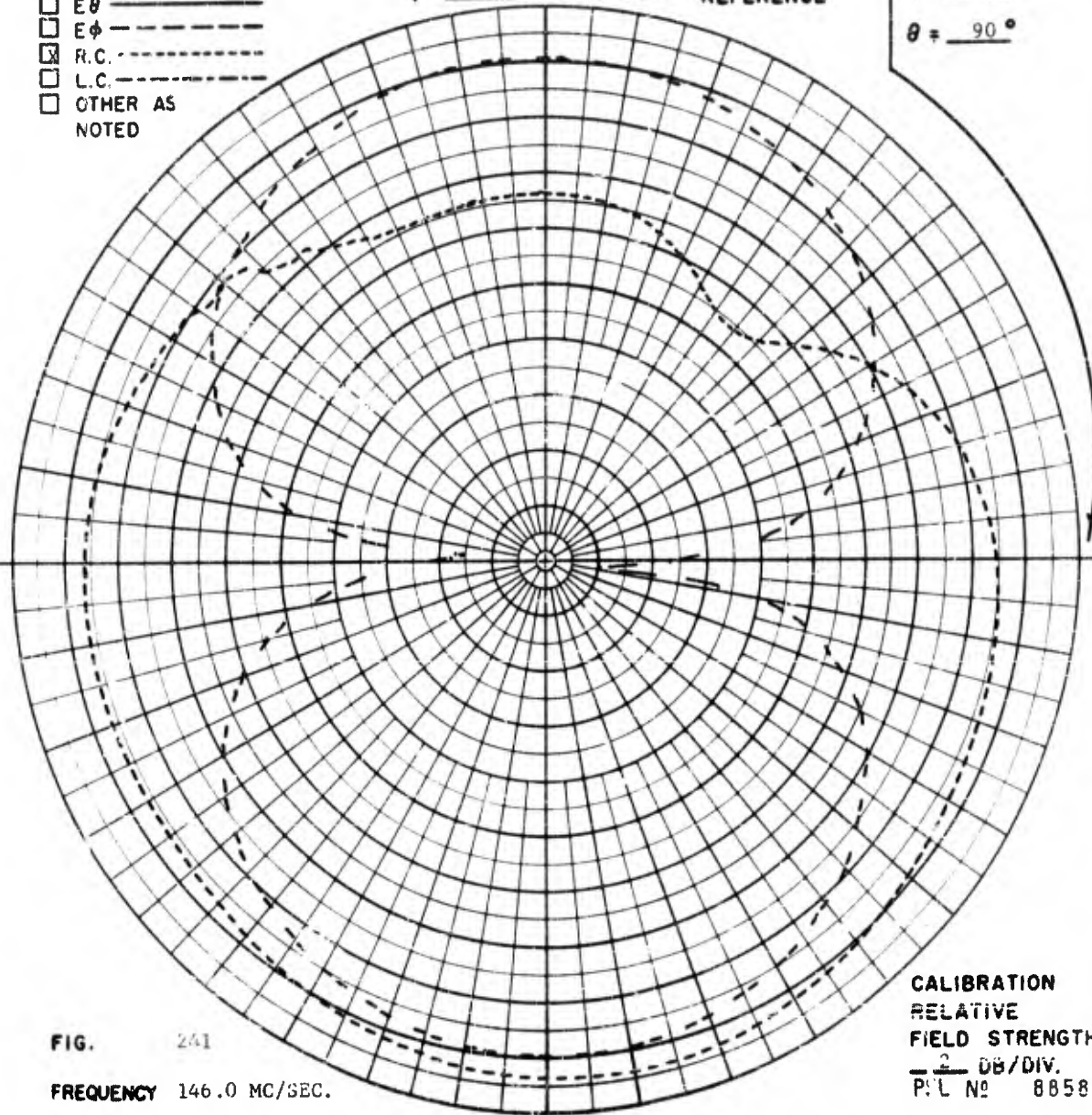


FIG. 241

FREQUENCY 146.0 MC/SEC.

ANTENNA MODEL 20.004 FOUR ELEMENT ARRAY MOUNTED ON THE AO-10 MOCKUP.

REMARKS THE GAIN REFERENCE IS A STODDARD HALF-WAVE DIPOLE ILLUMINATED BY A RIGHT CIRCULAR HELIX.

CALIBRATION
RELATIVE
FIELD STRENGTH
 $\frac{2}{\text{DB/DIV.}}$
P.C. No 8858

POLARIZATION

- GAIN REF - - - -
 E_{θ} - - - -
 E_{ϕ} - - - -
 R.C. - - - -
 L.C. - - - -
 OTHER AS NOTED

$\phi = \underline{\quad}^{\circ}$ $\theta = \underline{0}^{\circ}$ COORDINATE REFERENCE

$\phi = \underline{0}^{\circ}$
 $\theta = \underline{90}^{\circ}$

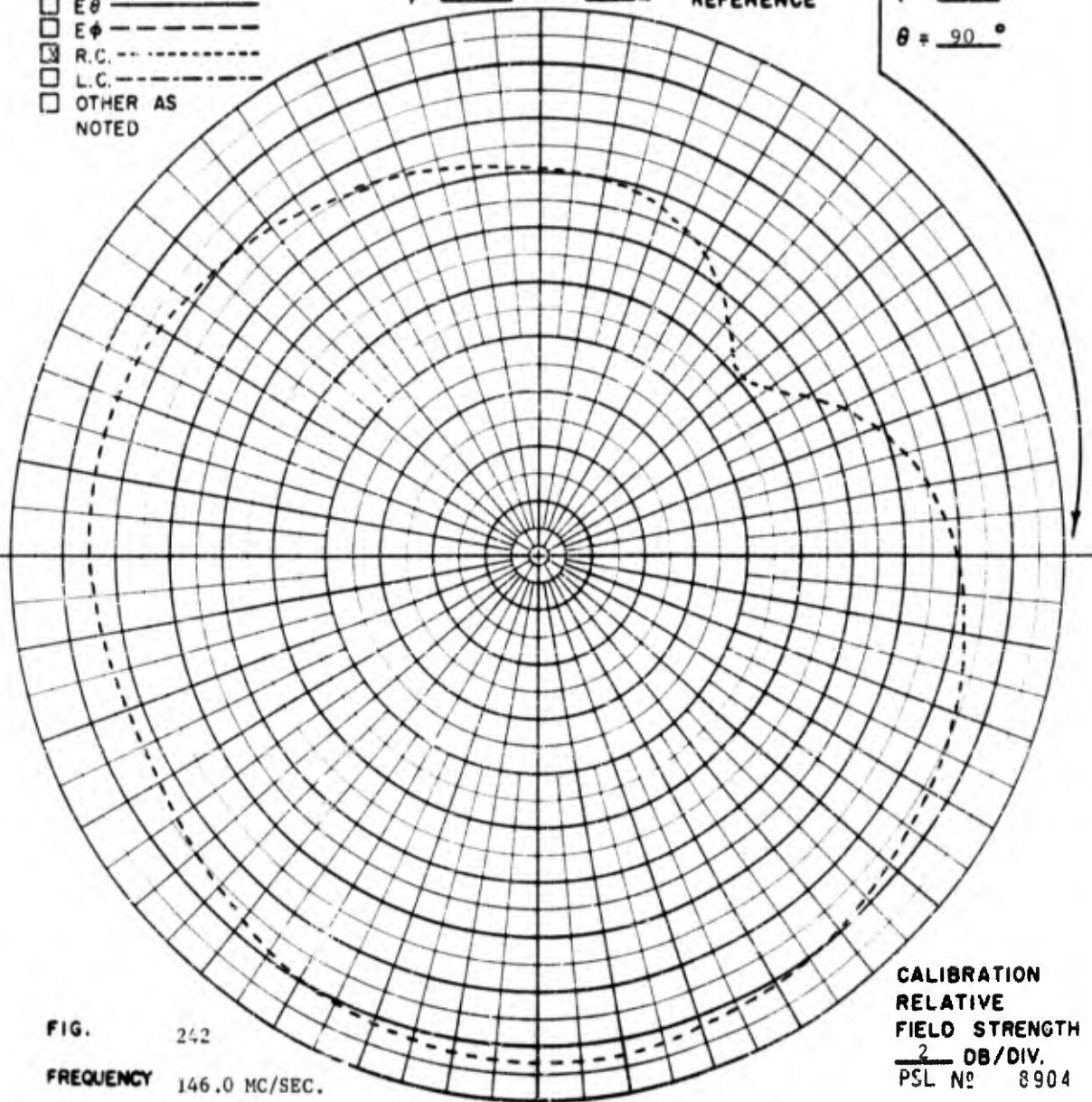


FIG. 242
 FREQUENCY 146.0 MC/SEC.

CALIBRATION
 RELATIVE
 FIELD STRENGTH
 2 DB/DIV.
 PSL No 8904

ANTENNA MODEL 20.004 FOUR ELEMENT ARRAY MOUNTED ON THE AO-10 MOCKUP.

REMARKS AT $\theta = 180^{\circ}$, $\phi = 0^{\circ}$ THE GAIN IS -2 DB WITH RESPECT TO THE REFERENCE DIPOLE.

POLARIZATION

- GAIN REF - - - -
 E_{θ} - - - -
 E_{ϕ} - - - -
 R.C. - - - -
 L.C. - - - -
 OTHER AS NOTED

$\phi = \underline{\quad}^{\circ}$ $\theta = \underline{0}^{\circ}$ COORDINATE REFERENCE

$\phi = \underline{90}^{\circ}$
 $\theta = \underline{90}^{\circ}$

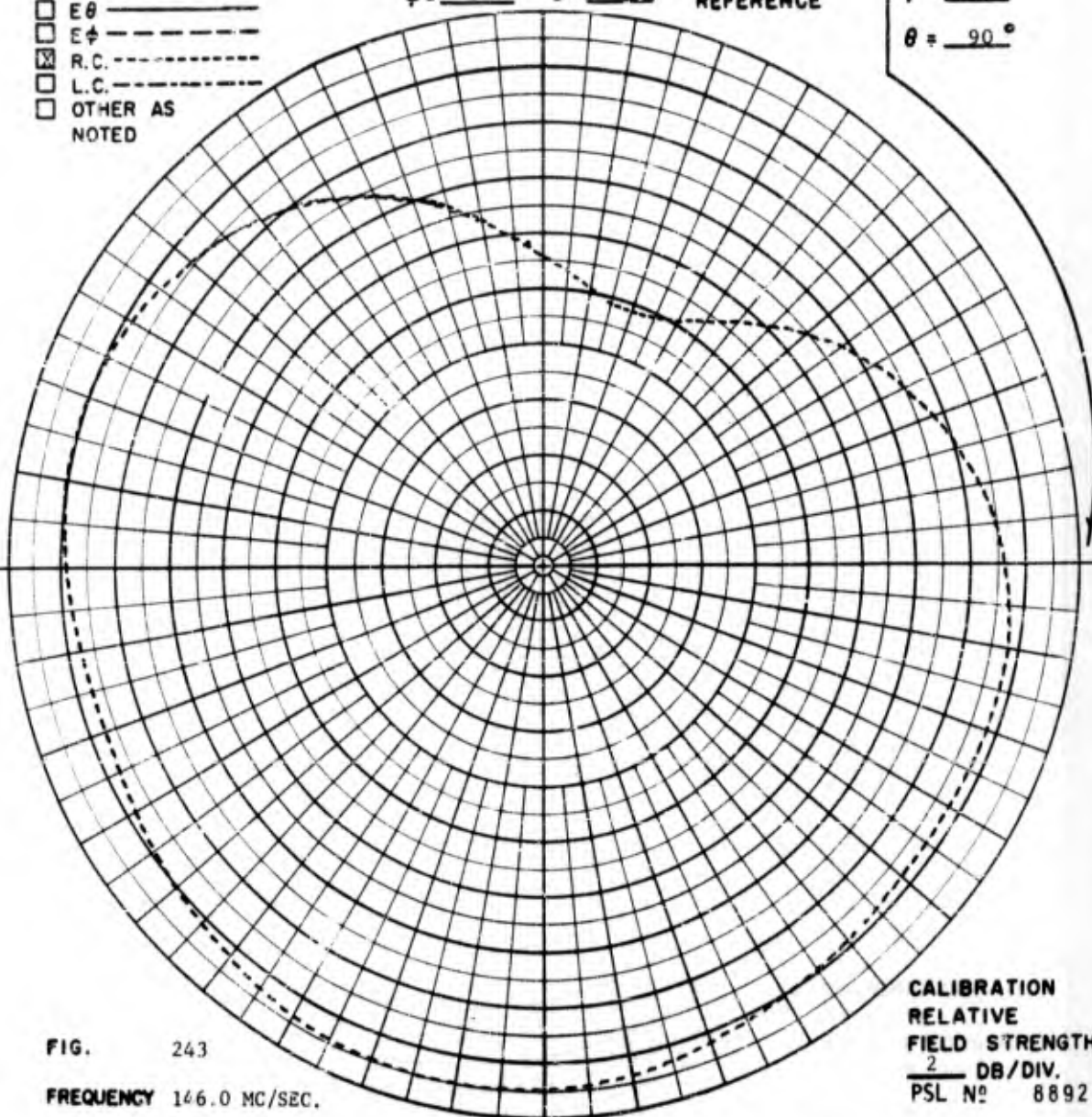


FIG. 243

FREQUENCY 146.0 MC/SEC.

ANTENNA MODEL 20.004 FOUR ELEMENT ARRAY MOUNTED ON THE AO-10 MOCKUP.

REMARKS

CALIBRATION
 RELATIVE
 FIELD STRENGTH
 2 DB/DIV.
 PSL No 8892

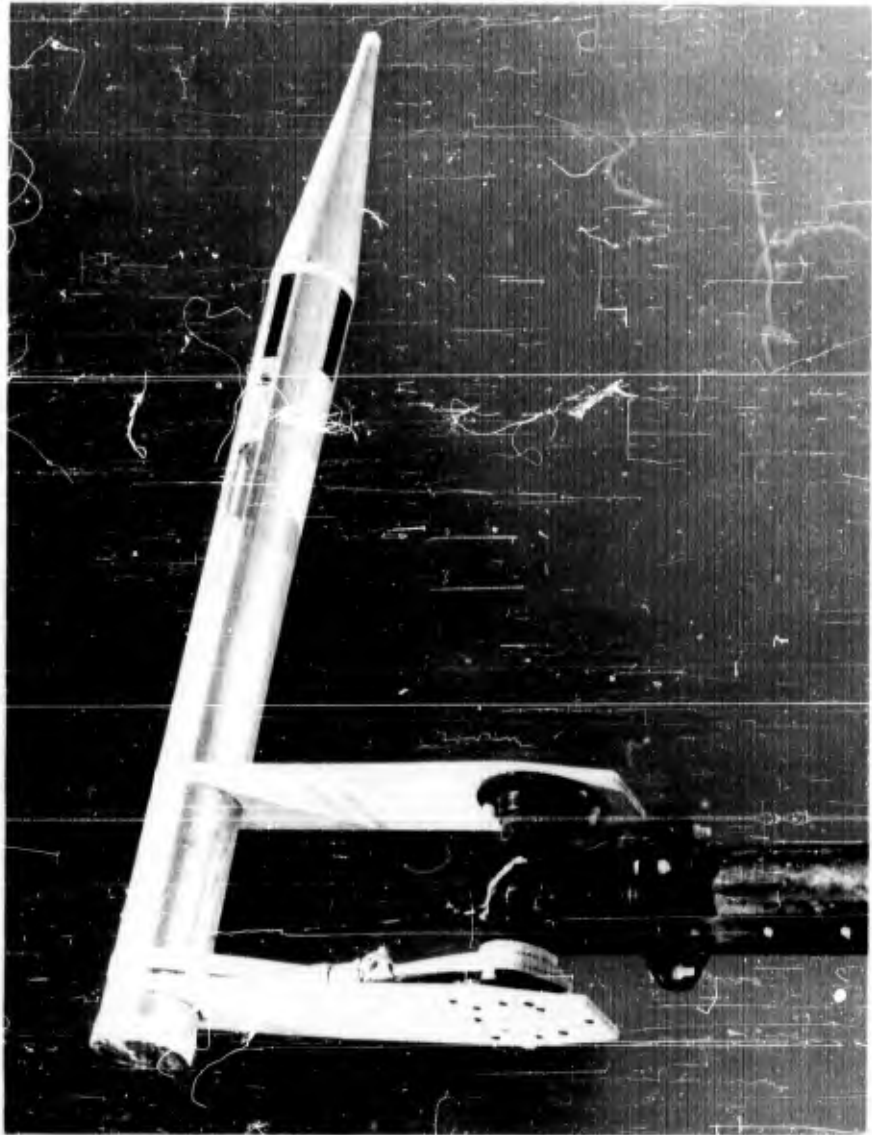


FIG. 244 - PHOTOGRAPH OF THE EXOS VEHICLE MOCKUP WITH THE FLAPS
CLOSED USED FOR RADIATION PATTERN MEASUREMENTS

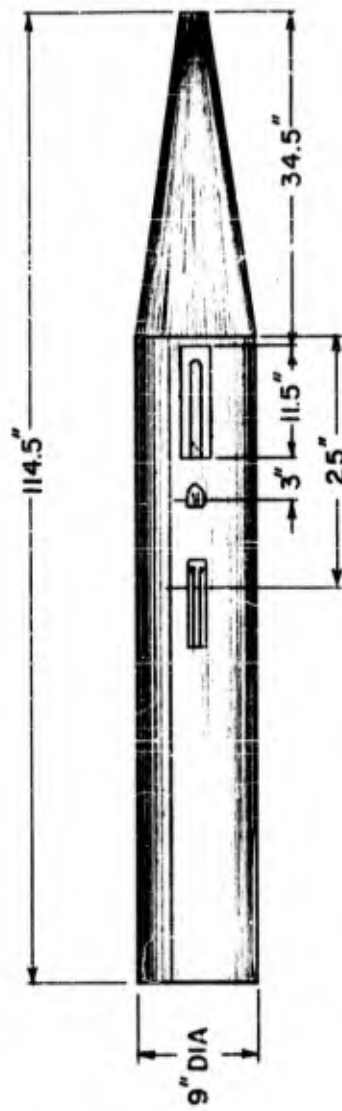


FIG. 245 - SKETCH OF THE EXOS VEHICLE MOCKUP USED FOR RADIATION PATTERN MEASUREMENTS

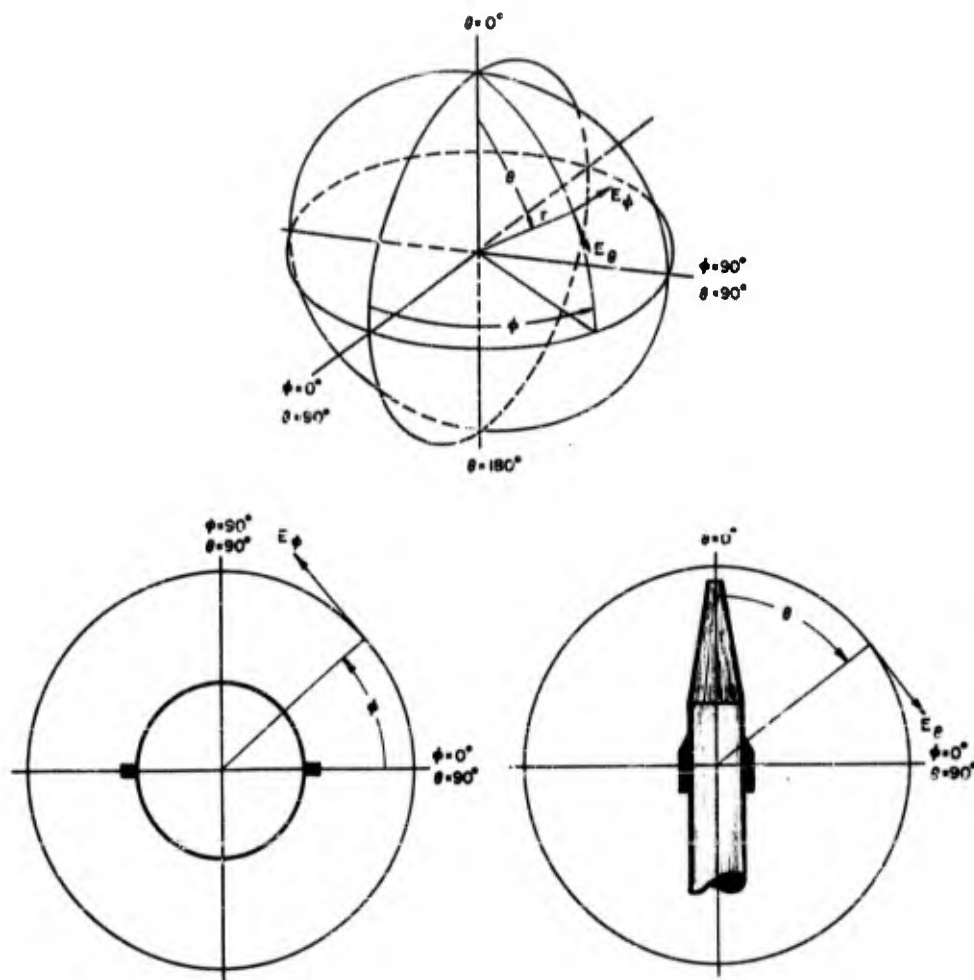


FIG. 246 - POSITION COORDINATES OF THE MODEL 2.036 ANTENNAS
FLAPS CLOSED CONFIGURATION

POLARIZATION

- GAIN REF - - - - -
 E θ - - - - -
 E ϕ - - - - -
 R.C. - - - - -
 L.C. - - - - -
 OTHER AS NOTED

$\phi = \underline{\quad}^\circ$ $\theta = \underline{0}^\circ$ COORDINATE REFERENCE

$\phi = \underline{0}^\circ$
 $\theta = \underline{90}^\circ$

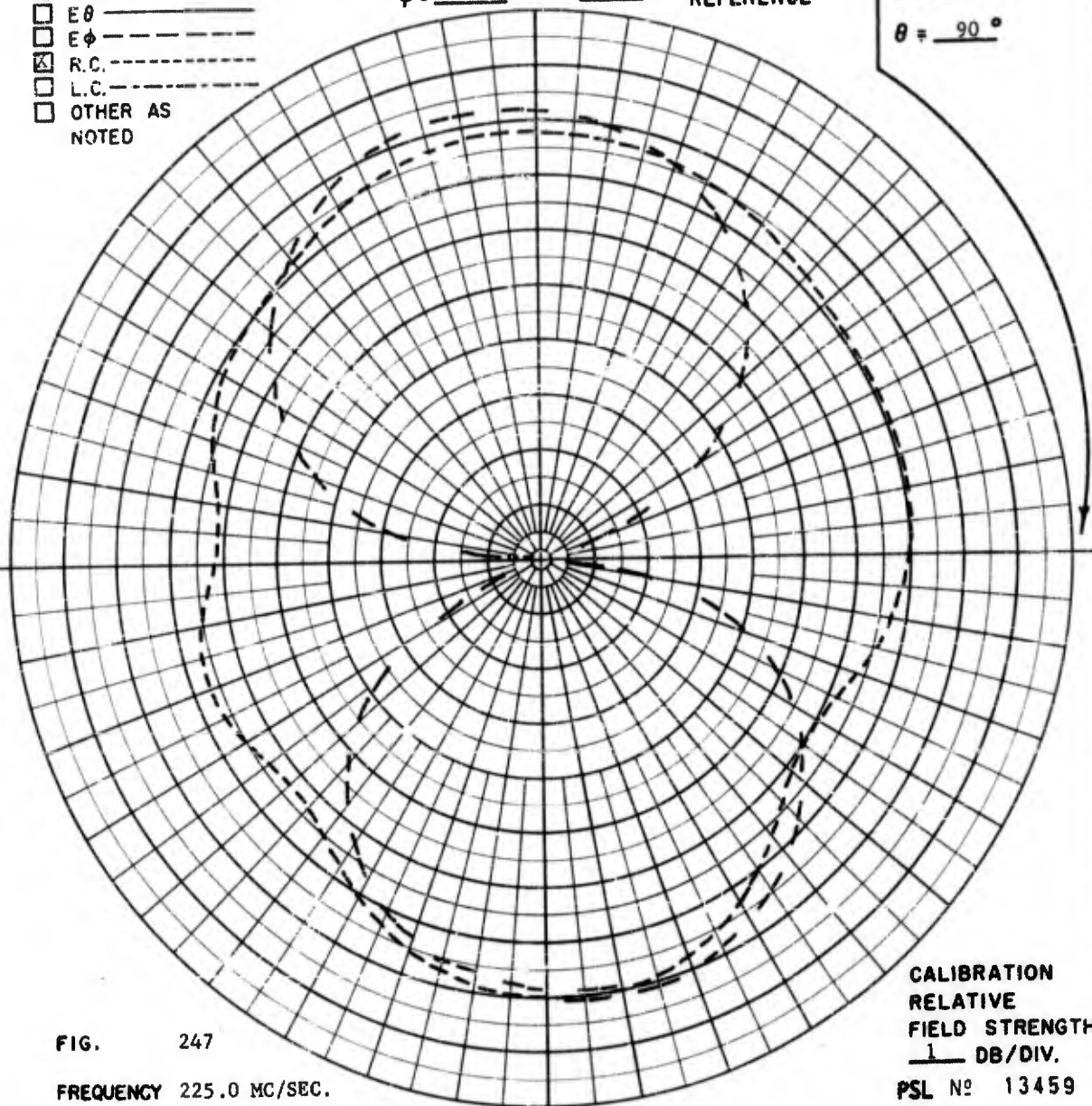


FIG. 247
 FREQUENCY 225.0 MC/SEC.

CALIBRATION
 RELATIVE
 FIELD STRENGTH
 1 DB/DIV.
 PSL No 13459

ANTENNA MODEL 2.036 TWO ELEMENT ARRAY MOUNTED ON THE EXOS MOCKUP WITH THE VEHICLE FLAPS CLOSED.
REMARKS THE GAIN REFERENCE ANTENNA IS A STODDARD HALF-WAVE DIPOLE ILLUMINATED BY A RIGHT CIRCULAR RELIX.

POLARIZATION

- GAIN REF -----
 E_{θ} -----
 E_{ϕ} -----
 R.C. -----
 L.C. -----
 OTHER AS NOTED

$\phi = \underline{\quad\quad}^{\circ}$ $\theta = \underline{0}^{\circ}$ COORDINATE REFERENCE

$\phi = \underline{0}^{\circ}$
 $\theta = \underline{90}^{\circ}$

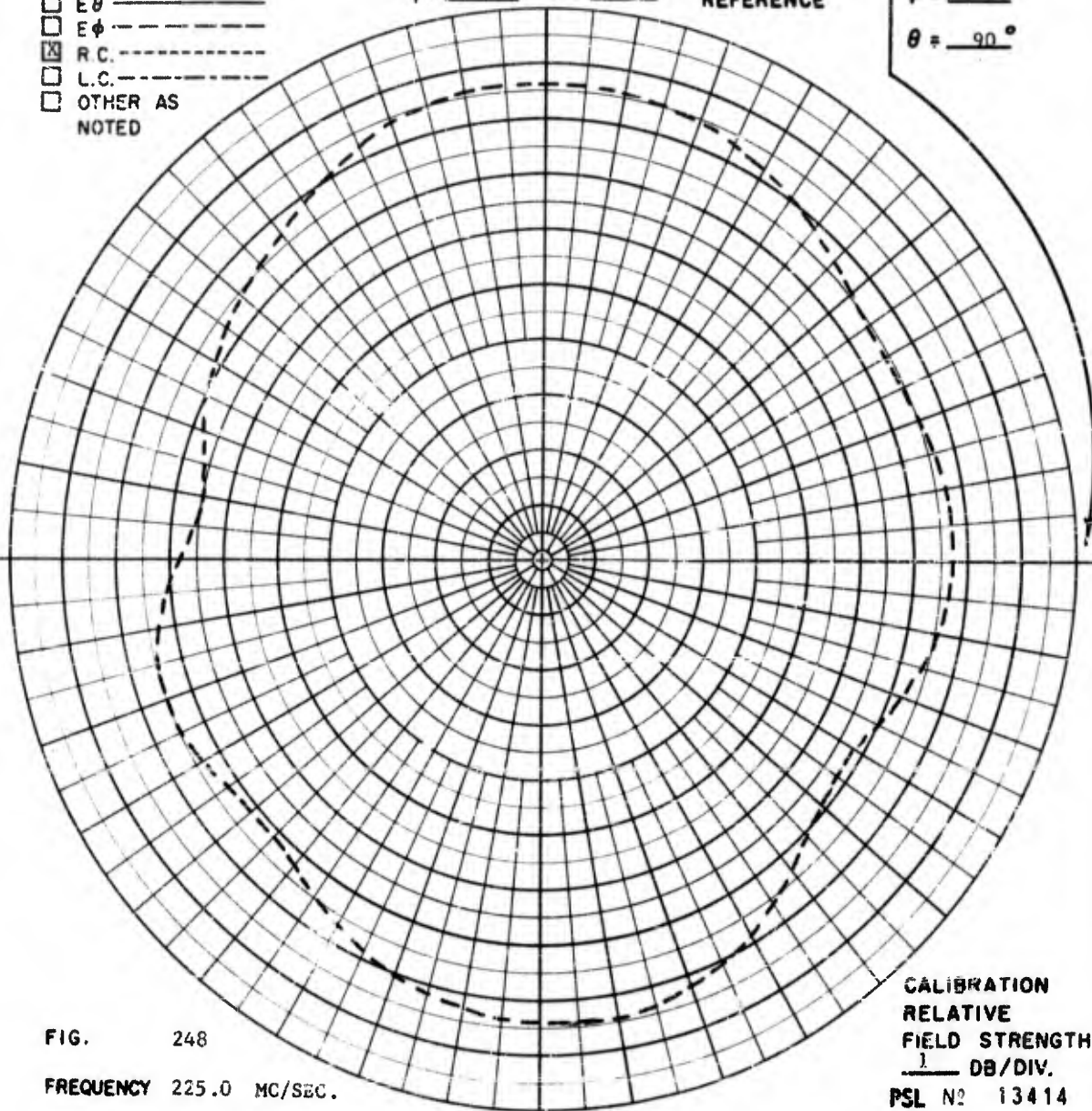


FIG. 248
 FREQUENCY 225.0 MC/SEC.

CALIBRATION
 RELATIVE
 FIELD STRENGTH
 1 DB/DIV.
 PSL N^o 13414

ANTENNA MODEL 2.036 TWO ELEMENT ARRAY MOUNTED ON THE EXOS MOCKUP WITH THE VEHICLE FLAPS CLOSED.

REMARKS AT $\theta = 180^{\circ}$, $\phi = 0^{\circ}$ THE GAIN IS EQUAL TO THAT OF THE REFERENCE DIPOLE.

POLARIZATION

- GAIN REF - - - - -
 E θ - - - - -
 E ϕ - - - - -
 R.C. - - - - -
 L.C. - - - - -
 OTHER AS NOTED

 $\phi = \underline{\hspace{1cm}}^\circ$ $\theta = \underline{\hspace{1cm}}^\circ$

COORDINATE REFERENCE

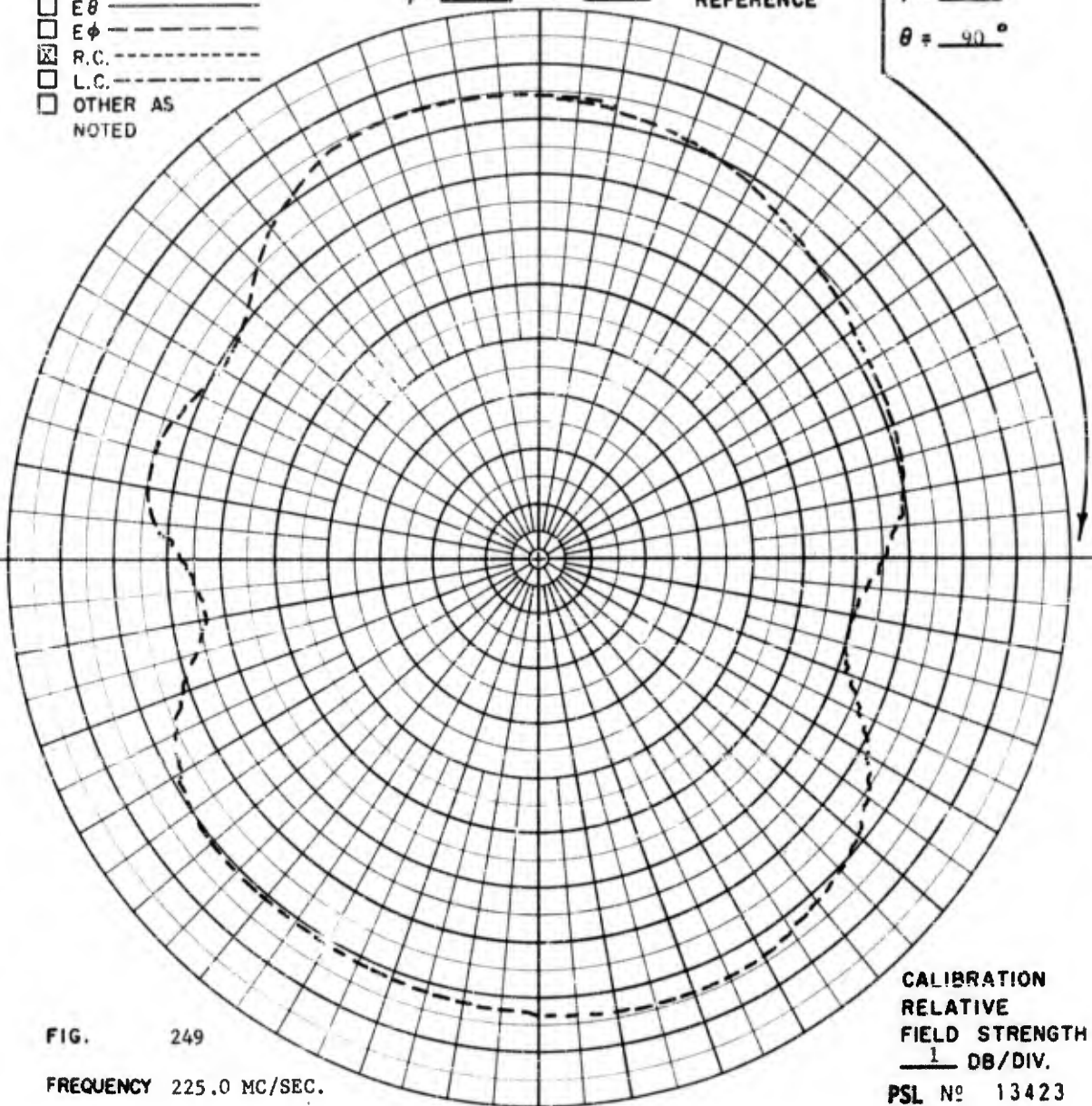
 $\phi = \underline{90}^\circ$
 $\theta = \underline{90}^\circ$


FIG. 249

FREQUENCY 225.0 MC/SEC.

ANTENNA MODEL 2.036 TWC ELEMENT ARRAY MOUNTED ON THE EXOS MOCKUP WITH VEHICLE FLAPS CLOSED.

REMARKS

 CALIBRATION
 RELATIVE
 FIELD STRENGTH
 1 DB/DIV.

PSL No 13423

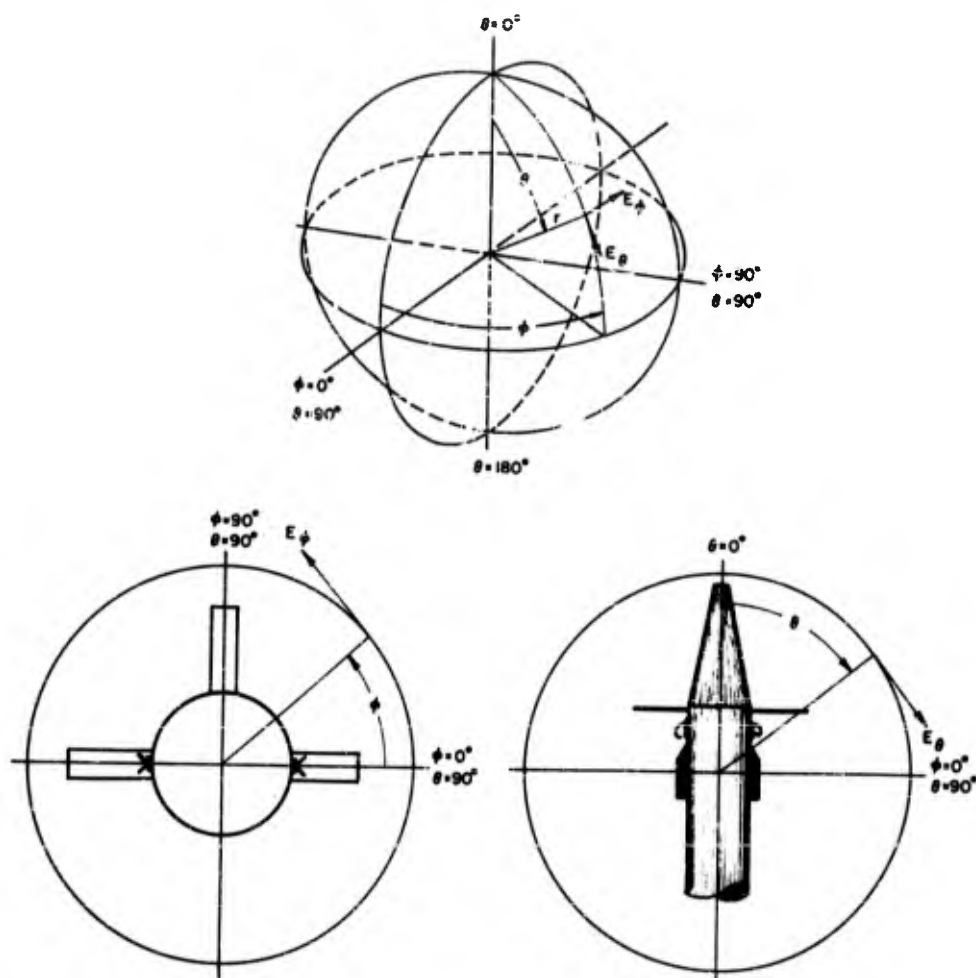


FIG. 251 - POSITION COORDINATES OF THE MODEL 2.036 ANTENNA FLAPS OPEN CONFIGURATION

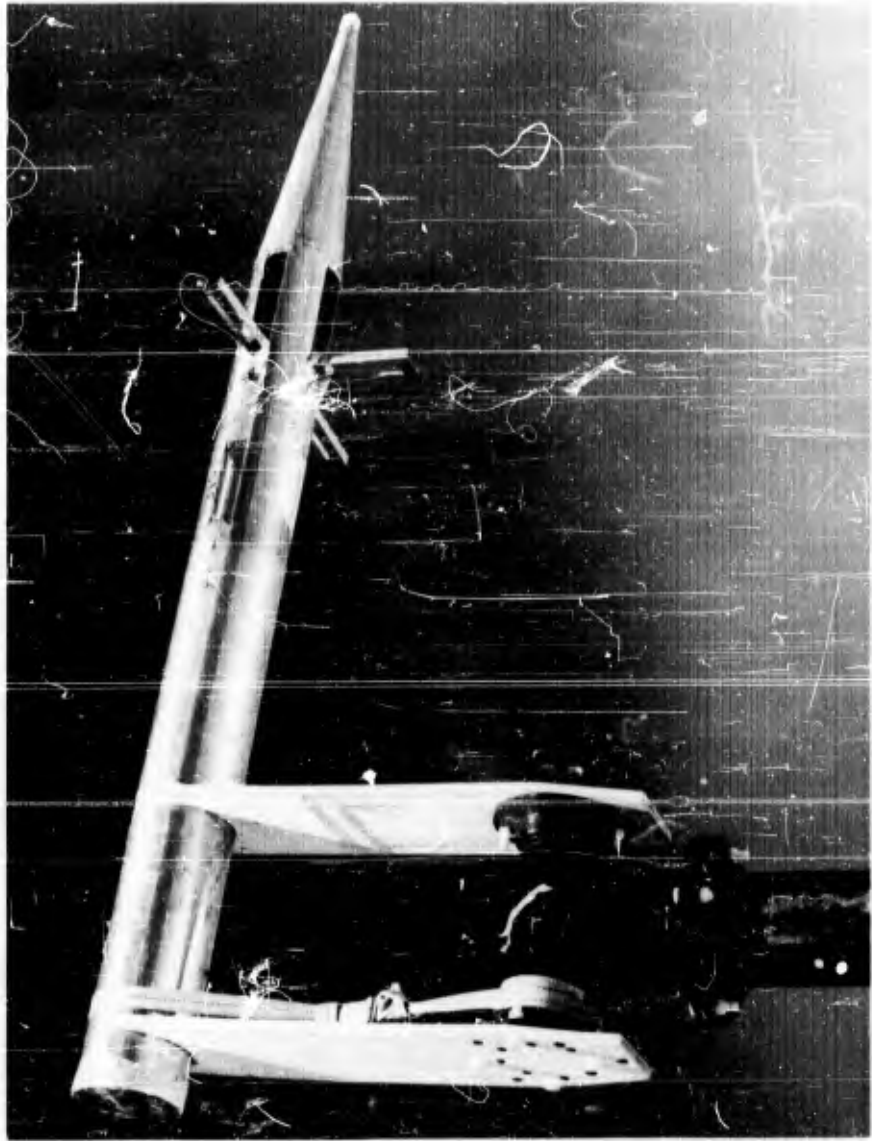


FIG. 250 - PHOTOGRAPH OF THE EXOS VEHICLE MOCKUP WITH THE FLAPS
OPEN USED FOR RADIATION PATTERN MEASUREMENTS

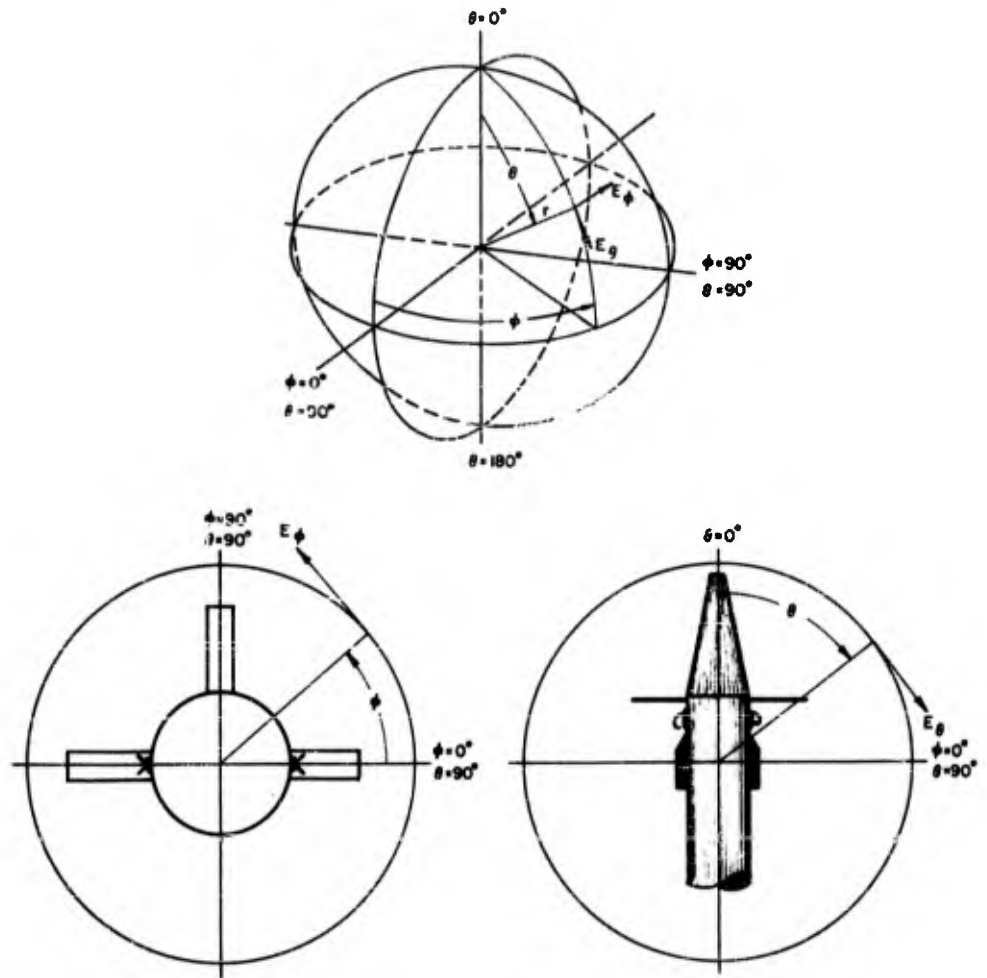


FIG. 251 - POSITION COORDINATES OF THE MODEL 2,036 ANTENNA
FLAPS OPEN CONFIGURATION

POLARIZATION

- GAIN REF - - - - -
 E_{θ} - - - - -
 E_{ϕ} - - - - -
 R.C. - - - - -
 L.C. - - - - -
 OTHER AS NOTED

$\phi = \underline{\quad}^{\circ}$ $\theta = \underline{0}^{\circ}$ COORDINATE REFERENCE

$\phi = \underline{0}^{\circ}$
 $\theta = \underline{90}^{\circ}$

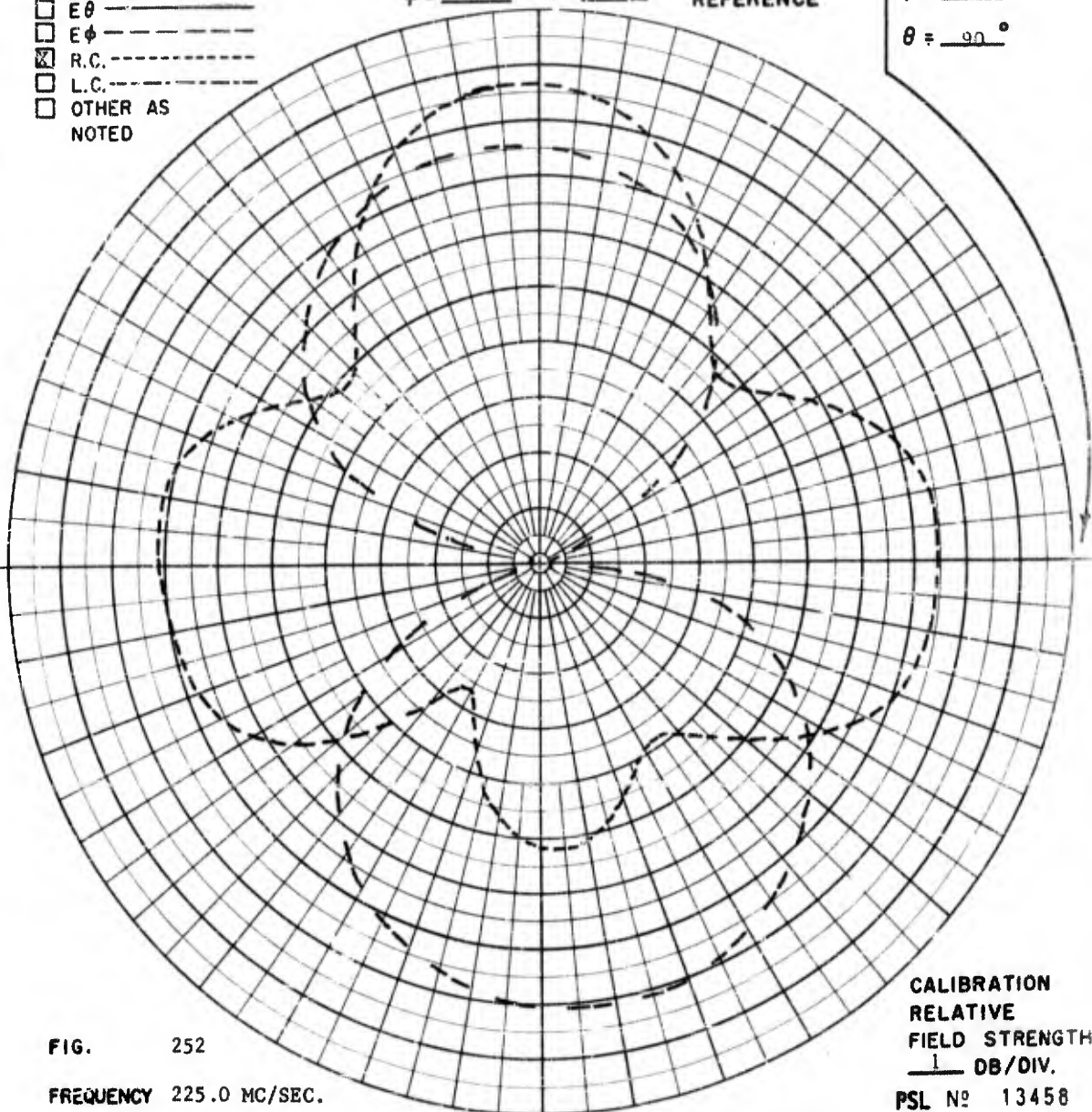


FIG. 252
 FREQUENCY 225.0 MC/SEC.

CALIBRATION
 RELATIVE
 FIELD STRENGTH
 1 DB/DIV.
 PSL No 13458

ANTENNA MODEL 2.036 TWO ELEMENT ARRAY MOUNTED ON THE EXOS MOCKUP WITH THE VEHICLE FLAPS OPEN.

REMARKS THE GAIN REFERENCE ANTENNA IS A STODDARD HALFWAVE DIPOLE ILLUMINATED BY A RIGHT CIRCULAR HELIX.

POLARIZATION

- GAIN REF - - - - -
 E θ - - - - -
 E ϕ - - - - -
 R.C. - - - - -
 L.C. - - - - -
 OTHER AS NOTED

$\phi = \underline{\quad}^\circ$ $\theta = \underline{0}^\circ$ COORDINATE REFERENCE

$\phi = \underline{0}^\circ$
 $\theta = \underline{90}^\circ$

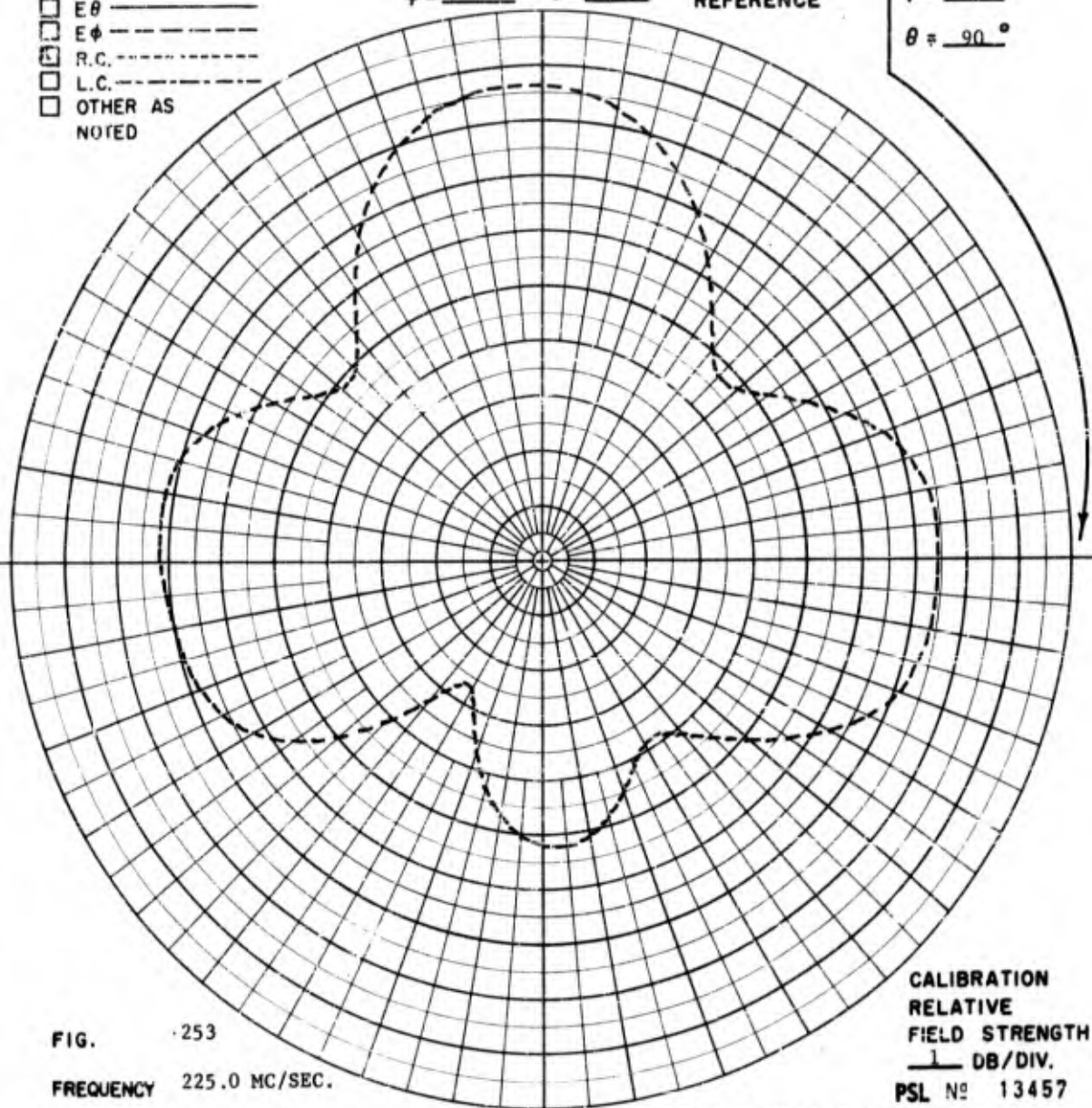


FIG. 253

FREQUENCY 225.0 MC/SEC.

ANTENNA MODEL 2.036 TWO ELEMENT ARRAY MOUNTED ON THE EXOS MOCKUP WITH THE VEHICLE FLAPS OPEN.

REMARKS AT $\theta = 180^\circ$, $\phi = 0^\circ$ THE GAIN IS -6 DB WITH RESPECT TO THE REFERENCE DIPOLE.

CALIBRATION
 RELATIVE
 FIELD STRENGTH
 1 DB/DIV.
 PSL No 13457

POLARIZATION

- GAIN REF - - - - -
- E θ - - - - -
- E ϕ - - - - -
- R.C. - - - - -
- L.C. - - - - -
- OTHER AS NOTED

$\phi = \underline{\hspace{1cm}}^\circ \quad \theta = \underline{0}^\circ$

COORDINATE REFERENCE

$\phi = \underline{90}^\circ$
 $\theta = \underline{90}^\circ$

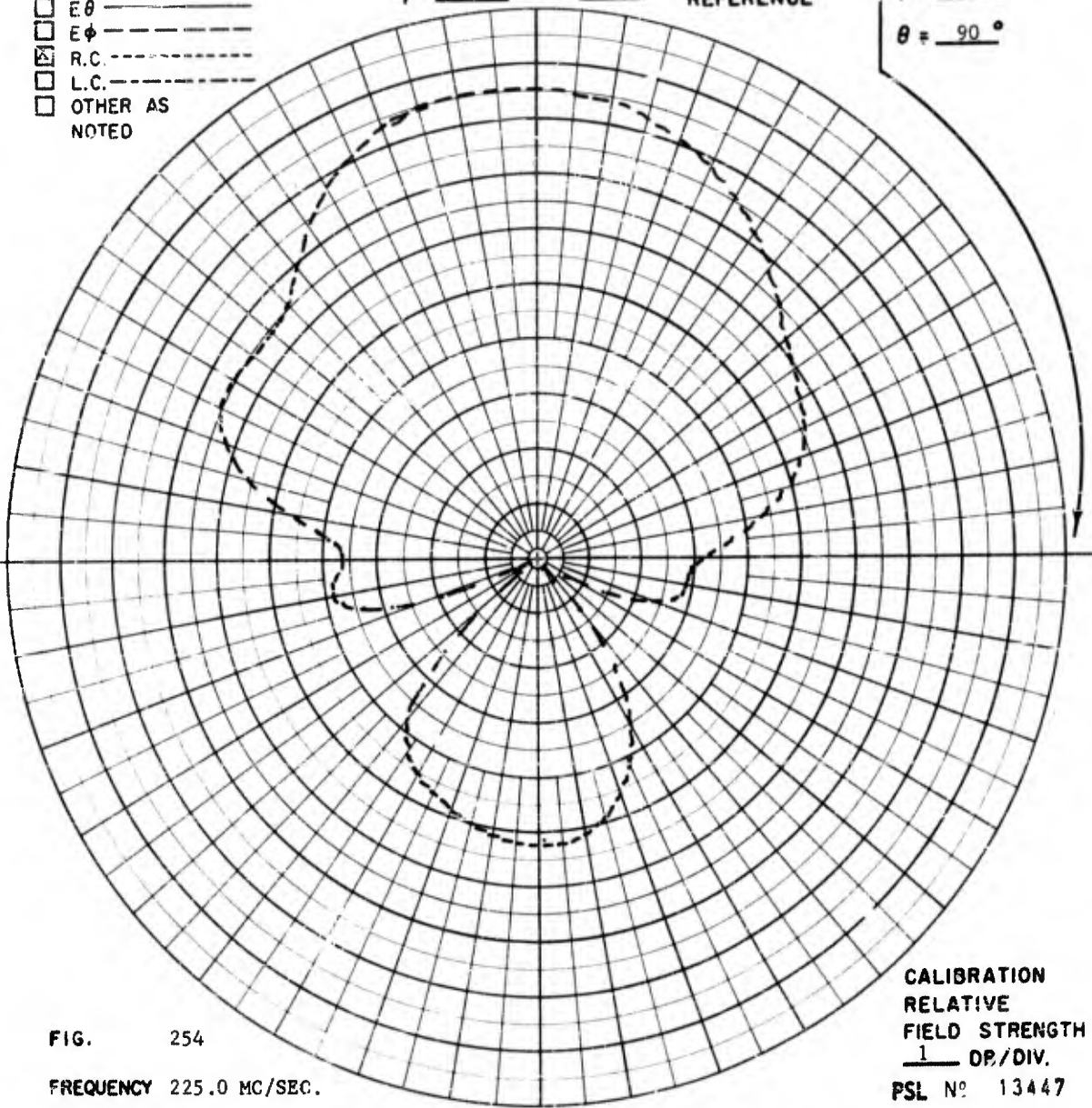


FIG. 254
 FREQUENCY 225.0 MC/SEC.
 ANTENNA MODEL 2.036 TWO ELEMENT ARRAY MOUNTED ON THE EXOS MOCKUP WITH FLAPS OPEN.
 REMARKS

CALIBRATION
 RELATIVE
 FIELD STRENGTH
1 DB/DIV.
 PSL NO 13447

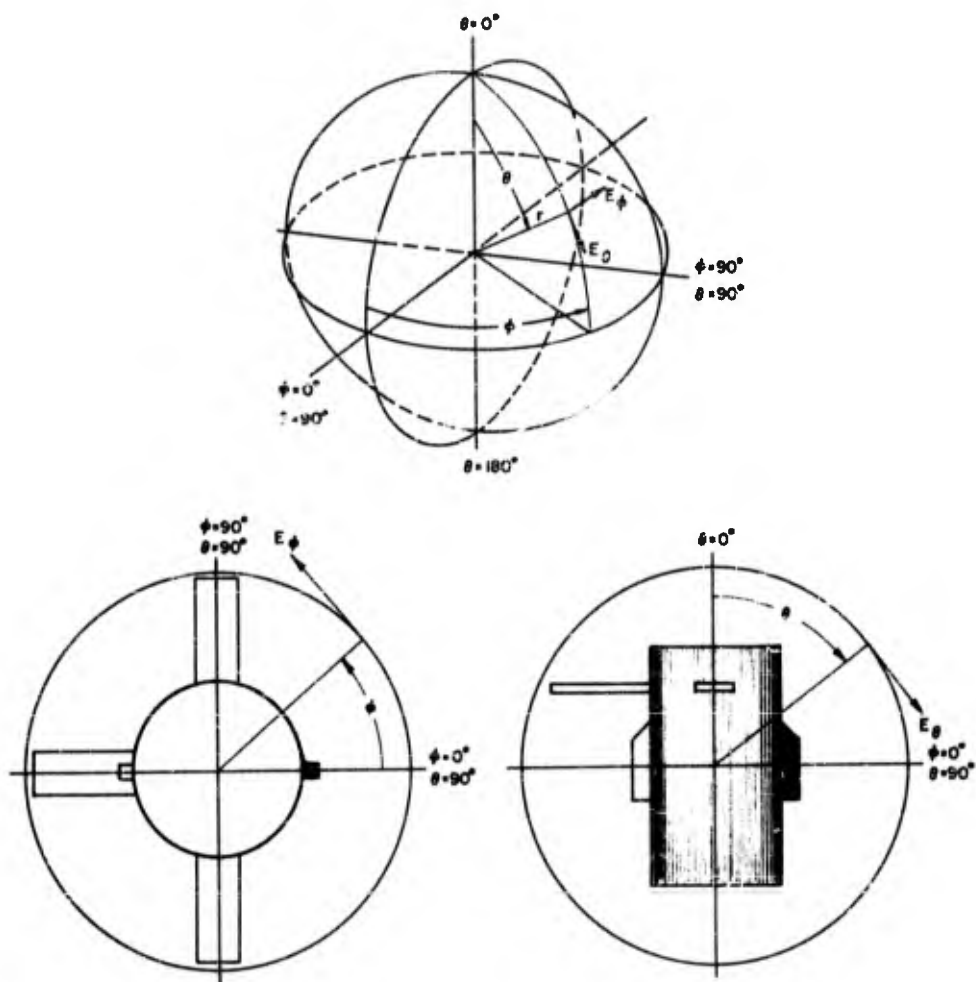


FIG. 255 - POSITION COORDINATES OF THE MODEL 2.007 ANTENNAS ON THE EXOS VEHICLE MOCKUP WITH THE FLAPS OPEN

POLARIZATION

- GAIN REF ---
 E θ ———
 E ϕ - - - -
 R.C. - - - -
 L.C. - - - -
 OTHER AS NOTED

 $\phi = \underline{\quad}^\circ$ $\theta = \underline{0}^\circ$

COORDINATE REFERENCE

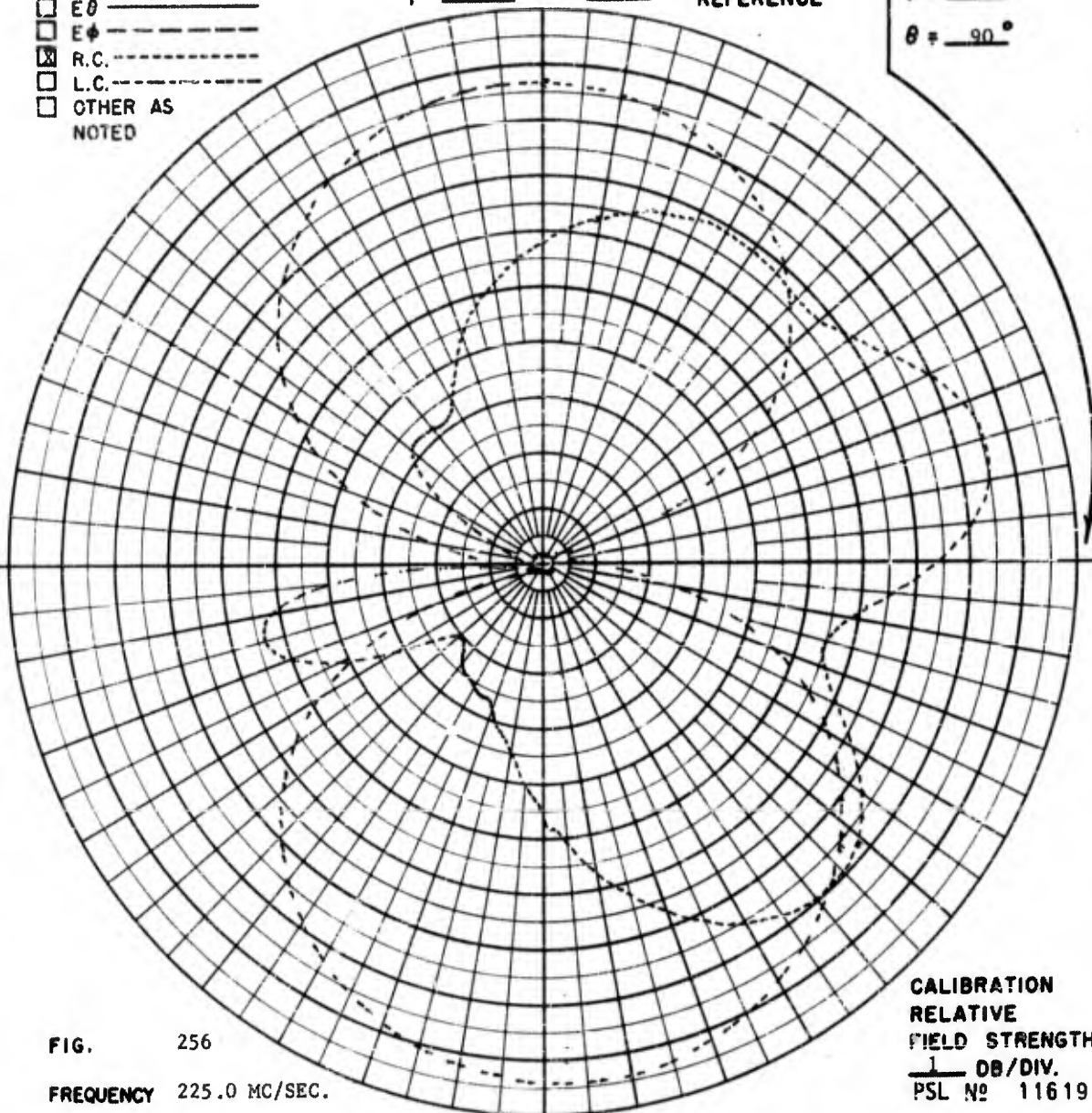
 $\phi = \underline{0}^\circ$
 $\theta = \underline{90}^\circ$


FIG. 256
 FREQUENCY 225.0 MC/SEC.

CALIBRATION
 RELATIVE
 FIELD STRENGTH
 1 DB/DIV.
 PSL No 11619

ANTENNA MODEL 2.007 UNIT RADIATOR MOUNTED ON THE EXOS MOCKUP WITH THE VEHICLE FLAPS OPEN.

REMARKS THE GAIN REFERENCE ANTENNA IS A STODDARD HALF-WAVE DIPOLE ILLUMINATED BY A RIGHT CIRCULAR HELIX.

POLARIZATION

- GAIN REF - - - - -
 E_{θ} - - - - -
 E_{ϕ} - - - - -
 R.C. - - - - -
 L.C. - - - - -
 OTHER AS NOTED

$\phi = \underline{\quad}^{\circ}$ $\theta = \underline{0}^{\circ}$ COORDINATE REFERENCE

$\phi = \underline{0}^{\circ}$
 $\theta = \underline{90}^{\circ}$

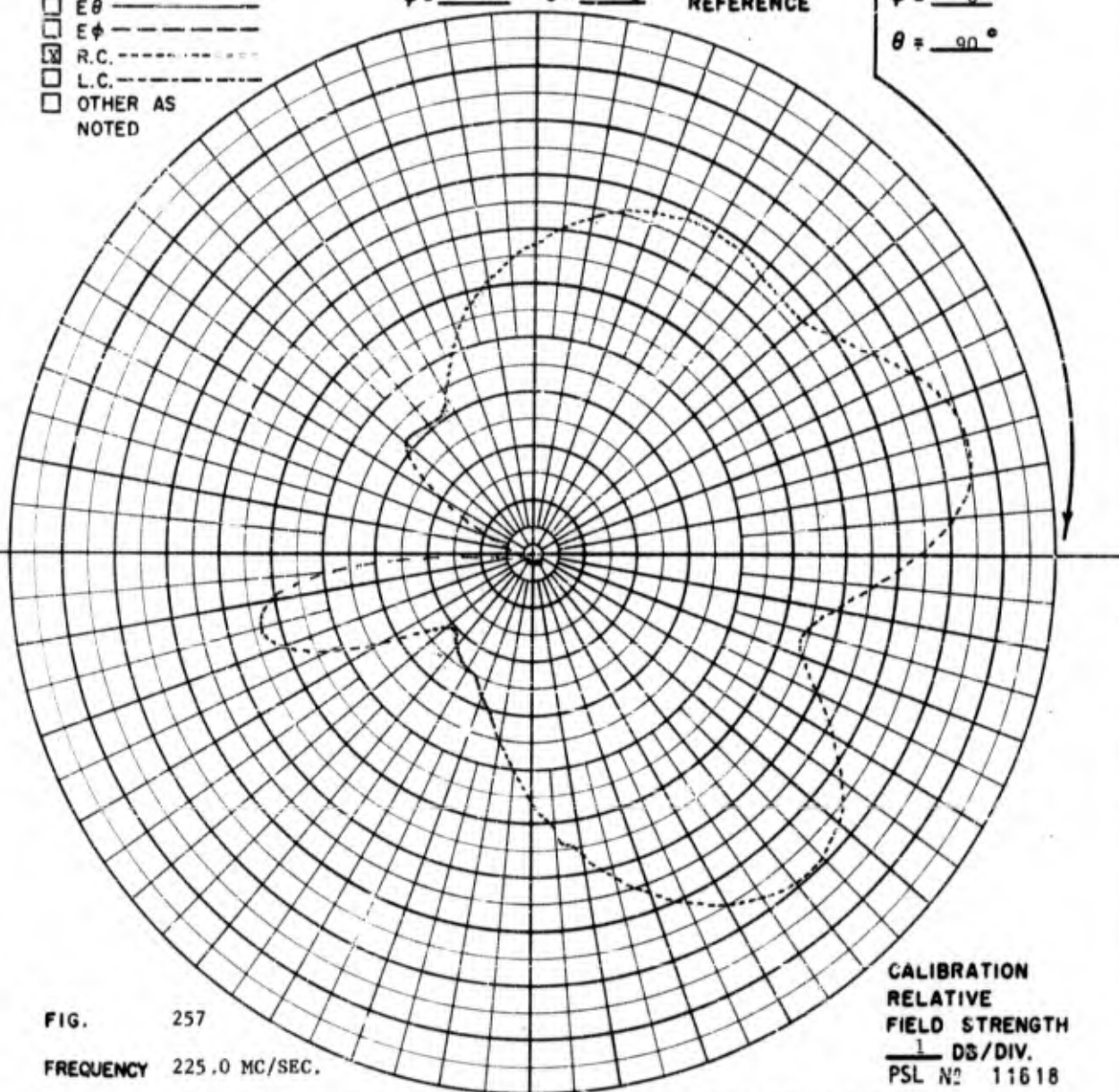


FIG. 257

FREQUENCY 225.0 MC/SEC.

ANTENNA MODEL 2.007 UNIT RADIATOR MOUNTED ON THE EXOS MOCKUP WITH THE VEHICLE FLAPS OPEN.

REMARKS At $\theta = 180^{\circ}$, $\phi = 0^{\circ}$ THE GAIN IS -10 DB WITH RESPECT TO THE REFERENCE DIPOLE.

CALIBRATION
 RELATIVE
 FIELD STRENGTH
 1 DB/DIV.
 PSL No 11618

POLARIZATION

- GAIN REF - - - -
 $E\theta$ - - - -
 $E\phi$ - - - -
 R.C. - - - -
 L.C. - - - -
 OTHER AS NOTED

$\phi = \underline{\hspace{1cm}}^\circ$ $\theta = \underline{0}^\circ$

COORDINATE
REFERENCE

$\phi = \underline{90}^\circ$
 $\theta = \underline{90}^\circ$

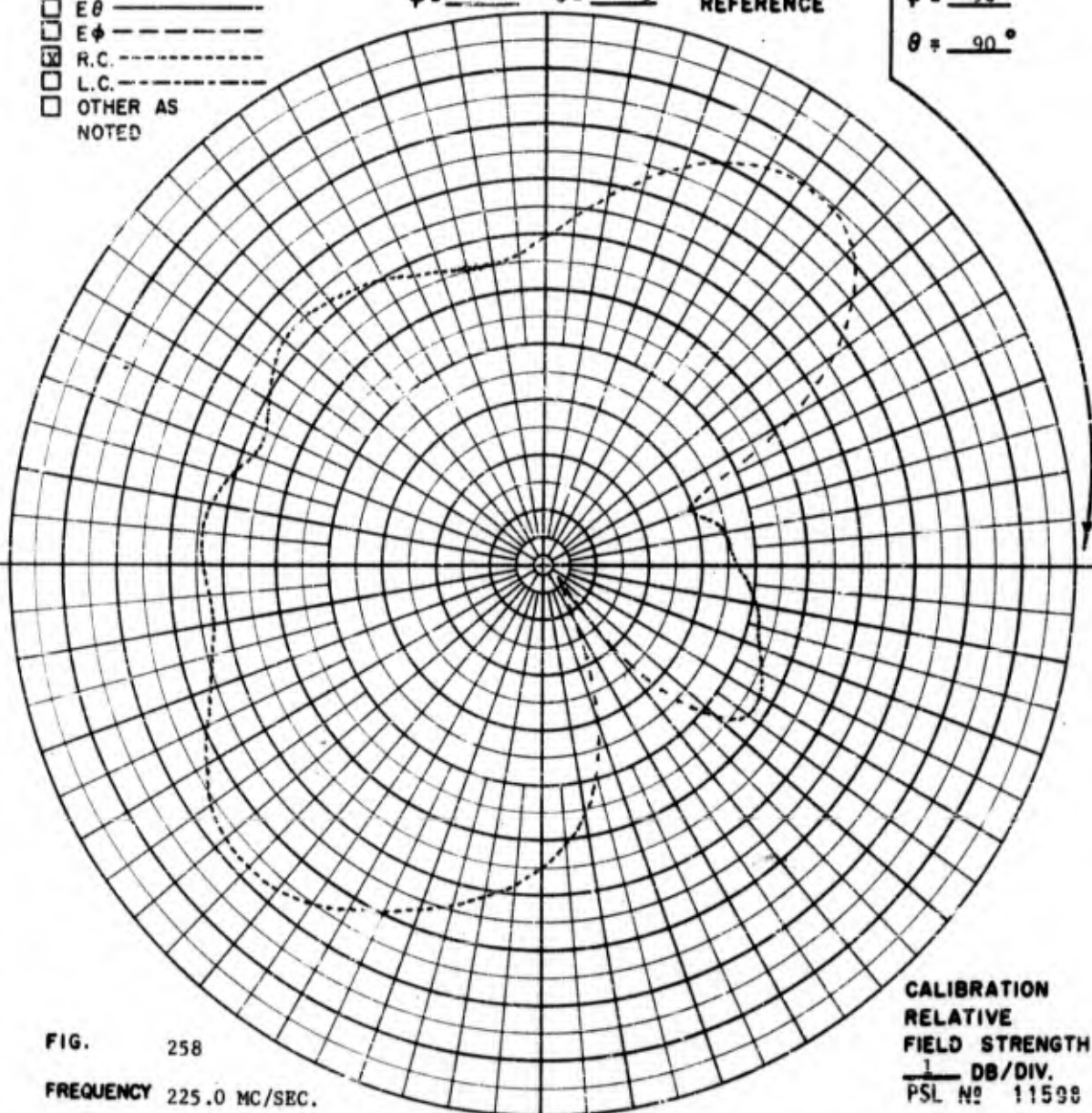


FIG. 258
 FREQUENCY 225.0 MC/SEC.

CALIBRATION
 RELATIVE
 FIELD STRENGTH
 1 DB/DIV.
 PSL No 11598

ANTENNA MODEL 2.007 UNIT RADIATOR MOUNTED ON THE EXOS MOCKUP WITH VEHICLE FLAPS OPEN.

REMARKS

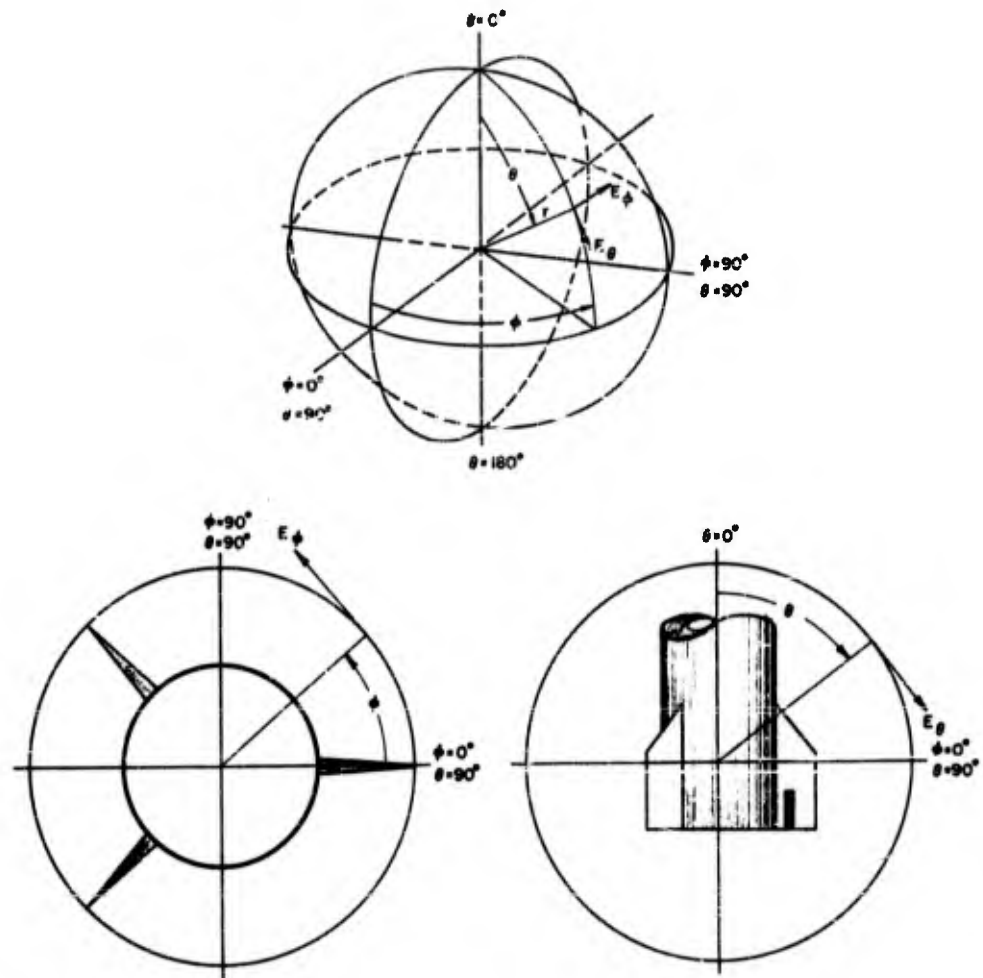


FIG. 259 - POSITION COORDINATES OF THE COMMAND CONTROL FIN NOTCH ANTENNA ON THE AEROBEE 150 MOCKUP FOR PATTERN MEASUREMENTS

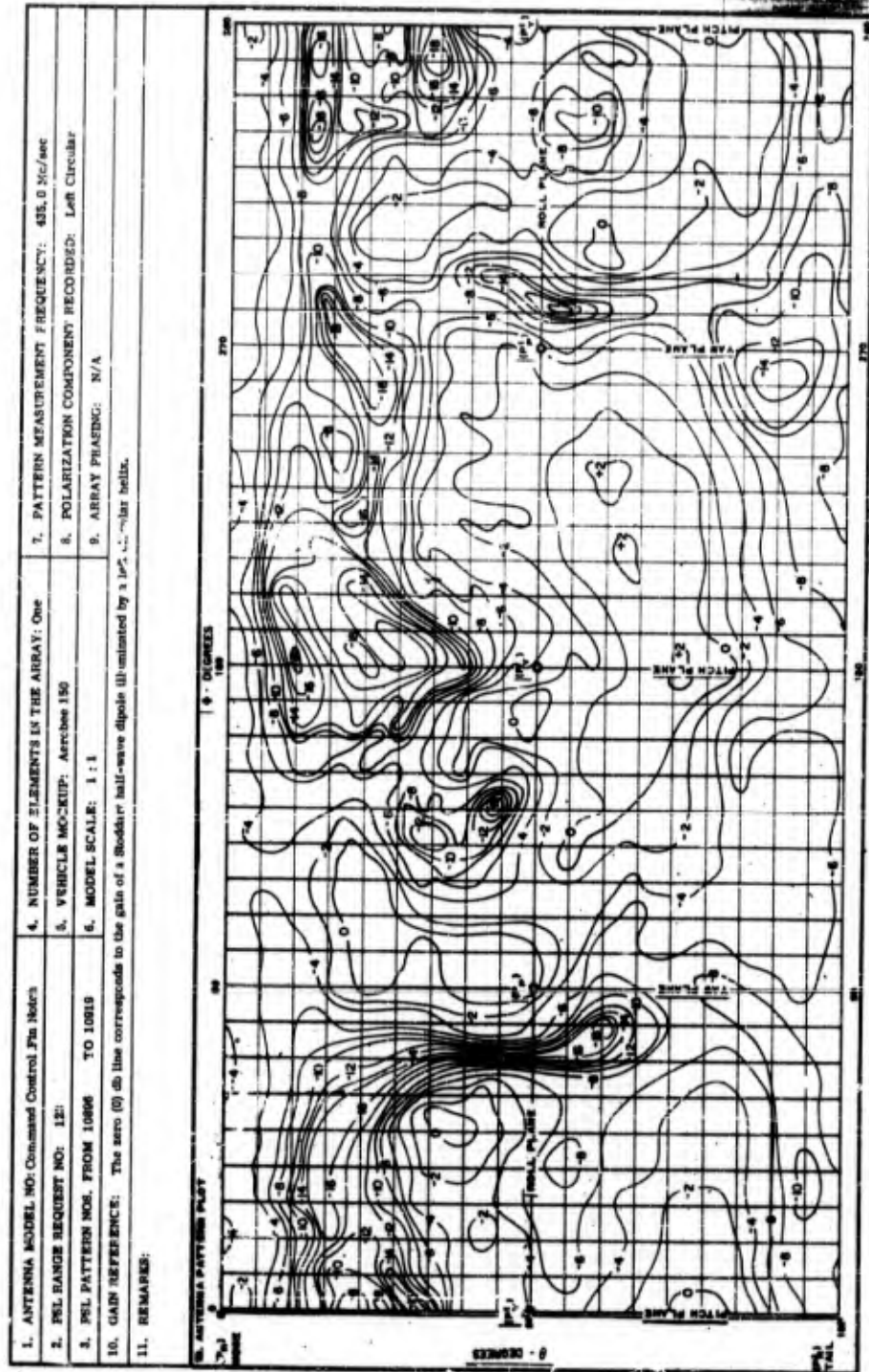
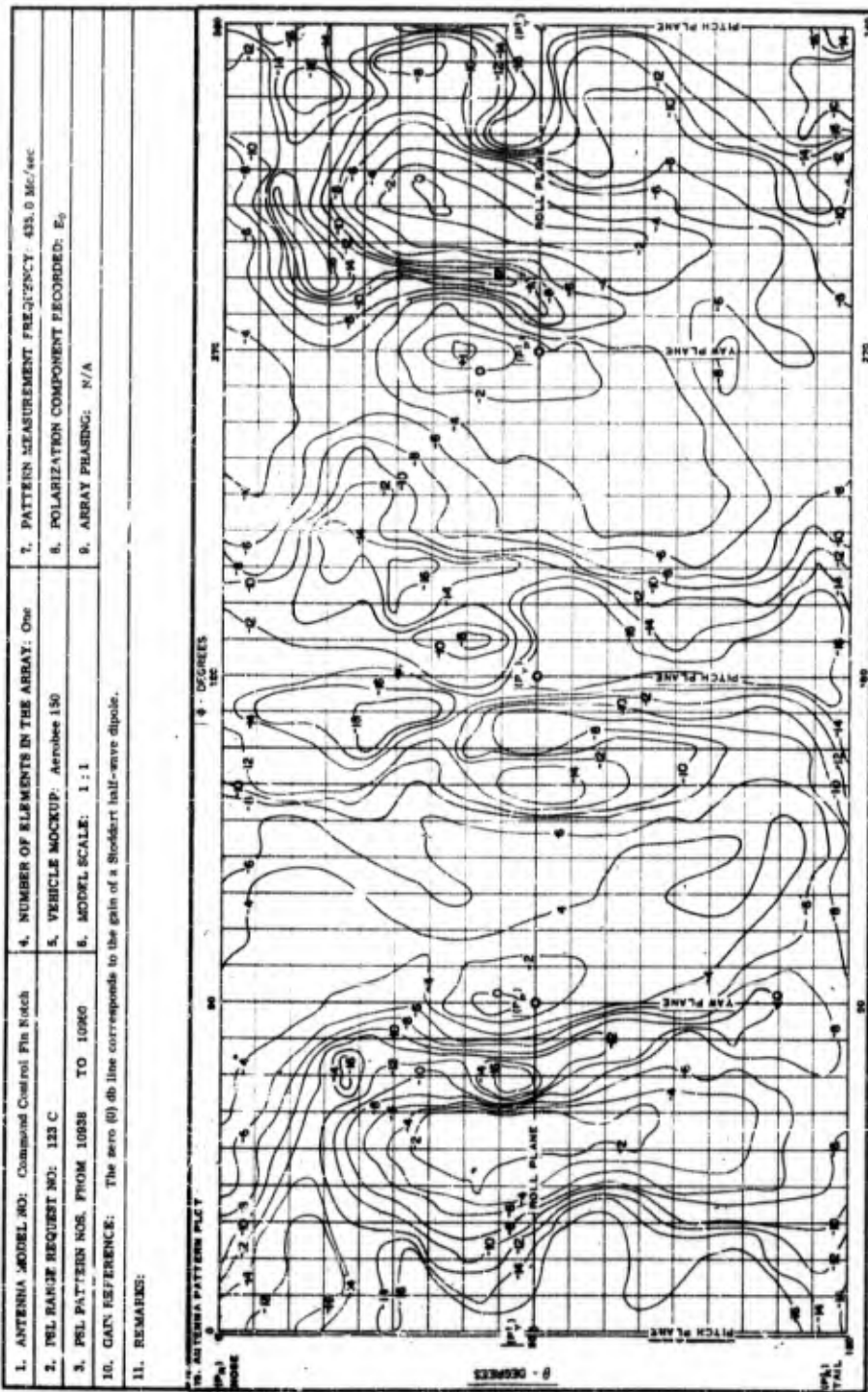


FIG. 260 - POWER CONTOUR PLOT OF THE COMMAND CONTROL FIN NOTCH ANTENNA FOR THE LEFT CIRCULAR COMPONENT, AT 435.0 MC/SEC



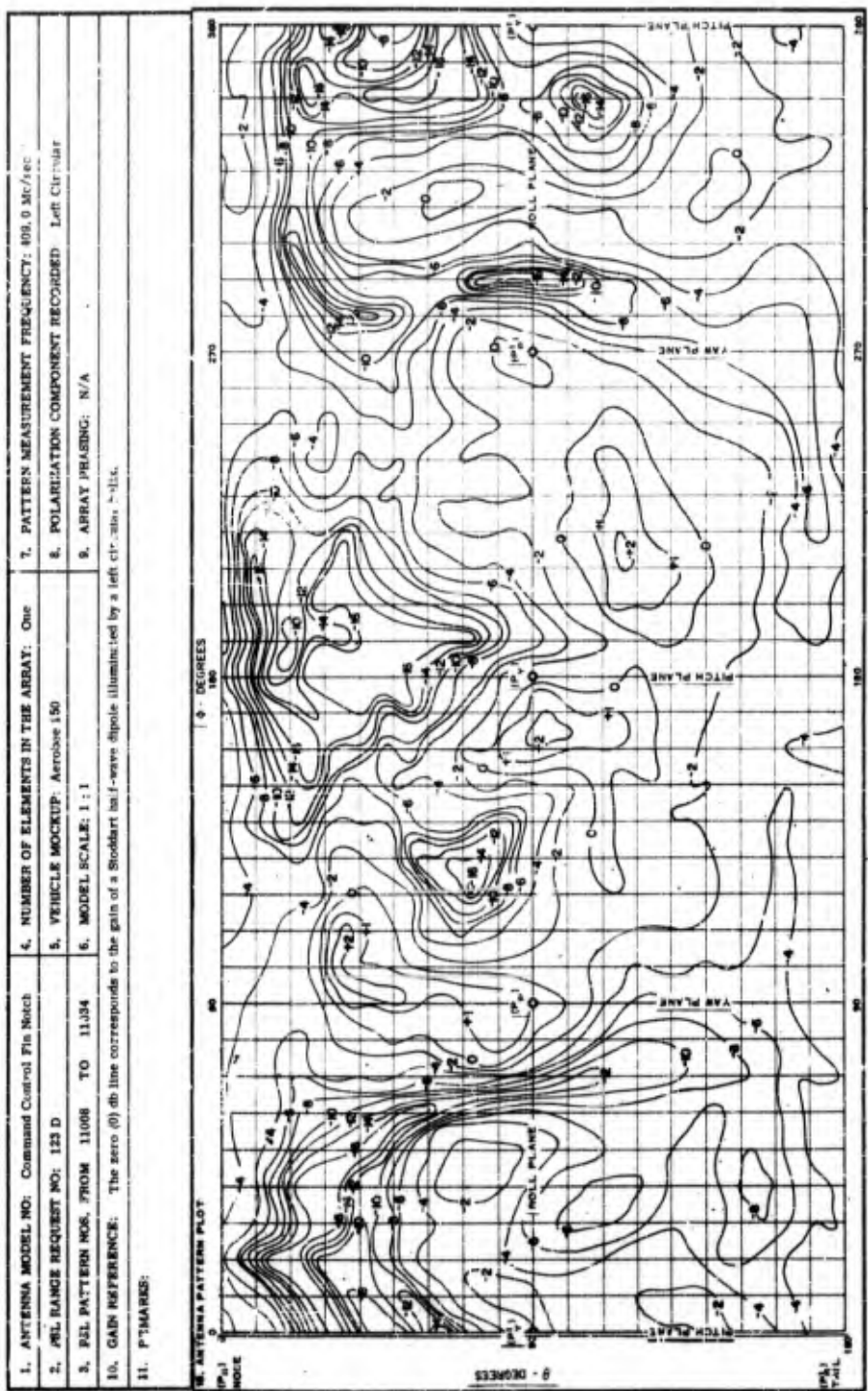


FIG. 263 - POWER CONTOUR PLOT OF THE COMMAND CONTROL FIN NOTCH ANTENNA FOR THE LEFT CIRCULAR COMPONENT AT 409.0 MC/SEC

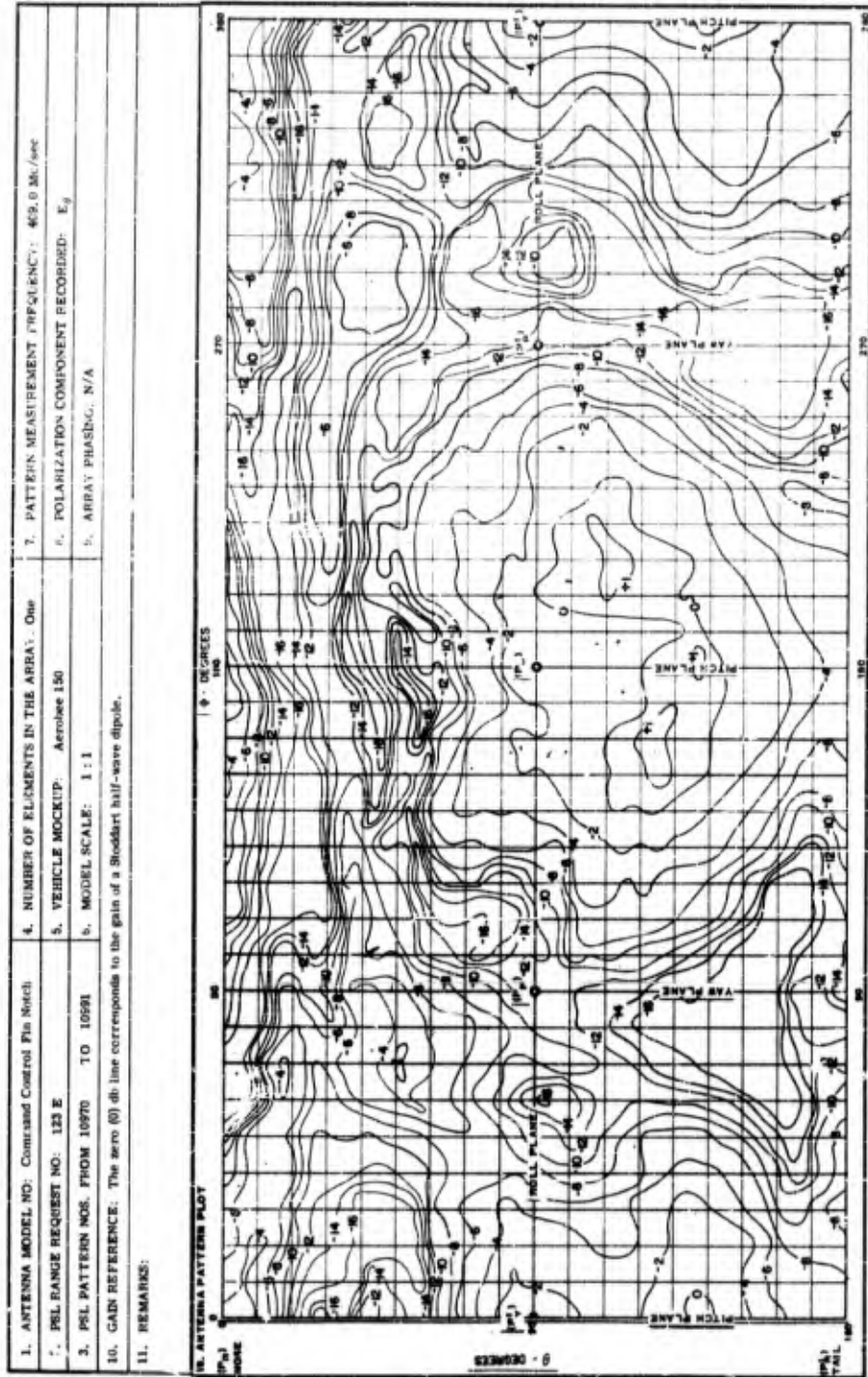


FIG. 264 - POWER CONTOUR PLOT OF THE COMMAND CONTROL FIN NOTCH ANTENNA
FOR THE E_{θ} COMPONENT AT 409.0 MC/SEC

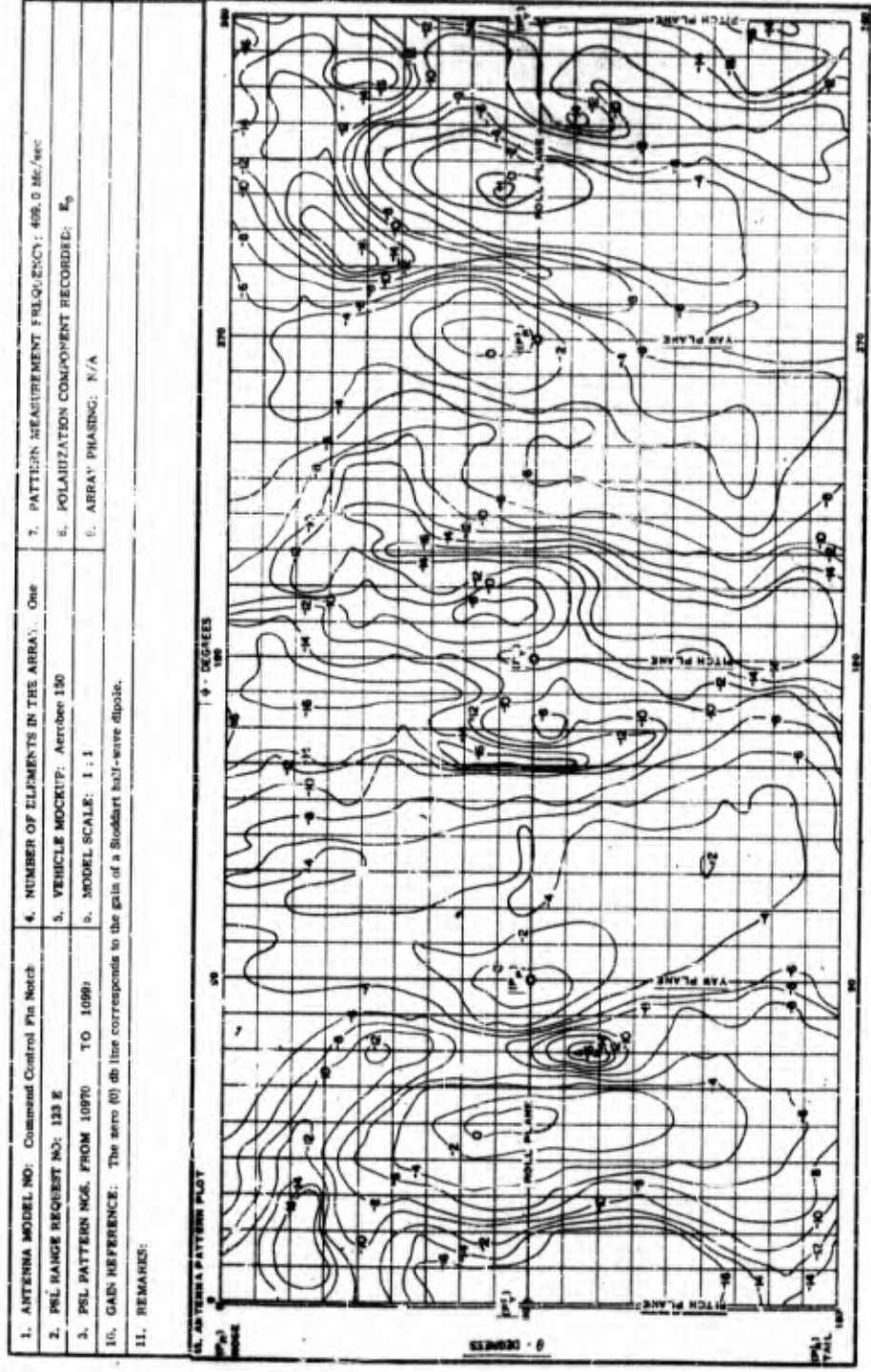


FIG. 265 - POWER CONTOUR PLOT OF THE COMMAND CONTROL FIN NOTCH ANTENNA FOR THE E_0 COMPONENT AT 409.0 MC/SEC

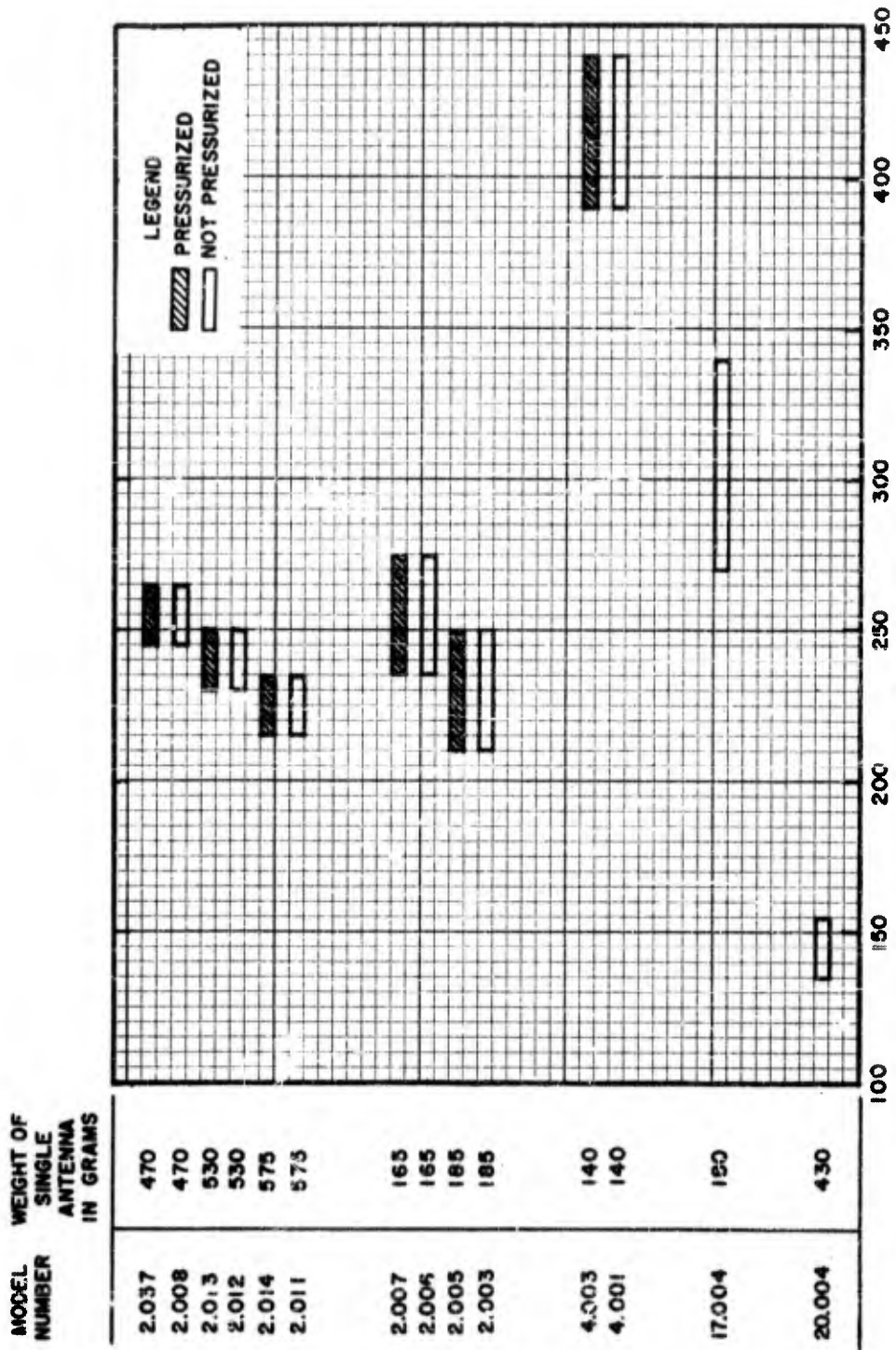


FIG. 266 - GRAPH SHOWING THE TUNING RANGE, THE WEIGHT AND THE TYPE OF SEAL FOR THE STANDARD ANTENNAS IN THE 135-440 MC/SEC FREQUENCY RANGE

APPENDIX I

ANTENNA REFERENCE INDEX TO THE QUARTERLY PROGRESS REPORTS

Quadraloop Telemetry Antennas, 1.5-Inches High

<u>MODEL</u>	<u>REPORT</u>	<u>DATE</u>	<u>SECTION</u>
II-short	3*	1960	1.0
	1	1961	2.7.1(a)
II-A (2.037)	1	1961	2.7.1(b)
II-B	1	1961	2.7.1(c)
II-C	1	1961	2.7.1(d)
II-D	1	1961	2.7.1(e)
II-E	1	1961	2.7.1(f)
2.002	1	1961	2.7.1(g)
	2	1961	2.2
2.011	8	1962	2.6
2.014	8	1962	2.6
2.013	4	1961	2.4

Quadraloop Telemetry Antennas, 1.0-Inch High

A-2	1	1961	2.4
	1	1961	2.7.2(a)
A-3	1	1961	2.7.2(b)
2.001	1	1961	2.7.2(b)
2.003	2	1961	2.1
	3	1961	2.1
	4	1961	2.2
2.004	2	1961	2.1
	3	1961	2.1
	4	1961	2.2

Note: Report 3, 1960 covers the period from 1 July 1960 through 30 September 1960. Report 3*, 1960 covers the period from 1 October 1960 through 31 December 1960.

Quadraloop Telemetry Antennas, 1.0-Inch High
(Continued)

<u>MODEL</u>	<u>REPORT</u>	<u>DATE</u>	<u>SECTION</u>
2.005	3	1961	2.1
	4	1961	2.2
	9	1963	2.5
2.009	4	1961	2.2
2.025	6	1962	2.5
	8	1962	2.1
	9	1963	2.1
2.032	8	1962	2.5
2.035	9	1963	2.3

Quadraloop Telemetry Antennas, 0.5-Inch High

2.019	4	1961	2.3
	5	1962	2.3
2.026	5	1962	2.3
2.030	6	1962	2.2
	7	1962	2.1
2.031	7	1962	2.1

Quadraloop Telemetry Antennas, Flush Mounted

III-B-1	1	1961	2.7.3(a)
III-C	3	1960	1.0
	1	1961	2.7.3(b)
III-D	3	1960	2.0
	1	1961	2.7.3(c)
III-F	1	1961	2.5
	2	1961	3.0
	4	1961	2.5
	5	1962	3.0
	6	1962	2.3
	7	1962	2.2

Quadraloop Telemetry Antennas, Flush Mounted
(Continued)

<u>MODEL</u>	<u>REPORT</u>	<u>DATE</u>	<u>SECTION</u>
III-G	1	1961	2.7.3(d)

Quadraloop Command Control Antennas

IV	1	1961	2.7.4(a)
IV	3*	1960	2.0
	1	1961	2.7.4(f)
4.001	1	1961	2.7.4(c)

Quadraloop Telemetry Antennas, Semiflush Mounted

V-B	1	1960	1.0
V-C	1	1960	3.0
	2	1960	1.0
	3*	1960	3.0
V-F	2	1960	1.0
V-G	1	1961	2.7.3(e)

Quadraloop Beacon Antennas, S-Band

IA3b	1	1961	2.6
	2	1961	4.0
6.007	6	1962	2.4
	7	1962.	2.3
6.011	9	1963	2.5

C-Band Beacon Antennas

7.001	2	1961	5.0
	3	1961	2.2
	4	1961	2.1
	5	1962	2.1
7.002	5	1962	2.2

C-Band Beacon Antennas
(Continued)

<u>MODEL</u>	<u>REPORT</u>	<u>DATE</u>	<u>SECTION</u>
7.004	6	1962	2.1
7.007	9	1963	2.3
7.008	9	1963	2.5
Circumferential Quadraloop DOVAP Antenna			
10.004	8	1962	2.5
10.005	8	1962	2.5
10.006	8	1962	2.5
Gap Fed Oblique Stub Telemetry Antennas			
23.005	9	1963	2.4
23.006	8	1962	2.2
	9	1963	2.2
Quadraloop Telemetry Antenna, Light Weight			
24.001	8	1962	2.1
	9	1963	2.1

APPENDIX II
VEHICLE REFERENCE INDEX TO THE QUARTERLY PROGRESS REPORTS

<u>VEHICLE</u>	<u>REPORT</u>	<u>DATE</u>	<u>SECTION</u>
AEROBEE 150	1	1961	2.6
	2	1961	4.0
	4	1961	2.4
	6	1962	2.4
	7	1962	2.3
AO-10	6	1962	2.5
AP/3	6	1962	2.5
	8	1962	2.1
	8	1962	2.1
	9	1963	2.1
	9	1963	2.1
AP/5	6	1962	2.5
	8	1962	2.2
	9	1963	2.2
ASP	3	1960	2.0
ASTROBEE 200	3*	1960	1.0
	2	1961	2.2
	2	1961	5.0
ASTROBEE 500	1	1960	3.0
	2	1960	3.0
	3*	1960	2.0
ASTROBEE 1500	2	1961	2.1
BLACK BRANT II-A	2	1961	2.1
CAJUN	4	1961	2.3
	5	1962	2.3
	5	1962	2.3
	6	1962	2.2
	6	1962	2.2
	7	1962	2.1
	7	1962	2.1
	8	1962	2.4
	9	1963	2.4

<u>VEHICLE</u>	<u>REPORT</u>	<u>DATE</u>	<u>SECTION</u>
EXOS	3*	1960	3.0
	1	1961	2.5
	2	1961	3.0
	4	1961	2.5
	5	1962	3.0
	6	1962	2.3
	7	1962	2.2
	8	1962	2.3
	9	1963	2.3
	9	1963	2.3
JAVELIN	8	1962	2.5
	8	1962	2.5
	8	1962	2.5
	8	1962	2.5
	9	1963	2.5
	9	1963	2.5
	9	1963	2.5

Note: Report 3, 1960 covers the period from 1 July 1960 through 30 September 1960. Report 3*, 1960 covers the period from 1 October 1960 through 31 December 1960.

APPENDIX III
ANTENNA MODEL LISTINGS

Model	PSL Assembly or Mounting Drawing	PSL Photo Number	Tuning or operating range in Mc/sec	Weight in gm
II-short *	1152-3	2979		615
II-short	1250-3			
II-short	1251-3			
II-short	1252-3			
II-short	1253-3			
II-short	1254-3			
II-short	1255-3			
II-A (2.037)	003950		244-264	470
II-B	1258-3		228-248	
II-C	1410-4		215-227	
II-D	1315-3			
II-E	1280-3		222-242	550
2.002	1325-3			
2.008 *	004223	4465	244-264	470
2.010	003962	4467	224-244	540
2.011	003965	5594	215-235	575
2.012 *	004145	5352	228-248	530
2.013 *	004346	5880	228-248	530
2.014	004316	5315	215-235	575
2.018	1512-3		228-248	

* Starred antennas are not discussed in the quarterly progress reports.

Model	PSL Assembly or Mounting Drawing	PSL Photo Number	Tuning or operating range in Mc/sec	Weight in gm
A-2		4034		275
A-3	1311-4			
2.001	1342-4	4175		
2.003	004232		210-250	185
2.004	1364-4			
2.005	004233		210-250	185
2.006 *	004330	5767	235-275	165
2.007 *	004327	5314	235-275	165
2.009	1451-4			
2.023	1606-4			
2.025	004483	4735		
2.032	004230	5141		220
2.035				
2.036 *	004591	5821		815
2.019	1737-4	4694		110
2.026	1687-3	4748		160
2.030	1792-4			
2.031	1825-4	5069		135
III-B *	1030-3	3189		
III-B-1	1031-3			
III-C	1046-3	3476		465

Model	PSL Assembly or Mounting Drawing	PSL Photo Number	Tuning or operating range in Mc/sec	Weight in gm
III-D	1137-3	3558		
III-F	1746-3	4893		
III-G	1194-3			
3.001*	1523-3	4838		290
IV	750-3	2839		
IV-B	1079-4			
4.001	004222	5910	390-440	140
4.002*	1179-4	4889	390-418	150
4.003*	004575	5909	390-440	140
V	747-3	3145		840
V-B		3257		
V-C	1042-3	3536		
V-F		3442		
V-G	1062-3			
IA7b	994-3	4177		55
IIB7b	994-3			
6.005*	1620-4	5825	2750-2950	34
6.006	1643-4	4646		65
6.007	1751-4	4963		40
6.010*	003881	5260		145
6.011	004350	5915		36

Model	PSL Assembly or Mounting Drawing	PSL Photo Number	Tuning or operating range in Mc/sec	Weight in gm
7.001	1322-2	4900		31
7.002	1577-3	4765		21
7.003*	1573-2			
7.004	004480	4767	5650-5800	56
7.005*	004373		5650-580	56
7.007	004303			
7.008	004775	5597		
7.009*	004921	5798		
10.023 *	004964			
10.004		5051		
10.005		5181		
10.006		5183		
10.009*		5656		
10.013*		5654		
10.014*		5654		
10.016*		5656		
10.023 *	004564			
17.004 *	1664-4	4714	267-340	180
20.004 *	004499	5921	135-155	430
23.005	003973	5916		355
23.006	004077	5967		30
23.007 *				
24.001	SK 4207	5540	103-250	

APPENDIX IV
"STANDARD" ANTENNA MODELS

Model	PSL Assembly or Mounting Drawing	PSL Photo Number	Tuning or operating range in Mc/sec	Single Antenna Weight in gm	Seal
2.037	003950	5968	244-264	470	P.
2.008	004223	4465	244-264	470	N. P.
2.013	004346	5880	228-248	530	P.
2.012	004345	5352	228-248	530	N. P.
2.014	004316	5315	215-235	575	P.
2.011	003965	5594	215-235	575	N. P.
2.007	004327	5314	235-275	165	P.
2.006	004330	5767	235-275	165	N. P.
2.005	004233	4333	210-250	185	P.
2.003	004232	5996	210-250	185	N. P.
4.001	004222	5910	390-440	140	N. P.
4.003	004575	5909	390-440	140	P.
6.005	1620-4	5825	2750-2950	34	P.
7.004	004480	4767	5650-5800	56	N. P.
7.005	004373	4767	5650-5800	56	P.
17.004	1664-4	4714	267-340	180	N. P.

APPENDIX V
LIST OF ANTENNA SHIPMENTS

Model	Number of Antenna Units Shipped
II-short	14 pr.
2.002	2 pr.
2.010	4 pr.
A-3	1 pr.
2.003	2 pr.
2.004	1 pr.
2.005	16 pr.
2.009	4 pr.
2.023	2 pr.
2.025	2 pr.
2.019	1 ea.
2.026	7 pr.
III-C	1 pr.
III-F	3 pr.
IV	1 pr.
IV	1 pr.
V	1 pr.
V-B	1 pr.
V-C	12 pr.
IA3b	19 pr.
IIB3b	1 pr.
6.006	1 pr.

Model	Number of Antenna Units Shipped
7.001	11 pr.
7.004	14 pr.
20.004	8 ea.
23.006	1 ea.
Telemetry Notch	42 ea.
Command Control Notch	50 ea.

APPENDIX VI
ANTENNA INFORMATION WORK SHEET

Edition No. _____ Date _____

Supersedes Editions Prior To _____

Project Identification: _____
_____**Antenna Information Work Sheet****PSL/NMSU Electromagnetics Group**

The purpose of these work sheets is to provide this laboratory and associated agencies with a functional interchange of information and design requirements. It is also valuable if both parties at telephone terminals have a common reference form. These work sheets will be updated as often as necessary and all concerned are cordially invited to submit addenda for maximum effectiveness.

1.0 GENERAL INFORMATION**1.1 Contracting Agency****1.2 Project Name****1.3 Contract No.****1.4 Shipping Address****1.5 Number of Antennas Required****1.6 Time Schedule****1.6.1****1.6.2****1.6.3****1.7 Names and Phone Numbers of Personnel Cognizant of Project****Please include Area Code, exchange and extension number.****1.7.1 Scientific Officer _____****1.7.2****1.7.3**

1.8 Address

Physical Science Laboratory
New Mexico State University
University Park, New Mexico
P. O. Box 548

Attn: _____, Project Engineer

Telephone: 505-524-2851

PSL Project Engineer Extension No. : _____

1.9 Special Shipping Instructions

Urgent air shipments for immediate pickup, ship to El Paso, Texas, per address in paragraph 1.8. Mark: 'Notify Purchasing Agent,' collect telephone call 505-524-2851.

2.0 THE VEHICLE AND ANTENNA MOUNTING

2.1 Vehicle Designation

2.2 Vehicle Drawings

Make dimensioned outline drawings of the various changes in vehicle configuration during the period when the antenna is in operation. Since the antenna can generally be tuned to optimum for one configuration only, indicate the preferred one. State the configurations for which pattern and/or impedance measurements are required.

Show on the drawing which parts of the vehicle are metal and which are dielectric. Indicate the locations at which the antennas may be mounted and show the preferred position. Give the vehicle skin thickness at the various antenna locations. Indicate the available space inside the vehicle.

2.3 Temperature and/or Velocity Profile

2.4 Vehicle Trajectory Relative to Launch Site

2.5 Vehicle Trajectory Relative to Pertinent Antennas

2.6 Vehicle Spin Rate

2.7 Pressurization Requirements

Unpressurized

Vacuum Seal

2.8 Maximum Allowable Drag Profile for the Antenna

3.0 VEHICLE INSTRUMENTATION

3.1 The Transmitter

- 3.1.1 Model
- 3.1.2 Operating Frequency
- 3.1.3 Power Output
- 3.1.4 Modulation
- 3.1.5 Bandwidth Requirement
- 3.1.6 Allowable Mismatch
 - (a) Continuous
 - (b) Intermittent

3.2 The Receiver

- 3.2.1 Model
- 3.2.2 Operating Frequency
- 3.2.3 Sensitivity

3.3 The Transponder

- 3.3.1 Model
- 3.3.2 Transmit Frequency
- 3.3.3 Transmit Power

- 3.3.4 Transmit Modulation
- 3.3.5 Bandwidth Requirement
- 3.3.6 Allowable Mismatch
 - (a) Continuous
 - (b) Intermittent
- 3.3.7 Receive Frequency
- 3.3.8 Receive Sensitivity
- 3.3.9 Isolation Requirements

4.0 GROUND INSTRUMENTATION

4.1 Location of Launch Site

4.2 Receiving System

4.2.1 Antenna Model

4.2.2 Polarization

4.2.3 Antenna Measured Gain (not directivity)

4.2.4 Sensitivity

4.3 Transmitting System

4.3.1 Antenna Model

4.3.2 Polarization

4.3.3 Antenna Measured Gain (not directivity)

4.3.4 Transmitted Power

4.4 Radar System

4.4.1 Antenna Model or Designation

4.4.2 Polarization

4.4.3 Antenna Measured Gain (not directivity)

4.4.4 Transmitted Power

4.4.5 Receiver Sensitivity in dbm

4.4.6 Pulse Repetition Rate

4.4.7 Memory Time

4.4.8 Nutation or Scan Rate

4.4.9 Ground Antenna Servo Resonant Frequency (to be considered with antenna lobes and spin rate of vehicle).

5.0 THE ANTENNA PATTERN

5.1 Antenna Position in the Coordinate System

On pages 10 through 12 are standard coordinate systems. The coordinate system is fixed with respect to the vehicle. Show an outline of the vehicle in the coordinate system and superimpose the desired radiation pattern. It is general practice to locate the nose of a missile $\theta = 0^\circ$ and one of the antennas at $\phi = 0^\circ$. For a nose spike or similar ϕ symmetric antennas some other reference point may be chosen.

5.2 Aspect Data

Include curves showing the aspect angles as a function of vehicle distance from the ground station for the various ground stations.

5.3 Indicate What ϕ Cut Increments are Desired: Degrees

5.4 Check Desired Polarization

5.4.1 E_θ

5.4.2 E_ϕ

5.4.3 Right Circular

5.4.4 Left Circular

5.5 Power Contour Plot Is Required

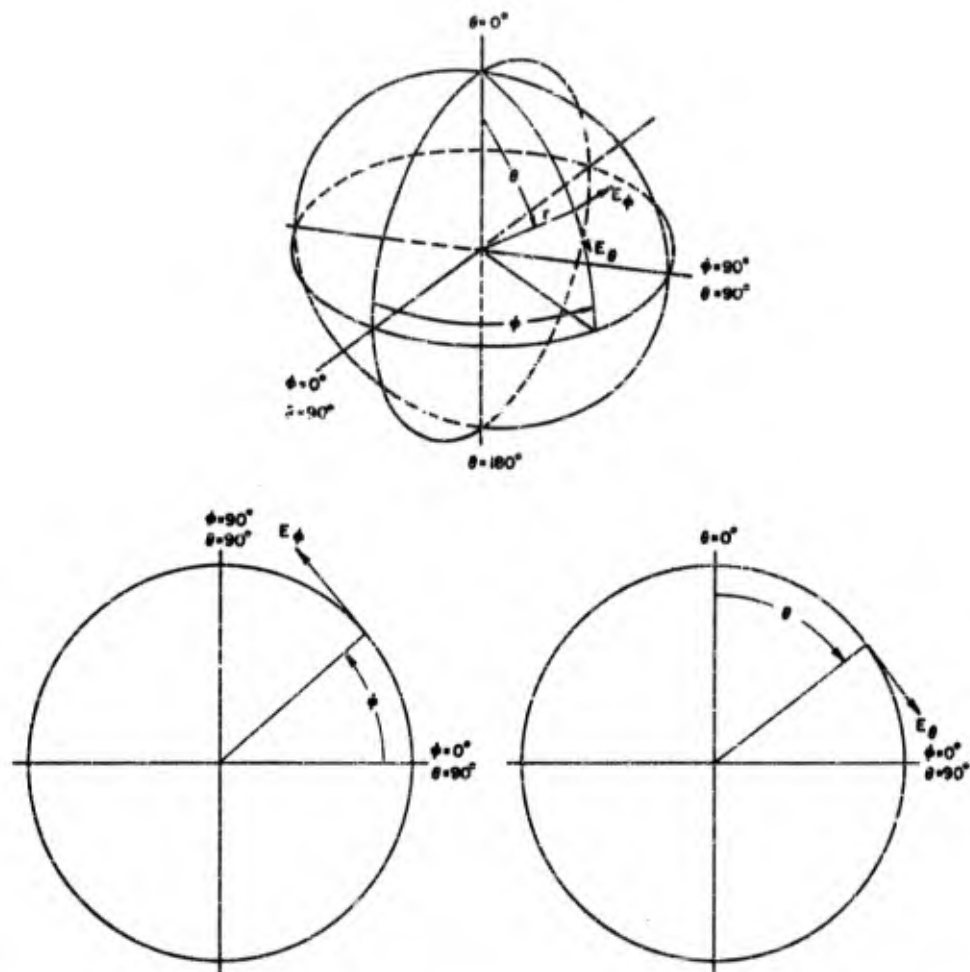
YES

NO

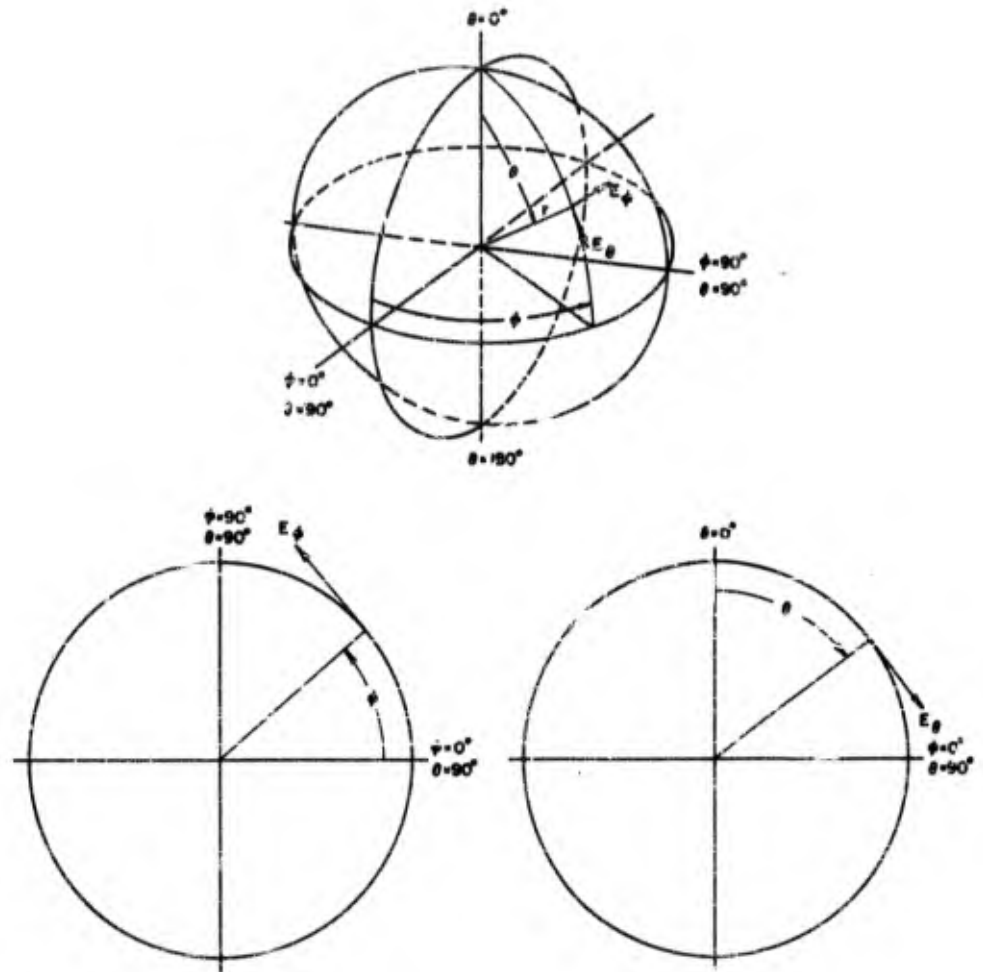
5.6 Distribution List

Give a distribution list for the above data.

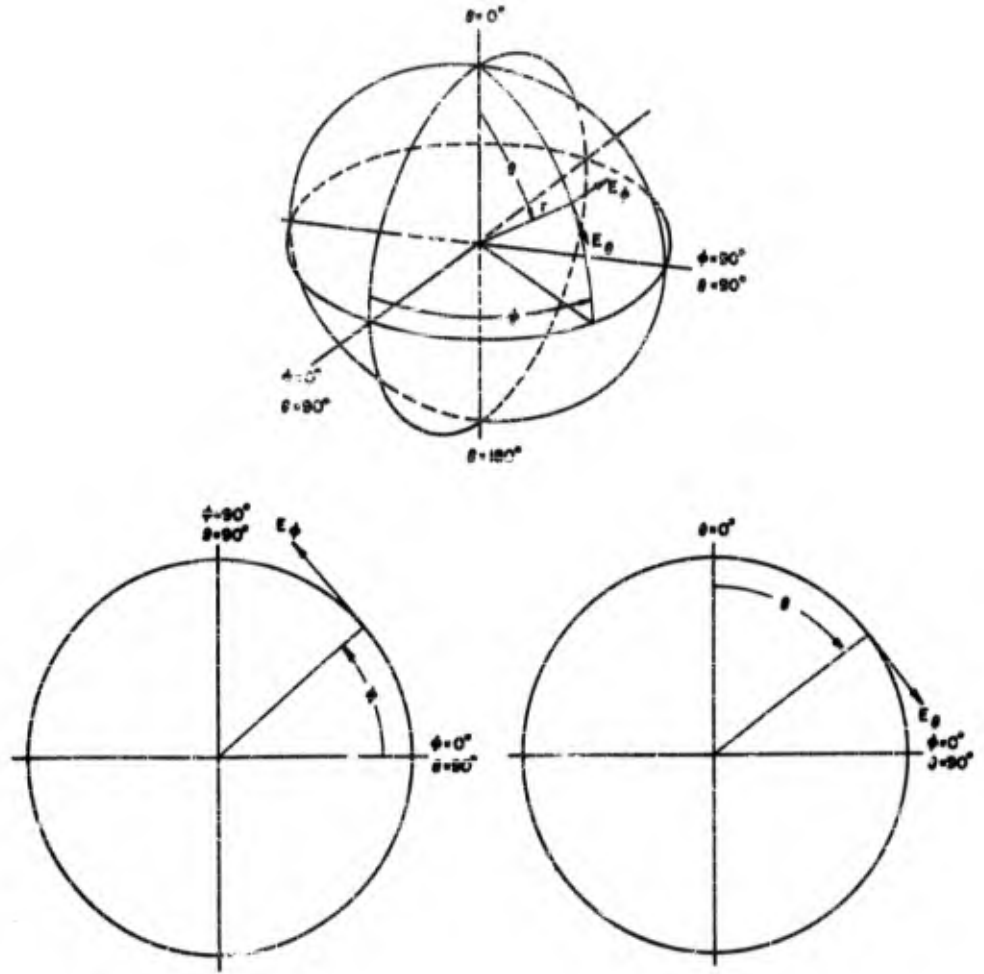
Paragraphs 5.1 and 5.5 per IRIG Document No. 102-61.



RADIATION PATTERN FOR RIGHT CIRCULAR
(LEFT CIRCULAR) POLARIZATION



RADIATION PATTERN FOR LINEAR E_θ POLARIZATION



RADIATION PATTERN FOR LINEAR E_0 POLARIZATION

6.0 THE ANTENNA HARNESS

6.1 Standard Harness

If no special request is made, the harness for telemetry and S-Band antennas is built with RG 142/U cable and BNC connectors, the harness for the C-Band antennas is built with 9/64 diameter copper jacket cable and TNC or TM connectors.

6.2 Cable Type

6.3 Connector Type

6.4 Specific Connector Required to Mate With the Transmitter or Receive Connector

6.5 Required Cable Length From the Harness Junction to the Transmitter or Receiver

7.0 RADIO FREQUENCY BREAKDOWN

7.1 Description of Breakdown

Two types of breakdown may occur. Multipacting breakdown which will be sustained in a vacuum once it is started and diffusion breakdown which is a function of power and altitude. The multipacting breakdown can usually be corrected. The diffusion breakdown depends on the antenna type. There is no simple way to correct it. The diffusion breakdown terminates spontaneously after the vehicle reaches a particular altitude which depends on the antenna type and the power fed to the antenna. Optimum breakdown conditions exist at an altitude which is defined by the equation below:

$$fd = 52.5$$

where f is the frequency in megacycles per second,

d is the mean free path of the neutral particles in centimeters.

The two consequences of breakdown usually important to the experimenter are the attenuation or loss of signal and large mismatch with respect to the transmitter.

Please check below, the type of breakdown information required.

7.2 No Breakdown Data Required

7.3 Nominal Breakdown Data Obtained From Similar Antennas

7.4 Specific Breakdown Data

7.5 Correlation Between Measured and Flight Data

It should be noted with regard to the measurements above that all data are obtained in a vacuum chamber which can only approximate the actual flight conditions. However, in the past the breakdown in the belljar is apparently more severe than in flight.

8.0 VIBRATION TESTS

8.1 Nominal Vibration Data Obtained From the Antenna Type Are Sufficient

8.2 Specific Vibration Data for Each Antenna Are Required; Specify Required Data

9.0 SPECIAL ANTENNA PROPERTIES

9.1 Non-magnetic

YES

NO

ACKNOWLEDGEMENT

The persons who have contributed to this report are H. W. Haas, B. M. Keenan, R. C. Lanphere, Jr., C. C. Post, J. E. Shannon, L. L. Snow and H. D. Weinschel and numerous student Scientific Aides from New Mexico State University.

BIBLIOGRAPHY

- Duncan, R. H. and Haas, H. W. , Volume I Quadraloop Antennas, Part I- The Design and Performance of Quadraloop Antennas. Part II- Telemetering Quadraloop Antennas for Project Vanguard. Part III- and IV-Issued as a supplementary classified report. , 1957
- Henry, D. G. , Duncan, R. H. and Haas, H. W. , The Design and Performance of Quadraloop Telemetry and Control Antennas for the Aerobee HI and Spaerobee Rockets, 1960
- Keenan, B. M. and Haas, H. W. , Design and Performance of the Models 2.003, 2.004, 2.005 and 2.009 Telemetry Quadraloop Antennas , 1961
- Weinschel, H. D. and Haas, H. W. , Design and Performance of Models II-A, II-B, II-C Telemetry Antennas for Aerobee and Calch Vehicles, 1962
- Weinschel, H. D. and Haas, H. W. , Telemetry and Command Control Antennas for the Guided Flight Vehicle, 1962
- Weinschel, H. D. and Haas, H. W. , Design and Performance of Model 2.007 Telemetry Antennas for the AFSWC-EOS Payload, 1962
- Weinschel, H. D. and Haas, H. W. , Design and Performance of Model 4.001 Command Control Antenna for ARGO D8-F1 Vehicle, 1961
- Haas, H. W. , Telemetering Notch Antenna 225.0 Mc/Sec Aerobee HI Rocket
- Henry, D. G. , Duncan, R. H. and Haas, H. W. , 400 Mc/Sec Cutoff Notch Antenna Aerobee HI, 1960
- Henry, D. G. , Duncan, R. H. and Haas, H. W. , The Design and Performance of Telemetry and Command Control Fin Notch Antennas for Aerobee 150-A, 1960
- Smith, H. D. and Duncan, R. H. , Radiation Pattern Measurements of an S-Band Quadraloop Two-Element Antenna Array Mounted on an Aerobee Rocket, 1958
- Weinschel, H. D. and Haas, H. W. , S-Band Beacon Antennas for Aerobee 150, 1962
- Sanchez, M. J. and Haas, H. W. , Speedball missile-Borne Scimitar Antennas, 1961
- Henry, D. G. , Diel, J. H. and Haas, H. W. , C-Band Beacon Antennas for Project 6.13 of Operation Washbowl, 1962

- Henry, D. G., Diel, J. H. and Haas, H. W., C-Band Beacon Antennas for Damp in Connection with Operation Fishbowl, 1962
- Duncan, R. H. and Haas, H. W., Radio Frequency Diffusion Breakdown Analysis Martin Company Telemetry Quadraloop Antenna Design Project Vanguard, 1958
- Haas, H. W., Antenna Breakdown, 1960
- Williams, H. Bartel, Investigation of the Secondary Electron Resonance Mechanism and Its Role in High Frequency-Low Pressure Gas Breakdown, 1951
- Radiation Pattern Measurement Procedure for PSL Antenna Range, (Internal PSL Document), 1961
- Haas, H. W., An Antenna Radiation Pattern Measuring Research Instrument, 1963
- King, R., Morrison, C. W., Jr., and Denton, D. H., Jr., Transmission Line Missile Antennas, Volume AP-8, January 1960, Number 1
- U. S. Standard Atmosphere, 1962, Prepared under sponsorship of NASA, U. S. Air Force and the U. S. Weather Bureau
- Jackson, J. E. and Kane, J. A., Breakdown and Detuning of Transmitting Antennas in the Ionosphere, Upper Atmosphere Research Report No. XXXVI, 1959

DISTRIBUTION LIST

Copy No.

1-100

Headquarters
Air Force Cambridge Research Laboratories
Office of Aerospace Research
Laurence G. Hanscom Field
Bedford, Massachusetts
Attention: CRZEL/Raymond E. Wilton

UNCLASSIFIED

UNCLASSIFIED